

14

OSU

The Ohio State University

AD-A163 027

SURFACE SHIP CLASSIFICATION
USING MULTIPOLARIZATION,
MULTIFREQUENCY SKY-WAVE RESONANCE RADAR

by

Neil F. Chamberlain

The Ohio State University

ElectroScience Laboratory

Department of Electrical Engineering
Columbus, Ohio 43212

Project No. 714190-9

Contract No. N00014-82-K-0037

October 1984

DTIC FILE COPY

Office of Naval Research
800 North Quincy Street
Arlington, Virginia 22217

DTIC
ELECTE
JAN 08 1986
S D E

This document has been approved
for public release and its
distribution is unlimited.

85 11 08 001

NOTICES

When Government drawings, specifications, or other data are used for any purpose other than in connection with a definitely related Government procurement operation, the United States Government thereby incurs no responsibility nor any obligation whatsoever, and the fact that the Government may have formulated, furnished, or in any way supplied the said drawings, specifications, or other data, is not to be regarded by implication or otherwise as in any manner licensing the holder or any other person or corporation, or conveying any rights or permission to manufacture, use, or sell any patented invention that may in any way be related thereto.

REPORT DOCUMENTATION PAGE		1. REPORT NO. <i>AD-A163 027</i>		3. Recipient's Accession No.	
4. Title and Subtitle SURFACE SHIP CLASSIFICATION USING MULTIPOLARIZATION, MULTIFREQUENCY SKY-WAVE RESONANCE RADAR				5. Report Date October 1984	
7. Author(s)				6.	
9. Performing Organization Name and Address The Ohio State University ElectroScience Laboratory Dept. of Electrical Engineering 1320 Kinnear Road Columbus, Ohio 43212				8. Performing Organization Rept. No. 714190-9	
12. Sponsoring Organization Name and Address Office of Naval Research 800 North Quincy Street Arlington, Virginia 22217				10. Project/Task/Work Unit No.	
				11. Contract(C) or Grant(G) No. (C) N00014-82-K-0037 (G)	
15. Supplementary Notes				13. Type of Report & Period Covered Technical Report	
16. Abstract (Limit: 200 words) Experiments investigating the classification of surface ships using processed radar returns are described. The calibrated and scaled backscatter measurements of scale-model ships at several aspect and elevation angles are used to establish a catalog representing the HF sky-wave resonance region radar returns of actual ship targets. The performance of both the nearest neighbour algorithm, (using frequency domain data), and a correlation algorithm (using time domain data), is investigated. The effects of wave polarization, aspect angle, elevation angle and other key parameters are examined. The consequences of introducing forced errors into the estimates of aspect and elevation angle are studied. A novel feature set employing the ratio of vertically and horizontally polarized radar returns is described, and its classification performance is examined. In general, classification is found to be very much dependent on the particular aspect angle and polarization of interest. The time domain algorithm, vertical polarization, and bow and stern aspects are the parameters which yield best all-round classification performance. Increasing the number of classification frequencies improves performance, but only to a limit. Errors in aspect angle and especially in elevation angle are found to significantly degrade classification performance. A number of suggestions for improving the classification process are discussed. <i>X</i>					
17. Document Analysis a. Descriptors					
b. Identifiers/Open-Ended Terms					
c. COSATI Field/Group					
18. Availability Statement			19. Security Class (This Report) Unclassified		21. No of Pages 372
			20. Security Class (This Page) Unclassified		22. Price

TABLE OF CONTENTS

		<u>PAGE</u>
	LIST OF TABLES.....	vi
	LIST OF FIGURES.....	vii
<u>CHAPTER</u>		
I	INTRODUCTION.....	1
II	SKY-WAVE RESONANCE RADAR.....	5
	2.1 INTRODUCTION.....	5
	2.2 HF RADAR SPECIFICATIONS.....	7
	2.3 MEASUREMENT OF HF AMPLITUDE AND PHASE RETURNS.....	11
	2.4 MEASUREMENT OF PHASE RETURNS.....	15
	2.5 CHOICE OF FREQUENCIES IN SKY-WAVE RADAR.....	16
III	GENERATING A DATA BASE.....	19
	3.1 INTRODUCTION.....	19
	3.2 MEASUREMENT OF DATA.....	20
	3.3 CALIBRATING THE DATA.....	24
	3.3-1 THE GROUNDPLANE.....	26
	3.3-2 CHECKING CALIBRATED RESPONSES.....	37
	3.4 DATA SCALING.....	41
	A SUMMARY OF SCALED DATA GENERATION.....	43
IV	TARGET CLASSIFICATION.....	44
	4.1 INTRODUCTION.....	44
	4.2 CLASSIFICATION IN THE FREQUENCY DOMAIN.....	46
	4.3 CLASSIFICATION IN THE TIME DOMAIN.....	49
	4.4 RELATIVE AMPLITUDE FEATURE.....	51

	<u>PAGE</u>
V EXPERIMENTAL CONSIDERATIONS.....	52
5.1 INTRODUCTION.....	52
5.2 CHOICE OF EXPERIMENTAL FREQUENCIES.....	55
5.3 SELECTION OF β IN NEAREST NEIGHBOUR ALGORITHM.....	56
5.4 NOISE MODEL.....	57
5.5 POST-PROCESSING SIGNAL TO NOISE RATIO.....	63
5.6 ESTIMATION OF THE PROBABILITY OF MISCLASSIFICATION	66
VI EXPERIMENTS.....	69
6.1 INTRODUCTION.....	69
6.1.2 INTERPRETATION OF HEADERS IN MISCLASSIFICATION PERCENTAGE VERSUS SIGNAL TO NOISE RATIO CURVES.....	74
6.2 FREQUENCY BAND.....	76
6.2.1 INTRODUCTION.....	76
6.2.2 RESULTS AND CONCLUSIONS.....	77
6.3 COMPARISON WITH PREVIOUS WORK.....	81
6.3.1. INTRODUCTION.....	81
6.3.2 RESULTS AND CONCLUSIONS.....	82
6.4 ELEVATION ANGLE.....	90
6.4.1 INTRODUCTION.....	90
6.4.2 RESULTS AND CONCLUSIONS.....	91
6.5 POLARIZATION.....	101
6.5.1 INTRODUCTION.....	101
6.5.2 RESULTS AND CONCLUSIONS.....	103
6.6 ASPECT ZONE.....	108
6.6.1 INTRODUCTION.....	108
6.6.2 RESULTS AND CONCLUSIONS.....	108
6.7 ERROR IN ASPECT.....	113
6.7.1 INTRODUCTION.....	113
6.7.2 RESULTS AND CONCLUSIONS.....	115
VII CONCLUSIONS.....	124

REFERENCES..... 137

APPENDICES

A. CLASSIFICATION RESULTS..... 139

B. AMPLITUDE AND PHASE RETURNS..... 277

C. PROGRAMS..... 288

Accession For	
NTIS GRA&I <input checked="" type="checkbox"/>	
DTIC TAB <input type="checkbox"/>	
Unannounced <input type="checkbox"/>	
Justification <i>per</i>	
By _____	
Distribution/	
Availability Codes	
Dist	Avail and/or Special
<i>A-1</i>	



LIST OF TABLES

<u>TABLE</u>		<u>PAGE</u>
2.1	SPECIFICATIONS OF HF RADARS (from [1]).....	8
3.1	SUMMARY OF TARGET SPECIFICATIONS.....	23
3.2	SCALE FACTORS FOR MODEL SHIPS AND ASSOCIATED FREQUENCY BANDS.....	41
5.1	RANGE OF FREQUENCIES USED IN EXPERIMENTS.....	56
6.1	DEFINITIONS.....	70
B.1	AVERAGE AMPLITUDES FOR VARIOUS CATALOGS, CONTAINING SIX SHIPS.....	287

LIST OF FIGURES

<u>FIGURE</u>	<u>PAGE</u>
1.1. Block diagram of target classification system. The catalog contains returns of some preselected targets ($\hat{A}, \hat{\theta}$). The output of the signal processor is a set of amplitude and phase returns of the inknown target. (from [1]).....	4
2.1. The resolution cell of a sky-wave radar, shown by the shaded area (from [1]).....	10
2.2. A doppler spectrum is shown in which a ship target return is separated from the clutter. The reference here is the larger first order sea scatter. The doppler frequency is normalized to the 1 st order sea scatter doppler frequency; that is $f_r = -1$ (from [11]).....	14
3.1. Schematic diagram of the compact range system.....	21
3.2. Silhouettes of the six ships used in measurements and classifications, shown for a scale of 1:1700 (from [23])....	25
3.3. The groundplane and its low profile supporting structure....	27
3.4. An example of how the impulse respone of a ship retains groundplane edge residuals (at ± 3 ns.) after calibration. The main response of the ship is constrained within ± 0.5 ns, and decays into clutter after 1.5 ns.....	30
3.5. The impulse response, 2-18 GHz, of an uncalibrated target on groundplane after background subtraction, showing the location in time of all major scatterers and the pre-calibration Hanning window. The response from -50 ns to 50 ns is the continuation of the response from 0 ns to 50 ns.....	31
3.6. An uncalibrated six-inch sphere with background and path delay removed showing the occurrence of phase steps at the 4, 8, and 12.4 GHz receives band edges.....	33
3.7. Calibrated ship data using a narrow ± 3 ns pre-calibration window to remove groundplane edge residuals, resulting in in the occurrence of spikes at the receiver band edges.....	35

<u>FIGURE</u>	<u>PAGE</u>
3.9. Resultant frequency response when a flat 2 to 18 GHz frequency response is windowed in the time domain with a ± 3 ns Hanning window.....	38
3.10. A ship scaled 1:1 with its impulse response in order to check a calibration.....	40
4.1. Basic process of a pattern classification system.....	45
5.1. A flow chart of the experimental process of classification.	53
5.2. Schematic diagram summarizing the various stages of noise contamination after the initial scattering of radar energy by a ship.....	58
5.3. The distribution of the noise on an I-Q plane (from [1])....	61
6.1. Misclassification percentage versus post-processing SNR for 3 sub-bands in the 2-7 MHz band.....	78
6.2. Average misclassification percentages at 10 dB post-processing SNR for 3 bands, as a function of aspect zone.....	79
6.3. Average misclassification percentages at 10 dB post-processing SNR for 3 bands, as a function of algorithm.....	80
6.4. Average misclassification percentages at 10 dB post-processing SNR for 3 bands, as a function of polarization.....	80
6.5. Misclassification percentage versus post-processing SNR for 4 different numbers of frequencies, using amplitudes only...	83
6.6. Misclassification percentage versus post-processing SNR for 4 different numbers of frequencies, using the time domain algorithm.....	84
6.7. Average misclassification percentages at 10 dB post-processing SNR for 3 different numbers of frequencies as a function of algorithm (from Chen [1]).....	85
6.8. Average misclassification percentages at 10 dB post-processing SNR for 3 different numbers of frequencies as a function of algorithm.....	85

<u>FIGURE</u>	<u>PAGE</u>
6.9. Misclassification percentage versus post-processing SNR for known and unknown aspect angles.....	88
6.10. Average misclassification percentages at 10 dB post-processing SNR for known and unknown aspect angles as a function of algorithm (from [1]).....	89
6.8. Average misclassification percentages at 10 dB post-processing SNR for 3 different numbers of frequencies as a function of algorithm.....	85
6.9. Misclassification percentage versus post-processing SNR for known and unknown aspect angles.....	88
6.10. Average misclassification percentages at 10 dB post-processing SNR for known and unknown aspect angles as a function of algorithm (from [1]).....	89
6.11. Average misclassification percentages at 10 dB post-processing SNR for known and unknown aspect angles as a function of algorithm.....	89
6.12. Average misclassification percentage versus the number of frequencies used.....	90
6.13. Misclassification percentage versus post-processing SNR for various elevation angles.....	92
6.14. Misclassification percentage versus post-processing SNR for various elevation angles.....	93
6.16. Misclassification percentage versus post-processing SNR for various elevation angles.....	95
6.17. Average misclassification percentages at 10 dB post-processing SNR for various elevation angles as a function of aspect zone.....	96
6.18. Average misclassification percentages at 10 dB post-processing SNR for various elevation angles as a function of polarization.....	96
6.19. Average misclassification percentages at 10 dB post-processing SNR for various elevation angles as a function of algorithm.....	97

<u>FIGURE</u>	<u>PAGE</u>
6.20. Average misclassification percentages at 10 dB post-processing SNR for an elevation error of $\pm 12^\circ$ as a function of aspect zone and polarization.....	97
6.21. Average misclassification percentages at 10 dB post-processing SNR for an elevation error of $\pm 12^\circ$ as a function of aspect zone and algorithm.....	98
6.22. Misclassification percentage versus post-processing SNR for various polarizations.....	104
6.23. Average misclassification percentage at 10 dB post-processing SNR for various polarizations as a function of aspect zone.....	105
6.24. Average misclassification percentage at 10 dB post-processing SNR for various polarizations as a function of algorithm.....	105
6.25. Misclassification percentage versus post-processing SNR for various aspect zones using vertical polarization.....	110
6.26. Misclassification percentage versus post-processing SNR for various aspect zones using V/H polarization.....	111
6.27. Average misclassification percentage at 10 dB post-processing SNR for various aspect zones, as a function of polarization.....	112
6.28. Average misclassification percentage at 10 dB post-processing SNR for various aspect zones, as a function of algorithm.....	112
6.29. A ship travelling with velocity V_s from point P_1 to point P_2 has an apparent aspect angle of θ_a degrees owing to the sea current having a velocity V_c	114
6.30. Misclassification percentage versus post-processing SNR for various aspect errors, near to 0° aspect, using vertical polarization.....	116
6.31. Misclassification percentage versus post-processing SNR for various aspect errors, near to 0° aspect, using cross polarization.....	117
6.32. Misclassification percentage versus post-processing SNR for an aspect error of $\pm 10^\circ$ at various aspect zone.....	118

<u>FIGURE</u>	<u>PAGE</u>
6.33. Average misclassification percentage at 10 dB post-processing SNR for various aspect errors, near to 0° aspect, as a function of polarization.....	119
6.34. Average misclassification percentage at 10 dB post-processing SNR for various aspect errors, near to 0° aspect, as a function of algorithm.....	119
6.35. Average difference in misclassification percentage at 10 dB post-processing SNR between classifications having a 0° aspect error and classifications having a ±10° aspect error, at various aspect zones, as a function of polarization.....	122
6.36. Average difference in misclassification percentage at 10 dB post-processing SNR between classifications having a 0° aspect error and classifications having a ±10° aspect error, at various aspect zones, as a function of algorithm.....	122
7.1. Variation of normalization constant, derived from the variances of the noise contaminated amplitudes (A_n) and differential phases (W_n), with post-processing SNR. The curves are representative of 2 and 8 frequencies using the AW feature in the NN algorithm, for ships at 0°, 90° and 180° aspect angles and 27° elevation angle.....	136

<u>FIGURE</u>	<u>PAGE</u>
A.1. Misclassification percentage versus post-processing SNR, comparing the performance of 3 sub-bands in the 2-7 MHz band.....	140
A.2. Misclassification percentage versus post-processing SNR, comparing the performance of 3 sub-bands in the 2-7 MHz band.....	141
A.3. Misclassification percentage versus post-processing SNR, comparing the performance of 3 sub-bands in the 2-7 MHz band.....	142
A.4. Misclassification percentage versus post-processing SNR, comparing the performance of 3 sub-bands in the 2-7 MHz band.....	143
A.5. Misclassification percentage versus post-processing SNR, comparing the performance of 3 sub-bands in the 2-7 MHz band.....	144
A.6. Misclassification percentage versus post-processing SNR, comparing the performance of 3 sub-bands in the 2-7 MHz band.....	145
A.7. Misclassification percentage versus post-processing SNR, comparing the performance of 3 sub-bands in the 2-7 MHz band.....	146
A.8. Misclassification percentage versus post-processing SNR, comparing the performance of 3 sub-bands in the 2-7 MHz band.....	147
A.9. Misclassification percentage versus post-processing SNR, comparing the performance of 3 sub-bands in the 2-7 MHz band.....	148
A.10. Misclassification percentage versus post-processing SNR, comparing the performance of different numbers of frequencies.....	149
A.11. Misclassification percentage versus post-processing SNR, comparing the performance of different numbers of frequencies.....	150
A.12. Misclassification percentage versus post-processing SNR, comparing the performance of different numbers of frequencies.....	151

<u>FIGURE</u>	<u>PAGE</u>
A.13. Misclassification percentage versus post-processing SNR, comparing the performance of different numbers of frequencies.....	152
A.14. Misclassification percentage versus post-processing SNR, comparing the performance of different algorithms.....	153
A.15. Misclassification percentage versus post-processing SNR, comparing the performance of different algorithms.....	154
A.16. Misclassification percentage versus post-processing SNR, comparing the performance of different algorithms.....	155
A.17. Misclassification percentage versus post-processing SNR, comparing the performance of known and unknown aspect angles.....	156
A.18. Misclassification percentage versus post-processing SNR, comparing the performance of known and unknown aspect angles.....	157
A.19. Misclassification percentage versus post-processing SNR, comparing the performance of known and unknown aspect angles.....	158
A.20. Misclassification percentage versus post-processing SNR, comparing the performance of known and unknown aspect angles.....	159
A.21. Misclassification percentage versus post-processing SNR, comparing the performance of known and unknown aspect angles.....	160
A.22. Misclassification percentage versus post-processing SNR, comparing the performance of various elevation angles.....	161
A.23. Misclassification percentage versus post-processing SNR, comparing the performance of various elevation angles.....	162
A.24. Misclassification percentage versus post-processing SNR, comparing the performance of various elevation angles.....	163
A.25. Misclassification percentage versus post-processing SNR, comparing the performance of various elevation angles.....	164
A.26. Misclassification percentage versus post-processing SNR, comparing the performance of various elevation angles.....	165

<u>FIGURE</u>	<u>PAGE</u>
A.27. Misclassification percentage versus post-processing SNR, comparing the performance of various elevation angles.....	166
A.28. Misclassification percentage versus post-processing SNR, comparing the performance of various elevation angles.....	167
A.29. Misclassification percentage versus post-processing SNR, comparing the performance of various elevation angles.....	168
A.30. Misclassification percentage versus post-processing SNR, comparing the performance of various elevation angles.....	169
A.31. Misclassification percentage versus post-processing SNR, comparing the performance of various elevation angles.....	170
A.32. Misclassification percentage versus post-processing SNR, comparing the performance of various elevation angles.....	171
A.33. Misclassification percentage versus post-processing SNR, comparing the performance of various elevation angles.....	172
A.34. Misclassification percentage versus post-processing SNR, comparing the performance of various elevation angles.....	173
A.35. Misclassification percentage versus post-processing SNR, comparing the performance of various elevation angles.....	174
A.36. Misclassification percentage versus post-processing SNR, comparing the performance of various elevation angles.....	175
A.37. Misclassification percentage versus post-processing SNR, comparing the performance of various elevation angles.....	176
A.38. Misclassification percentage versus post-processing SNR, comparing the performance of various elevation angles.....	177
A.39. Misclassification percentage versus post-processing SNR, comparing the performance of various elevation angles.....	178
A.40. Misclassification percentage versus post-processing SNR, comparing the performance of various elevation angles.....	179
A.41. Misclassification percentage versus post-processing SNR, comparing the performance of various elevation angles.....	180
A.42. Misclassification percentage versus post-processing SNR, comparing the performance of various elevation angles.....	181

<u>FIGURE</u>	<u>PAGE</u>
A.43. Misclassification percentage versus post-processing SNR, comparing the performance of various elevation angles.....	182
A.44. Misclassification percentage versus post-processing SNR, comparing the performance of various elevation angles.....	183
A.45. Misclassification percentage versus post-processing SNR, comparing the performance of various elevation angles.....	184
A.46. Misclassification percentage versus post-processing SNR, comparing the performance of various elevation angles.....	185
A.47. Misclassification percentage versus post-processing SNR, comparing the performance of various elevation angles.....	186
A.48. Misclassification percentage versus post-processing SNR, comparing the performance of various elevation angles.....	187
A.49. Misclassification percentage versus post-processing SNR, comparing the performance of various elevation angles.....	188
A.50. Misclassification percentage versus post-processing SNR, comparing the performance of various elevation angles.....	189
A.51. Misclassification percentage versus post-processing SNR, comparing the performance of various elevation angles.....	190
A.52. Misclassification percentage versus post-processing SNR, comparing the performance of various elevation angles.....	191
A.53. Misclassification percentage versus post-processing SNR, comparing the performance of various elevation angles.....	192
A.54. Misclassification percentage versus post-processing SNR, comparing the performance of various elevation angles.....	193
A.55. Misclassification percentage versus post-processing SNR, comparing the performance of various elevation angles.....	194
A.56. Misclassification percentage versus post-processing SNR, comparing the performance of various elevation angles.....	195
A.57. Misclassification percentage versus post-processing SNR, comparing the performance of various elevation angles.....	196
A.58. Misclassification percentage versus post-processing SNR, comparing the performance of various elevation angles.....	197

<u>FIGURE</u>	<u>PAGE</u>
A.59. Misclassification percentage versus post-processing SNR, comparing the performance of various elevation angles.....	198
A.60. Misclassification percentage versus post-processing SNR, comparing the performance of various elevation angles.....	199
A.61. Misclassification percentage versus post-processing SNR, comparing the performance of various elevation angles.....	200
A.62. Misclassification percentage versus post-processing SNR, comparing the performance of various elevation angles.....	201
A.63. Misclassification percentage versus post-processing SNR, comparing the performance of various elevation angles.....	202
A.64. Misclassification percentage versus post-processing SNR, comparing the performance of various elevation angles.....	203
A.65. Misclassification percentage versus post-processing SNR, comparing the performance of various elevation angles.....	204
A.66. Misclassification percentage versus post-processing SNR, comparing the performance of various polarizations.....	205
A.67. Misclassification percentage versus post-processing SNR, comparing the performance of various polarizations.....	206
A.68. Misclassification percentage versus post-processing SNR, comparing the performance of various polarizations.....	207
A.69. Misclassification percentage versus post-processing SNR, comparing the performance of various polarizations.....	208
A.70. Misclassification percentage versus post-processing SNR, comparing the performance of various polarizations.....	209
A.71. Misclassification percentage versus post-processing SNR, comparing the performance of various polarizations.....	210
A.72. Misclassification percentage versus post-processing SNR, comparing the performance of various polarizations.....	211
A.73. Misclassification percentage versus post-processing SNR, comparing the performance of various polarizations.....	212
A.74. Misclassification percentage versus post-processing SNR, comparing the performance of various polarizations.....	213

<u>FIGURE</u>	<u>PAGE</u>
A.75. Misclassification percentage versus post-processing SNR, comparing the performance of various polarizations.....	214
A.76. Misclassification percentage versus post-processing SNR, comparing the performance of various polarizations.....	215
A.77. Misclassification percentage versus post-processing SNR, comparing the performance of various polarizations.....	216
A.78. Misclassification percentage versus post-processing SNR, comparing the performance of various polarizations.....	217
A.79. Misclassification percentage versus post-processing SNR, comparing the performance of various polarizations.....	218
A.80. Misclassification percentage versus post-processing SNR, comparing the performance of various polarizations.....	219
A.81. Misclassification percentage versus post-processing SNR, comparing the performance of various polarizations.....	220
A.82. Misclassification percentage versus post-processing SNR, comparing the performance of various polarizations.....	221
A.83. Misclassification percentage versus post-processing SNR, comparing the performance of various aspect zones.....	222
A.84. Misclassification percentage versus post-processing SNR, comparing the performance of various aspect zones.....	223
A.85. Misclassification percentage versus post-processing SNR, comparing the performance of various aspect zones.....	224
A.86. Misclassification percentage versus post-processing SNR, comparing the performance of various aspect zones.....	225
A.87. Misclassification percentage versus post-processing SNR, comparing the performance of various aspect zones.....	226
A.88. Misclassification percentage versus post-processing SNR, comparing the performance of various aspect zones.....	227
A.89. Misclassification percentage versus post-processing SNR, comparing the performance of various aspect zones.....	228
A.90. Misclassification percentage versus post-processing SNR, comparing the performance of various aspect zones.....	229

<u>FIGURE</u>	<u>PAGE</u>
A.91. Misclassification percentage versus post-processing SNR, comparing the performance of various aspect zones.....	230
A.92. Misclassification percentage versus post-processing SNR, comparing the performance of various aspect zones.....	231
A.93. Misclassification percentage versus post-processing SNR, comparing the performance of various aspect zones.....	232
A.94. Misclassification percentage versus post-processing SNR, comparing the performance of various aspect zones.....	233
A.95. Misclassification percentage versus post-processing SNR, comparing the performance of various aspect zones.....	234
A.96. Misclassification percentage versus post-processing SNR, comparing the performance of various aspect zones.....	235
A.97. Misclassification percentage versus post-processing SNR, comparing the performance of various aspect zones.....	236
A.98. Misclassification percentage versus post-processing SNR, comparing the performance of various aspect zones.....	237
A.99. Misclassification percentage versus post-processing SNR, comparing the performance of various aspect zones.....	238
A.100. Misclassification percentage versus post-processing SNR, comparing the performance of various aspect zones.....	239
A.101. Misclassification percentage versus post-processing SNR, comparing the performance of various aspect zones.....	240
A.102. Misclassification percentage versus post-processing SNR, comparing the performance of various aspect zones.....	241
A.103. Misclassification percentage versus post-processing SNR, comparing the performance of various aspect zones.....	242
A.104. Misclassification percentage versus post-processing SNR, comparing the performance of various aspect zones.....	243
A.105. Misclassification percentage versus post-processing SNR, comparing performance with various aspect angle errors, near to 0° aspect.....	244

<u>FIGURE</u>	<u>PAGE</u>
A.106. Misclassification percentage versus post-processing SNR, comparing performance with various aspect angle errors, near to 0° aspect.....	245
A.107. Misclassification percentage versus post-processing SNR, comparing performance with various aspect angle errors, near to 0° aspect.....	246
A.108. Misclassification percentage versus post-processing SNR, comparing performance with various aspect angle errors, near to 0° aspect.....	247
A.109. Misclassification percentage versus post-processing SNR, comparing performance with various aspect angle errors, near to 0° aspect.....	248
A.110. Misclassification percentage versus post-processing SNR, comparing performance with various aspect angle errors, near to 0° aspect.....	249
A.111. Misclassification percentage versus post-processing SNR, comparing performance with various aspect angle errors, near to 0° aspect.....	250
A.112. Misclassification percentage versus post-processing SNR, comparing performance with various aspect angle errors, near to 0° aspect.....	251
A.113. Misclassification percentage versus post-processing SNR, comparing performance with various aspect angle errors, near to 0° aspect.....	252
A.114. Misclassification percentage versus post-processing SNR, comparing performance with various aspect angle errors, near to 0° aspect.....	253
A.115. Misclassification percentage versus post-processing SNR, comparing performance with various aspect angle errors, near to 0° aspect.....	254
A.116. Misclassification percentage versus post-processing SNR, comparing performance with various aspect angle errors, near to 0° aspect.....	255
A.117. Misclassification percentage versus post-processing SNR, comparing performance with various aspect angle errors, near to 0° aspect.....	256

<u>FIGURE</u>	<u>PAGE</u>
A.118. Misclassification percentage versus post-processing SNR, comparing performance with various aspect angle errors, near to 0° aspect.....	257
A.119. Misclassification percentage versus post-processing SNR, comparing performance with a $\pm 10^\circ$ aspect error at various aspect zones.....	258
A.120. Misclassification percentage versus post-processing SNR, comparing performance with a $\pm 10^\circ$ aspect error at various aspect zones.....	259
A.121. Misclassification percentage versus post-processing SNR, comparing performance with a $\pm 10^\circ$ aspect error at various aspect zones.....	260
A.122. Misclassification percentage versus post-processing SNR, comparing performance with a $\pm 10^\circ$ aspect error at various aspect zones.....	261
A.123. Misclassification percentage versus post-processing SNR, comparing performance with a $\pm 10^\circ$ aspect error at various aspect zones.....	262
A.124. Misclassification percentage versus post-processing SNR, comparing performance with a $\pm 10^\circ$ aspect error at various aspect zones.....	263
A.125. Misclassification percentage versus post-processing SNR, comparing performance with a $\pm 10^\circ$ aspect error at various aspect zones.....	264
A.126. Misclassification percentage versus post-processing SNR, comparing performance with a $\pm 10^\circ$ aspect error at various aspect zones.....	265
A.127. Misclassification percentage versus post-processing SNR, comparing performance with a $\pm 10^\circ$ aspect error at various aspect zones.....	266
A.128. Misclassification percentage versus post-processing SNR, comparing performance with a $\pm 10^\circ$ aspect error at various aspect zones.....	267
A.129. Misclassification percentage versus post-processing SNR, comparing performance with a $\pm 10^\circ$ aspect error at various aspect zones.....	268

<u>FIGURE</u>	<u>PAGE</u>
A.130. Misclassification percentage versus post-processing SNR, comparing performance with a $\pm 10^\circ$ aspect error at various aspect zones.....	269
A.131. Misclassification percentage versus post-processing SNR, comparing performance with a $\pm 10^\circ$ aspect error at various aspect zones.....	270
A.132. Misclassification percentage versus post-processing SNR, comparing performance with a $\pm 10^\circ$ aspect error at various aspect zones.....	271
A.133. Misclassification percentage versus post-processing SNR, comparing performance with a $\pm 10^\circ$ aspect error at various aspect zones.....	272
A.134. Misclassification percentage versus post-processing SNR, comparing the performance of various algorithms using unknown aspect.....	273
A.135. Misclassification percentage versus post-processing SNR, comparing the performance of various algorithms using unknown aspect.....	274
A.136. Misclassification percentage versus post-processing SNR, comparing the performance of various algorithms using unknown aspect.....	275
A.137. Misclassification percentage versus post-processing SNR, comparing the performance of various algorithms using unknown aspect.....	276
B.1. Ship at 0 degree aspect, vertical polarization.....	278
B.2. Ship at 90 degree aspect, vertical polarization.....	279
B.3. Ship at 180 degree aspect, vertical polarization.....	280
B.4. Ship at 0 degree aspect, horizontal polarization.....	281
B.5. Ship at 90 degree aspect, horizontal polarization.....	282
B.6. Ship at 180 degree aspect, horizontal polarization.....	283
B.7. Ship at 0 degree aspect, horizontal polarization.....	284
B.8. Ship at 90 degree aspect, horizontal polarization.....	285
B.9. Ship at 180 degree aspect, horizontal polarization.....	286

CHAPTER I

INTRODUCTION

The general radar problem has, conventionally, been one of finding the spatial location, or velocity or both, of some target. This information can be extended to include a knowledge of the target's identity, if the operating frequencies of the radar are properly chosen. More specifically, if the wavelength of the radar energy is comparable to the maximum dimension of the target (i.e., in the resonance region), then certain essential information, relating to the target's dimensions and shape, will be imbedded in the radar return. Radars operating in the HF band (3 to 30 MHz) have wavelengths ranging from 10 to 100 m; hence missiles, aircraft and ships are potential candidates for resonance region target identification. Furthermore, frequencies in the HF band are capable of propagation over large distances (perhaps up to 4000 km) and thus, with an HF radar system we have, *prima facie*, the potential for identifying ships and aircraft, etc., at very long ranges. Figure 1.1 shows a diagram of an HF radar target classification system.

Chen [1] studied the available techniques for measuring and processing the radar returns of targets in the HF band. He concluded that sufficient signal-to-noise ratio could be attained after processing (in a reasonable amount of time) to permit target classification. He developed algorithms to implement target classification and, in conjunction with simulated radar returns of ships and aircraft, studied classification performance as a function of post-processed signal-to-noise ratio.

Chen's investigations involved the use of data for ships and aircraft at zero degrees elevation angle, using vertical polarization. Hence, for the case of ships, the data was representative of surface-wave radar returns. HF radiation can also propagate by means of sky-waves, that is, by ionospheric refraction, and target classification for this mode of propagation is the subject of investigation in this report. Classification at various polarizations and aspect angles are also considered. Hence, the problem addressed here is one of studying the classification of ship targets in a representatively noisy environment, using simulated multiple-frequency, multiple-polarization, sky-wave resonance radar returns.

Chapter II discusses the general nature and limitations of the HF sky-wave radar system and how these relate to the measurement of phase and amplitude returns. Chapter III describes the generation of a database of ship amplitude and phase returns, with particular reference to problems incurred by the use of a groundplane to simulate the surface of the sea. Chapter IV details the classification algorithms used in

experiments. Chapter V describes the experimental procedure and other considerations, such as the specifications of the noise model, which relate to the HF resonance radar detection problem. Chapter VI summarizes the results of the various classification experiments and draws conclusions from these and other observations. Representative curves of misclassification percentage versus post-processing signal-to-noise ratio are included in Chapter VI, but the majority of these plots are appended, owing to their sheer bulk. Chapter VII presents a summary of the work, emphasizing the more important findings of Chapter VI, with conclusions and a set of recommendations for future work.

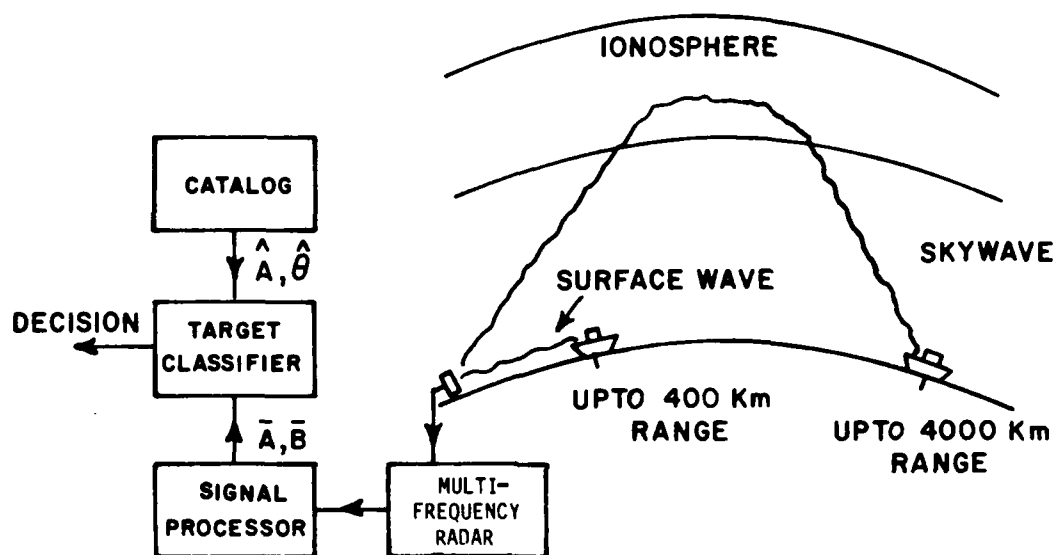


Figure 1.1. Block diagram of target classification system. The catalog contains returns of some preselected targets ($\hat{A}, \hat{\theta}$). The output of the signal processor is a set of amplitude and phase returns of the unknown target. (from [1])

CHAPTER II

SKY-WAVE RESONANCE RADAR

2.1 INTRODUCTION

Resonance radar is a technique whereby characteristic information of an object is gained by illuminating it with electromagnetic energy of certain wavelengths. These frequencies are commonly called resonance region frequencies, and are defined by the relation $L/\lambda \approx 1$, where L is the maximum dimension of the target and λ is the wavelength of the energy [3,4]. Hence, resonance radar extends our knowledge of a target beyond the conventional information concerning presence, location and velocity, and tells us something of the target's identity.

The principle of resonance region radar is applicable across the entire electromagnetic spectrum. For example, ships and aircraft can be interrogated with high frequencies (HF) [5,10], ground vehicles with very high frequencies (VHF) [20], satellites with ultra-high frequencies (UHF) and insects with microwaves. The technique is applicable to acoustic environments so that underwater objects could be investigated with resonant region SONAR sound waves. This report is concerned with HF resonance region radar used for the detection of ships.

Many of the first radar systems operated in the HF band (3-30 MHz). This is because microwave devices, such as the magnetron, were not available at that time. Generally it is more advantageous, in terms of directivity for a given antenna size and unhampered propagation [8], to use microwave frequencies for radar detection. However, HF radiation has the property of propagation beyond the line of sight by either surface-waves or ionospheric refraction (sky-waves). In fact, ship detection has been accomplished using a sky-wave radar system under a variety of atmospheric (and sea state) conditions by the Naval Research Laboratory [9]. Furthermore, wavelengths in the HF region (ranging from 10 to 100 m), are comparable to the dimensions of ships, missiles and aircraft, and are therefore suited to the resonance region techniques mentioned earlier. Chen [1] showed that reliable classification of ships can be achieved by processing representative resonance region multi-frequency radar returns. Ksienski and Lin [10] demonstrated similar results for aircraft. This chapter summarizes current techniques for measuring and processing HF radar returns, and discusses some of the limitations pertinent to sky-wave propagation.

2.2 HF RADAR SPECIFICATIONS

Table 2.1 lists and compares the specifications of sky-wave and surface-wave HF radar systems. The second is characterized by a range of 200-400 km. The limitation in range (compared with sky-wave radar) is due to the exponential attenuation of surface waves [8]. The work on the classification of ships and aircraft at an elevation angle of 0 degrees [1], is applicable to a surface-wave radar system. The data used in the experimental work of this report represents radar returns of ships at elevation angles above 0°, hence, sky-wave propagation and, in particular, ionospheric refraction is considered here.

The maximum range of a sky-wave radar is stated as 4000 km [9]. This value applies to a single skip (skip distance is the distance between radar and target after refraction from the ionosphere) and could be obtained by using an elevation angle of about 8° and a frequency of 23 MHz [9]. In general, it must be remembered that range is a function of both the ionospheric condition and the propagation frequency.

The antenna of a sky-wave radar must have a large aperture (about 1-2 km) in order to provide high gain and narrow azimuthal beamwidth. High gain (20 to 30 dB) is necessary to ensure adequate signal level in the noisy HF environment. Narrow azimuthal beamwidth is necessary for high azimuthal resolution and, in conjunction with range resolution, determines the cell size of a particular scan. Range resolution is limited by the instantaneous bandwidth, B, of the ionospheric

TABLE 2.1
SPECIFICATIONS OF HF RADARS (from [1])

	SKY-WAVE RADAR	SURFACE-WAVE RADAR
TRANSMITTED POWER	SEVERAL HUNDRED kW	HIGHER
RANGE	500 km to 4000 km	200-400 km
Antenna gain	20 to 30 dB	same
Antenna horizontal length	about 1 km	about 1 km
Waveform	can be pulsed sinusoidal waves	can be pulsed sinusoidal waves
Bandwidth	5 to 100 kHz	can be wider
pulse width	200 μ s to 10 μ s	can be narrower
Range resolution	2 to 40 km	can be smaller
Doppler resolution	0.01 to 0.1 Hz	can be less than 0.1 Hz
PRF	about 30 Hz	about 300 Hz
Targets	aircraft, ships, missiles	same
Antenna Azimuth beamwidth	about 1°	about 1°

propagation path, and is given by [8]

$$\Delta R = \frac{C}{2B \cos \phi} \quad (2.1)$$

where C is the speed of light, and ϕ is the elevation angle. For example, if $B = 100$ khz and $\phi = 30^\circ$, then $\Delta R = 1.7$ km. Figure 2.1 shows the effective cell size for a particular range R . Azimuth resolution is given by [8]

$$\Delta A_z = R \theta_B \quad (2.2)$$

where θ_B is the azimuth beamwidth. Using a 1° beamwidth antenna at a range of 2000 km yields an azimuth resolution of 35 km. Hence, a typical minimum cell size has an area on the order of 60 km².

The work of this report is concerned with the identification of single targets. It is quite conceivable that several ships could amass in a typical resolution cell and the resulting radar returns would then be a complex representation of a number of ships. This problem is considered as too complicated for a primary analysis, and thus is not addressed here.

Cell size also affects the signal-to-clutter ratio since a signal in a larger cell will inherently acquire more clutter. Clutter can be reduced by filtering in the doppler domain, and the resolution attainable in doppler frequency is inversely proportional to the coherent observation time.

The pulse repetition frequency (PRF) must be kept low to avoid range ambiguities. Maximum unambiguous range is given by [8]

$$R_{un} = \frac{C}{2 \text{ PRF}} \quad (2.3)$$

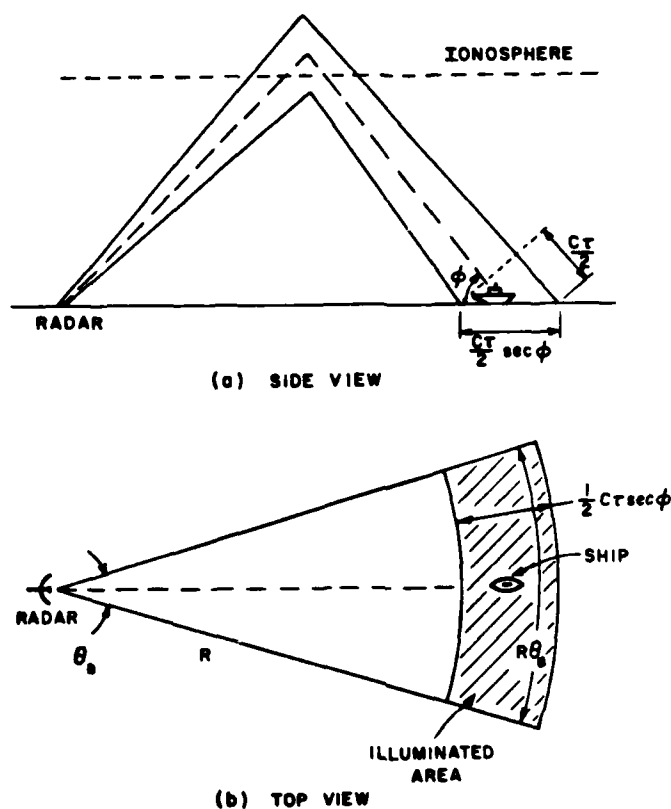


Figure 2.1. The resolution cell of a sky-wave radar, shown by the shaded area (from [1]). Note here that

- ϕ = elevation angle
- τ = pulse width
- C = speed of light
- R = wavepath length
- θ_B = antenna azimuth beam width

The PRF for an unambiguous maximum range of 4000 km is 37 Hz. A low PRF can lead to doppler ambiguities [8] and generally a compromise must be made between range and doppler ambiguity. The narrow bandwidth criterion imposed by the dispersive nature of the ionosphere requires that pulse widths should be about 10 μ s. For a square pulse of width τ , the null-to-null bandwidth is given by

$$B = 1/\tau \quad (2.4)$$

A narrow pulse width is an aid to improving signal to clutter ratio, however a long pulse is important for achieving the energy required for long-range detection.

2.3 MEASUREMENT OF HF AMPLITUDE AND PHASE RETURNS

The amplitude return, A , is defined as the square root of the radar cross section σ , where σ is given by

$$\sigma = \frac{\text{Scattered Power}}{\text{Incident Power Density at the Target}} \quad (2.5)$$

$$A \equiv \sqrt{\sigma} = \sqrt{\frac{p^r (4\pi)^3 R^4 L_p^2 L_s}{P_T G_T G_R \lambda^2 G_A}} \quad (2.6)$$

where:

P_T = Transmitter power

G_T = Transmitting antenna gain

G_R = Receiving antenna gain

λ = Wavelength of propagating energy

G_A = Receiver power gain

p^r = Power received

R = Range of target

L_p = One-way propagation loss

L_s = System loss

Equation 2.6 shows that the amplitude return depends on many parameters, some of which are difficult to estimate. The propagation loss, L_p , for example, is dependent on the continually changing state of the ionosphere for sky-wave radar. To obviate the need for such estimates, a reference signal return of another object close to the target is often used. The radar cross section of the reference target is given by

$$\sigma_{\text{ref}} = \frac{p^{\text{ref}} (4\pi)^3 R^4 L_p^2 L_s}{P_T G_T G_R \lambda^2 G_A} \quad (2.7)$$

The range and propagation loss in equations 2.6 and 2.7 are approximately equal, and other parameters P_T , G_T , G_R , G_A and L_s are similar by virtue of the fact that the reference and the target are illuminated at the same time and are thus contained in the same resolution cell. Radar cross section can then be defined as

$$\sigma = \frac{p^r}{p^{\text{ref}}} \sigma_{\text{ref}}. \quad (2.8)$$

p^r and p^{ref} are the received powers of the target and reference signals respectively, and σ^{ref} is estimated from a priori information or theoretical calculations.

Trizna [11] proposed a method for calibrating a target cross section by using the sea scatter as a reference. Essentially, the sea surface behaves like a diffraction grating and the moving water waves impart a doppler shift to the incident electromagnetic wave. Figure 2.2 shows a representative doppler spectrum for a ship and its reference sea echo. The doppler shifts depend upon the radial components (i.e., with respect to the direction of radar wave propagation) of the velocities of the ship and of the sea. The theoretical doppler spectrum of wind waves for a given sea state can then be computed using 1st and 2nd order radar cross section terms of the sea, in the manner described by Maresca and Barnum [12]. The calculated sea scatter cross section, σ_c , at a doppler shift of f_r Hz is then used in the calibration equation (Equation (2.8)) to find the calibrated target cross section

$$\sigma_t = \sigma_s - (\sigma_r - \sigma_c) \quad \text{dBm}^2 \quad (2.9)$$

Usually the reference return is on the order of 20 to 40 dB greater than the ship return. Typical figures taken from [11] give $\sigma_s = 40 \text{ dBm}^2$, $\sigma_r = 62 \text{ dBm}^2$ and $\sigma_c = 51 \text{ dBm}^2$ for a frequency of 21.8 MHz, vertically polarized, at 1600 km range, using a 17 second integration time. The resulting ship cross section, about 30 dBm^2 is typical of one of the smaller ships in the measured data set, for an aspect angle of 0° using vertical polarization. It is also

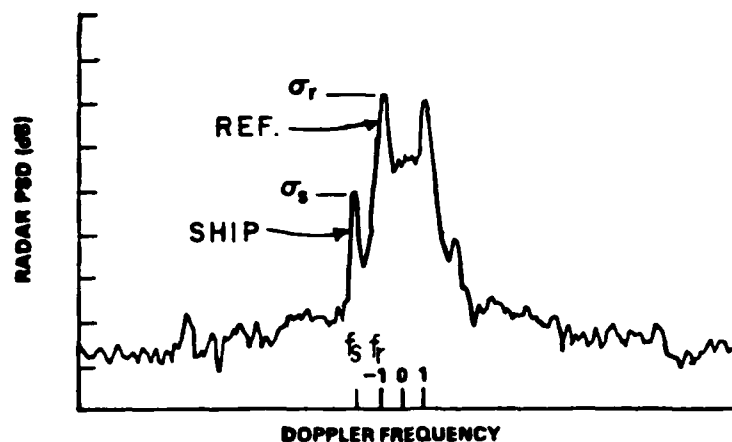


Figure 2.2. A doppler spectrum is shown in which a ship target return is separated from the clutter. The reference here is the larger first order sea scatter. The doppler frequency is normalized to the 1st order sea scatter doppler frequency; that is $f_r = -1$ (from [11]).

evident from Figure 2.2 that certain combinations of wave and ship velocity will render the ship and reference returns indistinguishable. Maresca and Barnum [12] defined a blind doppler frequency as one for which $\sigma_c > \sigma_t - 10$ dB. They concluded that for ships with cross sections in the order of 50 dBm², there were very few combinations of ship and wave velocity that resulted in blind doppler frequencies. For ships with cross sections of about 30 dBm², detection is contingent on the sea state. In general, the result depends on the frequency used, and the above problems can be averted by the use of higher operating frequencies when available. Of course, it is impossible to completely characterize a ship with a single radar cross section. A ship's cross section

depends on its size and orientation, as well as the frequency and polarization used. Typical cross sections might vary from 20 dBm² to over 70 dBm² and consequently the magnitude of a ship's radar returns, for a given orientation, is a characteristic of that target.

The above discussion pertains to the use of sea scatter as a reference in the calibration process. Sea scatter may not be the only reference available; for example, another ship in the immediate vicinity with an on-board repeater might serve as a reference. Furthermore, it is possible that the use of V/H polarization, discussed in Chapter VI, Section 6.5, might obviate the need to use a reference altogether.

2.4 MEASUREMENT OF PHASE RETURNS

The total phase shift, comprising the path, target and equipment phase shifts, can be derived from the demodulated received carrier. Taking the ratio of in-phase (E_I) and quadrature (E_Q) components yields

$$\theta = \tan^{-1} \frac{E_Q}{E_I} = \frac{4\pi R}{\lambda} + \phi_i + \phi_e \quad (2.10)$$

where

$4\pi R$ = Wave path length for a range R

ϕ_i = Intrinsic target phase

ϕ_e = Equipment phase.

In practice, it is difficult to accurately estimate the range. However, a differential method [13] can be employed which exploits the fact that

the total phase shift in the Rayleigh region is independent of the co-polarized scattering matrix terms.

If $R = R_0$ is the nominal range in the Rayleigh region, then the intrinsic phase is given by

$$\phi_i = \frac{\lambda\theta - \lambda_0\theta_0}{\lambda} \quad (2.11)$$

where θ_0 is the total phase shift for a Rayleigh wavelength λ_0 . Unfortunately, for sky-wave propagation, R is not equal to R_0 owing to the frequency dependent path lengths through the ionosphere. Furthermore, the Rayleigh region return is generally lower in amplitude than a resonance region return, and may not be measurable. This would suggest the choice of subtrahend wavelength much closer to the original wavelength λ to minimize the dependence of radar cross sections on path lengths. This technique is described in a subsequent chapter.

In conclusion, it is difficult to recover the intrinsic phase from a sky-wave radar return. However, this does not preclude the use of phase data in subsequent experimental classification procedures.

2.5 CHOICE OF FREQUENCIES IN SKY-WAVE RADAR

There are a number of factors which influence the choice of operating frequencies in sky-wave resonance radar. The most important of these is the ionosphere [9]. The electron density of this medium varies with height and with the solar illumination angle. Lower electron densities require lower frequencies for refraction, and vice versa. Consequently, elevation angle, and hence range, is dependent on

the condition of the ionosphere. The ionosphere is a dispersive medium (i.e., the velocity of a wave is a function of its frequency) and this limits the instantaneous bandwidth (or minimum pulse width) and the frequency sampling interval. A bandwidth of 100 KHz which corresponds to a pulse width of 10 μ s is considered to be the maximum signal bandwidth [11].

Certain areas of the HF spectrum are subject to interference from other HF band signals, to deviative absorption in the ionosphere, and to natural forms of interference such as auroral ionization. This may necessitate a choice of frequencies that avoids the bands where these phenomena are prevalent.

Maresca and Barnum [12] showed that the sea state can be a critical factor in the detection of small ships (those with radar cross section approximately 30 dBm²). Higher frequencies may be used to avoid this problem by increasing the doppler separation between the sea echo (or Bragg return), and the ship return.

In addition to the above limitations, the operating frequencies should be in the resonance region of the target. This is, approximately, the region between $1 < L/\lambda < 10$, where L is the maximum dimension of the target. The 6 ships used in the classification experiments discussed below average about 150 m in length. This defines an operating frequency band of 2 to 20 MHz. Furthermore, lower frequencies are preferable because there is a more distinct and reliable variation of radar cross section per unit bandwidth, and this is an aid to classification.

The above effects constrain frequency selection and thus, the choice of frequencies should be matched to these continually changing conditions. It may be necessary to sense the environment in real time to permit this matching.

CHAPTER III

GENERATING A DATA BASE

3.1 INTRODUCTION

In order to build a catalog of reference ship responses, a large amount of experimental data collection and processing using scaled model ships is necessary.

Firstly, the phase and amplitude returns of each model ship are measured at all frequencies, polarizations, aspect angles and elevation angles of interest. The raw data are calibrated to remove unwanted background and system response effects, and are converted into absolute radar cross section magnitude and phase. The calibrated data are then scaled in magnitude and frequency so that the responses are representative of real ship returns measured in the HF band.

The following discussion on calibration techniques is detailed for two reasons. First the calibration process is the most critical and intricate step in producing meaningful scaled cross section data. Second, this is the first time that a groundplane has been used in the measurement of ship radar cross section data.

The entire calibration process, including the development of software, experimentation and processing of data, represents approximately 40% of the total work done on this report.

3.2 MEASUREMENT OF DATA

The backscatter data of ships, calibration targets and backgrounds were measured using the compact radar range, described by Walton and Young, [18], of the ElectroScience Laboratory at the Ohio State University. The term 'backscatter' is used to describe radiation which is scattered by the target back in the direction of the transmitting antenna. A 12' x 12' parabolic reflector generates a plane wave and thus simulates an antenna at a much larger distance (hence the compact feature). The radar transmissions are of the continuous wave (CW) type, possessing no modulation. A more detailed account of the system, including system specifications, is given by Kimball [2]. Figure 3.1 summarizes the key features of the compact radar range by means of a schematic diagram.

Measurements of the amplitude and phase of the returns were made monostatically (i.e., transmitting and receiving horns were at the same location and orientation). The frequency band used was 2-18 GHz (continuous), with 10 MHz frequency increments. The continuous band avoids the need for taking measurements in sub-bands, a common practice in the past, and simplifies the subsequent calibration procedure.

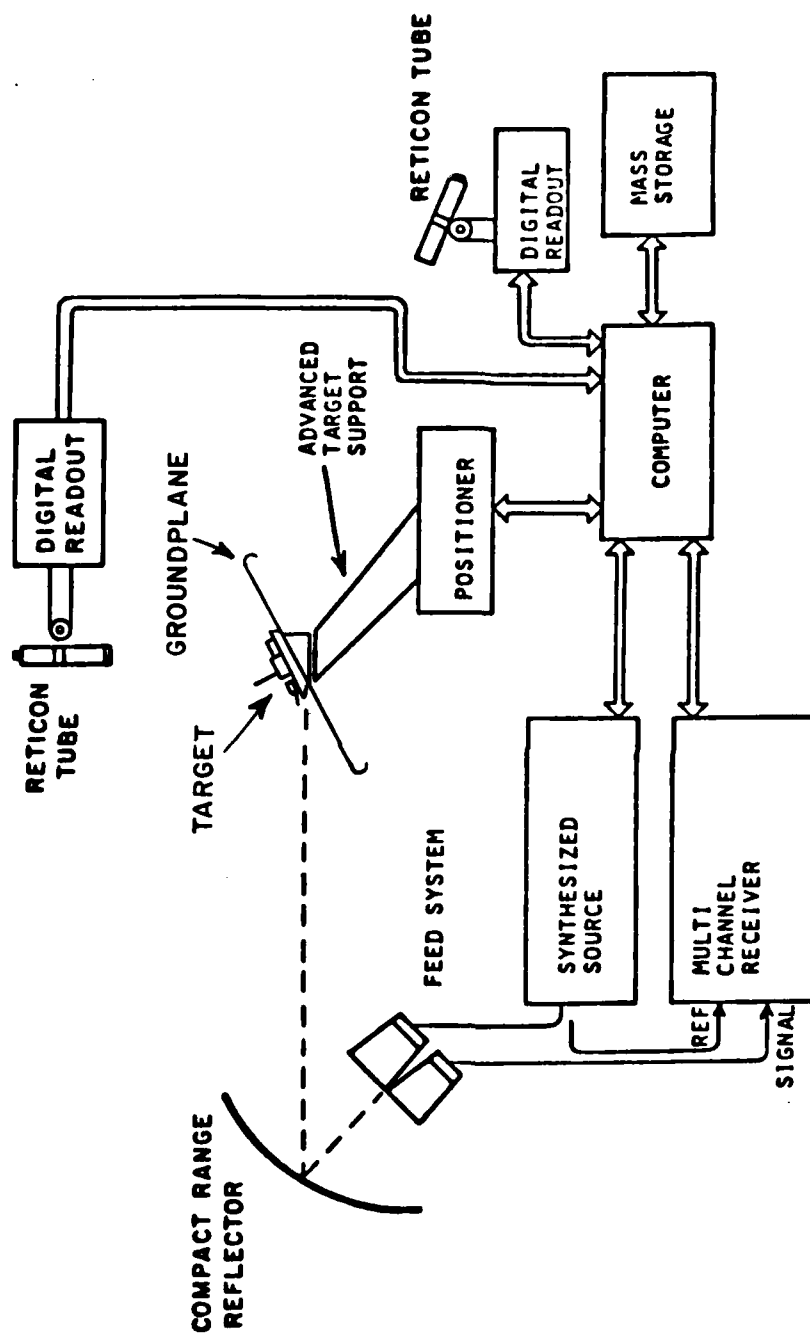


Figure 3.1. Schematic diagram of the compact range system.

All of the data were taken prior to the modifications made on the edge of the reflector dish during August 1984, which were designed to reduce edge diffraction terms.

Amplitude data were recorded in units of dB cm², and phase data were registered in degrees. Both were recorded sequentially onto a PDP-11/23 floppy disk (i.e., amplitude at f_1 , phase at f_1 , amplitude at f_2 , phase at f_2 , etc). The PDP-11 computer served mainly to control the system and observe the response as the measurements progressed; it was used for only limited processing at the time the data were taken.

Table 3.1 shows a summary of the of target measurements. These sum to 366 data files; however the total files including backgrounds and calibration targets number 649. The average time for the collection of a single file, including setting up the target and taking the measurements is estimated to be 15 minutes. Thus, at least 162 hours, not including re-runs, were spent in acquiring the raw (measured) amplitude and phase returns. These data then needed to be calibrated and scaled before they were used in classification experiments.

Aspect angle was varied by rotating the ship about an axis perpendicular to the centre of the groundplane. Elevation angle was set by tilting the entire groundplane to the desired angle. Three polarization schemes were employed:

1. Transmit vertical, receive vertical - vertical (V) polarization
2. Transmit horizontal, receive horizontal - horizontal (H) polarization
3. Transmit vertical, receive horizontal - cross (X) polarization

TABLE 3.1
SUMMARY OF TARGET SPECIFICATIONS

Elevation = 15°			Elevation = 27°		
V	H	X	V	H	X
Aspect (degrees)			Aspect (degrees)		
0	0	0	0	0	0
10	10	10	10	10	10
15	15	15	15	15	15
			20	20	
			30	30	30
			40	40	40
			45	45	45
			50	50	
			60		
80	80	80	80	80	80
90	90	90	90	90	90
100	100	100	100	100	100
170	170	170	170	170	170
180	180	180	180	180	180

A polarization was selected by rotating the horns of the transmitting and receiving antennas appropriately.

Figure 3.2 shows silhouettes of the six ships used in classification. These models were made from die-cast aluminum. A ship was attached to the groundplane by means of a highly conductive silver paste.

3.3 CALIBRATING THE DATA

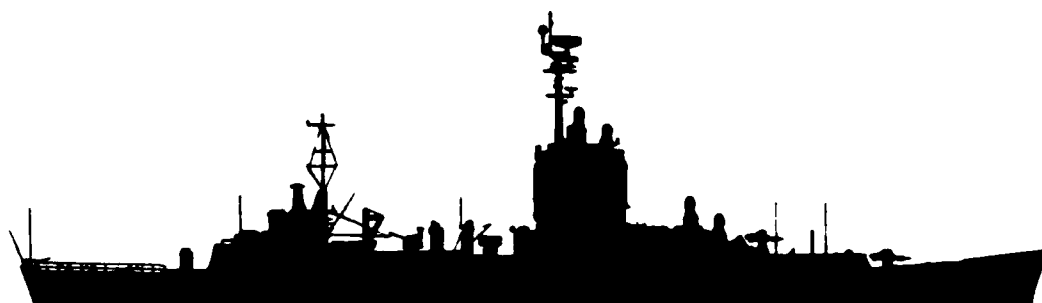
The purpose of calibrating frequency data is to remove the imbedded system characteristic. Kimball [2] describes the process in detail, and it is summarized as follows.

1. Remove the range delay from the measured data.
2. Subtract backgrounds from target and calibration target.
3. Remove invalid points from resulting subtractions.
4. Filter (in range) the subtracted files to further reduce background terms.
5. Calibrate the target of interest according to equation 3.1.
6. Filter (in range) the calibrated data again if necessary.

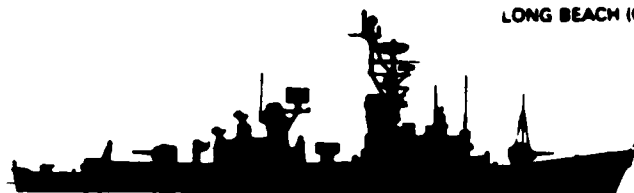
The calibration equation is given by

$$\tilde{T}_C = \frac{\tilde{E} (\tilde{T} - \tilde{B}_T)}{(\tilde{S} - \tilde{B}_S)} \quad (3.1)$$

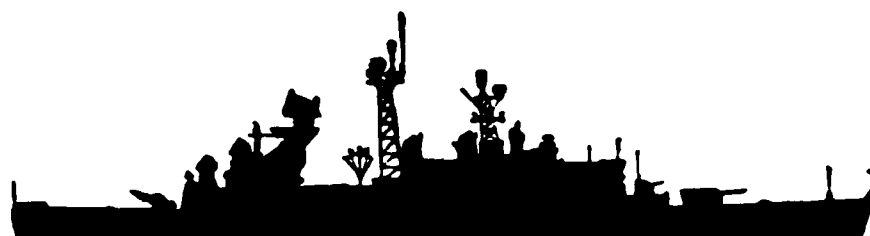
where \tilde{T}_C , \tilde{E} , \tilde{T} , \tilde{B}_T , \tilde{S} , and \tilde{B}_S are complex phasors for each frequency defined as;



LONG BEACH (CGN 9) (1980)



WADDELL (DDG 24) "Charles F. Adams" Class



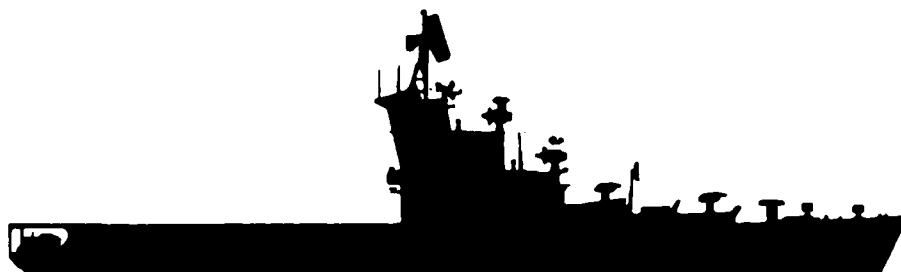
LITTLE ROCK



"KNOX" Class (improved)



"MODIFIED RASHIN" Class



"MOSKVA" Class

Figure 3.2. Silhouettes of the six ships used in measurements and classifications, shown for a scale of 1:1700 (from [23]).

\tilde{T}_C , the signal voltage measured with the calibration target installed.

\tilde{E} , the computed (exact) backscatter σ : in units of meters and absolute phase (deg.), from the calibration target.

\tilde{T} , the signal voltage measured with the target installed.

\tilde{B}_T , the signal voltage measured for the background (no target installed) associated with the target.

\tilde{S} , the signal voltage measured with the calibration target installed.

\tilde{B}_S , the signal voltage measured for the background (no target installed) associated with the calibration target.

3.3-1 THE GROUNDPLANE

For this particular set of ship measurements, a large flat, circular groundplane (Figure 3.3) was used to simulate the surface of the sea. This approach is valid because the $\sigma/\omega\epsilon$ ratio for salt water at frequencies in the HF band is about 1000, indicating that it is a good conductor [21]. Doppler processing is normally used to separate the ship return from the ocean wave spectrum [11]. This allows, as a first-order approximation, the sea to be represented as a flat surface in measurements. (A discussion on scattering from rough surfaces is given by [19]).

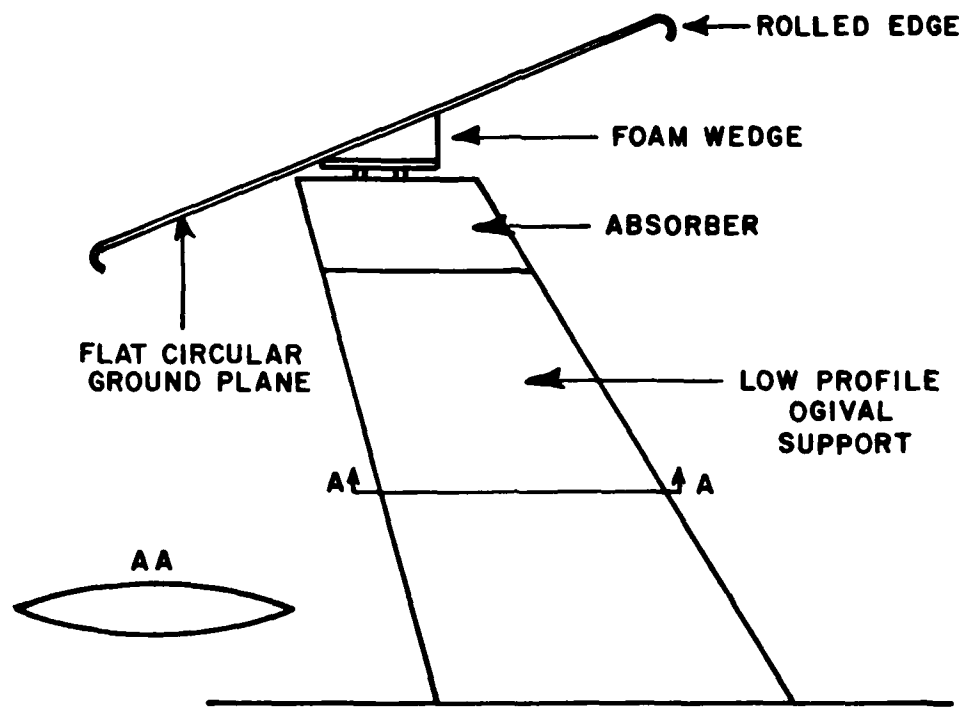


Figure 3.3. The groundplane and its low profile supporting structure.

Chen [1], in his analysis of ship classification at zero degrees elevation angle was able to simulate the effect of the surface of the sea by attaching a mirror image of the ship directly beneath the actual target. This technique is only applicable at zero degrees elevation and for vertical polarization, thus for the elevation angles of 15° and 27° , a groundplane must be used.

The groundplane has a diameter of about 3.4'. Walton and Young [5] found that the transient response of a scatterer typically dies out after $T = 6\tau$ where $\tau = L/C$, C is the speed of light and L is the maximum target dimension. With a maximum ship length of six inches, the impulse response would be zero after about 3 ns (one-way). The edge of the groundplane is about $1.7n$ ns from $T = 0$ meaning that, using this rule of thumb, the transient and groundplane edge responses might interfere. However, in the case of the 'low Q' ship targets considered here, the transient response can be shown to be indistinguishable from clutter after about 1 ns (one way) for the six inch targets (see Figure 3.4). Consequently, the ship response does not interfere with the groundplane edge.

The term \tilde{T} in Equation 3.1 is a combination of backscatter from the ship and groundplane, and the term \tilde{B}_T is the backscatter from the groundplane alone. Hence, a background (groundplane) subtraction should yield the ship backscatter. Unfortunately, owing to target-groundplane edge interactions and the unavoidable positional disturbance of the groundplane when the targets were installed or moved, some residual response remains at the location of the groundplane edges after the

subtraction and calibration. Sometimes this residual can have a peak magnitude similar to that of the ship (see Figure 3.4). Time domain windowing is necessary to remove these residuals as they represent a distortion of the desired ship data, and would be particularly disruptive in the time domain algorithm discussed later. Although smoothing, that is, convolution in the frequency domain with a Hanning window, (see Kimball [2]), which is equivalent to time domain windowing, is performed in the scaling routine, it is desirable to remove residuals before this stage is reached. The main reason for this is that existing software formatted the scaled data in such a way as to be incompatible with available fast Fourier transform programs. Hence, if the data was smoothed in the scaling routine to remove residuals, there would be no way (without extensive alterations to software) of performing an inverse Fourier transform to check the result.

Initially, it was thought that the residuals could be removed by using a sufficiently narrow window (or large number of smoothing points) in step 4 of the calibration process described earlier. To see how this would work, consider the impulse response of a typical target-on-groundplane shown in Figure 3.5. The purpose of the Hanning window outlined over the target area is to window out the effect of the antenna coupling and reflector terms. If made sufficiently narrow, the window might also remove the groundplane residuals. This was tried by setting the first null points of the window to ± 3 ns; the points in time corresponding to the groundplane residuals. The residuals were removed successfully, but another problem was spawned in doing so, owing to receiver hardware problems.

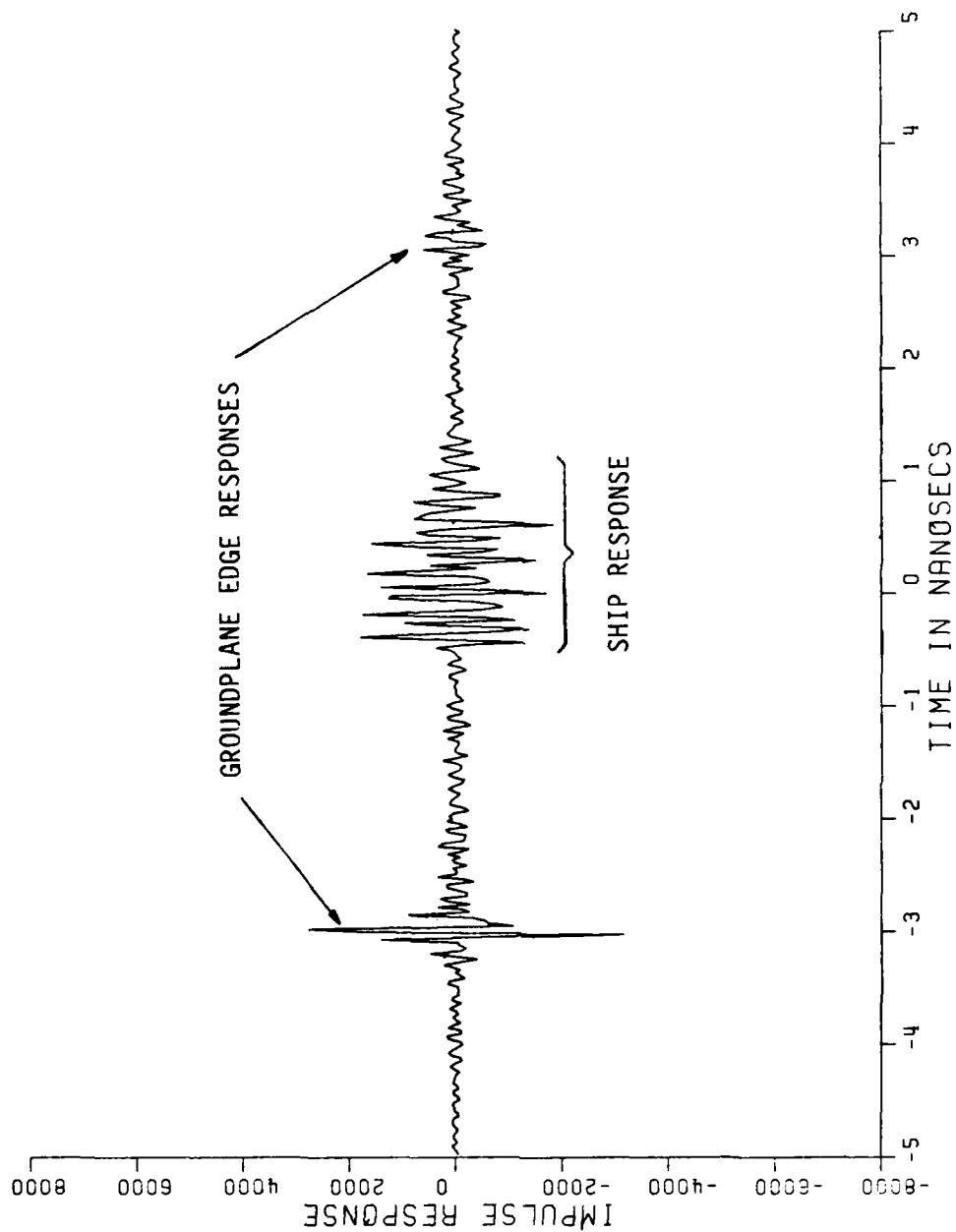


Figure 3.4. An example of how the impulse response of a ship retains groundplane edge residuals (at ± 3 ns.) after calibration. The main response of the ship is constrained within ± 0.5 ns, and decays into clutter after 1.5 ns. Vertical polarization was used.

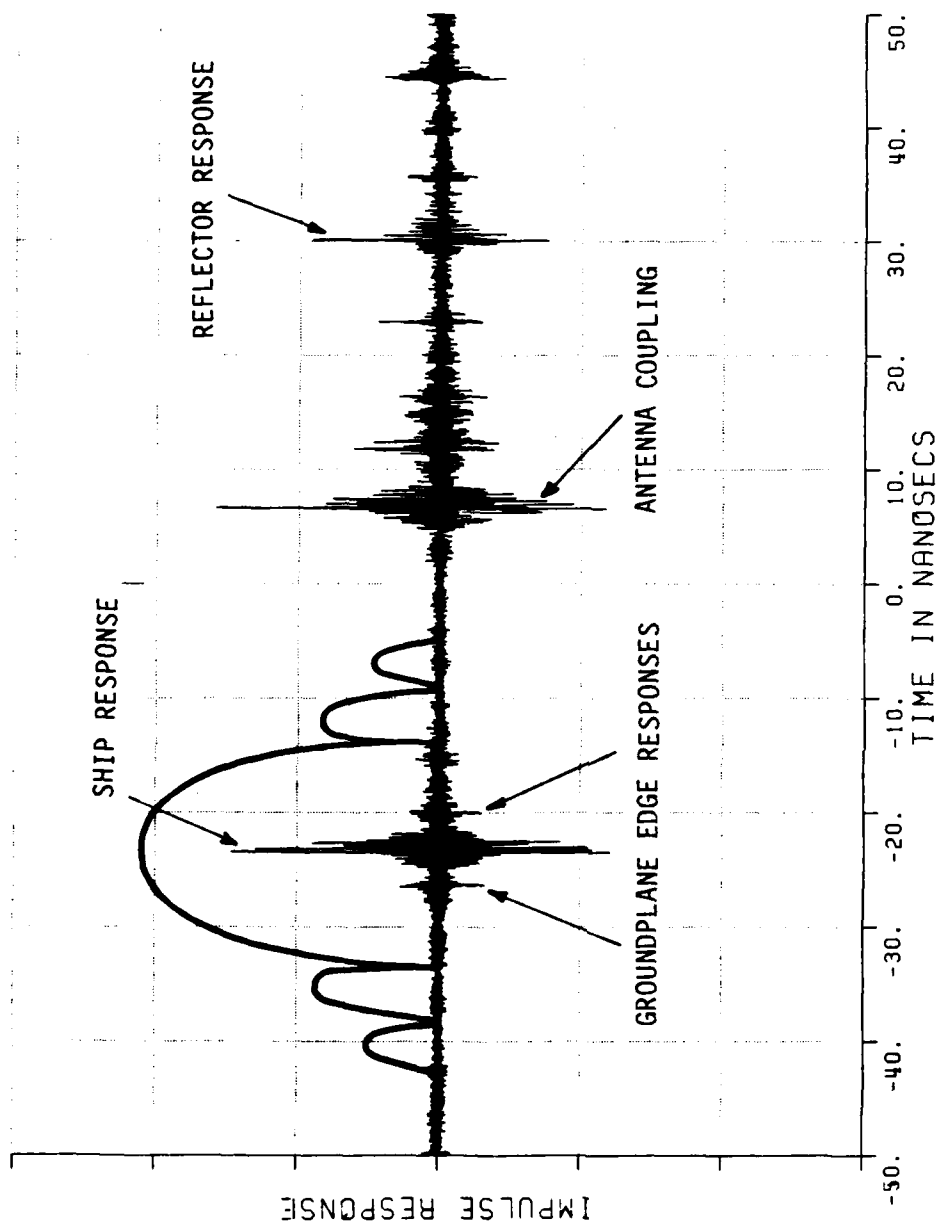


Figure 3.5. The impulse response, 2-18 GHz, of an uncalibrated target on groundplane after background subtraction, showing the location in time of all major scatterers and the pre-calibration Hanning window. The response from -50 ns to 50 ns is the continuation to the response from 0 ns to 50 ns.

The receiver used in the measurement process had band edges located at 2, 4, 8, 12.4 and 18 GHz. These band edges caused a step type pattern in the phase response (shown in Figure 3.6 for a raw 6" sphere data file with range delay removed). Narrow windowing, or convolution over a large number of frequencies (as the smoothing is actually performed), emphasized these steps differently for both the calibration target and the target of interest. The net result after calibration was a series of spikes of up to 10 dBm² in magnitude, located at or near the receiver band edge frequencies. Clearly then, narrow pre-calibration smoothing was not practical.

The edge residuals must then be removed in step 6 of the calibration process. The existing calibration software, (CAL 53 due to Kimball) achieved this by convolution in the frequency domain. This program was upgraded to permit the windowing to be done in the time domain, for two reasons.

1. The process is computationally more efficient.
2. The process is conceptually more relevant to the problem, i.e., the groundplane edges are recognizable as time domain phenomena, so it is logical to deal with them in the time domain.

Computational efficiency is a function of the number of frequencies, or data points. A fast Fourier transform requires $N \log_2 N$ operations, while a convolution requires NM operations, where N is the total number of data points and M is the size of the convolution window (in data points). However, for time domain windowing, both forward and

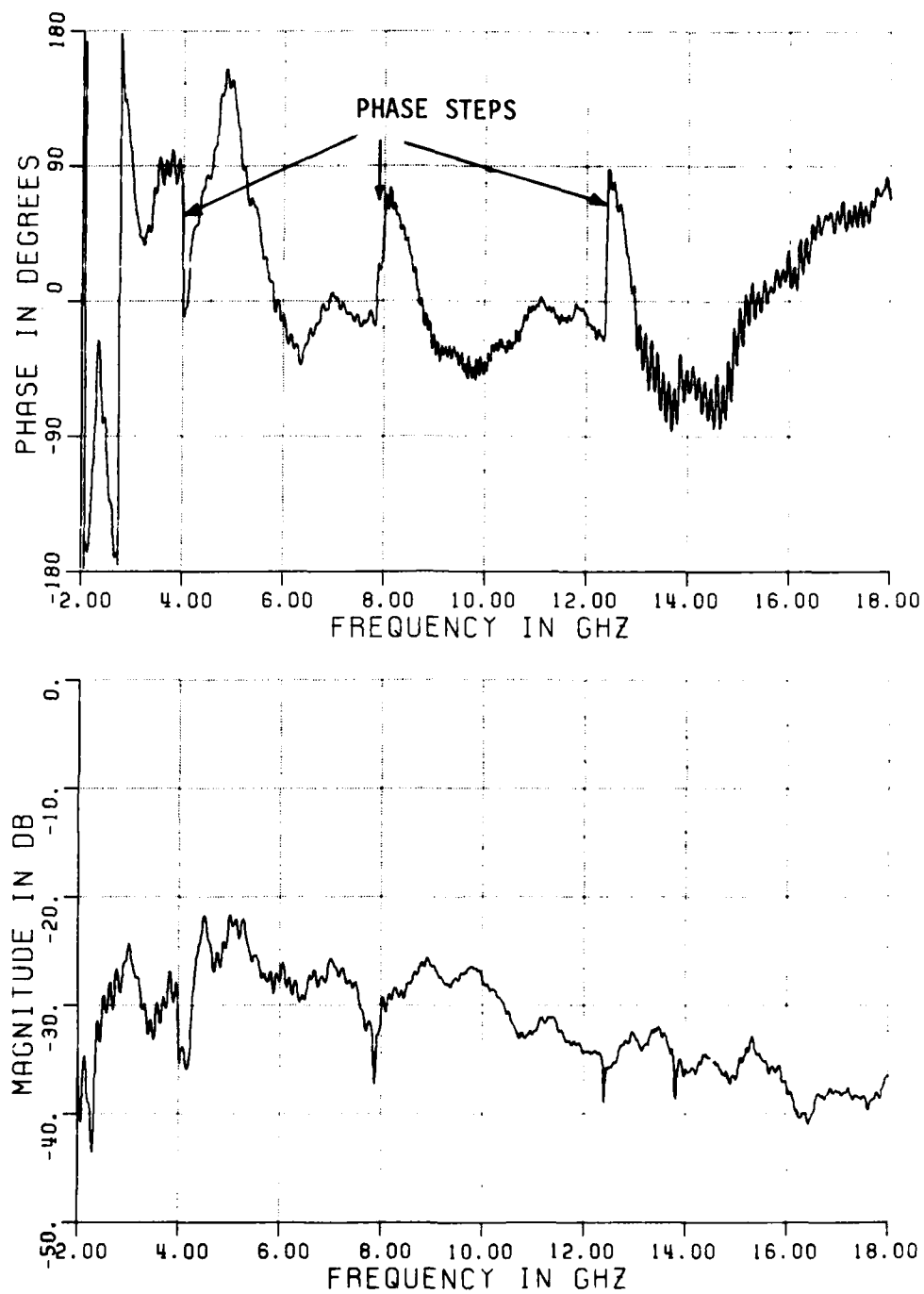


Figure 3.6. An uncalibrated six-inch sphere with background and path delay removed showing the occurrence of phase steps at the 4, 8, and 12.4 GHz receives band edges.

inverse transforms as well as a multiplication over the number of data points in the time domain array (4096 in this case), which represents the actual windowing, are necessary. The total number of operations for the time and frequency domain smoothing routines are given by

$$N_t = 2N \log_2 N + 4096 \quad (3.2)$$

$$N_f = NM \quad (3.3)$$

A total of 1601 data points (sample frequencies) were used, with a ± 3 ns window in the time domain corresponding to a 65 point convolution window. Substituting these values in 3.2 and 3.3 yields 38180 operations required for time domain windowing and 104065 operations for frequency convolution. Setting the first null points of the Hanning window to ± 3 ns removed the residuals completely (see Figure 3.8). For the largest target, most of the response was confined to ± 0.5 ns with the transient decaying into clutter at 1.5 ns (1.5 ns is the 6 dB down point of the Hanning window). However, close examination of a six inch ship response with the narrow ± 3 ns window revealed no discernable difference from the same response processed with a much wider ± 20 ns window.

There is a consequence of using the time domain technique which should be noted. Figure 3.9 shows the resultant frequency response after a perfectly flat 2-18 GHz frequency response (phase= 0°) is inverse Fourier transformed, windowed with a ± 3 ns window, and then forward transformed. The first and last 0.3 GHz of the band are unuseable owing to the drop off caused by a narrow time window. This problem is somewhat precluded with the use of frequency domain convolution since

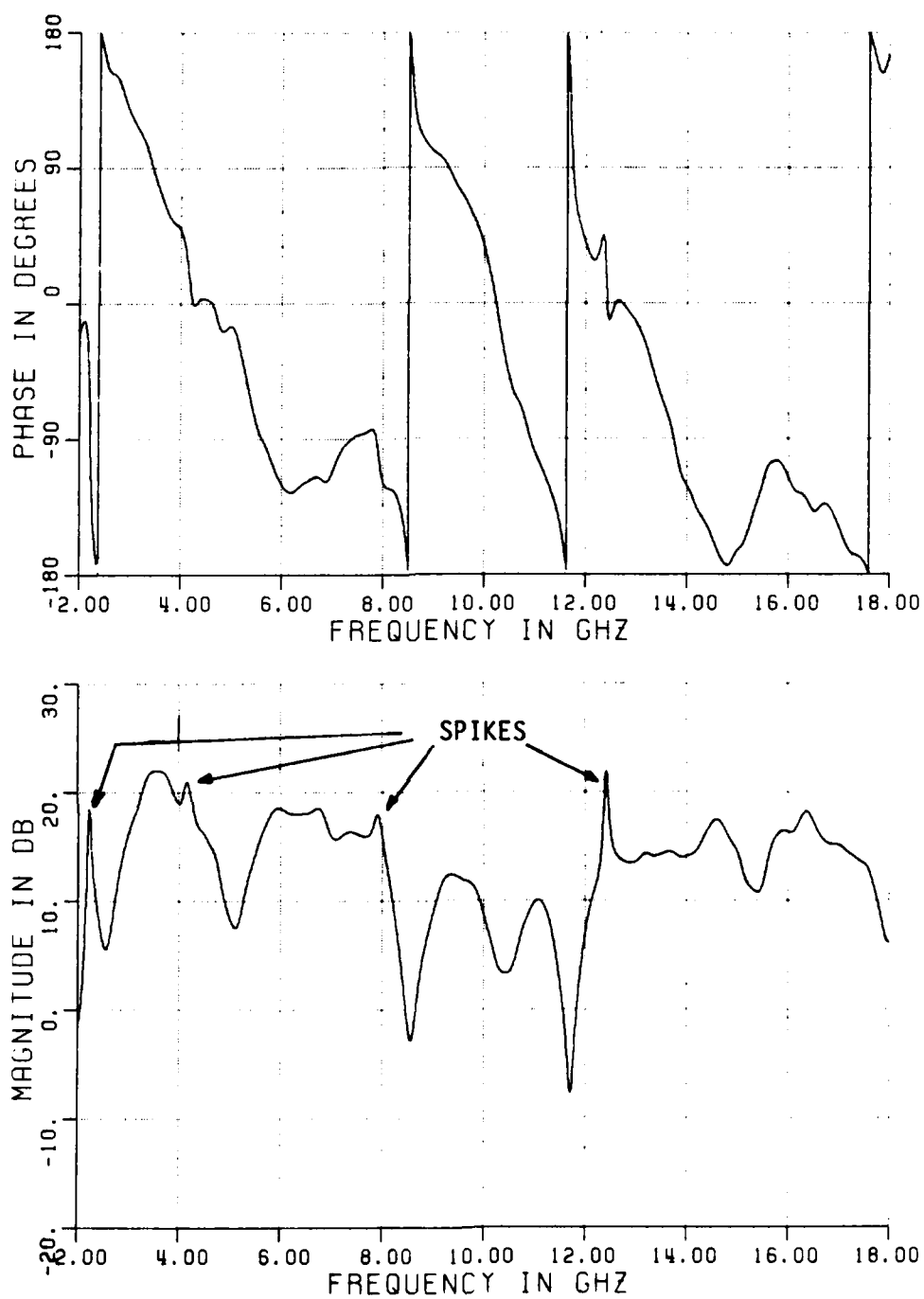


Figure 3.7. Calibrated ship data using a narrow ± 3 ns pre-calibration window to remove groundplane edge residuals, resulting in the occurrence of spikes at the receiver band edges.

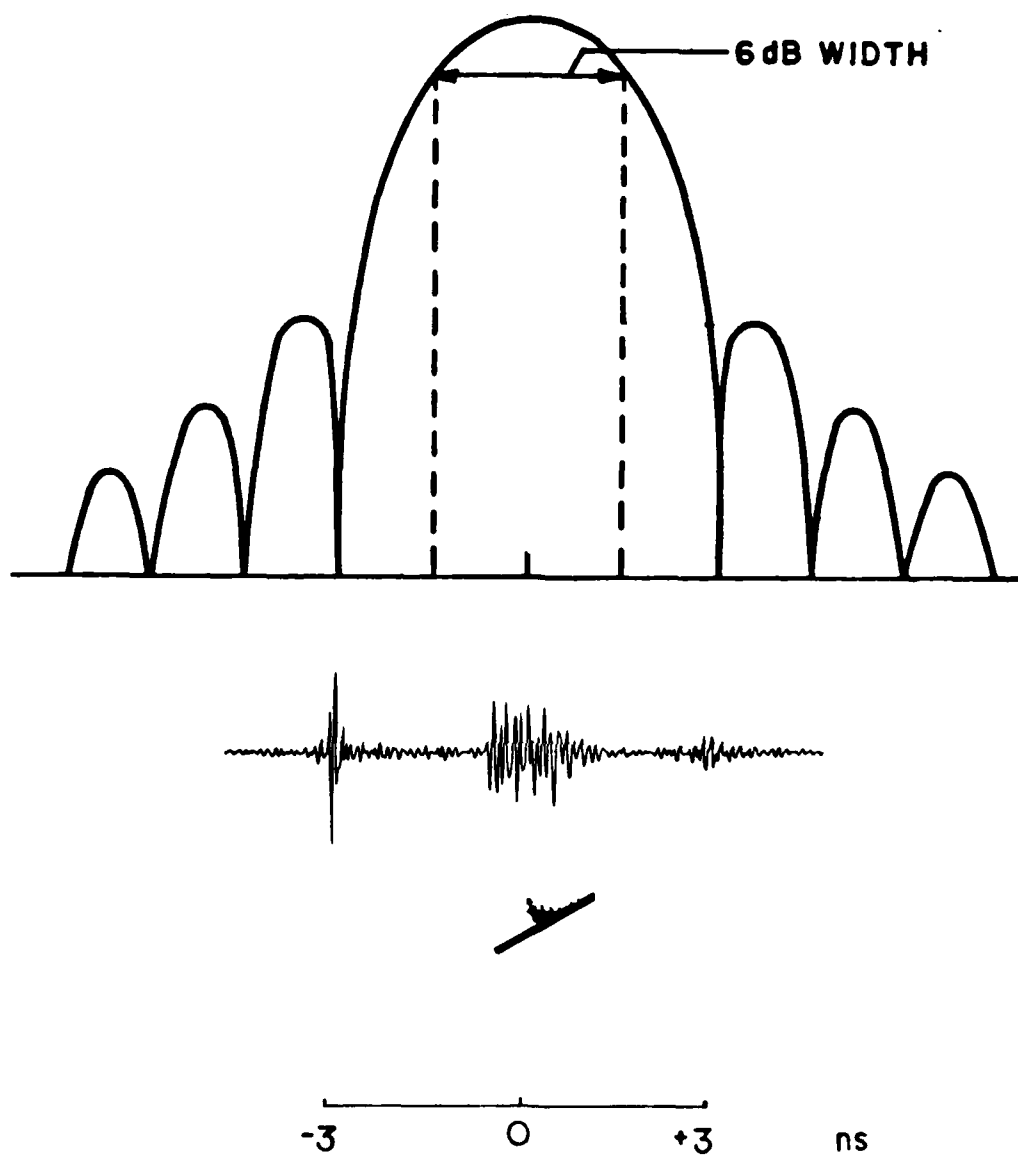


Figure 3.8. Use of a Hanning window after calibration to remove the ground plane edge residuals at ± 3 ns.

the frequencies near the band edges are reflected to permit the convolution, showing convolution and time domain gating, as implemented in our software, not to be exact transform pairs. However, the validity of data taken immediately adjacent to band edges is not certain, so it is good policy to ignore these regions irrespective of the technique used to perform the smoothing or windowing.

3.3-2 CHECKING CALIBRATED RESPONSES

Once a particular ship had been calibrated, its frequency and impulse response were then generated as plots. The frequency responses were examined for 'glitches', i.e., large spikes of about 10-100 MHz bandwidth and 10 to 30 dB in extent, caused by receiver hardware problems. Generally a glitch is hard to deal with because the phase and amplitude responses affect up to 10 points. If the glitch exists in a background or calibration target file then an alternative data file might be used. A bad glitch in a ship data file might require a new set of measurements. Small glitches, both in amplitude and bandwidth, at frequencies lower than 4 GHz can be tolerated.

The time response was the main tool for checking the validity of calibrations because the transient response gives an intuitive geometric guide to the mechanisms which cause scattering. Figure 3.9 shows a typical response, scaled 1 to 1 with the ship overlaid. Using templates in this way shows whether the main response confines itself to the length of the ship, and if structures likely to cause large amounts

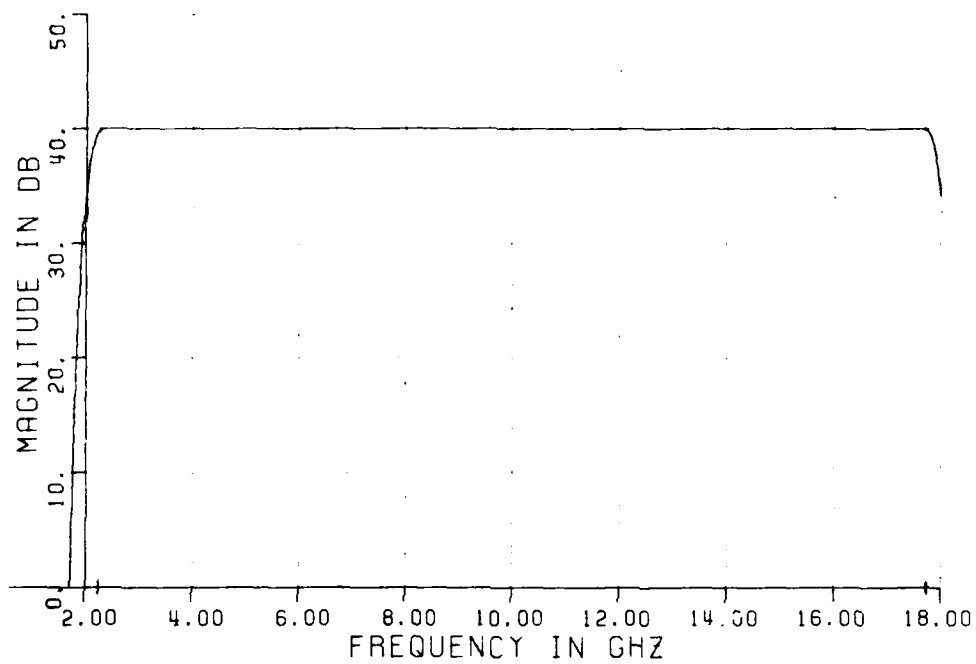


Figure 3.9. Resultant frequency response when a flat 2 to 18 GHz frequency response is windowed in the time domain with a ± 3 ns Hanning window.

of scattering are indeed doing so. The bandwidth of the responses is sufficiently large to provide the necessary resolution to make these judgements. Resolution in time is given by

$$\tau \approx 1/B \quad (3.4)$$

For $B = 16$ GHz, then $\tau = 62.5$ p seconds, which at the speed of light corresponds to 1.875 cm. Most of the major features on the ship models, such as masts, gun turrets, etc., are separated by about 1 to 2 cm. There was not always a 1:1 relationship between the physical features of a ship and its time response; partly owing to the resolution limit and partly because of the complex scattering interactions and interferences. Certain aspect angles, particularly those close to 90° were harder to judge than others. No standard procedure could be developed under which to judge a calibrated result, although the presence of significant precursors or other unusual phenomena would tend to indicate a bad calibration.

An alternative method for judging the validity of the calibration, based on comparing a measured hemisphere-on-a-groundplane with its theoretical counterpart, was found to be unsatisfactory. The measured and theoretical responses were too dissimilar to be meaningful. Much work was done in the pursuit of finding the mechanism responsible for the differences. However, no conclusive evidence was found and this particular technique was dropped in favour of the time domain method.

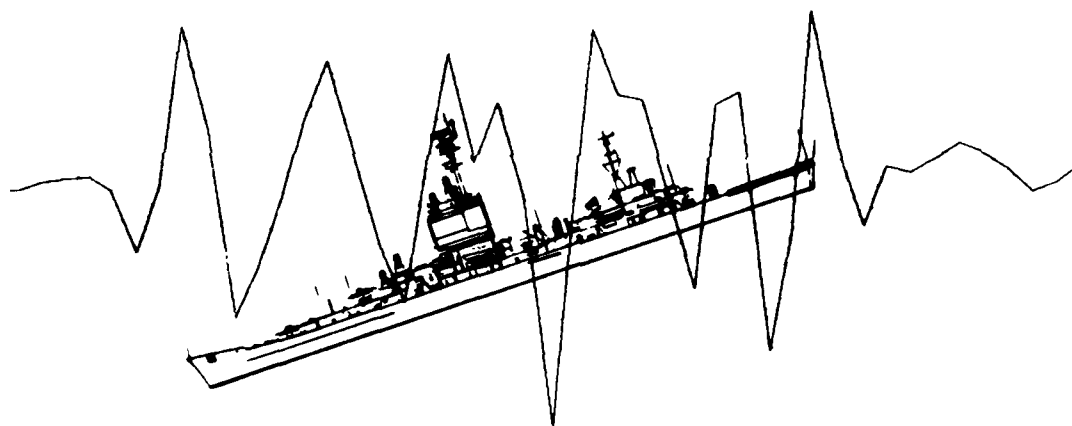


Figure 3.10. A ship scaled 1:1 with its impulse response in order to check a calibration.

3.4 DATA SCALING

Data collected and calibrated in the microwave region must be scaled before being used in classification algorithms. A data point is scaled in two ways. Firstly, its amplitude is multiplied by the scale factor, and secondly, the frequency it represents is divided by the scale factor. Data measured in the 2 to 18 GHz microwave band was collected for models having scale factors of 1:1200 and 1:2400. The resulting HF bands are shown in Table 3.2.

TABLE 3.2
SCALE FACTORS FOR MODEL SHIPS AND ASSOCIATED FREQUENCY BANDS

Scale Factor	1:1200	1:2400
f_{\min}	1.667 MHz	0.833 MHz
f_{\max}	15 MHz	7.5 MHz

The figures presented above were rounded to one decimal place, and a frequency increment was selected. Since frequencies may have been selected which were not actually represented by data points, it was necessary to interpolate between data points by means of a Hamming window. Chen [1] also used a Hamming window to remove noise and clutter from the calibrated data. As explained earlier, it was necessary to perform smoothing during the calibration process.

A frequency increment of 1/32 MHz was selected for each band. Window widths of 0.5 MHz and 0.25 MHz were selected for the 1.7 to 15 MHz band and 0.8 to 7.5 MHz band respectively. The shape of the scaled data curves differed little from the calibrated data curves. This is to be expected as the window to bandwidth ratios for each are 1:27 and 1:25 respectively. Representative scaled frequency and phase returns are shown in Appendix B.

The useable bandwidth for classification must overlap both scaled bands; this is 1.7 to 7.5 MHz. For reasons mentioned in the discussion of the calibration procedure, frequencies near the band edges are avoided, so the net useable bandwidth is about 2 to 7 MHz.

A SUMMARY OF SCALED DATA GENERATION

1. Measured Data (m)

Amplitudes	A_m	
Phases	θ_m	
(at) frequencies	f_m	: 2 - 18 GHz, 10 MHz steps = 1601 data points

2. Calibrated Data (c)

A_c	
θ_c	
f_c	: 2 - 18 GHz, 10 MHz steps

Smoothing	± 3 ns (first nulls) Hanning window equivalent to 65 point smoothing, gives a 1:25 window to bandwidth ratio.
-----------	--

3. Scaled Data (s)

$A_s = A_c$	SF	
$\theta_s = \theta_c$		
$f_s = f_c/SF$		(SF = Scale Factor)

$$SF = 1:1200$$

1.7 - 15 MHz, 1/32 MHz steps
426 data points
Interpolation using 0.5 MHz Hamming window

$$SF = 1:2400$$

0.8 - 7.5 MHz, 1/32 MHz steps
214 data points.
Interpolation using 0.25 MHz Hamming window

Net useable common bandwidth : 2 - 7 MHz.

CHAPTER IV

TARGET CLASSIFICATION

4.1 INTRODUCTION

The basic process of target classification is illustrated in Figure 4.1. The measurement system in this case is a compact radar range. It produces a measurement vector m , which is a set of amplitudes and phases at a number of frequencies, aspect angles, elevation angles, and polarizations. Each measurement vector is a point in M -dimensional space (also called the observation space). The feature extractor reduces the dimensionality of the measurement vector to produce a feature vector n , which is a point in N -dimensional space ($M > N$). For example, if the amplitudes and phase returns of a ship were measured at 2 polarizations, 2 elevation angles, 3 aspect angles and 4 frequencies, and it is assumed polarization and elevation are known and only amplitudes are used to classify the target, then the feature extractor reduces a 96-dimensional space to 12-dimensional space (4 frequencies x 3 aspect angles). Essentially, the feature extractor is

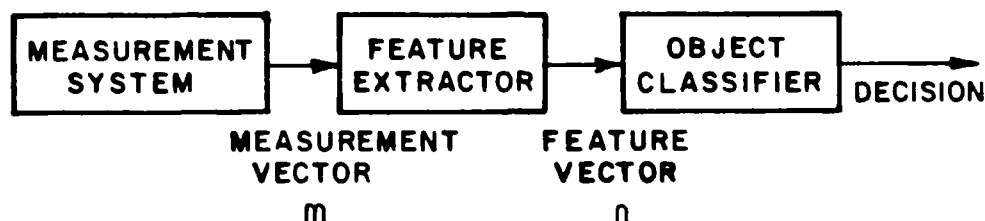


Figure 4.1. Basic process of a pattern classification system.

the mechanism by which a particular data file is addressed, since a measurement vector is usually dispersed amongst several data files.

The feature vector is then passed to the object classifier which uses a particular algorithm to make a decision as to the identity of the object. The decision can be either, 1) the object is classified as a known member of a catalog or, 2) the object belongs to some other 'uncatalogued' class. The classification of catalogued and uncatalogued classes is discussed by Lin [6]. For this particular application, only catalogued classification is considered.

The ultimate goal of a classification system is to identify targets with a minimum probability of error. Since the noise in these tests was simulated, the classification could have been a parametric procedure. However, in practice, the exact probability distributions of features in

the feature space after contamination by noise are not known, thus we must resort to non-parametric methods of classification. Two such methods which do not require knowledge of probabilistic information are the nearest neighbour algorithm [1] and the time domain correlation algorithm [1], and are discussed below.

4.2 CLASSIFICATION IN THE FREQUENCY DOMAIN

The nearest neighbour (NN) algorithm uses amplitude and phase returns measured at a series of frequencies $f = f_1, f_2, \dots, f_N$. (Note that, in general, the NN algorithm is applicable to both the frequency and the time domain.) The amplitude is defined as the square root of the measured target cross section. For sky-wave radars, it is difficult to recover the intrinsic phase of a target, because of the dispersive and variable nature of the ionosphere and because the wave path lengths are difficult to estimate accurately. Hence a measurement of both the actual (intrinsic) phase, or relative phase may contain unacceptable errors. To circumvent these difficulties, the differential quantity W is used and is defined as:

$$W_i = \theta_i \lambda_i - \theta_{i+1} \lambda_{i+1} \quad (4.1)$$

where

θ_i is the measured phase at $\lambda = \lambda_i$,

R_i is the Wave path length at $\lambda = \lambda_i$, and

$i = 1, \dots, N - 1$ (where N = Number of frequencies).

Equation (4.1) assumes that R_i and R_{i+1} differ by a small amount. This is true for sky-wave radars only when λ_i and λ_{i+1} differ by a small amount and the radar operating frequencies are chosen carefully.

A feature space for a given orientation and polarization can be defined as,

$$(A_1, A_2, \dots, A_N, KW_1, KW_2, \dots, KW_{N-1})$$

where

N is the number of frequencies.

K is a normalization constant relating the variances of A and W .

$$K = \sqrt{\frac{\text{VAR}(A)}{\beta \text{VAR}(W)}} \quad (4.2)$$

$$\beta = \frac{\text{VAR}(A)}{\text{VAR}(KW)} \quad (4.3)$$

The parameter β is a variable ranging from 0 to ∞ and its value depends on the reliability of amplitude and phase information.

$\beta = \infty$ corresponds to using amplitudes only

$\beta = 0$ corresponds to using differential phase only

$\beta = 1$ corresponds to the use of amplitudes and phases with equal weighting in the respective variances.

In practical use of the algorithm, the stated limits of β (i.e., 0 and ∞) are not substituted into Equation 4.2 in order to select either the amplitudes-only feature or differential-phases-only feature from the

feature space; these features are selected directly and are independent of K . It is worth mentioning that a value of $\beta = 0.01$ gives classification results virtually indistinguishable from the differential-phases-only feature, and $\beta = 100$ does the same for the amplitudes-only feature. K is calculated only when both amplitudes and phases are used, and for all of the experiments done here, β was set to 1.

Let $A_t(f_i)$, $\theta_t(f_i)$ be the target amplitude and phase returns, where $i = 1, 2, \dots N$. Let $A_j(f_i)$, $\theta_j(f_i)$ be the data base amplitude and phase returns, where j is the target index, $j = 1, 2, \dots M$. The NN algorithm is as follows:

1. Compute the differential phases

$$W_i^t = \lambda_i \theta_t(f_i) - \lambda_{i+1} \theta_t(f_{i+1})$$

$$W_i^j = \lambda_i \theta_j(f_i) - \lambda_{i+1} \theta_j(f_{i+1})$$

$$i = 1, 2, \dots N-1$$

$$j = 1, 2, \dots M$$

2. Calculate the sample averages of A and W in the data base.

$$\text{Avg}(A) = \frac{1}{MN} \sum_{j=1}^M \sum_{i=1}^N A_j(f_i) = \bar{A}$$

$$\text{Avg}(W) = \frac{1}{M(N-1)} \sum_{j=1}^M \sum_{i=1}^{N-1} W_i^j = \bar{W}$$

3. Calculate the sample variances of A and W in the database.

$$\text{Var (A)} = \frac{1}{MN} \sum_{j=1}^M \sum_{i=1}^N (A_j (f_i) - \bar{A})^2$$

$$\text{Var (W)} = \frac{1}{M(N-1)} \sum_{j=1}^M \sum_{i=1}^{N-1} (W_i^j - \bar{W})^2$$

4. Select β and calculate K.

$$K = \sqrt{\frac{\text{VAR}(A)}{\beta \text{VAR}(W)}}$$

5. Compute the distance between the target and each class in the data base.

$$d_{t,j} = \sqrt{\sum_{i=1}^N (A_t(f_i) - A_j(f_i))^2 + \sum_{i=1}^{N-1} (KW_i^t - KW_i^j)^2}.$$

$$j = 1, 2, \dots, M.$$

6. Apply the nearest neighbour rule:

Choose smallest $d_{t,j}$ $j = 1, 2, \dots, M$.

If $d_{t,m} = \min (d_{t,j})$ classify the target (t) as m.

4.3 CLASSIFICATION IN THE TIME DOMAIN

The inverse Fourier transform of the frequency and phase responses mentioned in the previous section yields the impulse response of the target. This is the time-dependent field intensity produced when a plane electromagnetic wave washes over the object.

In the frequency domain, differential phase was used to reduce the phase error introduced when the path length varies. This error manifests itself as a time shift in the canonical time domain, and is removable by means of a correlation process. (Note that the correlation process is applicable to both the time and the frequency domain). Chen [1] discussed the correlation process; a summary of its implementation is given below.

1. Compute the correlation function.

$$\rho_{t,r}(k) = \frac{\text{DIFT} [X(m) Y^*(m)]}{2 \sqrt{\sum_{m=1}^M |X(m)|^2} \sqrt{\sum_{m=1}^M |Y(m)|^2}}$$

where

$$X(m) = A_t(f_k) e^{j\theta_t(f_k)} \quad t = \text{target index}$$

$$Y(m) = A_r(f_k) e^{j\theta_r(f_k)} \quad r = \text{catalog index}$$

$$k = 1, 2, \dots, M$$

$$M = \text{Number of frequencies}$$

$$m = f_1/\Delta f, f_2/\Delta f, \dots, f_M/\Delta f$$

$$\Delta f = f_i - f_{i-1} \quad i = 1, 2, \dots, M$$

and DIFT is the Discrete Inverse Fourier Transform of the frequency domain data $(X(m) Y^*(m))$. Y^* is the complex conjugate of Y .

2. Choose the time shift constant k such that $\rho(k)$ is maximized.

For a particular set of two targets this yields $\rho_{t,r}^{\max}$.

$r = 1, \dots, N$, where N = number of catalog members.

3. Choose the largest $\rho_{t,r}^{\max}$. If $\rho_{t,q}^{\max} = \text{Max}(\rho_{t,r}^{\max})$, classify the target (t) as q.

The DIFT will work with as few as 2 frequencies, however, this low number of frequency samples is insufficient to provide any useable resolution. Recall that the cross section data, as originally measured, were sampled at 1601 frequencies from 2 to 18 GHz with a 10 MHz interval. This amount of sampling provided the necessary resolution to distinguish between individual scattering centers on the target (which allowed the calibrations to be checked). A much lower number of samples still provides scattering information of the target, but relates more to the overall dimensions rather than individual structures.

4.4 RELATIVE AMPLITUDE FEATURE

The relative amplitude feature was developed to reduce the effects of a possible multiplicative bias in the amplitude data. It is defined as follows:

$$\bar{A}_i = A_i/A_{i+1} \quad ; \quad i = 1, 2, \dots, N-1.$$

Such a bias might be due to an error in estimating the sea state, which would cause a local shift of amplitudes in the frequency response. The relative amplitude feature was not designed to remove the complex multiplicative terms impressed by the ionosphere.

CHAPTER V

EXPERIMENTAL CONSIDERATIONS

5.1 INTRODUCTION

Figure 5.1 summarizes the experimental classification procedure in the form of a flow chart. Data for M ships at a total of N frequencies are contained in the data base. The data base is a directory of 366 scaled data files, each corresponding to a ship at a particular aspect angle, elevation angle and polarization. Amplitudes and phases at the desired frequencies, aspect and elevation angles, and polarizations are selected for each ship in the data base to form a catalog (this is equivalent to feature extraction, see Chapter IV, Section 4.1). This selection, in a practical situation, would be based on all of the a priori information pertaining to the unknown target. Gaussian noise is then added to the entire catalog to produce a set of test targets. Classification proceeds for each noisy test target and decision statistics are compiled. It is worth emphasizing that in the following experiments, the whole catalog of ship amplitude and phase returns is corrupted by noise and classification proceeds for each ship target in

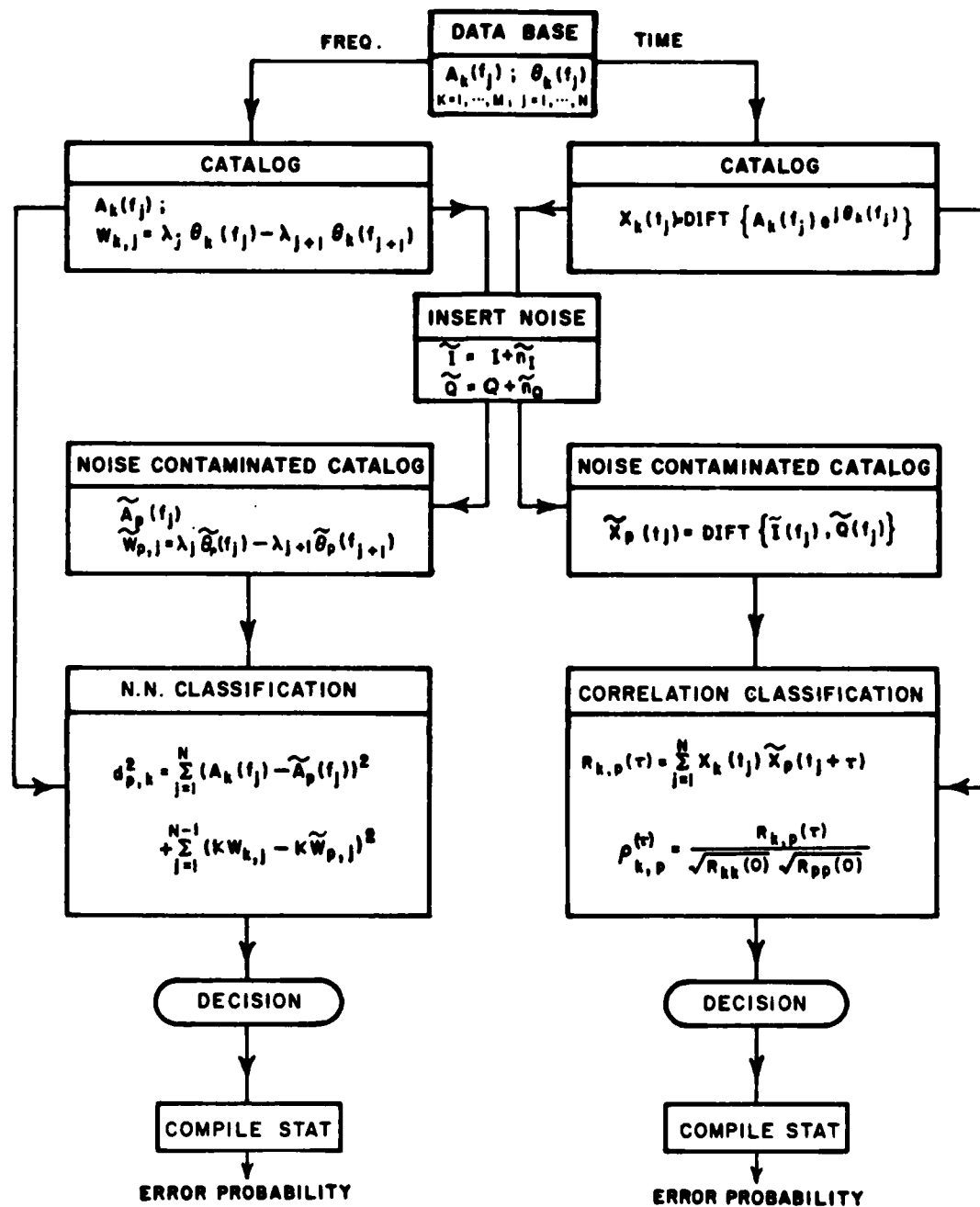


Figure 5.1. A flow chart of the experimental process of classification.

that 'noisy catalog'. At this point there are two catalogs; one a noise-contaminated version of the other. The returns of the first noisy ship are compared (by some algorithm) with those of the M noise-free ships, and a decision is made as to the identity of the test target. Since we added the noise to the test target, we know its identity a priori, and can therefore determine if the classification was either correct or incorrect. We say a target has been identified correctly if we choose the right ship at the right aspect and elevation angle. A target is misclassified if we choose either the wrong ship, or the right ship at the wrong elevation or aspect angle. This decision process is justified on the basis that we are investigating the classification properties of parameters, such as aspect angle, polarization etc., rather than the classification properties of individual ships.

The process is then repeated for subsequent members of the noisy catalog until all M noise-contaminated test targets have been classified. The number of misclassifications is recorded for the particular level of injected noise power. Hence the statistics of the experiments apply to the collection of ships as a whole and classification properties between individual ships, although of interest, are not investigated here.

The experiment is repeated a number of times in order to compile meaningful statistics, or representative curves (see below). The entire process is then repeated for a different injected noise power so that curves of misclassification percentage versus post-processing SNR can be drawn. The software needed to perform this process is listed with comments in Appendix C.

5.2 CHOICE OF EXPERIMENTAL FREQUENCIES

The discussion in Chapter III concluded with a summary of the data-base generation procedure, which showed that our data has a useable band of 2-7 MHz. An important concern here is that the classification frequencies should be in the lower part of the resonance region, i.e., close to $L/\lambda = 1$, where L is the maximum dimension of the dominant scattering structures of the target. The increment between sample frequencies is also an important parameter.

The experimental time domain ramp response in our ship data base, as previously mentioned, has a duration of less than 6 transit times across a target of length L , i.e.,

$$R(t, t_0) \approx 0; \quad t_0 > t > t_0 + 6L/C$$

where C is the speed of light and t_0 is a time reference. (This is a worst-case rule of thumb; there are many exceptions, including the case at hand.) For the preceding time limited expression, Shannon's sampling theorem [22] requires that the frequency sampling interval should satisfy

$$\Delta f < C/6L \quad . \quad (5.1)$$

The ships dimensions are in the order of 100 m, implying

$$\Delta f < 0.5 \text{ MHz}.$$

Thus, $\Delta f = 0.4 \text{ MHz}$ was selected as the frequency increment. The corresponding selection of frequencies is given in Table 5.1.

TABLE 5.1

RANGE OF FREQUENCIES USED IN EXPERIMENTS

N = 2	2.0 MHz < f < 2.4 MHz
N = 4	2.0 MHz < f < 3.2 MHz
N = 8	2.0 MHz < f < 4.8 MHz
N = 12	2.0 MHz < f < 6.4 MHz

Note that 2.0 MHz corresponds to a wavelength of 150 m, and 4.8 MHz (N = 8 frequencies was the most commonly used number) corresponds to a wavelength of 62.5 m. Hence, with $0.7 < L/\lambda < 1.6$, the lower resonance region criterion is satisfied.

5.3 SELECTION OF β IN NEAREST NEIGHBOUR ALGORITHM

As discussed earlier, the selection of β is relevant only for the case where both amplitudes and (differential) phases are used in the nearest neighbour algorithm. $\beta = 1$ corresponds to using amplitudes and phases with equal weighting in variance. Classification with β at some intermediate value represents a weighting towards either feature depending upon the reliability of that features' measurement. Chen [1] acknowledged that his estimate for K was not optimal.

$$K = \sqrt{\frac{\text{VAR}(A)}{\beta \text{VAR}(W)}} \quad (5.2)$$

An optimal expression for K , in addition to a carefully selected value of β might provide an optimal use of the AW feature. This possibility is not explored in this work, but is discussed in the conclusion.

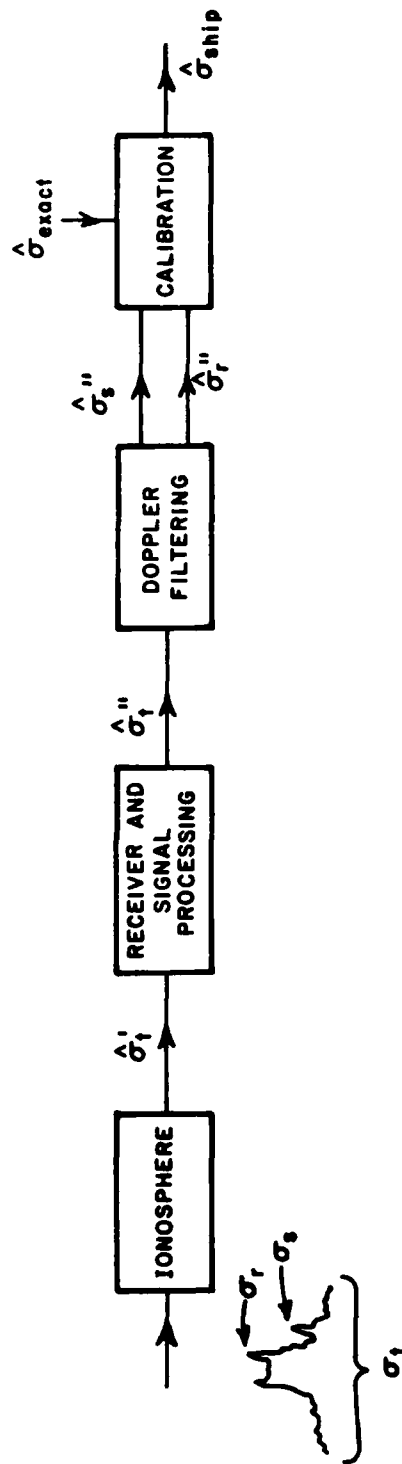
5.4 NOISE MODEL

Before discussing the specific characteristics of the noise model, it is appropriate to define exactly what is meant by noise and signal-to-noise-ratio.

Figure 5.2 summarizes the various channel and processing stages in a radar system. Assume that, immediately after the incident radar wave impinges on a target, a radar cross section σ_t is generated, where σ_t comprises the ship return σ_s and sea echo σ_r . If it were possible to be exactly adjacent to the target at this point in time, we could measure, with a hypothetically perfect system, the exact values of σ_s and σ_r . Knowing the exact state of the sea would allow us to compute σ_{exact} precisely from a perfect theoretical model of the sea scattering process. The (exact) radar cross section of the ship would then be given by

$$\sigma_{\text{ship}} = \frac{\sigma_s}{\sigma_r} \sigma_{\text{exact}} \quad (5.3)$$

This, of course, is not the case and the initial radar cross section σ_t is corrupted by the ionosphere and various stages of signal processing. After doppler filtering, the resultant radar cross section $\hat{\sigma}_t$ is separated into its components $\hat{\sigma}_s$ and $\hat{\sigma}_r$. Using an imperfect estimate



- σ_t = Original target radar cross section comprising σ_r and σ_s
 σ_r = Sea echo radar cross section
 σ_s = Ship radar cross section
 $\hat{\sigma}_{exact}$ = Estimate of theoretical exact sea echo
 $\hat{\sigma}_{ship}$ = Post-processed radar cross section of ship.

Figure 5.2. Schematic diagram summarizing the various stages of noise contamination after the initial scattering of radar energy by a ship.

of the exact theoretical sea-echo cross section $\hat{\sigma}_{\text{exact}}$, the resultant calibration yields

$$\hat{\sigma}_{\text{ship}} = \frac{\hat{\sigma}_s''}{\hat{\sigma}_r''} \hat{\sigma}_{\text{exact}} \quad (5.4)$$

Assuming that multiplicative noise terms can be ignored (for the sake of conceptualizing), Equations (5.3) and (5.4) are related by

$$\hat{\sigma}_{\text{ship}} = \sigma_{\text{ship}} + \epsilon \quad (5.5)$$

Here ϵ represents the remaining errors after the processing system has done its best to minimize the effects of various 'noises' accumulated after the initial scattering of energy from the target. The term ϵ is defined as post-processing noise and consequently, in the context of processed radar returns, the term post-processing signal-to-noise ratio is used.

Pre-processing noise is noise present in the returned signal before any processing, such as filtering, is done to reduce the effect of this contamination. For example, a lightning strike might add 10 dBm² of pre-processed noise to a scattered radar signal, and this would eventually become a component, to some degree, of post-processed noise ϵ .

Chen [1] concluded that the total noise power (i.e., the error variance of the final estimation of radar cross section σ) rather than the specific noise characteristics, has the most impact on the performance of classification algorithms. He went on to say that, because there are

numerous independent noise sources, none of which dominate, the Central Limit Theorem can be applied and the sum of these noises can be approximately described as Gaussian.

Headrick and Skolnik [9] commented that the effect of external (pre-processed) noise sources such as lightning, man-made noise and other HF transmissions, can be significantly greater than that of the internal (pre-processed) Gaussian receiver noise. The ionosphere contributes to signal distortion by introducing complex multiplicative terms by dispersion and by polarization rotation. These errors will appear, to a certain degree, in the final post-processed estimate of the radar cross section. A complete, representative model for post-processed sky-wave path distortion is clearly needed, however, a sufficiently detailed model has not yet been developed. In view of this, and based on Chen's initial conclusion, the Gaussian model was used.

Figure 5.3 shows a noise-free vector which is contaminated by adding in-phase and quadrature Gaussian noise components. The resultant vector has real and imaginary terms thus

$$\tilde{I} = A \cos \theta + \tilde{n}_I \quad (5.6)$$

$$\tilde{Q} = A \sin \theta + \tilde{n}_Q \quad (5.7)$$

where \tilde{n}_I and \tilde{n}_Q are independent Gaussian-distributed random variables with zero mean and variance σ^2 . The power in component \tilde{n}_I is equal to that of \tilde{n}_Q . The noise amplitude is given as

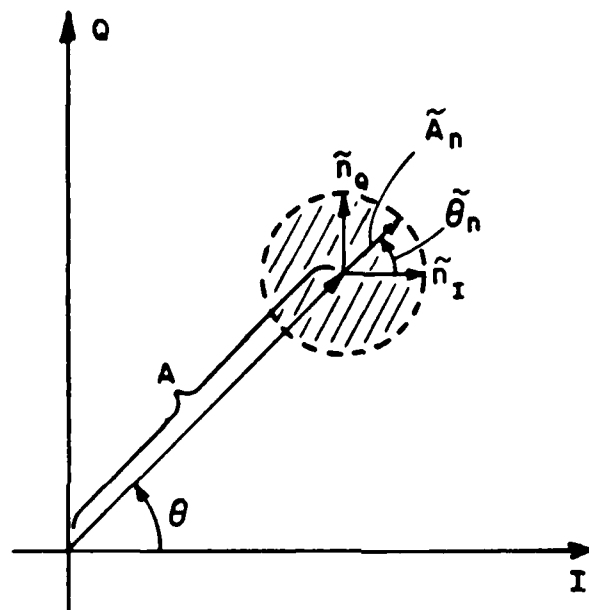


Figure 5.3. The distribution of the noise on an I-Q plane (from [1]).

$$\tilde{A}_n = \sqrt{n_I^2 + n_Q^2} \quad (5.8)$$

and is Rayleigh distributed [15]. The noise phase is given as

$$\tilde{\theta}_n = \tan^{-1} \left[\frac{\tilde{n}_Q}{\tilde{n}_I} \right] \quad (5.9)$$

and is uniformly distributed [15]. An expression for signal to noise ratio is given as

$$\frac{S}{N} = \frac{I^2 + Q^2}{\text{VAR}(\tilde{n}_I) + \text{VAR}(\tilde{n}_Q)} = \frac{A^2}{\alpha^2} \quad (5.10)$$

where

α^2 is the noise power, and

A^2 is the average signal power estimated as

$$A^2 = \sum_{i=1}^{NF} \sum_{j=1}^{NS} A_{ij}^2 \quad (5.11)$$

where

A_{ij} is the amplitude for the i^{th} frequency and the j^{th} ship.

i is a frequency index, $i = 1, 2, \dots, NF$ = NUMBER OF FREQUENCIES,

and,

j is a target index, $j = 1, 2, \dots, NS$ = NUMBER OF SHIPS.

5.5 POST-PROCESSING SIGNAL-TO-NOISE RATIO

From the previous discussion, we define post-processing signal-to-noise ratio (post-processing SNR) as the ratio of signal power to error variance after the received waveform has been processed to produce a final best estimate of the amplitude or phase, or both, of the target radar cross section.

From [1] post-processing SNR can be estimated as

$$\frac{S}{N} \approx \frac{M}{\sqrt{M+2}} \quad (5.12)$$

where M is the number of samples for a particular frequency. Using a typical sample time of 10 seconds and taking $M=100$ samples, (a total observation time of 16 minutes) yields a post-processing SNR of

$$\frac{S}{N} \approx \frac{100}{\sqrt{102}} \approx 10 = 10 \text{ dB.}$$

This value is used as a reference point in the experiments discussed below.

Post-processing SNR is limited by the total time available to take the M samples and by the duration of a sample. Assuming that the sea state is used as a reference, then the total time available is limited to between 1 and 12 hours; the period over which the sea state statistics are stationary [16]. The sample duration is the inverse of doppler resolution.

$$t_s = 1/T_d \quad (5.13)$$

where t_s is the coherent sampling interval (seconds) and T_d is the doppler resolution (Hz). The upper bound on t_s is set by the maximum coherent observation time through the ionosphere. This depends on the particular ionization layer; 25 seconds is a typical maximum for F-layer [11] and 100 seconds is possible for E-layer [11]. The lower bound, set by the required doppler resolution depends on the radial component of ships velocity, and of the sea state [12]. Generally 10 seconds ($T_d=0.1$ Hz) is a safe minimum. Assuming a 12 hour interval, the maximum attainable SNR is then

$$\frac{S}{N} \approx \sqrt{\frac{(12 \times 3600 / 10)}{(12 \times 3600 / 10) + 2}} \approx 18 \text{ dB} .$$

In view of the fact that the radar system will usually scan thousands of square miles of ocean and possibly need to identify several targets, it might not be possible to devote 12 hours to observing one target at one frequency. Consequently, the figure of 18 dB would then be an unrealistic upperlimit. For a maximum observation time of 1 hour, post-processing SNR has a maximum of 13 dB.

Another important consideration concerning (post-processing) SNR is the variability of signal powers between individual frequencies, between ships and between classes of ships.

From Figure B.1 in Appendix B it is evident that signal powers of returns at individual frequencies can vary from 0 to 40 dBm². The average signal power for this ship might be 30 dBm², and so for a 10 dB post processing SNR, it is necessary to add 20 dBm² of noise power to

each amplitude. This yields SNRs for individual amplitude returns ranging from -20 dB to 20 dB. Clearly the lower amplitudes are much more distorted than the larger ones, for a particular level of injected noise power. This is reasonable since for a given noise environment, weaker returns are more susceptible to degradation by noise. The same argument can be developed for ships; the individual amplitude returns of larger ships over several frequencies are, on average, larger than amplitude returns of smaller ships. And finally, we consider the case of classes. If a classification is performed using a catalog comprising ships at aspect angles 0° , 90° , and 180° , then the average signal power, used to determine the amount of noise required for a given post-processing SNR, would be based on the average power for the 3 classes. The 90° aspect angle amplitude returns are generally higher than those of 0° and 180° aspect angles, consequently we would maintain a constant level of noise power amongst the 3 classes, but SNR would vary from class to class and the resulting classification curve would not be representative of any one particular aspect angle.

In general, the signal level of a received amplitude return (not including the noise power) can be estimated with a useful degree of accuracy. This information can be used, a priori, with the estimates of aspect and elevation angles to reduce the size of the catalog. As a consequence, we are interested in the classification of ships at specific aspect and elevation angles, rather than over a group of markedly different aspect or elevation angles. Hence if we compare classification results for 90° aspect with a classification results

for 180° aspect at a given post-processing SNR, we must bear in mind that the amount of injected noise differs for each case.

The consequences of this discussion are somewhat dependent on the effect of the difference in average signal powers, (between any two given ships), on classification errors. One way to access the importance of this difference would be to compare classifications where all catalog members are normalized with respect to their own average signal powers, with classifications where the variability of average signal power is retained.

5.6 ESTIMATION OF THE PROBABILITY OF MISCLASSIFICATION

Chen [1] used the Maximum Likelihood Estimate (MLE) [14] as the estimate of probability of error for a given target;

$$PE \cong \hat{P}_E$$

where PE is the probability of error and \hat{P}_E is the MLE of the probability of error. The proximity of the terms expressed in the equation above is usually stated in terms of confidence interval. A $(1-\alpha)$ confidence interval for PE is given as

$$\hat{P}_E \pm \xi_\alpha \sqrt{\frac{\hat{P}_0(1-\hat{P}_0)}{Mn}} \quad (5.14)$$

where

M = number of targets

n = number of experiments

\hat{P}_0 = probability for which the confidence interval is desired

ξ_α is such that

$$\Phi(\xi_\alpha) = 1 - \alpha/2 = \frac{1}{\sqrt{2\pi}} \int_{-\infty}^{\xi_\alpha} e^{-x^2/2} dx \quad (5.15)$$

where Φ is the standard (zero mean, unit variance) normal distribution.

For example, the calculated 90% confidence interval at 30% error (a typical error value) for 18 targets and 50 experiments is found as

$$\alpha = 1 - 0.9 = 0.1$$

$$\Phi(\xi_\alpha) = 1 - \alpha/2 = 0.95$$

$$\xi_\alpha = 1.65$$

$$P_0 = 30\% = 0.3$$

$$PE = \hat{P}_E \pm 1.65 \sqrt{\frac{0.3(1-0.3)}{18 \times 50}}$$

$$PE = \hat{P}_E \pm 2.5\%$$

Clearly, the result is made more accurate by increasing the number of experiments. It must be emphasized that the confidence interval is not an expression of probability, i.e., the above calculation does not show that 9 times out of 10 the actual probability of error at 30% misclassification will be within $\pm 2.5\%$ (or $27.5\% < PE < 32.5\%$). DeGroot [17] pointed out that "confidence" is a more subtle and less defined

term than "probability" and that under certain experimental conditions, the term "confidence" interval can be misleading. In regard to this, we must view confidence interval as a measure of accuracy for the measured result, not as an absolute probability.

In his experiments, Chen [1] used $M=15$ experiments. The significant increase to $M=50$ for this work is for two reasons. Firstly, the curves are more reliable, especially when close together, if the confidence interval is smaller. A $\pm 5.6\%$ confidence interval (using $M=15$) in some cases meant that two curves, representing the same experiment, using the same parameters but with different random number seeds, differed by 11%. Using $M=50$ experiments cuts this worst case error by half, and makes conclusions about particular sets of curves more reliable. More importantly, the large number of classification runs required that curves be plotted automatically after each run. Hence it is desirable to have a high degree of similarity between curves from different runs representing the same classification parameters.

CHAPTER VI

EXPERIMENTS

6.1 INTRODUCTION

This chapter presents most of the original work done in this report. The purpose of the experiments discussed here is to study classification behaviour under a wide variety of the available classification parameters. These are listed below (a list of commonly used terms is given in Table 6.1).

1. Frequency Band (in the allotted 2-7 MHz)
2. Comparisons with previous work on ships
3. Elevation Angle (known, unknown and with error)
4. Polarization
5. Aspect Zone (known, unknown)
6. Aspect Error (magnitude of error and location in aspect zone).

TABLE 6.1
DEFINITIONS

1. ASPECT ZONE: A small range of aspect angles centred on or adjacent to a particular aspect angle.

<u>ASPECT ZONE</u>	<u>NAME</u>	<u>ASPECT ANGLES</u>
0°	BOW	0°, 10°
90°	BROADSIDE	80°, 90°, 180°
180°	STERN	170°, 180°

2. KNOWN ASPECT: If ship data having more than one aspect angle is used in a classification, then the aspect angle is assumed known when the algorithm only allows comparisons between an 'unknown' noisy target at aspect θ_K , with 'noise-free' catalog targets at the same aspect angle θ_K . The same follows for known elevation.
3. UNKNOWN ASPECT: If ship data having more than one aspect angle is used in a classification, then the aspect angle is assumed unknown when the algorithm permits comparisons between an 'unknown' noisy target at θ_K with all 'noise-free' catalog targets at all aspect angles used in the classification.
4. ALGORITHM: One of the following:
 1. Nearest neighbour (NN), using any of the features listed in 5.
 2. Time domain (T)
5. NN ALGORITHM FEATURES:
 - A Amplitude only
 - W Differential phase only
 - AW Amplitude and differential phase
 - \bar{A} Relative amplitude
 - $\bar{A}W$ Relative amplitude and differential phase.

TABLE 6.1

(Continued)

Note that, in general, the term 'feature', in the context of resonance region radar returns, applies to any property or quality associated with the returns. This includes, for example, the magnitudes of the time domain impulse response.

6. PARAMETER: A variable in the measurement or classification process such as frequency, aspect angle, elevation angle, polarization, feature or algorithm.
7. DATA BASE: A collection of data files containing a measurement vector for each ship.
8. CATALOG: A single 2 dimensional complex array containing the amplitudes and phases of all ships at the selected frequencies, and other parameters.
9. FEATURE VECTOR: A single vector for a particular target, dimensional in frequency or time, derived from the catalog by selecting a particular feature.
10. POLARIZATION: One of the following:
 1. Vertical, V
 2. Horizontal, H
 3. Cross, X
 4. Vertical divided by horizontal, V/H.

The term described in 4 is not really a polarization scheme, in the sense of the preceding three terms, but is called a polarization for convenience. Strictly speaking, the polarization of a wave describes the instantaneous orientation of the electric field vector; the terms listed above refer to a particular measurement scheme or use of radar cross section returns, with respect to polarization.

If each of these parameters were to be assessed in terms of the others, over 10,000 curves would be needed. Clearly this is not practical; however, an intelligent approach toward choosing the experiments allows a thorough investigation without incurring too much processing of data.

First, experimenting with a sub-band in the 2-7 MHz band indicates the best region of frequencies (if any) for a particular type of classification. Second, an evaluation of classification performance as a function of the number of frequencies (NF) provides a comparison with work presented in [1] and also establishes the ranking of a particular number of frequencies. Hence we can choose $NF=8$ for subsequent experiments and refer to this section for results pertaining to other values of NF. The problem of choosing the desired classification frequencies is thus solved. Next, a study of elevation angle and its effect on classification allows classification using only one elevation in subsequent experiments. The remaining parameters are then classified using various features and algorithms, polarizations and aspect zones. Sometimes it is useful to reduce the number of features in the NN algorithm by eliminating W and $\bar{A}W$, or W and \bar{A} . W is generally the least useful of NN features and it is unlikely that only phase would be measured practical situation.

It must be remembered that certain parameters, such as relative amplitude (\bar{A}), and V/H polarization, are not really tested in these experiments since the difficulties which they were designed to overcome were not simulated. This should be taken into consideration when making comparisons between features such as A and \bar{A} , or polarizations such as V

and V/H. For example, V/H polarization purportedly has the property that multiplicative errors cancel out by virtue of the division of a vertically polarized phasor by a horizontally polarized phasor. To test the validity of this assumption, the ship data must be contaminated with multiplicative noise before classification proceeds. For reasons mentioned earlier, multiplicative noise models were excluded from this analysis, and what we are really measuring is the 'insertion loss' of the algorithm which uses this parameter.

In the following sections, each experiment is introduced, detailing the aim of the experiments with a brief discussion of any relevant points. The results of all experiments in the form of misclassification percentage versus post-processing SNR curves, are contained in Appendix A. These results are summarized by means of histograms representing averaged misclassification percentage at 10 dB post-processing SNR, and are presented, along with typical misclassification curves.

Conclusions drawn from the histograms often compare the classification performance of one parameter with the performance of another by saying that misclassification percentage (at 10 dB post-processing SNR) is higher or lower by $x\%$; here x is always the difference between two misclassification percentages, not the percentage increase of one misclassification percentage compared with another.

6.1.2 INTERPRETATION OF HEADERS IN CLASSIFICATION RESULTS

The data presented in subsequent sections were plotted with an automatic header system to aid the batch processing of classification experiments. The header comprises of up to 11 lines and these are described as follows:

1. LINE 1. TARGET TYPE. i.e., ships, aircraft, ground vehicles, etc.
2. LINE 2. POLARIZATION. This can be either vertical ('V'), horizontal ('H'), cross('X') or vertical divided by horizontal ('V/H'). The polarization for each curve is printed if this varies from curve to curve.
3. LINE 3. A PRIORI KNOWLEDGE OF ELEVATION ANGLE. This can be either 'known', 'unknown', or 'known/unknown' if some of the curves use known elevation angle and others use unknown elevation angle. The system is specific about which is known and which is unknown only if 2 curves are present.
4. LINE 4. ELEVATION ANGLE(S). This can be '15' for 15° elevation data, '27' for 27° elevation data or '15,27' if both elevation angles are used. Elevation angle is printed if it varies between curves, so if there were 5 curves and only two entries in LINE 4, say '15,27' and '27', the last 4 curves would be representative of 27° elevation data.
5. LINE 5. A PRIORI KNOWLEDGE OF ASPECT ANGLE. This is compiled in the same way as LINE 3.

6. LINE 6. MINIMUM, MAXIMUM AND INCREMENT OF ASPECT. The minimum and maximum aspect angles can be any of those listed in Table 3.1. If these parameters vary from curve to curve, they are printed out for each curve in the same way as LINE 4 (or LINE 2).
7. LINE 7. NUMBER OF FREQUENCIES. This is printed for each curve.
8. LINE 8. NUMBER OF TARGETS. This is always a multiple of 6, the number of ships. (No. of targets = 6 x No. aspect angles x No. elevation angles). This is printed for each curve.
9. LINE 9. 90% CONFIDENCE INTERVAL AT 30% MISCLASSIFICATION. This is calculated according to the discussion in 5.6, and is printed for each curve.
10. LINE 10. CLASSIFICATION FEATURES. These are listed as:

'A' Amplitudes only 'W' Differential phases only 'AW' Amplitudes and phases 'R' Relative Amplitude 'RW' Relative Amplitude and phase 'T' Time domain algorithm.]	NN algorithm
--	---	-----------------
11. LINE 11. IDENTITY OF CURVES WITH ASPECT OR ELEVATION ANGLE ERRORS. This is printed only if there is an error in elevation angle or aspect angle. Note that the classification software does not allow both types of errors at once. For example, if 3 curves were plotted and the last two had aspect errors, LINE 11 would read

'ASPECT ERR IN CURVE 2 3'

Curves are identified as follows:

_____	Curve 1
-----	Curve 2
-----	Curve 3
.....	Curve 4
-----	Curve 5
-----	Curve 6

6.2 FREQUENCY BAND

6.2.1 INTRODUCTION

This set of experiments was designed to examine the effect of choosing a particular frequency band for various aspect angles, polarizations and algorithms. (The term algorithm implies the use of various features in the NN algorithm; see Table 6.1).

The available band of 2 to 7 MHz was split into 3 non-overlapping sub-bands, each containing 4 discrete frequencies separated by 0.4 MHz. These were

Band 1: 2 - 3.2 MHz

Band 2: 4 - 5.2 MHz

Band 3: 5.8 - 7.0 MHz.

Generally, it is expected that the lower of frequencies will provide the best classification performance. This is because the radar cross section at lower frequencies tends to vary less per unit bandwidth compared with higher frequencies. Consequently, for higher frequencies, (in the upper resonance region) a small change in a parameter such as aspect angle, or the addition of noise to the cross section amplitudes results in a greater change in the selected features compared to the change at lower frequencies. In this sense, the radar cross section frequency response is more reliable (i.e., impervious to small changes in orientation, frequency, etc.) at lower frequencies than at higher frequencies.

Note that for this experiment only a single elevation angle (27°) was used. This is justified by a study of the effect of elevation angle on classification presented below.

6.2.2 RESULTS AND CONCLUSIONS

Figure 6.1 shows a set of typical curves representing misclassification percentage versus post-processing SNR. Similar plots using other parameters are contained in Appendix A; the results for all curves have been summarized by compiling averages of misclassification percentage at 10 dB post-processing SNR and are presented in Figures 6.2 to 6.4.

From Figure 6.2 it is evident that for 0° and 180° aspect zones, there is no distinct preference for a particular frequency band. 90° aspect zone favours the lower bands, but not significantly. Taking an average across all 3 aspect zones results in a marginal preference for band 1, showing that in general, the performance for a given sub-band in the 2-7 MHz band is not significantly affected by aspect zone. This is encouraging in one respect; namely that if the ionosphere or range conditions necessitated the use of higher frequencies (in the 2-7 MHz band), then performance is not degraded for a particular azimuthal orientation of the target ship.

Figure 6.4 shows a clear preference for band 1 (2-3.2 MHz) for vertical and cross polarizations. For the other two polarizations, frequency band seems unimportant. In Figure 6.3, a clear precedence of band 1, band 2, followed by band 3 is set, for each algorithm. This seems to best conform to the initial expectation that classification is more reliable at lower frequencies (i.e., closest to $L/\lambda=1$). However, certain results show an insensitivity to frequency band, at least for the range of frequency bands available here. Choosing a band of much

CLASSIFICATION OF SHIPS
 POLARIZATION V
 ELEV ASSUMED KNOWN
 ELEVATION (DEG.) 27
 ASPECT ASSUMED KNOWN
 MIN,MAX,INC ASPECT 170 180 10
 NO OF FREQUENCIES 4 4 4
 NO OF TARGETS 12 12 12
 90% CI (±30%) +/- 3.1% 3.1% 3.1%
 CLASS. FEATURES A A A

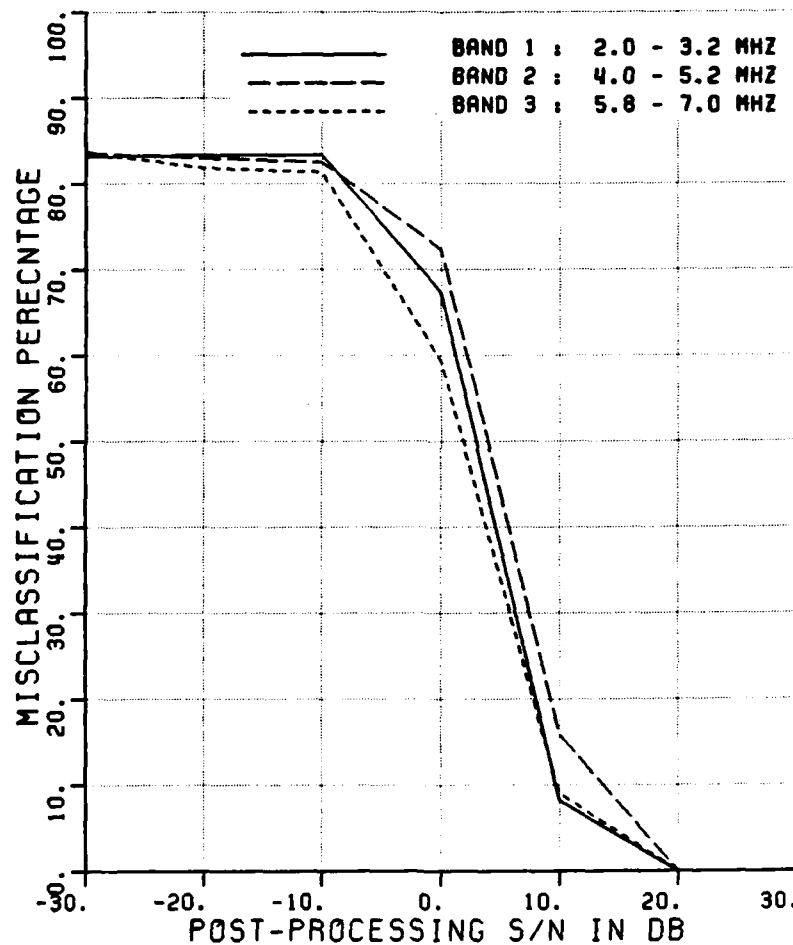


Figure 6.1. Misclassification percentage versus post-processing SNR for 3 sub-bands in the 2-7 MHz band.

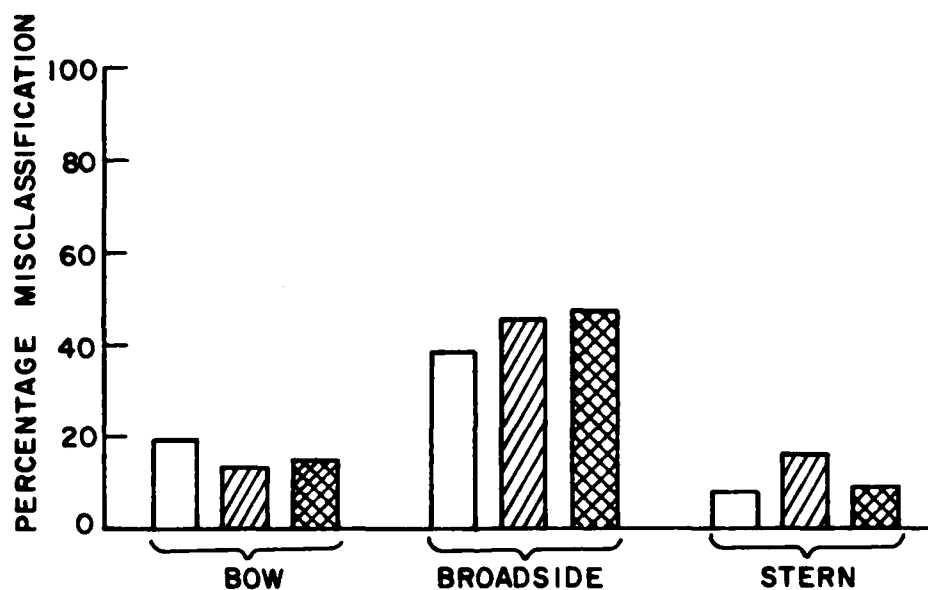
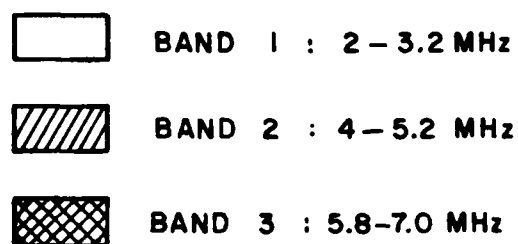


Figure 6.2. Average misclassification percentages at 10 dB post-processing SNR for 3 bands, as a function of aspect zone.

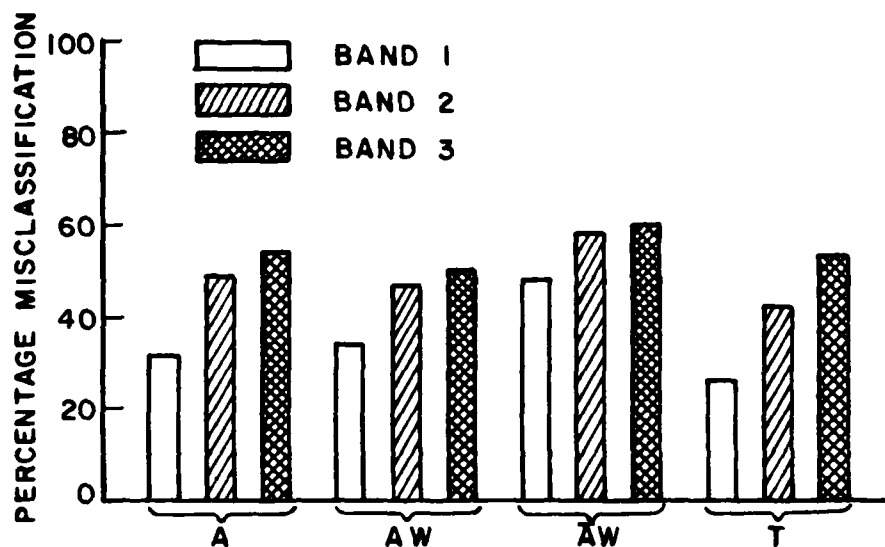


Figure 6.3. Average misclassification percentages at 10 dB post-processing SNR for 3 bands, as a function of algorithm.

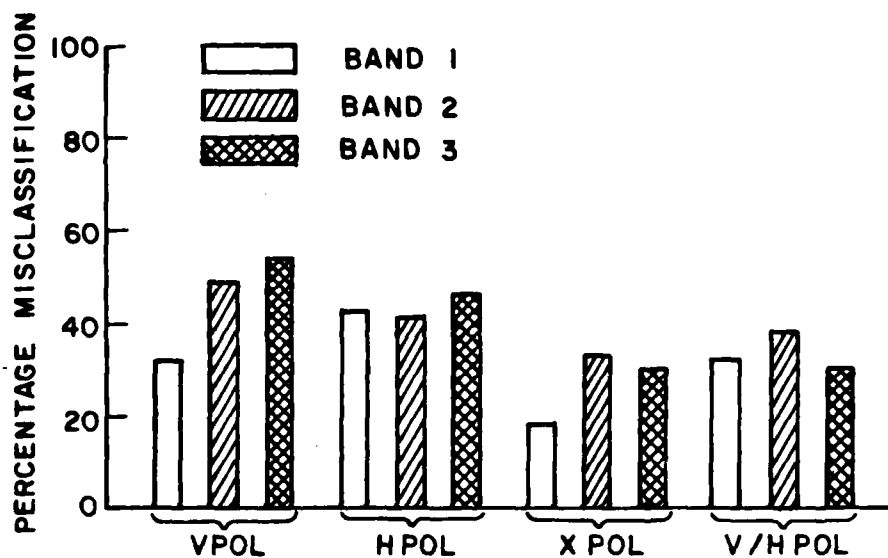


Figure 6.4. Average misclassification percentages at 10 dB post-processing SNR for 3 bands, as a function of polarization.

higher frequencies, for example 15 to 16.2 MHz, might show a dependence on frequency band not measurable here. In conclusion, certain parameters, such as vertical and cross polarizations, and the classification algorithm (i.e., A, AW, $\bar{A}W$, or T) are markedly dependent on the selection of frequencies in the 2 to 7 MHz band.

6.3 COMPARISON WITH PREVIOUS WORK

6.3.1. INTRODUCTION

The purpose of this experiment was to provide a direct comparison between the work done by Chen [1] and that done here. The essential difference between Chen's data and the data used here is that the former exclusively uses an elevation angle of 0° , while the latter has elevation angles of 15° and 27° . The comparison was done using 27° elevation only, since classification statistics are similar for 27° and 15° elevations.

Five features (A, AW, W, \bar{A} , and $\bar{A}W$) in the NN algorithm, and the time domain algorithm were evaluated at 2, 4, 6, 8 and 12 frequencies, using vertical polarization, 27° elevation and aspect angles of 0° , 90° and 180° (aspect angles assumed known). The frequencies selected by using the above numbers were discussed in Chapter V, Section 5.2. The data at aspect angles 0° , 90° and 180° are nearly independent so that the results do not pertain to a particular aspect zone. (Chen used this approach in most of his work.) The evaluation using 12 frequencies was included to see if performance could be improved.

Classification results using known and unknown aspect angles at 8 frequencies, and other parameters as above, were compared with those in [1]. When the aspect angle is known, a noise-corrupted target is compared only with catalog members of the same aspect angle. Unknown aspect implies that the noisy target is compared with members of the catalog at all aspects (see Table 6.1).

6.3.2 RESULTS AND CONCLUSIONS

Figures 6.5 and 6.6 show typical classification results. Figures 6.7 and 6.8 indicate a general increase in misclassification percentage when 27° elevation is used in comparison with 0° . This increase is about 6% for each selected number of frequencies. Chen used 5 ships compared with the 6 ships used here, which should account for 3% of the difference ($4/5 - 5/6$). This still leaves a 3% improvement for 0° elevation over 27° . Although this difference is apparent for all numbers of frequencies, it is not sufficiently large to be conclusive about the effect of elevation angle on classification. However, the tilting of a target when elevation angles above 0° are used is equivalent to a compression in range of the various scattering structures, from the point of view of an incident electromagnetic wave. Furthermore, structures that are vertical at 0° elevation (hence good scattering centres for vertically polarized waves) become weaker scatterers when tilted. Consequently, the process by which nulls and peaks are produced in the amplitude returns, which essentially characterize a particular target, is weakened. Intuitively

CLASSIFICATION OF SHIPS

POLARIZATION	V			
ELEV ASSUMED	KNOWN			
ELEVATION (DEG.)	27			
ASPECT ASSUMED	KNOWN			
MIN,MAX,INC ASPECT	0	180	90	
NO OF FREQUENCIES	2	4	8	12
NO OF TARGETS	18	18	18	18
90% CI (±30%) +/-	2.5%	2.5%	2.5%	2.5%
CLASS. FEATURES	A	A	A	A

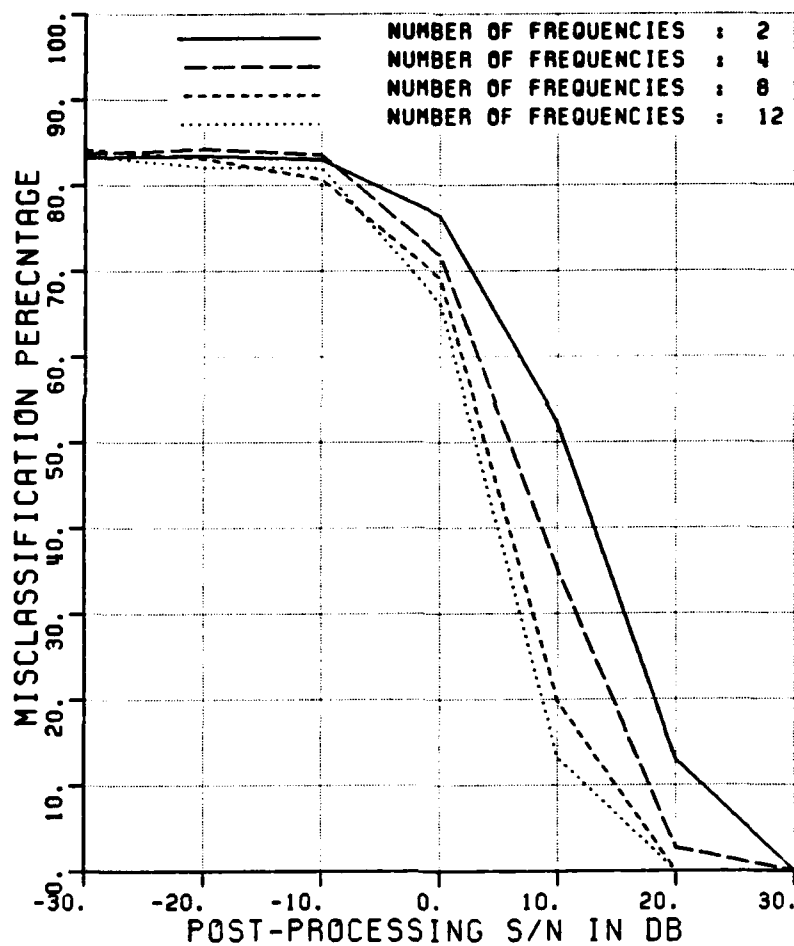


Figure 6.5. Misclassification percentage versus post-processing SNR for 4 different numbers of frequencies, using amplitudes only.

CLASSIFICATION OF SHIPS				
POLARIZATION	V			
ELEV ASSUMED	KNOWN			
ELEVATION (DEG.)	27			
ASPECT ASSUMED	KNOWN			
MIN,MAX,INC ASPECT	0	180	90	
NO OF FREQUENCIES	2	4	8	12
NO OF TARGETS	18	18	18	18
90% CI (@30%) +/-	2.5%	2.5%	2.5%	2.5%
CLASS. FEATURES	T	T	T	T

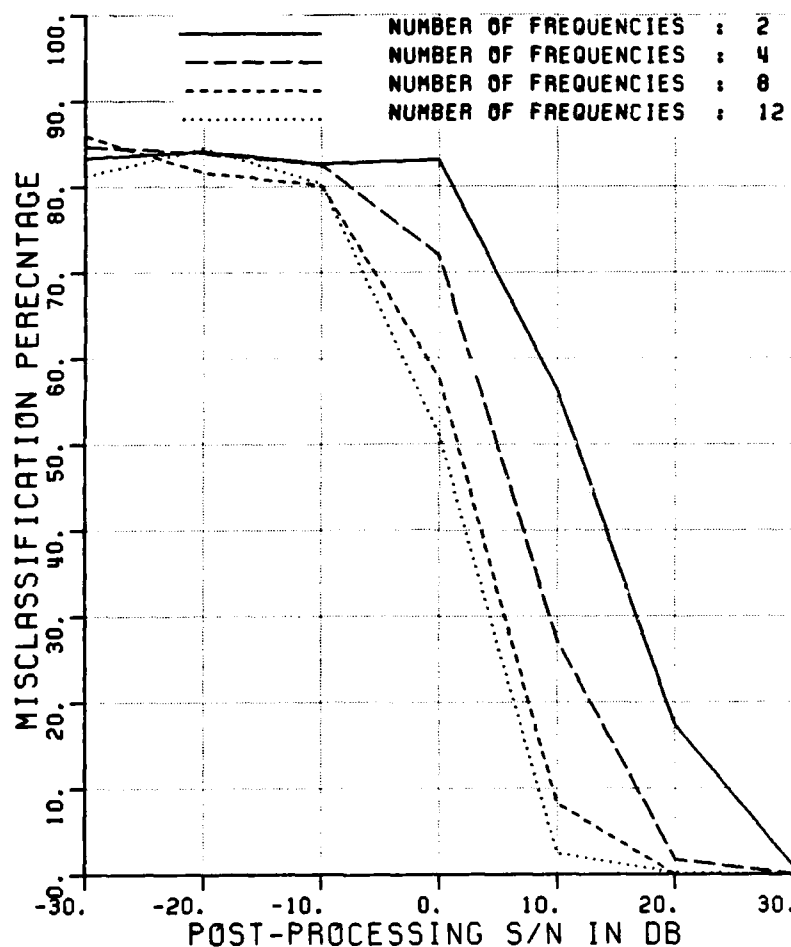


Figure 6.6. Misclassification percentage versus post-processing SNR for 4 different numbers of frequencies, using the time domain algorithm.

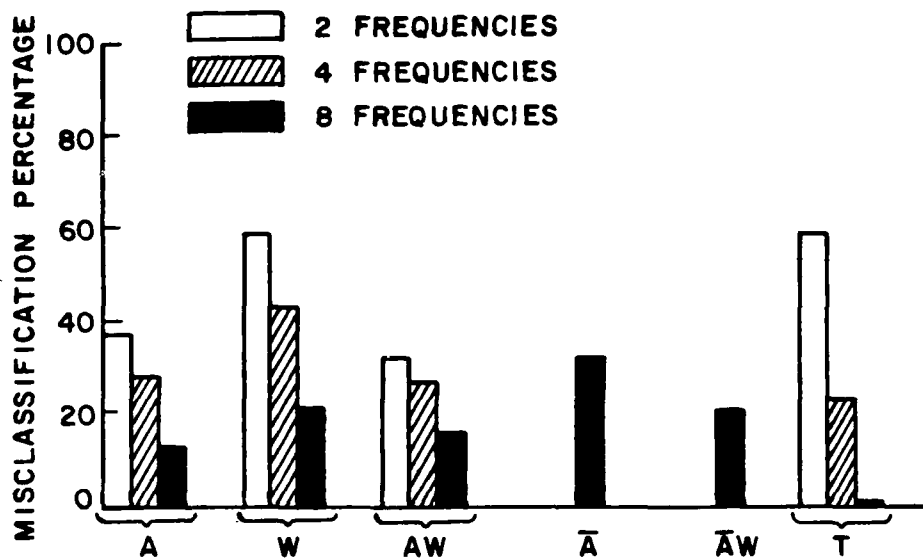


Figure 6.7. Average misclassification percentages at 10 dB post-processing SNR for 3 different numbers of frequencies as a function of algorithm (from Chen [1]).

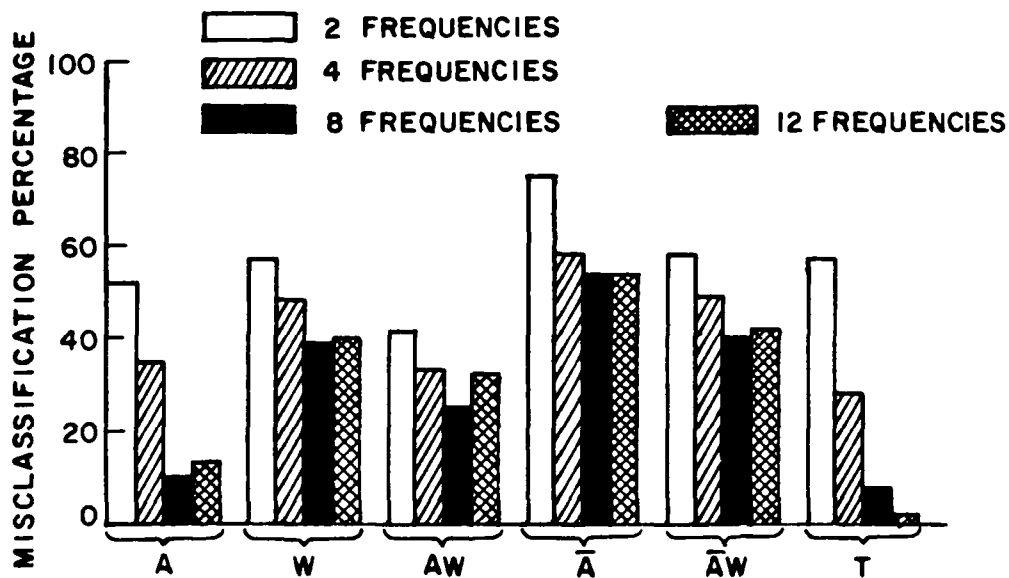


Figure 6.8. Average misclassification percentages at 10 dB post-processing SNR for 3 different numbers of frequencies as a function of algorithm.

classification is expected to be less reliable at higher elevation angles. Data sets at say 50° elevation might be taken to confirm this hypothesis.

Chen [1] established a ranking of features and algorithms in terms of lowest misclassification percentage for each number of frequencies. For $NF=2$, $AW < A < W < T$, for $NF=4$, $T < AW = A < W$, and for $NF=8$, $T < A < AW < W = \bar{AW} < \bar{A}$. Examination of Figures 6.7 and 6.8 shows this same ranking to hold at 27° as well. The time domain feature is still critically affected by the use of only 2 frequencies for 27° elevation (as one would expect, since this is the absolute minimum allowable to permit the operation of the DIFT).

For both 27° and 0° elevation it is evident that the addition of phase information (comparing A with AW) plays a more significant role at 2 frequencies than at a higher number of frequencies. For example, with $N=2$ and 27° elevation, AW produces 10% fewer misclassification errors than A alone. The contribution that phase information makes to classification performance seems to become smaller as the number of frequencies is increased. This phenomenon also manifests itself in the relative amplitude results. Using \bar{AW} gives an average improvement of 10% over \bar{A} , for $N=4, 8$, and 12 , but 15% for $N=2$. Phase information, therefore, could become particularly valuable when certain conditions constrain the measurements, such as being restricted to two frequency measurements or having a multiplicative bias in the amplitude data. Generally if 4 or more frequencies are available and phase information is at hand, it is best to use the time domain algorithm.

The addition of 4 extra frequencies above the previously used number of 8 yields a small improvement of 1%. In some cases, the use of 12 frequencies results in more classification errors than the use of 8 frequencies. Figure 6.12 shows the variation of average misclassification percentage with number of frequencies. The minimal increase in performance in going from 8 to 12 frequencies and, in general, from a lower to a higher number of frequencies, is consistent with the findings of the previous chapter. There it was shown that using lower frequencies in the allotted 2-7 MHz band resulted in better performance, depending on which parameters were used. Increasing the number of frequencies means that higher frequencies would be included, thus yielding a minimal improvement.

The number of frequencies is usually the most costly parameter (in terms of processing time) in a classification procedure. Bearing this in mind, and using results like those in Figure 6.12, it should be possible to obtain an optimal number of frequencies using counterposing weightings for the number of frequencies and the acceptable level of misclassification percentage. In subsequent classification experiments 8 frequencies are used. This tends to de-emphasize the affect of isolated errors or biases.

The difference in average misclassification percentage between classifications using known aspect and unknown aspect angle is about 6% for 27° elevation angle data, and 5% for 0° elevation angle data. Figure 6.9 shows a typical classification result and Figures 6.10 and 6.11 summarize the results of all curves produced in this part of the experiment, the remainder of which are contained in Appendix A.

CLASSIFICATION OF SHIPS
 POLARIZATION V
 ELEV ASSUMED KNOWN
 ELEVATION (DEG.) 27
 ASPECT ASSUMED KNOWN / UNKNOWN
 MIN,MAX,INC ASPECT 0 180 90
 NO OF FREQUENCIES 8
 NO OF TARGETS 18 18
 90% CI ($\pm 30\%$) $\pm 2.5\%$ $\pm 2.5\%$
 CLASS. FEATURES A A

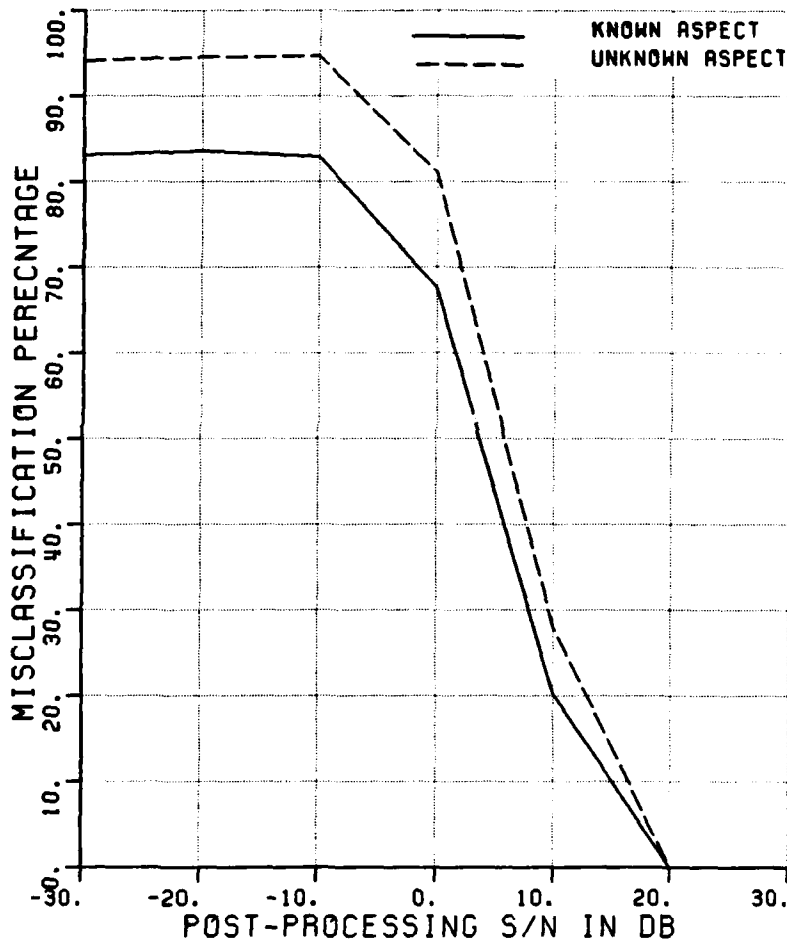


Figure 6.9. Misclassification percentage versus post-processing SNR for known and unknown aspect angles.

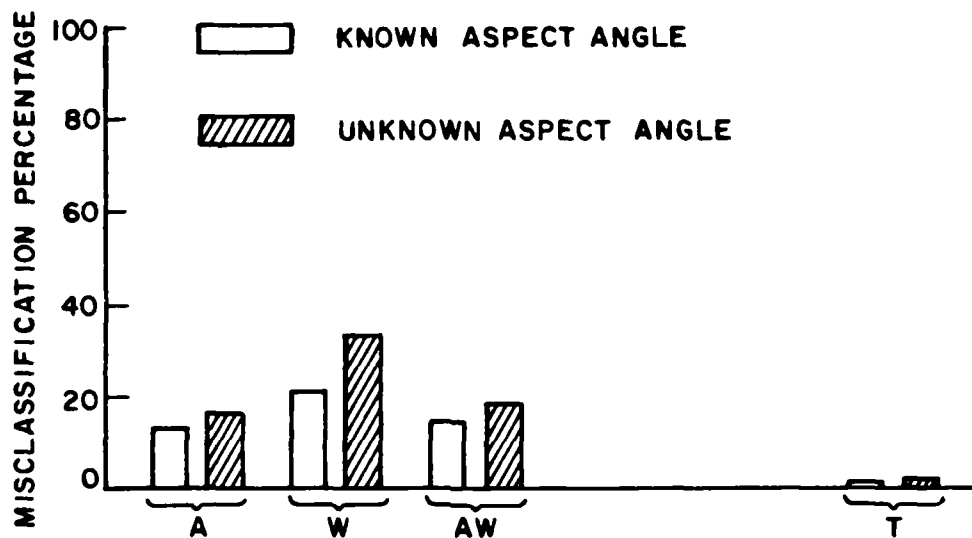


Figure 6.10. Average misclassification percentages at 10 dB post-processing SNR for known and unknown aspect angles as a function of algorithm (from [1]).

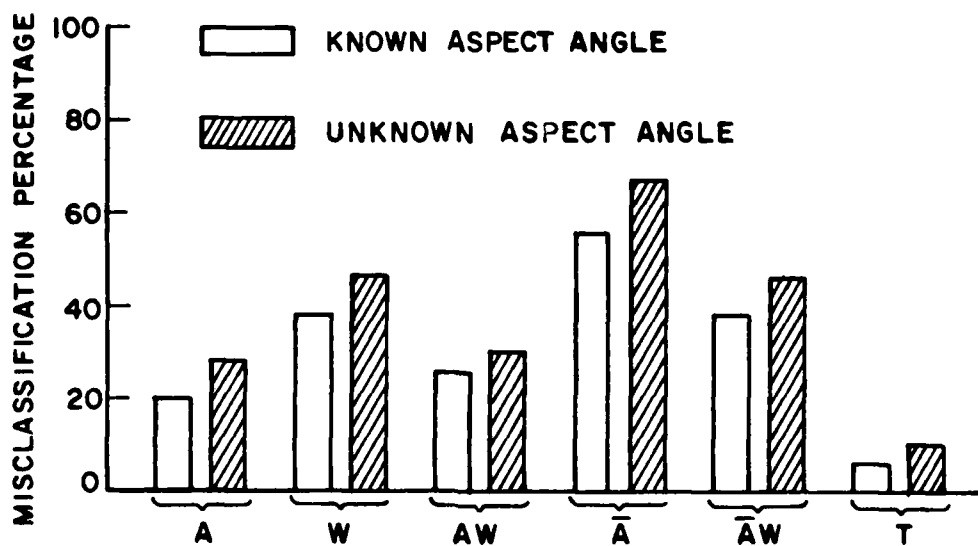


Figure 6.11. Average misclassification percentages at 10 dB post-processing SNR for known and unknown aspect angles as a function of algorithm.

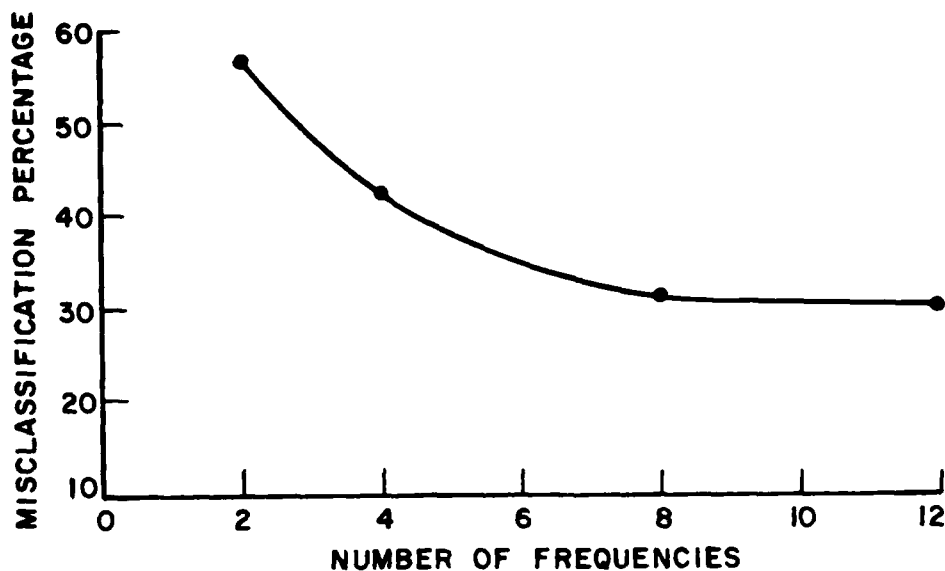


Figure 6.12. Average misclassification percentage versus the number of frequencies used.

6.4 ELEVATION ANGLE

6.4.1 INTRODUCTION

This experiment was divided into 3 parts. The first was designed to examine the differences in classification performance between ship data at elevation angles of 15° and 27° . The second part investigated classification performance when the elevation angle is known and unknown, and the final part measured the effect of having an error in elevation angle.

Each part of the experiment was conducted at the various aspect zones (0° , 90° , 180°), polarizations (V, H, X, V/H) and algorithms. In order to keep the data processing task to a manageable size,

only the A, AW and \bar{A} features of the nearest neighbour algorithm were considered. The time domain algorithm was also used. This combination alone leads to a total of 48 graphs, with each part of the experiment for a given set of parameters on the same graph.

Data for only 2 elevation angles, 15° and 27° were available. For the 'unknown elevation' case, data for a noise-contaminated target ship is compared to data for ships at 15° elevation, and 27° . The only error syndrome available was $\pm 12^\circ$. Hence, a noise-contaminated target ship known to be at 27° elevation would be compared with 15° elevation catalog members and vice versa. Chen's data [1] at 0° elevation were considered for use in this experiment but were ruled out on the grounds of the additional complexity necessary in the classification software for the minimal comparisons which would be obtained. (The data included 5 of the 6 ships used here, but only at vertical polarization and aspect angles of 0° , 90° and 180° .)

6.4.2 RESULTS AND CONCLUSIONS

Figures 6.13 to 6.16 show typical classification results (see Appendix A for others) and Figures 6.17 to 6.21 summarize all results in terms of the average misclassification percentage at 10 dB post-processing SNR.

Figures 6.17 to 6.19 show a high degree of similarity between classifications at 15° elevation and those at 27° . For aspect zone, polarization and algorithm, 15° elevation has, on average, an improvement of 1.7% fewer classification errors than 27° elevation. Although this improvement is small, it is consistent with all parameters

CLASSIFICATION OF SHIPS

POLARIZATION	V				
ELEV ASSUMED	KNOWN / UNKNOWN				
ELEVATION (DEG.)	15	27	15,27		
ASPECT ASSUMED	KNOWN				
MIN,MAX,INC ASPECT	0	10	10		
NO OF FREQUENCIES	8				
NO OF TARGETS	12	12	24	24	24
90% CI (@30%) +/-	3.1%	3.1%	2.2%	2.2%	2.2%
CLASS. FEATURES	A	A	A	A	
ELEV ERR IN CURVE	4				

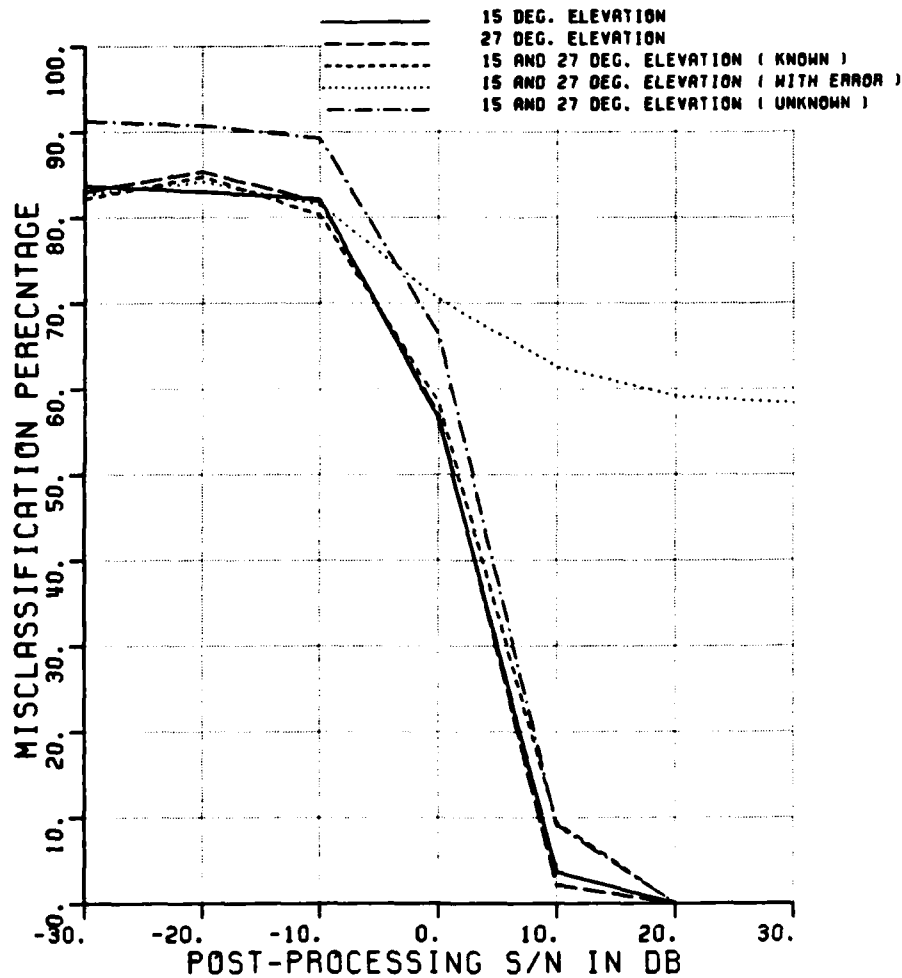


Figure 6.13. Misclassification percentage versus post-processing SNR for various elevation angles.

CLASSIFICATION OF SHIPS

POLARIZATION	H				
ELEV ASSUMED	KNOWN	/ UNKNOWN			
ELEVATION (DEG.)	15	27	15,27		
ASPECT ASSUMED	KNOWN				
MIN,MAX,INC ASPECT	0	10	10		
NO OF FREQUENCIES	8				
NO OF TARGETS	12	12	24	24	24
90% CI (@30%) +/-	3.1%	3.1%	2.2%	2.2%	2.2%
CLASS. FEATURES	A	A	A	A	A
ELEV ERR IN CURVE	4				

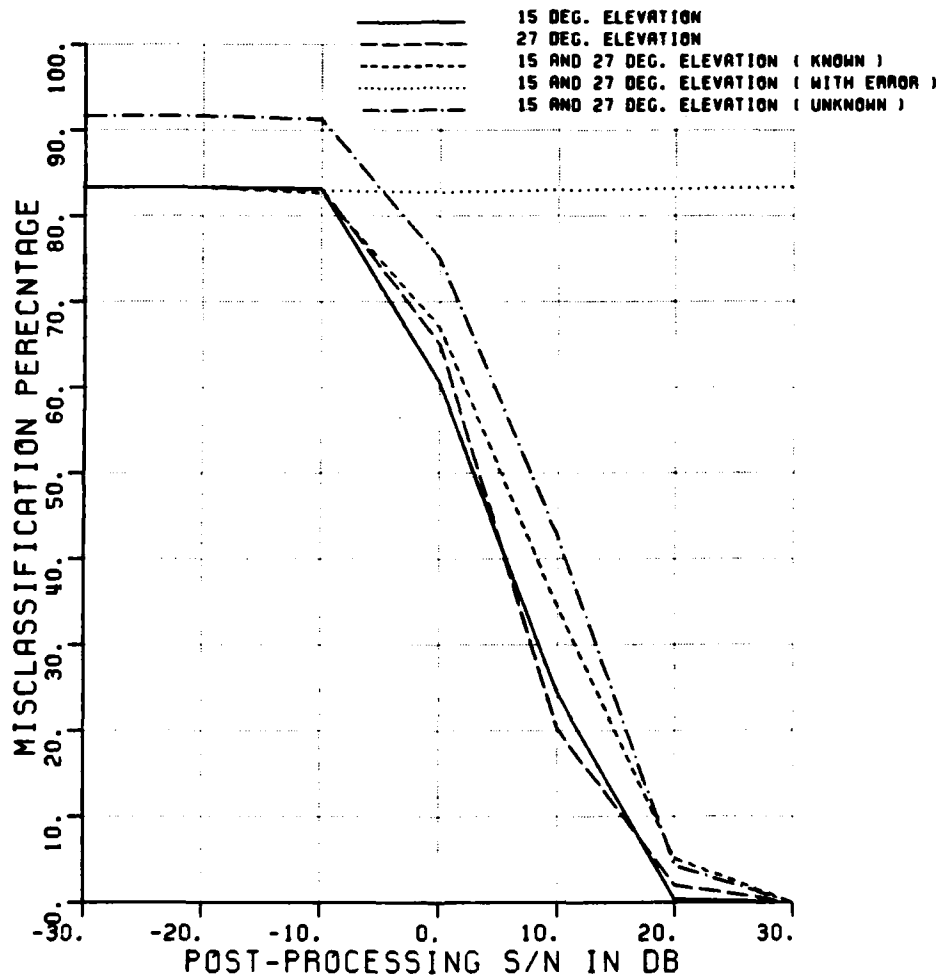


Figure 6.14. Misclassification percentage versus post-processing SNR for various elevation angles.

CLASSIFICATION OF SHIPS

POLARIZATION	X				
ELEV ASSUMED	KNOWN	/ UNKNOWN			
ELEVATION (DEG.)	15	27	15,27		
ASPECT ASSUMED	KNOWN				
MIN,MAX,INC ASPECT	0	10	10		
NO OF FREQUENCIES	8				
NO OF TARGETS	12	12	24	24	24
90% CI (@30%) +/-	3.1%	3.1%	2.2%	2.2%	2.2%
CLASS. FEATURES	A	A	A	A	
ELEV ERR IN CURVE	4				

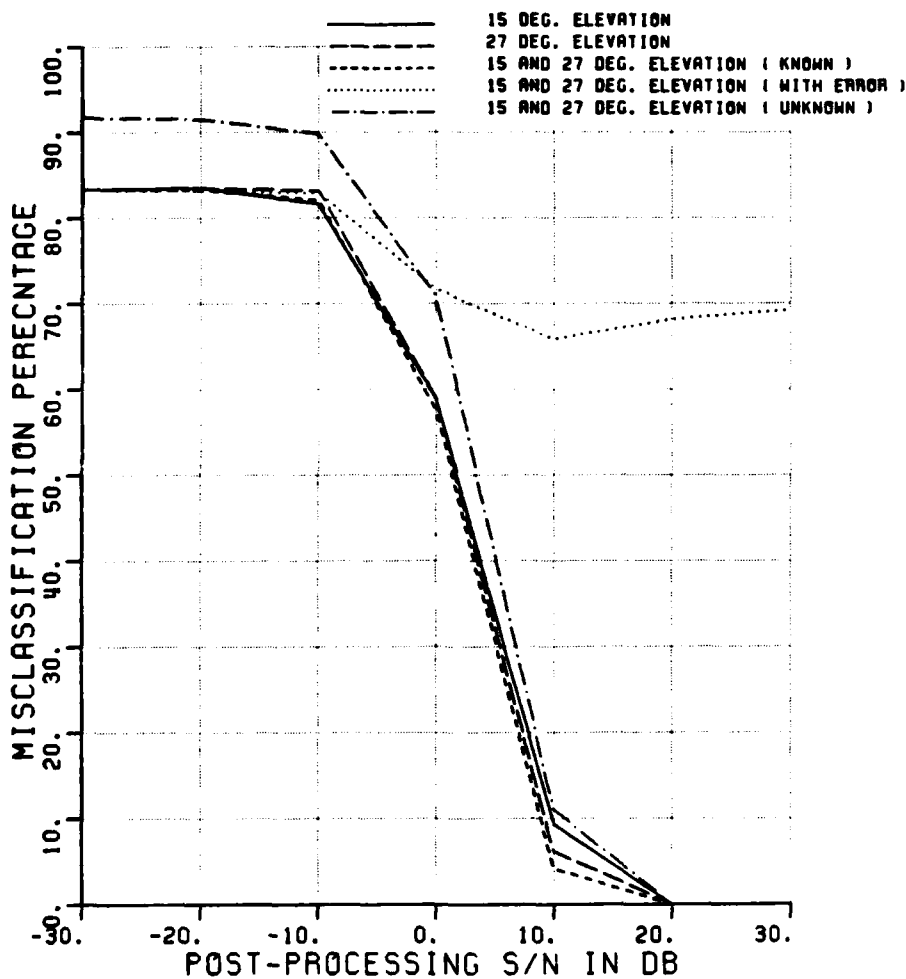


Figure 6.15. Misclassification percentage versus post-processing SNR for various elevation angles.

CLASSIFICATION OF SHIPS

POLARIZATION	V/H				
ELEV ASSUMED	KNOWN	/ UNKNOWN			
ELEVATION (DEG.)	15	27	15,27		
ASPECT ASSUMED	KNOWN				
MIN,MAX,INC ASPECT	0	10	10		
NO OF FREQUENCIES	8				
NO OF TARGETS	12	12	24	24	24
90% CI (±30%) +/-	3.1%	3.1%	2.2%	2.2%	2.2%
CLASS. FEATURES	A	A	A	A	A
ELEV ERR IN CURVE	4				

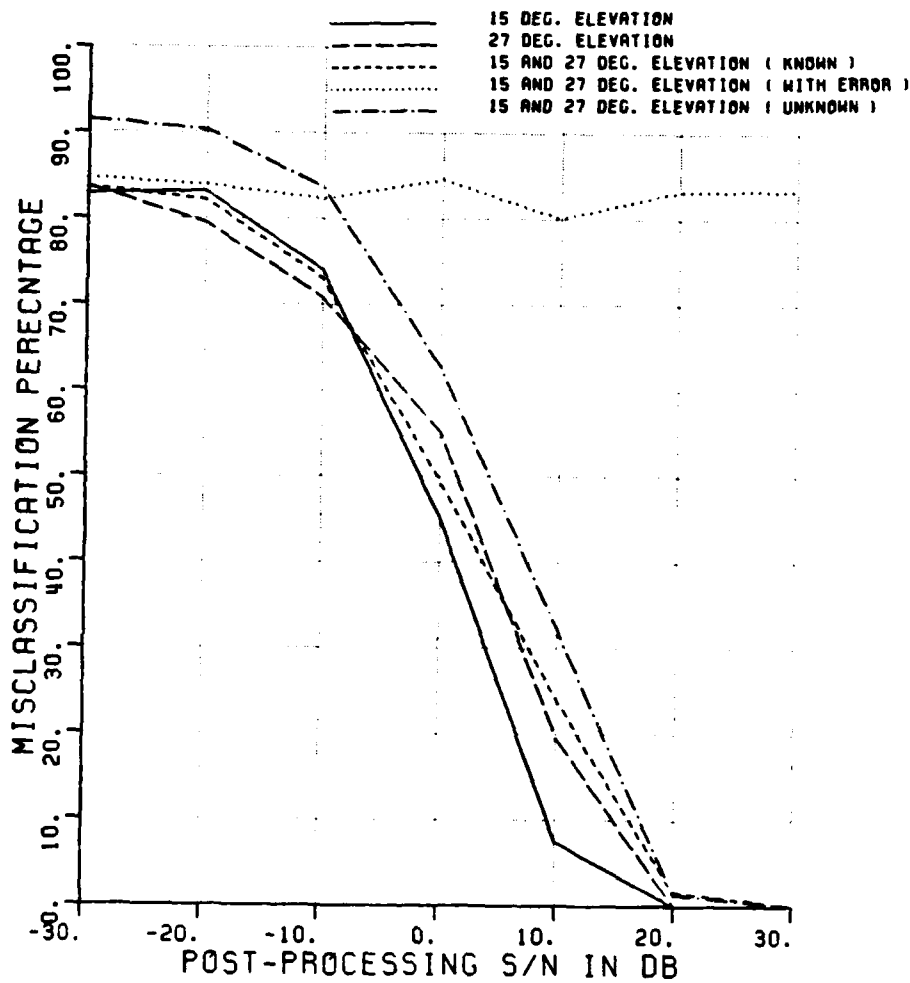


Figure 6.16. Misclassification percentage versus post-processing SNR for various elevation angles.

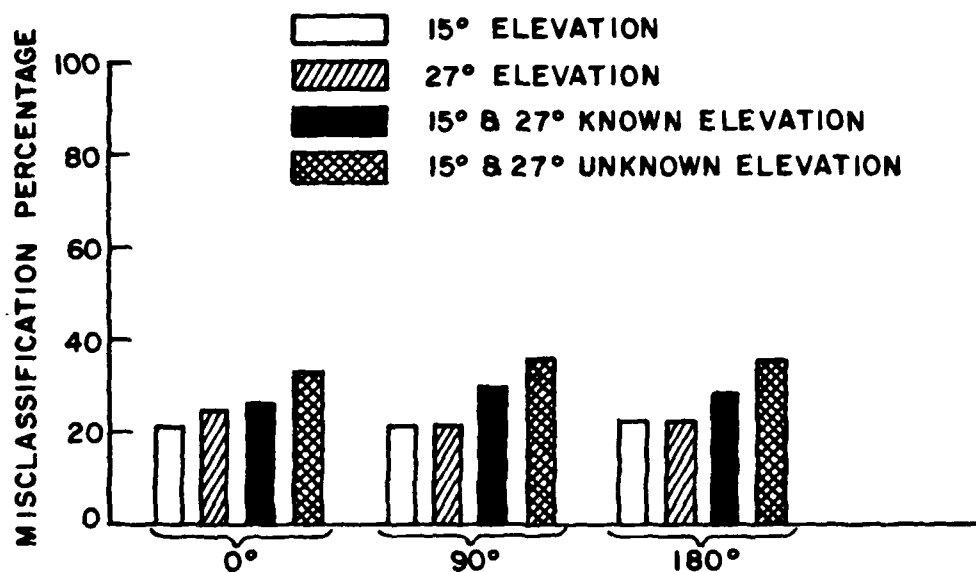


Figure 6.17. Average misclassification percentages at 10 dB post-processing SNR for various elevation angles as a function of aspect zone.

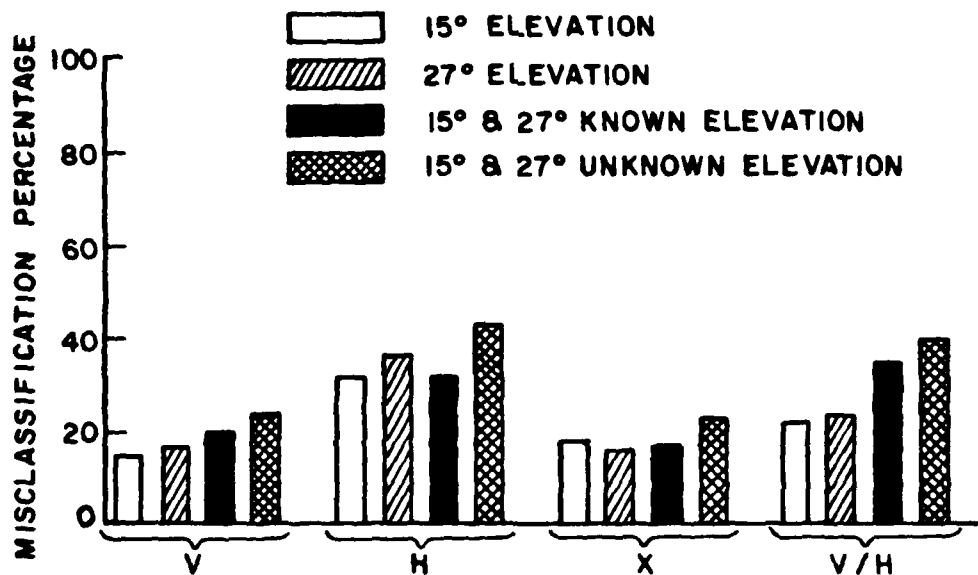


Figure 6.18. Average misclassification percentages at 10 dB post-processing SNR for various elevation angles as a function of polarization.

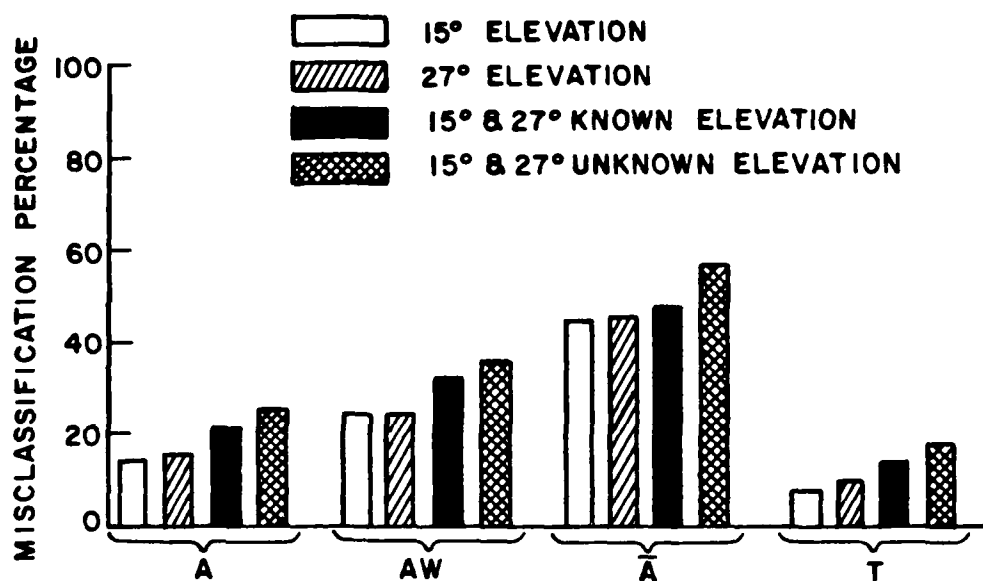


Figure 6.19. Average misclassification percentages at 10 dB post-processing SNR for various elevation angles as a function of algorithm.

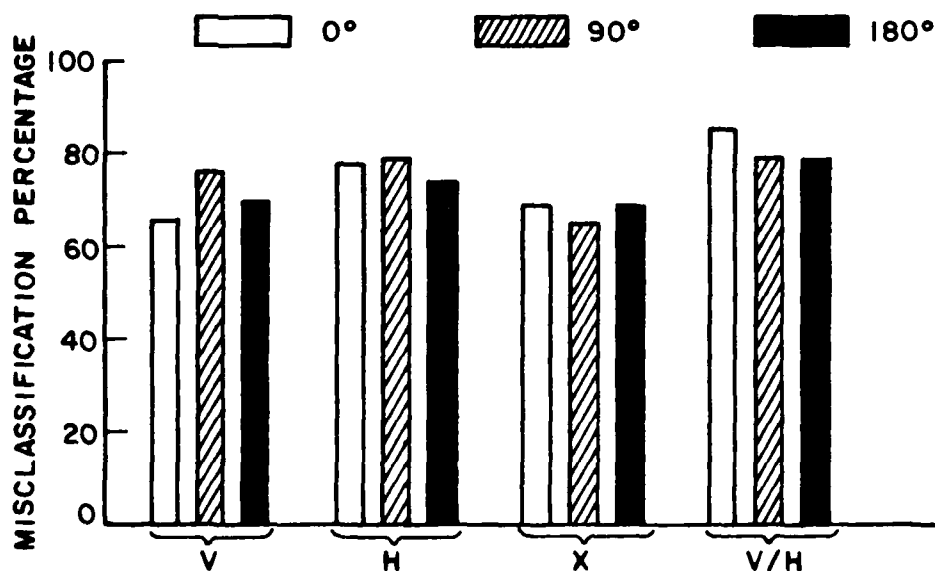


Figure 6.20. Average misclassification percentages at 10 dB post-processing SNR for an elevation error of $\pm 12^\circ$ as a function of aspect zone and polarization.

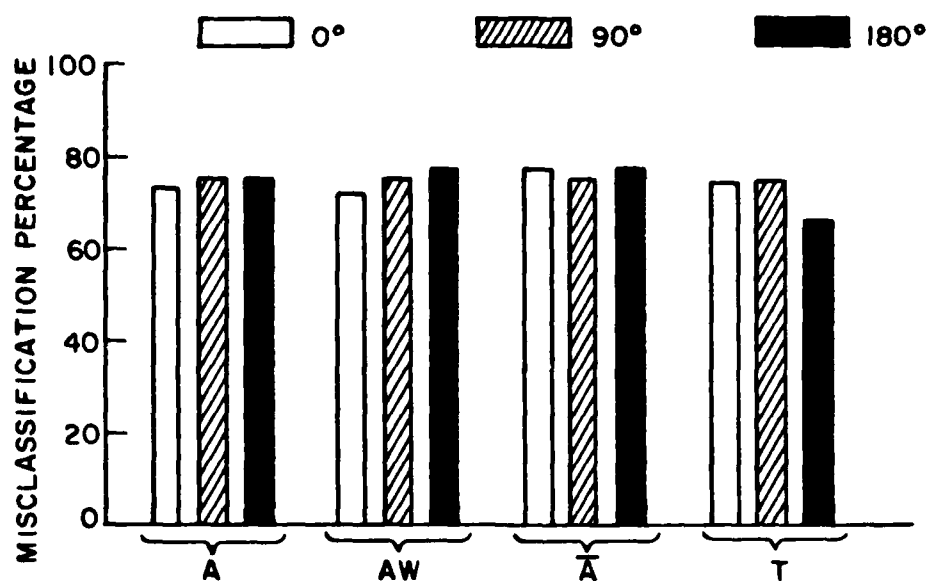


Figure 6.21. Average misclassification percentages at 10 dB post-processing SNR for an elevation error of $\pm 12^\circ$ as a function of aspect zone and algorithm.

except X polarization (where 27° is preferred), and it agrees with the results of the previous section where 0° elevation was found to have, on average, 3% less misclassification percentage as compared to 27° elevation. The difference in angle between 15° and 27° is clearly not large enough to provide a distinct change in classification performance.

Figures 6.17 to 6.19 also show the difference in misclassification percentage between known and unknown elevation angles when a data set comprising 2 elevation angles is used. Examining the known elevation results reveals an average classification error of 27%, which is 4% higher than the average of 15° and 27° elevations (23%) taken alone. Intuitively these would be expected to be the same since

algorithmically, known elevation (or aspect) simply compiles errors averaged over the known elevations (or aspects). The difference in performance is particularly distinct for the case of AW using V/H polarization at broadside (see Figure A.40), and this is a clue as to the cause of this discrepancy. The average of separate classifications at 15° and 27° elevation gives 15% classification error, while 15° and 27° known elevation gives 44% misclassification. Examining the average signal powers for each 'noise-free' data base yields 38 dB for 15°, 21 dB for 27° and 35 dB for 15° and 27° elevation (known). The average of 38 dB and 21 dB is

$$10 \text{ LOG}_{10} \left[\frac{10^{38/10} + 10^{21/10}}{2} \right] = 35 \text{ dB.}$$

Consider the case of 15° and 27° elevation (known). If a SNR of 10 dB is required, then 25 dBm² of noise power must be added to the data base amplitude (and phase) returns. However, this leads to 13 dB SNR for the 15° part of the data base, and -4 dB SNR for the 27° part of the data base. Consequently the 15° and 27° known elevation case is an average of a slightly better classification using 15° elevation data, and a very much poorer classification using 27° elevation data (at 10 dB SNR). In other words, the 15° and 27° known elevation result is only the average of the individual results when other parameters allow the average signal powers of the 'noise-free' data bases to be the same (X polarization is such a case).

This result follows directly from the discussion in Chapter 5.5 where two points were established. First, the classifications for classes having widely varying average signal powers have a constant injected noise power, but variable (post-processed) SNR for each class. Second, the separate classifications for the classes mentioned above will have constant (post-processed) SNR with corresponding different injected noise levels. Results due to Chen [1] and results established here can be used for meaningful comparisons if the above points are taken into consideration.

It is evident from Figures 6.17 to 6.19 that a priori knowledge of elevation angle results in 5% fewer in classification errors. This result is independent of aspect zone but does vary with polarization and algorithm. Specifically, H polarization, and relative amplitude \bar{A} , (not necessarily together) produce significant increases in misclassification percentage for an unknown elevation angle, where there is a 10% difference between the results for known and unknown elevation angle. These parameters are, in general, less favourable toward low misclassification and thus, classification without a priori knowledge of the elevation angle is particularly sensitive to 'adverse' parameters.

The high values of misclassification percentage when an error is made in elevation angle (see Figures 6.20 and 6.21) are due in part to the varying SNR problem mentioned earlier. However, note that for X polarization, where signal powers for 27° elevation and 15° elevation are equal (see Table B.1) and the special consideration does not apply, that classification error is still about 66%. Hence it must be

concluded that the majority of the classification errors introduced with an elevation ambiguity of $\pm 12^\circ$ stem from the dissimilarity of targets at 15° and 27° elevations. This might seem contrary to previous findings where classification performance at 15° was found to be very similar to classification performance at 27° . It must be noted that similarity in classification performance between two given parameters is not directly related to the similarity of the targets associated with those parameters.

Classification error, as a result of an elevation angle error of $\pm 12^\circ$, is about 74% on average. This result is independent of aspect zone and algorithm. Hence erroneous a priori elevation information has a catastrophic impact on classification; in such an event it would be better to discard the elevation angle information and assume that elevation were unknown, assuming there was no other recourse: (see the suggestions for future work in Chapter VII).

6.5 POLARIZATION

6.5.1 INTRODUCTION

The purpose of this experiment was to determine the relative classification performance of each polarization; vertical, horizontal, cross and vertical divided by horizontal, as a function of aspect zone and algorithm. An elevation of 27° was used in this experiment.

Corrupting features particular to the ionosphere, such as Faraday rotation, were not simulated here. Also, the fact that cross

polarization may not be practical in conjunction with ionospheric propagation did not preclude its investigation.

It is worth amplifying the purpose of using V/H polarization. Returns for this 'polarization' are produced by simply dividing the vertically polarized complex returns (A_V , θ_V) by the corresponding horizontally polarized complex returns (A_H , θ_H), i.e.,

$$A_{V/H}^i = A_V^i - A_H^i \quad \text{dBm}^2 \quad (6.1)$$

$$\theta_{V/H}^i = \theta_V^i - \theta_H^i \quad (6.2)$$

where i is the frequency index.

In general, a target scatters components of vertically and horizontally polarized electromagnetic energy when illuminated by radiation of a given polarization (vertical or horizontal). Since these components have the same frequency (and doppler shift), and are scattered simultaneously, they take the same ionospheric path and are hence subject to the same ionospheric distortion. This distortion can be approximately modeled as a complex multiplicative factor. If \tilde{A}_V^i and \tilde{A}_H^i are the complex target returns at a given frequency, and $Ce^{j\phi}$ is the appropriate ionospheric distortion factor, then the recieved returns are given by

$$\tilde{A}_{V,r}^i = \tilde{A}_V^i \cdot Ce^{j\phi} \quad (6.3)$$

$$\tilde{A}_{H,r}^i = \tilde{A}_H^i \cdot Ce^{j\phi} \quad (6.4)$$

Hence,

$$\begin{aligned}\tilde{A}_{V/H}^i &= \tilde{A}_{V,r}^i / \tilde{A}_{H,r}^i \\ &= \tilde{A}_V^i / \tilde{A}_H^i .\end{aligned}\tag{6.5}$$

and the multiplicative factor is removed. However, since multiplicative corruption was not simulated in this experiment, this hypothesis was not tested. Furthermore, this simple analysis might not adequately describe the corrupting nature of the ionospheric channel, although intuitively at least, one would expect some reduction in multiplicative factors by this type of operation.

6.5.2 RESULTS AND CONCLUSIONS

Figure 6.22 shows a typical result of classification performance using various polarizations the remainder of which are contained in Appendix A. Figures 6.23 and 6.24 summarize the classification performances at 10 dB post-processing SNR in terms of averages for a given parameter. On average, V polarization and X polarization rank first (with about 20% misclassification error), followed by V/H polarization (29%) then H polarization (44%). At 0° and 180°, V polarization and X polarization give similar performance, however at 90°, X polarization has 10% fewer classification errors compared with V polarization. V polarization and X polarization also give similar performances for all algorithms except \bar{A} (relative amplitude). It is significant that performance differs only when the parameters in question are particularly adverse toward classification (i.e.,

CLASSIFICATION OF SHIPS

POLARIZATION	V	H	X	V/H
ELEV ASSUMED	KNOWN			
ELEVATION (DEG.)	27			
ASPECT ASSUMED	KNOWN			
MIN,MAX,INC ASPECT	0	10	10	
NO OF FREQUENCIES	8			
NO OF TARGETS	12	12	12	12
90% CI (±30%) +/-	3.1%	3.1%	3.1%	3.1%
CLASS. FEATURES	A	A	A	A

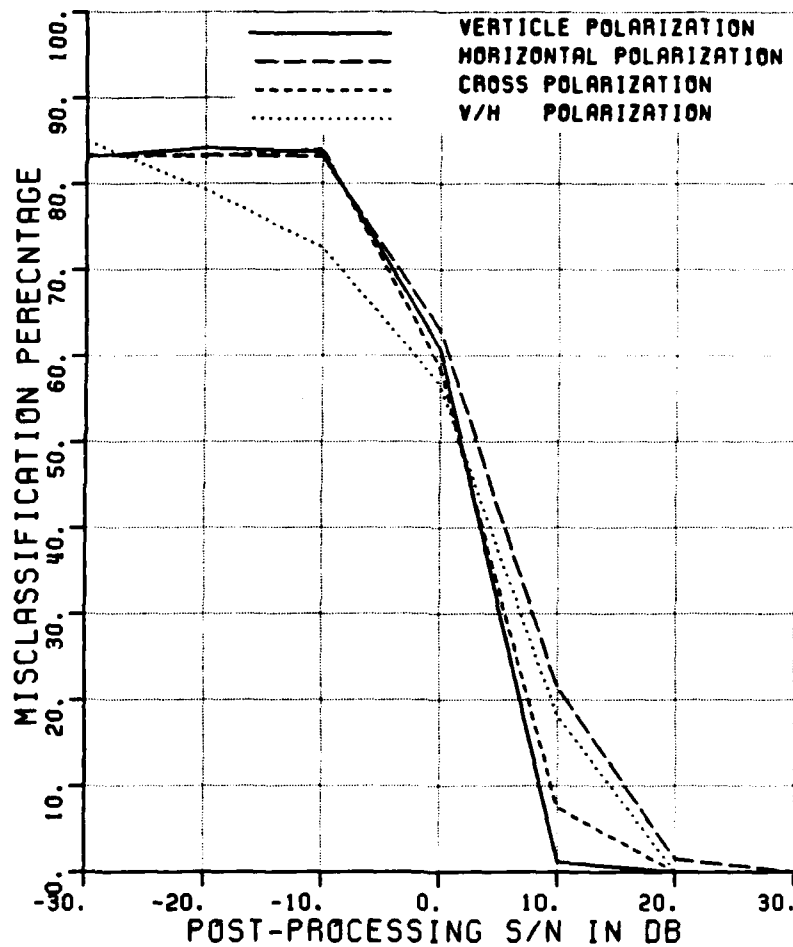


Figure 6.22. Misclassification percentage versus post-processing SNR for various polarizations.

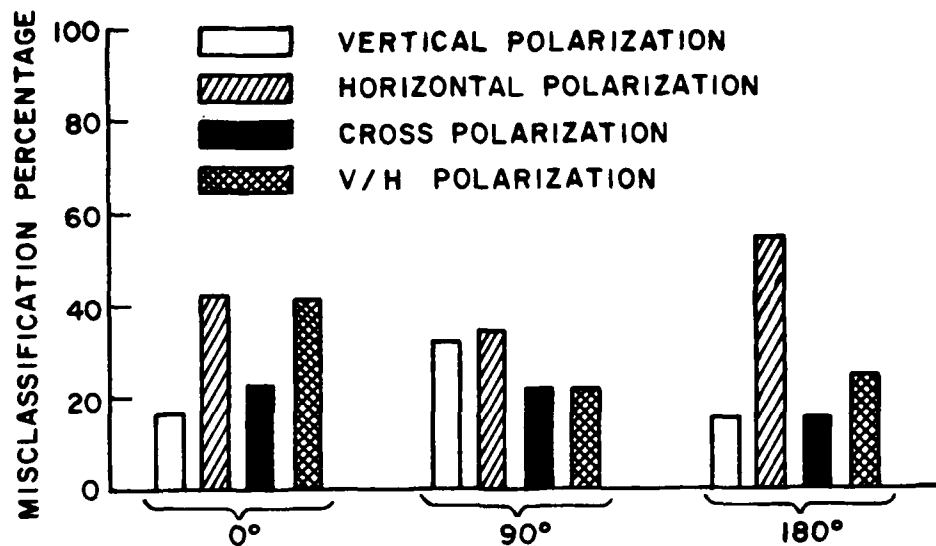


Figure 6.23. Average misclassification percentage at 10 dB post-processing SNR for various polarizations as a function of aspect zone.

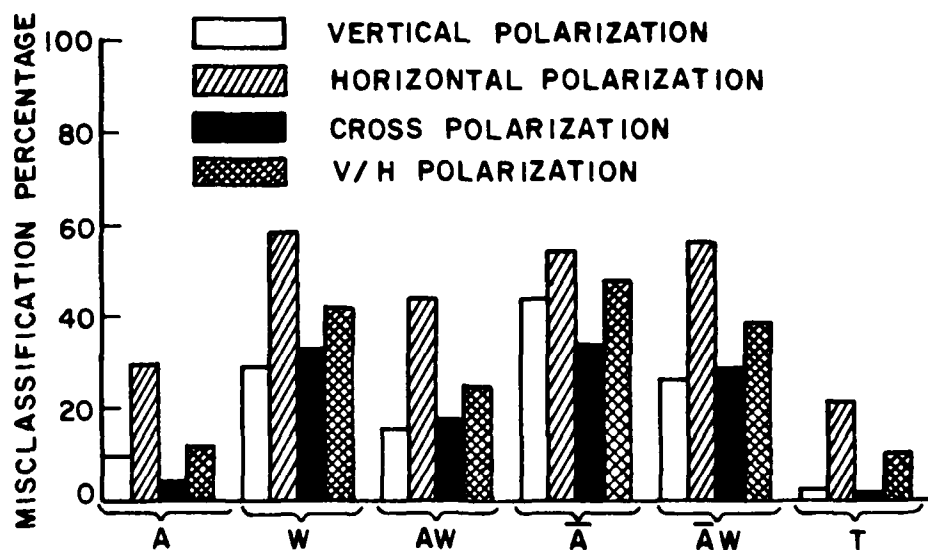


Figure 6.24. Average misclassification percentage at 10 dB post-processing SNR for various polarizations as a function of algorithm.

90° aspect zone or \bar{A}). This similarity in performance between V and X polarizations might stem from a combination of weaker scattering from the tilted vertical structures in the first case, and enhanced scattering from the tilted structures in the second case. Following this line of reasoning, V polarization might be expected to have better classification performance than X polarization, at zero degrees elevation angle.

H polarization consistently exhibits the poorest classification performance and this is particularly true at 0° and 180° aspect zones where H polarization is 20% and 30% worse than the V polarization results. This tends to reinforce the idea that, for bow and stern aspects, the major scatters are vertical and that these play a significant role in the classification process. H polarization exhibits its best performance at 90° aspect, where it has a similar misclassification percentage to V polarization (32%). At broadside, the ship's hull is a long horizontal structure, which is a good scatterer of horizontally polarized energy; at stern and bow aspects, there are few horizontal structures which may account for H polarization's preference for the 90° aspect zone. Data in Table B.1 in Appendix B support this conclusion. Radar cross sections for H polarization average to about 27 dBm², whilst those for V polarization average 20 dB higher. At 90° for H polarization, radar cross section is about 29 dBm², and for bow and stern, radar cross section is about 26 dBm².

X polarization has the best all-round performance. Although on average X and V polarization has the same 20% classification error, V

polarization is particularly affected at 90° aspect zone, having an error of 30%, whereas X polarization stays at the average.

V/H polarization on average has a misclassification error of about 30% which is roughly half way between that of V polarization and H polarization (which intuitively would seem reasonable). However, when dealing with data from a real system, we may be able to estimate V/H amplitudes more accurately than V amplitudes, assuming that it is possible to measure both the horizontally and vertically polarized components of the scattered energy. The discussion in 6.5.1 showed that multiplicative errors, which are characteristic of the ionosphere, cancel (see Equations (6.1) to (6.5)) when using the V/H parameter. This same division may also eliminate the need to use a reference, (since it would also cancel out). Hence the use of V/H polarization, as opposed to say V polarization, according to this analysis, removes two of the major sources of error in our process, i.e., the ionosphere and the referencing system. This is, potentially, a very valuable feature and the extent to which these errors are removed or reduced is a potential subject of further research.

The discussion thus far has concentrated much on the relative performance of polarizations with respect to each other. It is not the intention here to find an optimal polarization and then build a system using it; the same is true of any of the other parameters of classification. Indeed, limitations in a real sky-wave radar system might require the use of a particular polarization, so it is desirable to know the associated classification performance resulting from such a restriction.

6.6 ASPECT ZONE

6.6.1 INTRODUCTION

This experiment was designed to investigate how classification is affected by a particular aspect zone. From the above experiments, it is evident that classification performance is very dependent on the azimuthal orientation of the ship (i.e., aspect angle). Furthermore, from the discussion in 6.4.2, it might not be meaningful to do classifications where the catalog contains data pertaining to ships at widely varying aspect angles (for example 0° and 90°). Hence, a thorough investigation of classification performance at given aspect angles is of interest.

An elevation angle of 27° was used, and classifications at the 3 aspect zones, bow, stern and broadside, were done for each polarization and algorithm. A 45° aspect zone, comprising angles 30° , 45° and 60° was also included for the case of vertical polarization.

Based on the work of previous experiments, it was expected that 0° and 180° aspect zones would have similar classification performance, and 90° aspect zone would be worse.

6.6.2 RESULTS AND CONCLUSIONS

Figures 6.25 and 6.26 show typical curves of misclassification percentage versus post-processing SNR, the remainder of which are contained in Appendix A. Figures 6.27 and 6.28 summarize the results of

this experiment in terms of the average error at 10 dB post-processing SNR, for various polarizations and algorithms.

The initial expectation that classification performance at 0° aspect zone would be similar to that at 180° is true in general; the average classification error at 0° is 31%, and 29% for 180° (averaged across all polarizations, or algorithms). However, in the particular case, the above is only true for vertical polarization, the amplitude-only (A) feature, or the time domain algorithm. These 3 classification variables are generally the most favourable towards achieving low misclassification percentage, and 0° aspect behaves like 180° only under these conditions.

90° aspect zone exhibits best classification performance, for H polarization and V/H polarization. This is complimentary to the finding of the previous section where the above polarizations had best performance at 90° aspect zone. This does not mean, however, that it is more advantageous to use H polarization if the target is known to be at broadside; from Figure 6.27, we see that either X or V/H polarization are the most advantageous.

For V/H and H polarizations, 90° aspect zone has 14% fewer classification errors on average, compared with bow and stem aspects. For V and X polarizations, 180° and 0° aspect zones are better than broadside by an average of about 9%. Hence when averages are compiled across polarizations to produce the figures used in Figure 6.28, the difference in performance between the two pairs of polarizations

CLASS.	FEATURES	A	A	A	A
--------	----------	---	---	---	---

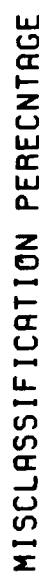


Figure 6.25. Misclassification percentage versus post-processing SNR for various aspect zones using vertical polarization.

CLASSIFICATION OF SHIPS
 POLARIZATION V/H
 ELEV ASSUMED KNOWN
 ELEVATION (DEG.) 27
 ASPECT ASSUMED KNOWN / KNOWN
 MIN,MAX,INC ASPECT 0 10 10, 80 100 10, 170 180 10
 NO OF FREQUENCIES 8
 NO OF TARGETS 12 18 12
 90% CI (±30%) +/- 3.1% 2.5% 3.1%
 CLASS. FEATURES A A A

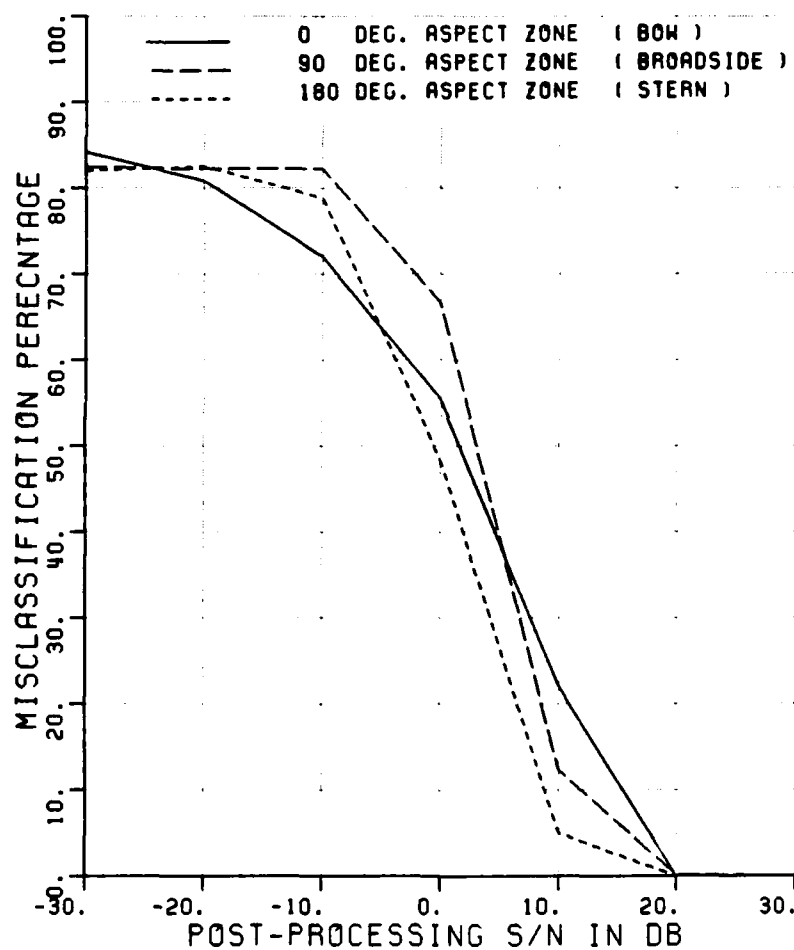


Figure 6.26. Misclassification percentage versus post-processing SNR for various aspect zones using V/H polarization.

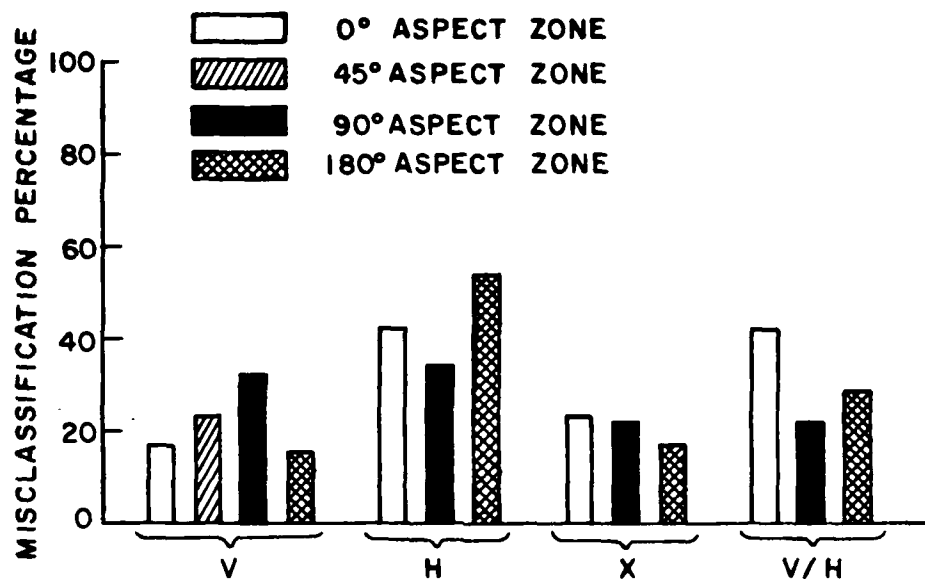


Figure 6.27. Average misclassification percentage at 10 dB post-processing SNR for various aspect zones, as a function of polarization.

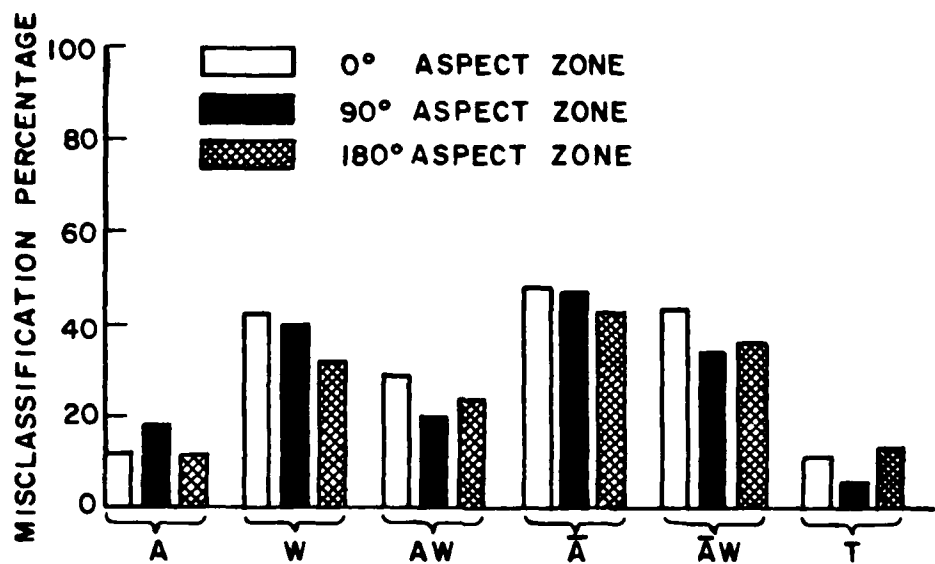


Figure 6.28. Average misclassification percentage at 10 dB post-processing SNR for various aspect zones, as a function of algorithm.

(i.e., V and X, compared to H and V/H) tends to enhance the performance 90° aspect zone. (See, for example, the time domain algorithm averages in Figure 6.28.) Consequently, when examining the performance of specific algorithms at various aspect zones, one should bear in mind the particular polarization used.

6.7 ERROR IN ASPECT

6.7.1 INTRODUCTION

The heading of a ship, and hence its aspect can be found quite accurately by simply plotting its position at two instances of time. Knowing the time interval and range between the reference positions allows the average velocity to be calculated, and this in conjunction with the doppler shifts at the two positions allows the aspect measurement to be refined.

An error in the aspect can be introduced when the heading of a ship is altered by a sea current. Figure 6.29 shows how this may happen. A ship traveling from P_1 to P_2 with velocity V_s is estimated to have an apparent aspect of θ_a . However, the component of sea current V_c forces the ship to take an aspect of $\theta_a + \theta_e$ in order to travel in the direction P_1 to P_2 .

$$\theta_e = \tan^{-1} \frac{V_c}{V_s} .$$

Typical values for V_c and V_s might be 5 and 20 knots, respectively, which leads to an error of $\theta_e = 14^\circ$.

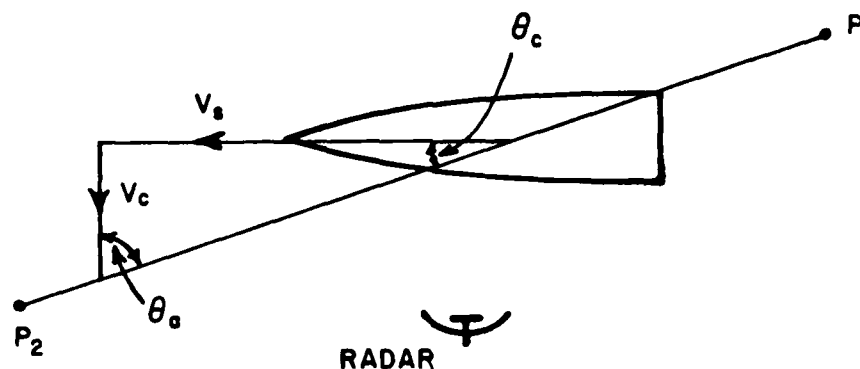


Figure 6.29. A ship travelling with velocity V_s from point P_1 to point P_2 has an apparent aspect angle of θ_a degrees owing to the sea current having a velocity V_c .

The purpose of this experiment was to examine classification performance as a function of various parameters when an aspect error is introduced. In general, for a given aspect, a $\pm\theta_e$ aspect error must be considered. For 0° aspect zone, using 0° and 10° aspects, a $\pm 10^\circ$ error was simulated by comparing 0° noise-contaminated ship returns with 10° catalog ship returns and vice versa. At broadside, where 3 aspects were used (80° , 90° and 100°), a $\pm 10^\circ$ aspect error was simulated by comparing 80° and 100° aspect noise-contaminated targets with a 90° catalog, and 90° aspect noise-contaminated targets with 80° and 100° catalogs. This represents performing an additional experiment for each ship and this

must be taken into consideration when calculating the average misclassification percentage for a given SNR.

This experiment was divided into 2 parts: the first to examine the effect of different aspect errors near to 0° aspect angle, and the second to examine the effect of 10° aspect errors at different aspect zones. Curves representing classification performance at 0° and 15° using unknown aspect for each of the parameters used in the above experiments, were derived in order to establish a threshold at which it would be wiser to stop estimating an aspect angle. An elevation angle of 27° was used in all experiments.

6.7.2 RESULTS AND CONCLUSIONS

Figures 6.30 to 6.32 show typical classification results for these experiments, the remainder of which are contained in Appendix A. Figures 6.33 and 6.34 show average misclassification percentages at 10 dB post-processing SNR for various errors in aspect near to 0° aspect. It is clear that performance is dependent on the particular polarization used. For V and H polarizations, a $\pm 10^\circ$ error is roughly equivalent to saying that the aspect is unknown. Hence for aspect angles near to 0° which can only be estimated with an accuracy of less than $\pm 10^\circ$, it would be better to re-evaluate the use of a priori aspect angle information. For X and V/H polarizations an error of $\pm 10^\circ$ aspect leads to a large increase in misclassification percentage (to about 60%) compared with 15% for V polarization. Based on the increase in misclassification

CLASSIFICATION OF SHIPS									
POLARIZATION	V								
ELEV ASSUMED	KNOWN								
ELEVATION (DEG.)	27								
ASPECT ASSUMED	KNOWN			/		KNOWN			
MIN,MAX,INC ASPECT	0	10	10,	0	15	15,	0	30	30
NO OF FREQUENCIES	8								
NO OF TARGETS	12	12			12				
90% CI (±30%) +/-	3.1%	3.1%			3.1%				
CLASS. FEATURES	A	A	A						
ASP ERR IN CURVE	2	3							

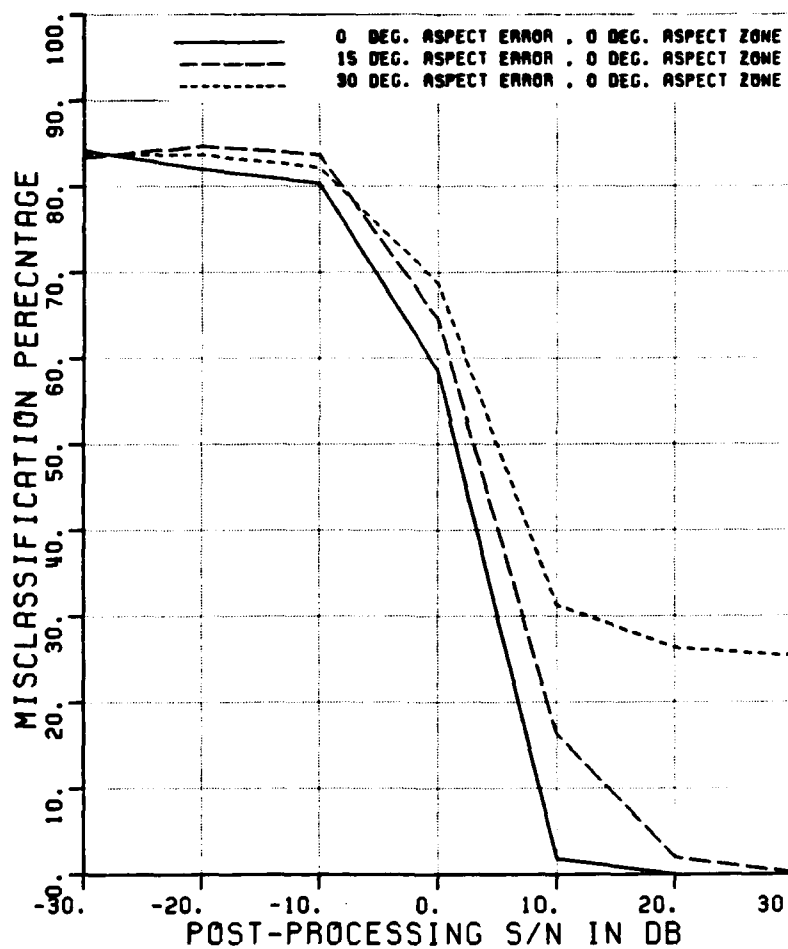


Figure 6.30. Misclassification percentage versus post-processing SNR for various aspect errors, near to 0° aspect, using vertical polarization.

CLASSIFICATION OF SHIPS									
POLARIZATION	X								
ELEV ASSUMED	KNOWN								
ELEVATION (DEG.)	27								
ASPECT ASSUMED	KNOWN / KNOWN								
MIN,MAX,INC ASPECT	0	10	10,	0	15	15,	0	30	30
NO OF FREQUENCIES	8								
NO OF TARGETS	12		12		12				
90% CI (@30%) +/-	3.1%		3.1%		3.1%				
CLASS. FEATURES	A	A	A						
ASP ERR IN CURVE	2		3						

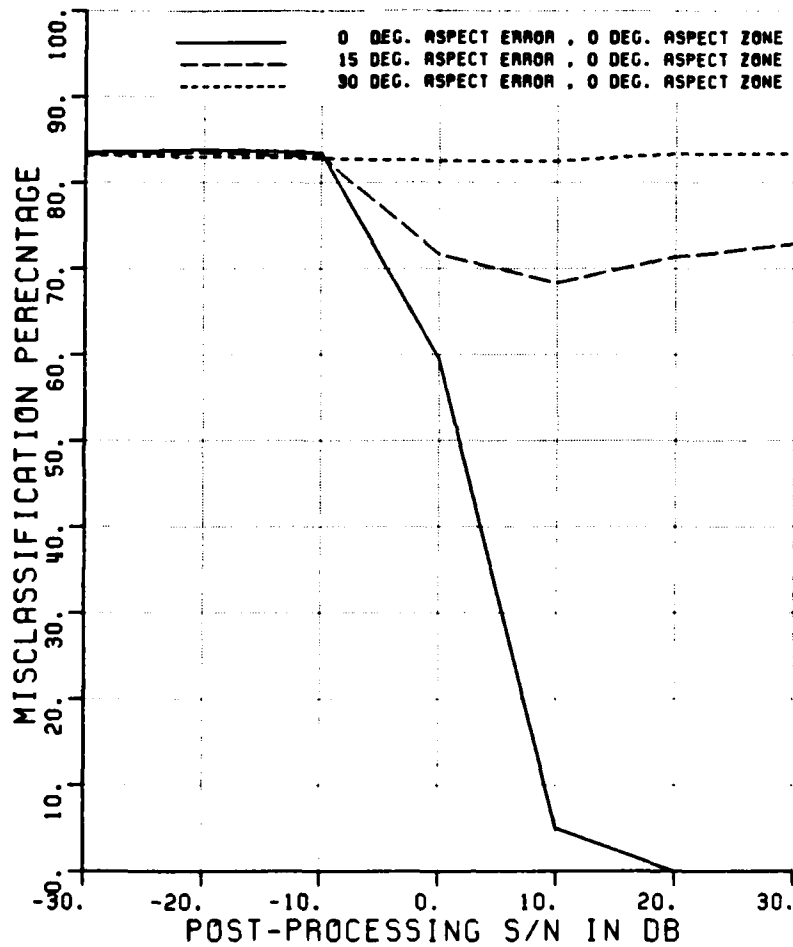


Figure 6.31. Misclassification percentage versus post-processing SNR for various aspect errors, near to 0° aspect, using cross polarization.

POLARIZATION	V
ELEV ASSUMED	KNOWN
ELEVATION (DEG.)	27

ASPECT ASSUMED	KNOWN			/	KNOWN									
MIN,MAX,INC ASPECT	0	10	10,		0	10	10,	80	100	10,	170	180	10	
NO OF FREQUENCIES	8													
NO OF TARGETS	12				18			12						
90% CI (±30%) +/-	3.1%				2.5%			3.1%						
CLASS. FEATURES	A				A									
ASP ERR IN CURVE	2				4									

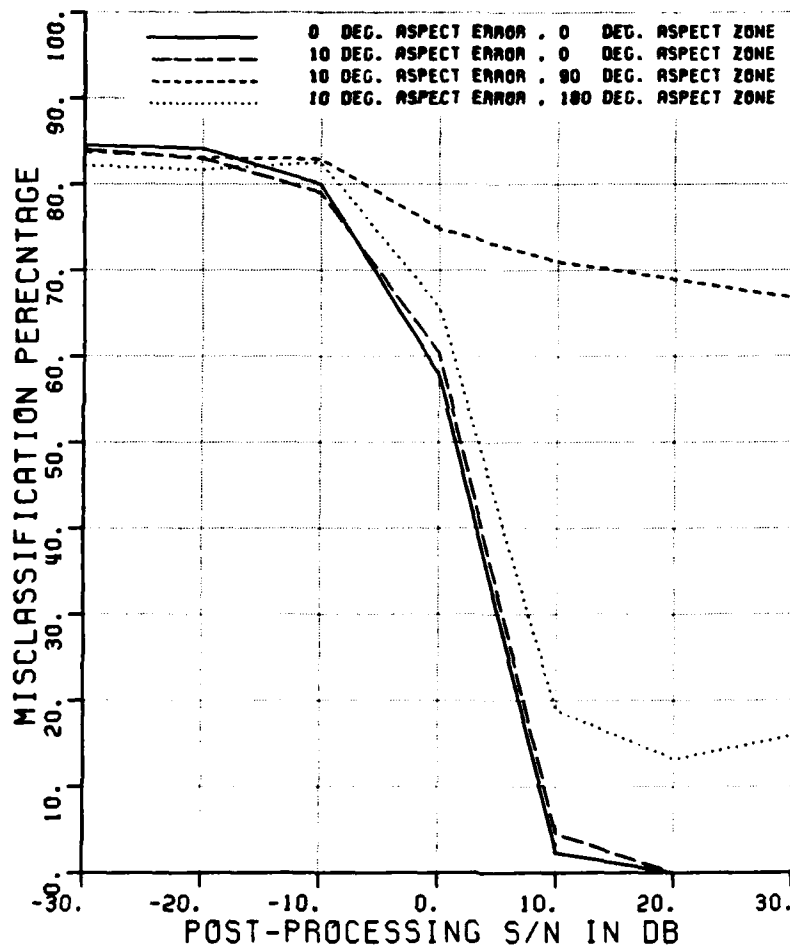


Figure 6.32. Misclassification percentage versus post-processing SNR for an aspect error of $\pm 10^\circ$ at various aspect zones.

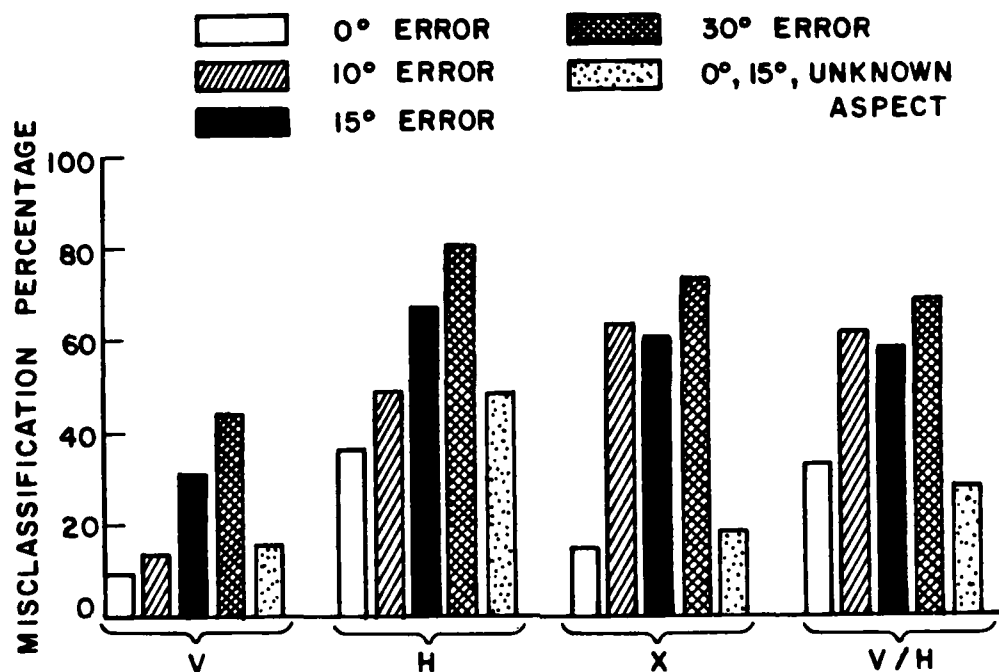


Figure 6.33. Average misclassification percentage at 10 dB post-processing SNR for various aspect errors, near to 0° aspect, as a function of polarization.

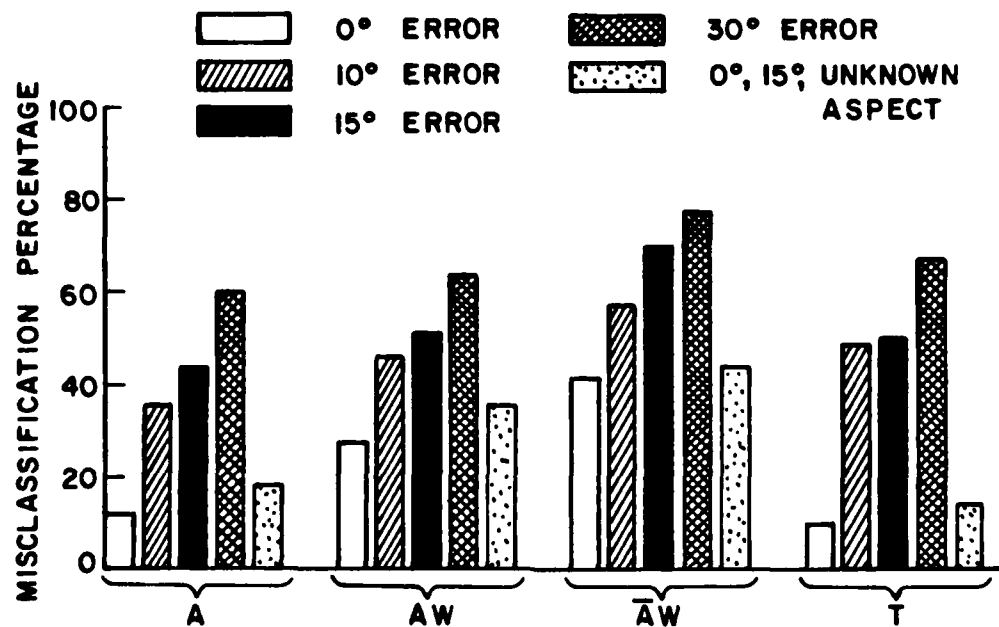


Figure 6.34. Average misclassification percentage at 10 dB post-processing SNR for various aspect errors, near to 0° aspect, as a function of algorithm.

percentage (shown in brackets) when an aspect error of $\pm 10^\circ$ is introduced, the polarizations acquire the following ranking

$$V(4\%) < H(13\%) < V/H(28\%) < X(48\%) \quad .$$

It is evident that X polarization, which was previously established as having good classification properties, is particularly susceptible to an error in aspect angle. Furthermore, V polarization is the only polarization with 30% or less misclassification for errors of $\pm 10^\circ$ or less.

Establishing a ranking of algorithms based on the increase in misclassification percentage when an error of $\pm 10^\circ$ is introduced yields

$$\bar{A}W(16\%) < AW(18\%) < A(24\%) < T(39\%) \quad .$$

This is the exact reverse order that these algorithms appear if there is no error in aspect. The time domain algorithm is more affected by an aspect error than the other algorithms. At 0° error, T has about 10% classification error on average, which is the same as A. However, at $\pm 10^\circ$ error T has about 50% error compared with 35% for A. In conclusion, for the aspect zone of 0° (bow), the parameters X polarization and the time domain algorithm, which previously had good records of classification performance, are particularly sensitive to errors in aspect angle.

Figures 6.35 and 6.36 show how a $\pm 10^\circ$ aspect error affects classification percentage at different aspect zones. Note that the histogram bars represent the difference between the results of classification at 0° error and classification at $\pm 10^\circ$ error. For X

polarization it has already been mentioned that classification performance is significantly degraded (by 45% on average) by the introduction of a $\pm 10^\circ$ error at 0° aspect zone. This is also true of X polarization for 90° and 180° aspect zones.

For the remaining polarizations it is also evident that 180° is more affected by an error of $\pm 10^\circ$ aspect error than is 0° aspect zone, and performance is poor (always above 50% classification error) irrespective of the polarization. V/H and H polarization have poor performance at all aspect zones when a $\pm 10^\circ$ aspect error is introduced; typically misclassification percentage is always above 50%.

Generally, the time domain algorithm is most affected by an aspect error of $\pm 10^\circ$, especially at 90° aspect zone. Based on the results, the choice of algorithms to provide lowest misclassification percentage at 0° , 90° and 180° aspect zones would be

	ASPECT ZONE		
	0°	90°	180°
ERROR			
0°	T	T	T
$\pm 10^\circ$	A	AW	T

Chen [1] also did an analysis of the affect of aspect errors. Using sets of ship data at 0° , 15° and 30° aspects (vertically polarized) he compared the no-noise distances and correlation coefficients for various ships and found that about 4 times out of 5, the closest neighbour to a particular ship was the same ship at a

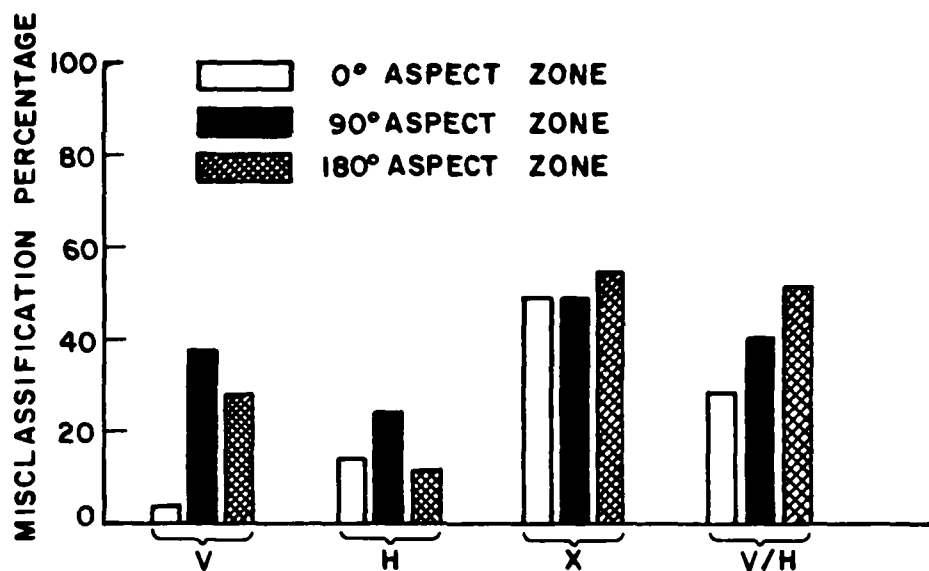


Figure 6.35. Average difference in misclassification percentage at 10 dB post-processing SNR between classifications having a 0° aspect error and classifications having a $\pm 10^\circ$ aspect error, at various aspect zones, as a function of polarization.

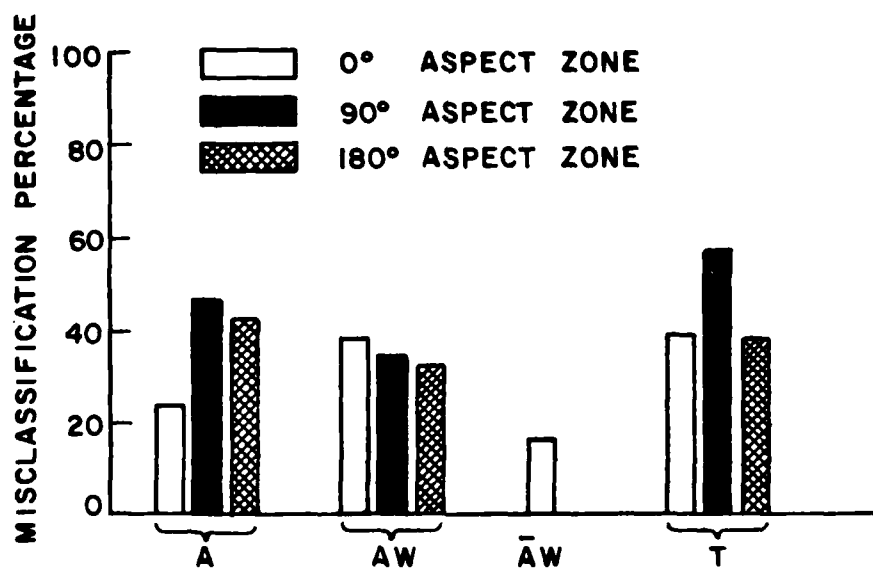


Figure 6.36. Average difference in misclassification percentage at 10 dB post-processing SNR between classifications having a 0° aspect error and classifications having a $\pm 10^\circ$ aspect error, at various aspect zones, as a function of algorithm.

different aspect angle, indicating a certain toleration towards errors in aspect angle. Results here would tend to confirm Chen's findings for the particular case of vertical polarization and 0° aspect zone (see Figure 6.33). However, for other polarizations and aspect zones, classification was found to be significantly degraded by the inclusion of an aspect error of $\pm 10^\circ$. Also, the inclusion of added noise in this analysis revealed a hitherto indistinguishable sensitivity in the particular algorithm (especially in the time domain algorithm) to errors in aspect angle.

CHAPTER VII

CONCLUSIONS

A series of experiments investigating the classification properties of a group of ships at various azimuthal and elevation angles, using a variety of polarizations, have been performed. These experiments, to a certain extent, were intended to represent classification based on HF sky-wave resonance radar returns.

The characteristics and specifications of an HF sky-wave radar system were discussed. These include the considerably longer range (compared with ground-wave propagation) afforded by sky-wave propagation, which is attained at the cost of contamination and dispersion by the ionosphere. These and other factors tend to severely restrict the range of operating frequencies available for classification purposes. The methods of measuring amplitude and phase returns and the use of a reference, such as sea-scatter, for calibration of the radar cross section amplitudes have been discussed. A technique using the ratio of the returns at vertical and horizontal polarizations has been suggested as a means of obviating the need to calibrate with a separate reference.

The construction of a data base, using radar backscatter measurements from scaled-model ships, has been described. The use of a groundplane to simulate the surface of the sea resulted in residual time responses corresponding to the location of the groundplane edges in the target's impulse response. Impulse responses were used to check the validity of calibrations. The calibration process was found to be both time consuming and intricate, but necessarily so in order to provide representative data. The calibration and scaling procedures converted measured ship amplitude and phase returns from 2 to 18 GHz into scaled amplitude and phase returns from 2 to 7 MHz.

Various sources of noise and errors have been discussed. Noise in the context of our classification experiments was defined as post-processing noise; the errors remaining after the processing system had done its best to minimize the various contaminations. A need was expressed to incorporate into the noise analysis a sufficiently detailed representation of the ionospheric channel and its associated distortions. No such model was available and in view of this and under other considerations, an independent additive Gaussian noise model was used.

In view of the limitations placed on available operating frequencies, the 2 to 7 MHz band was divided into 3 equal sub-bands of 4 frequencies to investigate the classification properties of each band. In general, the lower band (as expected) gave the lowest probabilities of misclassification, but in particular, the result depended on the parameter of interest. Vertical and cross polarizations each showed a

marked difference of about 16% in misclassification percentage between the lower and middle bands, whereas horizontal and V/H polarization had an average difference of about 3%. The difference in performance between band 1 and band 3 was not great (always less than 20%), hence if conditions dictated the use of higher frequencies in the 2-7 MHz band, then classification performance does not suffer badly.

The next set of experiments served as a comparison to previous work done by Chen [1]. In general the results using 27° elevation data, were similar to those of Chen's 0° elevation data. Increasing the number of frequencies was found to reduce misclassification percentage, but only to a limit. For example the use of 12 frequencies, compared to 8 frequencies, yielded a 1% improvement on average. The same ranking of algorithms established in [1] was also established here. For 2 frequencies this was, in terms of lowest misclassification percentage, $AW < A < W < T$ and for 8 frequencies, $T < A < AW < W$. Generally the addition of phase information (for example AW , or \bar{AW}) was found to be more significant in terms of improved classification performance, for a lower number of frequencies.

A priori knowledge of aspect angles provided a 6% decrease in misclassification percentage (compared to assuming the aspect angle as unknown), which was similar to Chen's finding. In general, there was a small but accountable improvement of about 3% less misclassification for the 0° data compared to the 27° data.

The investigation performed on classifications at elevation angles of 27° and 15°, revealed that there was a high degree of similarity

between the results for the two angles. A 1.7% reduction in classification error was established for the 15° elevation data over the 27° data; and this low value was representative of all polarizations, aspect zones and algorithms. When using a catalog containing data relating to two elevation angles, a 5% reduction in classification error resulted when the elevation angle was known a priori. This was comparable to the result for a priori knowledge of aspect angle. A $\pm 12^\circ$ error in elevation lead to a drastic degradation in classification performance; typically misclassification percentage was always worse than 65%, with some parameters, such as horizontal polarization being little better than random guessing (i.e., 5/6 or 88%), at 80% misclassification. No one polarization, aspect zone or algorithm showed any particular immunity to the effects of a $\pm 12^\circ$ error in elevation.

Vertical and cross polarizations were found to have similar classification properties, with about 20% classification error on average. V/H followed with 29%, and H polarization was consistently worst with 44% misclassification. These results were very much dependent on the particular aspect zone used, with vertical and cross polarizations doing best at 0° and 180° aspect zones, and horizontal and V/H polarizations doing best at 90° aspect zone.

V/H polarization was found to have a performance lying between that of vertical polarization and horizontal polarization. However, the V/H polarized amplitudes may, in practice, be measurable with a higher degree of accuracy than the vertically polarized amplitudes. This is because theoretically at least, multiplicative factors impressed by the

ionosphere should cancel out. Also the use of V/H polarization might preclude the need to use a reference. Unfortunately these sources of distortion could not be simulated here and so a real test of V/H polarization was not performed. However, it was established that the diversion of amplitudes in this manner does not drastically reduce their information content, otherwise the misclassification levels would have been much higher.

The analysis of classification performance at various aspect zones revealed a high degree of dependence on the particular aspect zone (0° , 90° or 180°). The initial expectation that 0° aspect zone would possess similar classification properties to 180° aspect zone was true only for vertical polarization, the amplitude only feature (A), or the time domain algorithm. These 3 classification variables generally were found to be the most favourable towards achieving low misclassification. The behaviour of 0° and 180° aspect zones for other parameters differed. 90° aspect zone favoured horizontal and V/H polarization. Its apparently good performance for certain features, such as AW in the nearest neighbour algorithm, was due to the relative performances of polarizations at certain aspect angles. As a result of this, the performance at a particular aspect zone needed to be judged with respect to a particular polarization, and averaging across polarizations tends to somewhat obscure the analysis.

Finally, the investigation of the effects of aspect errors revealed a particular sensitivity of some parameters to such errors. For example X polarization and the time domain algorithm both had a

misclassification percentage increase of more than 40% when a $\pm 10^\circ$ error was introduced. Vertical and horizontal polarizations had error levels of 13% and 49% respectively, which was equivalent to their performances when the aspect angle was assumed known. Generally, the levels of classification error, with the exception of vertical polarization, were quite high for a $\pm 10^\circ$ error, at all aspect zones; with misclassification levels of 50% and 60% being common.

The above results have illustrated how the classification of ships is dependent on the frequencies, polarizations aspect and elevation angles, and algorithms used in the classification process. Assuming that no errors have been made in estimating aspect and elevation angles, ship targets were correctly identified with a probability ranging approximately from 50% to 100%, depending on the prevailing conditions. Furthermore, the results presented here for the given catalog of ships are an 'upper-bound', for a variety of reasons. Firstly, in practice there would be a vast amount of a priori information, such as the knowledge of ship movements (perhaps from satellite photography), which could further reduce the catalog size. Estimation of the average amplitude returns for a ship, in conjunction with aspect and elevation angle information, could also allow further reduction of the catalog. In these experiments, a ship was considered misclassified even if the right ship was chosen at the wrong aspect or elevation angle; allowing such a decision to be considered as correct would also reduce the probability of making an incorrect decision. Finally, there is considerable potential for refining and optimizing the various algorithms for classification (some suggestions are discussed below).

Based on the experience gained whilst performing the various investigations of this report, it is suggested that future work be directed in the following areas.

The nearest neighbour technique for classifying targets involves calculating the distances at specific sample frequencies, between the test target and a particular catalog reference. The square root of the sum of distances over these frequencies is called 'the distance' between the unknown test target and the noise-free catalog member. This distance, compared with other such distances is used to make a classification decision. The following example is designed to demonstrate how the individual distances, for each frequency, contain useful information.

Consider 2 sets of arbitrary distances between an unknown target, (S_u), and 2 catalog targets, (S_1, S_2).

	$D_{u,1}$	$D_{u,2}$
f_1	3	8
f_2	2	8
f_3	4	10
f_4	72	10
Distance	9	6

On this basis, S_u would be classified as S_2 . Observe though that 3 out of the 4 frequencies suggest that S_u is S_1 and the fourth frequency

has biased the overall result sufficiently to change the classification. Such a syndrome is representative of impulsive noise, for example, lightning discharges which affect HF radar returns.

From the above demonstration, it is clear that the examination of distances for individual frequencies is necessary in order to deal with impulsive noise. A simple 'majority vote' system would be one way of implementing such a procedure. However, the majority vote system would involve extensive alterations to existing algorithms and software, and presents a problem in resolving ties.

One way around this problem would be to identify the 'rogue' distances on a statistical basis. For example, if a distance was more than, say, 1 standard deviation from the mean, then it could be set to some other value, perhaps the mean of the other distances. In the above example, the means are 20 and 9, and the standard deviations are 30 and 16 respectively. Hence all the frequencies of S_2 pass the test, but f_4 of S_1 has a distance which is 1.7 standard deviations above the mean. Consequently, it is set to 3, the average of the unaffected frequencies, resulting in a new total distance of 3.5. S_u is now closer to S_1 than S_2 .

Research is needed concerning the statistical distribution of individual target distances. The above test works with the arbitrary numbers presented, but may not do so with more practical figures. It would be undesirable to alter the distance of a particular target that is not subject to impulsive contamination.

From the previous discussion it is evident that information is contained in the actual values of NN distances (and correspondingly in time domain algorithm correlation coefficients). This information might further be exploited to reduce the sort of classification errors which are encountered when errors are made in the estimation of aspect and elevation angles. For example, if the heading of an unknown ship, S_u , is measurable to within $\pm 15^\circ$, then classification can proceed for each of 7 catalogs, C_1 to C_7 , one for the estimated aspect angle and the others at 5 degree increments above and below the estimate. From each catalog there would be a candidate classification, S_n , with a corresponding minimum distance (or maximum correlation coefficient), D_n , for $n = 1, 2, \dots, 7$. The choice of a particular candidate, for the case of the NN algorithm, would be based on these distances. Average distance in the NN algorithm is a function of post-processed SNR, hence if the latter could be estimated accurately, the candidate classification having a distance corresponding to the measured post-processing SNR (for a given angle) would be chosen.

Let $D_{n,\theta}(p)$ be the distance (generated by the NN algorithm) between the noise-free returns of a ship, n , at aspect angle θ , and the same returns contaminated by noise such that post-processing SNR was p dB. Assume for this example that p is 10 dB, and the aspect angle was estimated at 15° .

CATALOG	C ₁	C ₂	C ₃	C ₄	C ₅	C ₆	C ₇
ASPECT (θ)	0	5	10	15	20	25	30
S _n	S ₁	S ₂	S ₃	S ₄	S ₅	S ₆	S ₇
D _n	D ₁	D ₂	D ₃	D ₄	D ₅	D ₆	D ₇
D _{n,θ(10)}	D _{1,0}	D _{2,5}	D _{3,10}	D _{4,15}	D _{5,20}	D _{6,25}	D _{7,30}

Where

D_n = Distance between ships S_u and S_n

D_{n,θ(10)} = Distance between ships S_n and S_n^{*}

S_n^{*} is a noise-contaminated version of S_n.

The classification would proceed by choosing the smallest magnitude

$$| D_{n,\theta} - D_n | \quad \text{for } n = 1, 2, \dots, 7$$

$$\theta = 0, 5, \dots, 30.$$

Research is needed to examine the relationship between post-processing SNR and distance (or correlation coefficient), and how this varies with aspect and elevation angles and their increments.

Classification experiments thus far have produced misclassification percentages of between 0 to 50% for a nominal 6 ship catalog. In practice, even with a large amount of a priori information a working catalog size might be in the order of 100 ships or more. As a result, classification errors will be higher because of the greater chance that

the noise-contaminated returns of an unknown ship would look like the noise-free returns of a catalog ship.

Perhaps one way of addressing such a problem might be to investigate the classification properties of 'generic' ship targets. The term generic is used here to describe a set of amplitude and phase returns representative of a group of ships. Hence, a catalog would not contain the the returns of, say 30 destroyers, but rather the 'generic' returns of, say 3 representative destroyers.

The generic forms could be constructed from basic shapes representing what are thought to be the major scattering structures common to a group of targets. In a previous chapter, it was postulated that vertical structures, such as masts, play a significant part in classification using vertically polarized returns. The generic form could simulate, to varying degrees, such structures and this would help establish the extent to which the various features of a ship contribute to the characterisation of its amplitude and phase returns. In a sense, such experiments would investigate the 'resolution' of the classification system, i.e., the degree to which the system can distinguish between similar targets.

The use of the AW feature in the NN algorithm produces a hitherto unresolved effect. Referring to Figures A.14 and A.16, it is evident that for two frequencies the AW feature is always better than the A feature, whereas for 8 frequencies the A feature is better than the AW feature above 5 dB post-processing SNR. Intuitively, one would expect the AW feature to be better than the A feature because it appears to

contain more information about a target (having both amplitudes and phases).

This discrepancy is probably a consequence of Chen's assertion that the expression for normalizing constant, K (see Chapter IV Section 6.2) is not optimal. Since the relative performance of the A and AW features seems to be dependent on post-processing SNR, it is likely that a given amount of noise contaminates the A features and AW features to different extents.

Figure 7.1 shows the variation of noise-dependent normalizing constant K_n with post-processing SNR. Here the constant is determined from the variances of the noisy amplitudes and the noisy phases, rather than the noise-free ones. This figure shows that the amplitudes are much more affected by the addition of large amounts of noise than the differential phases, but only slightly more affected for small amounts of noise.

Compared with previous results, the use of this noise-dependent normalization constant results in a slight improvement in classification error of about 3 to 4% for the AW feature at post-processing SNRs of 10 to 20 dB. Further research might provide a substantially better implementation of the AW feature.

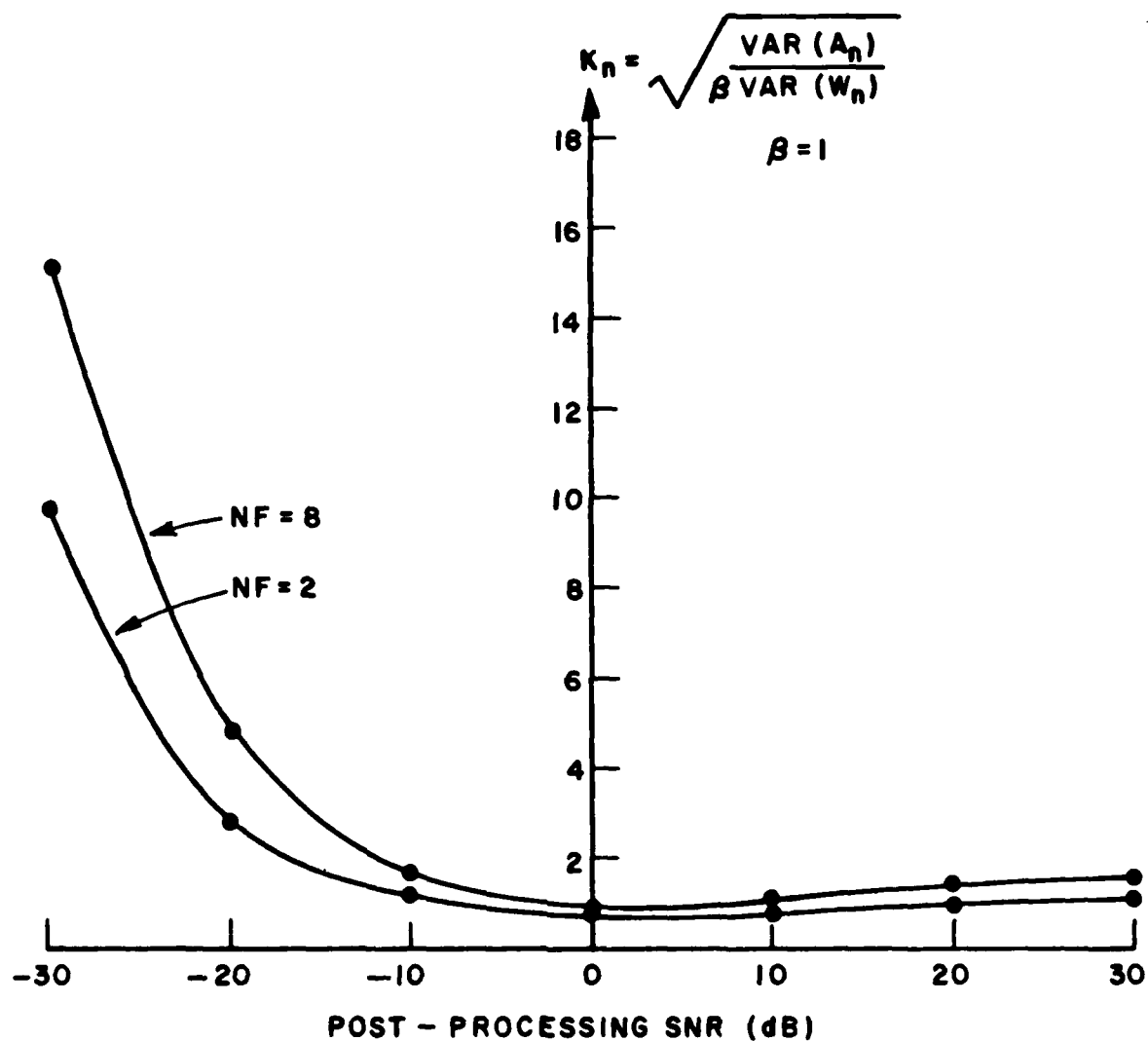


Figure 7.1. Variation of normalization constant, derived from the variances of the noise contaminated amplitudes (A_n) and differential phases (W_n), with post-processing SNR. The curves are representative of 2 and 8 frequencies using the AW feature in the NN algorithm, for ships at 0° , 90° and 180° aspect angles and 27° elevation angle.

REFERENCES

- [1] J. Chen, "Automatic Target Identification Using HF Multifrequency Radars," Ph.D. Dissertation, The Ohio State University, ElectroScience Laboratory, 1983.
- [2] D.F. Kimball, "Calibration Techniques For Broadband Radar Backscatter Measurements," M.S. Thesis, The Ohio State University, ElectroScience Laboratory, Autumn 1983.
- [3] E.M. Kennaugh and D.L. Moffatt, "Transient and Impulse Response Approximations," PROC. IEEE, Vol. 53, pp. 893-901, August 1965.
- [4] D.L. Moffatt, "Interpretation and Application of Transient and Impulse Response Approximations in Electromagnetic Scattering Problems," Report 2415-1, Dept. of Electrical Engineering, The Ohio State University, ElectroScience Laboratory, Columbus, Ohio, March 1968.
- [5] E.K. Walton and J.D. Young, "Surface Ship Target Classification Using HF Multifrequency Radar," Final Report 712352-1, The Ohio State University ElectroScience Laboratory, Columbus, Ohio, May 1980.
- [6] H.C. Lin, "Identification of Catalogued and Uncatalogued Classes," Ph.D. Dissertation, The Ohio State University, December 1978.
- [7] H. Lin and A.A. Ksienski, "Optimum Frequencies for Aircraft Classification," IEEE Trans. Aerospace and Electron. Sys., Vol. AES-17, No. 5, September 1981.
- [8] M.I. Skolnik, Introduction to Radar Systems, McGraw-Hill, New York, 1980.
- [9] J.M. Headrick and M.I. Skolnik, "Over-the-Horizon-Radar in the HF Band," PROC. IEEE, Vol. 62, pp. 664-673, No. 6, June 1974.
- [10] A.A. Ksienski, Y.T. Lin, and L.J. White, "Low-Frequency Approach to Target Identification," Proc. IEEE, Vol. 63, pp. 1651-1660, December 1975.
- [11] D.B. Trizna, "Estimation of the Sea Surface Radar Cross Section at HF from Second-Order Doppler Spectrum Characteristics," Naval Research Laboratory, Report 8579, May 1982.

- [12] J.W. Maresca, Jr., and J.R. Barnum, "Theoretical Limitation of the Sea on the Detection of Low Doppler Targets by Over-the-Horizon Radar," IEEE Trans. on Antenna Propagat., Vol. AP-30, No. 5, September, 1982.
- [13] W.B. Goggins, P. Blacksmith, and G.J. Sletten, "Phase Signature Radars," IEEE Trans. Antennas Propagat., Vol. AP-22, No. 6, November 1974.
- [14] H.L. Van Trees, Detection, Estimation, and Modulation Thoery, Part I, John Wiley & Sons, New York, 1968.
- [15] A. Papoulis, Signal Analysis, McGraw-Hill, New York, 1977.
- [16] D.E. Barrick and J.B. Snider, "The Statistics of H.F. Sea-Echo Doppler Spectra," IEEE Trans. Antennas Propagat., Vol. AP-25, January 1977.
- [17] M.H. DeGroot, Probability and Statistics, Addison-Wesley, 1975.
- [18] E.K. Walton, J.D. Young, "The Ohio State University Compact Radar Cross-Section Measurement Range," proposed paper for IEEE Trans. Antennas Propagat.
- [19] Beckmann and Spizzichino, The Scattering of Electromagnetic Waves from Rough Surfaces, McMillan, 1963.
- [20] E.K. Walton, "Processing and Analysis of VHF Radar Data for Target Classification," Report 712331-2, The Ohio State University ElectroScience Laboratory, March 1980.
- [21] J.D. Kraus and K.R. Carver, Electromagnetics, McGraw-Hill, 1973.
- [22] C.E. Shannon, "Communications in the Presence of Noise", Proc. IRE, Vol. 37, No. 1, pp. 10-21, January 1949.
- [23] Janes's Fighting Ships 1980-81, edited by Captain J. Moore RN, Jane's Publishing Co.

APPENDIX A

CLASSIFICATION RESULTS

This appendix contains plots of misclassification percentage versus post-processing signal-to-noise-ratio for the experiments of Chapter VI. A guide to interpreting the headers of these curves is given in Chapter VI, Section 6.1.2.

CLASSIFICATION OF SHIPS			
POLARIZATION	V		
ELEV ASSUMED	KNOWN		
ELEVATION (DEG.)	27		
ASPECT ASSUMED	KNOWN		
MIN,MAX,INC ASPECT	0	10	10
NO OF FREQUENCIES	4	4	4
NO OF TARGETS	12	12	12
90% CI (@30%) +/-	3.1%	3.1%	3.1%
CLASS. FEATURES	A	A	A

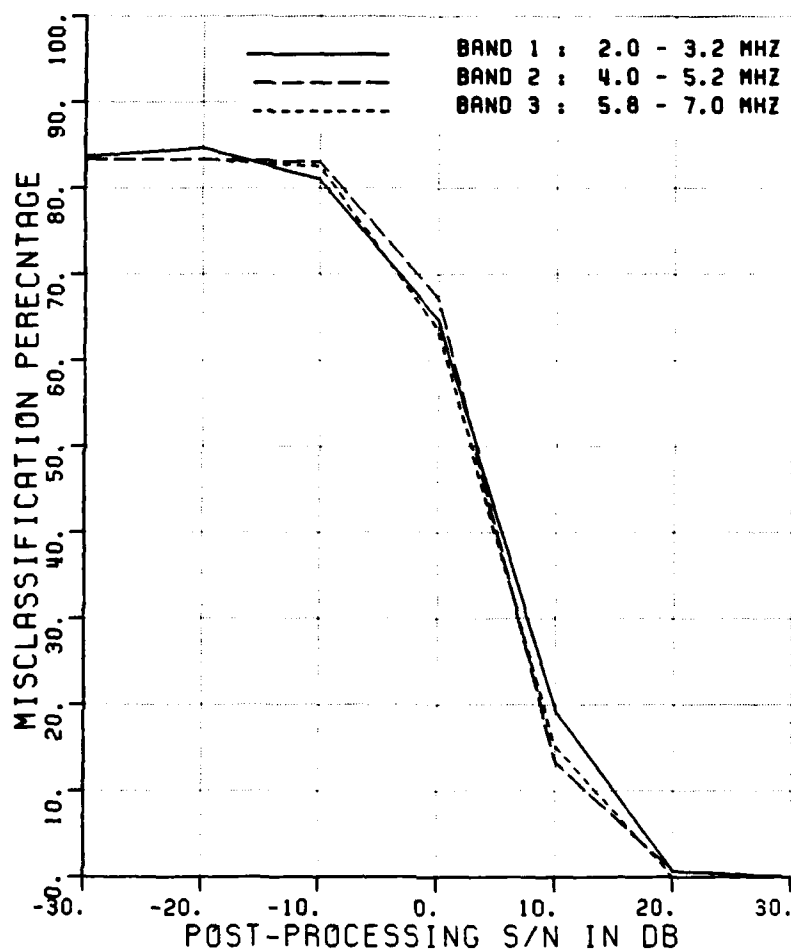


Figure A.1. Misclassification percentage versus post-processing SNR, comparing the performance of 3 sub-bands in the 2-7 MHz band.

CLASSIFICATION OF SHIPS			
POLARIZATION	V		
ELEV ASSUMED	KNOWN		
ELEVATION (DEG.)	27		
ASPECT ASSUMED	KNOWN		
MIN,MAX,INC ASPECT	80	100	10
NO OF FREQUENCIES	4	4	4
NO OF TARGETS	18	18	18
90% CI (±30%) +/-	2.5%	2.5%	2.5%
CLASS. FEATURES	A	A	A

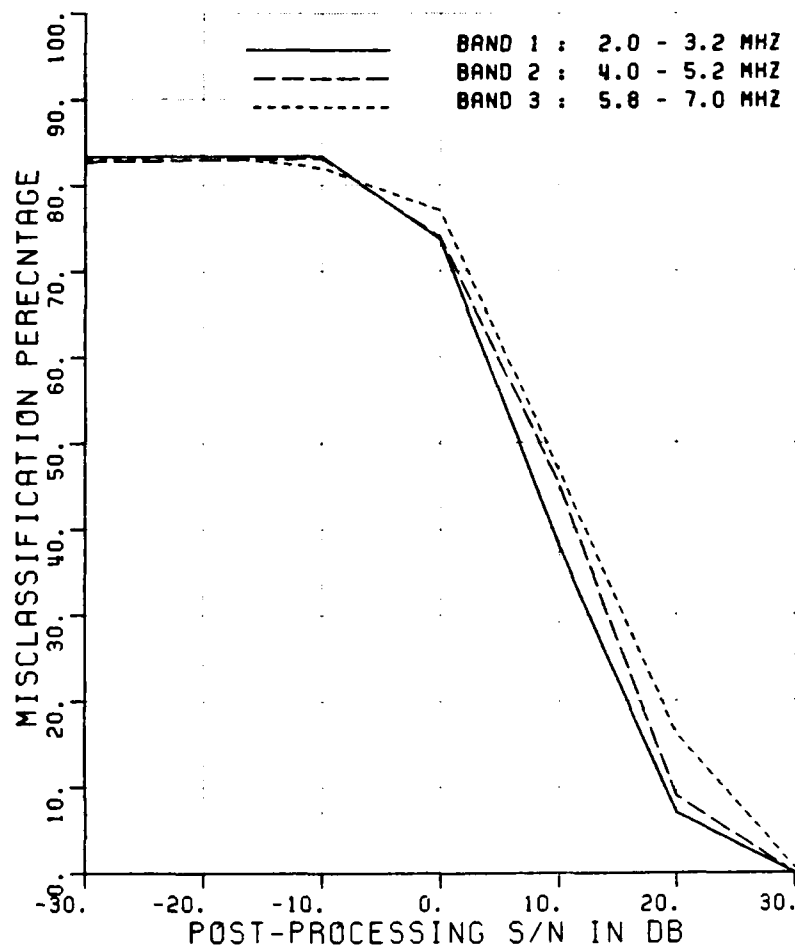


Figure A.2. Misclassification percentage versus post-processing SNR, comparing the performance of 3 sub-bands in the 2-7 MHz band.

CLASSIFICATION OF SHIPS			
POLARIZATION	V		
ELEV ASSUMED	KNOWN		
ELEVATION (DEG.)	27		
ASPECT ASSUMED	KNOWN		
MIN,MAX,INC ASPECT	0	180	90
NO OF FREQUENCIES	4	4	4
NO OF TARGETS	18	18	18
90% CI (±30%) +/-	2.5%	2.5%	2.5%
CLASS. FEATURES	A	A	A

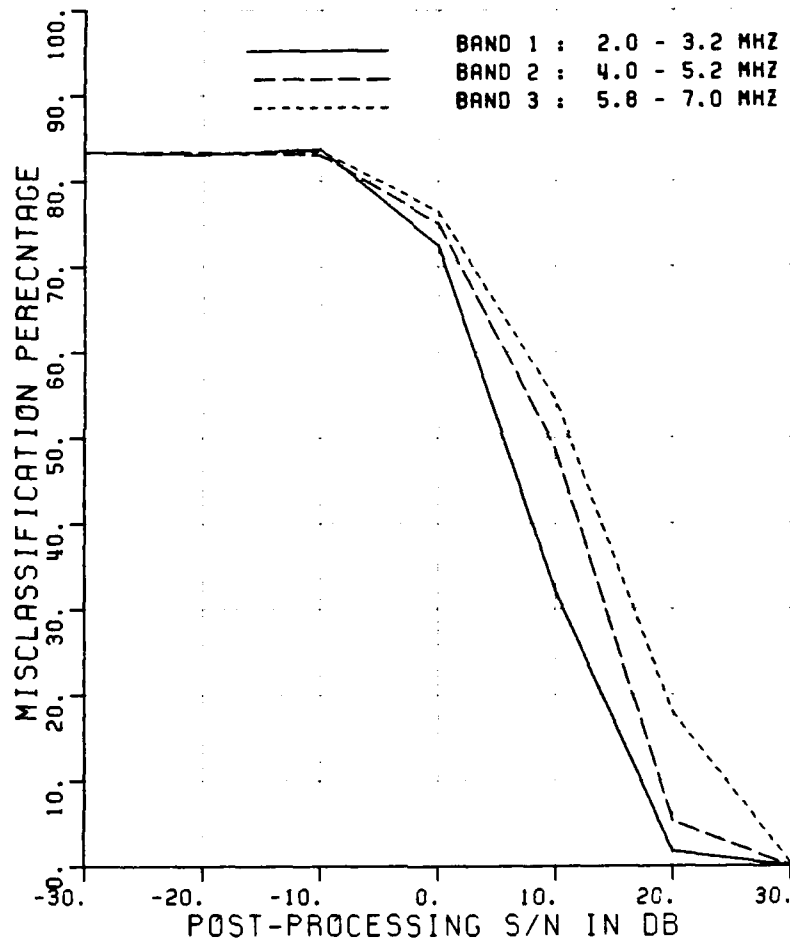


Figure A.3. Misclassification percentage versus post-processing SNR, comparing the performance of 3 sub-bands in the 2-7 MHz band.

CLASSIFICATION OF SHIPS

POLARIZATION	H		
ELEV ASSUMED	KNOWN		
ELEVATION (DEG.)	27		
ASPECT ASSUMED	KNOWN		
MIN,MAX,INC ASPECT	0	180	90
NO OF FREQUENCIES	4	4	4
NO OF TARGETS	18	18	18
90% CI (±30%) +/-	2.5%	2.5%	2.5%
CLASS. FEATURES	A	A	A

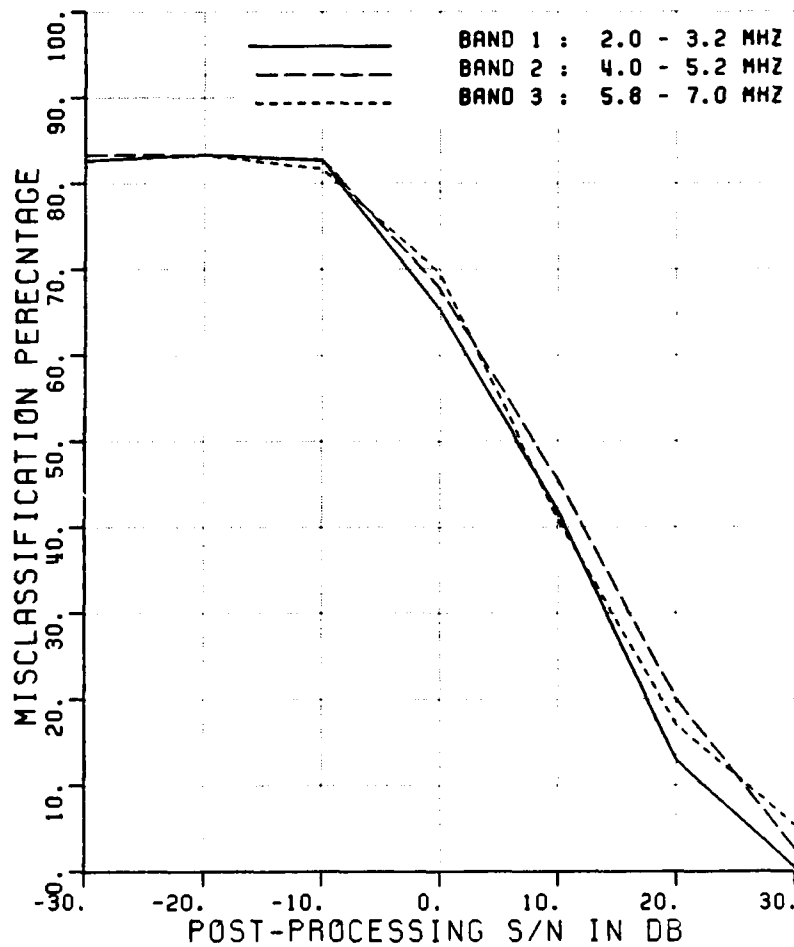


Figure A.4. Misclassification percentage versus post-processing SNR, comparing the performance of 3 sub-bands in the 2-7 MHz band.

CLASSIFICATION OF SHIPS

POLARIZATION	X		
ELEV ASSUMED	KNOWN		
ELEVATION (DEG.)	27		
ASPECT ASSUMED	KNOWN		
MIN,MAX,INC ASPECT	0	180	90
NO OF FREQUENCIES	4	4	4
NO OF TARGETS	18	18	18
90% CI (@30%) +/-	2.5%	2.5%	2.5%
CLASS. FEATURES	A	A	A

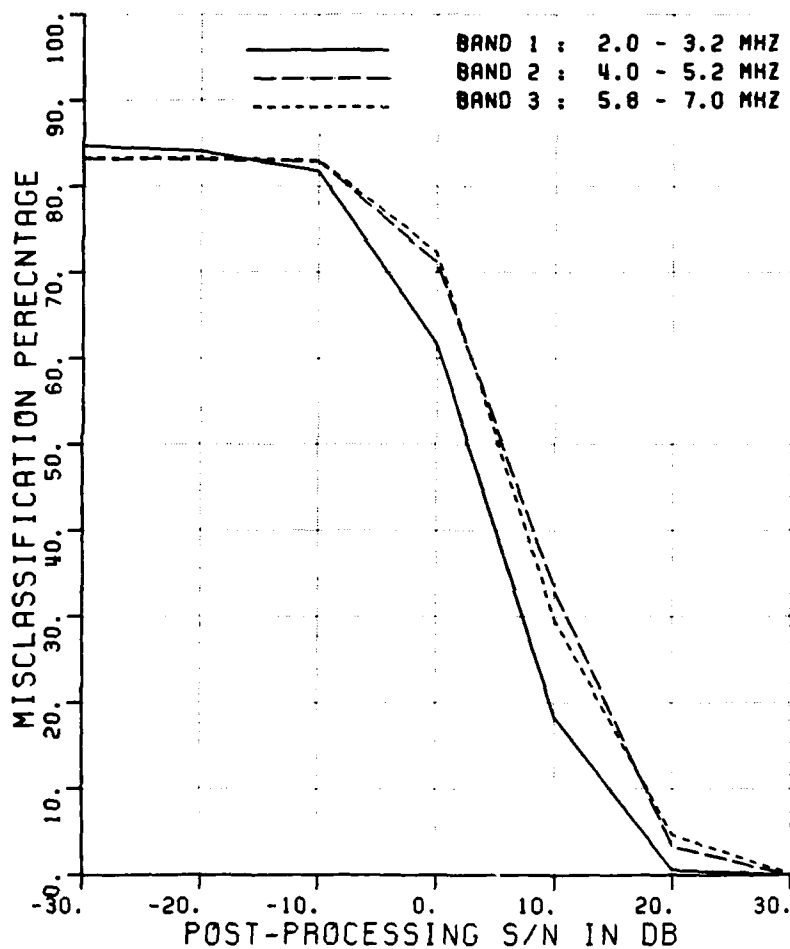


Figure A.5. Misclassification percentage versus post-processing SNR, comparing the performance of 3 sub-bands in the 2-7 MHz band.

CLASSIFICATION OF SHIPS
 POLARIZATION V/H
 ELEV ASSUMED KNOWN
 ELEVATION (DEG.) 27
 ASPECT ASSUMED KNOWN
 MIN,MAX,INC ASPECT 0 180 90
 NO OF FREQUENCIES 4 4 4
 NO OF TARGETS 18 18 18
 90% CI (±30%) +/- 2.5% 2.5% 2.5%
 CLASS. FEATURES A A A

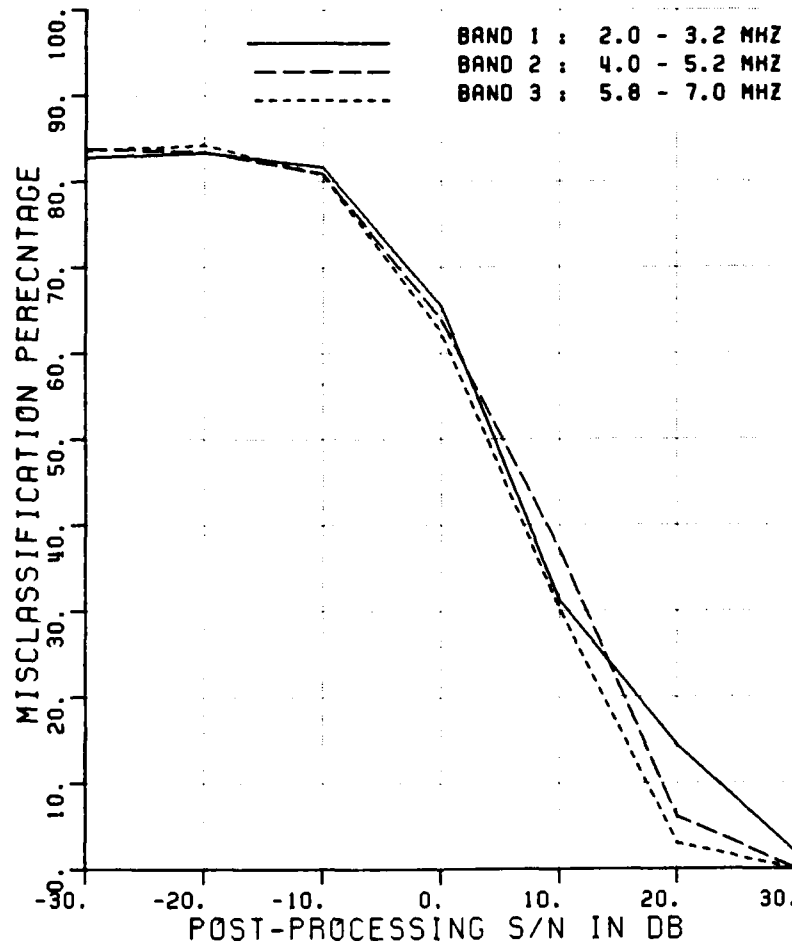


Figure A.6. Misclassification percentage versus post-processing SNR, comparing the performance of 3 sub-bands in the 2-7 MHz band.

CLASSIFICATION OF SHIPS			
POLARIZATION	V		
ELEV ASSUMED	KNOWN		
ELEVATION (DEG.)	27		
ASPECT ASSUMED	KNOWN		
MIN,MAX,INC ASPECT	0	180	90
NO OF FREQUENCIES	4	4	4
NO OF TARGETS	18	18	18
90% CI (#30%) +/-	2.5%	2.5%	2.5%
CLASS. FEATURES	T	T	T

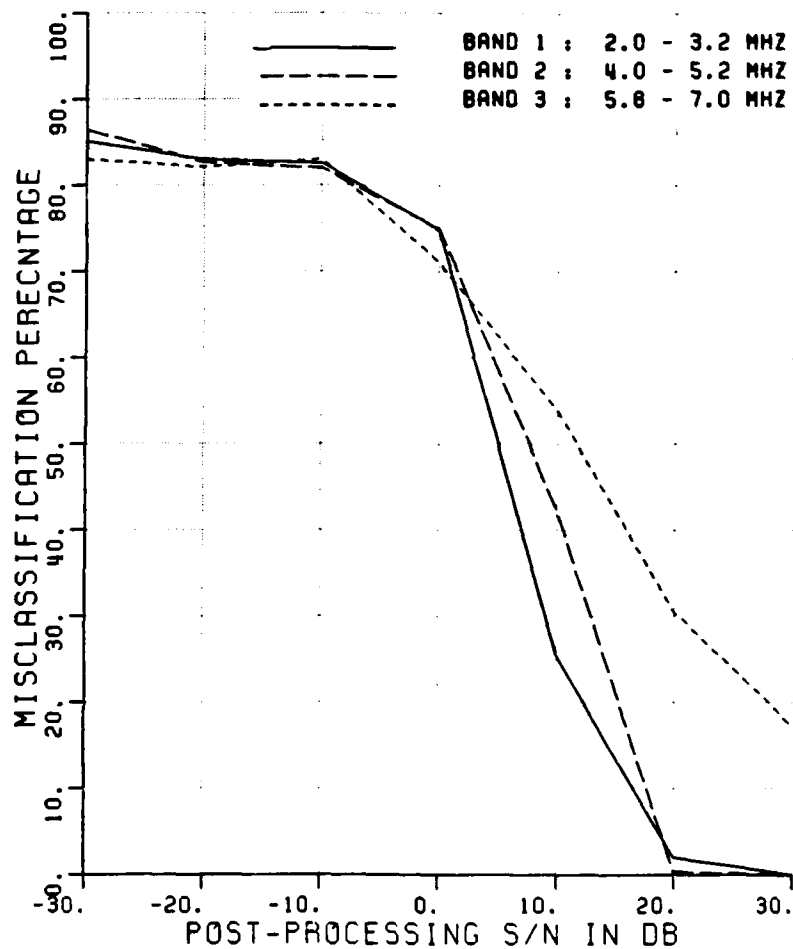


Figure A.7. Misclassification percentage versus post-processing SNR, comparing the performance of 3 sub-bands in the 2-7 MHz band.

CLASSIFICATION OF SHIPS
 POLARIZATION V
 ELEV ASSUMED KNOWN
 ELEVATION (DEG.) 27
 ASPECT ASSUMED KNOWN
 MIN,MAX,INC ASPECT 0 180 90
 NO OF FREQUENCIES 4 4 4
 NO OF TARGETS 18 18 18
 90% CI (@30%) +/- 2.5% 2.5% 2.5%
 CLASS. FEATURES R4W R4W R4W

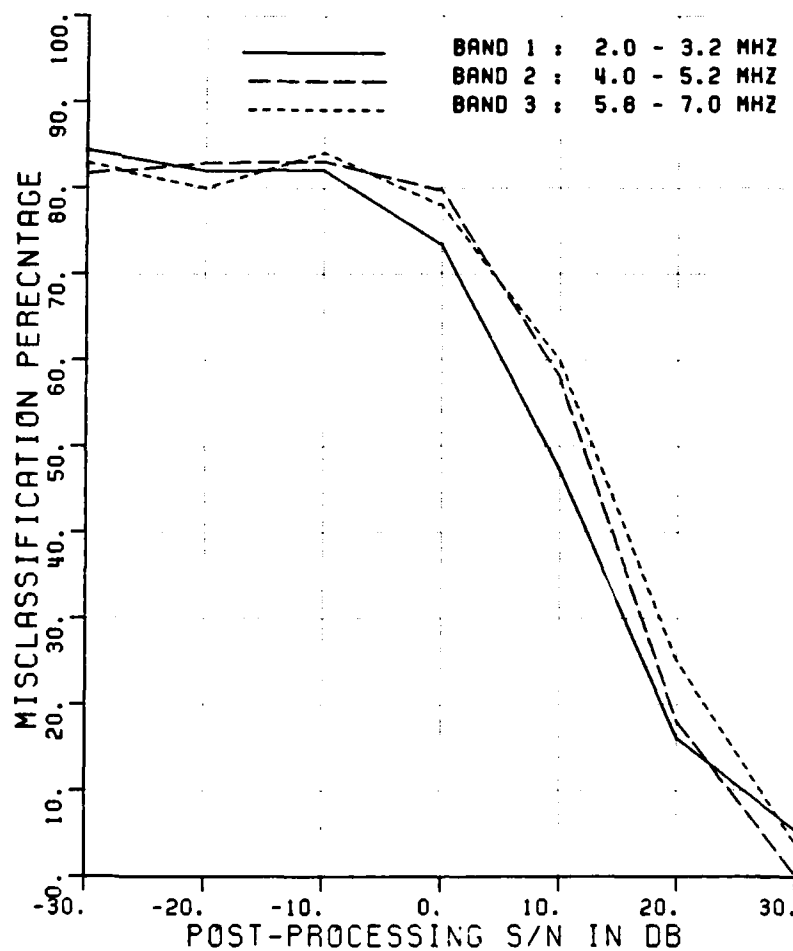


Figure A.8. Misclassification percentage versus post-processing SNR, comparing the performance of 3 sub-bands in the 2-7 MHz band.

CLASSIFICATION OF SHIPS			
POLARIZATION	V		
ELEV ASSUMED	KNOWN		
ELEVATION (DEG.)	27		
ASPECT ASSUMED	KNOWN		
MIN, MAX, INC ASPECT	0	180	90
NO OF FREQUENCIES	4	4	4
NO OF TARGETS	18	18	18
90% CI (±30%) +/-	2.5%	2.5%	2.5%
CLASS. FEATURES	A&W	A&W	A&W

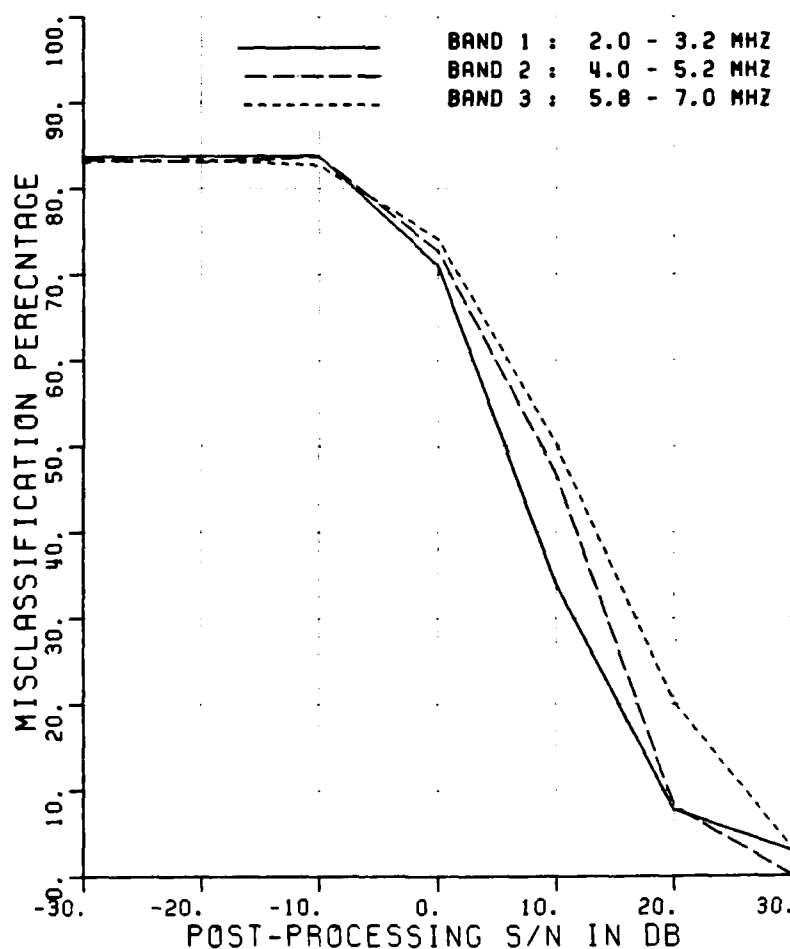


Figure A.9. Misclassification percentage versus post-processing SNR, comparing the performance of 3 sub-bands in the 2-7 MHz band.

CLASSIFICATION OF SHIPS

POLARIZATION	V			
ELEV ASSUMED	KNOWN			
ELEVATION (DEG.)	27			
ASPECT ASSUMED	KNOWN			
MIN,MAX,INC ASPECT	0 180 90			
NO OF FREQUENCIES	2	4	8	12
NO OF TARGETS	18	18	18	18
90% CI (±30%) +/-	2.5%	2.5%	2.5%	2.5%
CLASS. FEATURES	W	W	W	W

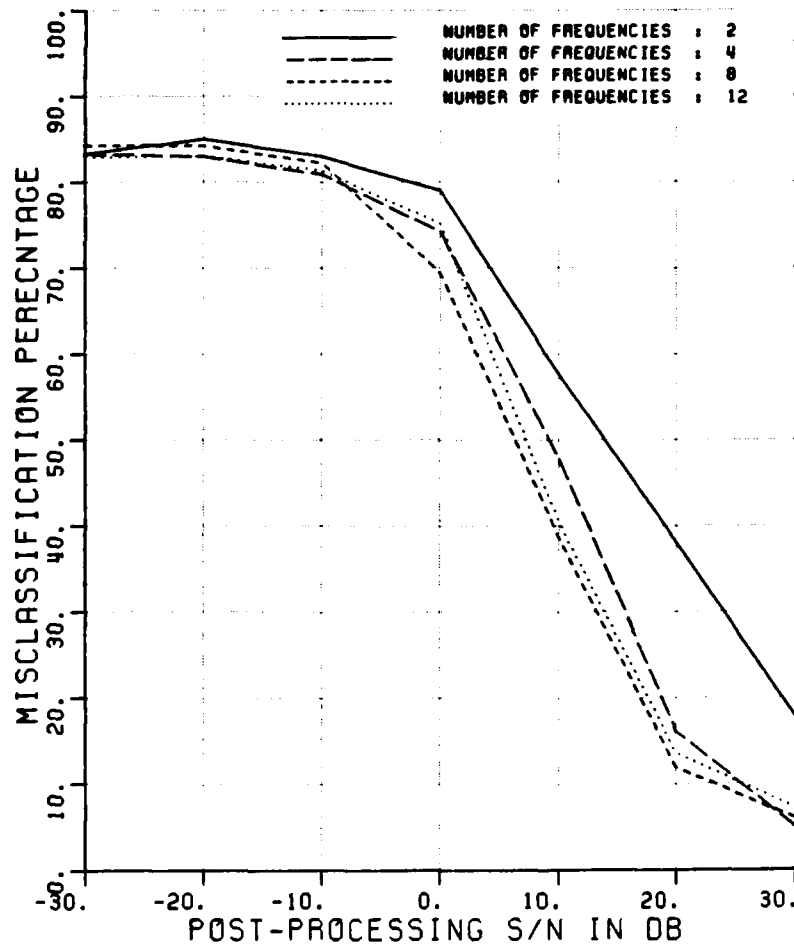


Figure A.10. Misclassification percentage versus post-processing SNR, comparing the performance of different numbers of frequencies.

CLASSIFICATION OF SHIPS

POLARIZATION	V			
ELEV ASSUMED	KNOWN			
ELEVATION (DEG.)	27			
ASPECT ASSUMED	KNOWN			
MIN,MAX,INC ASPECT	0	180	90	
NO OF FREQUENCIES	2	4	8	12
NO OF TARGETS	18	18	18	18
90% CI (±30%) +/-	2.5%	2.5%	2.5%	2.5%
CLASS. FEATURES	A&W	A&W	A&W	A&W

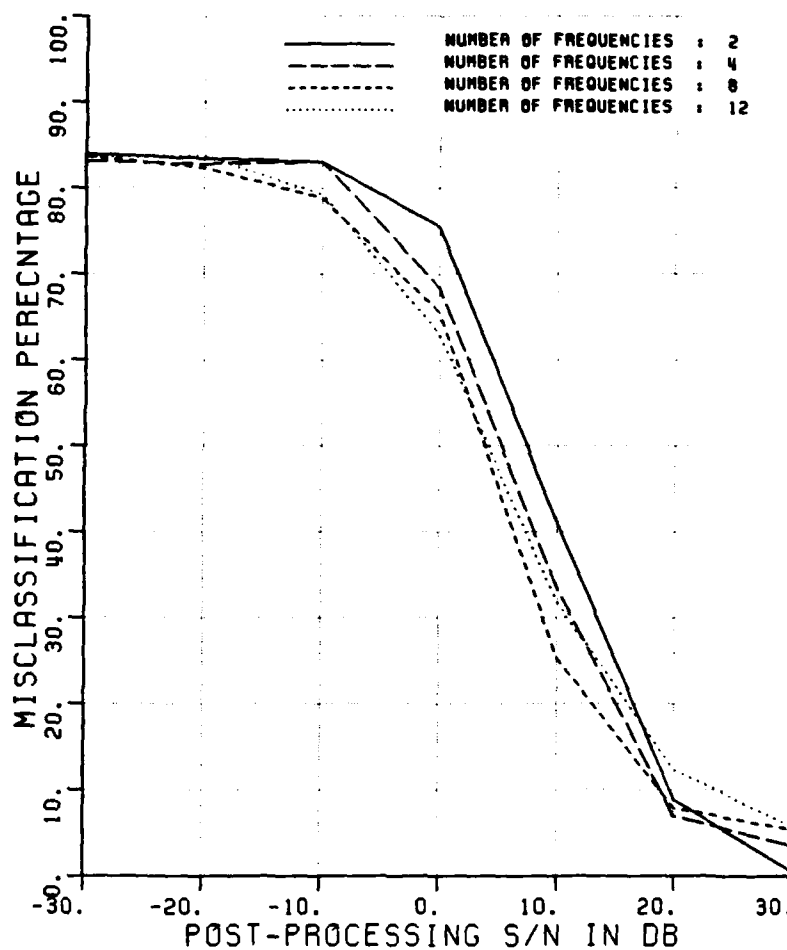


Figure A.11. Misclassification percentage versus post-processing SNR, comparing the performance of different numbers of frequencies.

CLASSIFICATION OF SHIPS

POLARIZATION	V				
ELEV ASSUMED	KNOWN				
ELEVATION (DEG.)	27				
ASPECT ASSUMED	KNOWN				
MIN,MAX,INC ASPECT	0 180 90				
NO OF FREQUENCIES	2	4	8	12	
NO OF TARGETS	18	18	18	18	18
90% CI (@30%) +/-	2.5%	2.5%	2.5%	2.5%	2.5%
CLASS. FEATURES	A	A	A	A	

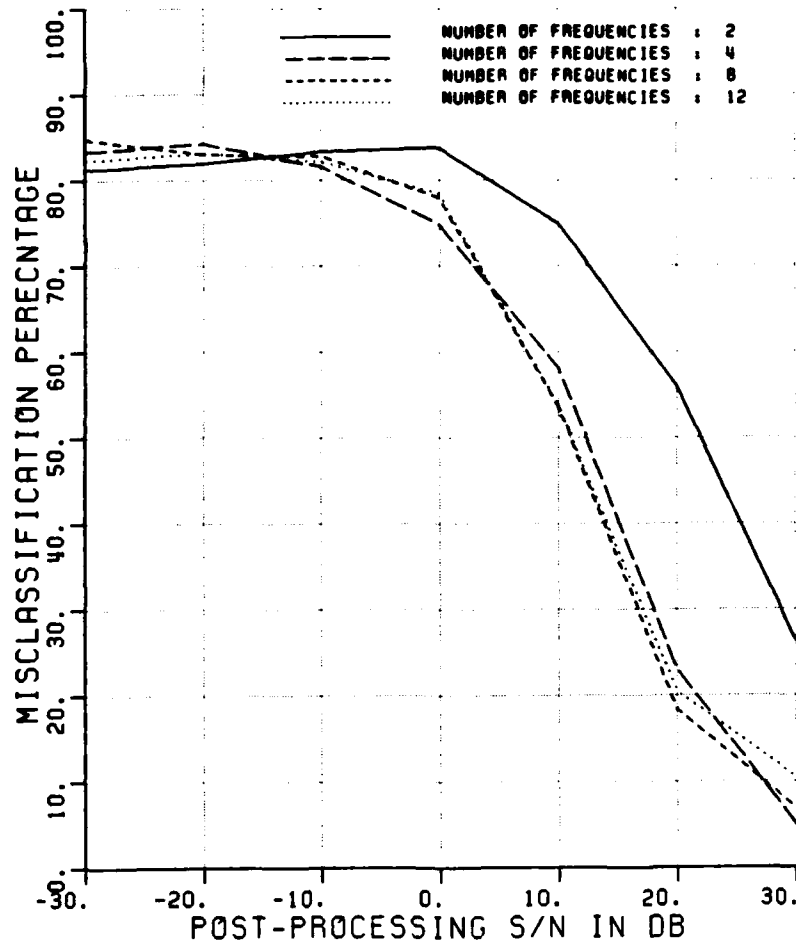


Figure A.12. Misclassification percentage versus post-processing SNR, comparing the performance of different numbers of frequencies.

CLASSIFICATION OF SHIPS

POLARIZATION V

ELEV ASSUMED KNOWN

ELEVATION (DEG.) 27

ASPECT ASSUMED KNOWN

MIN,MAX,INC ASPECT 0 180 90

NO OF FREQUENCIES 2 4 8 12

NO OF TARGETS 18 18 18 18

90% CI (±30%) +/- 2.5% 2.5% 2.5% 2.5%

CLASS. FEATURES R&W R&W R&W R&W

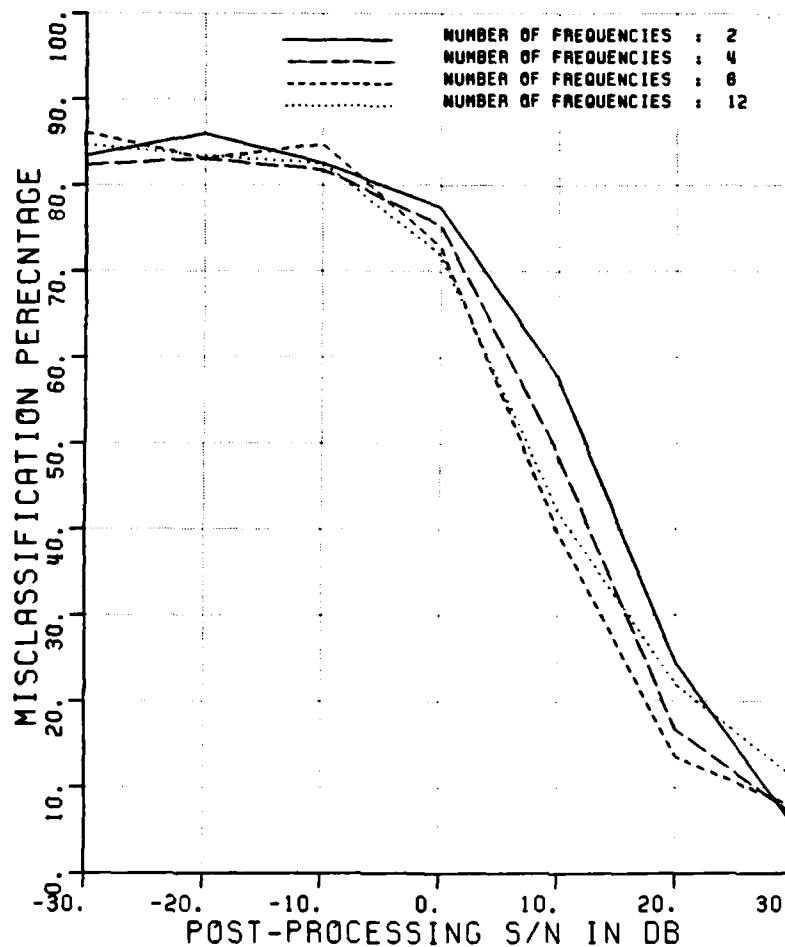


Figure A.13. Misclassification percentage versus post-processing SNR, comparing the performance of different numbers of frequencies.

CLASSIFICATION OF SHIPS
 POLARIZATION V
 ELEV ASSUMED KNOWN
 ELEVATION (DEG.) 27
 ASPECT ASSUMED KNOWN
 MIN,MAX,INC ASPECT 0 180 90
 NO OF FREQUENCIES 2
 NO OF TARGETS 18 18 18 18 18 18
 90% CI ($\pm 30\%$) +/- 2.5% 2.5% 2.5% 2.5% 2.5% 2.5%
 CLASS. FEATURES A W A&W R&W R T

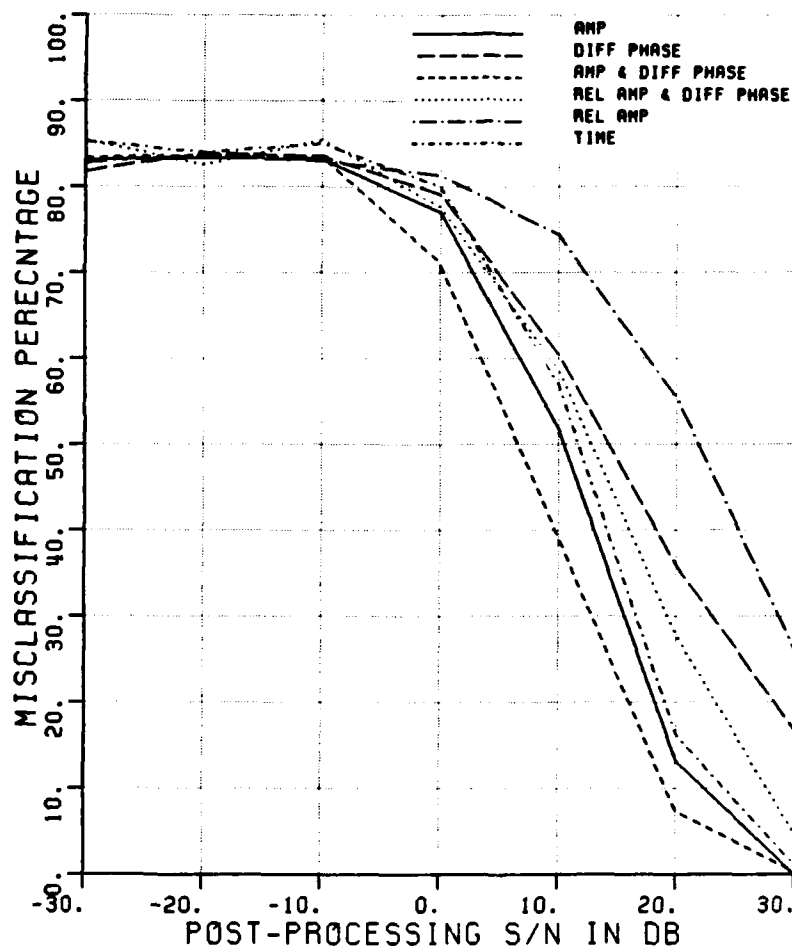


Figure A.14. Misclassification percentage versus post-processing SNR, comparing the performance of different algorithms.

CLASSIFICATION OF SHIPS
 POLARIZATION V
 ELEV ASSUMED KNOWN
 ELEVATION (DEG.) 27
 ASPECT ASSUMED KNOWN
 MIN,MAX,INC ASPECT 0 180 90
 NO OF FREQUENCIES 4
 NO OF TARGETS 18 18 18 18 18 18
 90% CI (±30%) +/- 2.5% 2.5% 2.5% 2.5% 2.5% 2.5%
 CLASS. FEATURES A W A&W A&W A T

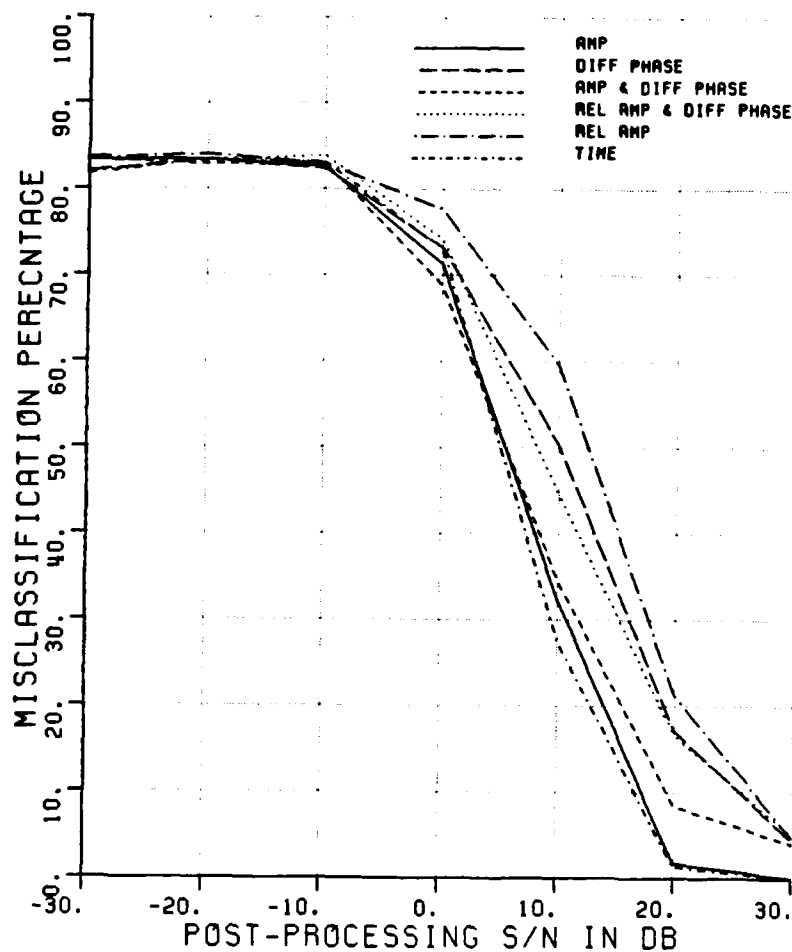


Figure A.15. Misclassification percentage versus post-processing SNR, comparing the performance of different algorithms.

CLASSIFICATION OF SHIPS

POLARIZATION	V						
ELEV ASSUMED	KNOWN						
ELEVATION (DEG.)	27						
ASPECT ASSUMED	KNOWN						
MIN,MAX,INC ASPECT	0	180	90				
NO OF FREQUENCIES	8						
NO OF TARGETS	18	18	18	18	18	18	16
90% CI (±30%) +/-	2.5%	2.5%	2.5%	2.5%	2.5%	2.5%	2.5%
CLASS. FEATURES	A	W	A&W	A&W	A	T	

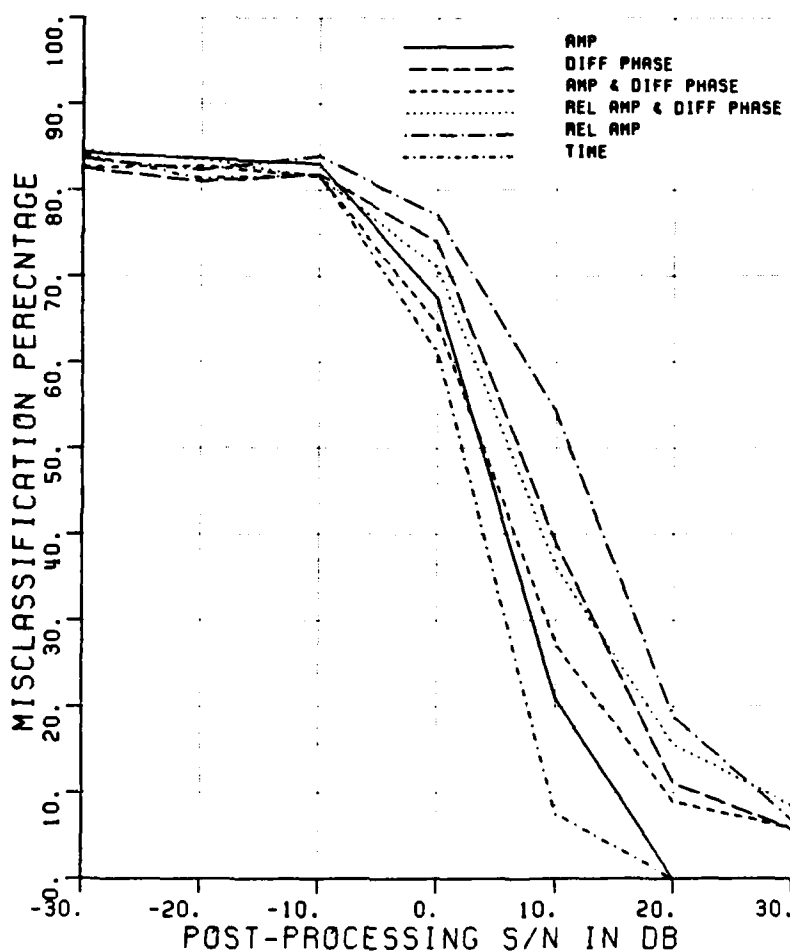


Figure A.16. Misclassification percentage versus post-processing SNR, comparing the performance of different algorithms.

CLASSIFICATION OF SHIPS
 POLARIZATION V
 ELEV ASSUMED KNOWN
 ELEVATION (DEG.) 27
 ASPECT ASSUMED KNOWN / UNKNOWN
 MIN,MAX,INC ASPECT 0 180 90
 NO OF FREQUENCIES 8
 NO OF TARGETS 18 18
 90% CI (@30%) +/- 2.5% 2.5%
 CLASS. FEATURES W W

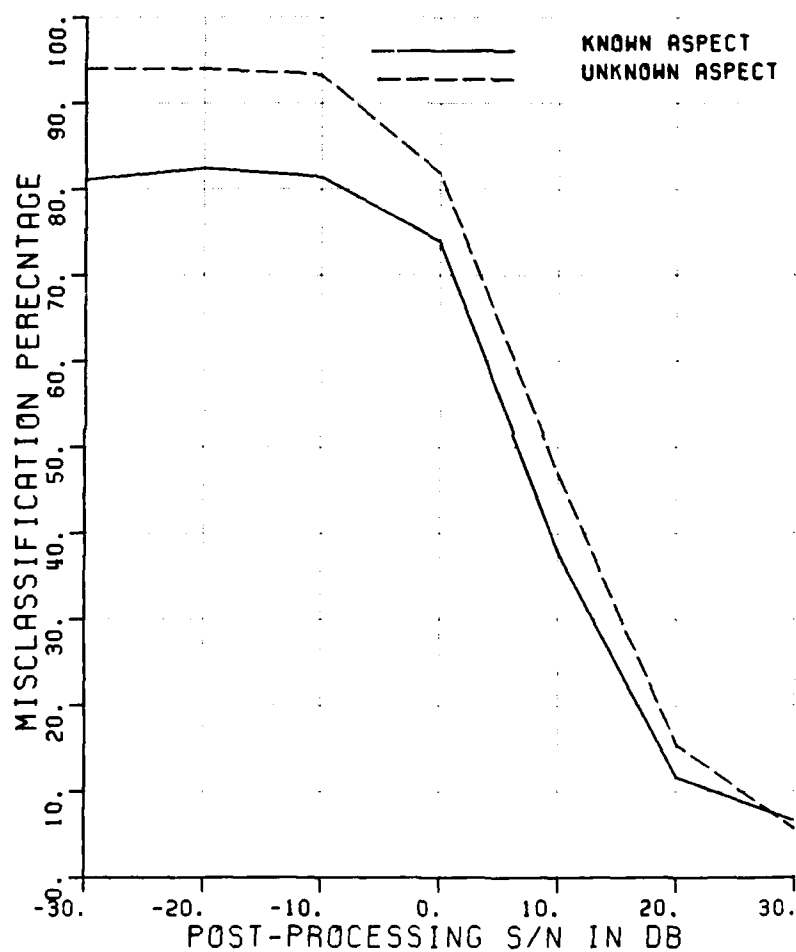


Figure A.17. Misclassification percentage versus post-processing SNR, comparing the performance of known and unknown aspect angles.

CLASSIFICATION OF SHIPS
 POLARIZATION V
 ELEV ASSUMED KNOWN
 ELEVATION (DEG.) 27
 ASPECT ASSUMED KNOWN / UNKNOWN
 MIN,MAX,INC ASPECT 0 180 90
 NO OF FREQUENCIES 8
 NO OF TARGETS 18 18
 90% CI ($\pm 30\%$) $\pm 2.5\%$ 2.5%
 CLASS. FEATURES A&W A&W

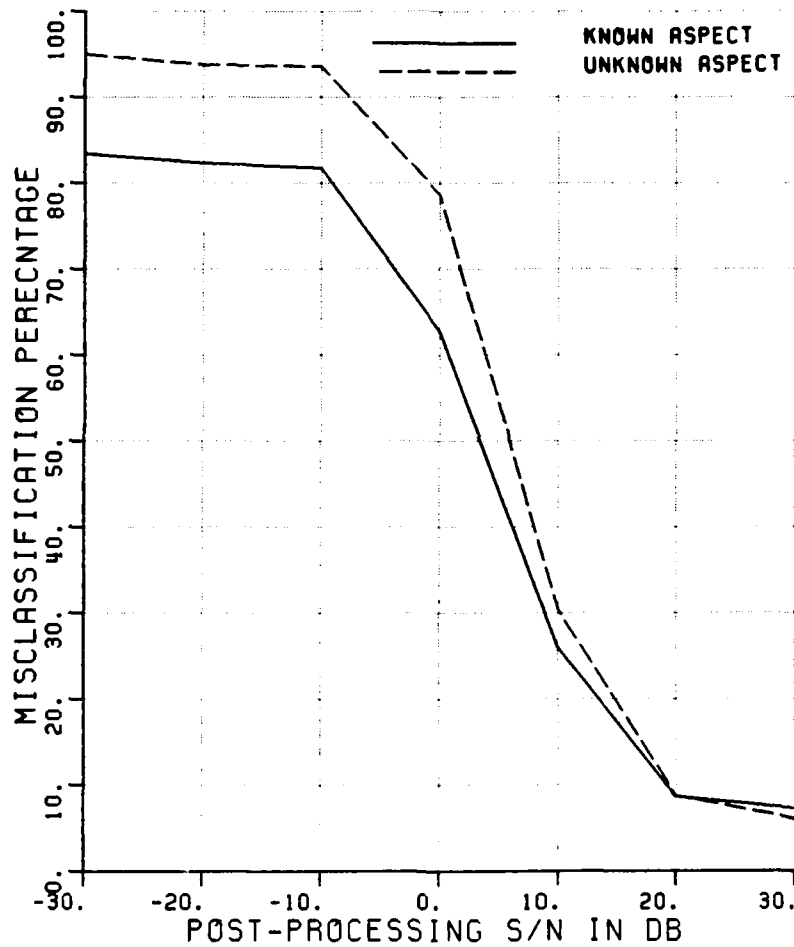


Figure A.18. Misclassification percentage versus post-processing SNR, comparing the performance of known and unknown aspect angles.

CLASSIFICATION OF SHIPS
 POLARIZATION V
 ELEV ASSUMED KNOWN
 ELEVATION (DEG.) 27
 ASPECT ASSUMED KNOWN / UNKNOWN
 MIN,MAX,INC ASPECT 0 180 90
 NO OF FREQUENCIES 8
 NO OF TARGETS 18 18
 90% CI (±30%) +/- 2.5% 2.5%
 CLASS. FEATURES R R

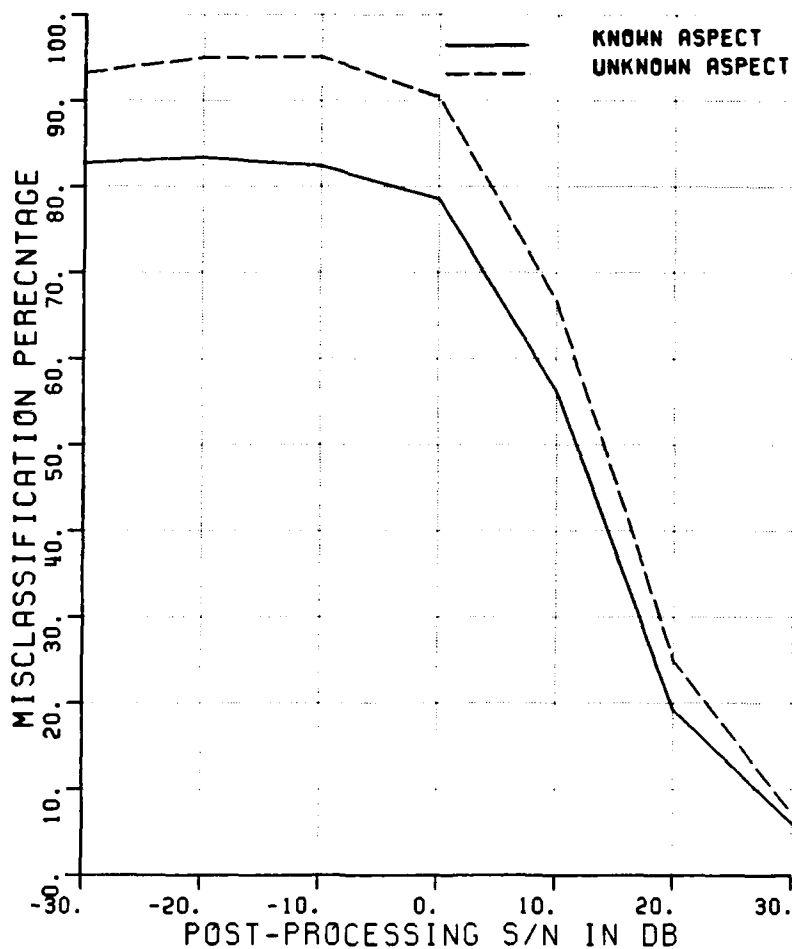


Figure A.19. Misclassification percentage versus post-processing SNR, comparing the performance of known and unknown aspect angles.

CLASSIFICATION OF SHIPS
 POLARIZATION V
 ELEV ASSUMED KNOWN
 ELEVATION (DEG.) 27
 ASPECT ASSUMED KNOWN / UNKNOWN
 MIN,MAX,INC ASPECT 0 180 90
 NO OF FREQUENCIES 8
 NO OF TARGETS 18 18
 90% CI (±30%) +/- 2.5% 2.5%
 CLASS. FEATURES R&W R&W

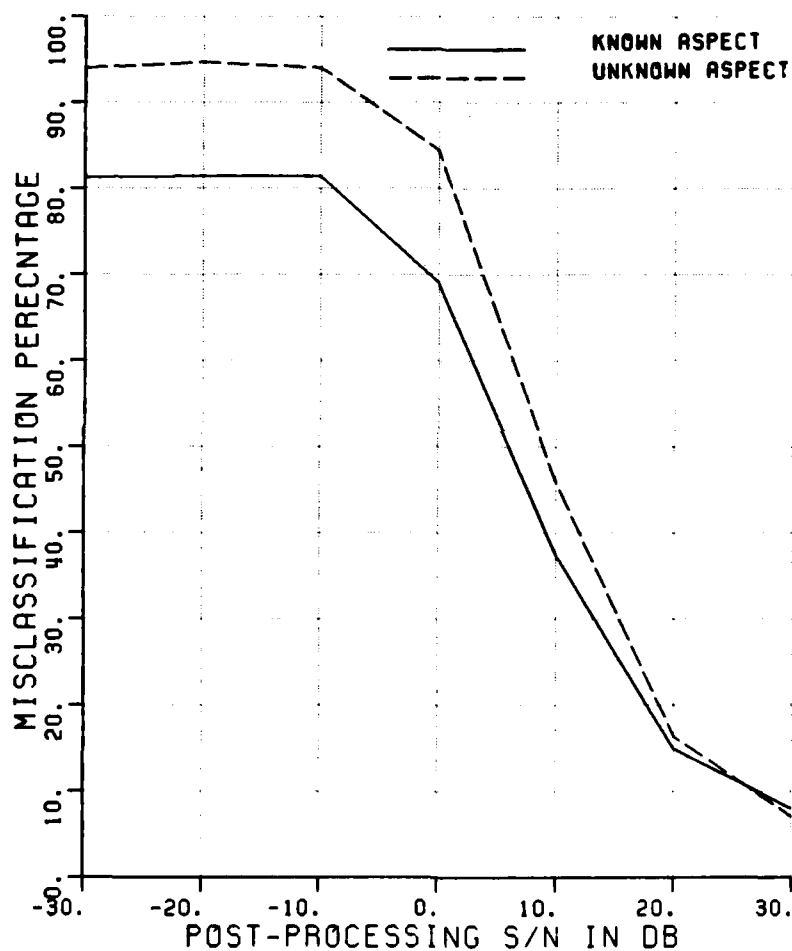


Figure A.20. Misclassification percentage versus post-processing SNR, comparing the performance of known and unknown aspect angles.

CLASSIFICATION OF SHIPS
 POLARIZATION V
 ELEV ASSUMED KNOWN
 ELEVATION (DEG.) 27
 ASPECT ASSUMED KNOWN / UNKNOWN
 MIN,MAX,INC ASPECT 0 180 90
 NO OF FREQUENCIES 8
 NO OF TARGETS 18 18
 90% CI (@30%) +/- 2.5% 2.5%
 CLASS. FEATURES T T

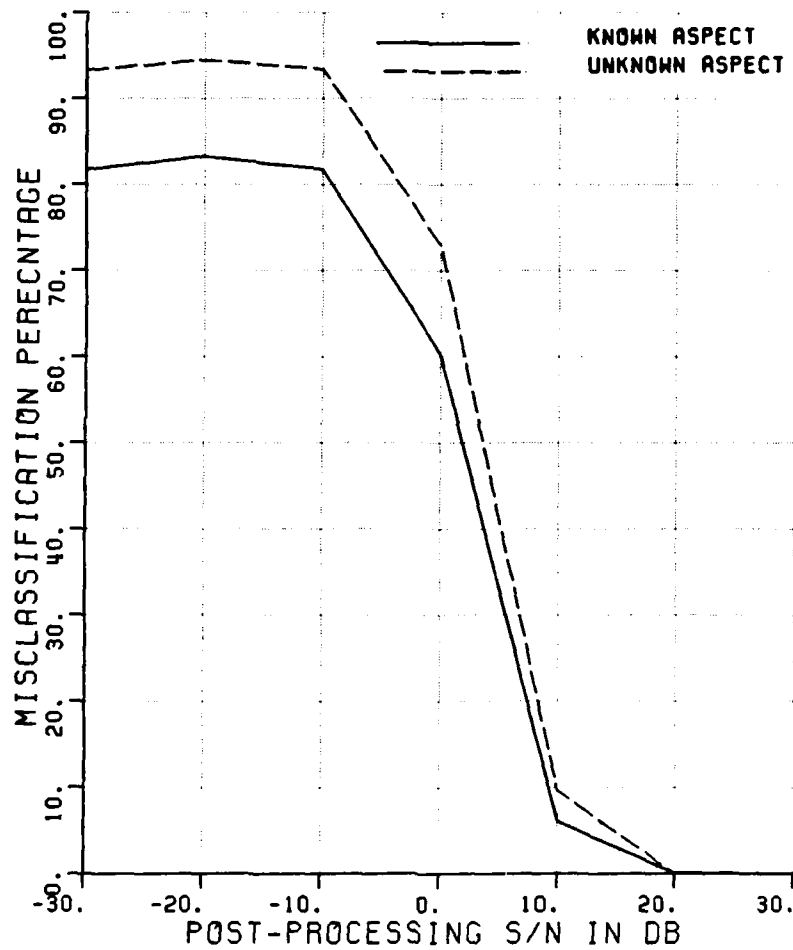


Figure A.21. Misclassification percentage versus post-processing SNR, comparing the performance of known and unknown aspect angles.

CLASSIFICATION OF SHIPS

POLARIZATION	V				
ELEV ASSUMED	KNOWN	/	UNKNOWN		
ELEVATION (DEG.)	15	27	15,27		
ASPECT ASSUMED	KNOWN				
MIN,MAX,INC ASPECT	80	100	10		
NO OF FREQUENCIES	8				
NO OF TARGETS	18	18	36	36	36
90% CI (+30%) +/-	2.5%	2.5%	1.8%	1.8%	1.8%
CLASS. FEATURES	A	A	A	A	A
ELEV ERR IN CURVE	4				

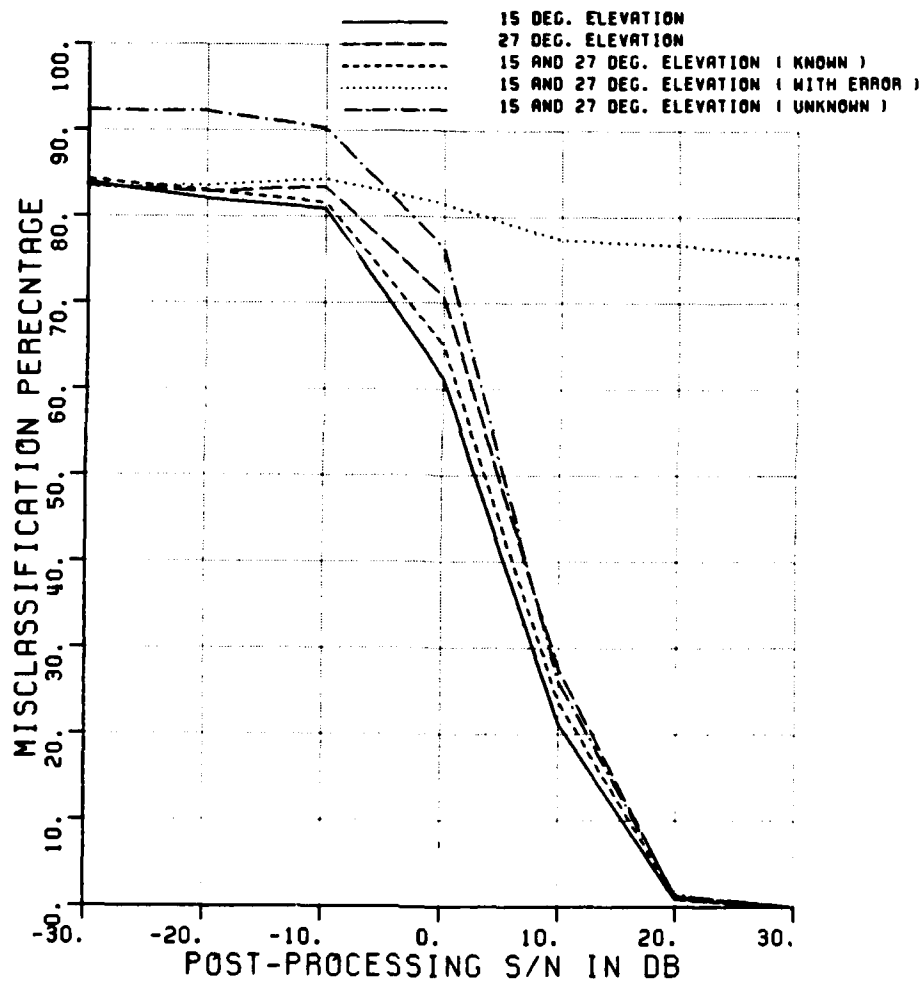


Figure A.22. Misclassification percentage versus post-processing SNR, comparing the performance of various elevation angles.

CLASSIFICATION OF SHIPS

POLARIZATION	V				
ELEV ASSUMED	KNOWN / UNKNOWN				
ELEVATION (DEG.)	15	27	15.27		
ASPECT ASSUMED	KNOWN				
MIN,MAX,INC ASPECT	170	180	10		
NO OF FREQUENCIES	8				
NO OF TARGETS	12	12	24	24	24
90% CI (±30%) +/-	3.1%	3.1%	2.2%	2.2%	2.2%
CLASS. FEATURES	A	A	A	A	A
ELEV ERR IN CURVE	4				

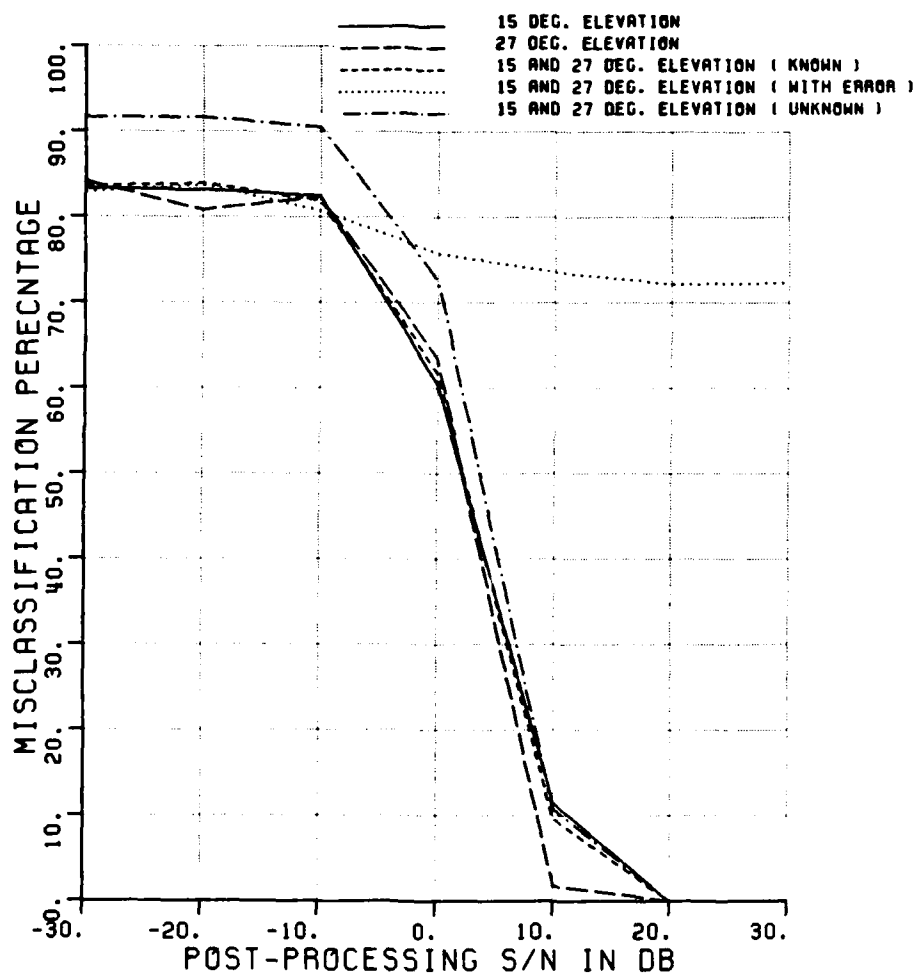


Figure A.23. Misclassification percentage versus post-processing SNR, comparing the performance of various elevation angles.

CLASSIFICATION OF SHIPS

POLARIZATION	H				
ELEV ASSUMED	KNOWN	/	UNKNOWN		
ELEVATION (DEG.)	15	27	15,27		
ASPECT ASSUMED	KNOWN				
MIN,MAX,INC ASPECT	80	100	10		
NO OF FREQUENCIES	8				
NO OF TARGETS	18	18	36	36	36
90% CI (±30%) +/-	2.5%	2.5%	1.8%	1.8%	1.8%
CLASS. FEATURES	A	A	A	A	A
ELEV ERR IN CURVE	4				

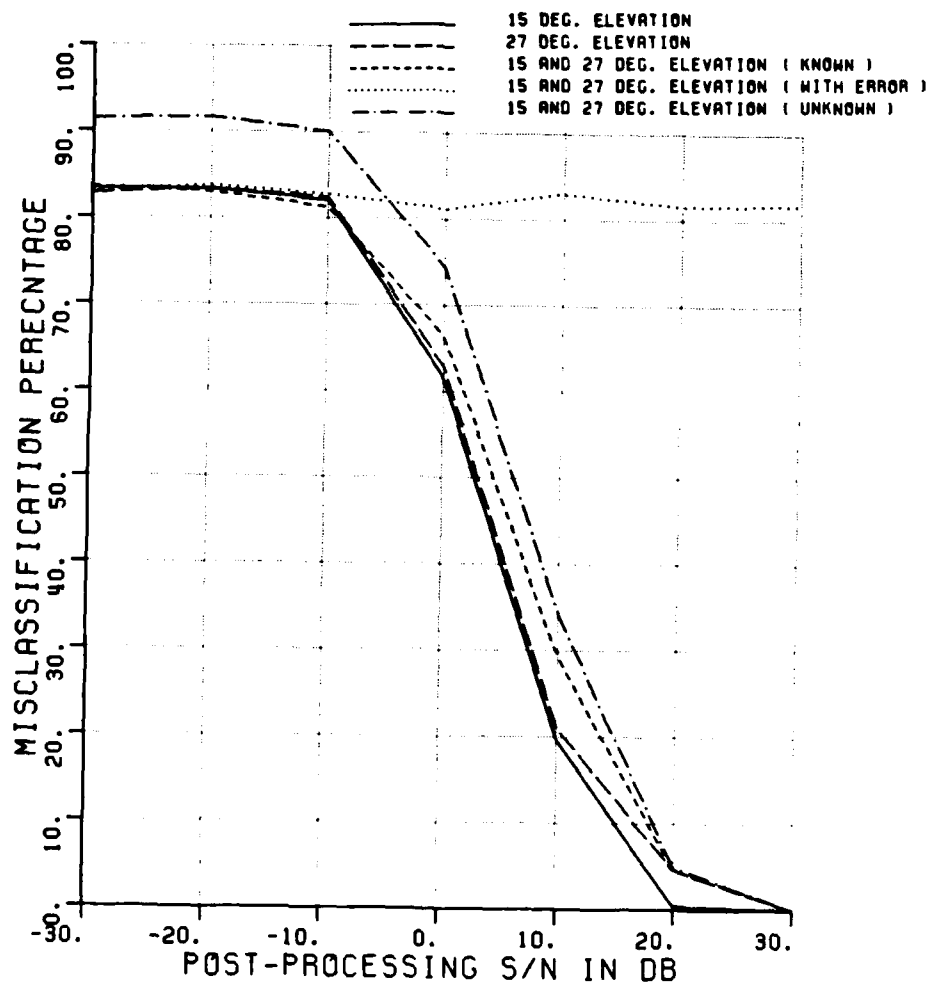


Figure A.24. Misclassification percentage versus post-processing SNR, comparing the performance of various elevation angles.

CLASSIFICATION OF SHIPS

POLARIZATION	H				
ELEV ASSUMED	KNOWN	/ UNKNOWN			
ELEVATION (DEG.)	15	27	15,27		
ASPECT ASSUMED	KNOWN				
MIN,MAX,INC ASPECT	170	180	10		
NO OF FREQUENCIES	8				
NO OF TARGETS	12	12	24	24	24
90% CI (±30%) +/-	3.1%	3.1%	2.2%	2.2%	2.2%
CLASS. FEATURES	A	A	A	A	A
ELEV ERR IN CURVE	4				

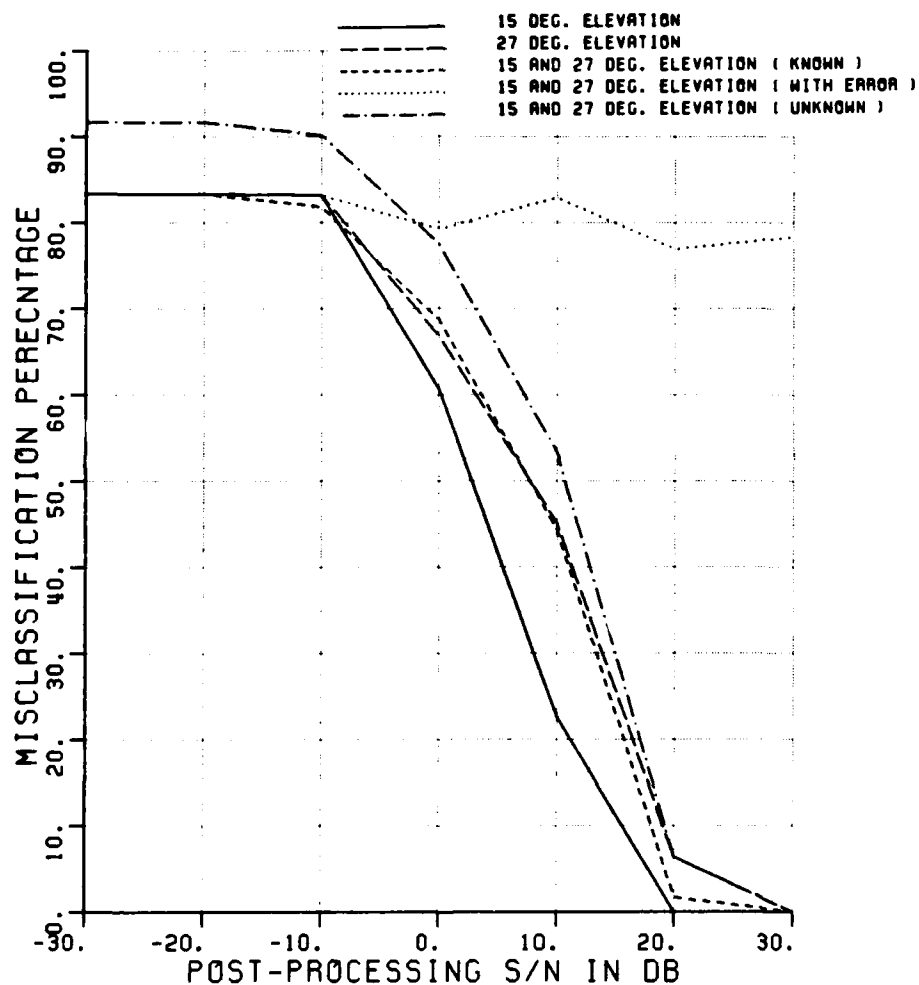


Figure A.25. Misclassification percentage versus post-processing SNR, comparing the performance of various elevation angles.

CLASSIFICATION OF SHIPS

POLARIZATION	X				
ELEV ASSUMED	KNOWN	/	UNKNOWN		
ELEVATION (DEG.)	15	27	15,27		
ASPECT ASSUMED	KNOWN				
MIN,MAX,INC ASPECT	80	100	10		
NO OF FREQUENCIES	8				
NO OF TARGETS	18	18	36	36	36
90% CI (±30%) +/-	2.5%	2.5%	1.8%	1.8%	1.8%
CLASS. FEATURES	A	A	A	A	A
ELEV ERR IN CURVE	4				

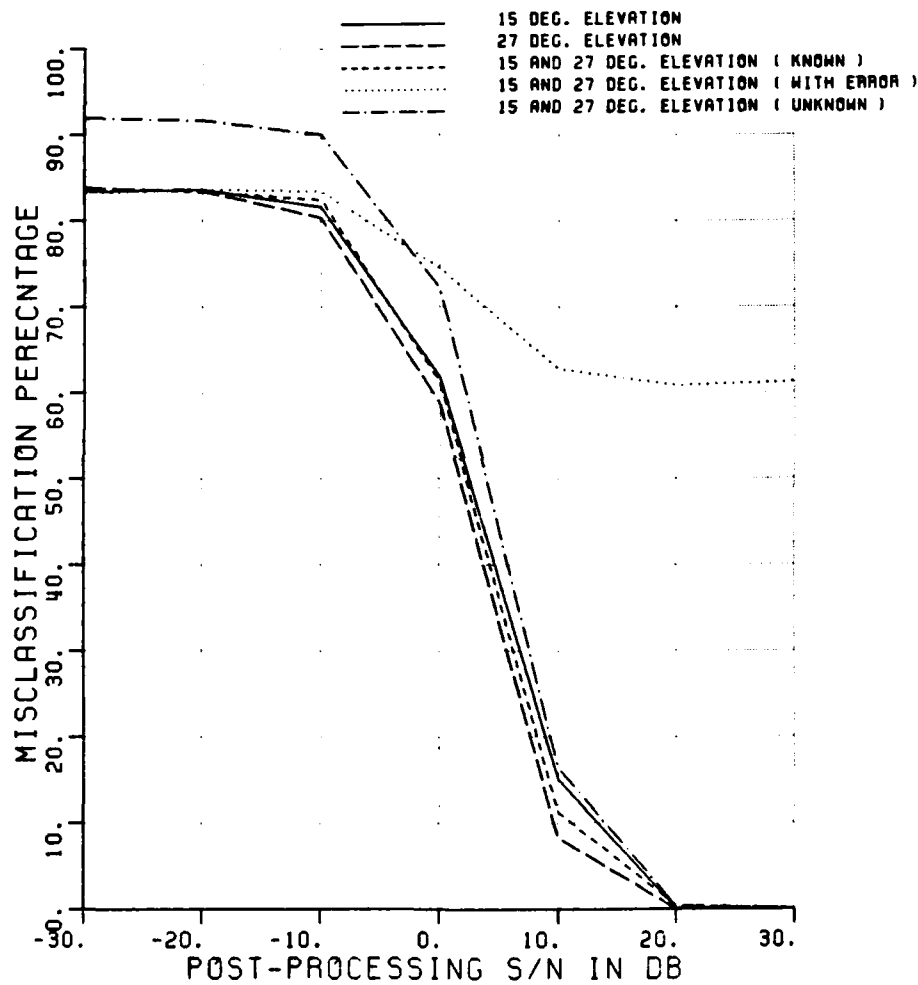


Figure A.26. Misclassification percentage versus post-processing SNR, comparing the performance of various elevation angles.

CLASSIFICATION OF SHIPS

POLARIZATION	X				
ELEV ASSUMED	KNOWN		/ UNKNOWN		
ELEVATION (DEG.)	15	27	15,27		
ASPECT ASSUMED	KNOWN				
MIN,MAX,INC ASPECT	170	180	10		
NO OF FREQUENCIES	8				
NO OF TARGETS	12	12	24	24	24
90% CI (@30%) +/-	3.1%	3.1%	2.2%	2.2%	2.2%
CLASS. FEATURES	A	A	A	A	
ELEV ERR IN CURVE	4				

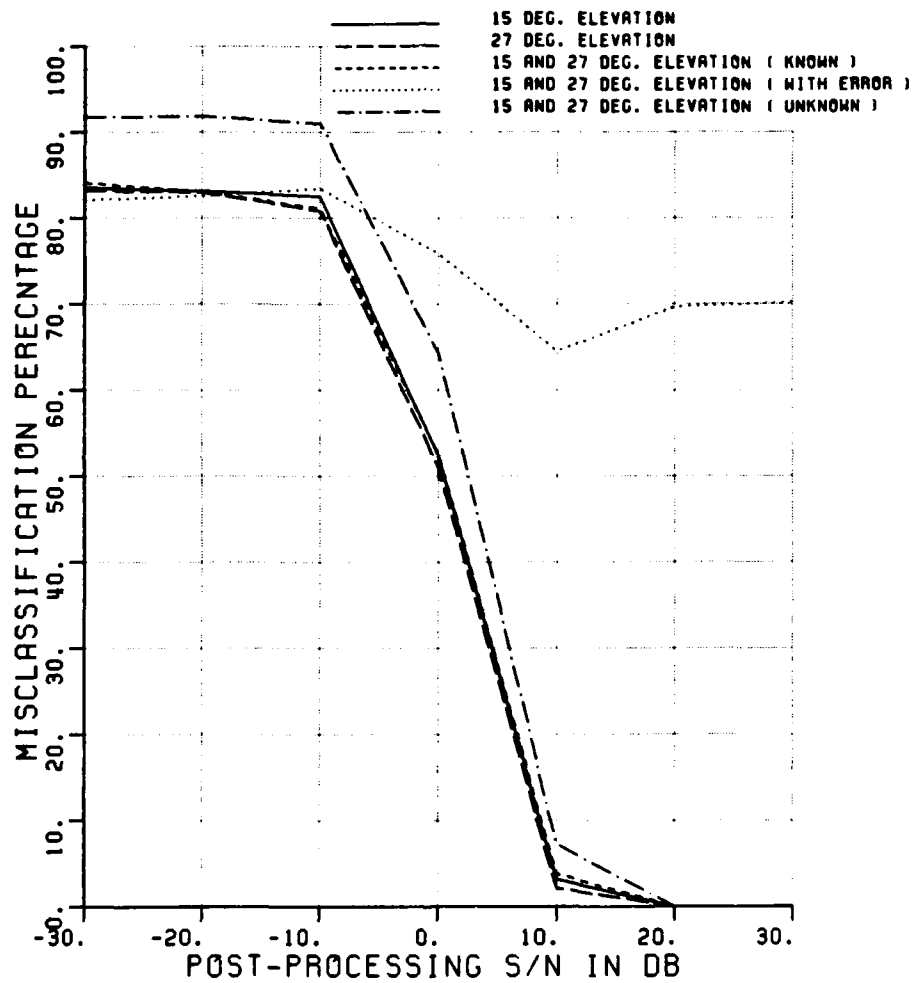


Figure A.27. Misclassification percentage versus post-processing SNR, comparing the performance of various elevation angles.

CLASSIFICATION OF SHIPS

POLARIZATION	V/H				
ELEV ASSUMED	KNOWN	/	UNKNOWN		
ELEVATION (DEG.)	15	27	15,27		
ASPECT ASSUMED	KNOWN				
MIN,MAX,INC ASPECT	80	100	10		
NO OF FREQUENCIES	8				
NO OF TARGETS	18	18	36	36	36
90% CI (@30%) +/-	2.5%	2.5%	1.8%	1.8%	1.8%
CLASS. FEATURES	A	A	A	A	
ELEV ERR IN CURVE	4				

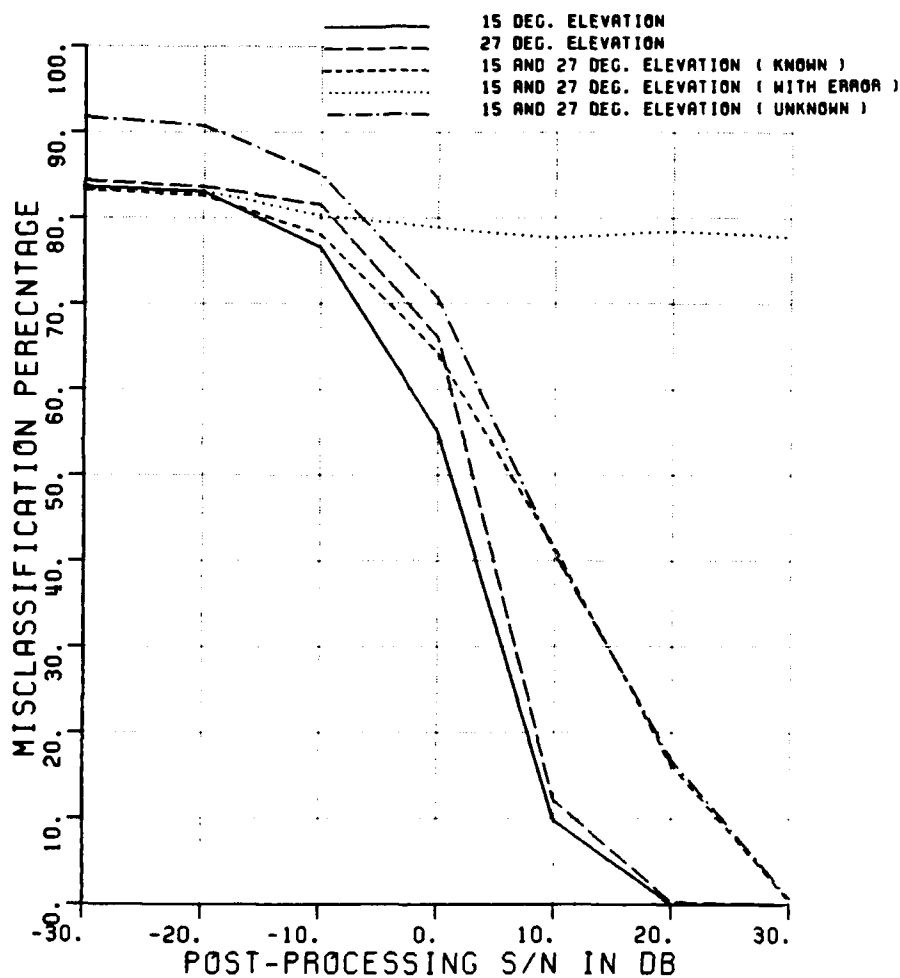


Figure A.28. Misclassification percentage versus post-processing SNR, comparing the performance of various elevation angles.

CLASSIFICATION OF SHIPS
 POLARIZATION V/H
 ELEV ASSUMED KNOWN / UNKNOWN
 ELEVATION (DEG.) 15 27 15,27
 ASPECT ASSUMED KNOWN
 MIN,MAX,INC ASPECT 170 180 10
 NO OF FREQUENCIES 8
 NO OF TARGETS 12 12 24 24 24
 90% CI (±30%) +/- 3.1% 3.1% 2.2% 2.2% 2.2%
 CLASS. FEATURES A A A A A
 ELEV ERR IN CURVE 4

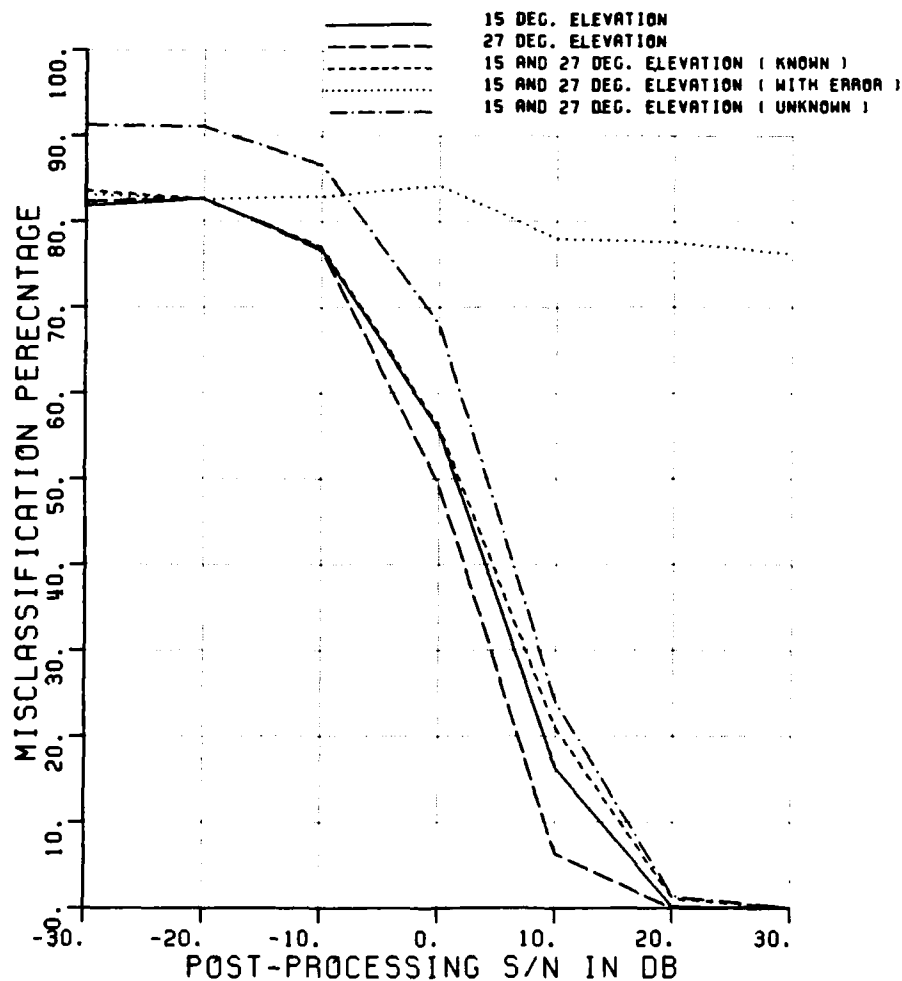


Figure A.29. Misclassification percentage versus post-processing SNR, comparing the performance of various elevation angles.

CLASSIFICATION OF SHIPS

POLARIZATION	V				
ELEV ASSUMED	KNOWN	/	UNKNOWN		
ELEVATION (DEG.)	15	27	15,27		
ASPECT ASSUMED	KNOWN				
MIN,MAX,INC ASPECT	0	10	10		
NO OF FREQUENCIES	8				
NO OF TARGETS	12	12	24	24	24
90% CI (±30%) +/-	3.1%	3.1%	2.2%	2.2%	2.2%
CLASS. FEATURES	A&W	A&W	A&W	A&W	A&W
ELEV ERR IN CURVE	4				

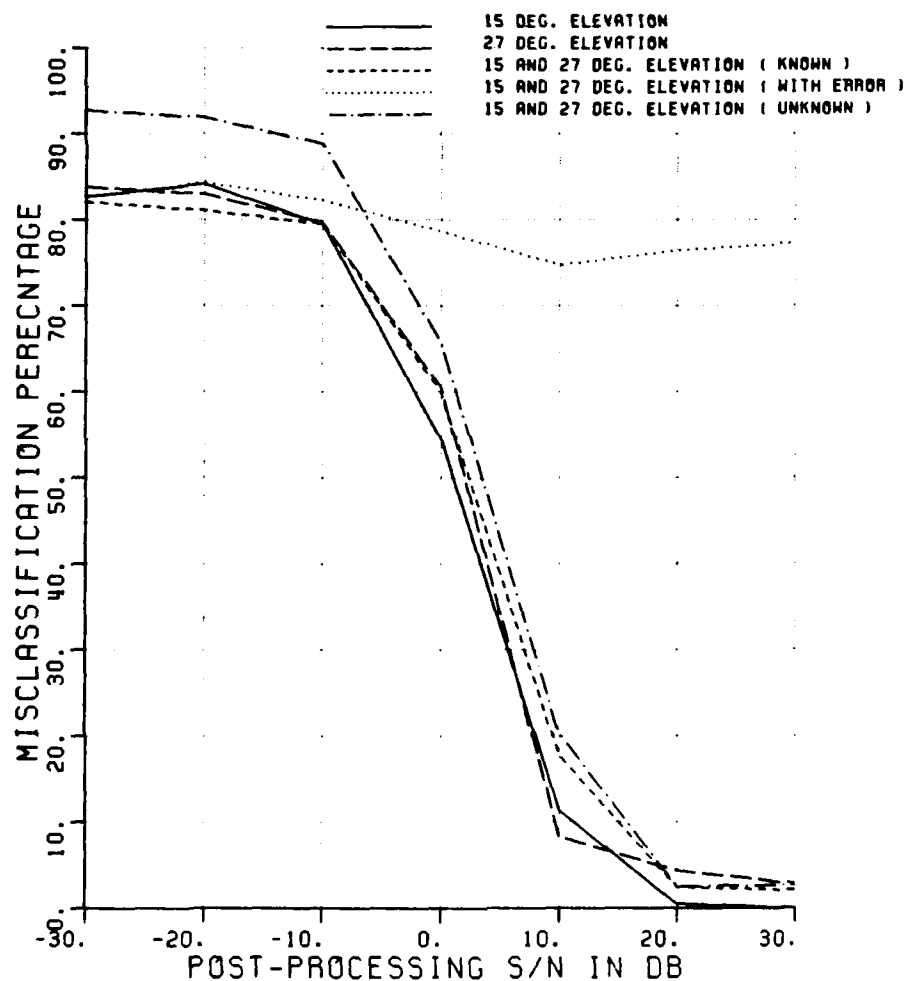


Figure A.30. Misclassification percentage versus post-processing SNR, comparing the performance of various elevation angles.

CLASSIFICATION OF SHIPS

POLARIZATION	V				
ELEV ASSUMED	KNOWN	/	UNKNOWN		
ELEVATION (DEG.)	15	27	15,27		
ASPECT ASSUMED	KNOWN				
MIN,MAX,INC ASPECT	80	100	10		
NO OF FREQUENCIES	8				
NO OF TARGETS	18	18	36	36	36
90% C1 (±30%) +/-	2.5%	2.5%	1.8%	1.8%	1.8%
CLASS. FEATURES	A&W	A&W	A&W	A&W	A&W
ELEV ERR IN CURVE	4				

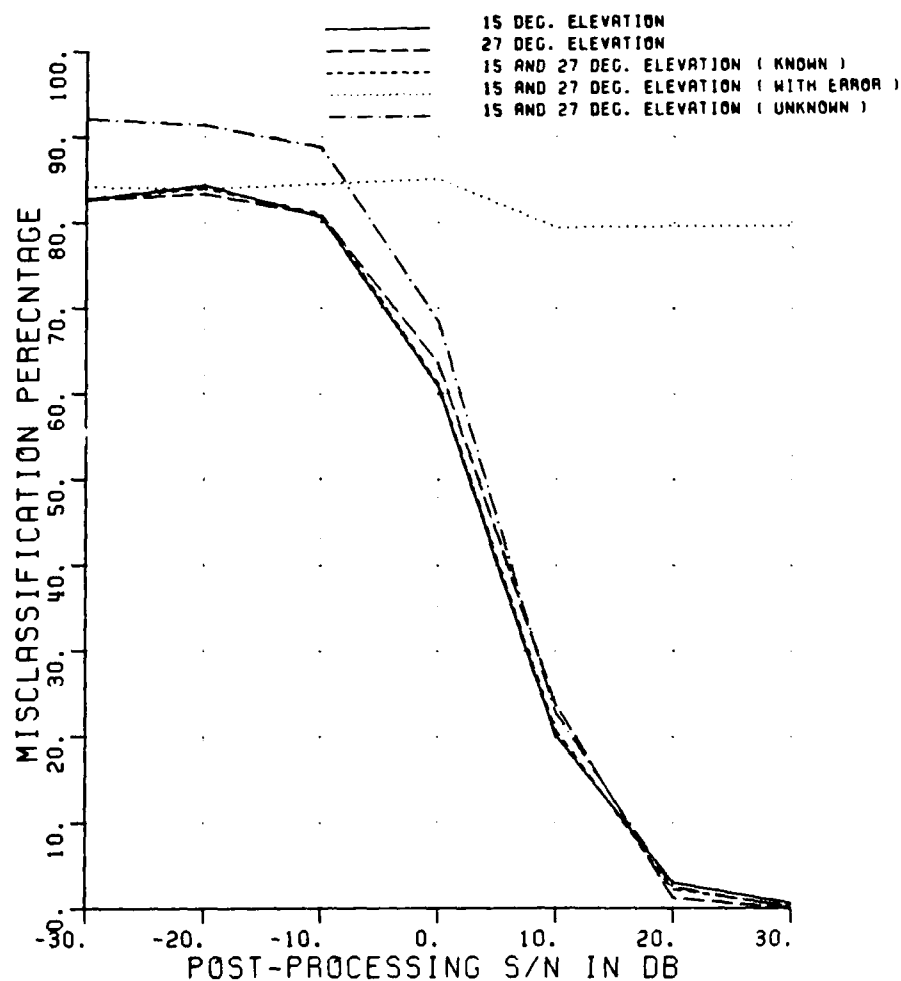


Figure A.31. Misclassification percentage versus post-processing SNR, comparing the performance of various elevation angles.

CLASSIFICATION OF SHIPS

POLARIZATION	V				
ELEV ASSUMED	KNOWN	/	UNKNOWN		
ELEVATION (DEG.)	15	27	15,27		
ASPECT ASSUMED	KNOWN				
MIN,MAX,INC ASPECT	170	180	10		
NO OF FREQUENCIES	8				
NO OF TARGETS	12	12	24	24	24
90% CI (@30%) +/-	3.1%	3.1%	2.2%	2.2%	2.2%
CLASS. FEATURES	A&W	A&W	A&W	A&W	A&W
ELEV ERR IN CURVE	4				

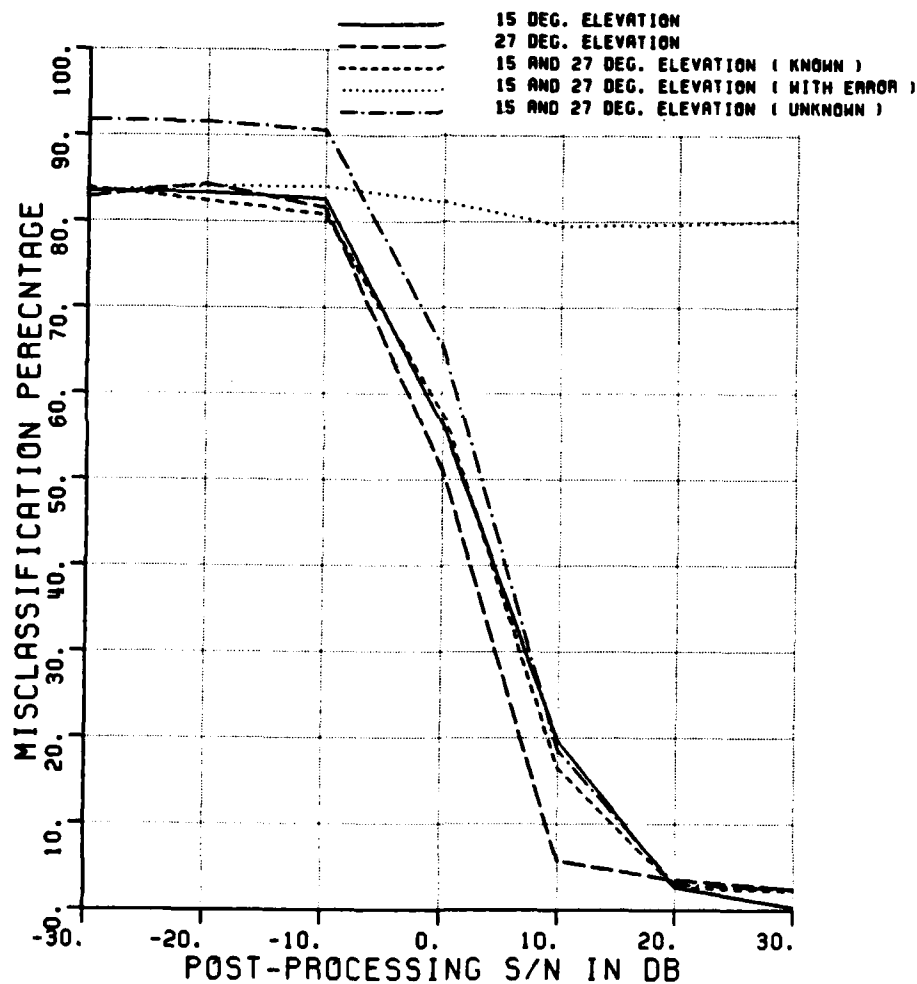


Figure A.32. Misclassification percentage versus post-processing SNR, comparing the performance of various elevation angles.

CLASSIFICATION OF SHIPS

POLARIZATION	H				
ELEV ASSUMED	KNOWN	/ UNKNOWN			
ELEVATION (DEG.)	15	27	15,27		
ASPECT ASSUMED	KNOWN				
MIN,MAX,INC ASPECT	0	10	10		
NO OF FREQUENCIES	8				
NO OF TARGETS	12	12	24	24	24
90% CI (±30%) +/-	3.1%	3.1%	2.2%	2.2%	2.2%
CLASS. FEATURES	A&W	A&W	A&W	A&W	A&W
ELEV ERR IN CURVE	4				

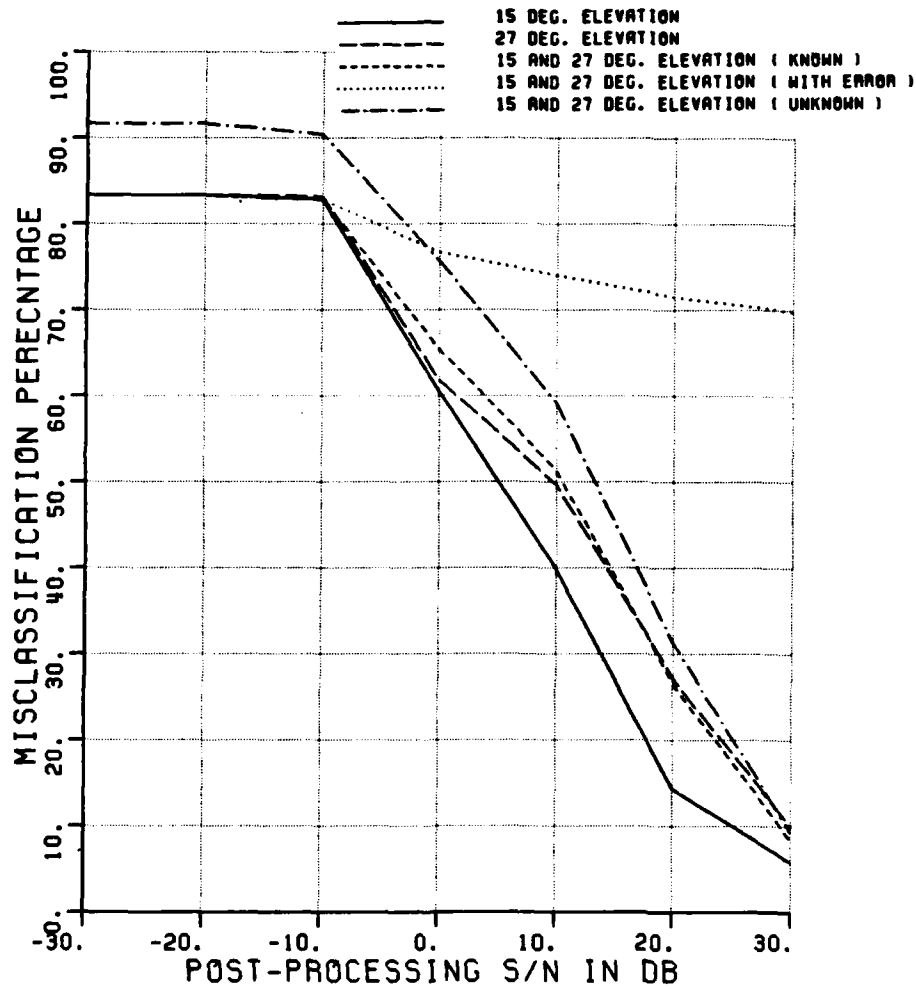


Figure A.33. Misclassification percentage versus post-processing SNR, comparing the performance of various elevation angles.

CLASSIFICATION OF SHIPS

POLARIZATION	H				
ELEV ASSUMED	KNOWN	/	UNKNOWN		
ELEVATION (DEG.)	15	27	15,27		
ASPECT ASSUMED	KNOWN				
MIN,MAX,INC ASPECT	80	100	10		
NO OF FREQUENCIES	8				
NO OF TARGETS	18	18	36	36	36
90% CI (@30%) +/-	2.5%	2.5%	1.8%	1.8%	1.8%
CLASS. FEATURES	A4W	A4W	A4W	A4W	A4W
ELEV ERR IN CURVE	4				

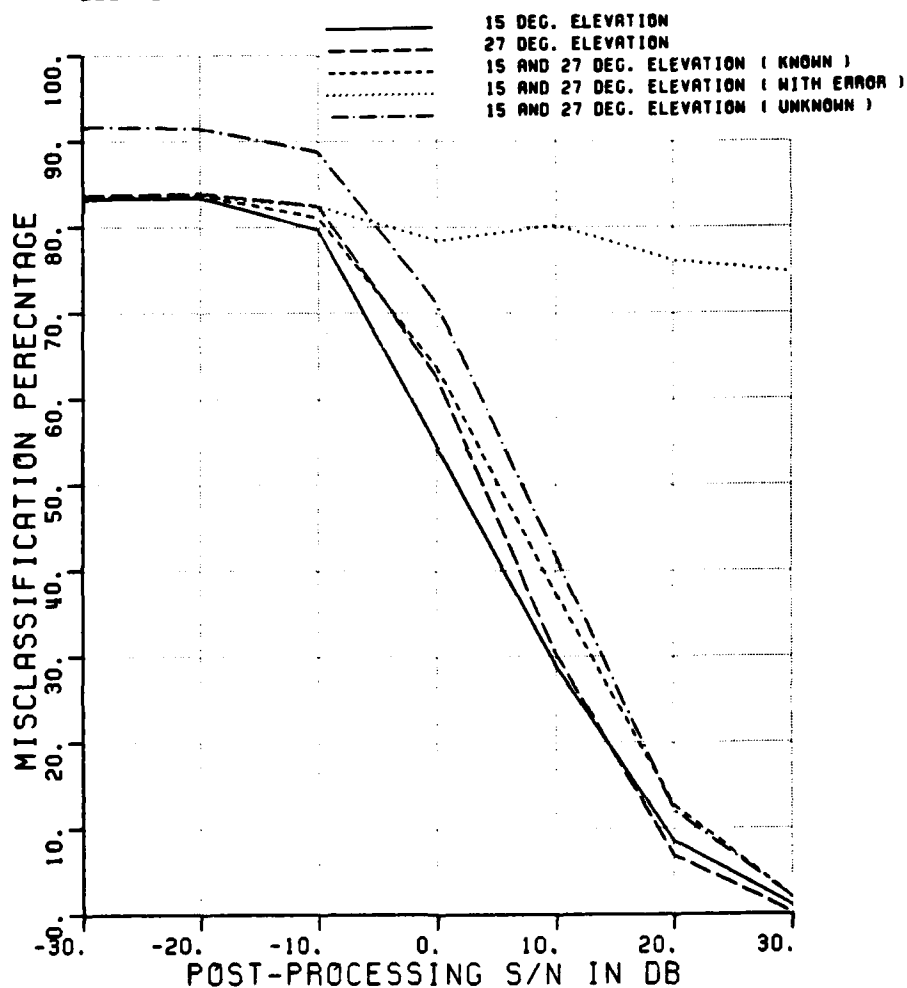


Figure A.34. Misclassification percentage versus post-processing SNR, comparing the performance of various elevation angles.

CLASSIFICATION OF SHIPS

POLARIZATION	H				
ELEV ASSUMED	KNOWN	/ UNKNOWN			
ELEVATION (DEG.)	15	27	15,27		
ASPECT ASSUMED	KNOWN				
MIN,MAX,INC ASPECT	170	180	10		
NO OF FREQUENCIES	8				
NO OF TARGETS	12	12	24	24	24
90% CI (±30%) +/-	3.1%	3.1%	2.2%	2.2%	2.2%
CLASS. FEATURES	A&W	A&W	A&W	A&W	A&W
ELEV ERR IN CURVE	4				

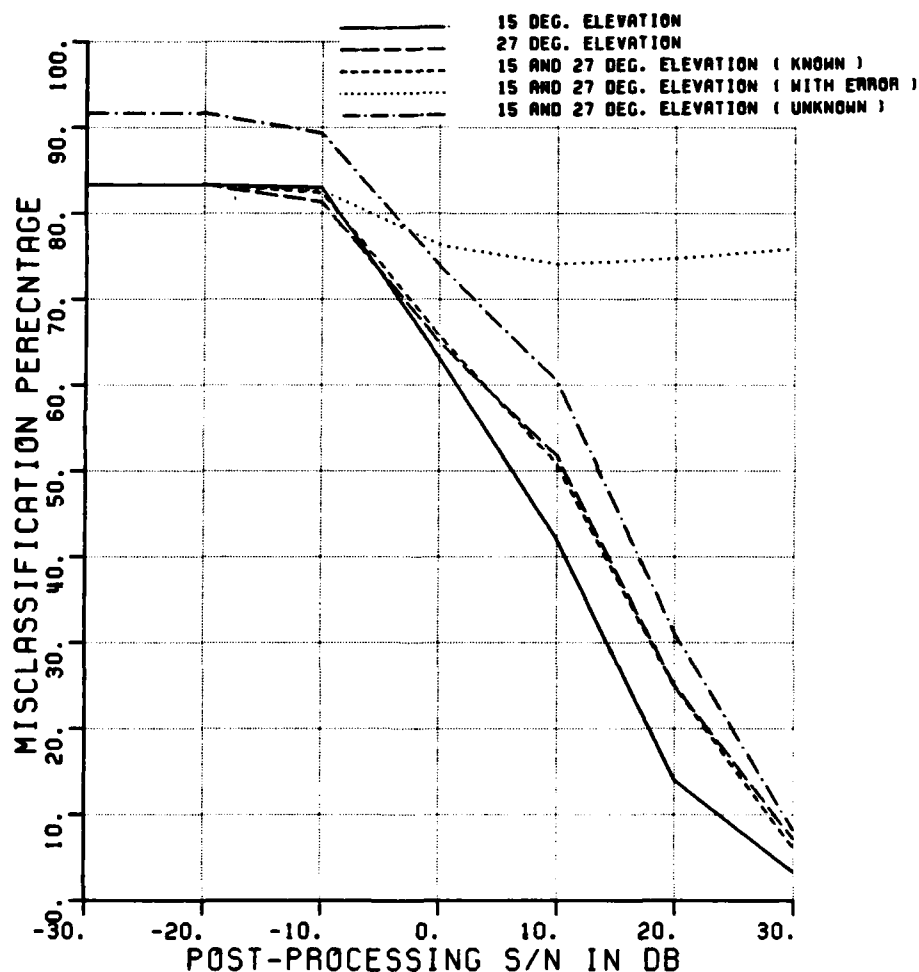


Figure A.35. Misclassification percentage versus post-processing SNR, comparing the performance of various elevation angles.

CLASSIFICATION OF SHIPS

POLARIZATION	X				
ELEV ASSUMED	KNOWN	/ UNKNOWN			
ELEVATION (DEG.)	15	27	15,27		
ASPECT ASSUMED	KNOWN				
MIN,MAX,INC ASPECT	0	10	10		
NO OF FREQUENCIES	8				
NO OF TARGETS	12	12	24	24	24
90% CI (@30%) +/-	3.1%	3.1%	2.2%	2.2%	2.2%
CLASS. FEATURES	A4W	A4W	A4W	A4W	A4W
ELEV ERR IN CURVE	4				

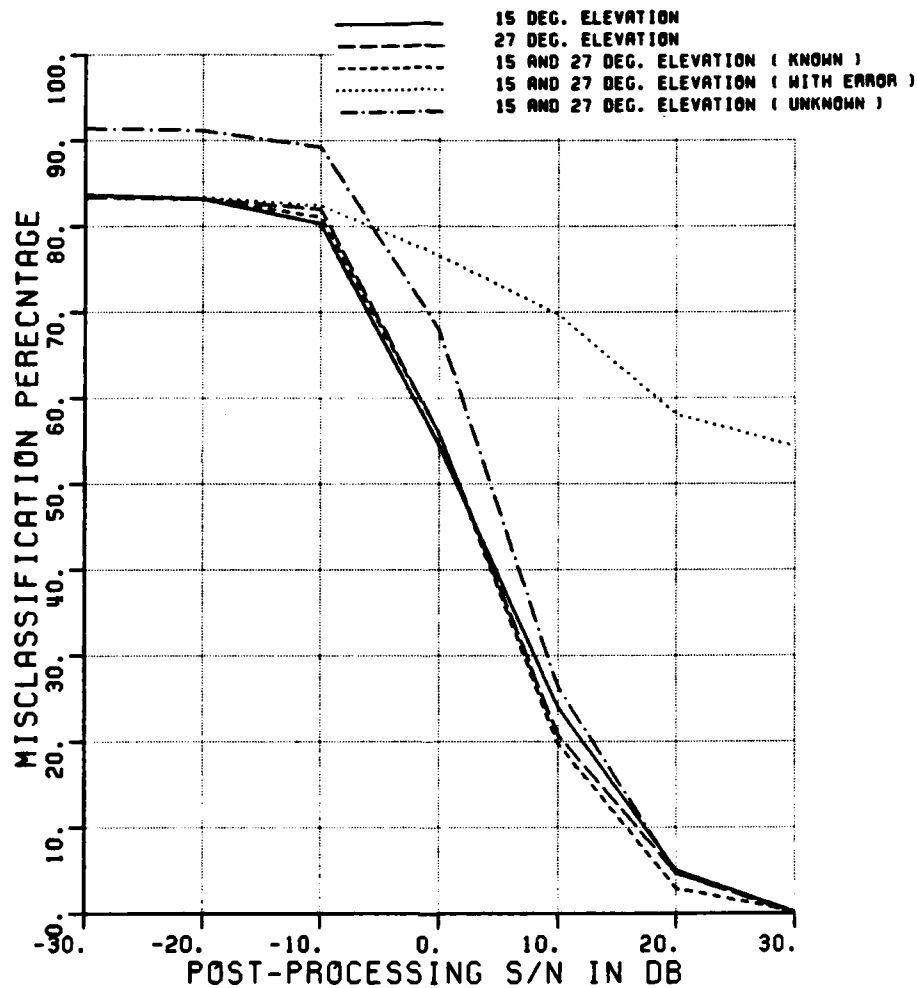


Figure A.36. Misclassification percentage versus post-processing SNR, comparing the performance of various elevation angles.

CLASSIFICATION OF SHIPS

POLARIZATION	X				
ELEV ASSUMED	KNOWN	/	UNKNOWN		
ELEVATION (DEG.)	15	27	15,27		
ASPECT ASSUMED	KNOWN				
MIN,MAX,INC ASPECT	80	100	10		
NO OF FREQUENCIES	8				
NO OF TARGETS	18	18	36	36	36
90% CI (±30%) +/-	2.5%	2.5%	1.8%	1.8%	1.8%
CLASS. FEATURES	A4W	A4W	A4W	A4W	A4W
ELEV ERR IN CURVE	4				

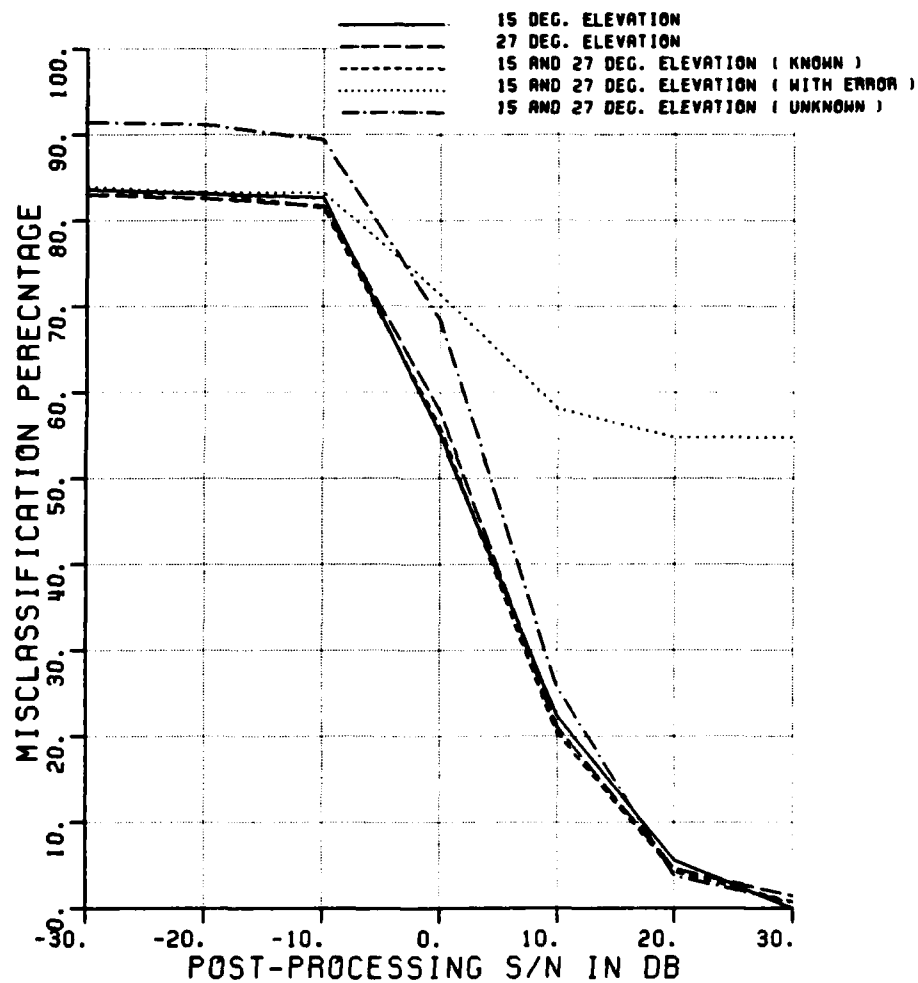


Figure A.37. Misclassification percentage versus post-processing SNR, comparing the performance of various elevation angles.

CLASSIFICATION OF SHIPS

POLARIZATION	X				
ELEV ASSUMED	KNOWN		/ UNKNOWN		
ELEVATION (DEG.)	15	27	15,27		
ASPECT ASSUMED	KNOWN				
MIN,MAX,INC ASPECT	170	180	10		
NO OF FREQUENCIES	8				
NO OF TARGETS	12	12	24	24	24
90% CI (±30%) +/-	3.1%	3.1%	2.2%	2.2%	2.2%
CLASS. FEATURES	A&W	A&W	A&W	A&W	A&W
ELEV ERR IN CURVE	4				

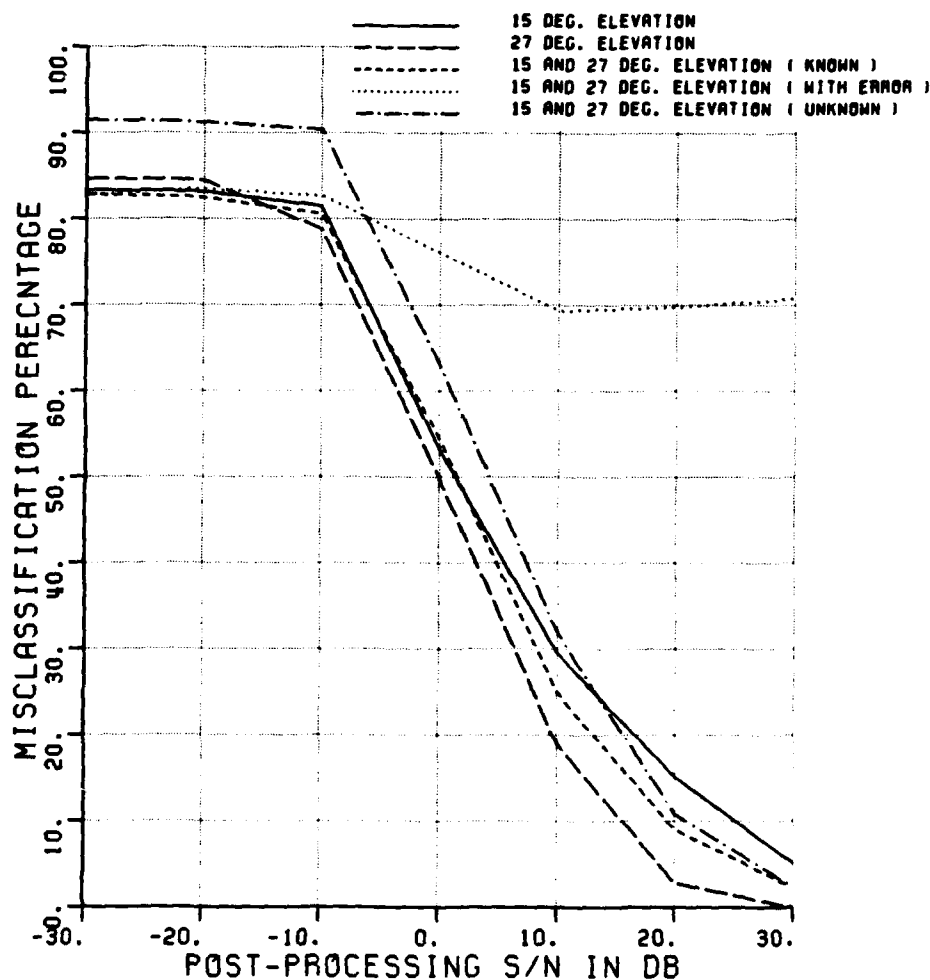


Figure A.38. Misclassification percentage versus post-processing SNR, comparing the performance of various elevation angles.

CLASSIFICATION OF SHIPS
 POLARIZATION V/H
 ELEV ASSUMED KNOWN / UNKNOWN
 ELEVATION (DEG.) 15 27 15.27
 ASPECT ASSUMED KNOWN
 MIN,MAX,INC ASPECT 0 10 10
 NO OF FREQUENCIES 8
 NO OF TARGETS 12 12 24 24 24
 90% CI (±30%) +/- 3.1% 3.1% 2.2% 2.2% 2.2%
 CLASS. FEATURES A&W A&W A&W A&W A&W
 ELEV ERR IN CURVE 4

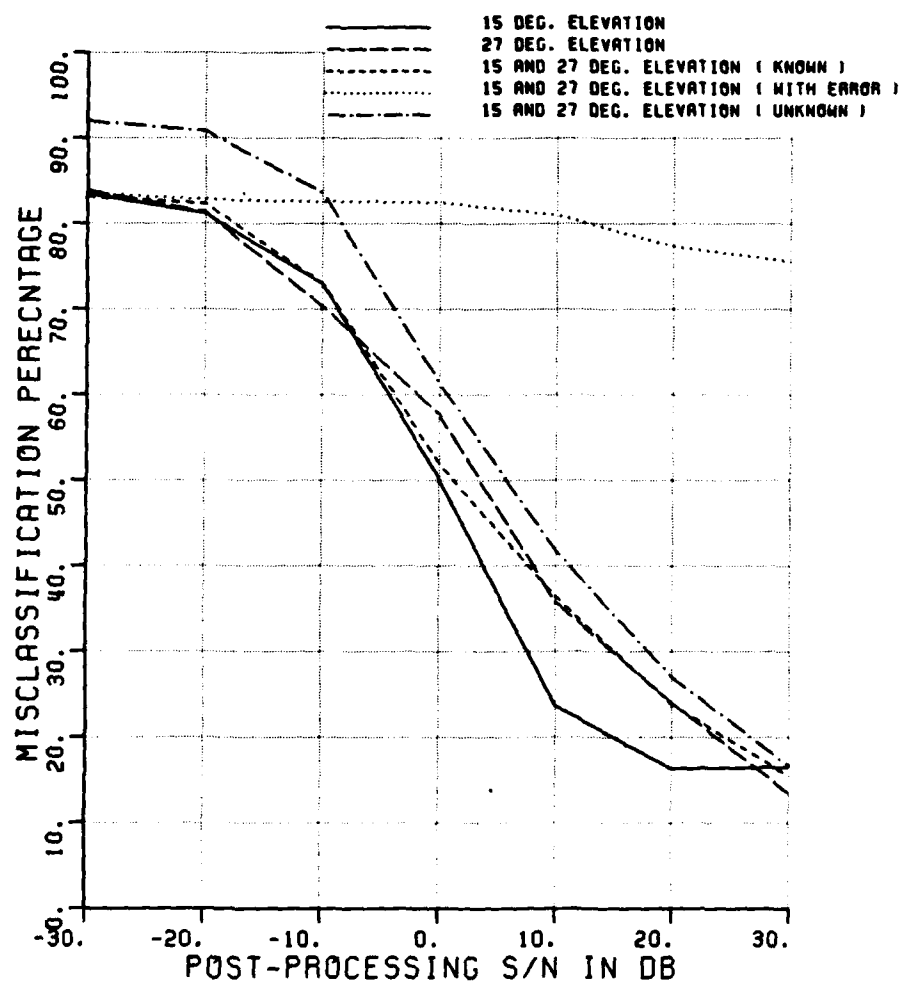


Figure A.39. Misclassification percentage versus post-processing SNR, comparing the performance of various elevation angles.

CLASSIFICATION OF SHIPS

POLARIZATION	V/H				
ELEV ASSUMED	KNOWN	/	UNKNOWN		
ELEVATION (DEG.)	15	27	15,27		
ASPECT ASSUMED	KNOWN				
MIN,MAX,INC ASPECT	80	100	10		
NO OF FREQUENCIES	8				
NO OF TARGETS	18	18	36	36	36
90% CI (@30%) +/-	2.5%	2.5%	1.8%	1.8%	1.8%
CLASS. FEATURES	A&W	A&W	A&W	A&W	A&W
ELEV ERR IN CURVE	4				

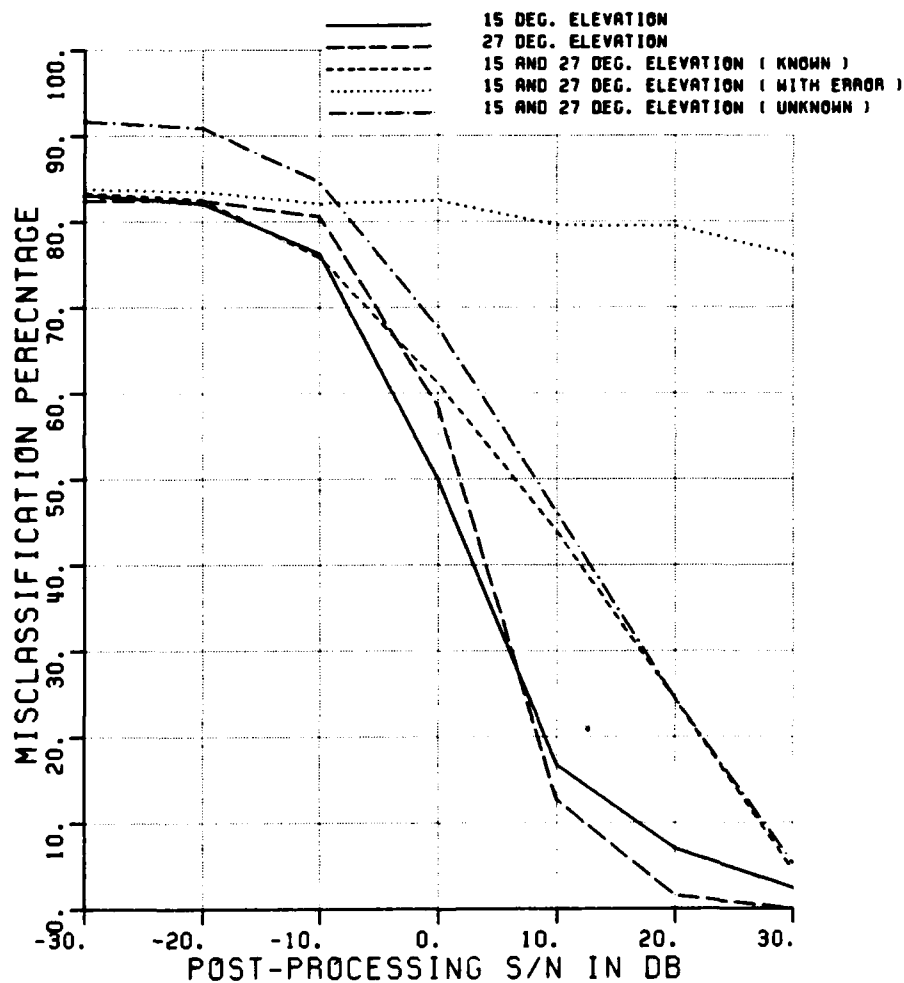


Figure A.40. Misclassification percentage versus post-processing SNR, comparing the performance of various elevation angles.

CLASSIFICATION OF SHIPS

POLARIZATION	V/H				
ELEV ASSUMED	KNOWN	/	UNKNOWN		
ELEVATION (DEG.)	15	27	15,27		
ASPECT ASSUMED	KNOWN				
MIN,MAX,INC ASPECT	170	180	10		
NO OF FREQUENCIES	8				
NO OF TARGETS	12	12	24	24	24
90% CI (@30%) +/-	3.1%	3.1%	2.2%	2.2%	2.2%
CLASS. FEATURES	A&W	A&W	A&W	A&W	A&W
ELEV ERR IN CURVE	4				

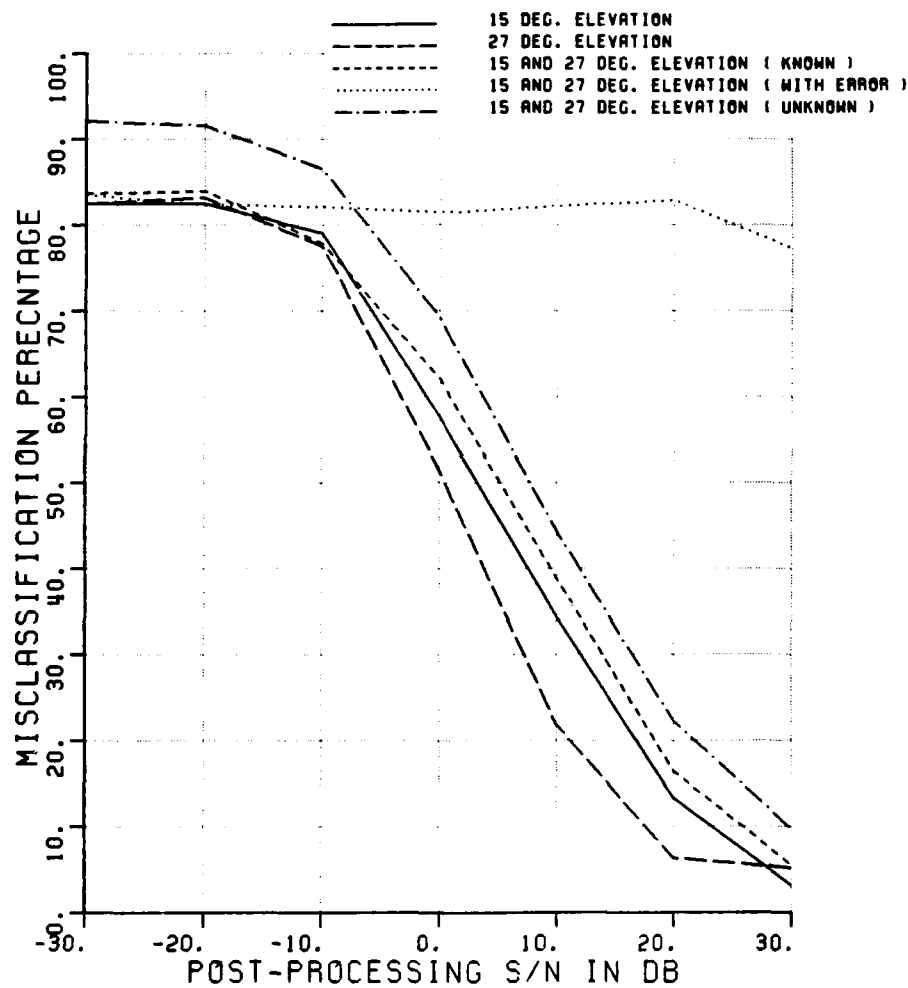


Figure A.41. Misclassification percentage versus post-processing SNR, comparing the performance of various elevation angles.

CLASSIFICATION OF SHIPS

POLARIZATION	V				
ELEV ASSUMED	KNOWN	/		UNKNOWN	
ELEVATION (DEG.)	15	27	15,27		
ASPECT ASSUMED	KNOWN				
MIN,MAX,INC ASPECT	0	10	10		
NO OF FREQUENCIES	8				
NO OF TARGETS	12	12	24	24	24
90% CI (@30%) +/-	3.1%	3.1%	2.2%	2.2%	2.2%
CLASS. FEATURES	R	R	R	R	R
ELEV ERR IN CURVE	4				

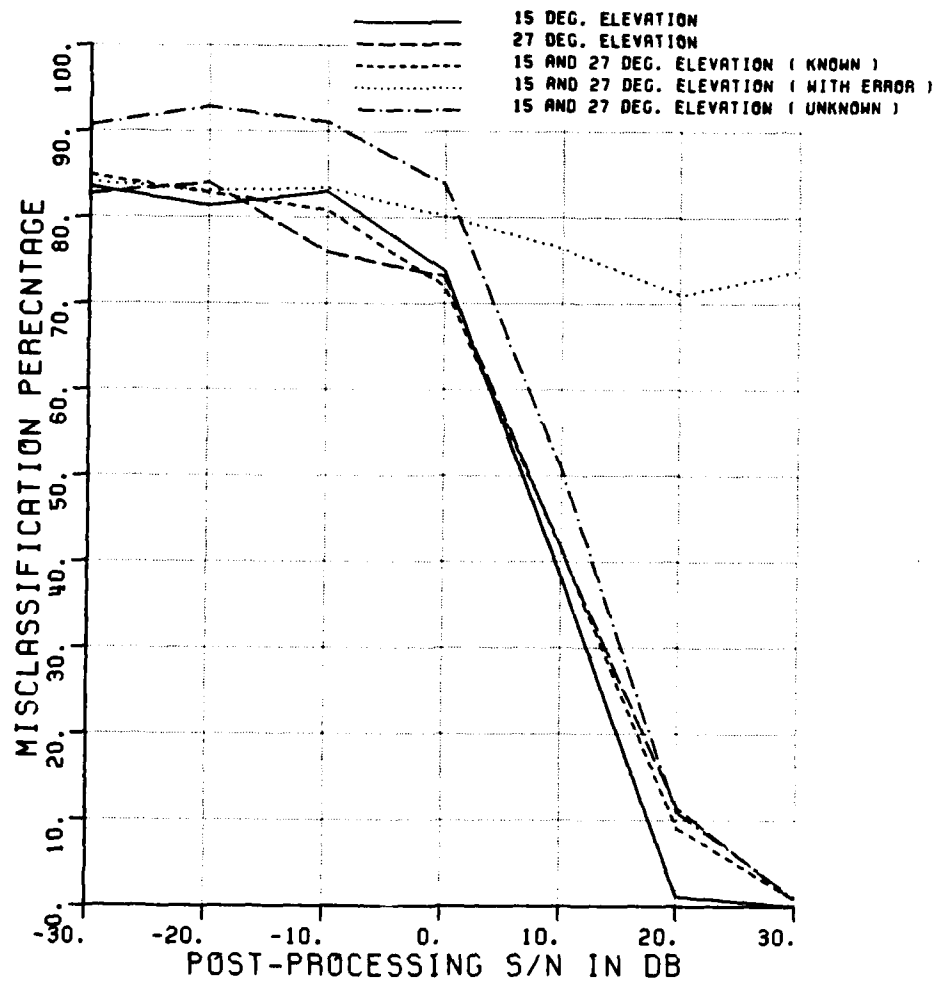


Figure A.42. Misclassification percentage versus post-processing SNR, comparing the performance of various elevation angles.

CLASSIFICATION OF SHIPS
 POLARIZATION V
 ELEV ASSUMED KNOWN / UNKNOWN
 ELEVATION (DEG.) 15 27 15,27
 ASPECT ASSUMED KNOWN
 MIN,MAX,INC ASPECT 80 100 10
 NO OF FREQUENCIES 8
 NO OF TARGETS 18 18 36 36 36
 90% CI ($\pm 30\%$) \pm 2.5% 2.5% 1.8% 1.8% 1.8%
 CLASS. FEATURES R R R R R
 ELEV ERR IN CURVE 4

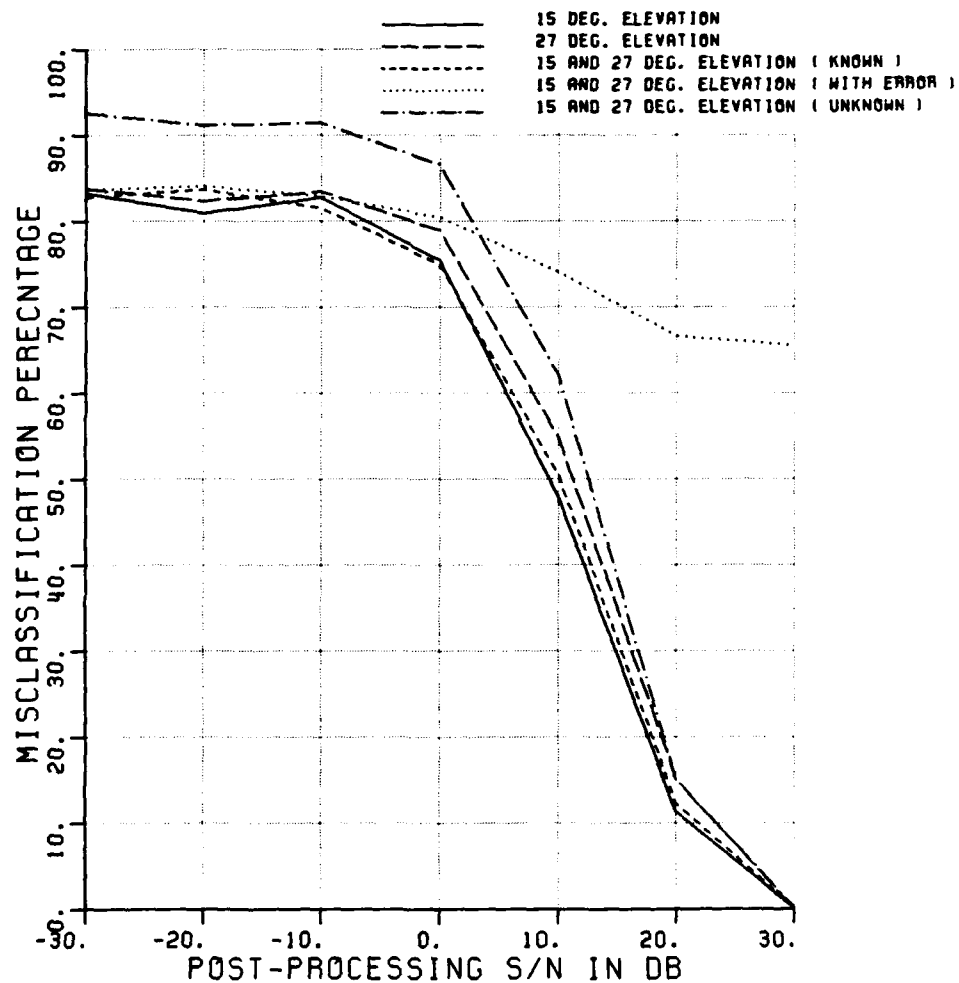


Figure A.43. Misclassification percentage versus post-processing SNR, comparing the performance of various elevation angles.

CLASSIFICATION OF SHIPS

POLARIZATION	V				
ELEV ASSUMED	KNOWN	/	UNKNOWN		
ELEVATION (DEG.)	15	27	15,27		
ASPECT ASSUMED	KNOWN				
MIN,MAX,INC ASPECT	170	180	10		
NO OF FREQUENCIES	8				
NO OF TARGETS	12	12	24	24	24
90% CI (±30%) +/-	3.1%	3.1%	2.2%	2.2%	2.2%
CLASS. FEATURES	A	A	A	A	A
ELEV ERR IN CURVE	4				

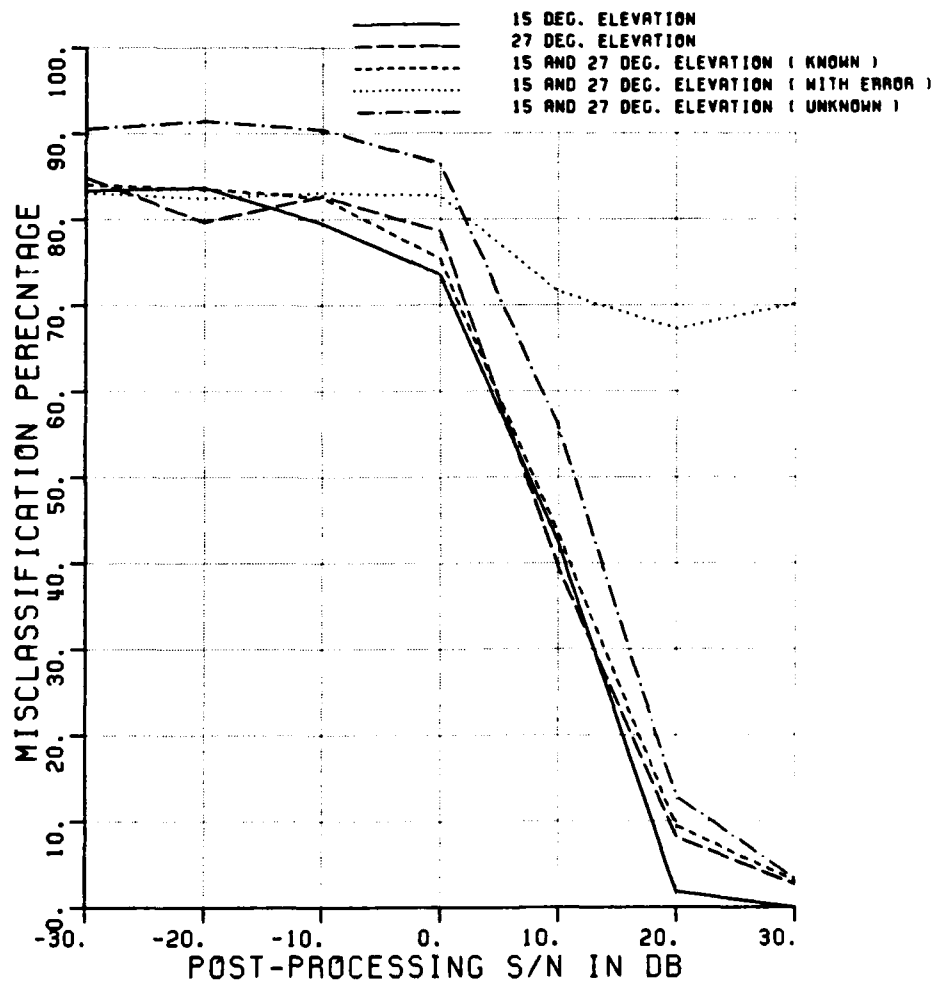


Figure A.44. Misclassification percentage versus post-processing SNR, comparing the performance of various elevation angles.

CLASSIFICATION OF SHIPS

POLARIZATION	H				
ELEV ASSUMED	KNOWN / UNKNOWN				
ELEVATION (DEG.)	15	27	15,27		
ASPECT ASSUMED	KNOWN				
MIN,MAX,INC ASPECT	0	10	10		
NO OF FREQUENCIES	8				
NO OF TARGETS	12	12	24	24	24
90% CI (±30%) +/-	3.1%	3.1%	2.2%	2.2%	2.2%
CLASS. FEATURES	A	A	A	A	A
ELEV ERR IN CURVE	4				

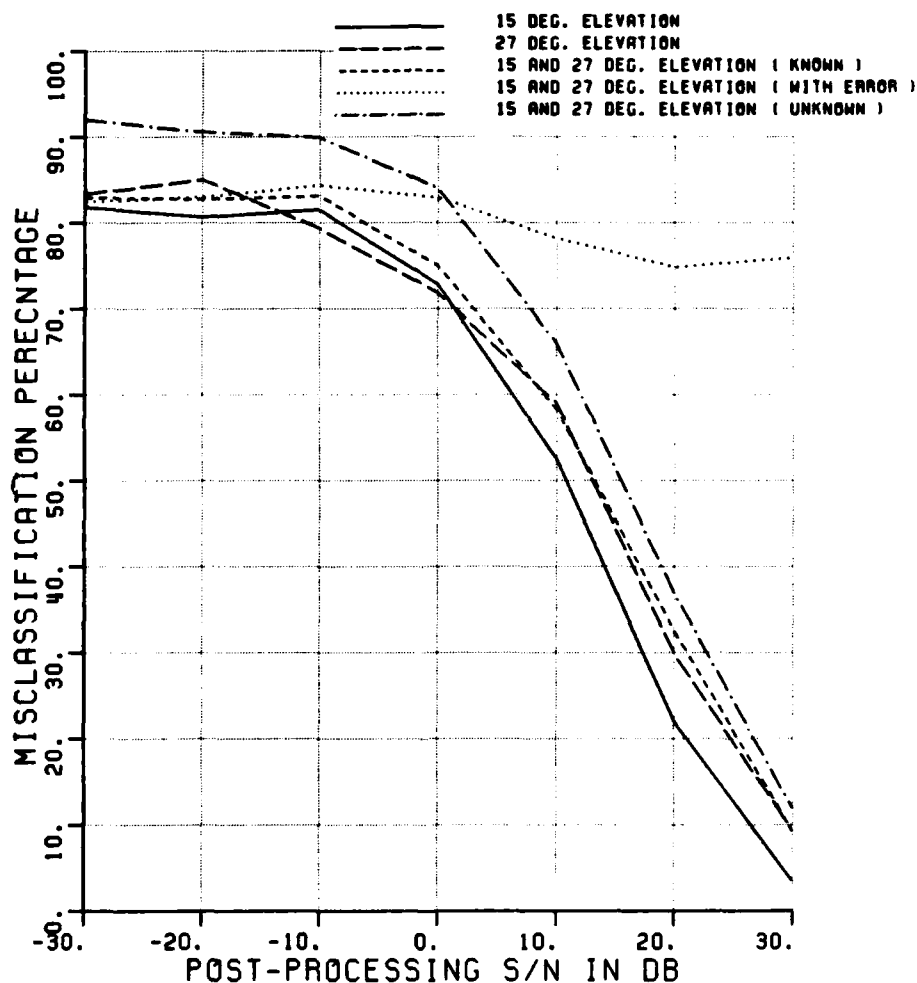


Figure A.45. Misclassification percentage versus post-processing SNR, comparing the performance of various elevation angles.

CLASSIFICATION OF SHIPS

POLARIZATION	H				
ELEV ASSUMED	KNOWN	/	UNKNOWN		
ELEVATION (DEG.)	15	27	15,27		
ASPECT ASSUMED	KNOWN				
MIN,MAX,INC ASPECT	80	100	10		
NO OF FREQUENCIES	8				
NO OF TARGETS	18	18	36	36	36
90% CI (@30%) +/-	2.5%	2.5%	1.8%	1.8%	1.8%
CLASS. FEATURES	R	R	R	R	
ELEV ERR IN CURVE	4				

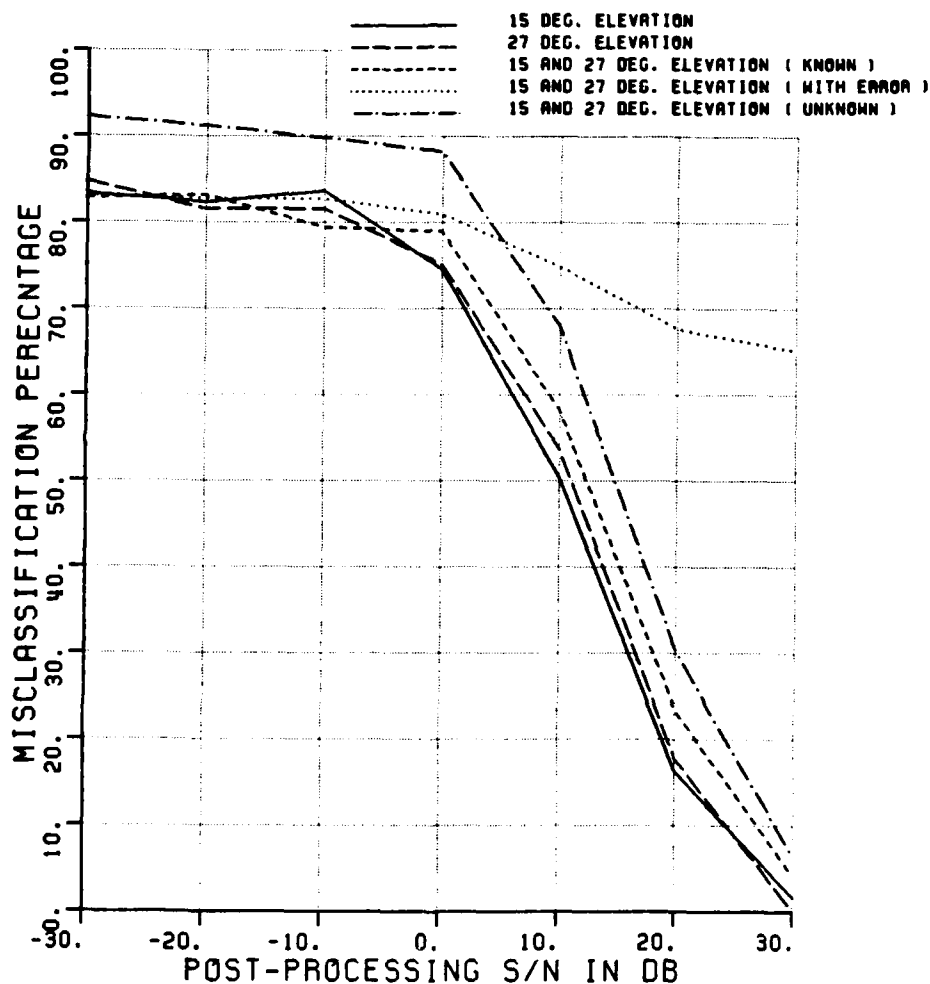


Figure A.46. Misclassification percentage versus post-processing SNR, comparing the performance of various elevation angles.

CLASSIFICATION OF SHIPS

POLARIZATION	H				
ELEV ASSUMED	KNOWN / UNKNOWN				
ELEVATION (DEG.)	15	27	15,27		
ASPECT ASSUMED	KNOWN				
MIN,MAX,INC ASPECT	170	180	10		
NO OF FREQUENCIES	8				
NO OF TARGETS	12	12	24	24	24
90% CI (±30%) +/-	3.1%	3.1%	2.2%	2.2%	2.2%
CLASS. FEATURES	A	A	A	A	
ELEV ERR IN CURVE	4				

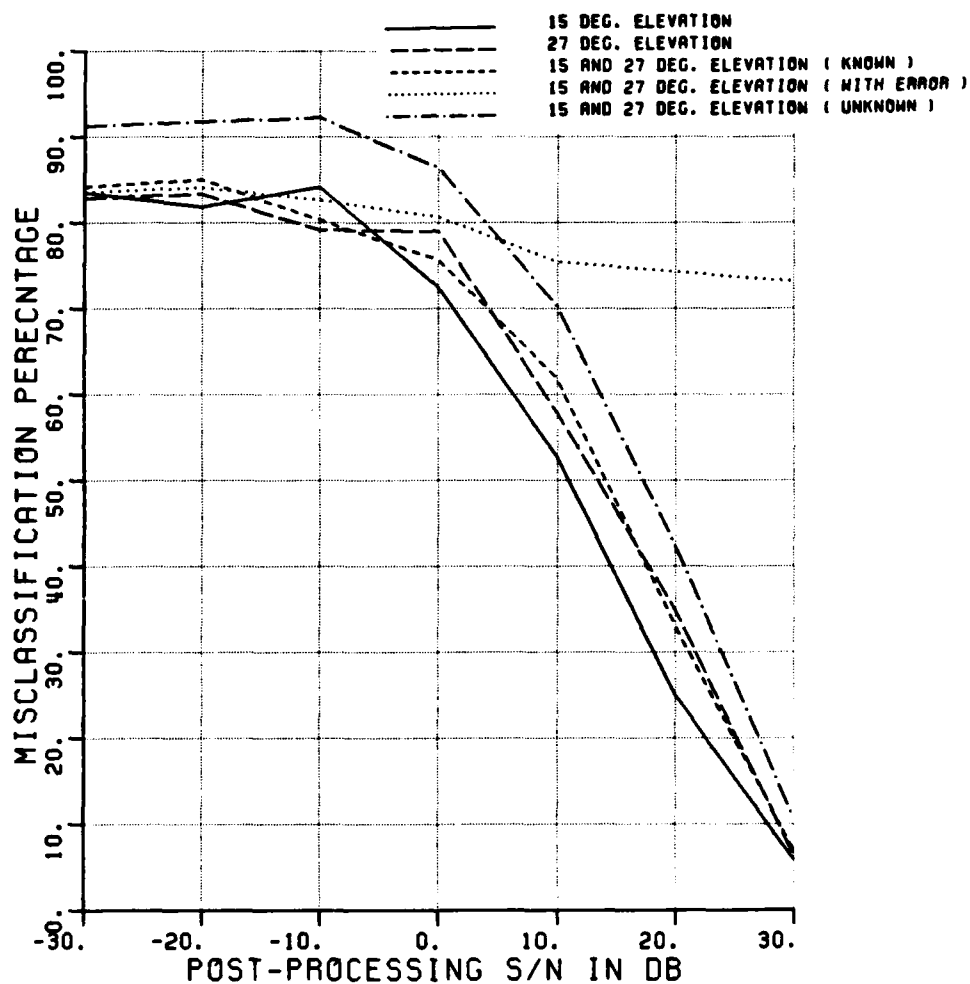


Figure A.47. Misclassification percentage versus post-processing SNR, comparing the performance of various elevation angles.

CLASSIFICATION OF SHIPS

POLARIZATION	X				
ELEV ASSUMED	KNOWN	/	UNKNOWN		
ELEVATION (DEG.)	15	27	15,27		
ASPECT ASSUMED	KNOWN				
MIN,MAX,INC ASPECT	0	10	10		
NO OF FREQUENCIES	8				
NO OF TARGETS	12	12	24	24	24
90% CI (±30%) +/-	3.1%	3.1%	2.2%	2.2%	2.2%
CLASS. FEATURES	A	A	A	A	A
ELEV ERR IN CURVE	4				

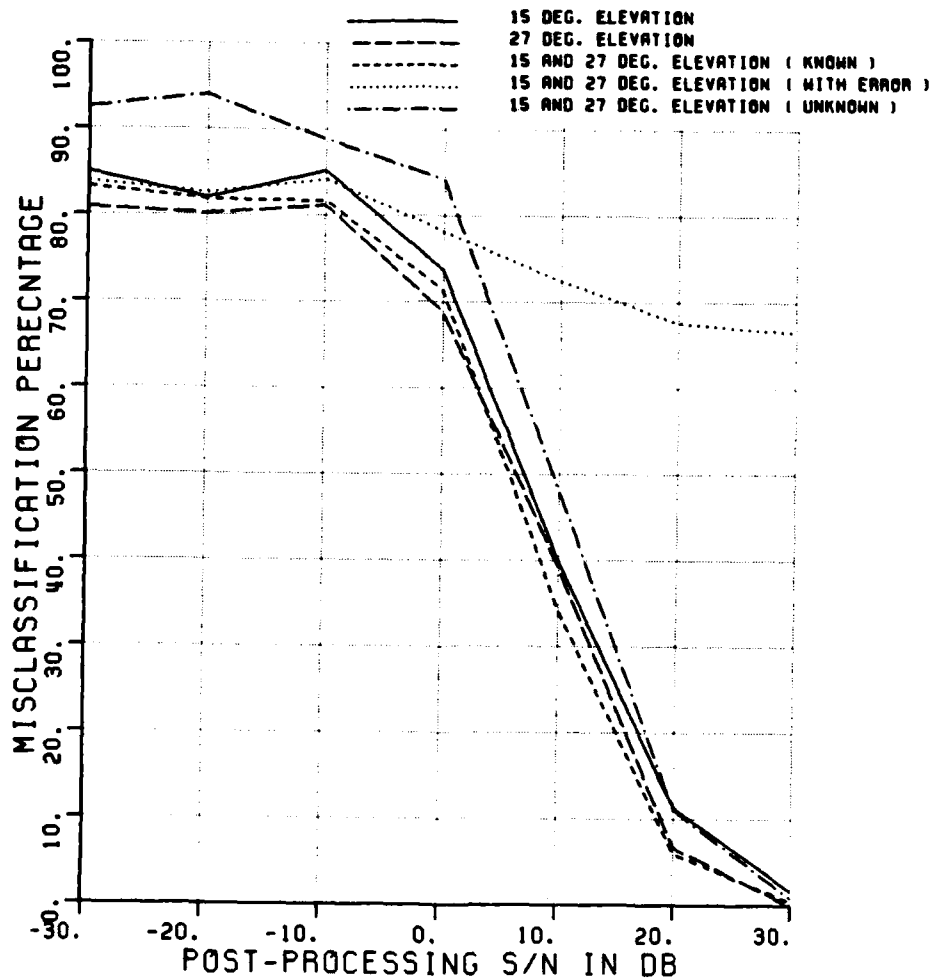


Figure A.48. Misclassification percentage versus post-processing SNR, comparing the performance of various elevation angles.

CLASSIFICATION OF SHIPS

POLARIZATION	X				
ELEV ASSUMED	KNOWN		/ UNKNOWN		
ELEVATION (DEG.)	15	27	15,27		
ASPECT ASSUMED	KNOWN				
MIN,MAX,INC ASPECT	80	100	10		
NO OF FREQUENCIES	8				
NO OF TARGETS	18	18	36	36	36
90% CI (@30%) +/-	2.5%	2.5%	1.8%	1.8%	1.8%
CLASS. FEATURES	R	R	R	R	R
ELEV ERR IN CURVE	4				

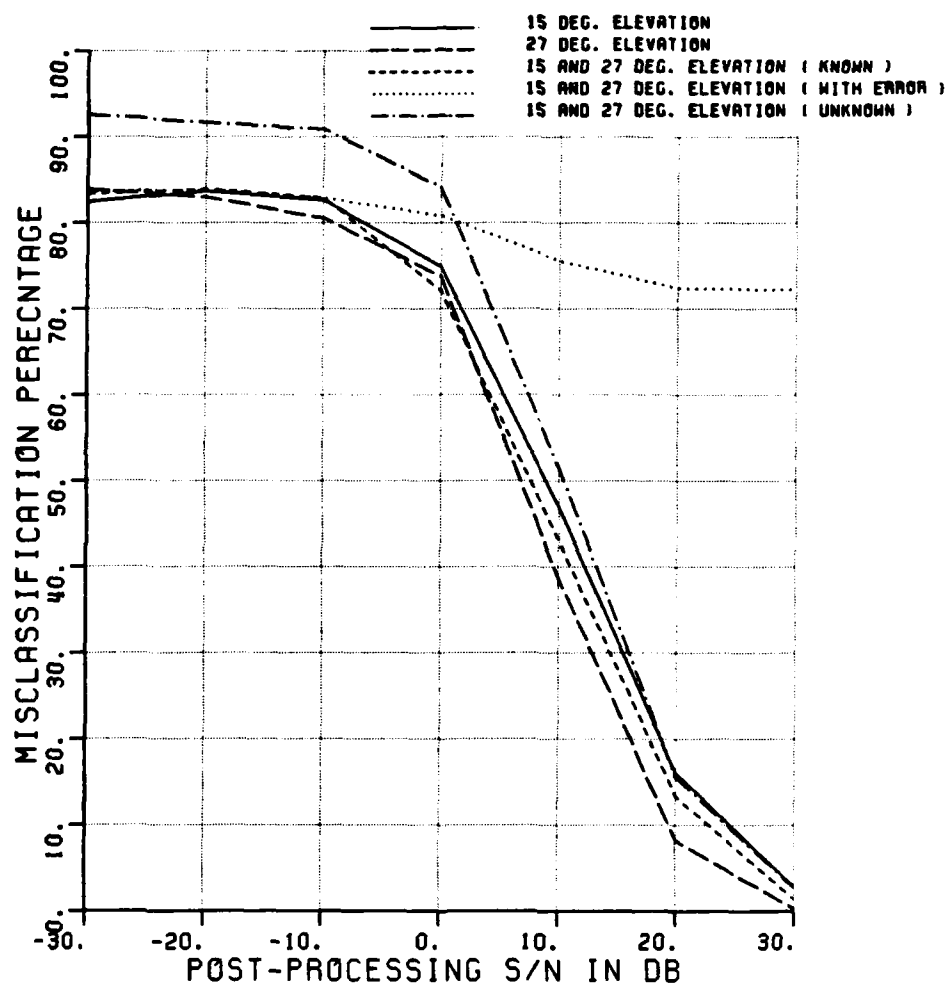


Figure A.49. Misclassification percentage versus post-processing SNR, comparing the performance of various elevation angles.

CLASSIFICATION OF SHIPS

POLARIZATION	X				
ELEV ASSUMED	KNOWN	/ UNKNOWN			
ELEVATION (DEG.)	15	27	15,27		
ASPECT ASSUMED	KNOWN				
MIN,MAX,INC ASPECT	170	180	10		
NO OF FREQUENCIES	8				
NO OF TARGETS	12	12	24	24	24
90% CI (±30%) +/-	3.1%	3.1%	2.2%	2.2%	2.2%
CLASS. FEATURES	R	R	R	R	
ELEV ERR IN CURVE	4				

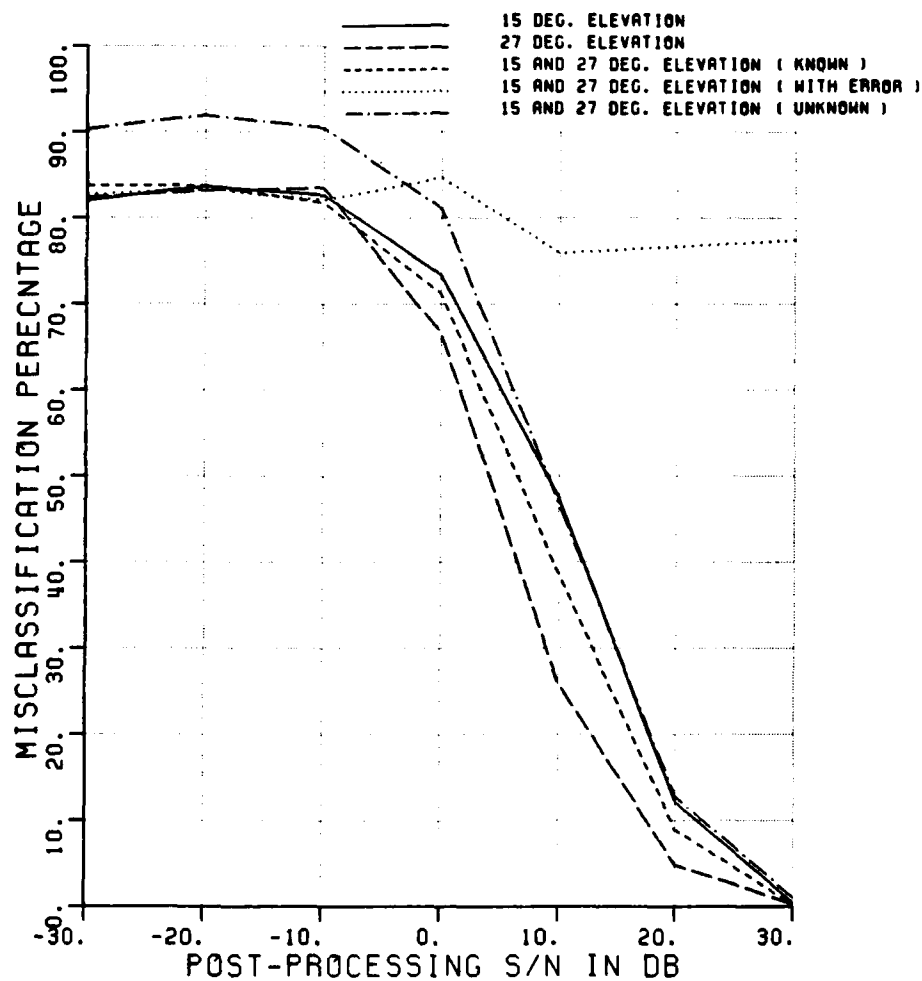


Figure A.50. Misclassification percentage versus post-processing SNR, comparing the performance of various elevation angles.

CLASSIFICATION OF SHIPS

POLARIZATION	V/H				
ELEV ASSUMED	KNOWN / UNKNOWN				
ELEVATION (DEG.)	15	27	15,27		
ASPECT ASSUMED	KNOWN				
MIN,MAX,INC ASPECT	0	10	10		
NO OF FREQUENCIES	8				
NO OF TARGETS	12	12	24	24	24
90% CI (±30%) +/-	3.1%	3.1%	2.2%	2.2%	2.2%
CLASS. FEATURES	A	A	A	A	A
ELEV ERR IN CURVE	4				

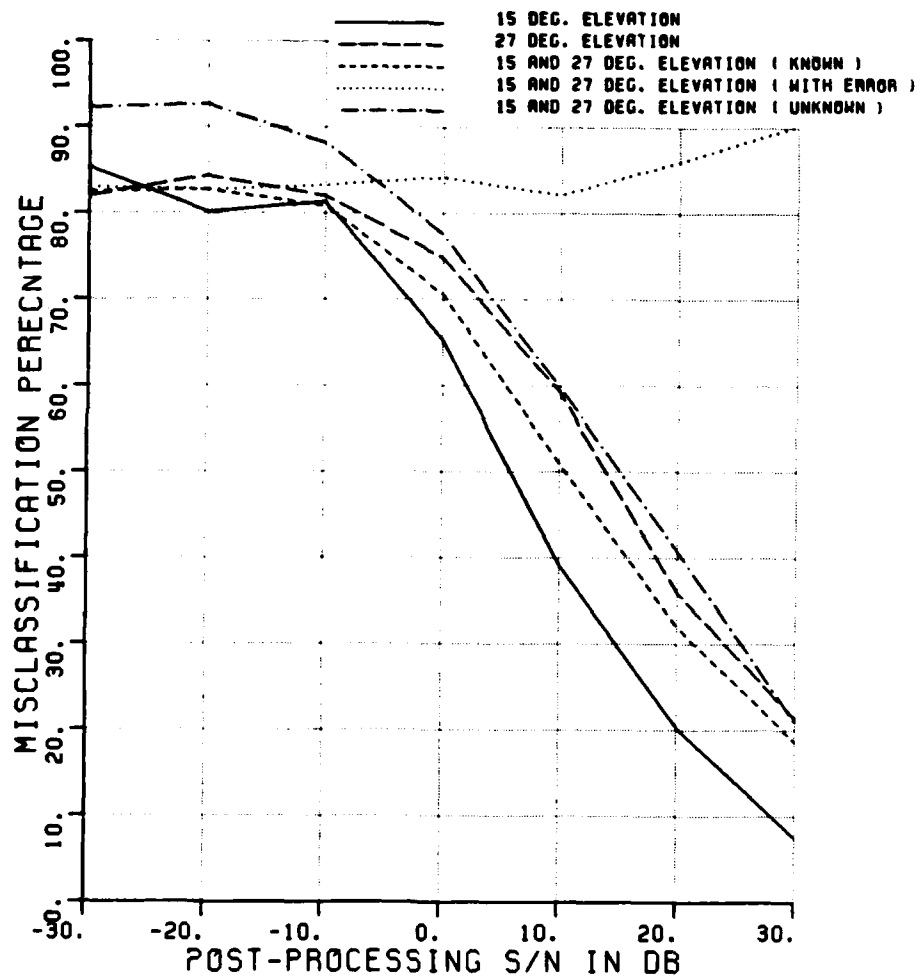


Figure A.51. Misclassification percentage versus post-processing SNR, comparing the performance of various elevation angles.

CLASSIFICATION OF SHIPS

POLARIZATION	V/H				
ELEV ASSUMED	KNOWN	/	UNKNOWN		
ELEVATION (DEG.)	15	27	15,27		
ASPECT ASSUMED	KNOWN				
MIN,MAX,INC ASPECT	80	100	10		
NO OF FREQUENCIES	8				
NO OF TARGETS	18	18	36	36	36
90% CI (@30%) +/-	2.5%	2.5%	1.8%	1.8%	1.8%
CLASS. FEATURES	R	R	R	R	
ELEV ERR IN CURVE	4				

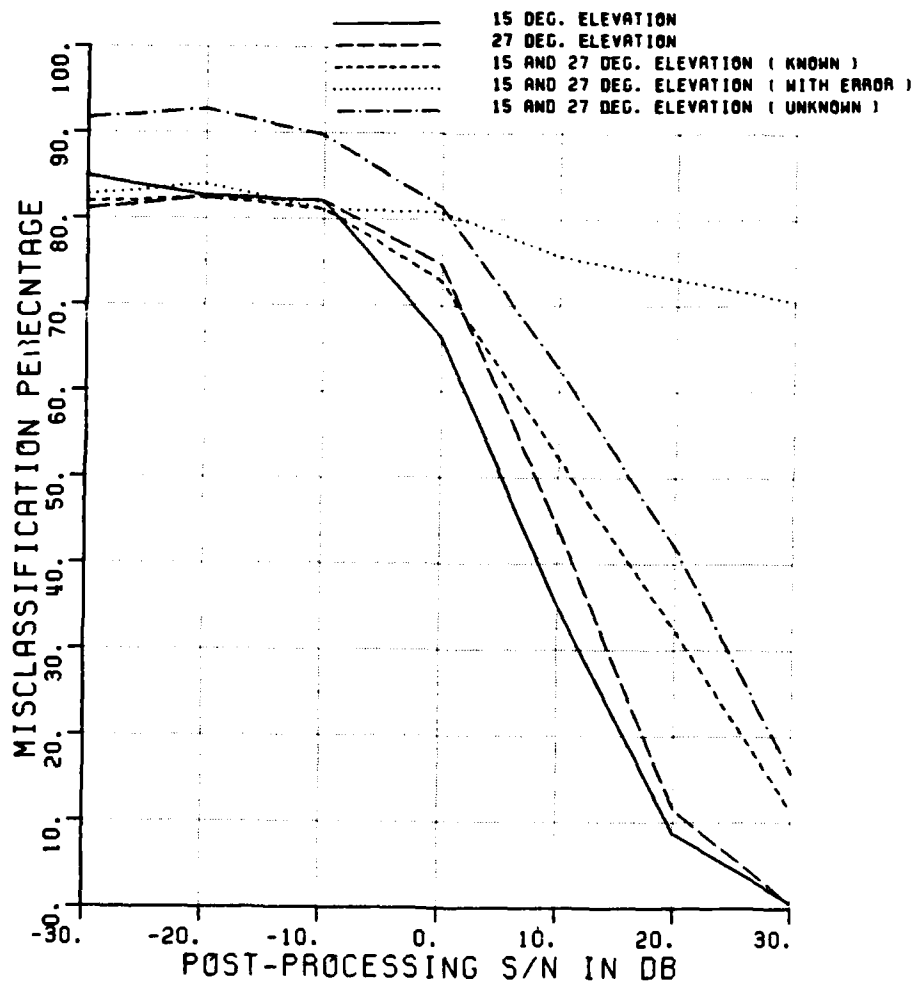


Figure A.52. Misclassification percentage versus post-processing SNR, comparing the performance of various elevation angles.

CLASSIFICATION OF SHIPS

POLARIZATION	V/H				
ELEV ASSUMED	KNOWN	/	UNKNOWN		
ELEVATION (DEG.)	15	27	15,27		
ASPECT ASSUMED	KNOWN				
MIN,MAX,INC ASPECT	170	180	10		
NO OF FREQUENCIES	8				
NO OF TARGETS	12	12	24	24	24
90% CI ($\pm 30\%$) \pm	3.1%	3.1%	2.2%	2.2%	2.2%
CLASS. FEATURES	R	R	R	R	
ELEV ERR IN CURVE	4				

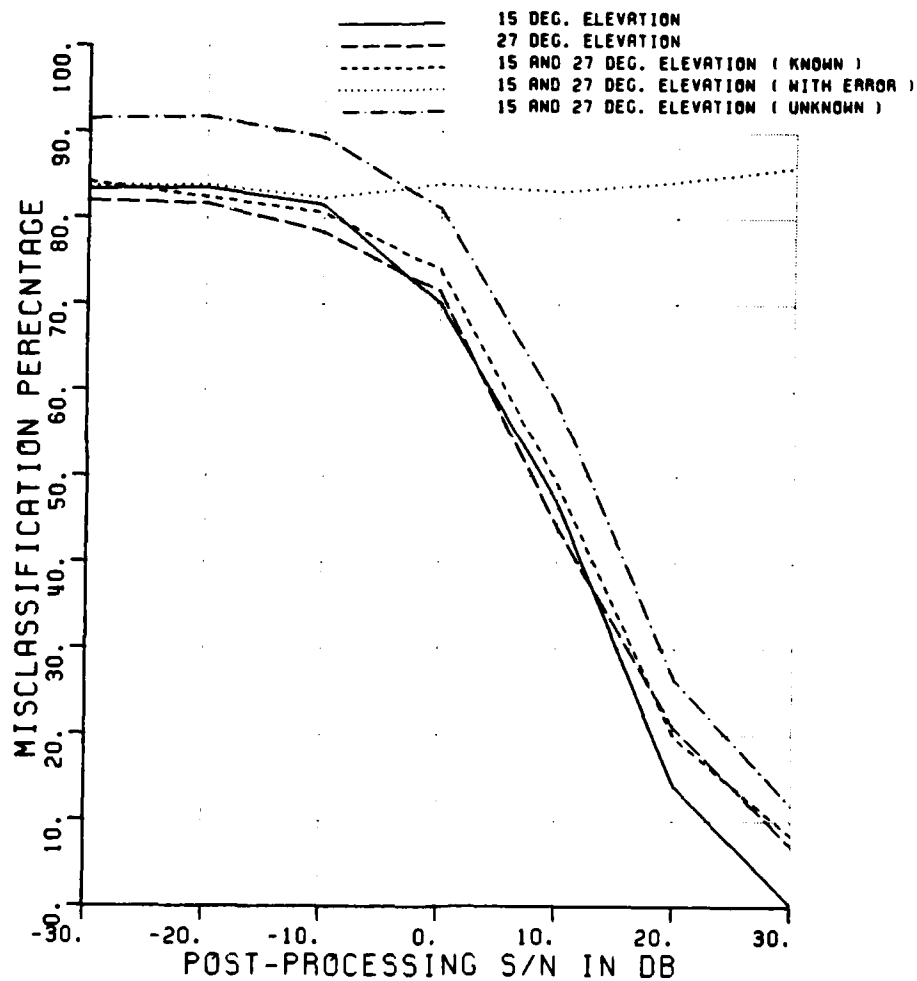


Figure A.53. Misclassification percentage versus post-processing SNR, comparing the performance of various elevation angles.

CLASSIFICATION OF SHIPS

POLARIZATION	V				
ELEV ASSUMED	KNOWN	/	UNKNOWN		
ELEVATION (DEG.)	15	27	15,27		
ASPECT ASSUMED	KNOWN				
MIN,MAX,INC ASPECT	0	10	10		
NO OF FREQUENCIES	8				
NO OF TARGETS	12	12	24	24	24
90% CI ($\pm 30\%$) +/-	3.1%	3.1%	2.2%	2.2%	2.2%
CLASS. FEATURES	T	T	T	T	T
ELEV ERR IN CURVE	4				

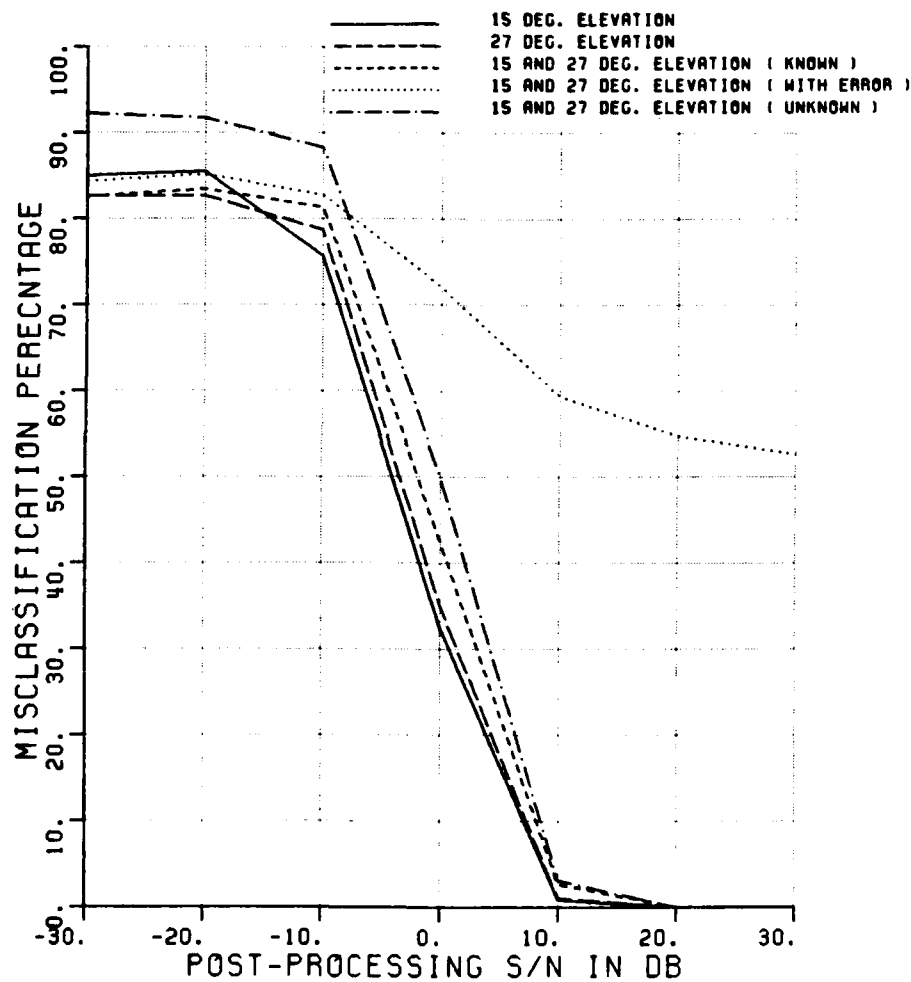


Figure A.54. Misclassification percentage versus post-processing SNR, comparing the performance of various elevation angles.

CLASSIFICATION OF SHIPS

POLARIZATION	V				
ELEV ASSUMED	KNOWN / UNKNOWN				
ELEVATION (DEG.)	15	27	15,27		
ASPECT ASSUMED	KNOWN				
MIN,MAX,INC ASPECT	80	100	10		
NO OF FREQUENCIES	8				
NO OF TARGETS	18	18	36	36	36
90% CI (±30%) +/-	2.5%	2.5%	1.8%	1.8%	1.8%
CLASS. FEATURES	T	T	T	T	T
ELEV ERR IN CURVE	4				

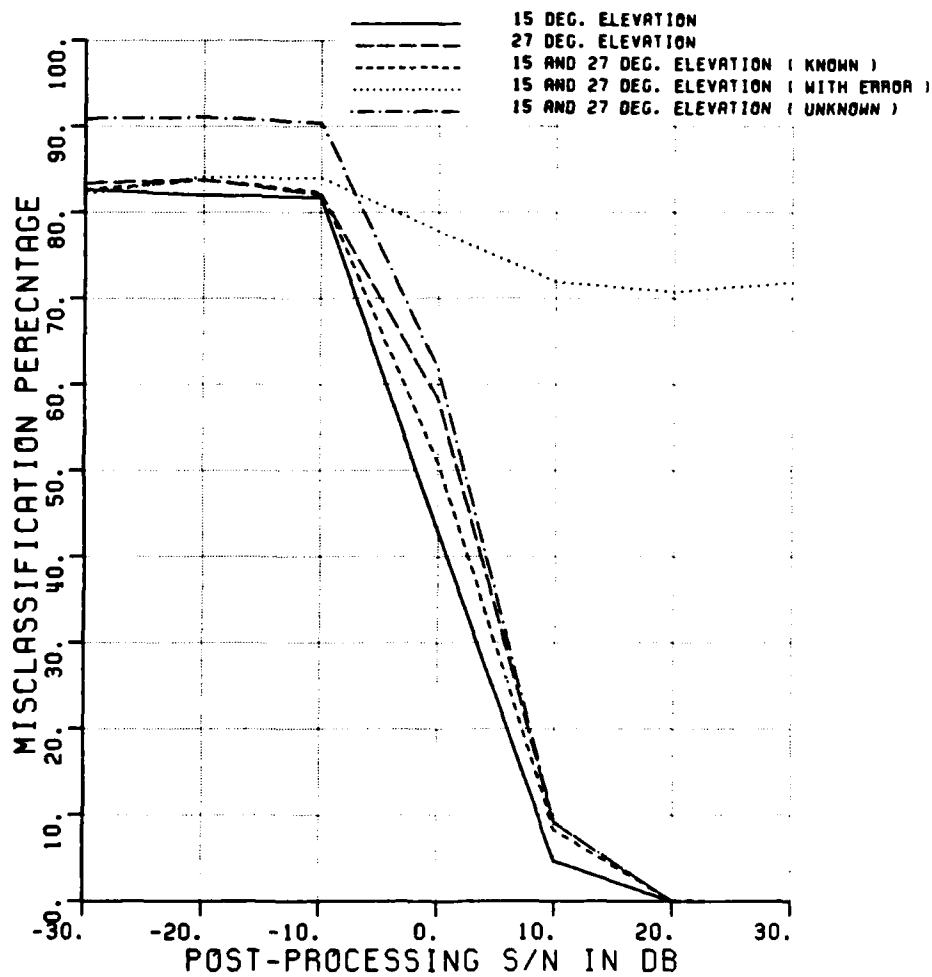


Figure A.55. Misclassification percentage versus post-processing SNR, comparing the performance of various elevation angles.

CLASSIFICATION OF SHIPS

POLARIZATION	V				
ELEV ASSUMED	KNOWN	/	UNKNOWN		
ELEVATION (DEG.)	15	27	15,27		
ASPECT ASSUMED	KNOWN				
MIN,MAX,INC ASPECT	170	180	10		
NO OF FREQUENCIES	8				
NO OF TARGETS	12	12	24	24	24
90% CI (±30%) +/-	3.1%	3.1%	2.2%	2.2%	2.2%
CLASS. FEATURES	T	T	T	T	T
ELEV ERR IN CURVE	4				

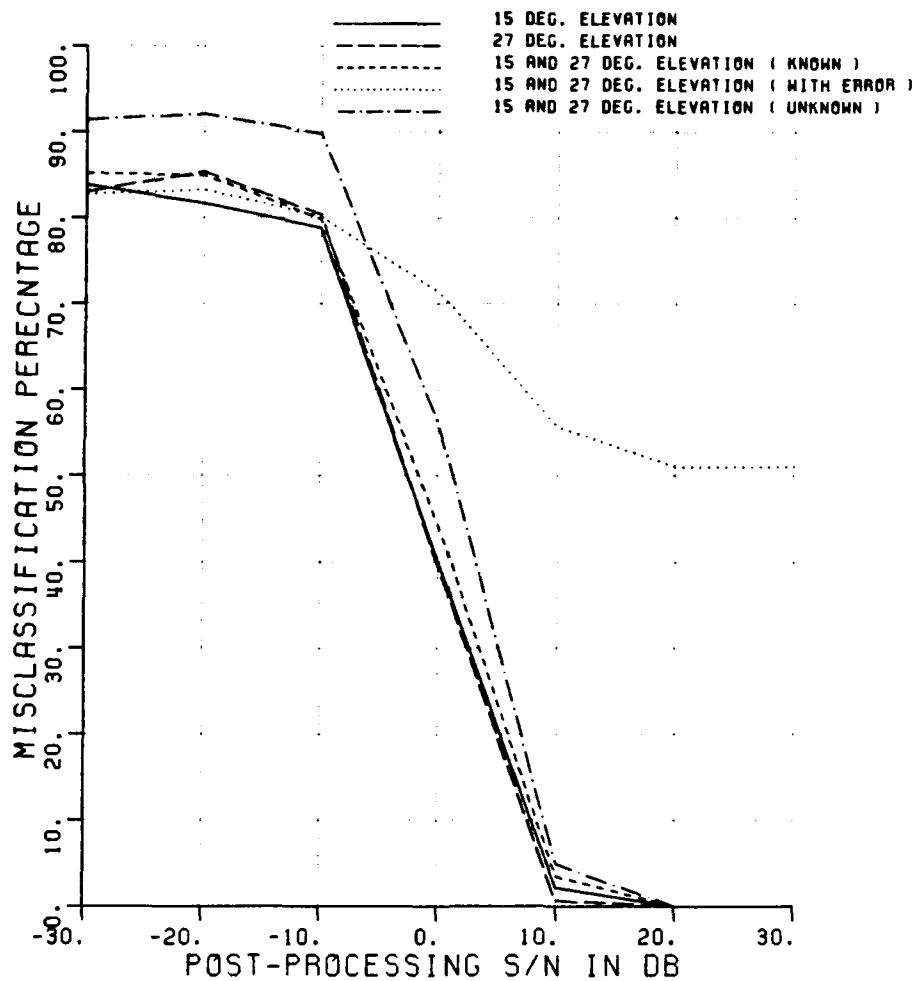


Figure A.56. Misclassification percentage versus post-processing SNR, comparing the performance of various elevation angles.

CLASSIFICATION OF SHIPS

POLARIZATION	H				
ELEV ASSUMED	KNOWN		/ UNKNOWN		
ELEVATION (DEG.)	15	27	15,27		
ASPECT ASSUMED	KNOWN				
MIN,MAX,INC ASPECT	0	10	10		
NO OF FREQUENCIES	8				
NO OF TARGETS	12	12	24	24	24
90% CI (±30%) +/-	3.1%	3.1%	2.2%	2.2%	2.2%
CLASS. FEATURES	T	T	T	T	T
ELEV ERR IN CURVE	4				

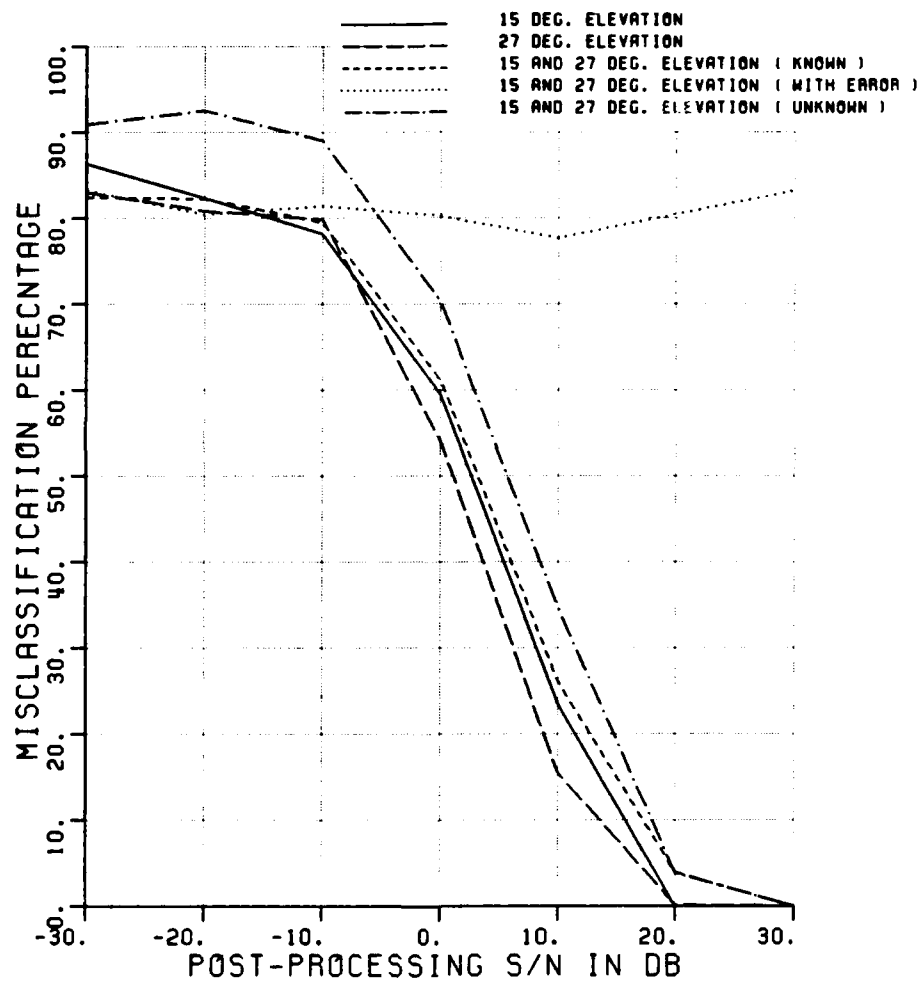


Figure A.57. Misclassification percentage versus post-processing SNR, comparing the performance of various elevation angles.

CLASSIFICATION OF SHIPS

POLARIZATION	H				
ELEV ASSUMED	KNOWN	/	UNKNOWN		
ELEVATION (DEG.)	15	27	15,27		
ASPECT ASSUMED	KNOWN				
MIN,MAX,INC ASPECT	80	100	10		
NO OF FREQUENCIES	8				
NO OF TARGETS	18	18	36	36	36
90% CI (±30%) +/-	2.5%	2.5%	1.8%	1.8%	1.8%
CLASS. FEATURES	T	T	T	T	T
ELEV ERR IN CURVE	4				

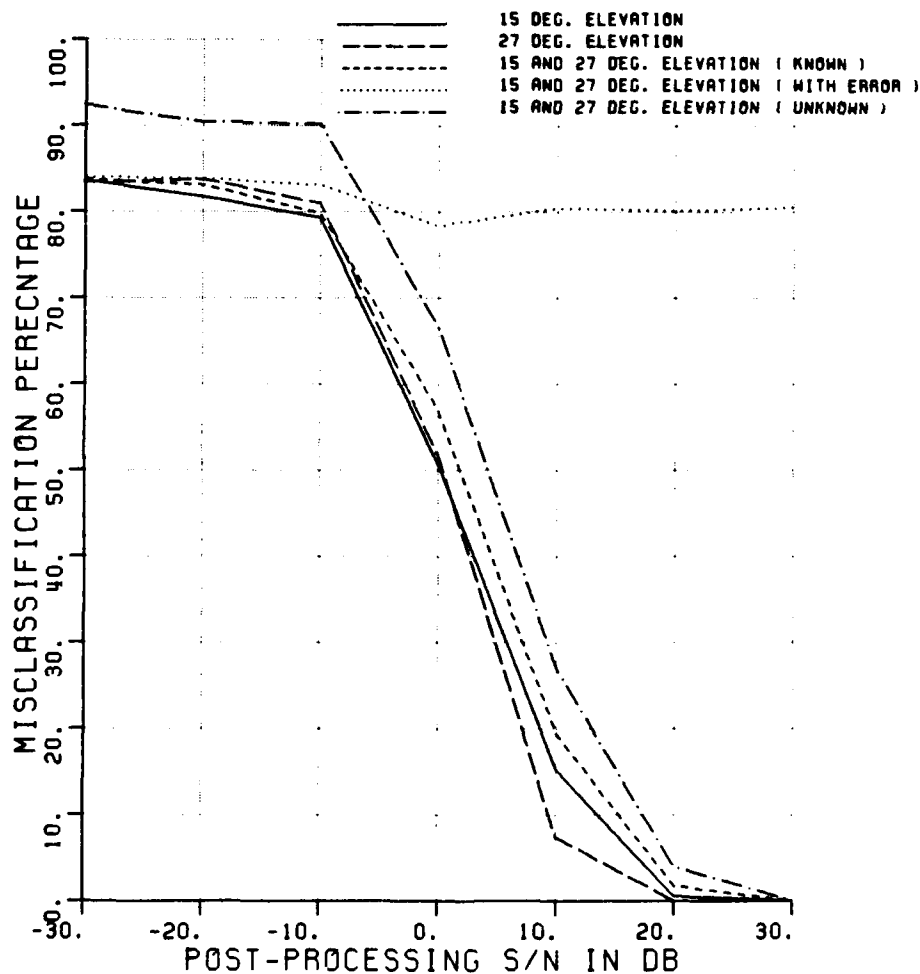


Figure A.58. Misclassification percentage versus post-processing SNR, comparing the performance of various elevation angles.

CLASSIFICATION OF SHIPS

POLARIZATION	H				
ELEV ASSUMED	KNOWN	/	UNKNOWN		
ELEVATION (DEG.)	15	27	15,27		
ASPECT ASSUMED	KNOWN				
MIN,MAX,INC ASPECT	170	180	10		
NO OF FREQUENCIES	8				
NO OF TARGETS	12	12	24	24	24
90% CI (±30%) +/-	3.1%	3.1%	2.2%	2.2%	2.2%
CLASS. FEATURES	T	T	T	T	T
ELEV ERR IN CURVE	4				

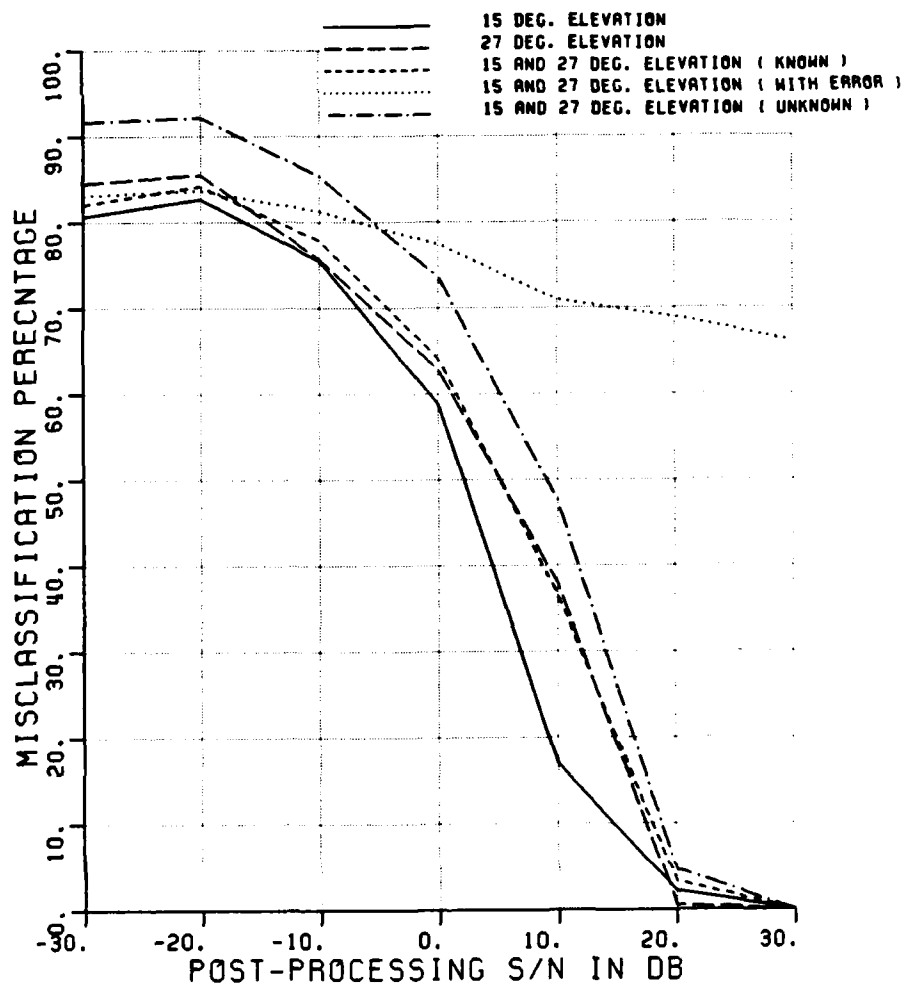


Figure A.59. Misclassification percentage versus post-processing SNR, comparing the performance of various elevation angles.

CLASSIFICATION OF SHIPS

POLARIZATION	X				
ELEV ASSUMED	KNOWN	/	UNKNOWN		
ELEVATION (DEG.)	15	27	15,27		
ASPECT ASSUMED	KNOWN				
MIN,MAX,INC ASPECT	0	10	10		
NO OF FREQUENCIES	8				
NO OF TARGETS	12	12	24	24	24
90% CI (±30%) +/-	3.1%	3.1%	2.2%	2.2%	2.2%
CLASS. FEATURES	T	T	T	T	
ELEV ERR IN CURVE	4				

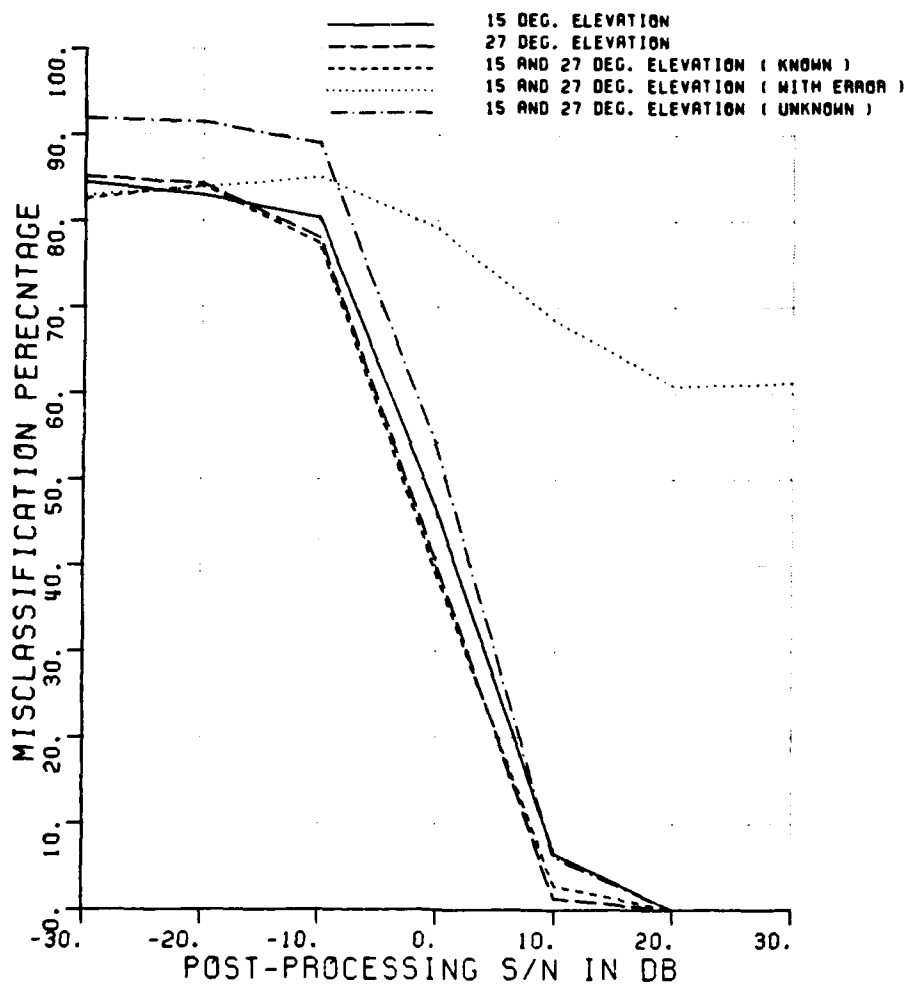


Figure A.60. Misclassification percentage versus post-processing SNR, comparing the performance of various elevation angles.

CLASSIFICATION OF SHIPS

POLARIZATION	X				
ELEV ASSUMED	KNOWN		/ UNKNOWN		
ELEVATION (DEG.)	15	27	15,27		
ASPECT ASSUMED	KNOWN				
MIN,MAX,INC ASPECT	80	100	10		
NO OF FREQUENCIES	8				
NO OF TARGETS	18	18	36	36	36
90% CI (±30%) +/-	2.5%	2.5%	1.8%	1.8%	1.8%
CLASS. FEATURES	T	T	T	T	T
ELEV ERR IN CURVE	4				

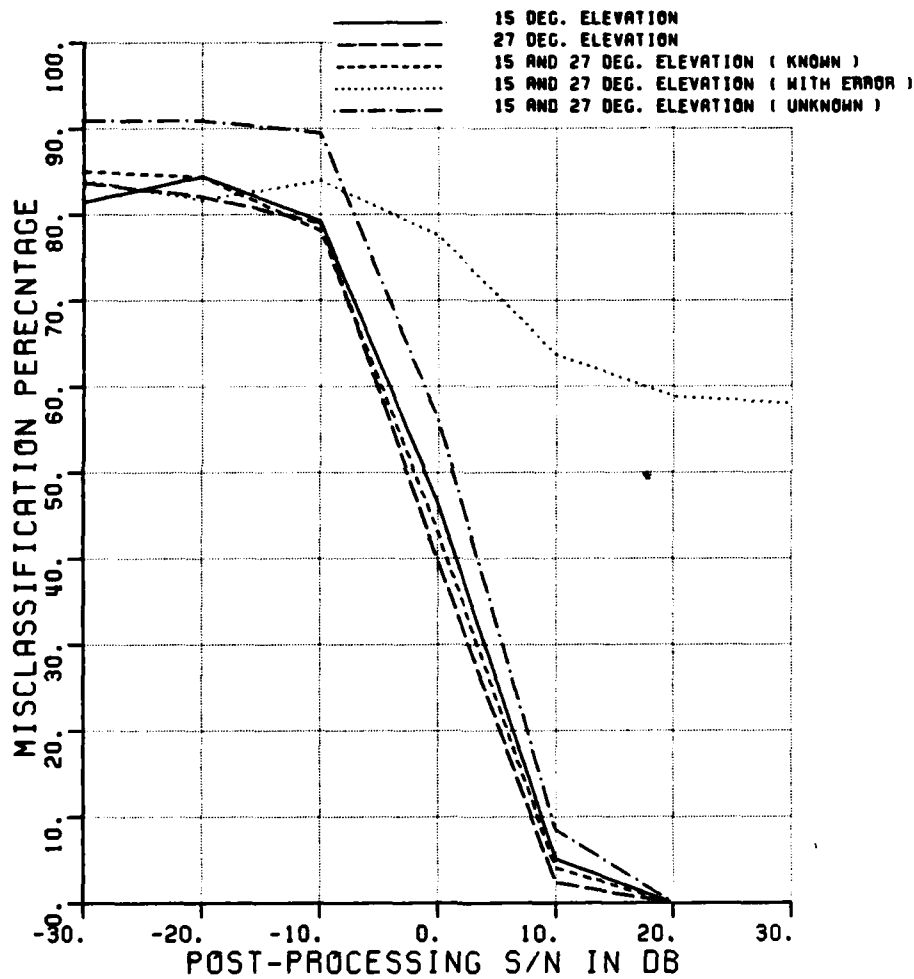


Figure A.61. Misclassification percentage versus post-processing SNR, comparing the performance of various elevation angles.

CLASSIFICATION OF SHIPS

POLARIZATION	X				
ELEV ASSUMED	KNOWN	/	UNKNOWN		
ELEVATION (DEG.)	15	27	15,27		
ASPECT ASSUMED	KNOWN				
MIN,MAX,INC ASPECT	170	180	10		
NO OF FREQUENCIES	8				
NO OF TARGETS	12	12	24	24	24
90% CI (±30%) +/-	3.1%	3.1%	2.2%	2.2%	2.2%
CLASS. FEATURES	T	T	T	T	T
ELEV ERR IN CURVE	4				

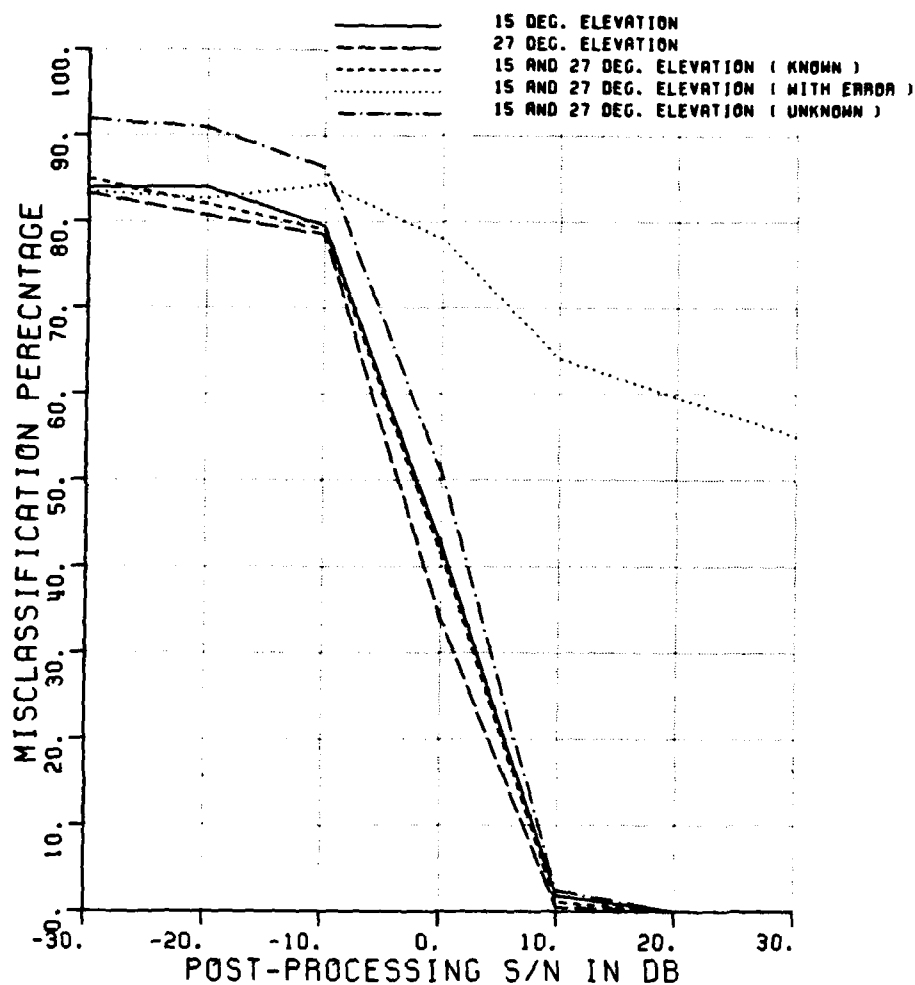


Figure A.62. Misclassification percentage versus post-processing SNR, comparing the performance of various elevation angles.

CLASSIFICATION OF SHIPS

POLARIZATION	V/H				
ELEV ASSUMED	KNOWN	/	UNKNOWN		
ELEVATION (DEG.)	15	27	15,27		
ASPECT ASSUMED	KNOWN				
MIN,MAX,INC ASPECT	0	10	10		
NO OF FREQUENCIES	8				
NO OF TARGETS	12	12	24	24	24
90% CI (±30%) +/-	3.1%	3.1%	2.2%	2.2%	2.2%
CLASS. FEATURES	T	T	T	T	
ELEV ERR IN CURVE	4				

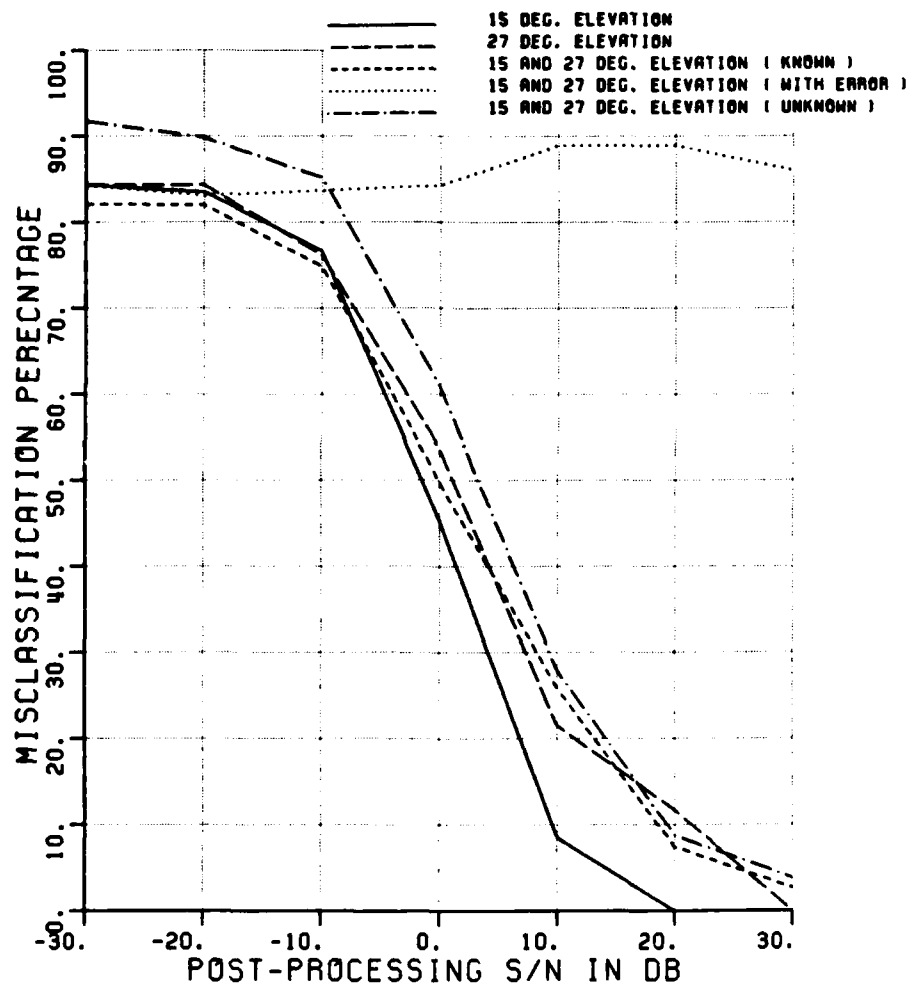


Figure A.63. Misclassification percentage versus post-processing SNR, comparing the performance of various elevation angles.

CLASSIFICATION OF SHIPS

POLARIZATION	V/H				
ELEV ASSUMED	KNOWN	/	UNKNOWN		
ELEVATION (DEG.)	15	27	15,27		
ASPECT ASSUMED	KNOWN				
MIN,MAX,INC ASPECT	80	100	10		
NO OF FREQUENCIES	8				
NO OF TARGETS	18	18	36	36	36
90% CI (@30%) +/-	2.5%	2.5%	1.8%	1.8%	1.8%
CLASS. FEATURES	T	T	T	T	T
ELEV ERR IN CURVE	4				

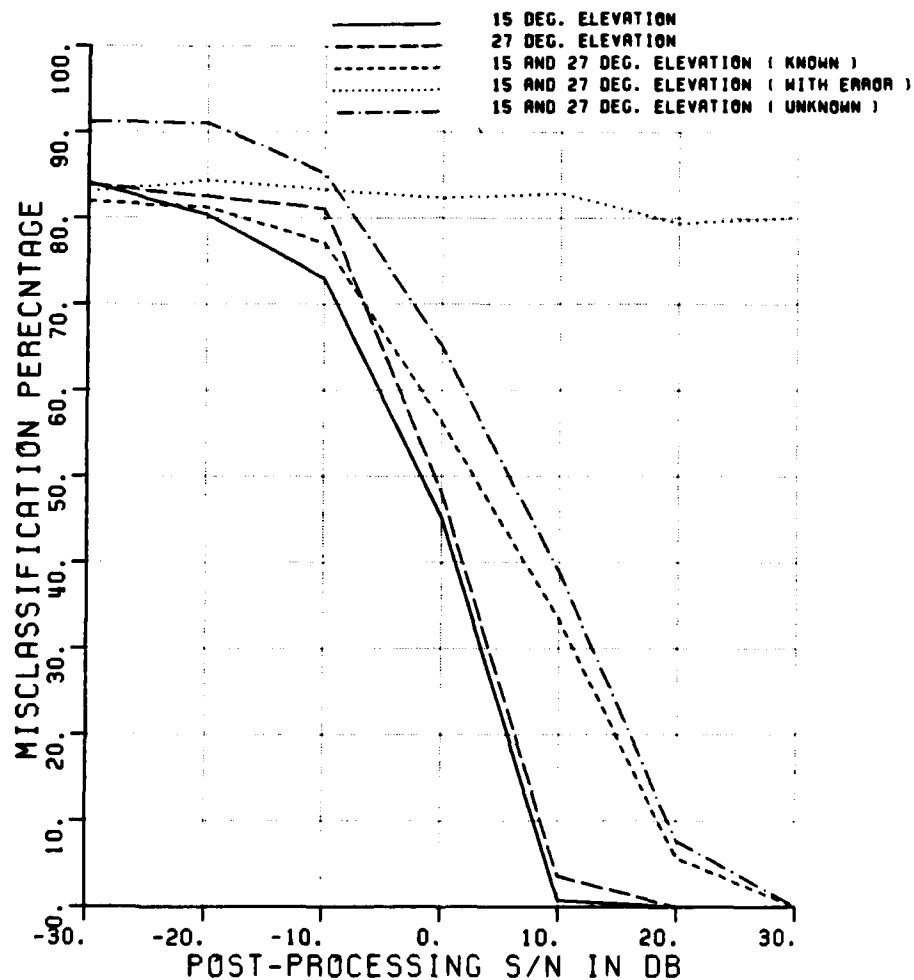


Figure A.64. Misclassification percentage versus post-processing SNR, comparing the performance of various elevation angles.

CLASSIFICATION OF SHIPS

POLARIZATION	V/H				
ELEV ASSUMED	KNOWN	/	UNKNOWN		
ELEVATION (DEG.)	15	27	15, 27		
ASPECT ASSUMED	KNOWN				
MIN, MAX, INC ASPECT	170	180	10		
NO OF FREQUENCIES	8				
NO OF TARGETS	12	12	24	24	24
90% CI (@30%) +/-	3.1%	3.1%	2.2%	2.2%	2.2%
CLASS. FEATURES	T	T	T	T	T
ELEV ERR IN CURVE	4				

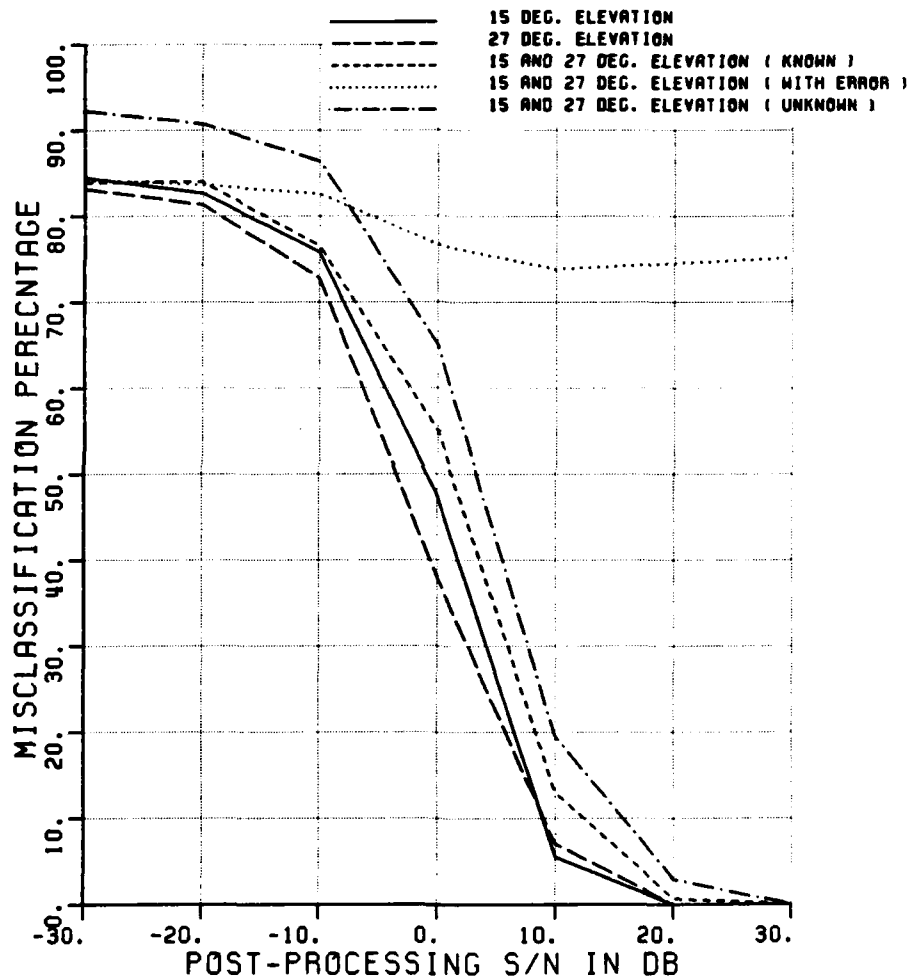


Figure A.65. Misclassification percentage versus post-processing SNR, comparing the performance of various elevation angles.

CLASSIFICATION OF SHIPS

POLARIZATION	V	H	X	V/H
ELEV ASSUMED	KNOWN			
ELEVATION (DEG.)	27			
ASPECT ASSUMED	KNOWN			
MIN,MAX,INC ASPECT	80	100	10	
NO OF FREQUENCIES	8			
NO OF TARGETS	18	18	18	18
90% CI (@30%) +/-	2.5%	2.5%	2.5%	2.5%
CLASS. FEATURES	A	A	A	A

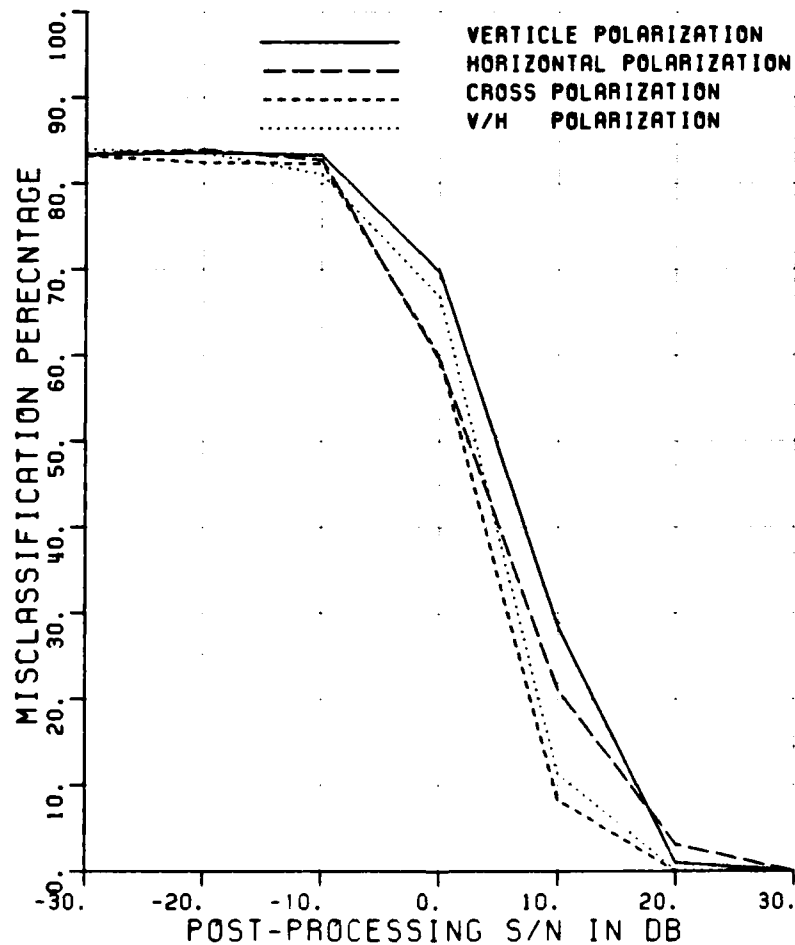


Figure A.66. Misclassification percentage versus post-processing SNR, comparing the performance of various polarizations.

CLASSIFICATION OF SHIPS				
POLARIZATION	V	H	X	V/H
ELEV ASSUMED	KNOWN			
ELEVATION (DEG.)	27			
ASPECT ASSUMED	KNOWN			
MIN,MAX,INC ASPECT	170	180	10	
NO OF FREQUENCIES	8			
NO OF TARGETS	12	12	12	12
90% CI (@30%) +/-	3.1%	3.1%	3.1%	3.1%
CLASS. FEATURES	A	A	A	A

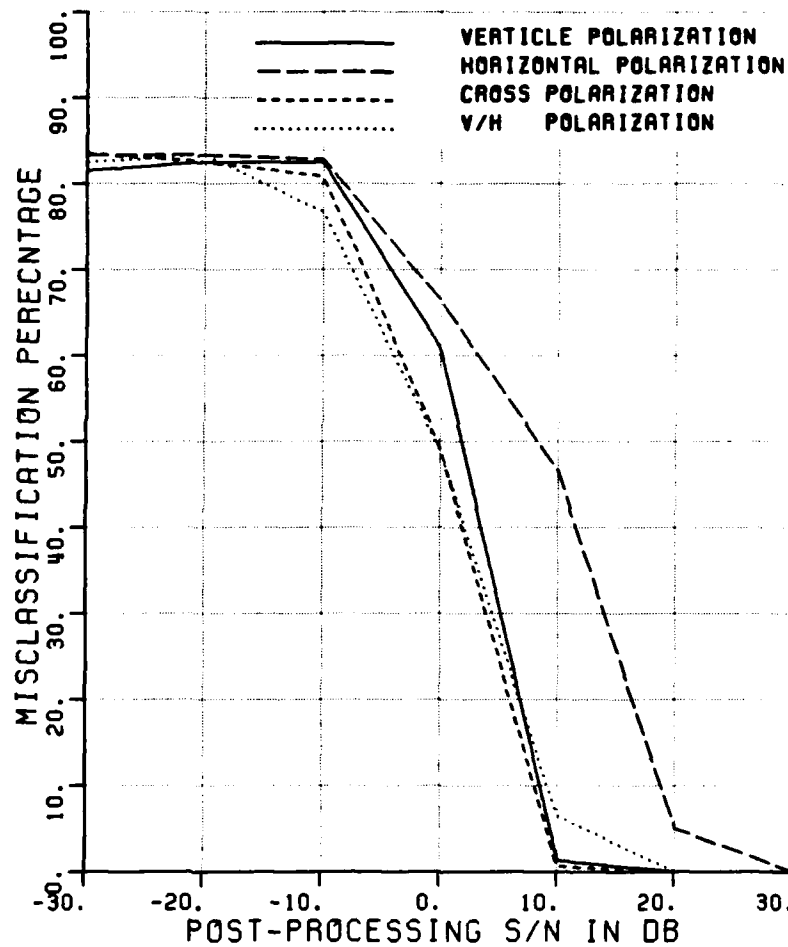


Figure A.67. Misclassification percentage versus post-processing SNR, comparing the performance of various polarizations.

CLASSIFICATION OF SHIPS

POLARIZATION	V	H	X	V/H
ELEV ASSUMED	KNOWN			
ELEVATION (DEG.)	27			
ASPECT ASSUMED	KNOWN			
MIN,MAX,INC ASPECT	0	10	10	
NO OF FREQUENCIES	8			
NO OF TARGETS	12		12	12
90% CI (±30%) +/-	3.1%	3.1%	3.1%	3.1%
CLASS. FEATURES	W	W	W	W

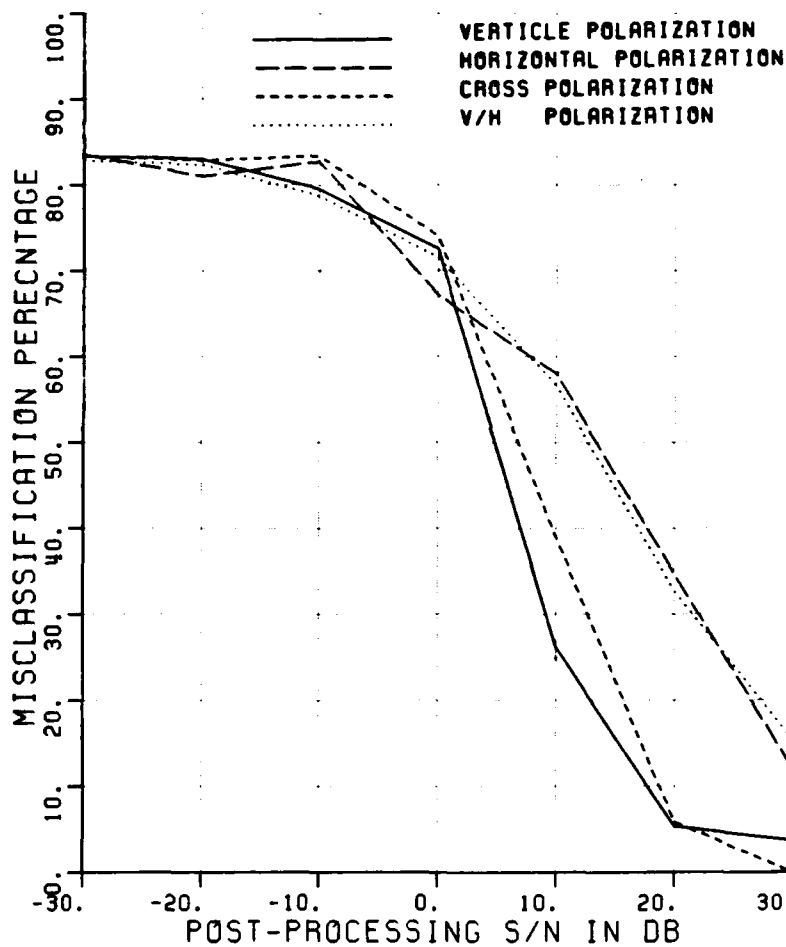


Figure A.68. Misclassification percentage versus post-processing SNR, comparing the performance of various polarizations.

CLASSIFICATION OF SHIPS

POLARIZATION	V	H	X	V/H
ELEV ASSUMED	KNOWN			
ELEVATION (DEG.)	27			
ASPECT ASSUMED	KNOWN			
MIN,MAX,INC ASPECT	80	100	10	
NO OF FREQUENCIES	8			
NO OF TARGETS	18	18	18	18
90% CI (±30%) +/-	2.5%	2.5%	2.5%	2.5%
CLASS. FEATURES	W	W	W	W

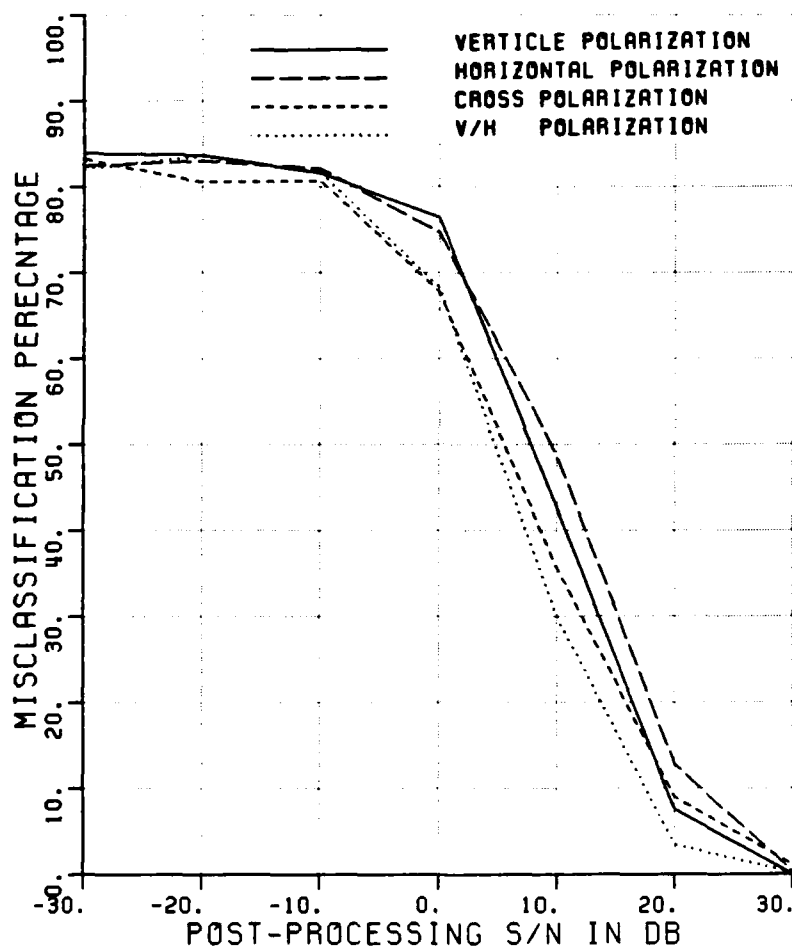


Figure A.69. Misclassification percentage versus post-processing SNR, comparing the performance of various polarizations.

CLASSIFICATION OF SHIPS

POLARIZATION	V	H	X	V/H
ELEV ASSUMED	KNOWN			
ELEVATION (DEG.)	27			
ASPECT ASSUMED	KNOWN			
MIN,MAX,INC ASPECT	170	180	10	
NO OF FREQUENCIES	8			
NO OF TARGETS	12	12	12	12
90% CI (@30%) +/-	3.1%	3.1%	3.1%	3.1%
CLASS. FEATURES	W	W	W	W

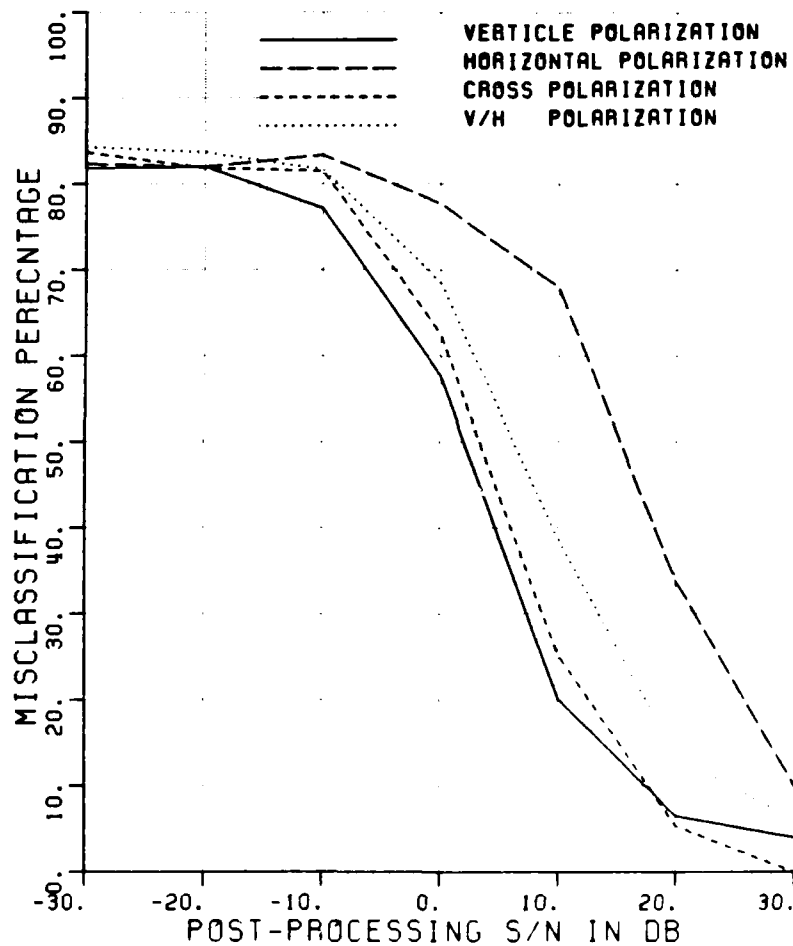


Figure A.70. Misclassification percentage versus post-processing SNR, comparing the performance of various polarizations.

CLASSIFICATION OF SHIPS

POLARIZATION	V	H	X	V/H
ELEV ASSUMED	KNOWN			
ELEVATION (DEG.)	27			
ASPECT ASSUMED	KNOWN			
MIN,MAX,INC ASPECT	0	10	10	
NO OF FREQUENCIES	8			
NO OF TARGETS	12	12	12	12
90% CI (±30%) +/-	3.1%	3.1%	3.1%	3.1%
CLASS. FEATURES	A&W	A&W	A&W	A&W

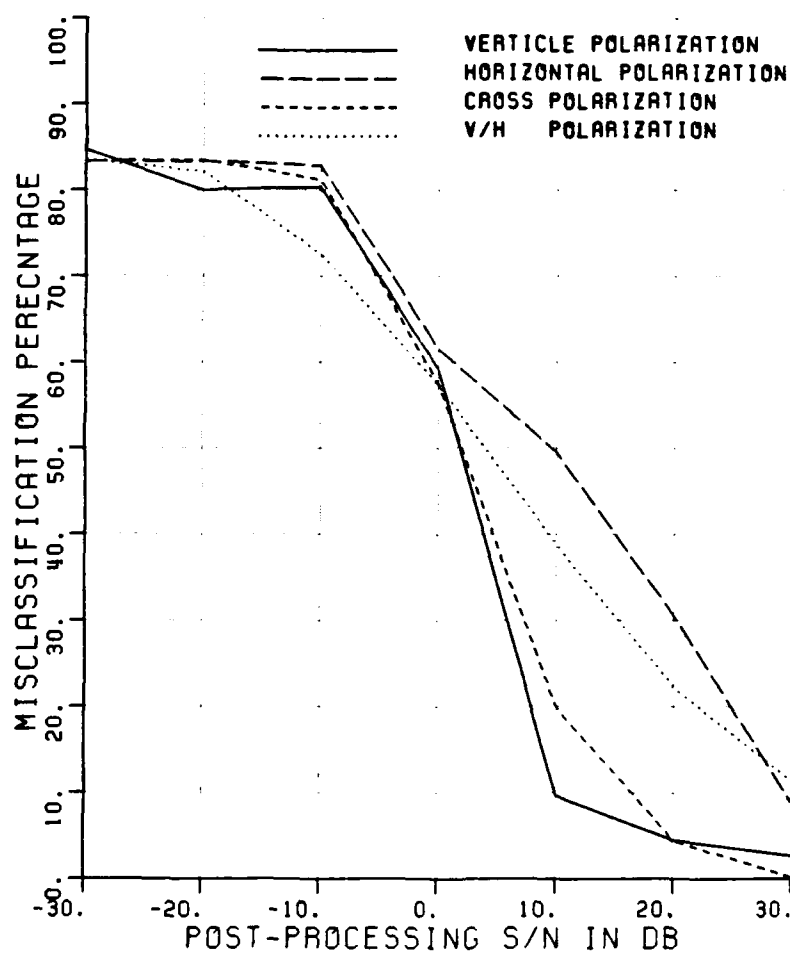


Figure A.71. Misclassification percentage versus post-processing SNR, comparing the performance of various polarizations.

CLASSIFICATION OF SHIPS

POLARIZATION	V	H	X	V/H
ELEV ASSUMED	KNOWN			
ELEVATION (DEG.)	27			
ASPECT ASSUMED	KNOWN			
MIN,MAX,INC ASPECT	80	100	10	
NO OF FREQUENCIES	8			
NO OF TARGETS	18	18	18	18
90% CI (±30%) +/-	2.5%	2.5%	2.5%	2.5%
CLASS. FEATURES	A&W	A&W	A&W	A&W

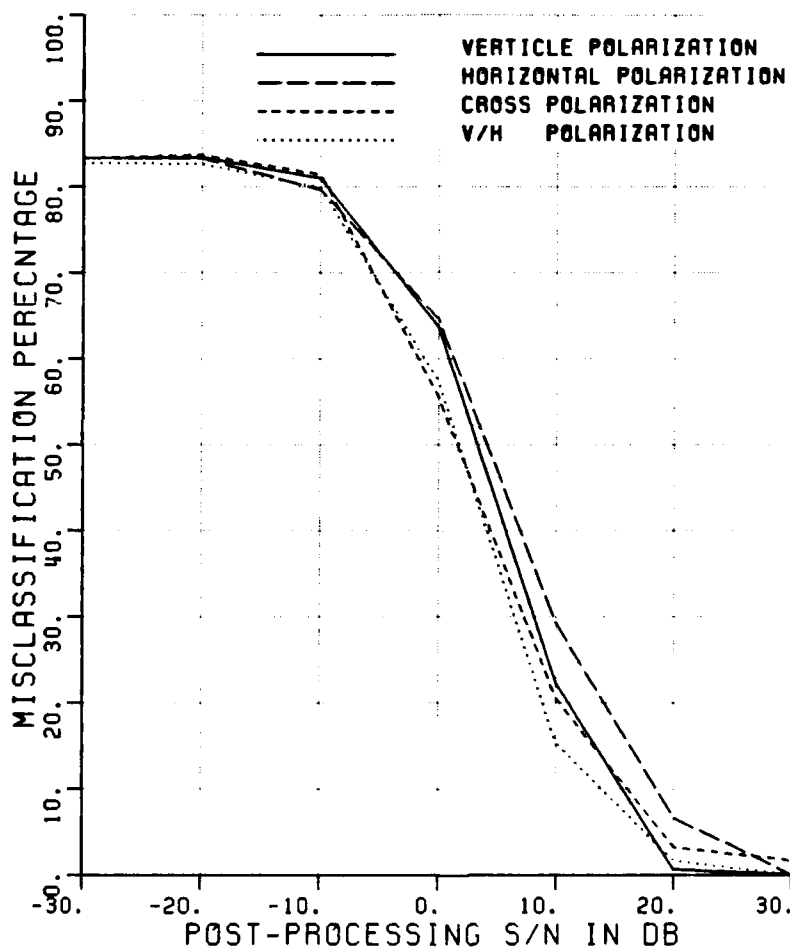


Figure A.72. Misclassification percentage versus post-processing SNR, comparing the performance of various polarizations.

CLASSIFICATION OF SHIPS

POLARIZATION	V	H	X	V/H
ELEV ASSUMED	KNOWN			
ELEVATION (DEG.)	27			
ASPECT ASSUMED	KNOWN			
MIN,MAX,INC ASPECT	170	180	10	
NO OF FREQUENCIES	8			
NO OF TARGETS	12	12	12	12
90% CI (@30%) +/-	3.1%	3.1%	3.1%	3.1%
CLASS. FEATURES	A&W	A&W	A&W	A&W

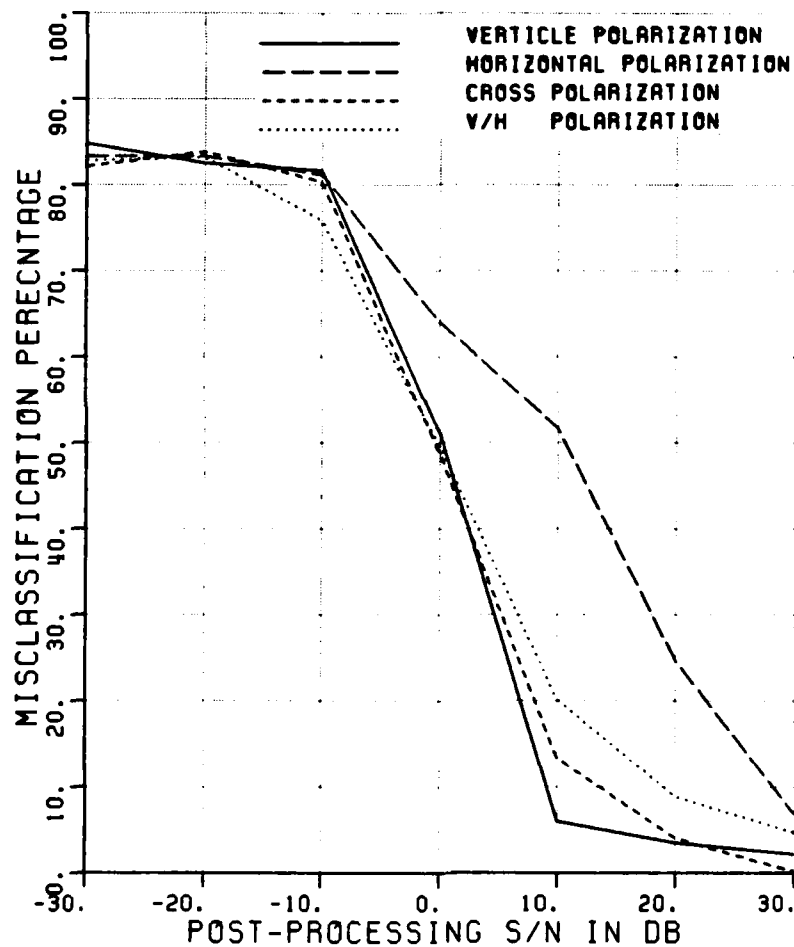


Figure A.73. Misclassification percentage versus post-processing SNR, comparing the performance of various polarizations.

CLASSIFICATION OF SHIPS

POLARIZATION	V	H	X	V/H
ELEV ASSUMED	KNOWN			
ELEVATION (DEG.)	27			
ASPECT ASSUMED	KNOWN			
MIN,MAX,INC ASPECT	0	10	10	
NO OF FREQUENCIES	8			
NO OF TARGETS	12		12	12
90% CI (±30%) +/-	3.1%		3.1%	3.1%
CLASS. FEATURES	R	R	R	R

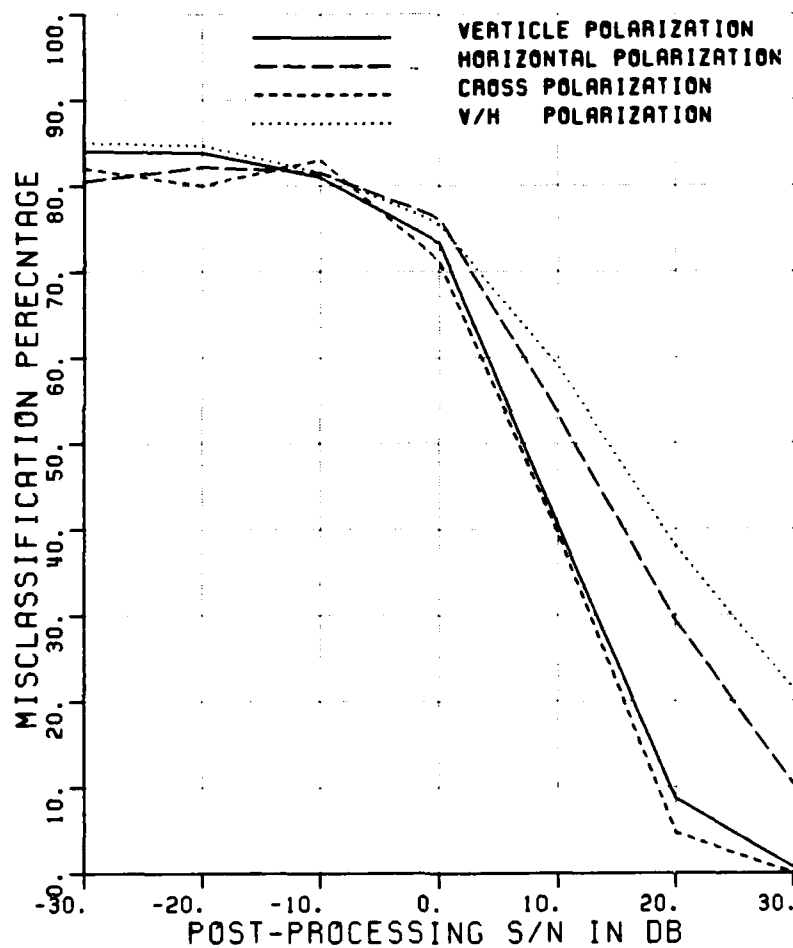


Figure A.74. Misclassification percentage versus post-processing SNR, comparing the performance of various polarizations.

CLASSIFICATION OF SHIPS

POLARIZATION	V	H	X	V/H
ELEV ASSUMED	KNOWN			
ELEVATION (DEG.)	27			
ASPECT ASSUMED	KNOWN			
MIN,MAX,INC ASPECT	80	100	10	
NO OF FREQUENCIES	8			
NO OF TARGETS	18	18	18	18
90% CI (±30%) +/-	2.5%	2.5%	2.5%	2.5%
CLASS. FEATURES	R	R	R	R

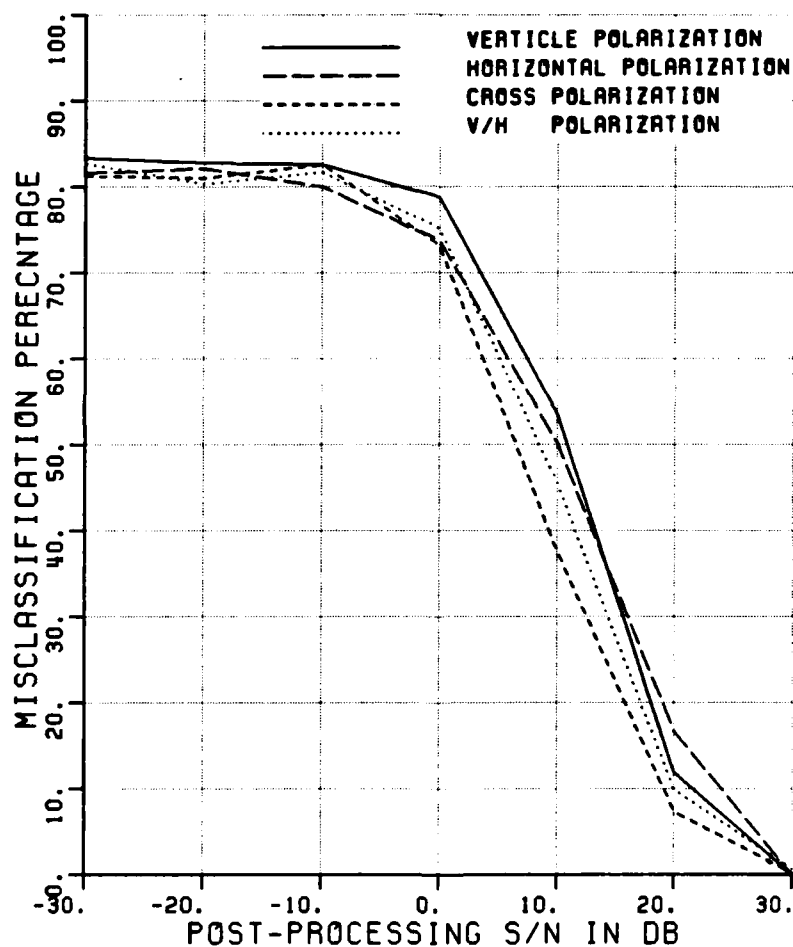


Figure A.75. Misclassification percentage versus post-processing SNR, comparing the performance of various polarizations.

CLASSIFICATION OF SHIPS

POLARIZATION	V	H	X	V/H
ELEV ASSUMED	KNOWN			
ELEVATION (DEG.)	27			
ASPECT ASSUMED	KNOWN			
MIN,MAX,INC ASPECT	170	180	10	
NO OF FREQUENCIES	8			
NO OF TARGETS	12		12	12
90% CI (±30%) +/-	3.1%		3.1%	3.1%
CLASS. FEATURES	A	A	A	A

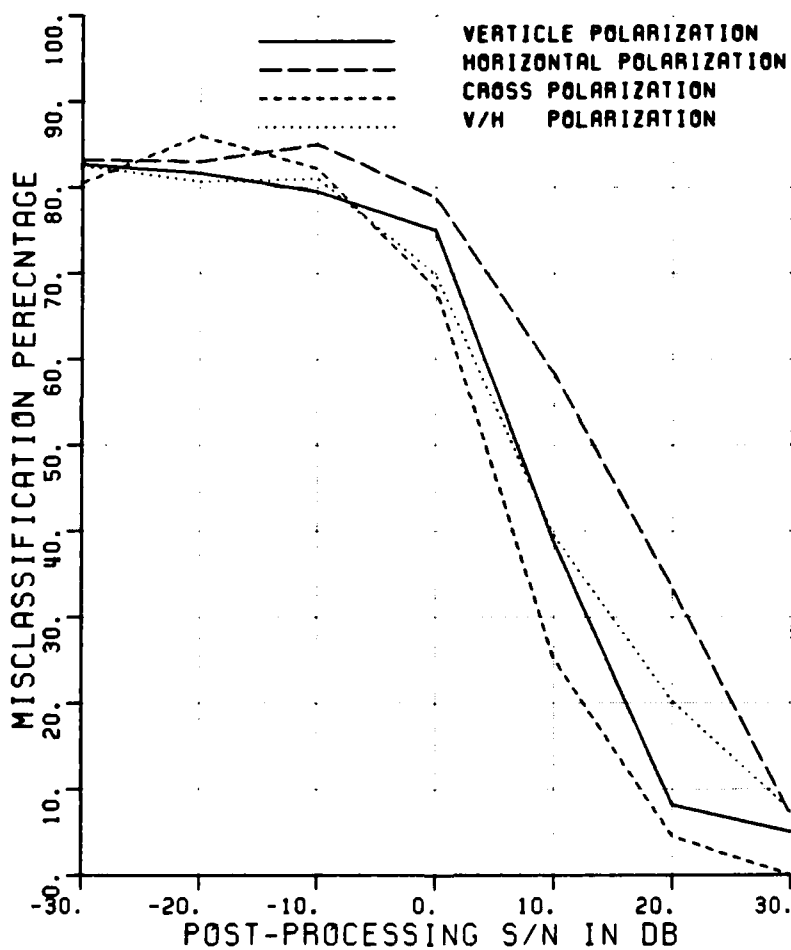


Figure A.76. Misclassification percentage versus post-processing SNR, comparing the performance of various polarizations.

CLASSIFICATION OF SHIPS

POLARIZATION	V	H	X	V/H
ELEV ASSUMED	KNOWN			
ELEVATION (DEG.)	27			
ASPECT ASSUMED	KNOWN			
MIN,MAX,INC ASPECT	0	10	10	
NO OF FREQUENCIES	8			
NO OF TARGETS	12	12	12	12
90% CI (±30%) +/-	3.1%	3.1%	3.1%	3.1%
CLASS. FEATURES	R4W	R4W	R4W	R4W

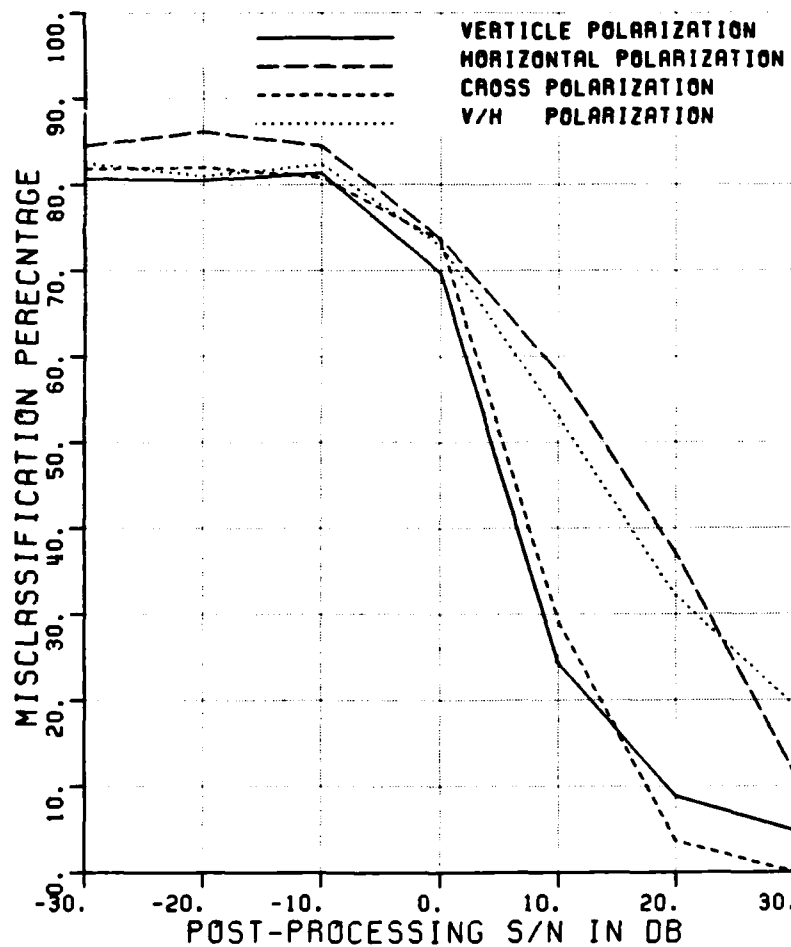


Figure A.77. Misclassification percentage versus post-processing SNR, comparing the performance of various polarizations.

CLASSIFICATION OF SHIPS

POLARIZATION	V	H	X	V/H
ELEV ASSUMED	KNOWN			
ELEVATION (DEG.)	27			
ASPECT ASSUMED	KNOWN			
MIN,MAX,INC ASPECT	80	100	10	
NO OF FREQUENCIES	8			
NO OF TARGETS	18	18	18	18
90% CI (@30%) +/-	2.5%	2.5%	2.5%	2.5%
CLASS. FEATURES	R4W	R4W	R4W	R4W

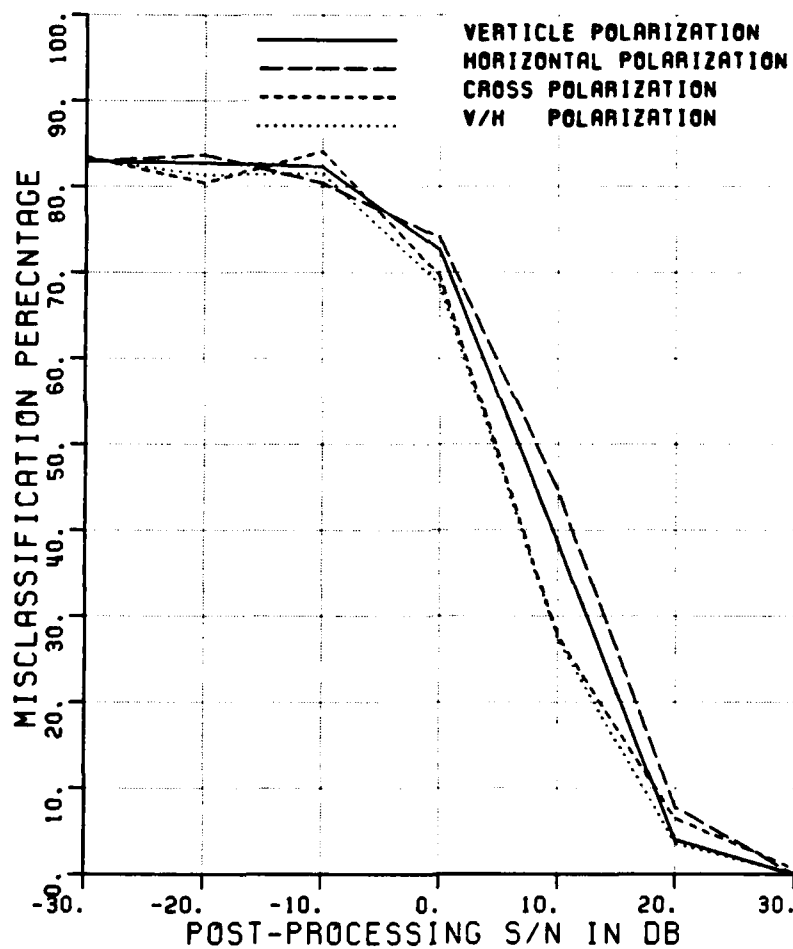


Figure A.78. Misclassification percentage versus post-processing SNR, comparing the performance of various polarizations.

CLASSIFICATION OF SHIPS

POLARIZATION	V	H	X	V/H
ELEV ASSUMED	KNOWN			
ELEVATION (DEG.)	27			
ASPECT ASSUMED	KNOWN			
MIN,MAX,INC ASPECT	170	180	10	
NO OF FREQUENCIES	8			
NO OF TARGETS	12	12	12	12
90% CI (+30%) +/-	3.1%	3.1%	3.1%	3.1%
CLASS. FEATURES	R4W	R4W	R4W	R4W

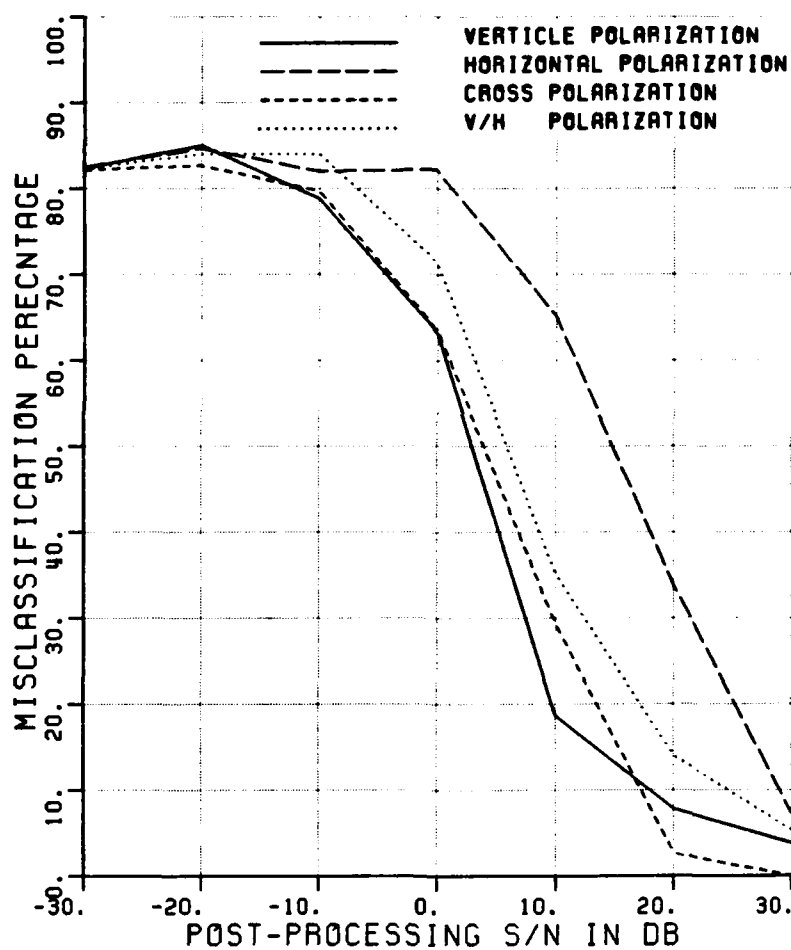


Figure A.79. Misclassification percentage versus post-processing SNR, comparing the performance of various polarizations.

CLASSIFICATION OF SHIPS

POLARIZATION	V	H	X	V/H
ELEV ASSUMED	KNOWN			
ELEVATION (DEG.)	27			
ASPECT ASSUMED	KNOWN			
MIN,MAX,INC ASPECT	0	10	10	
NO OF FREQUENCIES	8			
NO OF TARGETS	12		12	12
90% CI (±30%) +/-	3.1%		3.1%	3.1%
CLASS. FEATURES	T	T	T	T

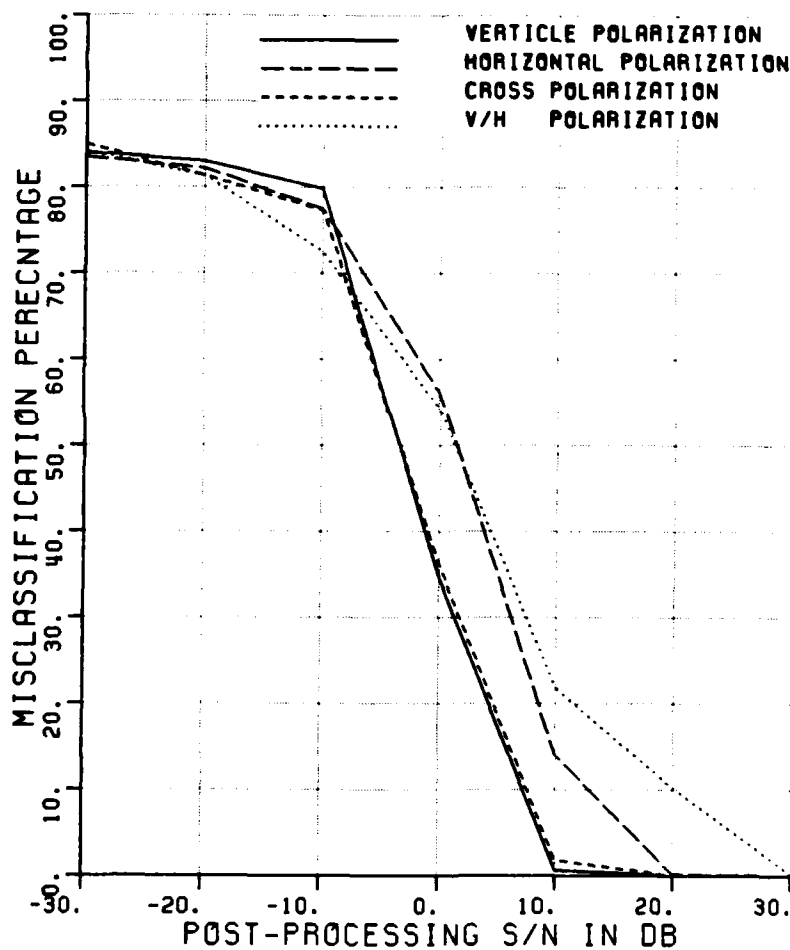


Figure A.80. Misclassification percentage versus post-processing SNR, comparing the performance of various polarizations.

CLASSIFICATION OF SHIPS

POLARIZATION	V	H	X	V/H
ELEV ASSUMED	KNOWN			
ELEVATION (DEG.)	27			
ASPECT ASSUMED	KNOWN			
MIN,MAX,INC ASPECT	80	100	10	
NO OF FREQUENCIES	8			
NO OF TARGETS	18	18	18	18
90% CI (±30%) +/-	2.5%	2.5%	2.5%	2.5%
CLASS. FEATURES	T	T	T	T

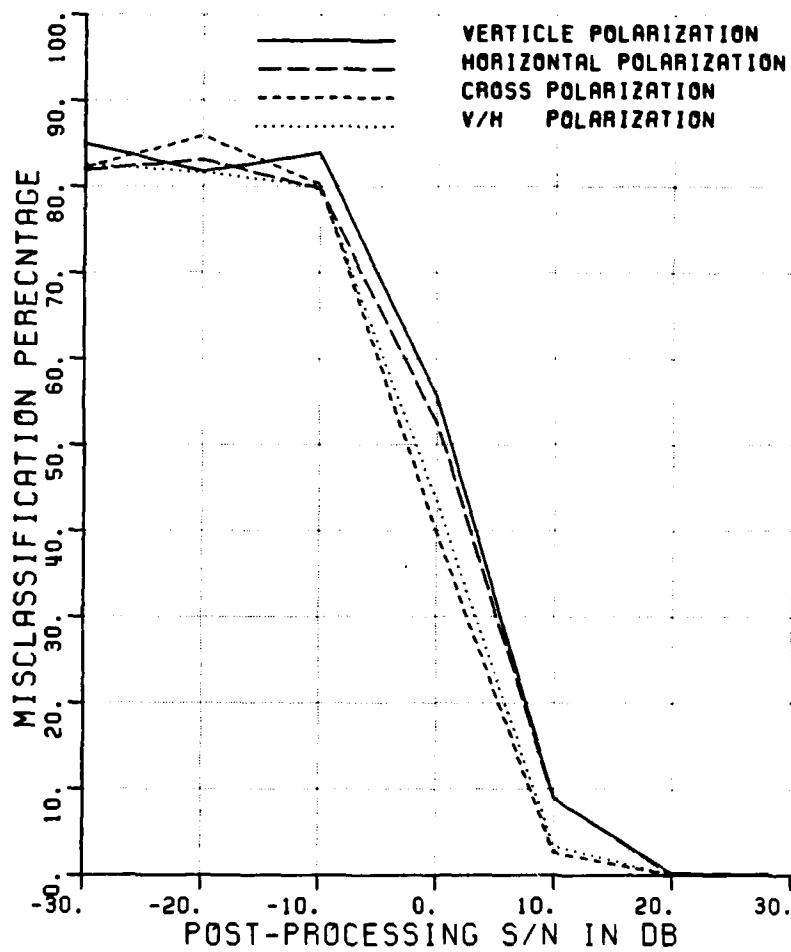


Figure A.81. Misclassification percentage versus post-processing SNR, comparing the performance of various polarizations.

CLASSIFICATION OF SHIPS

POLARIZATION	V	H	X	V/H
ELEV ASSUMED	KNOWN			
ELEVATION (DEG.)	27			
ASPECT ASSUMED	KNOWN			
MIN,MAX,INC ASPECT	170	180	10	
NO OF FREQUENCIES	8			
NO OF TARGETS	12	12	12	12
90% CI (±30%) +/-	3.1%	3.1%	3.1%	3.1%
CLASS. FEATURES	T	T	T	T

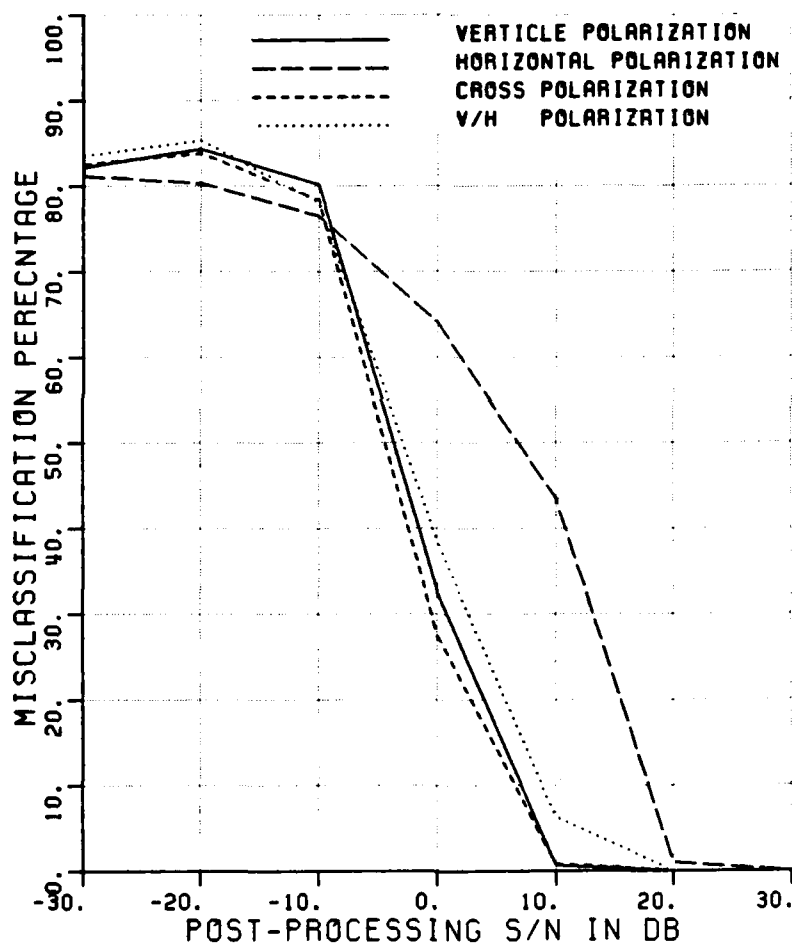


Figure A.82. Misclassification percentage versus post-processing SNR, comparing the performance of various polarizations.

CLASSIFICATION OF SHIPS

POLARIZATION	V												
ELEV ASSUMED	KNOWN												
ELEVATION (DEG.)	27												
ASPECT ASSUMED	KNOWN	/	KNOWN										
MIN,MAX,INC ASPECT	0	10	10.	30	60	15.	80	100	10.	170	180	10	
NO OF FREQUENCIES	8												
NO OF TARGETS	12		18		18		12						
90% CI (±30%) +/-	3.1%		2.5%		2.5%		3.1%						
CLASS. FEATURES	W	W	W	W									

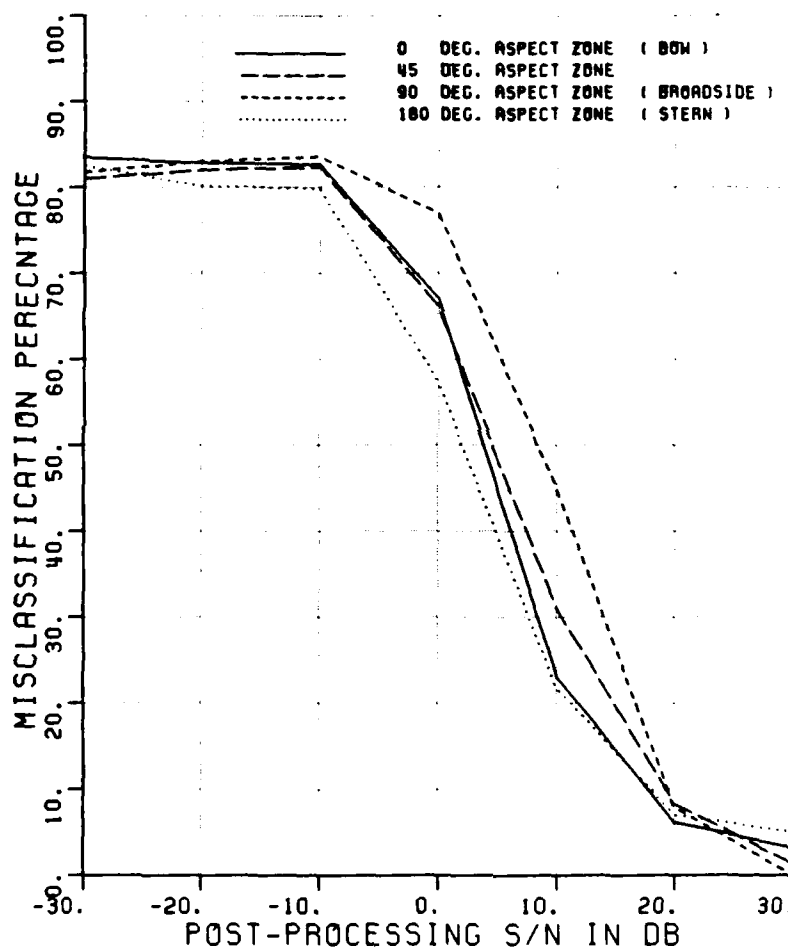


Figure A.83. Misclassification percentage versus post-processing SNR, comparing the performance of various aspect zones.

CLASSIFICATION OF SHIPS

POLARIZATION	V											
ELEV ASSUMED	KNOWN											
ELEVATION (DEG.)	27											
ASPECT ASSUMED	KNOWN			/			KNOWN					
MIN,MAX,INC ASPECT	0	10	10,	30	60	15,	80	100	10,	170	180	10
NO OF FREQUENCIES	8											
NO OF TARGETS	12			18			18			12		
90% CI (#30%) +/-	3.1%			2.5%			2.5%			3.1%		
CLASS. FEATURES	A4W			A4W			A4W			A4W		

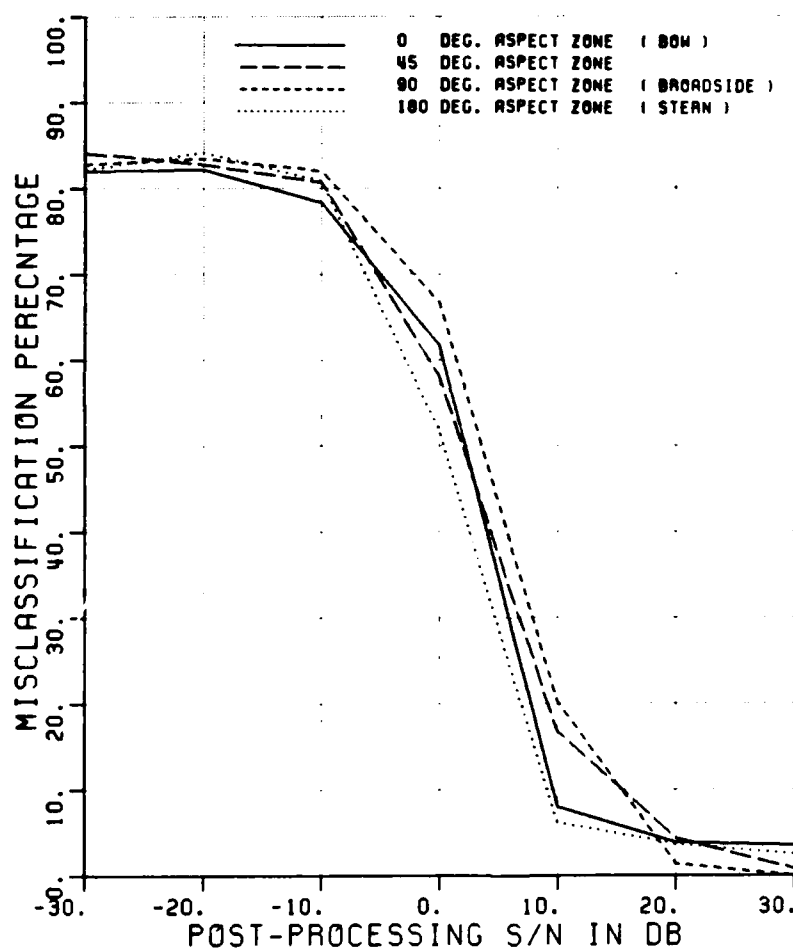


Figure A.84. Misclassification percentage versus post-processing SNR, comparing the performance of various aspect zones.

CLASSIFICATION OF SHIPS

POLARIZATION	V												
ELEV ASSUMED	KNOWN												
ELEVATION (DEG.)	27												
ASPECT ASSUMED	KNOWN	/	KNOWN										
MIN,MAX,INC ASPECT	0 10 10,	30 60 15,	80 100 10,	170 180 10									
NO OF FREQUENCIES	8												
NO OF TARGETS	12	18	18	12									
90% CI (±30%) +/-	3.1%	2.5%	2.5%	3.1%									
CLASS. FEATURES	R	R	R	R									

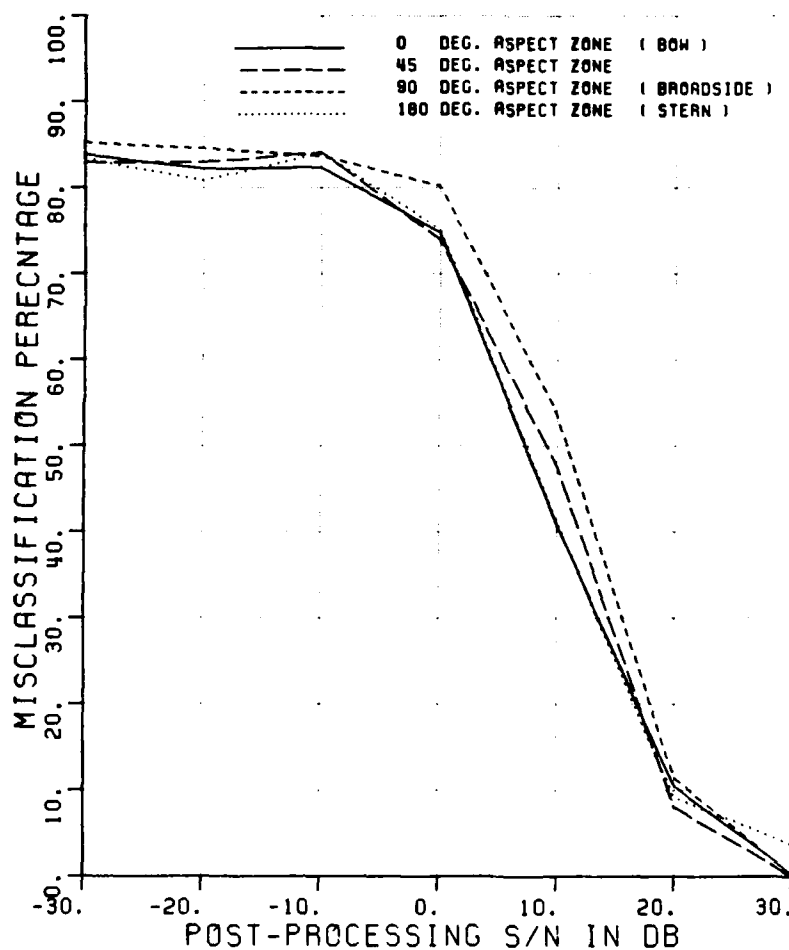


Figure A.85. Misclassification percentage versus post-processing SNR, comparing the performance of various aspect zones.

CLASSIFICATION OF SHIPS

POLARIZATION	V											
ELEV ASSUMED	KNOWN											
ELEVATION (DEG.)	27											
ASPECT ASSUMED	KNOWN / KNOWN											
MIN,MAX,INC ASPECT	0	10	10,	30	60	15,	80	100	10,	170	180	10
NO OF FREQUENCIES	8											
NO OF TARGETS	12		18		18		12					
90% CI (#30%) +/-	3.1%		2.5%		2.5%		3.1%					
CLASS. FEATURES	R&W		R&W		R&W		R&W					

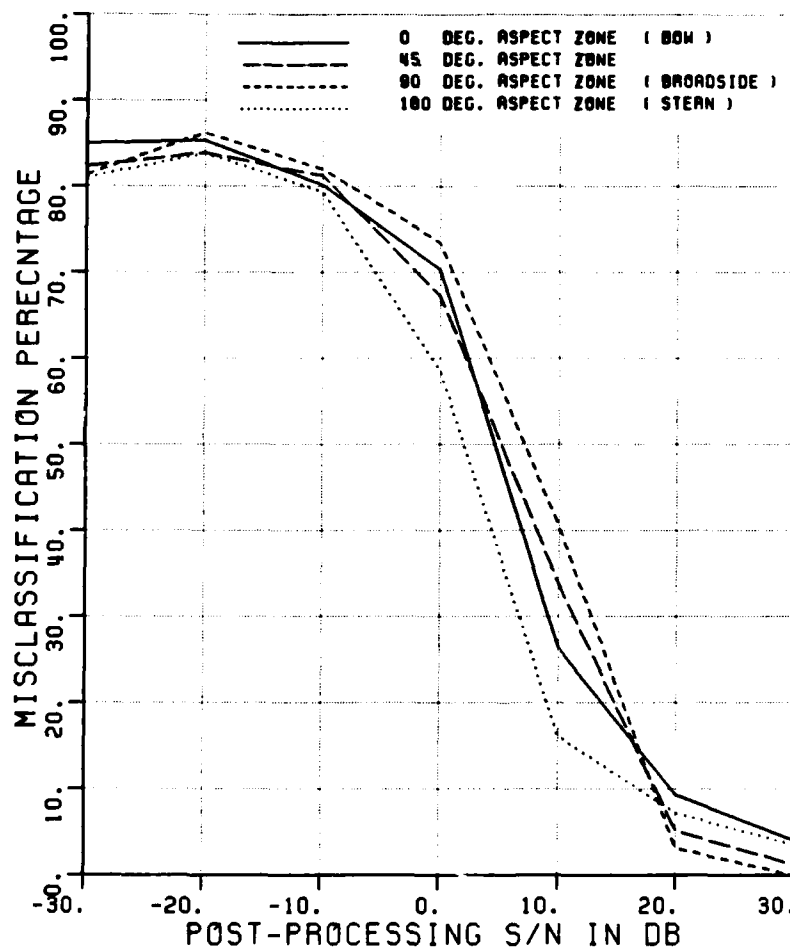


Figure A.86. Misclassification percentage versus post-processing SNR, comparing the performance of various aspect zones.

CLASSIFICATION OF SHIPS
 POLARIZATION V
 ELEV ASSUMED KNOWN
 ELEVATION (DEG.) 27
 ASPECT ASSUMED KNOWN / KNOWN
 MIN,MAX,INC ASPECT 0 10 10, 30 60 15, 80 100 10, 170 180 10
 NO OF FREQUENCIES 8
 NO OF TARGETS 12 18 18 12
 90% CI (±30%) +/- 3.1% 2.5% 2.5% 3.1%
 CLASS. FEATURES T T T T

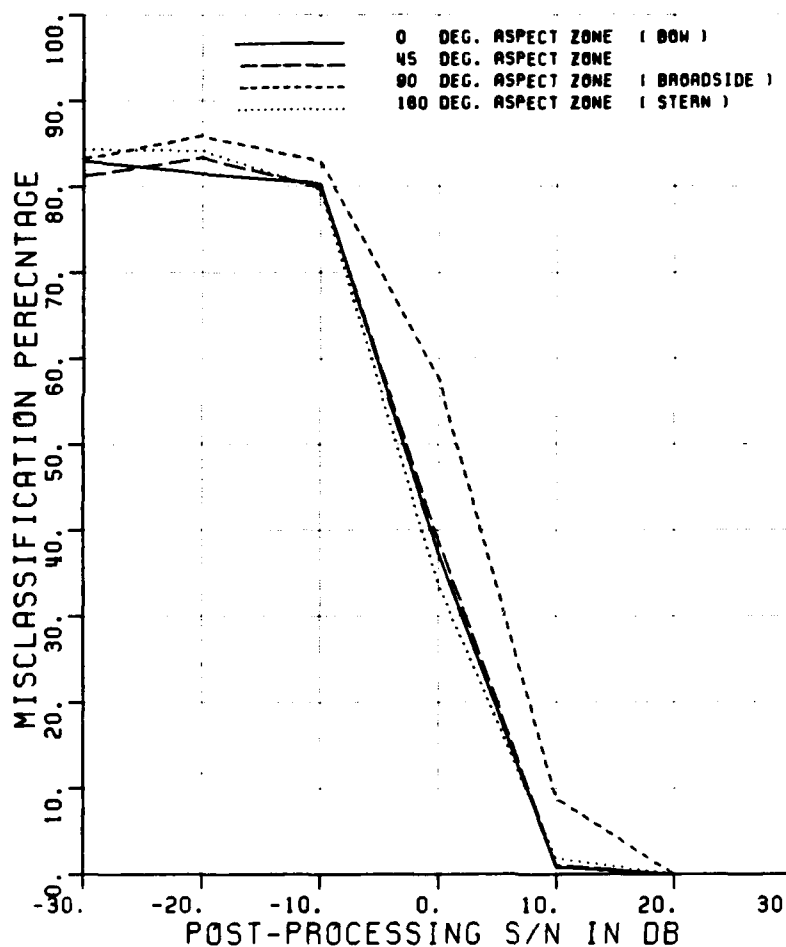


Figure A.87. Misclassification percentage versus post-processing SNR, comparing the performance of various aspect zones.

CLASSIFICATION OF SHIPS

POLARIZATION	H									
ELEV ASSUMED	KNOWN									
ELEVATION (DEG.)	27									
ASPECT ASSUMED	KNOWN / KNOWN									
MIN,MAX,INC ASPECT	0	10	10,	60	100	10,	170	180	10	
NO OF FREQUENCIES	8									
NO OF TARGETS	12		18		12					
90% CI (±30%) +/-	3.1%		2.5%		3.1%					
CLASS. FEATURES	A	A	A							

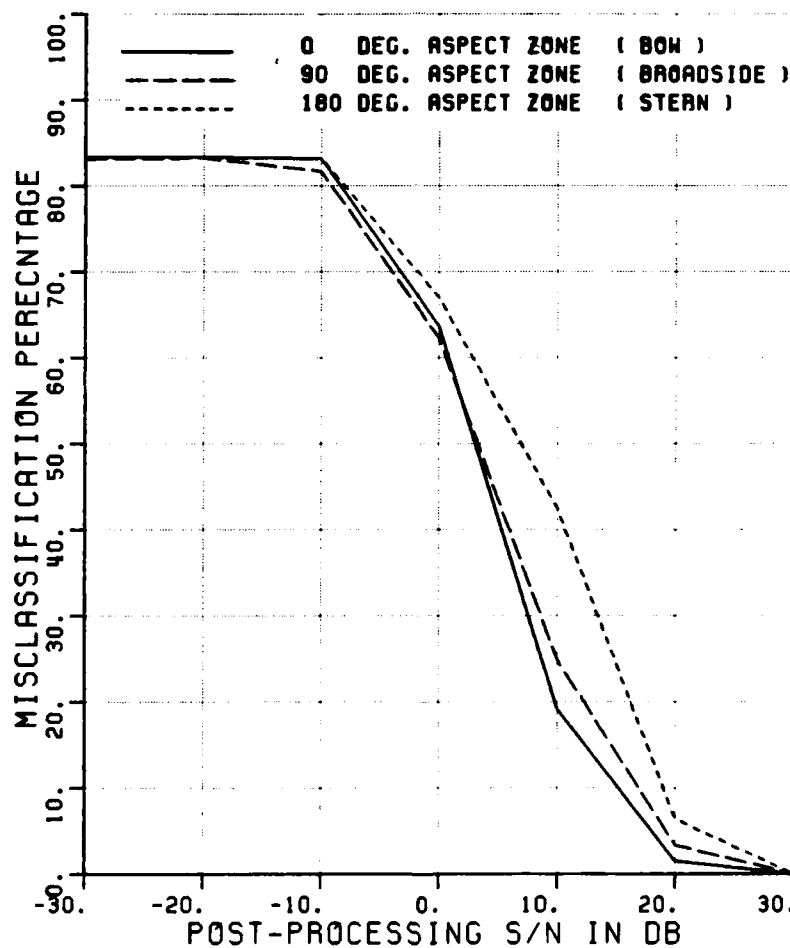


Figure A.88. Misclassification percentage versus post-processing SNR, comparing the performance of various aspect zones.

CLASSIFICATION OF SHIPS

POLARIZATION	H									
ELEV ASSUMED	KNOWN									
ELEVATION (DEG.)	27									
ASPECT ASSUMED	KNOWN					/ KNOWN				
MIN,MAX,INC ASPECT	0	10	10,	80	100	10,	170	180	10	
NO OF FREQUENCIES	8									
NO OF TARGETS	12			18			12			
90% CI (±30%) +/-	3.1%			2.5%			3.1%			
CLASS. FEATURES	W	W	W							

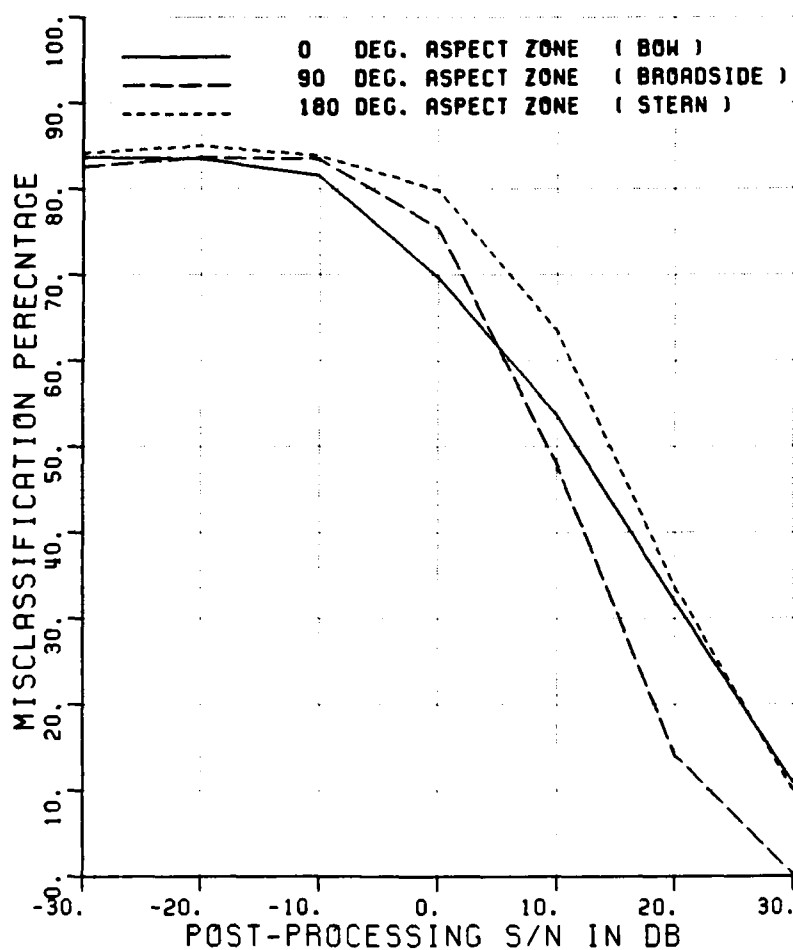


Figure A.89. Misclassification percentage versus post-processing SNR, comparing the performance of various aspect zones.

CLASSIFICATION OF SHIPS

POLARIZATION	H		
ELEV ASSUMED	KNOWN		
ELEVATION (DEG.)	27		
ASPECT ASSUMED	KNOWN	/	KNOWN
MIN,MAX,INC ASPECT	0 10 10,	80 100	10, 170 180 10
NO OF FREQUENCIES	8		
NO OF TARGETS	12	18	12
90% CI (@30%) +/-	3.1%	2.5%	3.1%
CLASS. FEATURES	A4W	A4W	A4W

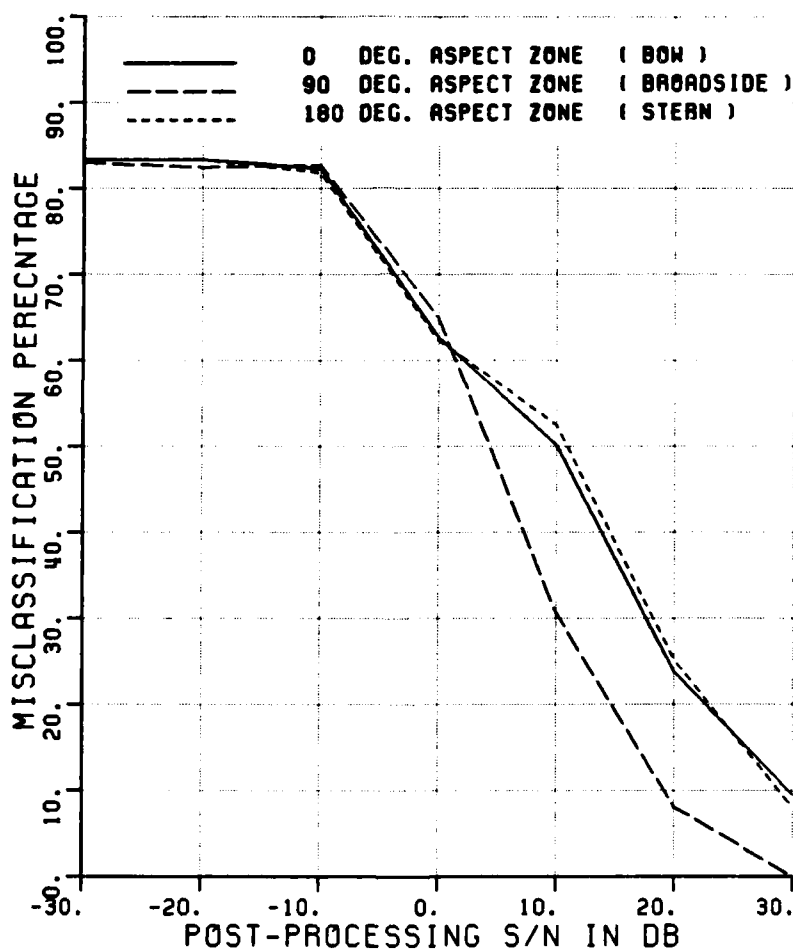


Figure A.90. Misclassification percentage versus post-processing SNR, comparing the performance of various aspect zones.

CLASSIFICATION OF SHIPS
 POLARIZATION H
 ELEV ASSUMED KNOWN
 ELEVATION (DEG.) 27
 ASPECT ASSUMED KNOWN / KNOWN
 MIN,MAX,INC ASPECT 0 10 10, 80 100 10, 170 180 10
 NO OF FREQUENCIES 8
 NO OF TARGETS 12 18 12
 90% CI (±30%) +/- 3.1% 2.5% 3.1%
 CLASS. FEATURES R R R

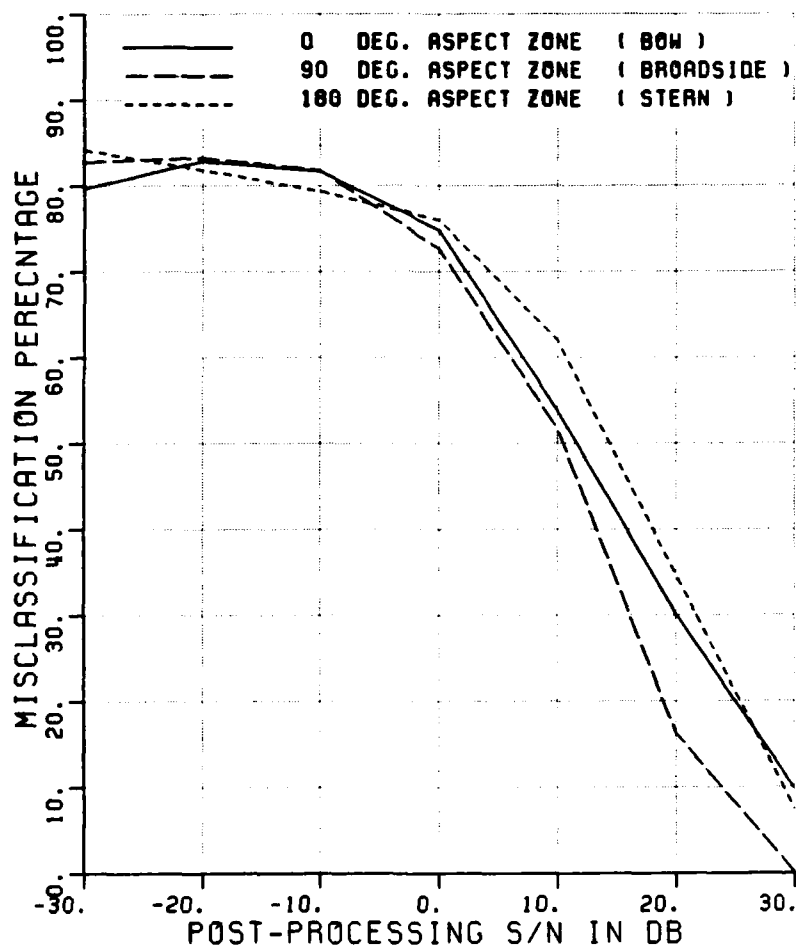


Figure A.91. Misclassification percentage versus post-processing SNR, comparing the performance of various aspect zones.

CLASSIFICATION OF SHIPS
 POLARIZATION H
 ELEV ASSUMED KNOWN
 ELEVATION (DEG.) 27
 ASPECT ASSUMED KNOWN / KNOWN
 MIN,MAX,INC ASPECT 0 10 10, 80 100 10, 170 180 10
 NO OF FREQUENCIES 8
 NO OF TARGETS 12 18 12
 90% CI (@30%) +/- 3.1% 2.5% 3.1%
 CLASS. FEATURES R&W R&W R&W

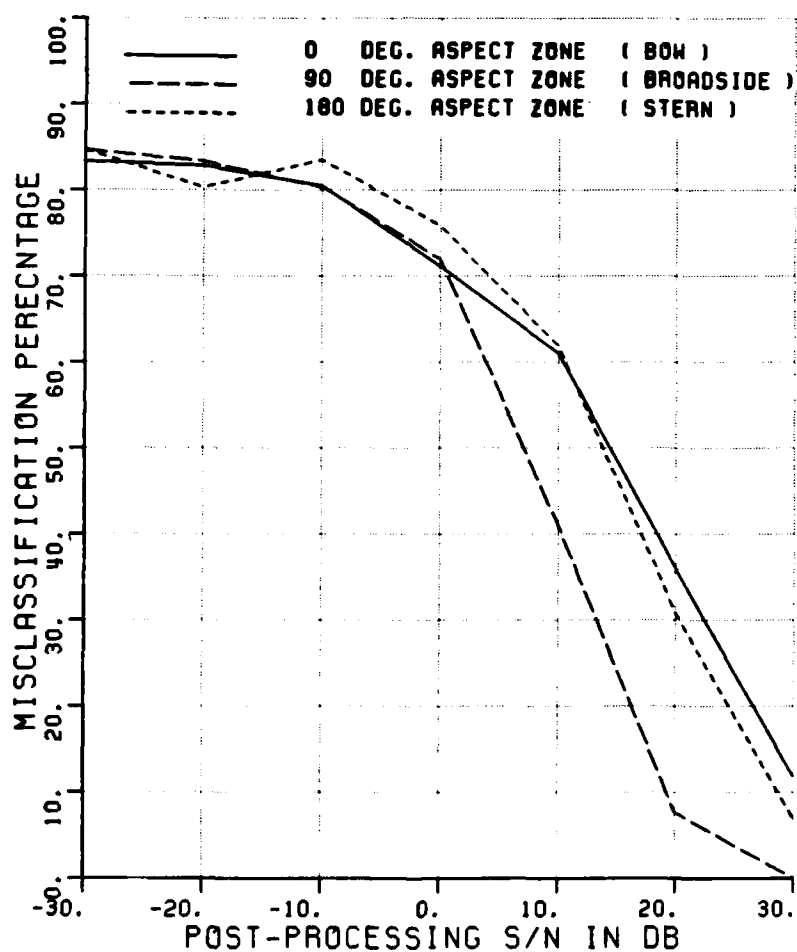


Figure A.92. Misclassification percentage versus post-processing SNR, comparing the performance of various aspect zones.

CLASSIFICATION OF SHIPS
 POLARIZATION H
 ELEV ASSUMED KNOWN
 ELEVATION (DEG.) 27
 ASPECT ASSUMED KNOWN / KNOWN
 MIN,MAX,INC ASPECT 0 10 10, 80 100 10, 170 180 10
 NO OF FREQUENCIES 8
 NO OF TARGETS 12 18 12
 90% CI (±30%) +/- 3.1% 2.5% 3.1%
 CLASS. FEATURES T T T

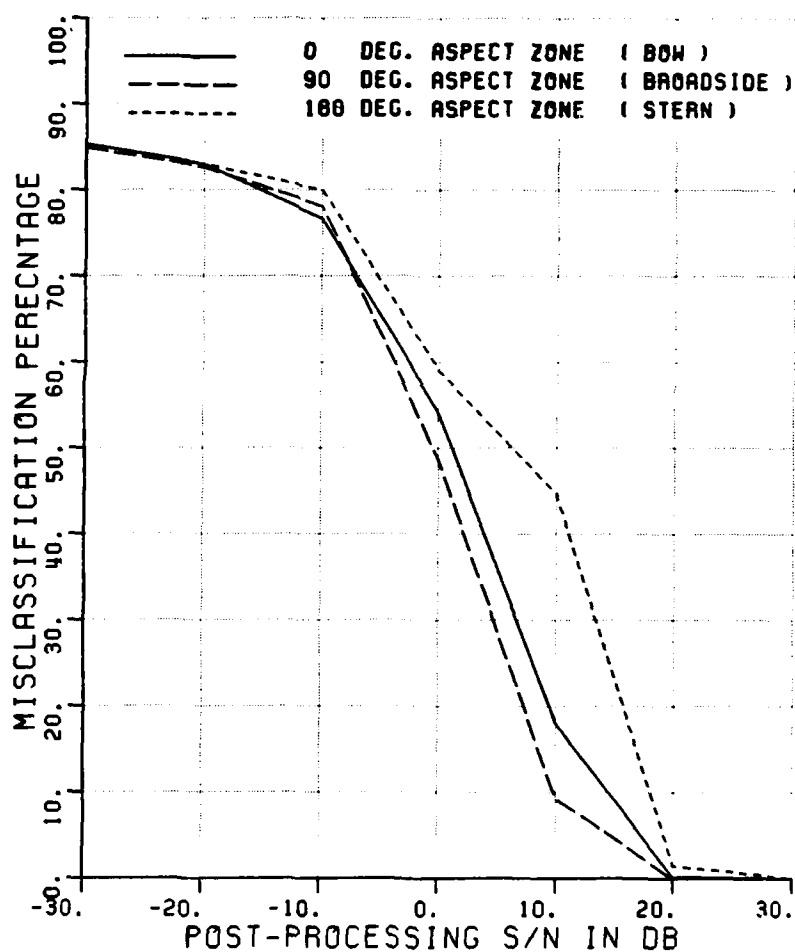


Figure A.93. Misclassification percentage versus post-processing SNR, comparing the performance of various aspect zones.

CLASSIFICATION OF SHIPS
 POLARIZATION X
 ELEV ASSUMED KNOWN
 ELEVATION (DEG.) 27
 ASPECT ASSUMED KNOWN / KNOWN
 MIN,MAX,INC ASPECT 0 10 10, 80 100 10, 170 180 10
 NO OF FREQUENCIES 8
 NO OF TARGETS 12 18 12
 90% CI (±30%) +/- 3.1% 2.5% 3.1%
 CLASS. FEATURES A A A

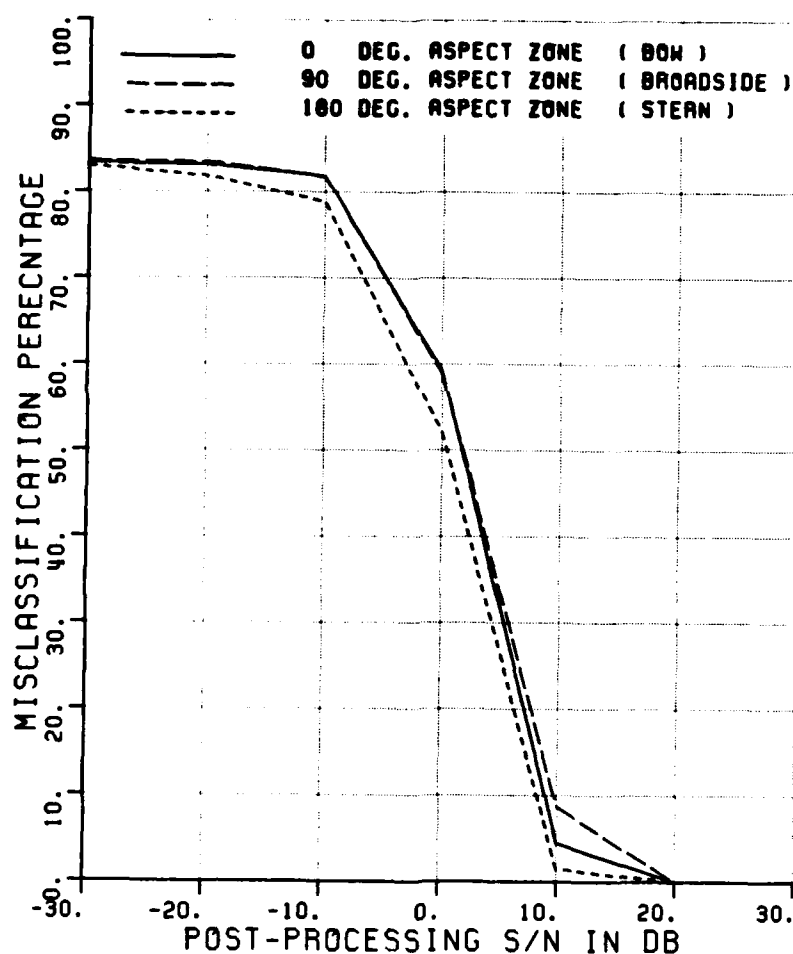


Figure A.94. Misclassification percentage versus post-processing SNR, comparing the performance of various aspect zones.

CLASSIFICATION OF SHIPS
 POLARIZATION X
 ELEV ASSUMED KNOWN
 ELEVATION (DEG.) 27
 ASPECT ASSUMED KNOWN / KNOWN
 MIN,MAX,INC ASPECT 0 10 10, 60 100 10, 170 180 10
 NO OF FREQUENCIES 8
 NO OF TARGETS 12 18 12
 90% CI (±30%) +/- 3.1% 2.5% 3.1%
 CLASS. FEATURES W W W

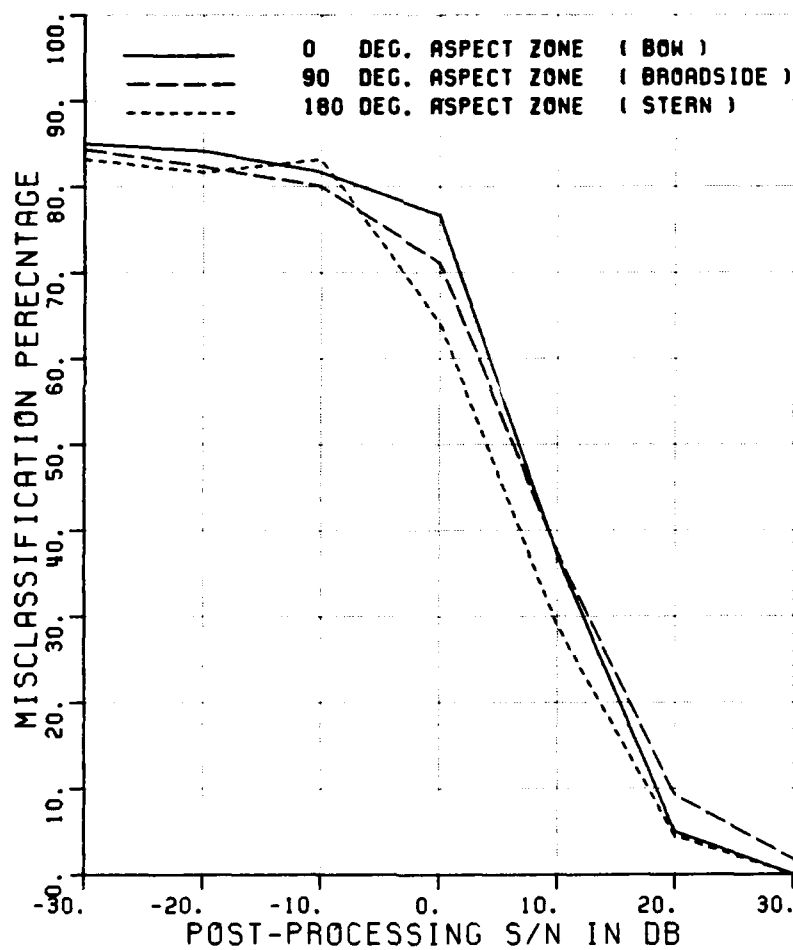


Figure A.95. Misclassification percentage versus post-processing SNR, comparing the performance of various aspect zones.

CLASSIFICATION OF SHIPS

POLARIZATION	X						
ELEV ASSUMED	KNOWN						
ELEVATION (DEG.)	27						
ASPECT ASSUMED	KNOWN			/	KNOWN		
MIN,MAX,INC ASPECT	0	10	10,	80	100	10,	170 180 10
NO OF FREQUENCIES	8						
NO OF TARGETS	12		18		12		
90% CI (±30%) +/-	3.1%		2.5%		3.1%		
CLASS. FEATURES	A&W		A&W		A&W		

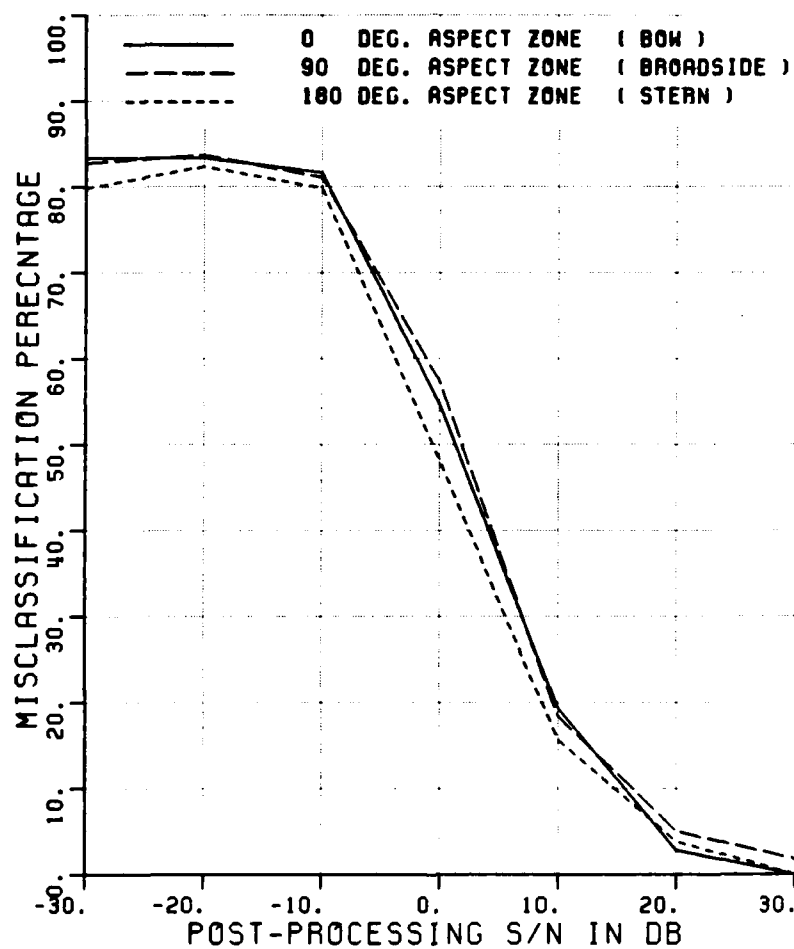


Figure A.96. Misclassification percentage versus post-processing SNR, comparing the performance of various aspect zones.

CLASSIFICATION OF SHIPS

POLARIZATION	X								
ELEV ASSUMED	KNOWN								
ELEVATION (DEG.)	27								
ASPECT ASSUMED	KNOWN	/	KNOWN						
MIN,MAX,INC ASPECT	0	10	10,	80	100	10,	170	180	10
NO OF FREQUENCIES	8								
NO OF TARGETS	12		18		12				
90% CI (±30%) +/-	3.1%		2.5%		3.1%				
CLASS. FEATURES	A	A	A						

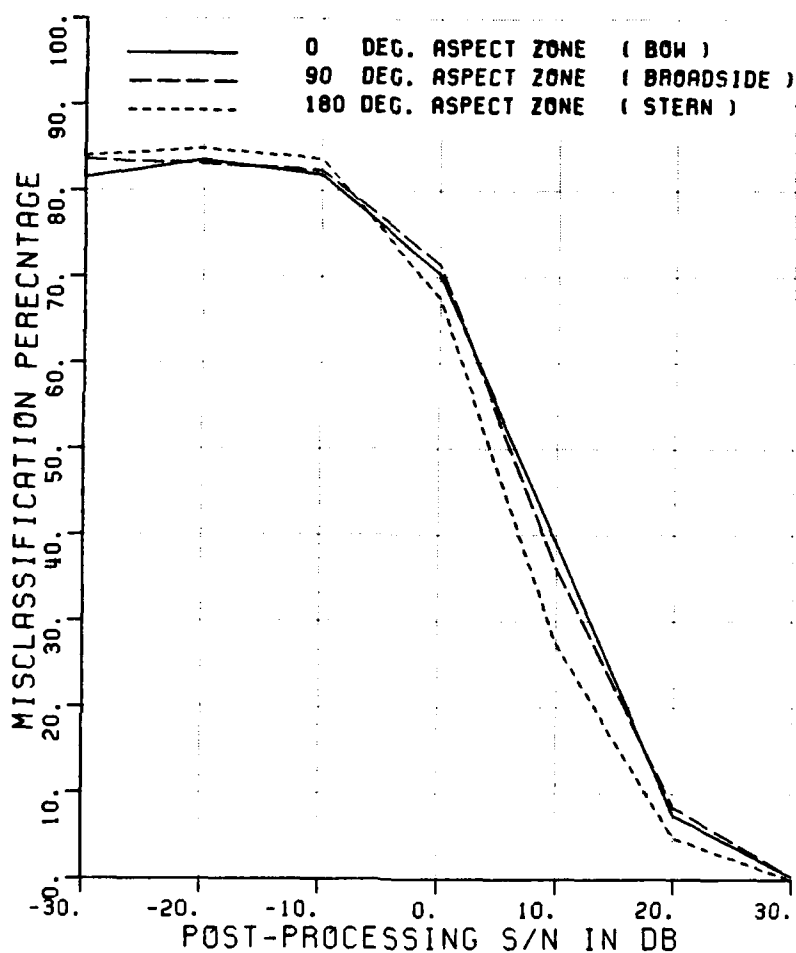


Figure A.97. Misclassification percentage versus post-processing SNR, comparing the performance of various aspect zones.

CLASSIFICATION OF SHIPS

POLARIZATION	X									
ELEV ASSUMED	KNOWN									
ELEVATION (DEG.)	27									
ASPECT ASSUMED	KNOWN / KNOWN									
MIN,MAX,INC ASPECT	0	10	10,	80	100	10,	170	180	10	
NO OF FREQUENCIES	8									
NO OF TARGETS	12		18		12					
90% CI (±30%) +/-	3.1%		2.5%		3.1%					
CLASS. FEATURES	R&W		R&W		R&W					

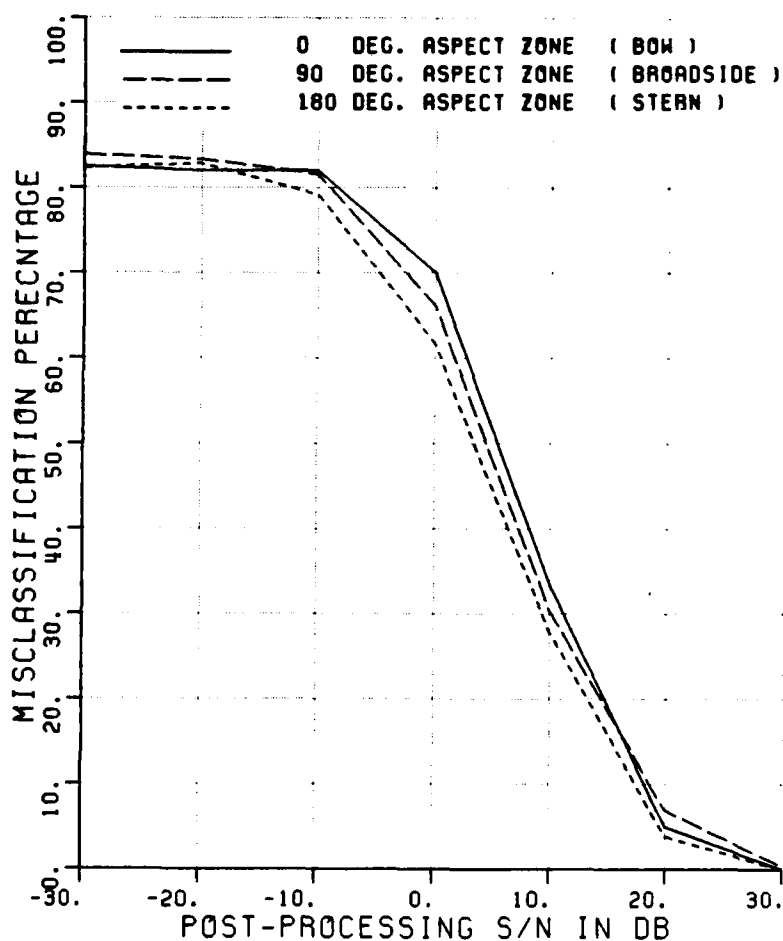


Figure A.98. Misclassification percentage versus post-processing SNR, comparing the performance of various aspect zones.

CLASSIFICATION OF SHIPS
 POLARIZATION X
 ELEV ASSUMED KNOWN
 ELEVATION (DEG.) 27
 ASPECT ASSUMED KNOWN / KNOWN
 MIN,MAX,INC ASPECT 0 10 10, 80 100 10, 170 180 10
 NO OF FREQUENCIES 8
 NO OF TARGETS 12 18 12
 90% CI (±30%) +/- 3.1% 2.5% 3.1%
 CLASS. FEATURES T T T

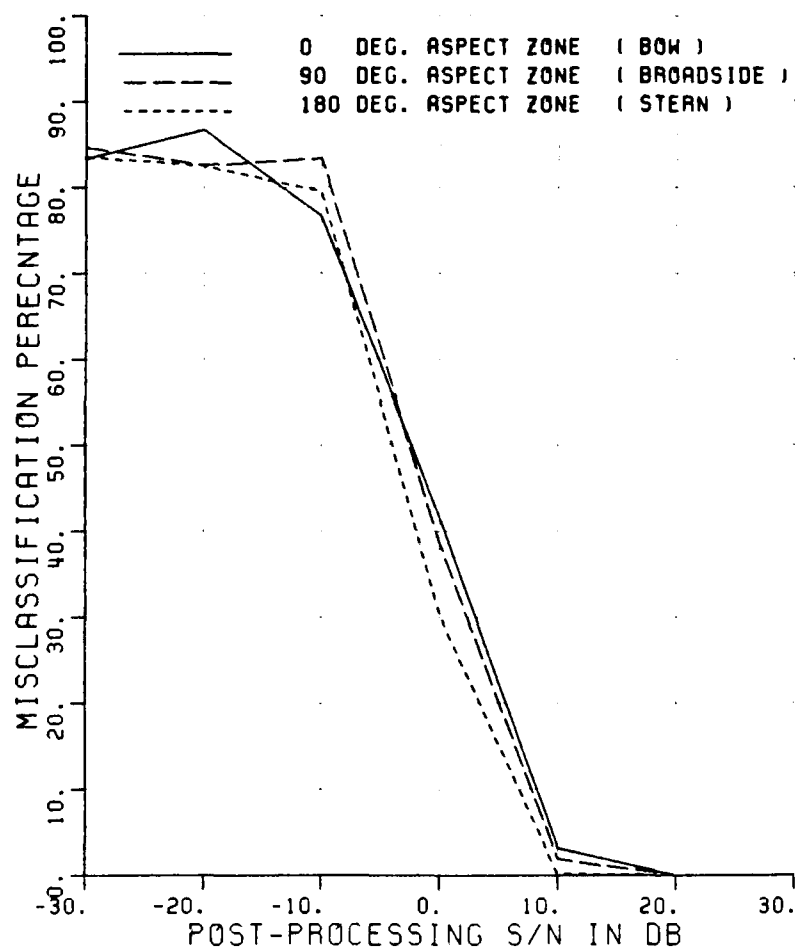


Figure A.99. Misclassification percentage versus post-processing SNR, comparing the performance of various aspect zones.

CLASSIFICATION OF SHIPS

POLARIZATION	V/H						
ELEV ASSUMED	KNOWN						
ELEVATION (DEG.)	27						
ASPECT ASSUMED	KNOWN / KNOWN						
MIN,MAX,INC ASPECT	0	10	10,	80	100	10,	170 180 10
NO OF FREQUENCIES	8						
NO OF TARGETS	12		18		12		
90% CI (±30%) +/-	3.1%		2.5%		3.1%		
CLASS. FEATURES	W	W	W				

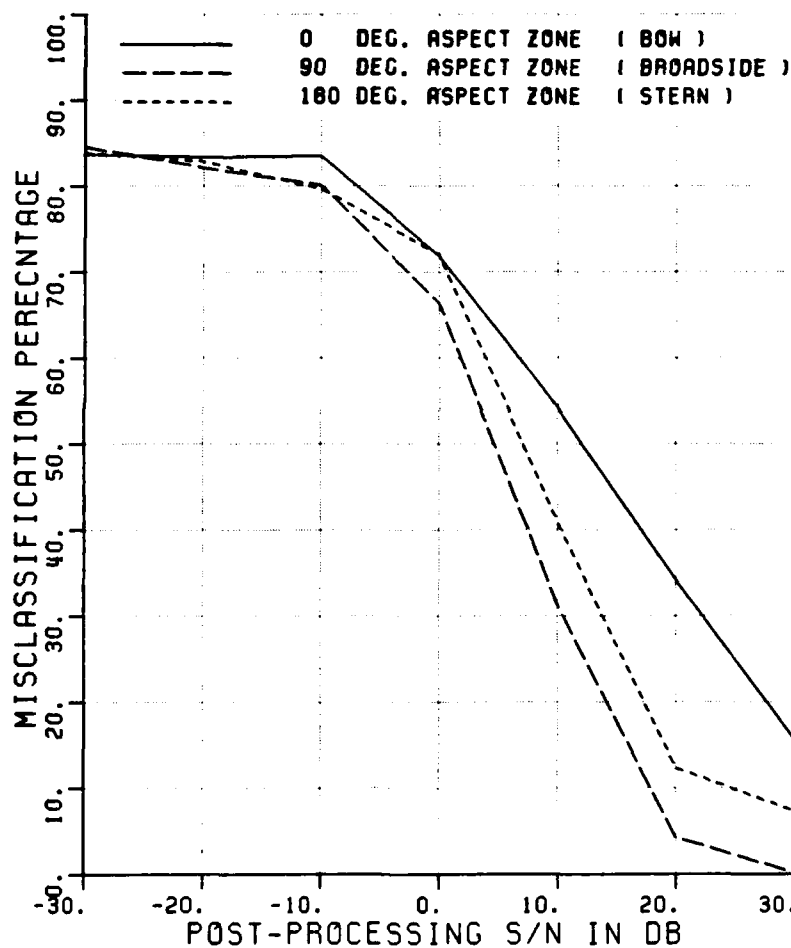


Figure A.100. Misclassification percentage versus post-processing SNR, comparing the performance of various aspect zones.

CLASSIFICATION OF SHIPS
 POLARIZATION V/H
 ELEV ASSUMED KNOWN
 ELEVATION (DEG.) 27
 ASPECT ASSUMED KNOWN / KNOWN
 MIN,MAX,INC ASPECT 0 10 10, 80 100 10, 170 180 10
 NO OF FREQUENCIES 8
 NO OF TARGETS 12 18 12
 90% CI (±30%) +/- 3.1% 2.5% 3.1%
 CLASS. FEATURES A&W A&W A&W

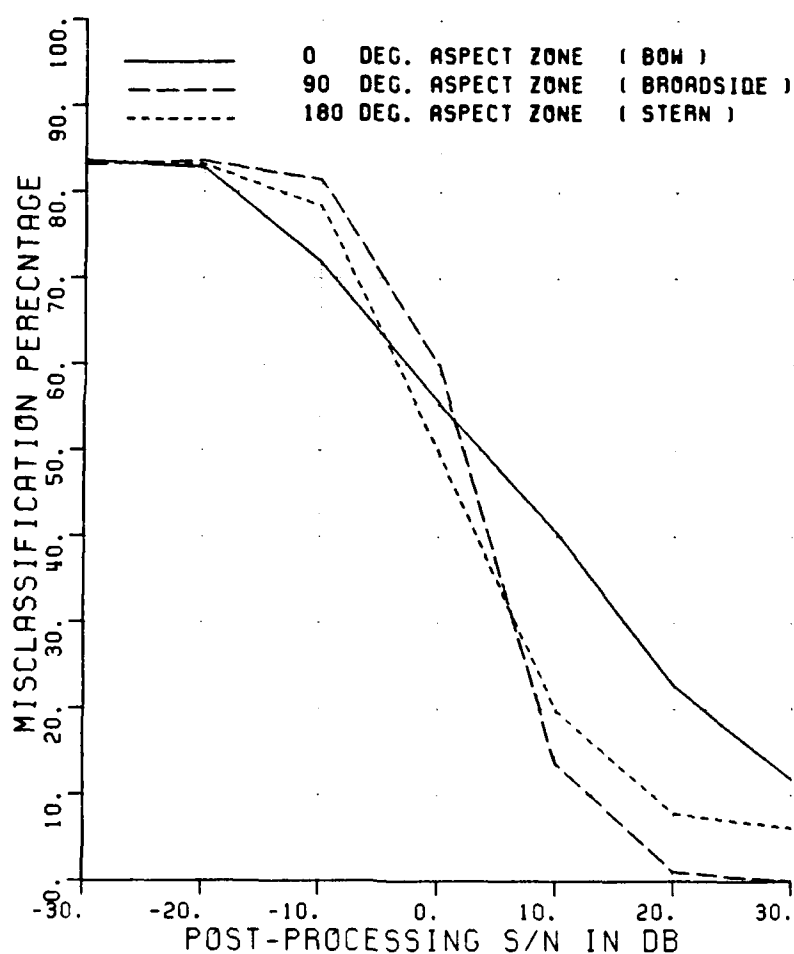


Figure A.101. Misclassification percentage versus post-processing SNR, comparing the performance of various aspect zones.

CLASSIFICATION OF SHIPS
 POLARIZATION V/H
 ELEV ASSUMED KNOWN
 ELEVATION (DEG.) 27
 ASPECT ASSUMED KNOWN / KNOWN
 MIN,MAX,INC ASPECT 0 10 10, 80 100 10, 170 180 10
 NO OF FREQUENCIES 8
 NO OF TARGETS 12 18 12
 90% CI (±30%) +/- 3.1% 2.5% 3.1%
 CLASS. FEATURES R R R

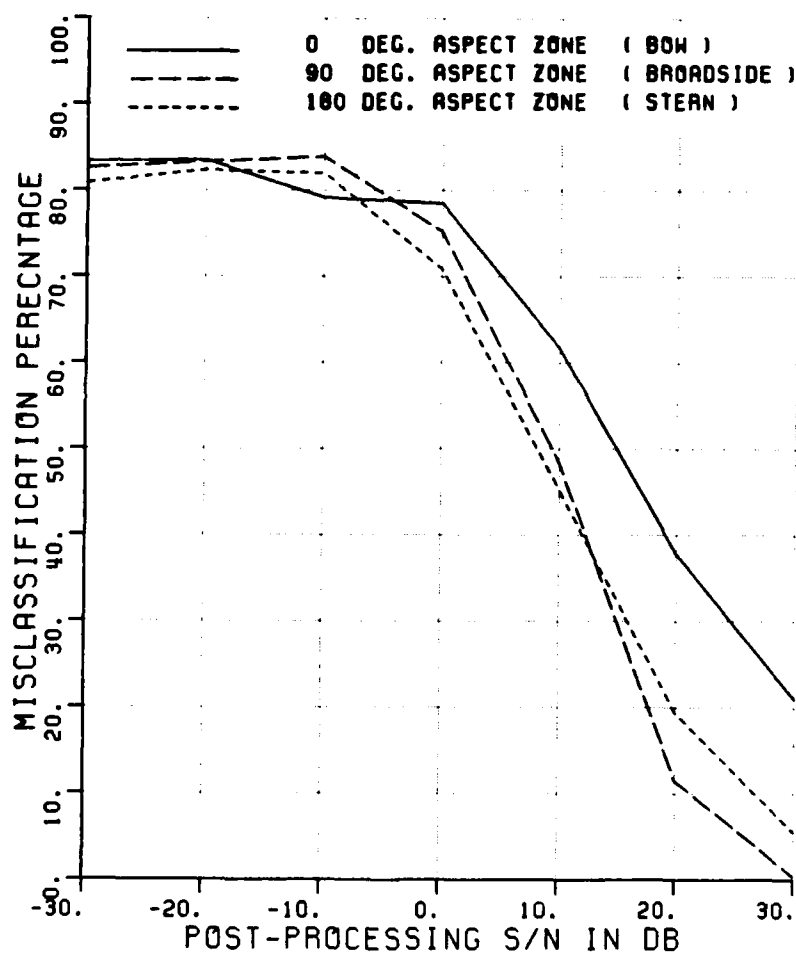


Figure A.102. Misclassification percentage versus post-processing SNR, comparing the performance of various aspect zones.

CLASSIFICATION OF SHIPS
 POLARIZATION V/H
 ELEV ASSUMED KNOWN
 ELEVATION (DEG.) 27
 ASPECT ASSUMED KNOWN / KNOWN
 MIN,MAX,INC ASPECT 0 10 10, 80 100 10, 170 180 10
 NO OF FREQUENCIES 8
 NO OF TARGETS 12 18 12
 90% CI (±30%) +/- 3.1% 2.5% 3.1%
 CLASS. FEATURES R4W R4W R4W

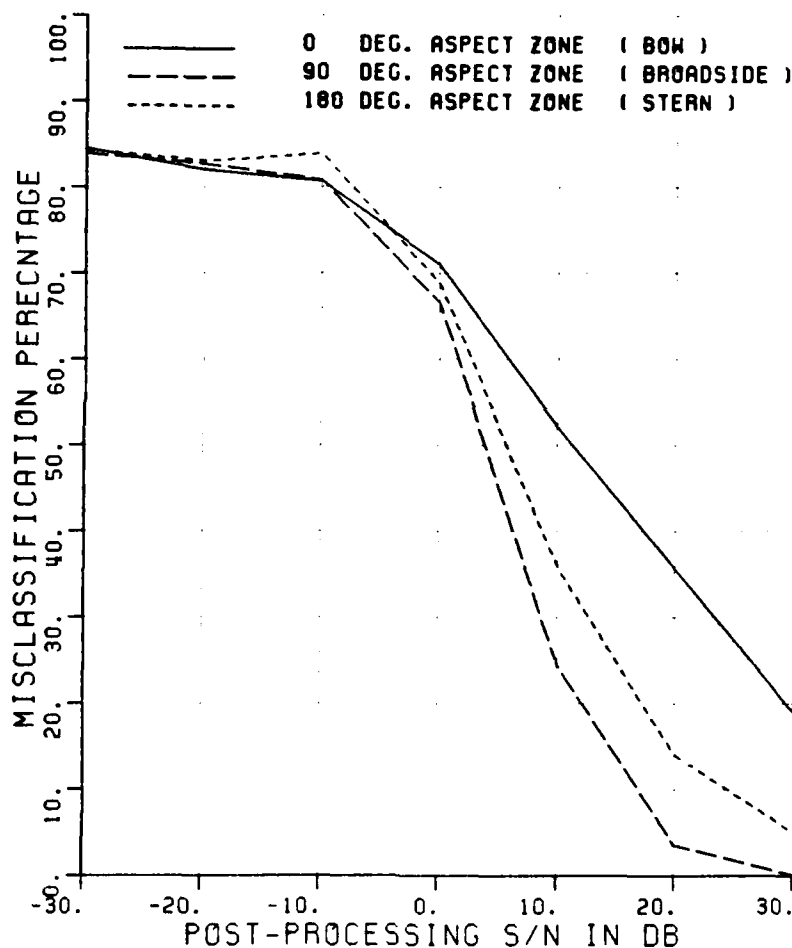


Figure A.103. Misclassification percentage versus post-processing SNR, comparing the performance of various aspect zones.

CLASSIFICATION OF SHIPS

POLARIZATION	V/H									
ELEV ASSUMED	KNOWN									
ELEVATION (DEG.)	27									
ASPECT ASSUMED	KNOWN / KNOWN									
MIN,MAX,INC ASPECT	0	10	10,	80	100	10,	170	180	10	
NO OF FREQUENCIES	8									
NO OF TARGETS	12		18		12					
90% CI (±30%) +/-	3.1%		2.5%		3.1%					
CLASS. FEATURES	T	T	T							

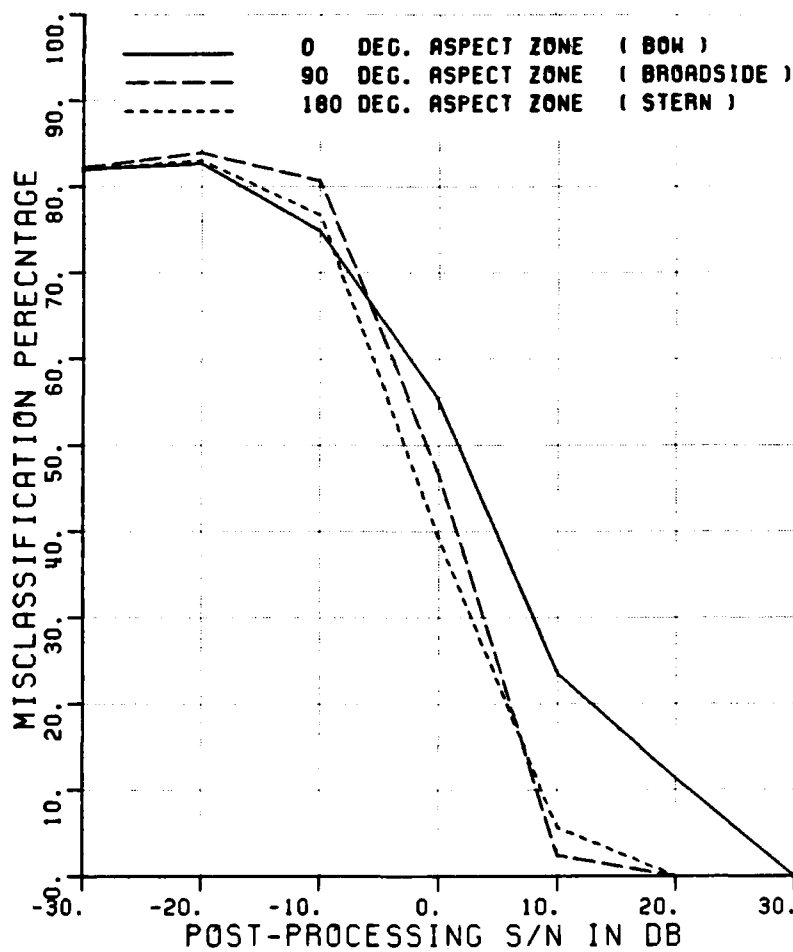


Figure A.104. Misclassification percentage versus post-processing SNR, comparing the performance of various aspect zones.

CLASSIFICATION OF SHIPS

POLARIZATION	H									
ELEV ASSUMED	KNOWN									
ELEVATION (DEG.)	27									
ASPECT ASSUMED	KNOWN					/ KNOWN				
MIN,MAX,INC ASPECT	0	10	10,	0	15	15,	0	30	30	
NO OF FREQUENCIES	8									
NO OF TARGETS	12		12		12					
90% CI (90%) +/-	3.1%		3.1%		3.1%					
CLASS. FEATURES	A	A	A							
ASP ERR IN CURVE	2		3							

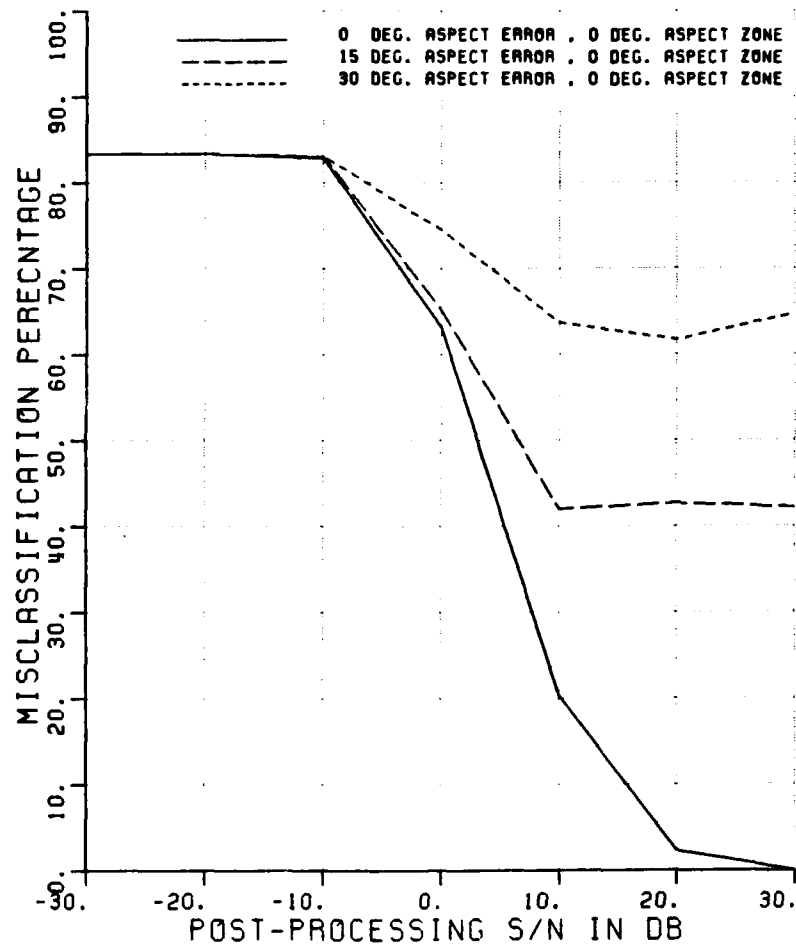


Figure A.105. Misclassification percentage versus post-processing SNR, comparing performance with various aspect angle errors, near to 0° aspect.

CLASSIFICATION OF SHIPS

POLARIZATION	V/H										
ELEV ASSUMED	KNOWN										
ELEVATION (DEG.)	27										
ASPECT ASSUMED	KNOWN					/ KNOWN					
MIN,MAX,INC ASPECT	0	10	10.	0	15	15.	0	30	30		
NO OF FREQUENCIES	8										
NO OF TARGETS	12		12		12						
90% CI (±30%) +/-	3.1%		3.1%		3.1%						
CLASS. FEATURES	A		A		A						
ASP ERR IN CURVE	2		3								

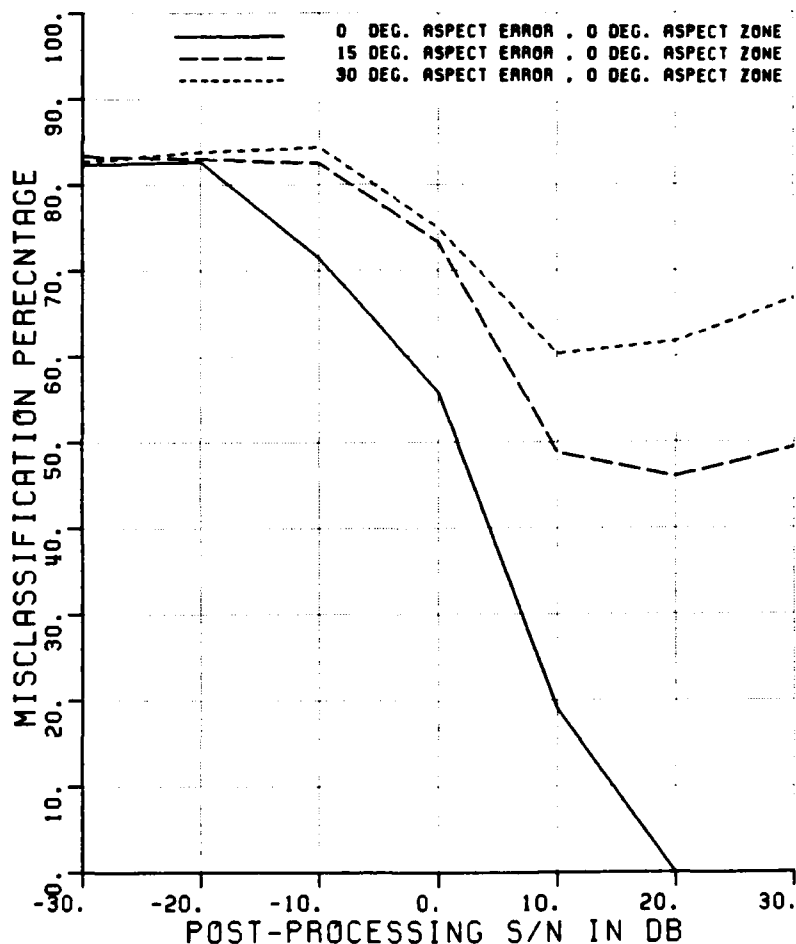


Figure A.106. Misclassification percentage versus post-processing SNR, comparing performance with various aspect angle errors, near to 0° aspect.

CLASSIFICATION OF SHIPS

POLARIZATION	V									
ELEV ASSUMED	KNOWN									
ELEVATION (DEG.)	27									
ASPECT ASSUMED	KNOWN / KNOWN									
MIN,MAX,INC ASPECT	0	10	10.	0	15	15.	0	30	30	
NO OF FREQUENCIES	8									
NO OF TARGETS	12	12				12				
90% CI (±30%) +/-	3.1%	3.1%				3.1%				
CLASS. FEATURES	A&W	A&W				A&W				
ASP ERR IN CURVE	2	3								

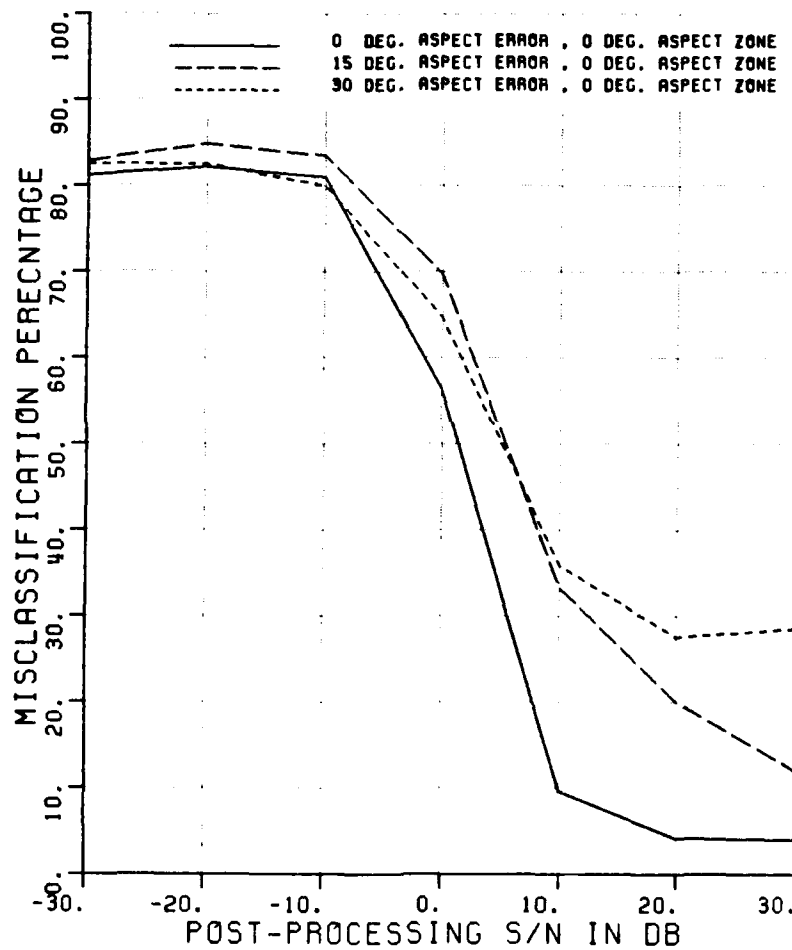


Figure A.107. Misclassification percentage versus post-processing SNR, comparing performance with various aspect angle errors, near to 0° aspect.

CLASSIFICATION OF SHIPS
 POLARIZATION H
 ELEV ASSUMED KNOWN
 ELEVATION (DEG.) 27
 ASPECT ASSUMED KNOWN / KNOWN
 MIN,MAX,INC ASPECT 0 10 10, 0 15 15, 0 30 30
 NO OF FREQUENCIES 8
 NO OF TARGETS 12 12 12
 90% CI (±30%) +/- 3.1% 3.1% 3.1%
 CLASS. FEATURES A&W A&W A&W
 ASP ERR IN CURVE 2 3

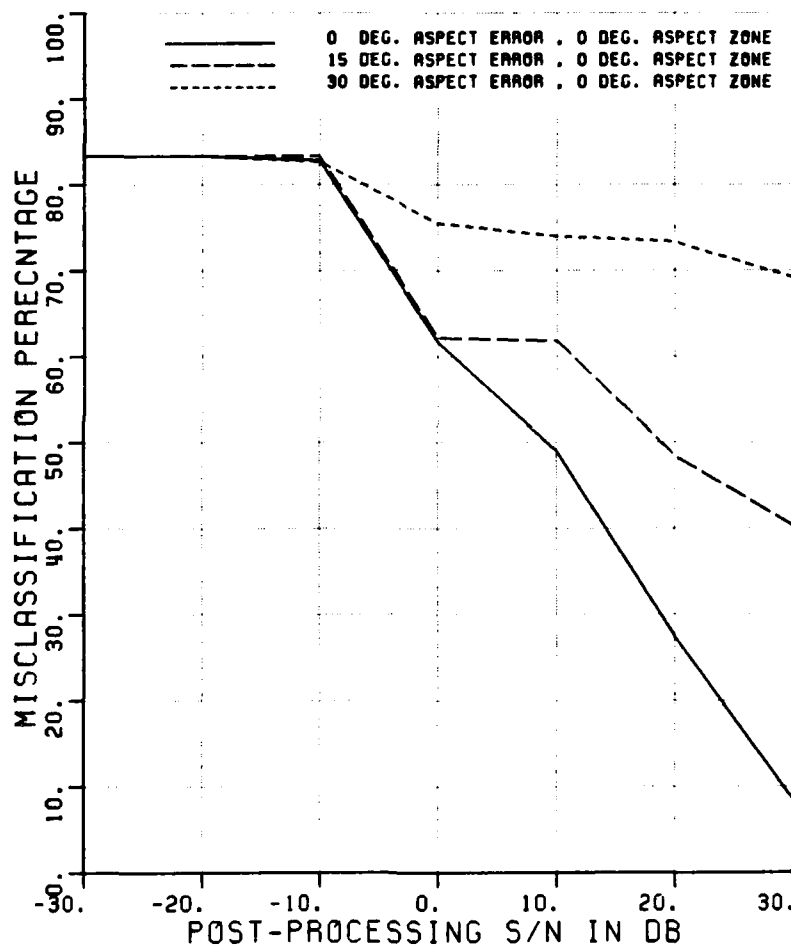


Figure A.108. Misclassification percentage versus post-processing SNR, comparing performance with various aspect angle errors, near to 0° aspect.

CLASSIFICATION OF SHIPS									
POLARIZATION	X								
ELEV ASSUMED	KNOWN								
ELEVATION (DEG.)	27								
ASPECT ASSUMED	KNOWN			/	KNOWN				
MIN,MAX,INC ASPECT	0	10	10.	0	15	15.	0	30	30
NO OF FREQUENCIES	8								
NO OF TARGETS	12	12			12				
90% CI (±30%) +/-	3.1%	3.1%			3.1%				
CLASS. FEATURES	A&W	A&W			A&W				
ASP ERR IN CURVE	2	3							

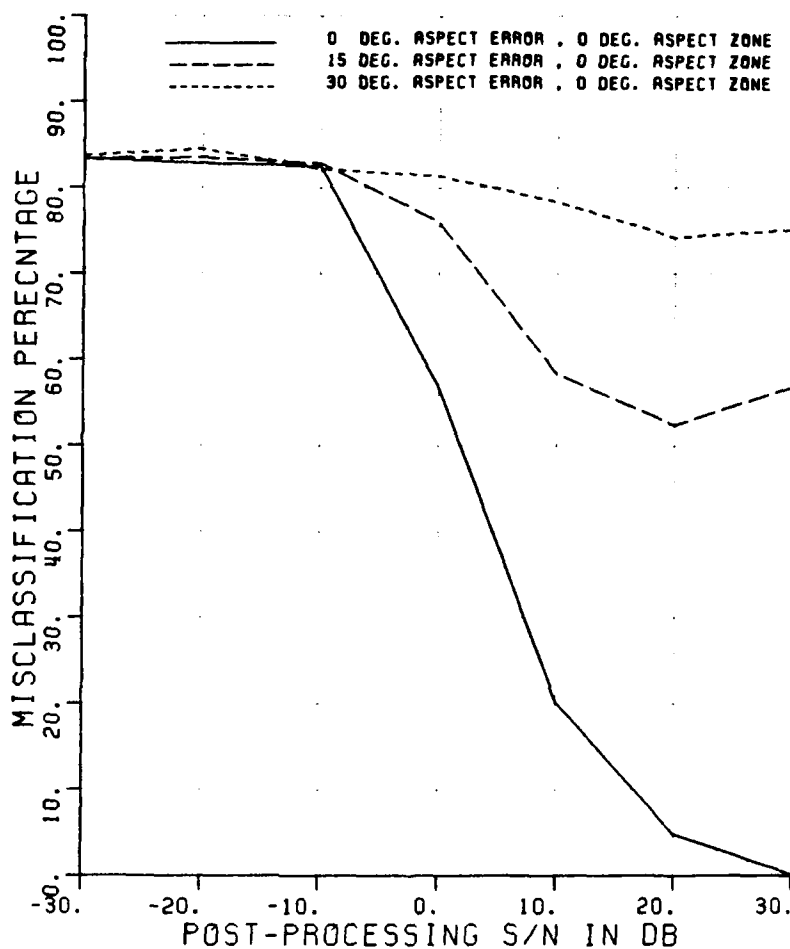


Figure A.109. Misclassification percentage versus post-processing SNR, comparing performance with various aspect angle errors, near to 0° aspect.

CLASSIFICATION OF SHIPS

POLARIZATION	V/H							
ELEV ASSUMED	KNOWN							
ELEVATION (DEG.)	27							
ASPECT ASSUMED	KNOWN	/	KNOWN					
MIN,MAX,INC ASPECT	0 10 10,	0 15 15,	0 30 30					
NO OF FREQUENCIES	8							
NO OF TARGETS	12	12	12					
90% CI (±30%) +/-	3.1%	3.1%	3.1%					
CLASS. FEATURES	A4W	A4W	A4W					
ASP ERR IN CURVE	2	3						

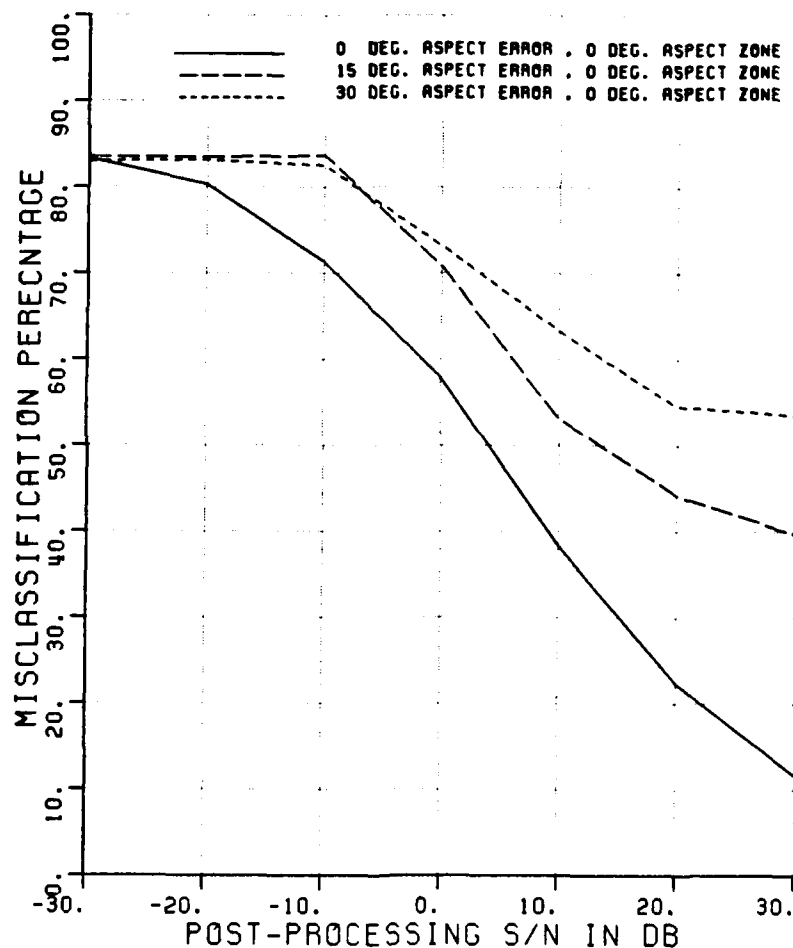


Figure A.110. Misclassification percentage versus post-processing SNR, comparing performance with various aspect angle errors, near to 0° aspect.

CLASSIFICATION OF SHIPS
 POLARIZATION V
 ELEV ASSUMED KNOWN
 ELEVATION (DEG.) 27
 ASPECT ASSUMED KNOWN / KNOWN
 MIN,MAX,INC ASPECT 0 10 10, 0 15 15, 0 30 30
 NO OF FREQUENCIES 8
 NO OF TARGETS 12 12 12
 90% CI (±30%) +/- 3.1% 3.1% 3.1%
 CLASS. FEATURES R&W R&W R&W
 ASP ERR IN CURVE 2 3

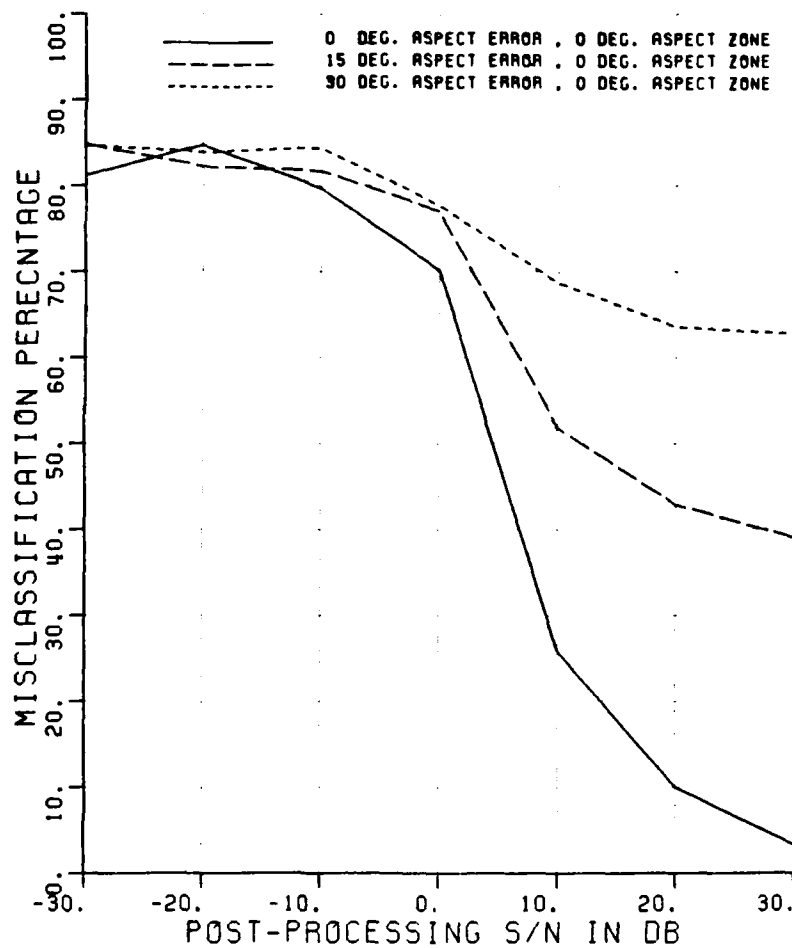


Figure A.111. Misclassification percentage versus post-processing SNR, comparing performance with various aspect angle errors, near to 0° aspect.

CLASSIFICATION OF SHIPS

POLARIZATION	H									
ELEV ASSUMED	KNOWN									
ELEVATION (DEG.)	27									
ASPECT ASSUMED	KNOWN					/ KNOWN				
MIN,MAX,INC ASPECT	0	10	10,	0	15	15,	0	30	30	
NO OF FREQUENCIES	8									
NO OF TARGETS	12					12				
90% CI (@30%) +/-	3.1%					3.1%				
CLASS. FEATURES	R&W					R&W				
ASP ERR IN CURVE	2					3				

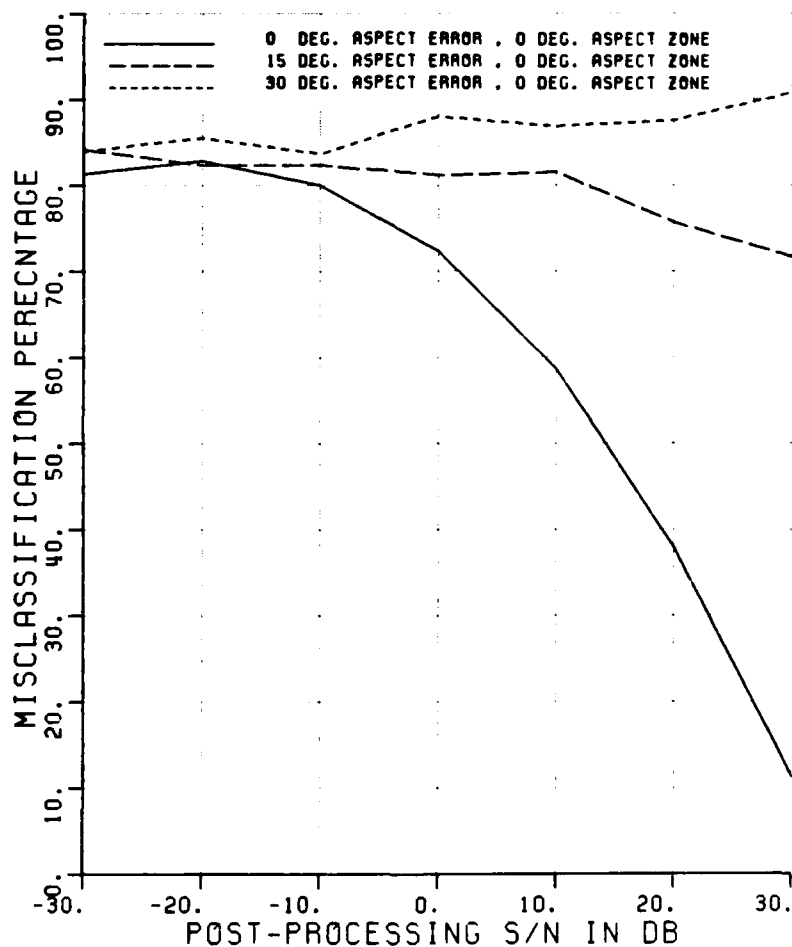


Figure A.112. Misclassification percentage versus post-processing SNR, comparing performance with various aspect angle errors, near to 0° aspect.

CLASSIFICATION OF SHIPS
 POLARIZATION X
 ELEV ASSUMED KNOWN
 ELEVATION (DEG.) 27
 ASPECT ASSUMED KNOWN / KNOWN
 MIN,MAX,INC ASPECT 0 10 10, 0 15 15, 0 30 30
 NO OF FREQUENCIES 8
 NO OF TARGETS 12 12 12
 90% CI (@30%) +/- 3.1% 3.1% 3.1%
 CLASS. FEATURES R&W R&W R&W
 ASP ERR IN CURVE 2 3

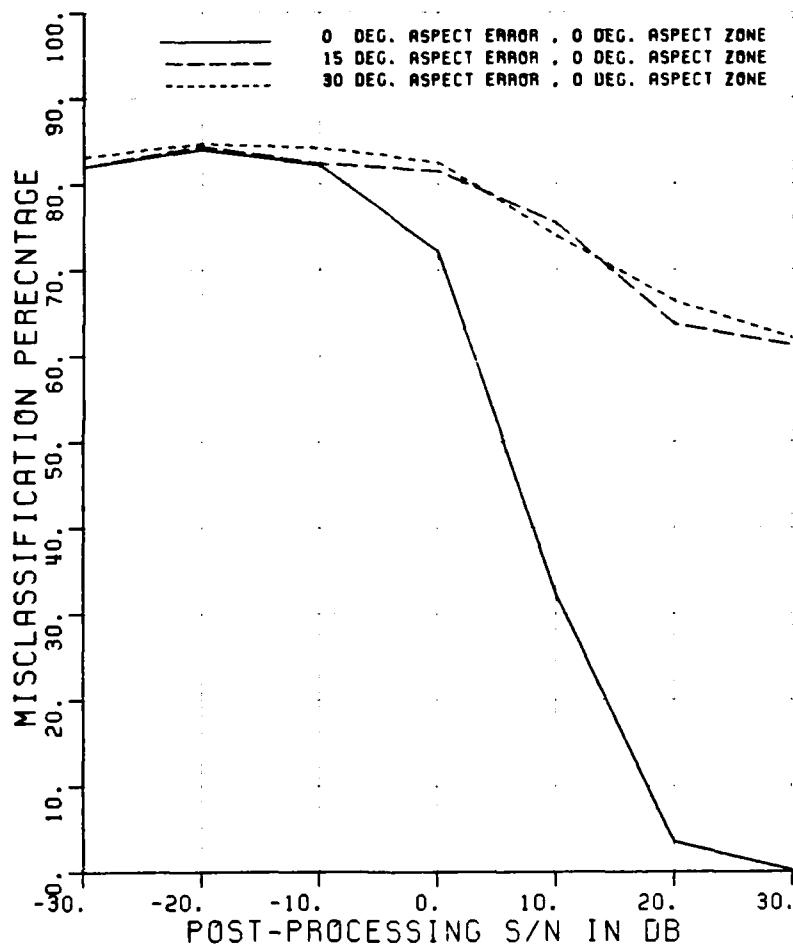


Figure A.113. Misclassification percentage versus post-processing SNR, comparing performance with various aspect angle errors, near to 0° aspect.

CLASSIFICATION OF SHIPS
 POLARIZATION V/H
 ELEV ASSUMED KNOWN
 ELEVATION (DEG.) 27
 ASPECT ASSUMED KNOWN / KNOWN
 MIN,MAX,INC ASPECT 0 10 10, 0 15 15, 0 30 30
 NO OF FREQUENCIES 8
 NO OF TARGETS 12 12 12
 90% CI (±30%) +/- 3.1% 3.1% 3.1%
 CLASS. FEATURES R&W R&W R&W
 ASP ERR IN CURVE 2 3

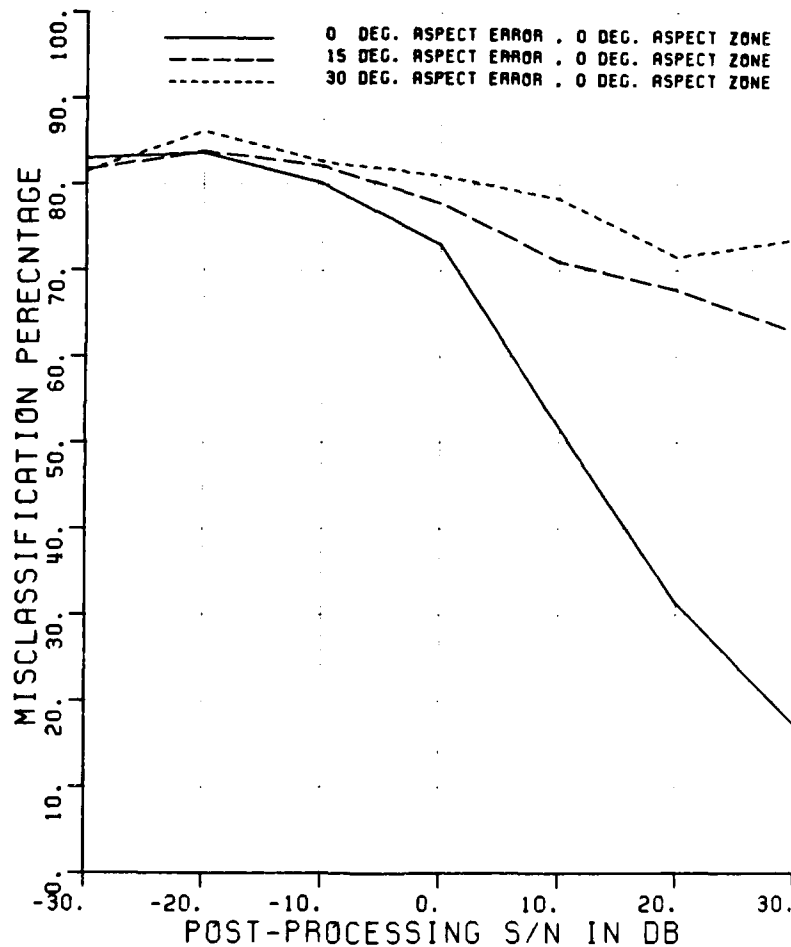


Figure A.114. Misclassification percentage versus post-processing SNR, comparing performance with various aspect angle errors, near to 0° aspect.

CLASSIFICATION OF SHIPS
 POLARIZATION V
 ELEV ASSUMED KNOWN
 ELEVATION (DEG.) 27
 ASPECT ASSUMED KNOWN / KNOWN
 MIN,MAX,INC ASPECT 0 10 10, 0 15 15, 0 30 30
 NO OF FREQUENCIES 8
 NO OF TARGETS 12 12 12
 90% CI (±30%) +/- 3.1% 3.1% 3.1%
 CLASS. FEATURES T T T
 ASP ERR IN CURVE 2 3

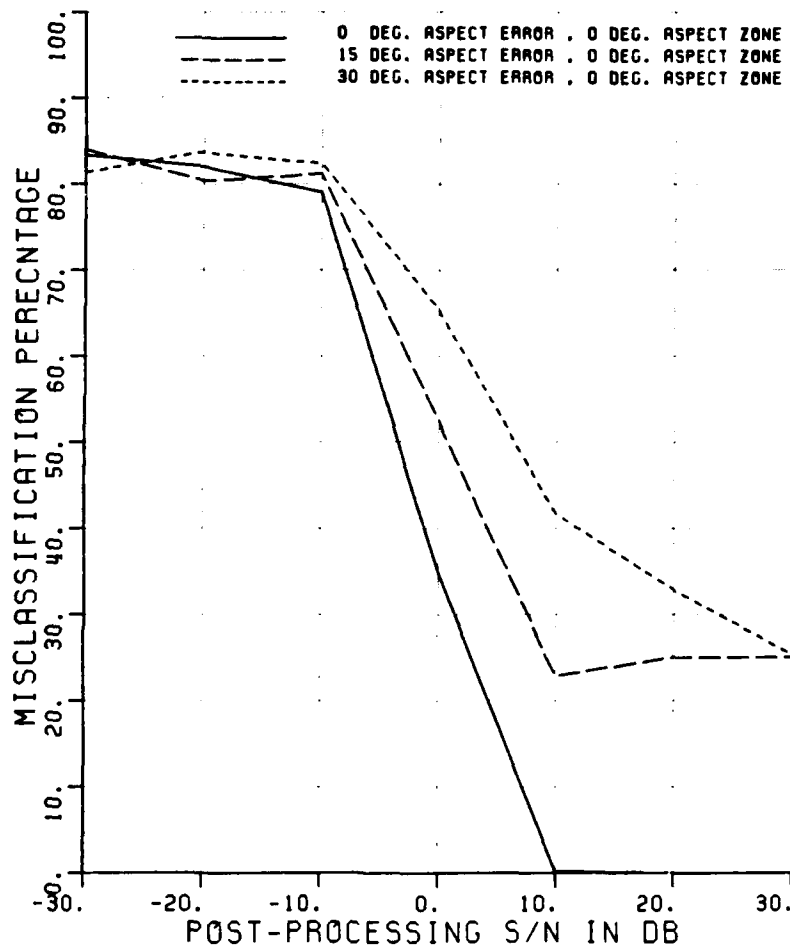


Figure A.115. Misclassification percentage versus post-processing SNR, comparing performance with various aspect angle errors, near to 0° aspect.

CLASSIFICATION OF SHIPS

POLARIZATION H
 ELEV ASSUMED KNOWN
 ELEVATION (DEG.) 27
 ASPECT ASSUMED KNOWN / KNOWN
 MIN,MAX,INC ASPECT 0 10 10, 0 15 15, 0 30 30
 NO OF FREQUENCIES 8
 NO OF TARGETS 12 12 12
 90% CI (±30%) +/- 3.1% 3.1% 3.1%
 CLASS. FEATURES T T T
 ASP ERR IN CURVE 2 3

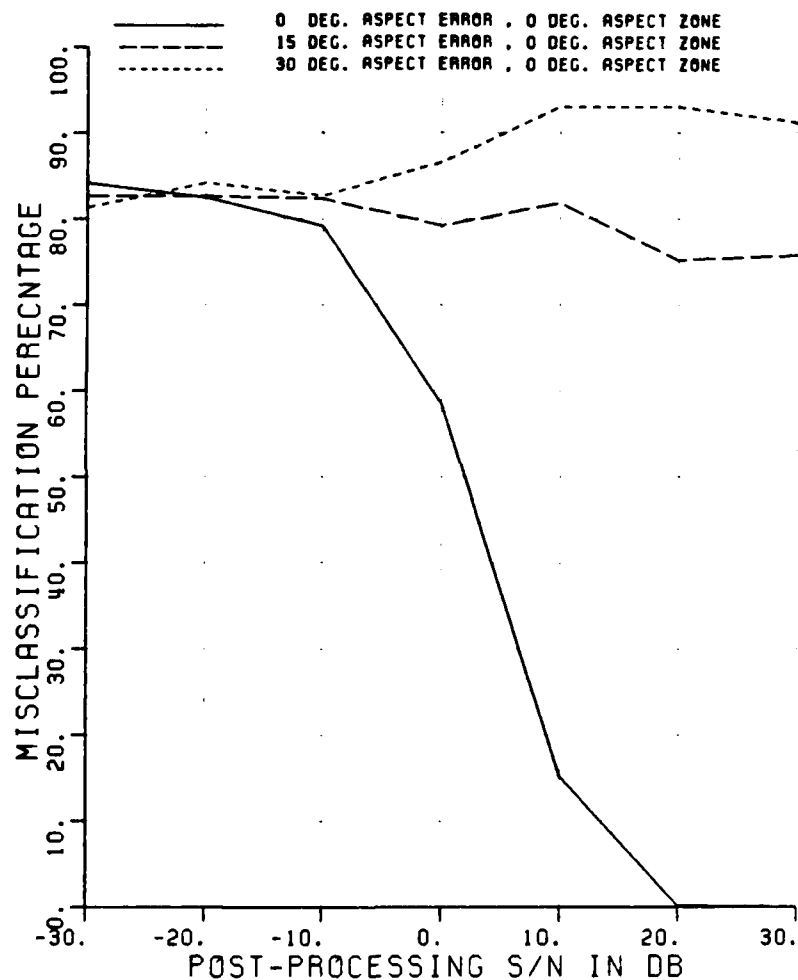


Figure A.116. Misclassification percentage versus post-processing SNR, comparing performance with various aspect angle errors, near to 0° aspect.

CLASSIFICATION OF SHIPS									
POLARIZATION	X								
ELEV ASSUMED	KNOWN								
ELEVATION (DEG.)	27								
ASPECT ASSUMED	KNOWN			/		KNOWN			
MIN,MAX,INC ASPECT	0	10	10,	0	15	15,	0	30	30
NO OF FREQUENCIES	8								
NO OF TARGETS	12			12			12		
90% CI (@30%) +/-	3.1%			3.1%			3.1%		
CLASS. FEATURES	T	T			T				
ASP ERR IN CURVE	2			3					

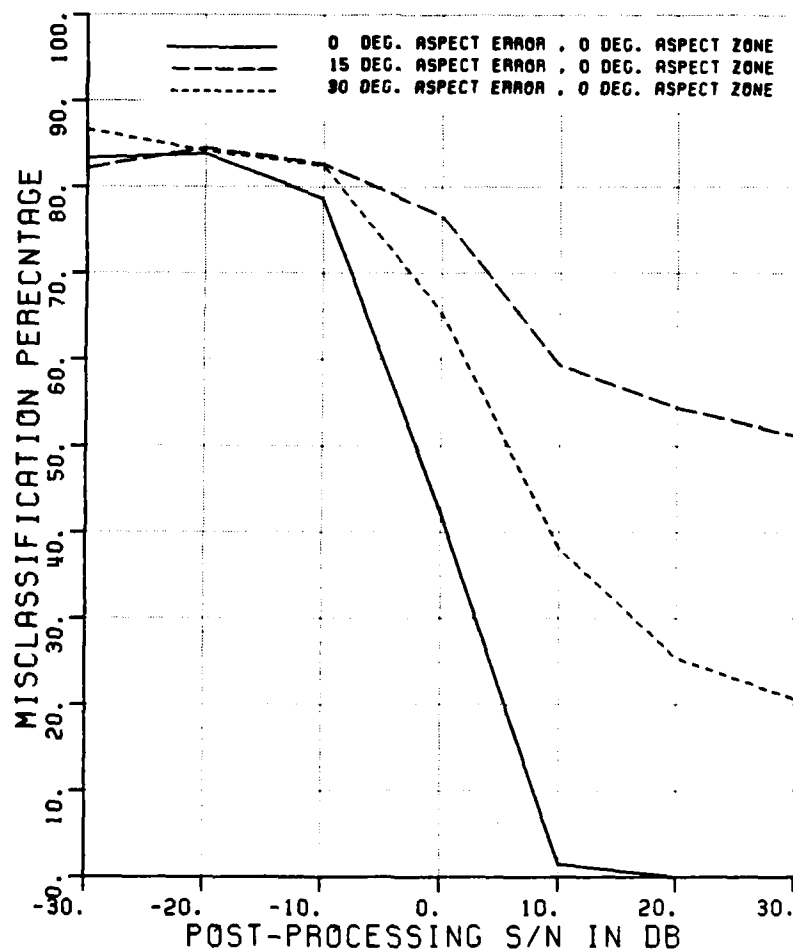


Figure A.117. Misclassification percentage versus post-processing SNR, comparing performance with various aspect angle errors, near to 0° aspect.

CLASSIFICATION OF SHIPS
 POLARIZATION V/H
 ELEV ASSUMED KNOWN
 ELEVATION (DEG.) 27
 ASPECT ASSUMED KNOWN / KNOWN
 MIN,MAX,INC ASPECT 0 10 10, 0 15 15, 0 30 30
 NO OF FREQUENCIES 8
 NO OF TARGETS 12 12 12
 90% CI (±30%) +/- 3.1% 3.1% 3.1%
 CLASS. FEATURES T T T
 ASP ERR IN CURVE 2 3

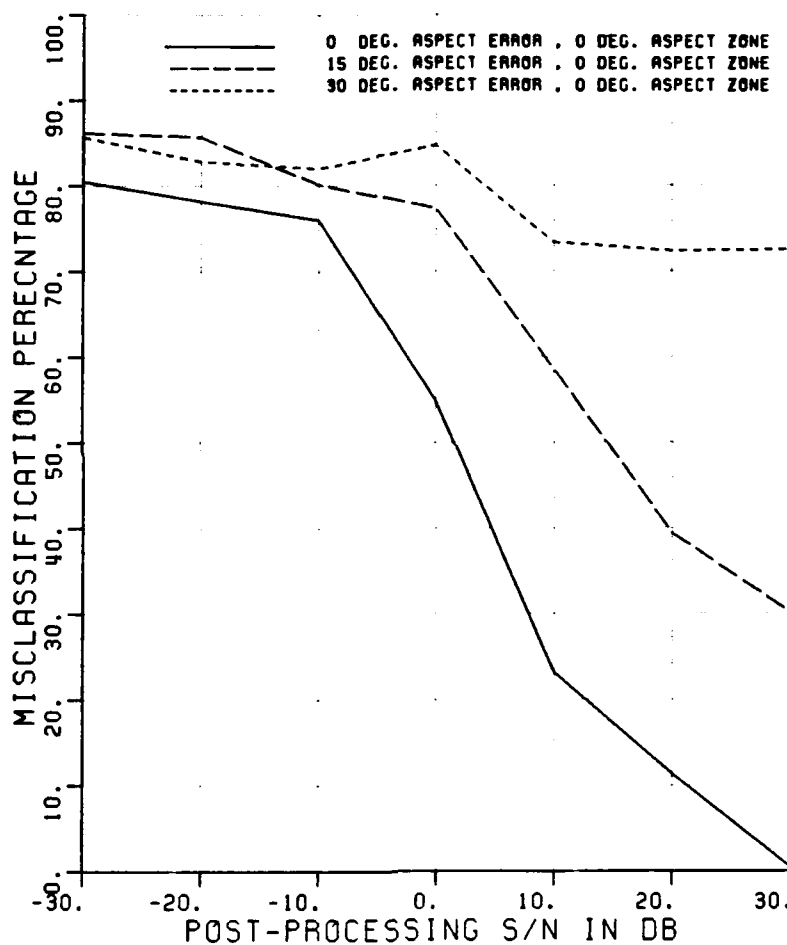


Figure A.118. Misclassification percentage versus post-processing SNR, comparing performance with various aspect angle errors, near to 0° aspect.

CLASSIFICATION OF SHIPS

POLARIZATION	H											
ELEV ASSUMED	KNOWN											
ELEVATION (DEG.)	27											
ASPECT ASSUMED	KNOWN					/ KNOWN						
MIN,MAX,INC ASPECT	0	10	10,	0	10	10,	80	100	10,	170	180	10
NO OF FREQUENCIES	8											
NO OF TARGETS	12		12		18		12					
90% CI (@30%) +/-	3.1%		3.1%		2.5%		3.1%					
CLASS. FEATURES	A	A	A		A							
ASP ERR IN CURVE	2		3		4							

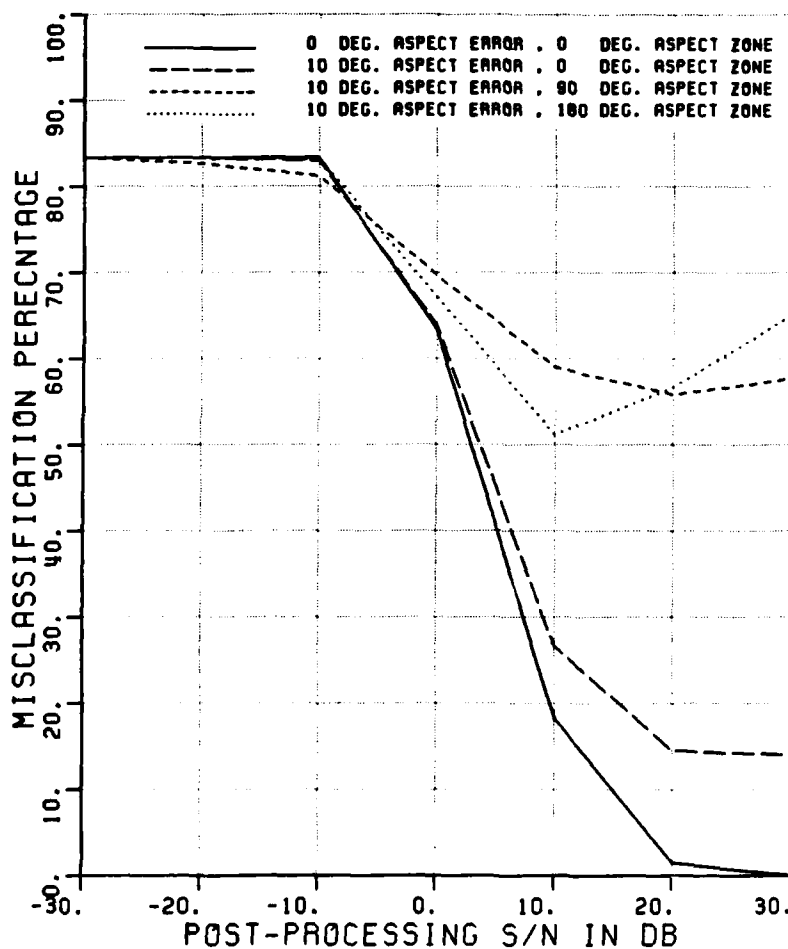


Figure A.119. Misclassification percentage versus post-processing SNR, comparing performance with a $\pm 10^\circ$ aspect error at various aspect zones.

CLASSIFICATION OF SHIPS

POLARIZATION	X											
ELEV ASSUMED	KNOWN											
ELEVATION (DEG.)	27											
ASPECT ASSUMED	KNOWN					/ KNOWN						
MIN,MAX,INC ASPECT	0	10	10,	0	10	10,	80	100	10,	170	180	10
NO OF FREQUENCIES	8											
NO OF TARGETS	12	12		18		12						
90% CI (±30%) +/-	3.1%	3.1%		2.5%		3.1%						
CLASS. FEATURES	A	A	A	A								
ASP ERR IN CURVE	2	3		4								

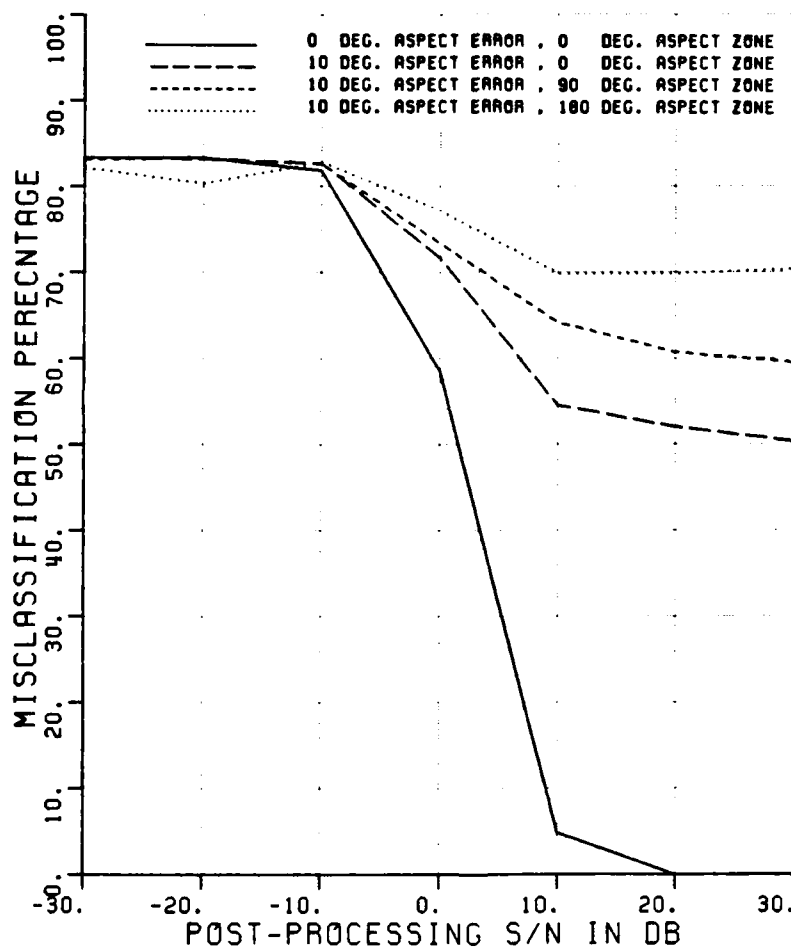


Figure A.120. Misclassification percentage versus post-processing SNR, comparing performance with a $\pm 10^\circ$ aspect error at various aspect zones.

CLASSIFICATION OF SHIPS

POLARIZATION	V/H											
ELEV ASSUMED	KNOWN											
ELEVATION (DEG.)	27											
ASPECT ASSUMED	KNOWN				/ KNOWN							
MIN,MAX,INC ASPECT	0	10	10,	0	10	10,	80	100	10,	170	180	10
NO OF FREQUENCIES	8											
NO OF TARGETS	12		12		18		12					
90% CI (±30%) +/-	3.1%		3.1%		2.5%		3.1%					
CLASS. FEATURES	A		A		A		A					
ASP ERR IN CURVE	2		3		4							

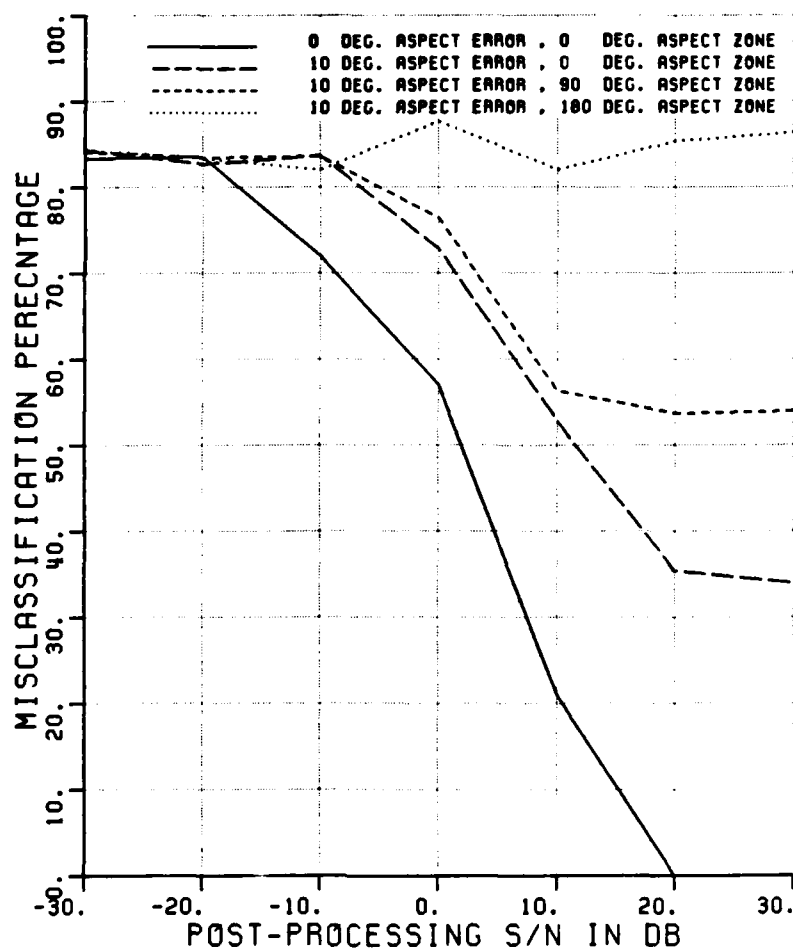


Figure A.121. Misclassification percentage versus post-processing SNR, comparing performance with a $\pm 10^\circ$ aspect error at various aspect zones.

CLASSIFICATION OF SHIPS												
POLARIZATION	V											
ELEV ASSUMED	KNOWN											
ELEVATION (DEG.)	27											
ASPECT ASSUMED	KNOWN				/		KNOWN					
MIN,MAX,INC ASPECT	0	10	10.	0	10	10.	80	100	10.	170	180	10
NO OF FREQUENCIES	8											
NO OF TARGETS	12			12			18			12		
90% CI (±30%) +/-	3.1%			3.1%			2.5%			3.1%		
CLASS. FEATURES	A&W			A&W			A&W			A&W		
ASP ERR IN CURVE	2			3			4					

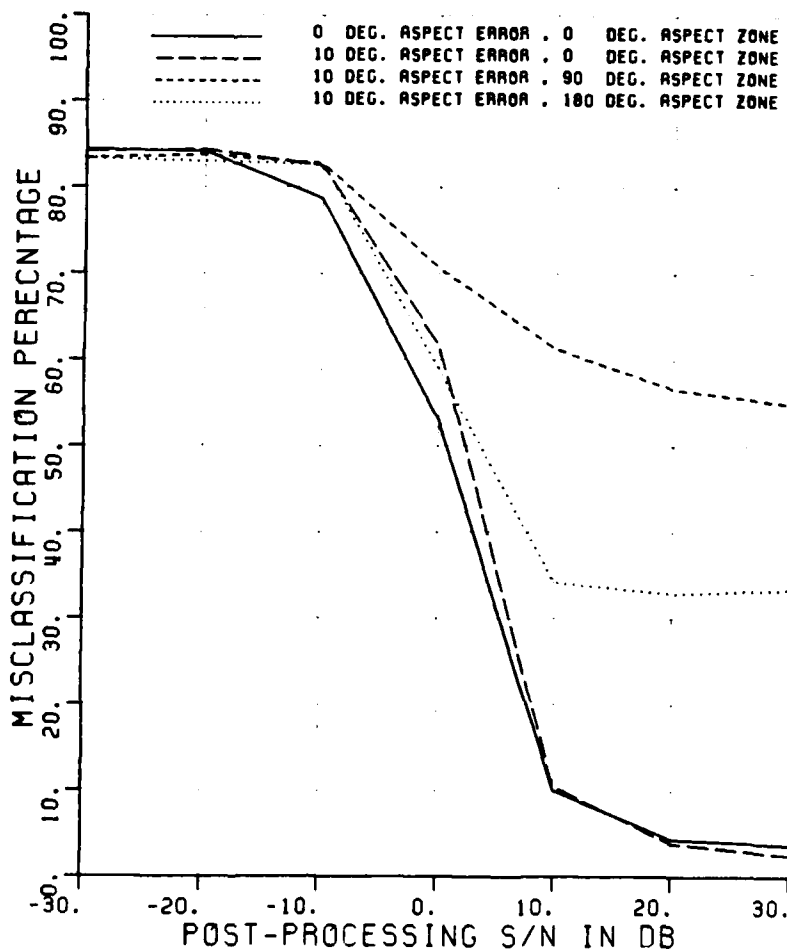


Figure A.122. Misclassification percentage versus post-processing SNR, comparing performance with a $\pm 10^\circ$ aspect error at various aspect zones.

CLASSIFICATION OF SHIPS

POLARIZATION	H											
ELEV ASSUMED	KNOWN											
ELEVATION (DEG.)	27											
ASPECT ASSUMED	KNOWN			/			KNOWN					
MIN, MAX, INC ASPECT	0	10	10,	0	10	10,	80	100	10,	170	180	10
NO OF FREQUENCIES	8											
NO OF TARGETS	12	12		18		12						
90% CI (±30%) +/-	3.1%	3.1%		2.5%		3.1%						
CLASS. FEATURES	A&W	A&W		A&W		A&W						
ASP ERR IN CURVE	2	3		4								

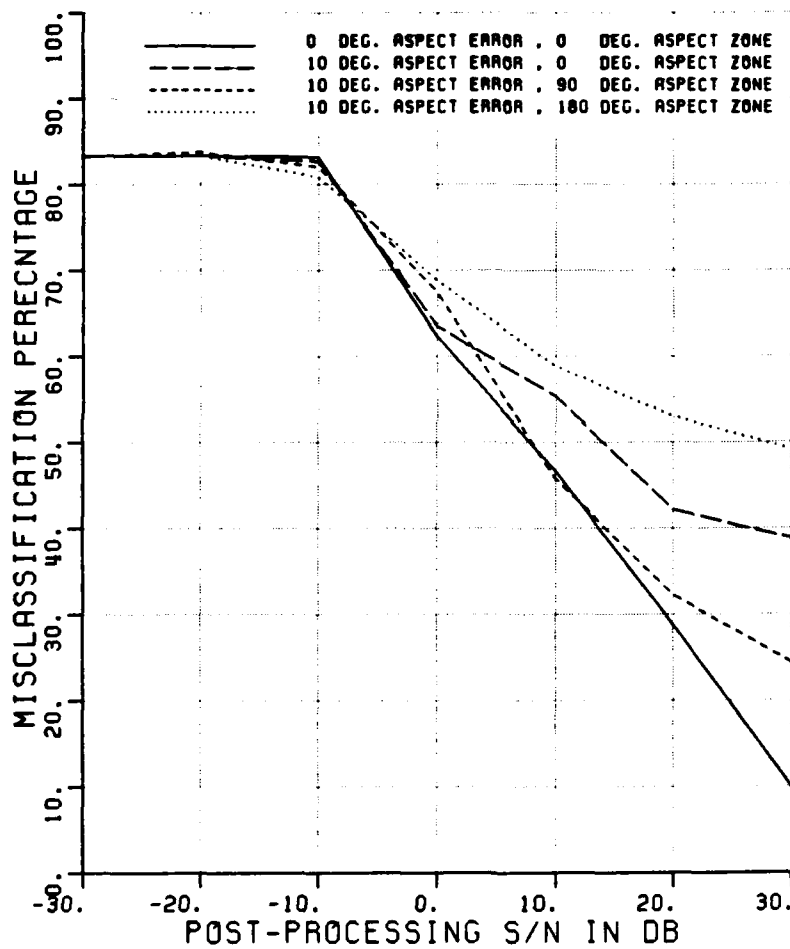


Figure A.123. Misclassification percentage versus post-processing SNR, comparing performance with a $\pm 10^\circ$ aspect error at various aspect zones.

CLASSIFICATION OF SHIPS

POLARIZATION	X													
ELEV ASSUMED	KNOWN													
ELEVATION (DEG.)	27													
ASPECT ASSUMED	KNOWN	/	KNOWN											
MIN,MAX,INC ASPECT	0	10	10,	0	10	10,	80	100	10,	170	180	10		
NO OF FREQUENCIES	8													
NO OF TARGETS	12		12		18		12							
90% CI (@30%) +/-	3.1%		3.1%		2.5%		3.1%							
CLASS. FEATURES	A4W		A4W		A4W		A4W							
ASP ERR IN CURVE	2		3		4									

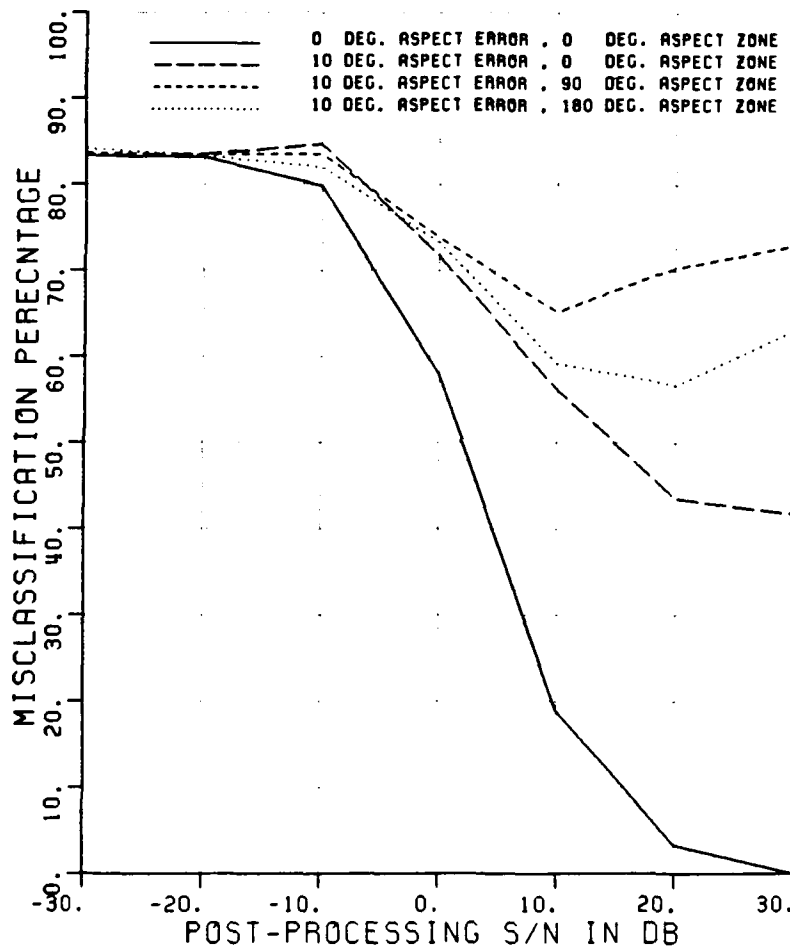


Figure A.124. Misclassification percentage versus post-processing SNR, comparing performance with a $\pm 10^\circ$ aspect error at various aspect zones.

CLASSIFICATION OF SHIPS

POLARIZATION	V/H											
ELEV ASSUMED	KNOWN											
ELEVATION (DEG.)	27											
ASPECT ASSUMED	KNOWN			/			KNOWN					
MIN,MAX,INC ASPECT	0	10	10,	0	10	10,	80	100	10,	170	180	10
NO OF FREQUENCIES	8											
NO OF TARGETS	12	12		18		12						
90% CI (±30%) +/-	3.1%	3.1%		2.5%		3.1%						
CLASS. FEATURES	A&W	A&W		A&W		A&W						
ASP ERR IN CURVE	2	3		4								

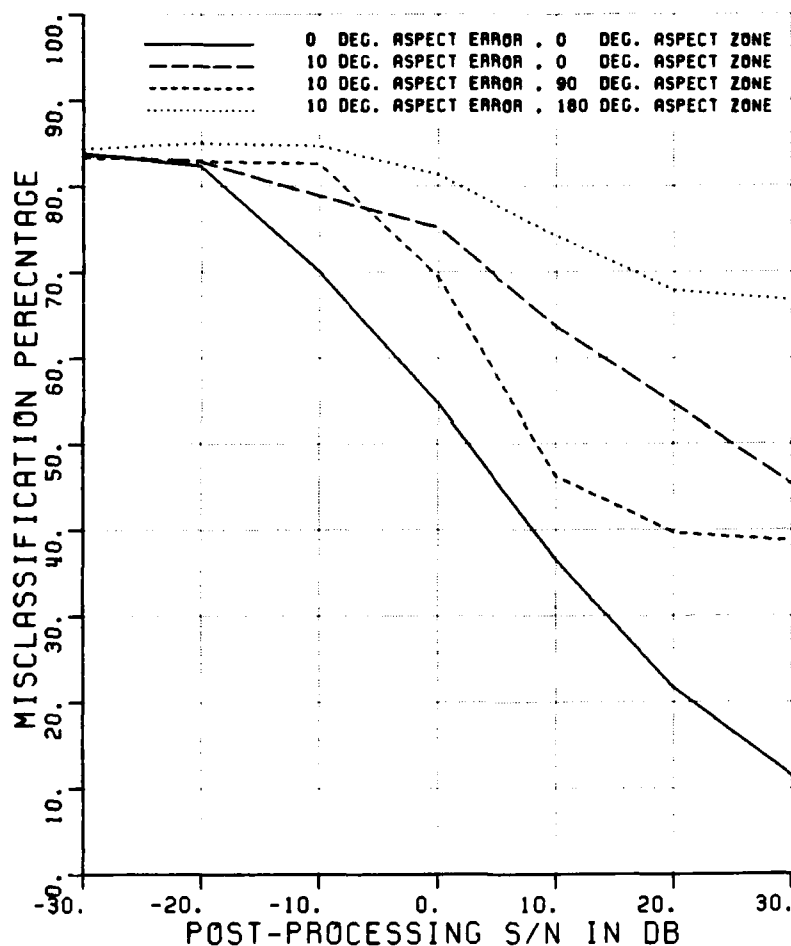


Figure A.125. Misclassification percentage versus post-processing SNR, comparing performance with a $\pm 10^\circ$ aspect error at various aspect zones.

CLASSIFICATION OF SHIPS

POLARIZATION	V												
ELEV ASSUMED	KNOWN												
ELEVATION (DEG.)	27												
ASPECT ASSUMED	KNOWN						/ KNOWN						
MIN,MAX,INC ASPECT	0	10	10.	0	10	10.	80	100	10.	170	180	10	
NO OF FREQUENCIES	8												
NO OF TARGETS	12	12				18				12			
90% CI (±30%) +/-	3.1%	3.1%				2.5%				3.1%			
CLASS. FEATURES	R&W	R&W				R&W				R&W			
ASP ERR IN CURVE	2	3				4							

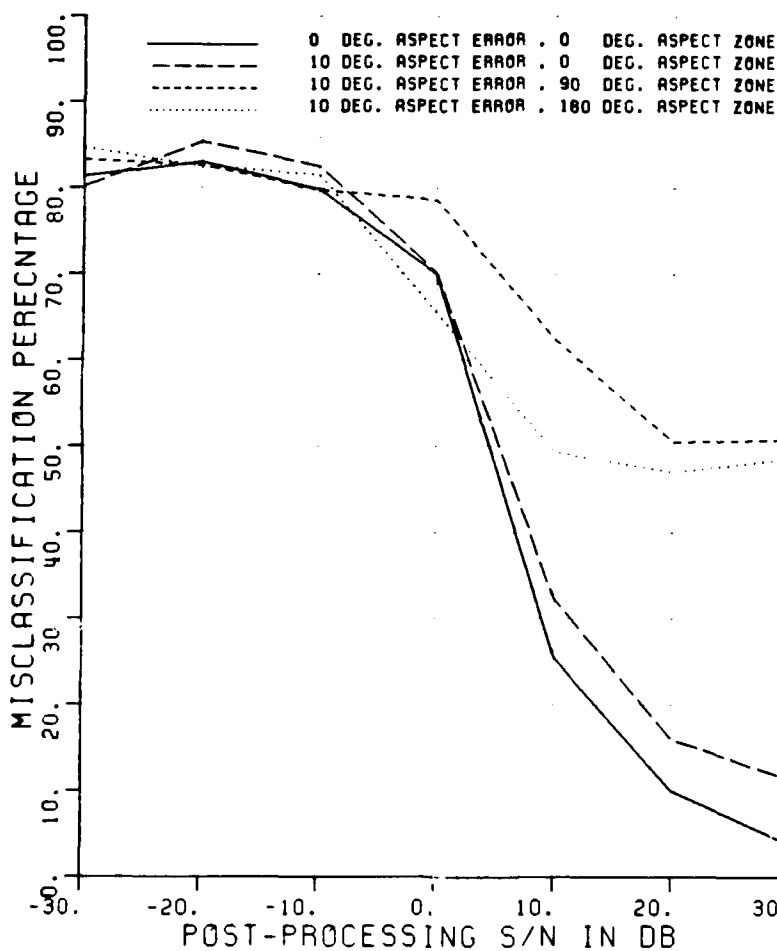


Figure A.126. Misclassification percentage versus post-processing SNR, comparing performance with a $\pm 10^\circ$ aspect error at various aspect zones.

CLASSIFICATION OF SHIPS
 POLARIZATION H
 ELEV ASSUMED KNOWN
 ELEVATION (DEG.) 27
 ASPECT ASSUMED KNOWN / KNOWN
 MIN,MAX,INC ASPECT 0 10 10, 0 10 10, 80 100 10, 170 180 10
 NO OF FREQUENCIES 8
 NO OF TARGETS 12 12 18 12
 90% CI (±30%) +/- 3.1% 3.1% 2.5% 3.1%
 CLASS. FEATURES R&W R&W R&W R&W
 ASP ERR IN CURVE 2 3 4

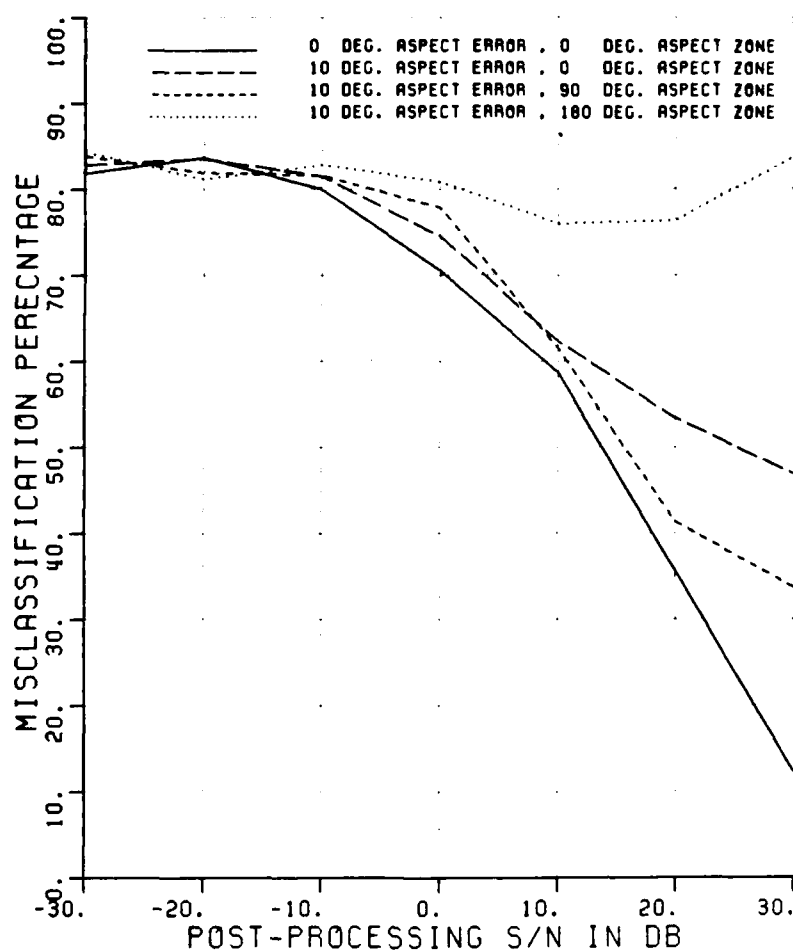


Figure A.127. Misclassification percentage versus post-processing SNR, comparing performance with a $\pm 10^\circ$ aspect error at various aspect zones.

CLASSIFICATION OF SHIPS										
POLARIZATION	X									
ELEV ASSUMED	KNOWN									
ELEVATION (DEG.)	27									
ASPECT ASSUMED	KNOWN		/		KNOWN					
MIN,MAX,INC ASPECT	0	10	10,	0	10	10,	80	100	10, 170 180	10
NO OF FREQUENCIES	8									
NO OF TARGETS	12	12		18		12				
90% CI (±30%) +/-	3.1%	3.1%		2.5%		3.1%				
CLASS. FEATURES	R4W	R4W	R4W		R4W					
ASP ERR IN CURVE	2	3		4						

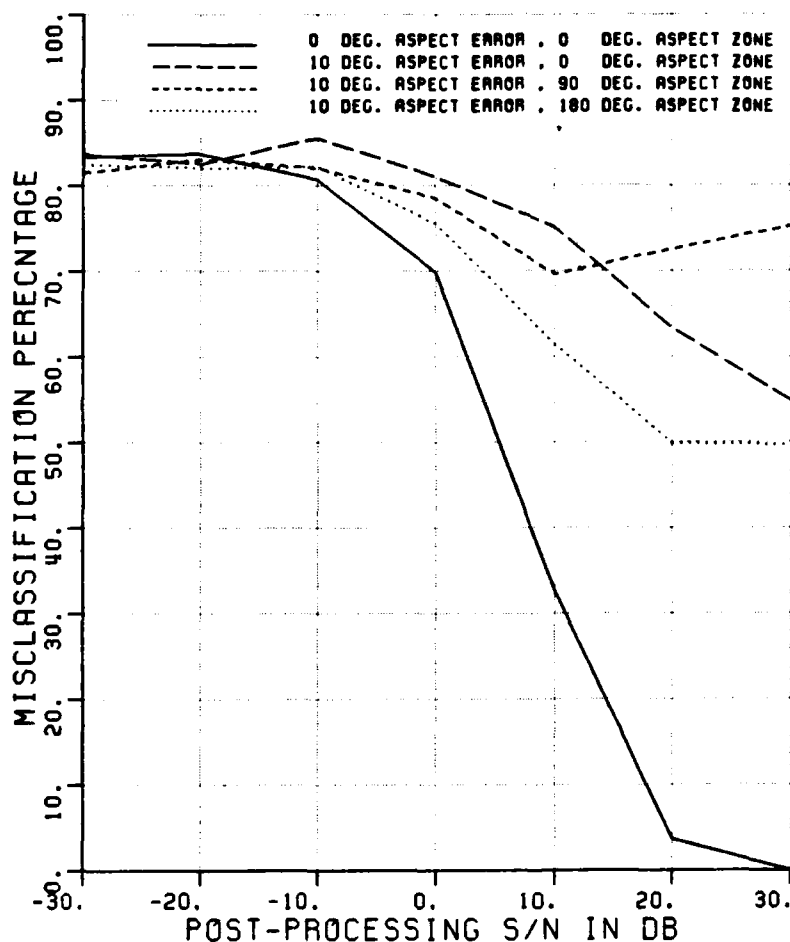


Figure A.128. Misclassification percentage versus post-processing SNR, comparing performance with a $\pm 10^\circ$ aspect error at various aspect zones.

POLARIZATION	V/H
ELEV ASSUMED	KNOWN
ELEVATION (DEG.)	27

ASPECT ASSUMED	KNOWN			/	KNOWN								
MIN,MAX,INC ASPECT	0	10	10.		0	10	10.	80	100	10.	170	180	10
NO OF FREQUENCIES	8												
NO OF TARGETS	12				18			12					
90% CI (±30%) +/-	3.1%		3.1%		2.5%		3.1%						
CLASS. FEATURES	R&W		R&W		R&W		R&W						
ASP ERR IN CURVE	2		3		4								

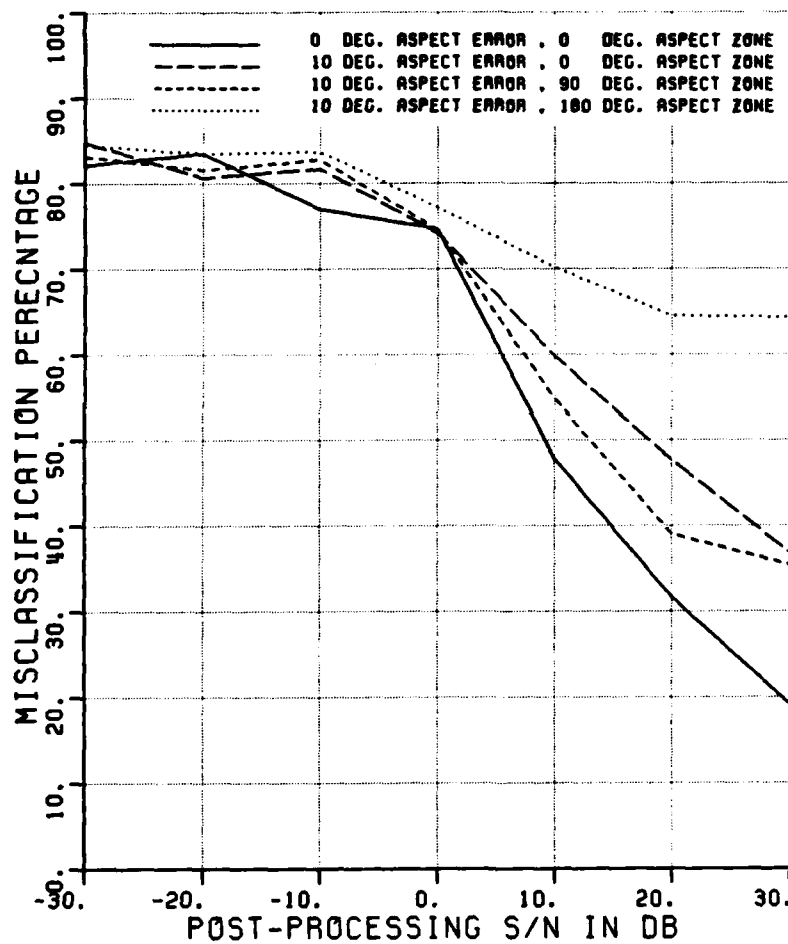


Figure A.129. Misclassification percentage versus post-processing SNR, comparing performance with a $\pm 10^\circ$ aspect error at various aspect zones.

CLASSIFICATION OF SHIPS
 POLARIZATION V
 ELEV ASSUMED KNOWN
 ELEVATION (DEG.) 27
 ASPECT ASSUMED KNOWN / KNOWN
 MIN,MAX,INC ASPECT 0 10 10, 0 10 10, 80 100 10, 170 180 10
 NO OF FREQUENCIES 8
 NO OF TARGETS 12 12 18 12
 90% CI (±30%) +/- 3.1% 3.1% 2.5% 3.1%
 CLASS. FEATURES T T T T
 ASP ERR IN CURVE 2 3 4

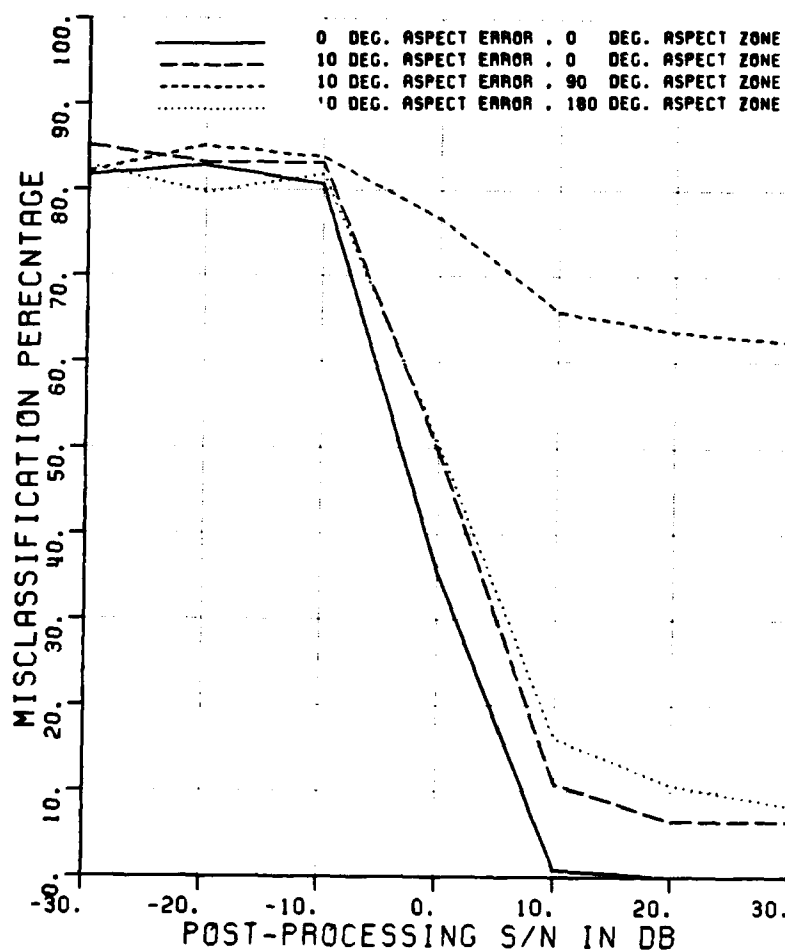


Figure A.130. Misclassification percentage versus post-processing SNR, comparing performance with a $\pm 10^\circ$ aspect error at various aspect zones.

CLASSIFICATION OF SHIPS
 POLARIZATION H
 ELEV ASSUMED KNOWN
 ELEVATION (DEG.) 27
 ASPECT ASSUMED KNOWN / KNOWN
 MIN,MAX,INC ASPECT 0 10 10, 0 10 10, 80 100 10, 170 180 10
 NO OF FREQUENCIES 8
 NO OF TARGETS 12 12 18 12
 90% CI (±30%) +/- 3.1% 3.1% 2.5% 3.1%
 CLASS. FEATURES T T T T
 ASP ERR IN CURVE 2 3 4

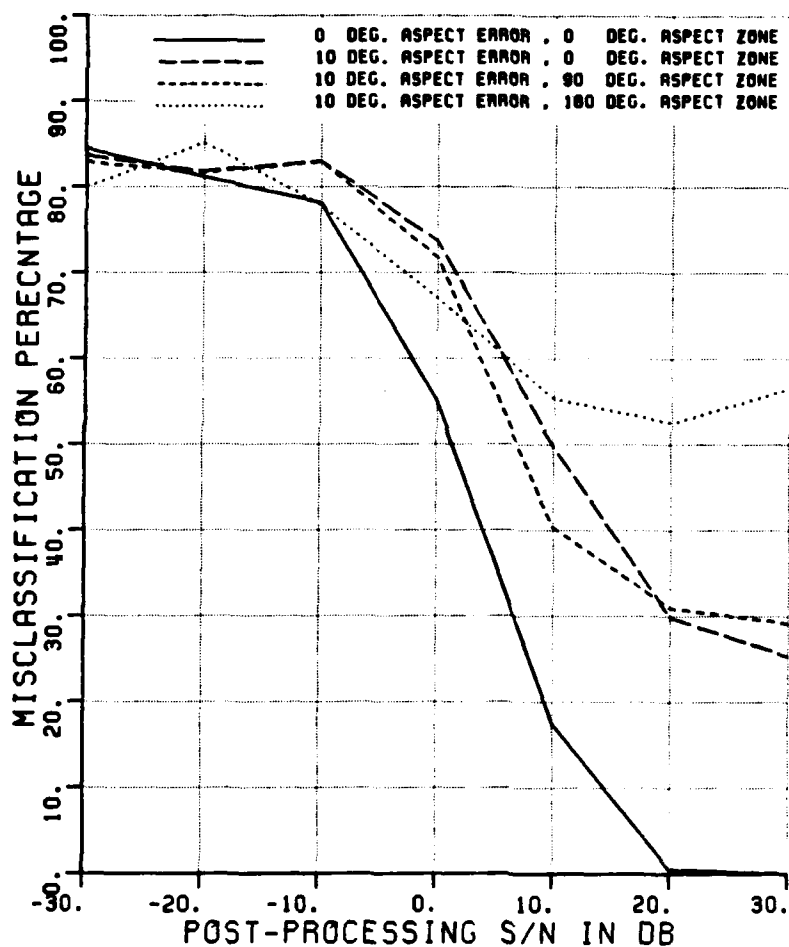


Figure A.131. Misclassification percentage versus post-processing SNR, comparing performance with a $\pm 10^\circ$ aspect error at various aspect zones.

CLASSIFICATION OF SHIPS

POLARIZATION	X											
ELEV ASSUMED	KNOWN											
ELEVATION (DEG.)	27											
ASPECT ASSUMED	KNOWN			/			KNOWN					
MIN,MAX,INC ASPECT	0	10	10,	0	10	10,	60	100	10,	170	180	10
NO OF FREQUENCIES	8											
NO OF TARGETS	12			12			18			12		
90% CI (+30%) +/-	3.1%			3.1%			2.5%			3.1%		
CLASS. FEATURES	T	T	T	T								
ASP ERR IN CURVE	2			3			4					

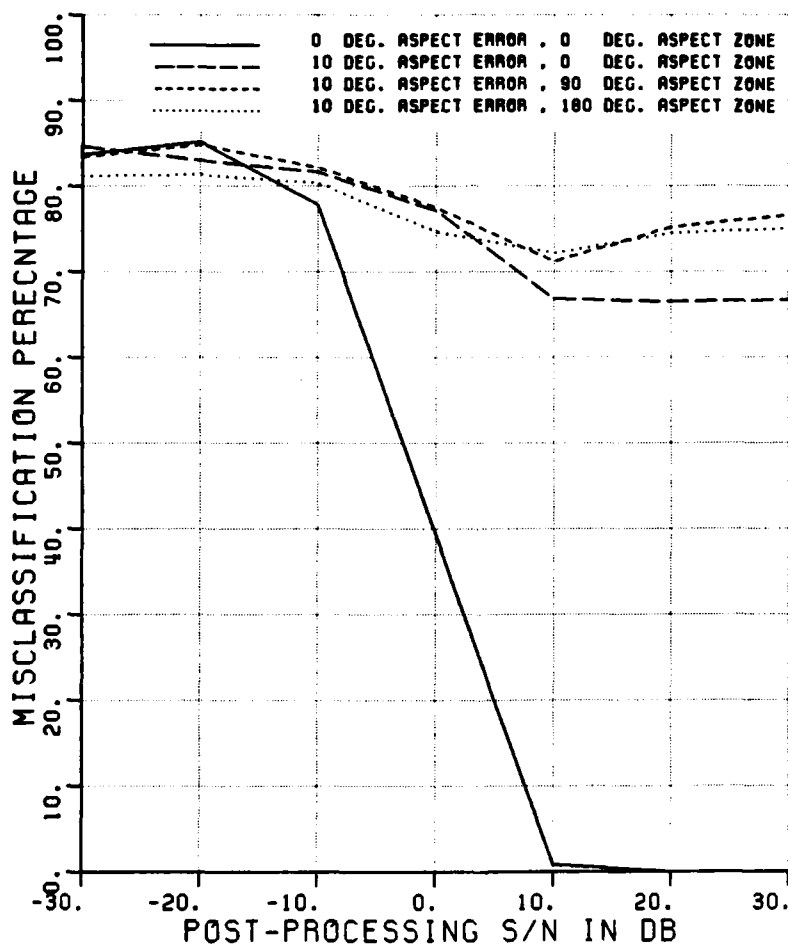


Figure A.132. Misclassification percentage versus post-processing SNR, comparing performance with a $\pm 10^\circ$ aspect error at various aspect zones.

POLARIZATION	V/H
ELEV ASSUMED	KNOWN

ELEVATION (DEG.)	27											
ASPECT ASSUMED	KNOWN				/ KNOWN							
MIN,MAX,INC ASPECT	0	10	10,	0	10	10,	80	100	10,	170	180	10
NO OF FREQUENCIES	8											
NO OF TARGETS	12				18				12			
90% CI (±30%) +/-	3.1%		3.1%		2.5%		3.1%					
CLASS. FEATURES	T	T	T	T								
ASP ERR IN CURVE	2		3		4							

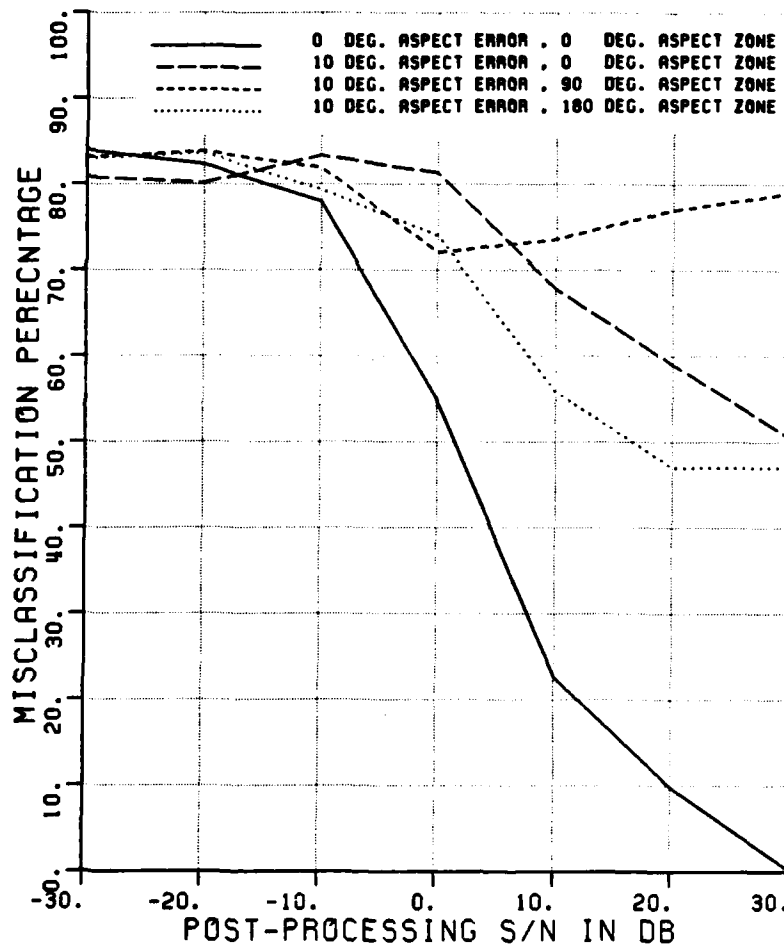


Figure A.133. Misclassification percentage versus post-processing SNR, comparing performance with a $\pm 10^\circ$ aspect error at various aspect zones.

CLASSIFICATION OF SHIPS				
POLARIZATION	V			
ELEV ASSUMED	KNOWN			
ELEVATION (DEG.)	27			
ASPECT ASSUMED	UNKNOWN			
MIN,MAX,INC ASPECT	0	15	15	
NO OF FREQUENCIES	8			
NO OF TARGETS	12	12	12	12
90% CI (±30%) +/-	3.1%	3.1%	3.1%	3.1%
CLASS. FEATURES	A	A&W	A&W	T

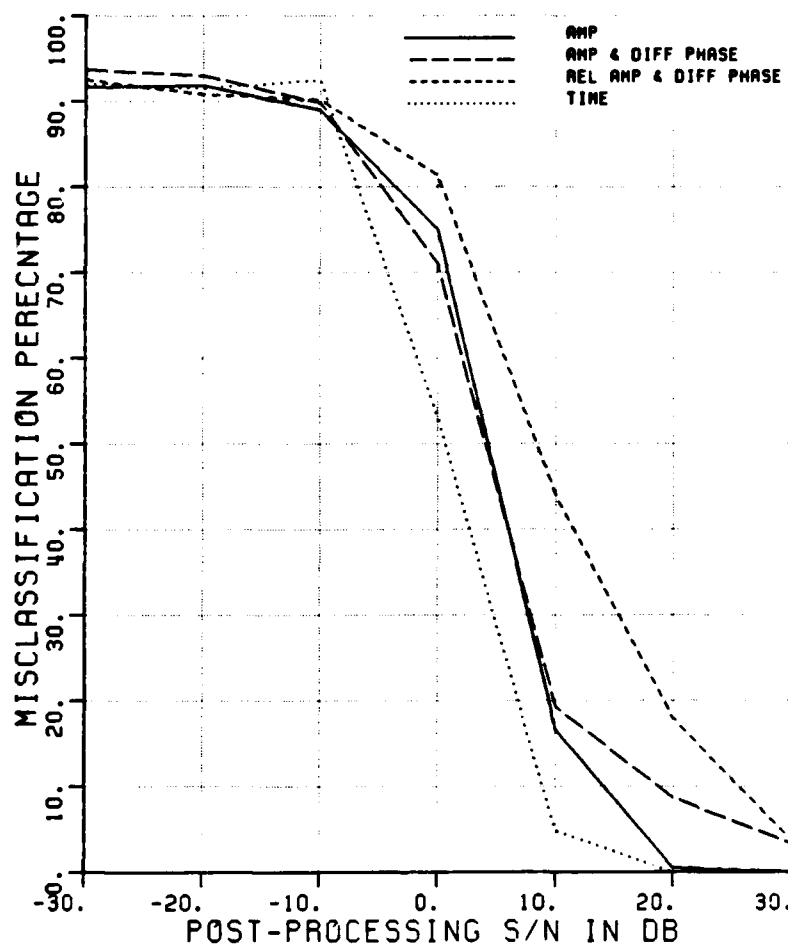


Figure A.134. Misclassification percentage versus post-processing SNR, comparing the performance of various algorithms using unknown aspect.

CLASSIFICATION OF SHIPS

POLARIZATION	H			
ELEV ASSUMED	KNOWN			
ELEVATION (DEG.)	27			
ASPECT ASSUMED	UNKNOWN			
MIN,MAX,INC ASPECT	0	15	15	
NO OF FREQUENCIES	8			
NO OF TARGETS	12	12	12	12
90% CI (±30%) +/-	3.1%	3.1%	3.1%	3.1%
CLASS. FEATURES	A	R&W	R&W	T

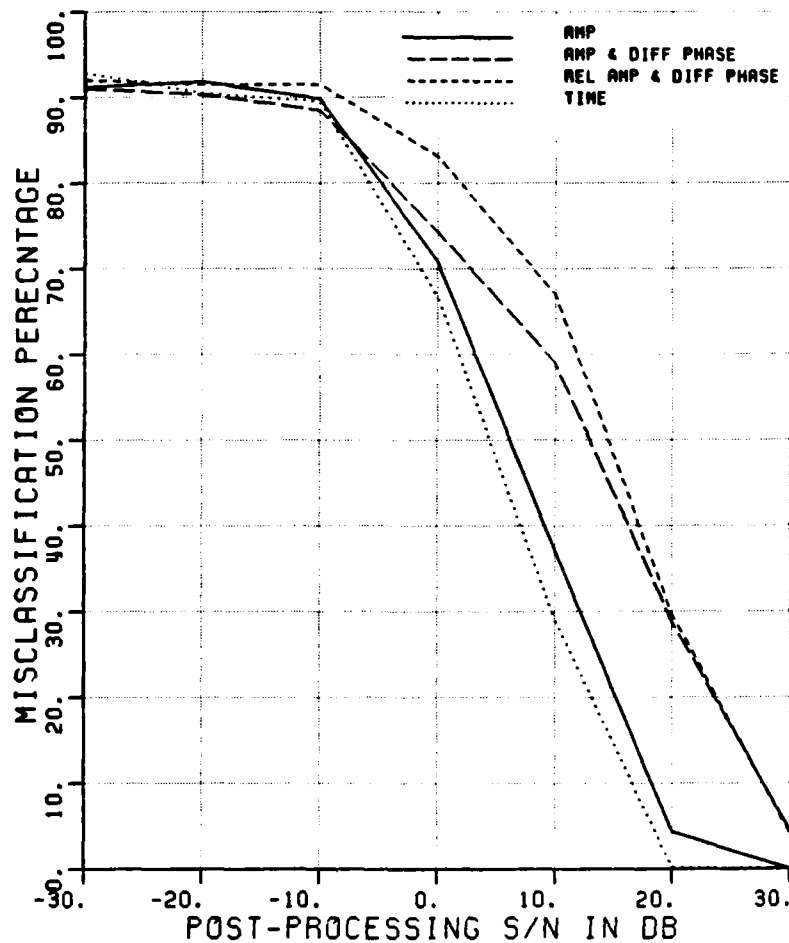


Figure A.135. Misclassification percentage versus post-processing SNR, comparing the performance of various algorithms using unknown aspect.

CLASSIFICATION OF SHIPS				
POLARIZATION	X			
ELEV ASSUMED	KNOWN			
ELEVATION (DEG.)	27			
ASPECT ASSUMED	UNKNOWN			
MIN,MAX,INC ASPECT	0	15	15	
NO OF FREQUENCIES	8			
NO OF TARGETS	12	12	12	12
90% CI (@30%) +/-	3.1%	3.1%	3.1%	3.1%
CLASS. FEATURES	A	A&W	A&W	T

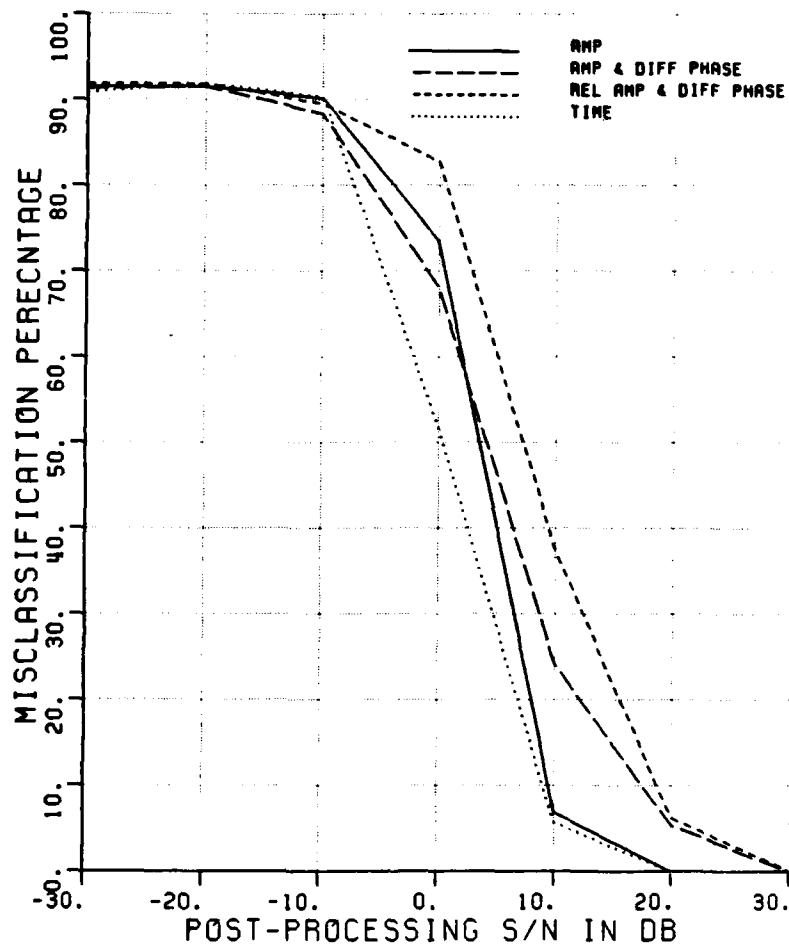


Figure A.136 Misclassification percentage versus post-processing SNR, comparing the performance of various algorithms using unknown aspect.

CLASSIFICATION OF SHIPS
 POLARIZATION V/H
 ELEV ASSUMED KNOWN
 ELEVATION (DEG.) 27
 ASPECT ASSUMED UNKNOWN
 MIN,MAX,INC ASPECT 0 15 15
 NO OF FREQUENCIES 8
 NO OF TARGETS 12 12 12 12
 90% CI (±30%) +/- 3.1% 3.1% 3.1% 3.1%
 CLASS. FEATURES A A&W R&W T

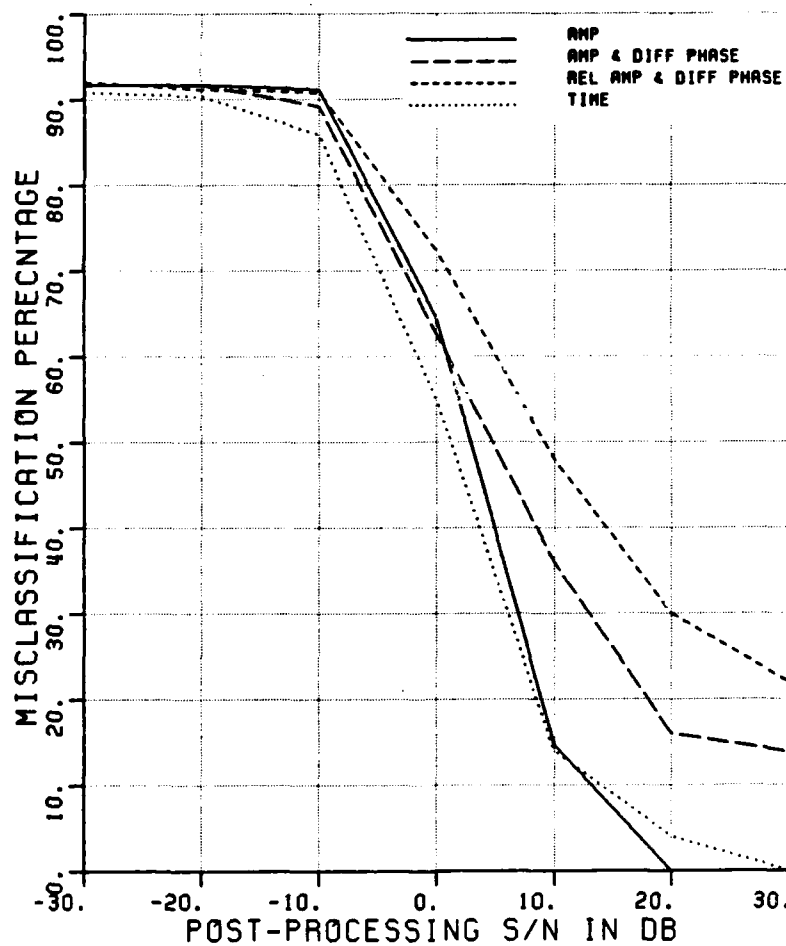


Figure A.137. Misclassification percentage versus post-processing SNR, comparing the performance of various algorithms using unknown aspect.

APPENDIX B

AMPLITUDE AND PHASE RETURNS

This appendix contains plots of the amplitudes and phases of processed radar returns for one ship, at 3 aspect angles, (0° , 90° and 180°), at 27° elevation angle, using vertical, horizontal and cross polarizations.

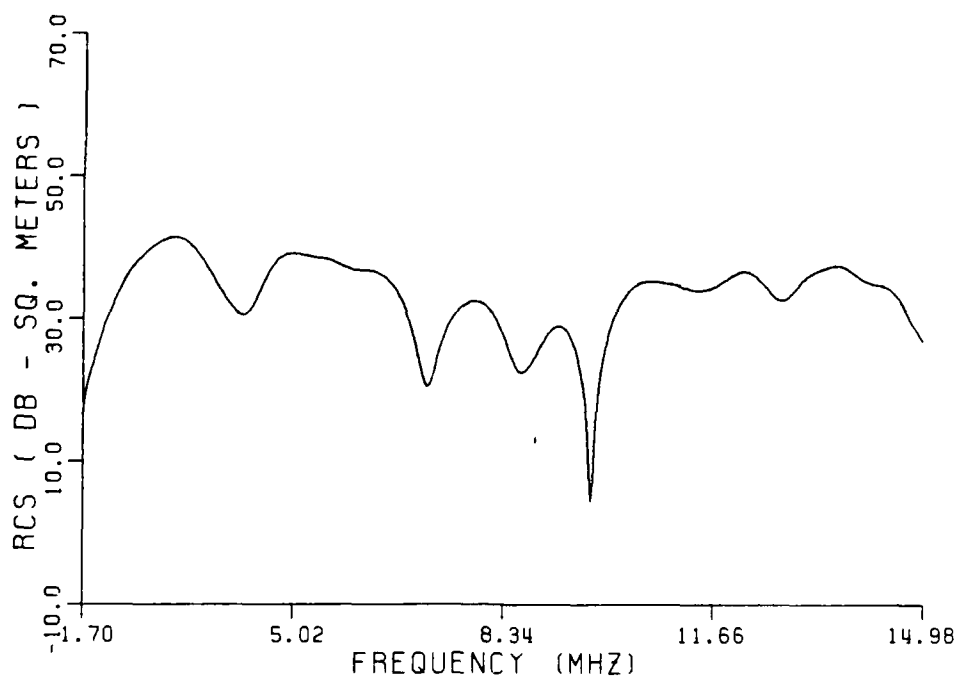
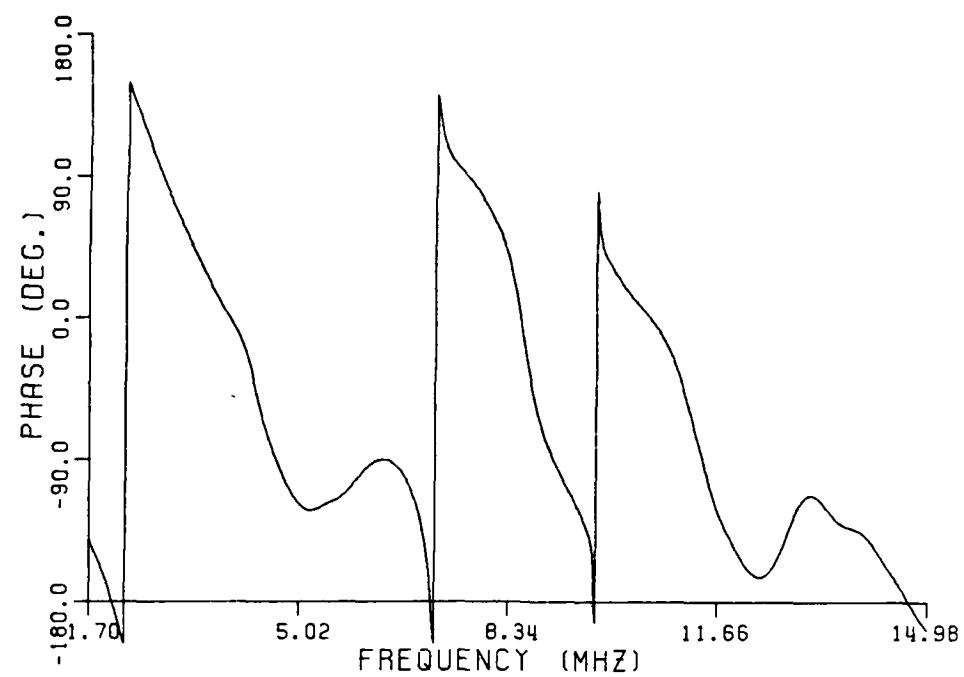


Figure B.1. Ship at 0 degree aspect, vertical polarization.

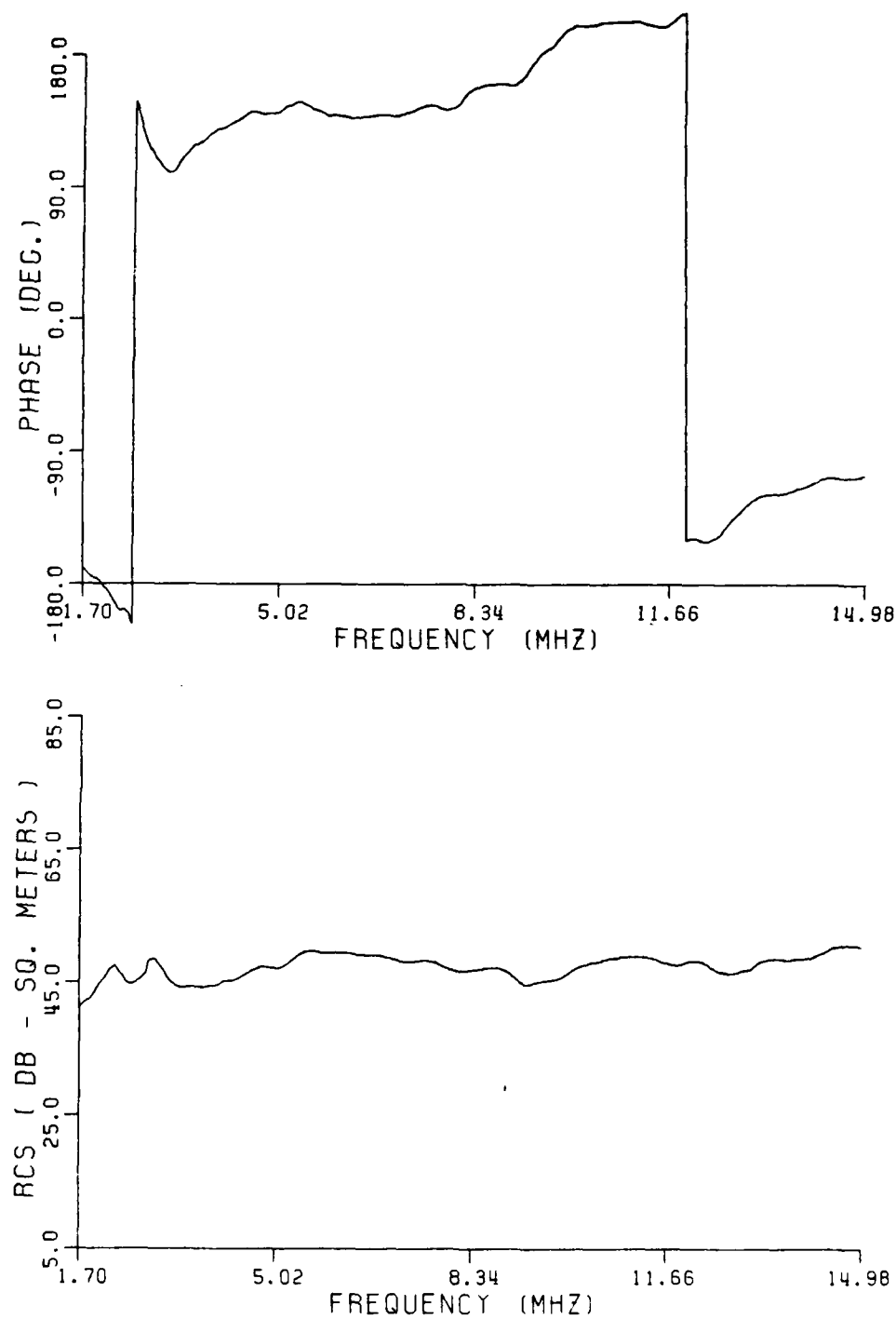


Figure B.2. Ship at 90 degree aspect, vertical polarization.

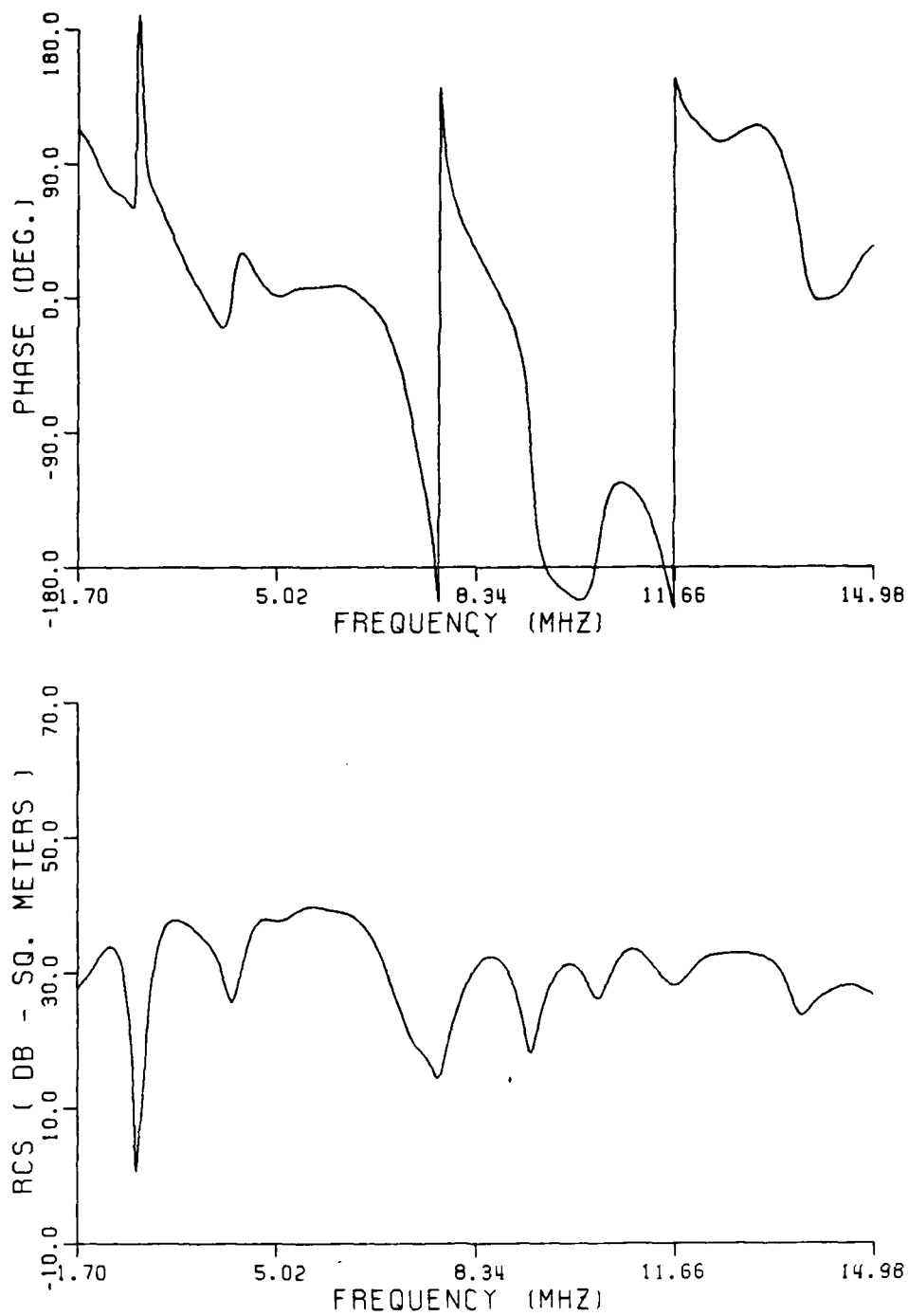


Figure B.3. Ship at 180 degree aspect, vertical polarization.

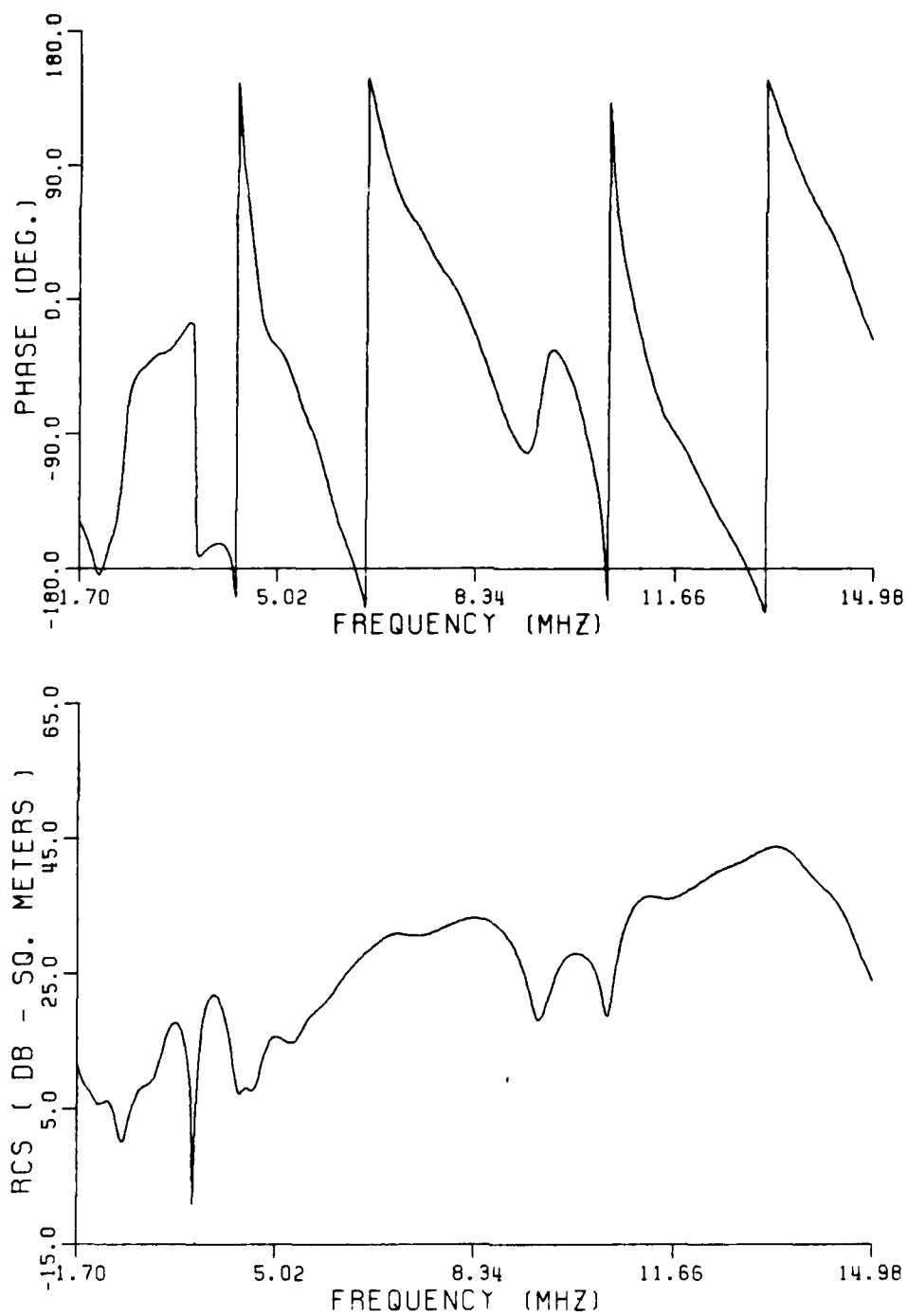


Figure B.4. Ship at 0 degree aspect, horizontal polarization.

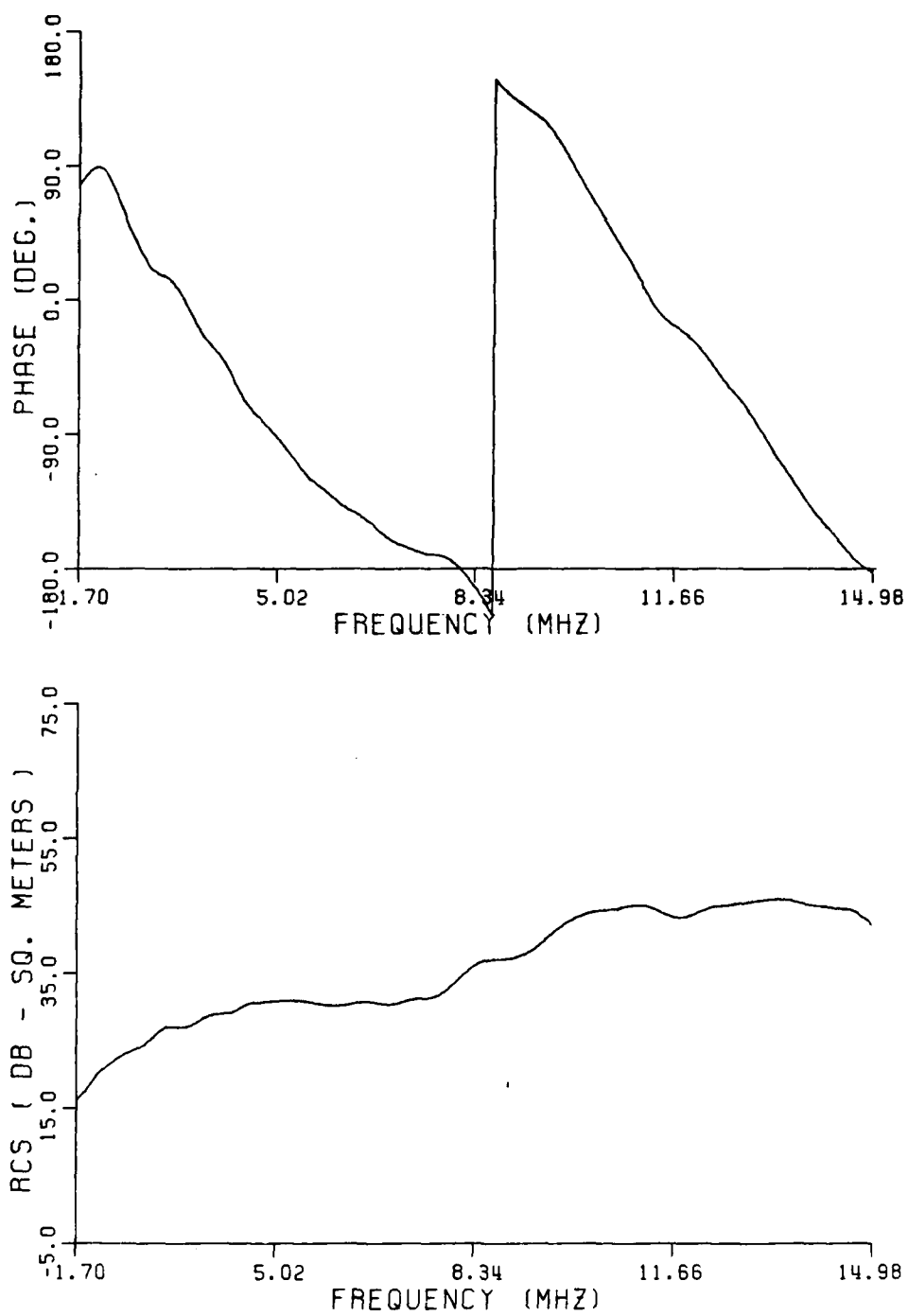


Figure B.5. Ship at 90 degree aspect, horizontal polarization.

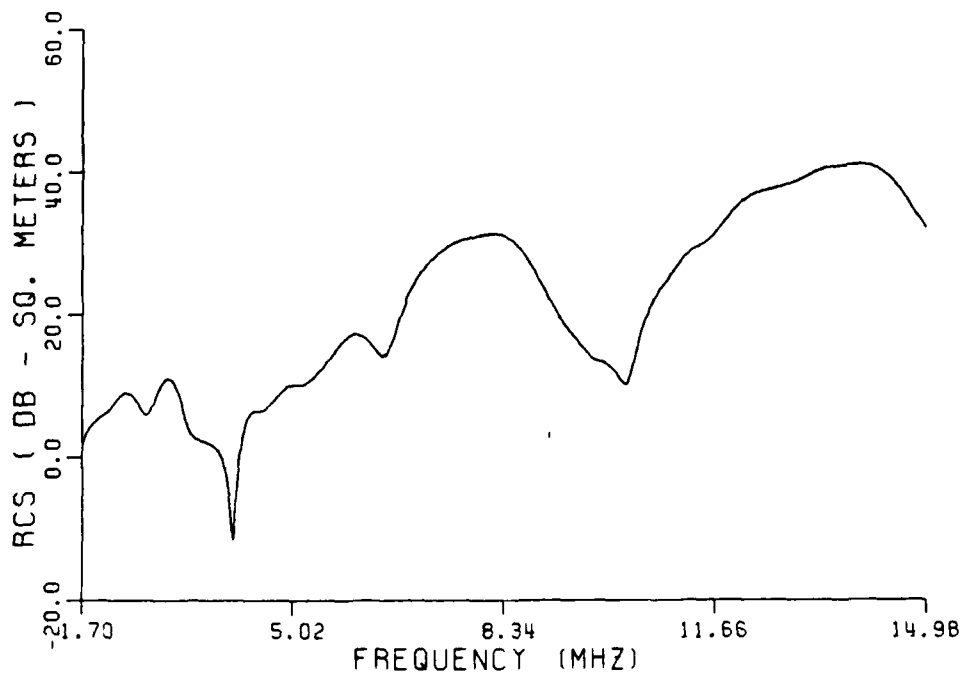
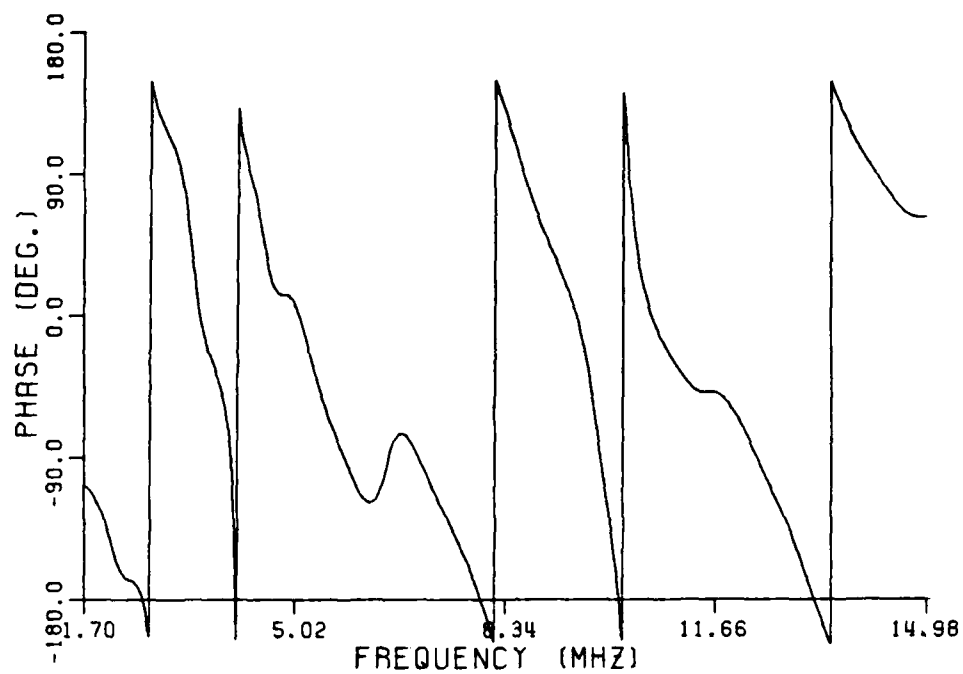


Figure B.6. Ship at 180 degree aspect, horizontal polarization.

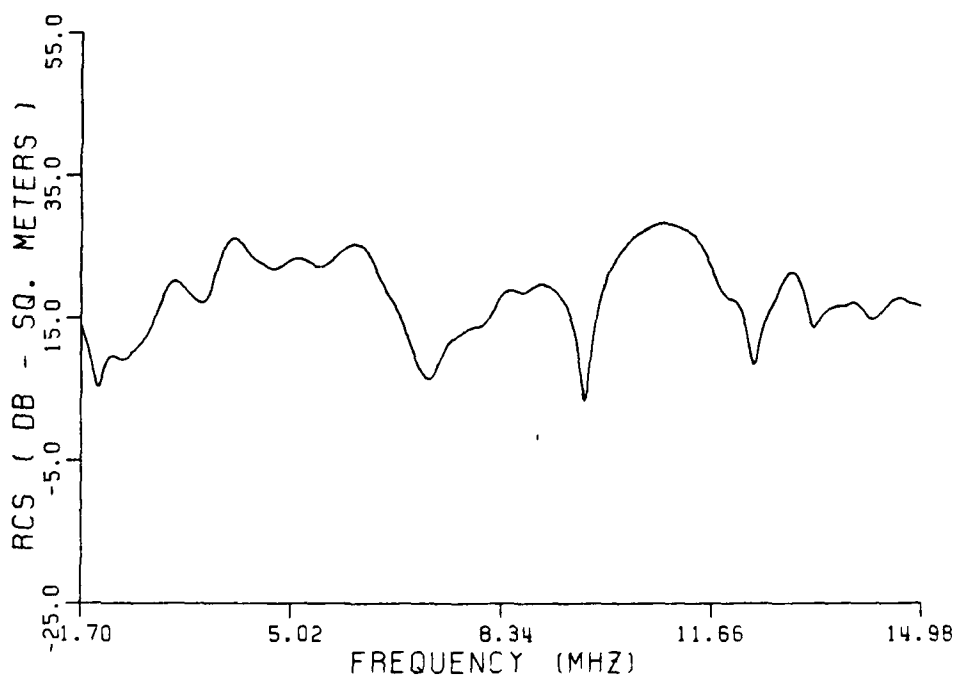
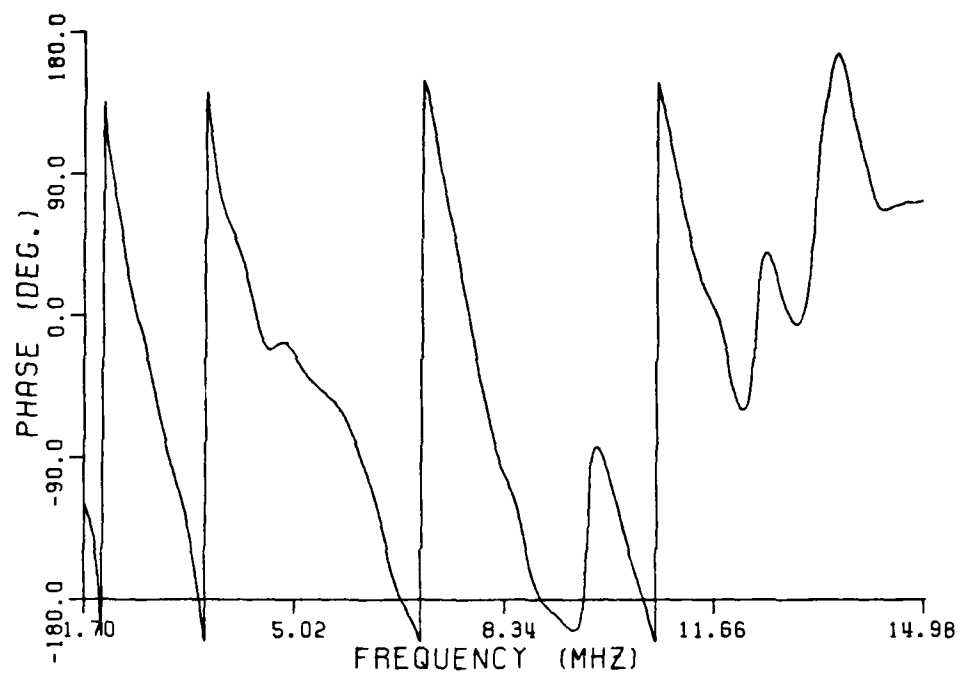


Figure B.7. Ship at 0 degree aspect, horizontal polarization.

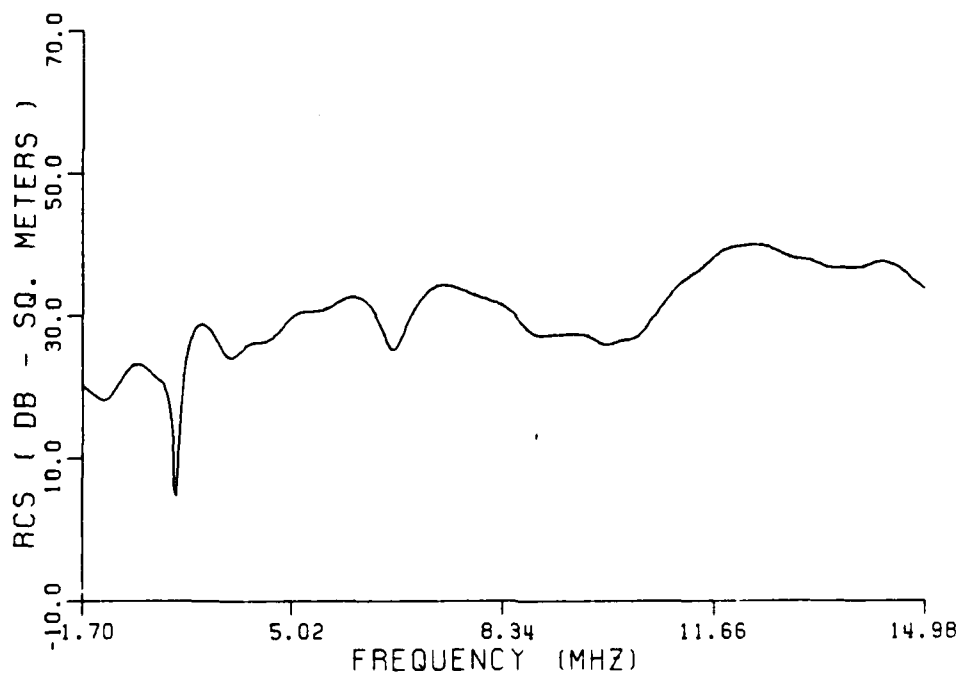
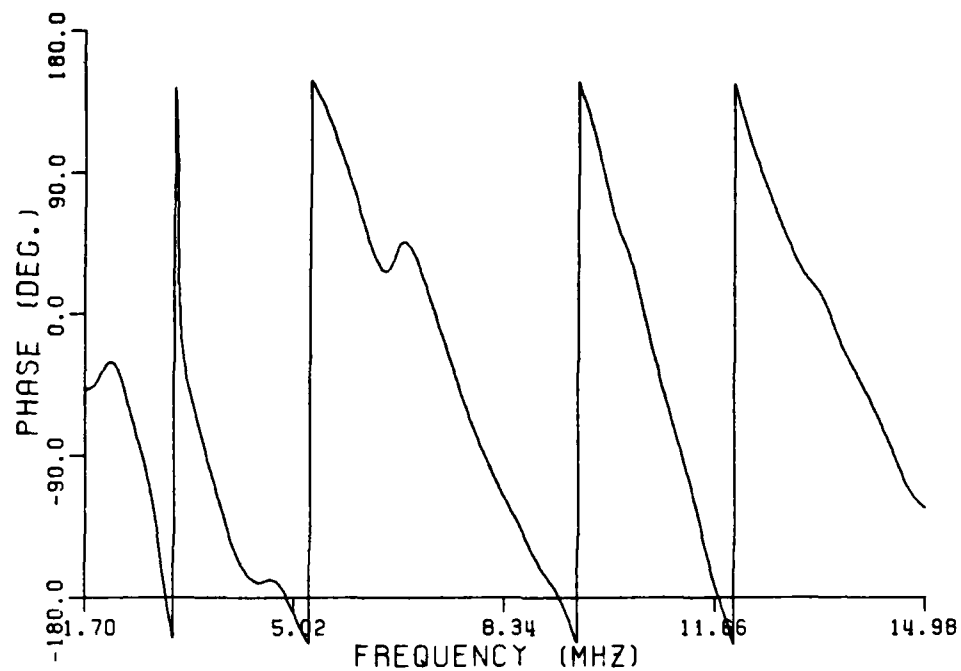


Figure B.8. Ship at 90 degree aspect, horizontal polarization.

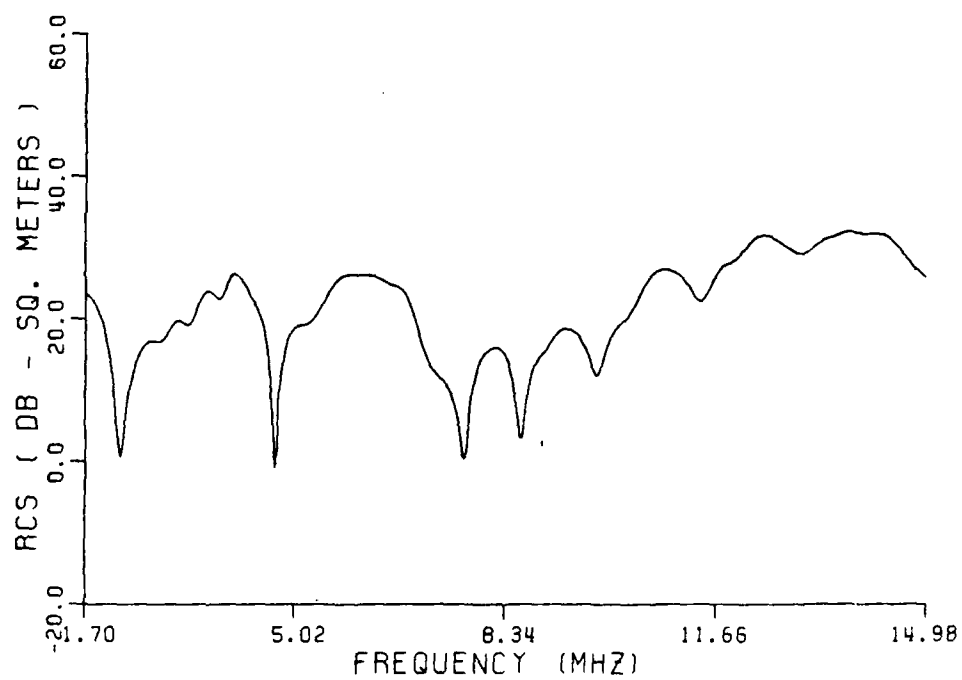
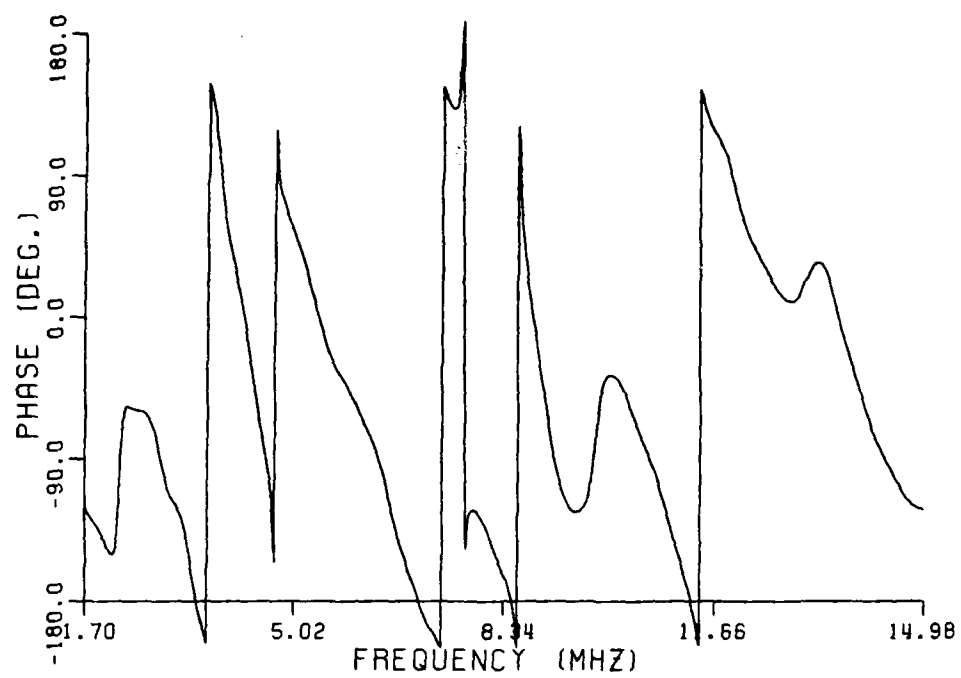


Figure B.9. Ship at 180 degree aspect, horizontal polarization.

TABLE B.1

AVERAGE AMPLITUDES FOR VARIOUS CATALOGS, CONTAINING SIX SHIPS

	0°		90°		180°		AVG
	15°	27°	15°	27°	15°	27°	
V	46	40	50	48	48	42	47
H	29	25	23	31	18	25	27
X	29	28	30	32	27	24	29
V/H	46	36	38	21	46	36	42
AVG	43	36	44	42	44	37	

APPENDIX C

PROGRAMS

The source codes, written in FORTRAN 7, developed for this research are listed in this appendix. Program names are CAL61.FOR, CATLOG.FOR and TAFCAL.FOR (Time and Frequency Classification Algorithm). All subroutines have been included, along with LINKING command procedures.

The command procedure FILESORT.COM is used to provide a directory file of file names to be used in conjunction with CATLOG.

```

C      PROGRAM NAME :- CAL81
C      THIS PROGRAM CALIBRATES THE RADAR CROSS-SECTION DATA FROM
C      MEASUREMENTS MADE ON THE COMPACT RADAR RANGE.
C      THE INPUT UNITS ARE IN DB AND DEGREES
C
C      ORIGINALLY CAL53,
C      MODIFIED 4 APRIL 1984 BY N.F.CHAMBERLAIN TO PERFORM
C      GATING IN THE TIME DOMAIN.
C
C      INCLUDE 'CALCOM.FOR'
C
C      Note CALCOM.FOR simply provides values for MD and other
C      dimensioning variables.
C
C      COMMON /BLK1/BUFF /BLK2/NP,FMIN,FINC /BLK3/IB
C      COMMON /BLK4/NDIM,ANST,AINC
C      COMMON /BLK5/ARRA,NRPT
C      COMMON /BLK6/PLOTOPT1,IP31,LPL1,NDIG1,FXB,FXE,FXS,FYB,FYE,FYS
C      COMMON /BLK7/PLOTOPT2,IP32,LPL2,NDIG2,TXB,TXE,TXS,TYB,TYE,TYS
C      INTEGER*2 TFILE(7),BTFILE(7),CFILE(7),EFILE(7),RFILE(16)
C      INTEGER*2 BCFILE(7),LINE2(30),INFILE(7)
C      BYTE LINE1(60),LINE3(60),BUFF(ID),TLINE1(60),TLINES(60),STRING(22)
C      INTEGER NSPKT(MD),NSPKC(MD)
C      EQUIVALENCE(LINE1(1),BUFF(1)),(LINE2(1),BUFF(61)),
2011 1(LINE3(1),BUFF(121))
C      COMPLEX*8 TA(MD),BT(MD),CAS(MD),BC(MD),EXS(MD),RS(5000)
C      COMPLEX*8 CMB(MD),TMB(MD)
C      DIMENSION ARRA(30)
C
C      TPI=6.2831853
C      CME=2.998E+08
C      CFT=9.836E+08
C      NP=MD
C
C      Initialise control variables.
C      ISUP=1 when SUP (set up command) is invoked.
C      KRPT is a counter which stops the repetition process
C      when NRPT repetitions are done.
C      NCSUP indexes ARRA(I) and increments after each command.
C
C      KSTP=0
2021 NCSUP=0
C      KRPT=1
C      ISUP=0
C      TYPE *, ' '
C      TYPE *, 'TYPE "HLP" TO PRINT LIST OF COMMANDS'
2020 IF(ISUP.EQ.1) THEN
C      NCSUP=NCSUP+1
C      CALL CSUP(ARR,NCSUP,KRPT,IEND,SPAG,KSTP)      I SUP control subroutine
C      IF(IEND.EQ.1) GOTO 287
C      GOTO 3863
C      END IF
C
287 TYPE 288
288 FORMAT(' ',/, ' COMMAND: ',*)

```

```

ACCEPT 3862,ARR
3862 FORMAT(A3)
1233 IF(ARR.EQ.'SUP') THEN
      CALL SUP(ISUP,ACFN,YDES,WTP,ALPHA,GWID1,GWID2,DEM0D,PAG)
      GOTO 2020
END IF
3863 IF(ARR.EQ.'FPL') TYPE *, 'TYPE "CHK" BEFORE ATTEMPTING FPL'
      IF(ARR.EQ.'CAL') TYPE *, 'TYPE "CHK" BEFORE ATTEMPTING CAL'
      IF(ARR.EQ.'WRT') TYPE *, 'DO CAL BEFORE WRITING FILE'
      IF(ARR.EQ.'TDW') TYPE *, 'DO CAL BEFORE TIME DOMAIN GATE'
      IF(ARR.EQ.'TPL') TYPE *, 'DO CAL BEFORE TIME DOMAIN PLOT'
1234 IF(ARR.EQ.'TAR') CALL TAR(TA,TFILE,TLINE1,TLINE3,NPT,&2020)
      IF(ARR.EQ.'BTA') CALL BTA(BT,BTFILE,NPBT,&2020)
      IF(ARR.EQ.'SPH') CALL SPH(CAS,CFILE,TFILE,TLINE1,TLINE3,NPC
        &2020)
      IF(ARR.EQ.'BSP') CALL BSP(BC,BCFILE,NPBC,&2020)
      IF(ARR.EQ.'EXA') CALL EXA(EXS,EFILE,NPE,&2020)
      IF(ARR.EQ.'CHK') GO TO 5762
      IF(ARR.EQ.'WIN') CALL WIN(DWIN,TDIST,TO,&2020)
      IF(ARR.EQ.'HLP') CALL HLP(&2020)
      IF(ARR.EQ.'EXIT') CALL EXIT
      TYPE *, '?'
      GO TO 2020
C
5762 IF(DWIN.NE.0.AND.FINC.NE.0) THEN
      FIN=FINC*1.E+08
      NS=2.*CFT/(FIN*DWIN)
      IF((NS/2)*2.EQ.NS)NS=NS+1
      IF(NS.LT.3)NS=3
      ELSE
      NS=0
      END IF
C
C      ICHK enables the checking of parameters to be done in
C      another part of the program
C
      ICHK=0
      ICHK2=0
1018 TYPE *, ' '
      TYPE *, 'LIST OF PARAMETERS'
      TYPE 3473,TDIST
3473 FORMAT(1X,/, ' TARGET DISTANCE IN METERS—————> ',F5.2)
      TYPE 3474,DWIN
3474 FORMAT(1X, ' WINDOW WIDTH IN FEET—————> ',F5.2)
      TYPE 3472,NS
3472 FORMAT(1X, ' NO. OF POINTS OF SMOOTHING—————> ',I4)
      TYPE *, ' '
      TYPE *, 'PRESENT INPUT DATA FILES'
      TYPE 3467,TFILE
3467 FORMAT(1X,/, ' "TAR", TARGET—————> ',7A2)
      TYPE 3468,BTFILE
3468 FORMAT(1X, ' "BTA", TARGET BACKGROUND—————> ',7A2)
      TYPE 3469,CFILE
3469 FORMAT(1X, ' "SPH", CALIBRATION TARGET—————> ',7A2)
      TYPE 3470,BCFILE

```

```

3470  FORMAT(1X,'BSP',CALIBRATION TARGET BACKGROUND-> ',7A2)
      TYPE 3471,EFILE
3471  FORMAT(1X,'EXA',EXACT CALIBRATION TARGET-----> ',7A2)
      IF(ICHK.EQ.1) GOTO 1028
      IF(ICHK2.EQ.1) GOTO 3333
C
      IF(ISUP.EQ.1) THEN
        NCSUP=NCSUP+1
        CALL CSUP(ARR,NCSUP,KRPT,IEND,SPAG,KSTP)
        IF(IEND.EQ.1) GOTO 1022
        GOTO 1023
      END IF
C
1022  TYPE 288
      ACCEPT 3862,ARR
1023  IF(ARR.EQ.'CAL') GOTO 1032
      IF(ARR.EQ.'HLP') THEN
        CALL HLP
        GOTO 1022
      END IF
      IF(ARR.EQ.'CHK') THEN
        ICHK2=1
        GOTO 1019
3333  ICHK2=0
        GOTO 1022
      END IF
      IF(ARR.NE.'WRT'.AND.ARR.NE.'TDW'.AND.ARR.NE.'FPL') GOTO 1234
      IF(ARR.NE.'TPL') GOTO 1234
      TYPE *,' '
      TYPE *,'DO CAL BEFORE WRT,FPL,TPL OR TDW'           ! Error checking
      GOTO 1022
C
1032  IF(ISUP.NE.1) THEN
      TYPE *,' '
      TYPE *,'TYPE Y OR N FOR AUTOMATIC CALIBRATED FILE NAMED'
      TYPE *,'FILE WILL BE NAMED *****CAL'
      ACCEPT 1122,ACFN
1122  FORMAT(A1)
      END IF
C
C      Note auto file namer can take directory prefixes and suffices
C      such that the total file name is 28 characters long.
C
      IF(ACFN.EQ.'N') THEN
        DO INOG=1,15
          RFILE(INOG)=' '
        END DO
        TYPE *,' '
        TYPE 52
52    FORMAT(1X,/, ' INPUT A FILE NAME FOR THE RESULT')
        ACCEPT 120,RFILE
        DO 10001 INOG=15,1,-1
          IF (RFILE(INOG).EQ.' ') THEN
            GOTO 10001
          ELSE

```

```

        IP3=IN06+1
        GOTO 10002
        END IF
10001    CONTINUE
10002    IP31=IP3
        IP32=IP3
        ELSE
C
C      Automatic calibrated file namer
C
        IP1=0
        IP2=0
        DO 171 I=1,7
        IF((TFILE(I).AND.'FF00'X).EQ.'2E00'X) IP2=I
        IF((TFILE(I).AND.'00FF'X).EQ.'002E'X) IP1=I
171      CONTINUE
        IF(IP1.NE.0) THEN
        DO 172 I=1,IP1-1
        RFILE(I)=TFILE(I)
172      CONTINUE
        RFILE(IP1)='C'
        RFILE(IP1+1)='AL'
        END IF
        IF(IP2.NE.0) THEN
        DO 173 I=1,IP2
        RFILE(I)=TFILE(I)
173      CONTINUE
        RFILE(IP2+1)='CA'
        RFILE(IP2+2)='L'
        END IF
        IP3=0
        IF(IP1+1.LT.15.AND.IP1.NE.0) IP3=IP1+2
        IF(IP2+2.LT.15.AND.IP2.NE.0) IP3=IP2+3
        IF(IP3.NE.0) THEN
        DO 174 I=IP3,15
        RFILE(IP3)=' '
174      CONTINUE
        IF(IP3.EQ.0) IP3=15
        IP31=IP3
        IP32=IP3
        END IF
C
        TYPE *,' '
        TYPE 118,RFILE
        END IF
118      FORMAT(1X,'CALIBRATED FILENAME',15A2)
120      FORMAT(15A2)
C
        NPMIN=MIND(NPT,NPBT,NPC,NPBC,NPE)
        IF(NPMIN.LT.1) NPMIN=NP
        NP=NPMIN
C
C      Remove background and target distance
C
711    DO 261 I=1,NPMIN

```

```

FREQ=(FINC*(FLOAT(I)-1.)*FMIN)*1.E+09*TP1
CMB(I)=(CAS(I)-BC(I))*CMPLX(COS(FREQ*T0),SIN(FREQ*T0))
TMB(I)=(TA(I)-BT(I))*CMPLX(COS(FREQ*T0),SIN(FREQ*T0))
IF(CAS(I).EQ.(0.,0.).AND.BC(I).EQ.(0.,0.)) CMB(I)=(1.,0.)
IF(TA(I).EQ.(0.,0.).AND.BT(I).EQ.(0.,0.)) TMB(I)=(1.,0.)
IF(I.NE.1) THEN
IF(CABS(CMB(I)).EQ.0.) CMB(I)=CMB(I-1)
IF(CABS(TMB(I)).EQ.0.) TMB(I)=TMB(I-1)
ELSE
IF(CABS(CMB(I)).EQ.0.) CMB(I)=(1.E-15,1.E-15)
IF(CABS(TMB(I)).EQ.0.) TMB(I)=(1.E-15,1.E-15)
END IF
281 CONTINUE
C
NREMOV=0
IF(ISUP.NE.1) THEN
TYPE *, ' '
TYPE *, 'REMOVE INVALID POINTS BEFORE CALIBRATION ? Y OR N'
6844 ACCEPT 6844,YDES
FORMAT(A1)
END IF
IF(YDES.EQ.'Y') THEN
TYPE *, ' '
TYPE *, 'POINT REMOVAL FROM TARGET-BACKGROUND TERM'
NRMT=0
IF(TMB(1).NE.(1.,0.)) CALL CREMOVE(TMB,NPMIN,NRMT,NSPKT,FINC)
TYPE *, ' '
TYPE *, 'POINT REMOVAL FROM CALIBRATION TARGET-BACKGROUND TERM'
NRMC=0
IF(CMB(1).NE.(1.,0.)) CALL CREMOVE(CMB,NPMIN,NRMC,NSPKC,FINC)
NREMOV=NRMT+NRMC
C TYPE *, 'DO YOU WANT TO RE-DO THE POINT REMOVAL Y OR N'
C ACCEPT 6844,YDES
C IF(YDES.EQ.'Y') GO TO 711
C END IF
C
TYPE *, ' '
TYPE *, 'CALIBRATING DATA'
IF(DWIN.EQ.0.) GO TO 1314
IF(CMB(1).NE.(1.,0.)) CALL HAMM(CMB,NPMIN,NS)
IF(TMB(1).NE.(1.,0.)) CALL HAMM(TMB,NPMIN,NS)
1314 DO 262 I=1,NPMIN
IF(CABS(EXS(I)).EQ.0.) EXS(I)=(1.,0.)
RS(I)=TMB(I)/CMB(I)*EXS(I)
262 CONTINUE
C
C FIND THE LOCATION OF THE PERIOD IN THE INPUT FILE NAMES
C
DO 113 I=1,6
IF((TFILE(I).AND.'FF00'X).EQ.'2E00'X) JTDOT=I
IF((TFILE(I).AND.'00FF'X).EQ.'002E'X) JTDOT=I
IF((BTFILE(I).AND.'FF00'X).EQ.'2E00'X) JBTDOT=I
IF((BTFILE(I).AND.'00FF'X).EQ.'002E'X) JBTDOT=I
IF((CFILE(I).AND.'FF00'X).EQ.'2E00'X) JCDDOT=I
IF((CFILE(I).AND.'00FF'X).EQ.'002E'X) JCDDOT=I

```

```

IF((BCFILE(I).AND.'FF00'X).EQ.'2E00'X) JBCDOT=I
IF((BCFILE(I).AND.'00FF'X).EQ.'002E'X) JBCDOT=I
IF((EFILE(I).AND.'FF00'X).EQ.'2E00'X) JEDOT=I
IF((EFILE(I).AND.'00FF'X).EQ.'002E'X) JEDOT=I
113 CONTINUE
JT=JTDOT-3
JBT=JBDOT-3
JC=JCDOT-3
JBC=JBCDOT-3
JE=JEDOT-3
IF(JT.LT.1) JT=1
IF(JBT.LT.1) JBT=1
IF(JC.LT.1) JC=1
IF(JBC.LT.1) JBC=1
IF(JE.LT.1) JE=1
LINE2(4)= ' '
LINE2(8)= ' '
LINE2(12)= ' '
LINE2(16)= ' '
DO 2855 I=20,30
2855 LINE2(I)= ' '
C
C STORE THE 1ST 6 CHARACTERS BEFORE THE PERIOD IN
C EACH OF THE INPUT DATA SET NAMES
C
DO 478 I=1,3
LINE2(I)=TFILE(JT-1+I)
LINE2(I+4)=BTFILE(JBT-1+I)
LINE2(I+8)=CFILE(JC-1+I)
LINE2(I+12)=BCFILE(JBC-1+I)
LINE2(I+16)=EFILE(JE-1+I)
478 CONTINUE
DO 2348 I=1,60
LINE1(I)=TLINE1(I)
2348 LINE3(I)=TLINE3(I)
C
C PUT TARGET DISTANCE AND WINDOW WIDTH AND PONTs REMOVED
C IN 3RD LINE OF HEADER
C
ENCODE(22,106,STRING)TDIST,DWIN,NREMOV
106 FORMAT(' TD=',F4.1,' W=',F4.1,' PR=',I2,X)
DO 727 NSTRG=1,15
727 BUFF(181-NSTRG)=BUFF(180-NSTRG)
DO 728 NSTRG=1,22
728 BUFF(144+NSTRG)=STRING(NSTRG)
C
1051 IF(IGUP.EQ.1) THEN
NCSUP=NCSUP+1
CALL CSUP(ARR,NCSUP,KRPT,IEND,SPAG,KSTP)
IF(IEND.EQ.1) GOTO 1981
GOTO 1052
END IF
1981 TYPE 288
ACCEPT 3862,ARR

```



```

C
C      Here begins the new order of post-calibration options
C
1052  IF (ARR.EQ.'WRT') THEN
      TYPE *, ' '
      TYPE *, 'WRITING FILE'
      CALL WRTFLE(RFILE,RS)
      IF(KSTP.EQ.0) THEN
        GOTO 2020
      ELSE
        GOTO 1051
      END IF
      END IF

C
      IF (ARR.EQ.'TDW') THEN                                ! Time domain window
        ITPL=0
        CALL TDW(INFILE,RS,NPMIN,ITPL,ISUP,GWID1,GWID2,WTP,ALPHA,DEM0D,SPAG
        $,PAG)
        END IF

C
      IF (ARR.EQ.'FPL') THEN                                ! Frequency plot
        NDIM=NP
        ANST=FMIN*1000.
        AINC=NINT(FINC*1000.)
        CALL APP(RFILE,RS,SPAG,PAG)
        END IF

C
      IF (ARR.EQ.'TPL') THEN                                ! Time plot
        ITPL=1
        CALL TDW(RFILE,RS,NPMIN,ITPL,ISUP,GWID1,GWID2,WTP,ALPHA,DEM0D,SPAG,PAG)

C
C      Note TPL uses a modified version of TDW to achieve a plot
C
      ITPL=0
      END IF

C
      IF (ARR.EQ.'CHK') THEN
        ICHK=1
        GOTO 1019
1028  ICHK=0
      END IF

C
      IF (ARR.EQ.'HLP') THEN
        CALL HLP
        END IF

C
      IF (ARR.EQ.'TDW'.OR.ARR.EQ.'FPL'.OR.ARR.EQ.'CHK') GOTO 1051
      IF (ARR.EQ.'TPL') GOTO 1051
      IF (ARR.EQ.'WIN'.OR.ARR.EQ.'EXA'.OR.ARR.EQ.'EXI') GOTO 1234
      IF (ARR.EQ.'TAR'.OR.ARR.EQ.'BTA'.OR.ARR.EQ.'SPH') GOTO 1234
      IF (ARR.EQ.'BSP') GOTO 1234
      IF (ARR.EQ.'SUP') THEN
        TYPE 5588
5588  FORMAT(1X,'Y OR N FOR NEW SET UP      ',*)
        ACCEPT 5588,NEW_SUP
      
```

```

5588  FORMAT(A1)
      IF(NEW_SUP.EQ.'Y') THEN
      IEND=0
      GOTO 1233
      END IF
      TYPE *, ' '
      TYPE 5577
5577  FORMAT(1X, 'TYPE NUMBER OF REPETITIONS ',*)
      ACCEPT *, NRPT
      NCSUP=0
      KSTP =0
      KRPT =1
      IEND =0
      ISUP =1
      GOTO 2020
      END IF

C
      TYPE *, '? '
      GOTO 1061
      END

C
      SUBROUTINE RDFLE(INFILE,CA)
      INCLUDE 'CALCOM.FOR'
      COMMON /BLK1/BUFF /BLK2/NP,FMIN,FINC /BLK3/IB
      INTEGER*2 INFILE(7)
      REAL*4 AP(JD),A(MD),P(MD)
      BYTE BUFF(ID),TBUFF(512)
      EQUIVALENCE (BUFF(361),AP(1))
      COMPLEX*8 CA(MD)
      INCLUDE 'SYS$LIBRARY:FORIOSDEF'
      INFILE(7)=0
      IB=1
      ICNT=0
810  OPEN(UNIT=8,NAME=INFILE,READONLY,TYPE='OLD',IOSTAT=IERR,ERR=8100)
82   IF(IB.EQ.1)LEN=512-8*4
      IF(IB.GT.1)LEN=512-26*4
      READ(8,80,END=80)(TBUFF(I),I=1,512)
80   FORMAT(512A1)
      DO 85 I=1,LEN
85   BUFF(ICNT+I)=TBUFF(I)
      IB=IB+1
      ICNT=ICNT+LEN
      GO TO 82
      DO 86 I=1,LEN
86   BUFF(ICNT+I)=TBUFF(I)
      DO 40 I=1,180
40   BUFF(I)=BUFF(2*I-1)
      TYPE 1982,(BUFF(I),I=1,180)
1982  FORMAT(1X,60A1)
      CALL DCDE
      PI=4.*ATAN(1.)
      DO 199 NN=1,NP
      ATMP=10.*(AP(2*NN-1)/20.)
      PTMP=AP(2*NN)/180.*PI
199  CA(NN)=CMPLX(ATMP*COS(PTMP),ATMP*SIN(PTMP))

```

```

      IB=IB+1
      GO TO 8017
8100  IF(IERR.EQ.FOR$IOS_FILNOTFOU)THEN
      TYPE 1112, (INFILE(IIT), IIT=1, 6)
1112  FORMAT(' FILE : ', 6A2, ' WAS NOT FOUND', '/', ' ENTER FILENAME AGAIN')
      ELSE IF (IERR.EQ.FOR$IOS_FILNAMSPE)THEN
      TYPE 1110, (INFILE(IIT), IIT=1, 6)
1110  FORMAT(' FILE : ', 6A2, ' WAS BAD,      ENTER NEW FILENAME')
      ELSE
      TYPE *, ' UNRECOVERABLE ERROR, CODE =', IERR
      STOP
      ENDIF
      ACCEPT 8816, (INFILE(IIT), IIT=1, 6)
8816  FORMAT(6A2)
      GO TO 810
8017  CLOSE(UNIT=8, DISP='SAVE')
      RETURN
      END

C
C
C
C
C
      SUBROUTINE WRTFILE(RFILE, CA, *)
      INCLUDE 'CALCOM.FOR'
      COMMON /BLK1/BUFF /BLK2/NP, FMIN, FINC /BLK3/IB
      COMPLEX*8 CA(5000)
      BYTE LINE1(60), LINE2(60), LINE3(60), BUFF(ID), TBUFF(512)
      CHARACTER*1 YN
      REAL*4 AP(JD)
      INTEGER*2 RFILE(15)
      EQUIVALENCE(LINE1(1), BUFF(1)), (LINE2(1), BUFF(61)),
1(LINE3(1), BUFF(121)), (AP(1), BUFF(361))
      NB=IB*256
      IBS=IB
      RFILE(15)=0
      PI=4.*ATAN(1.)
      DO 210 I=1, NP
      AP(2*I)=ATAN2(AIMAG(CA(I)), REAL(CA(I)))/PI*180.
210  AP(2*I-1)=20.*ALOG10(CABS(CA(I)))
C      TYPE *, 'DO YOU WANT TO EDIT THE HEADER ? Y OR N'
C      ACCEPT 111, YN
111  FORMAT(A1)
      IF(YN.NE.'Y')GO TO 122
      TYPE 112
112  FORMAT(1X, '/', ' INPUT A HEADER FOR THE RESULT ( 1 LINE)')
      ACCEPT 128, (LINE1(I), I=1, 60)
128  FORMAT(60A1)
122  OPEN(UNIT=18, NAME=RFILE, TYPE='NEW', RECORDSIZE=NB)
      IB=1
      ICNT=0
      DO 40 I=180, 1, -1
40  BUFF(2*I-1)=BUFF(I)
82  IF(IB.EQ.1)LEN=512-8*4
      IF(IB.GT.1)LEN=512-26*4

```

```

      DO 85 I=1,LEN
85      TBUF(I)=BUF(ICNT+I)
          IB=IB+1
          ICNT=ICNT+LEN
          WRITE(19,81)(TBUF(I),I=1,512)
81      FORMAT(512A1)
          IF(IB.LE.IBS)GO TO 82
80      CLOSE(UNIT=19,DISP='SAVE')
          RETURN
      END

C
C
C
C
      SUBROUTINE DCDE
      INCLUDE 'CALCOM.FOR'
      COMMON /BLK1/BUF /BLK2/NP,FMIN,FINC /BLK3/IB
      BYTE BUF(ID)
      INTEGER*4 IMIN,IINC,NP

C
C      NO. OF DATA POINTS IS STORED IN THREE CHARACTERS, AND
C      STARTING FREQ. AND FREQ. INC. IN 5 CHARACTERS
C

      CHARACTER*4 CNL
      CHARACTER*5 CFF,CINC
      EQUIVALENCE (BUF(123),CNL),(BUF(131),CFF),(BUF(140),CINC)

C
C      CONVERT CHARACTERS TO THEIR NUMERICAL EQUIVALENTS
C

      IF(BUF(123).EQ.' ') BUF(123)=' '
      DECODE(4,100,CNL)NPP
      NP=MINO(NP,NPP)
100      FORMAT(I5)
          DECODE(5,100,CFF)IMIN
          DECODE(5,100,CINC)IINC
          FMIN=FLOAT(IMIN)/1000.
          FINC=FLOAT(IINC)/1000.
          RETURN
      END

C
C      K=TOTAL NO. OF POINT
C      N=NO. OF POINTS OF SMOOTHING
C

      SUBROUTINE HAMM(CS,K,N)
      INCLUDE 'CALCOM.FOR'
      COMMON /BLK1/BUF /BLK2/NP,FMIN,FINC /BLK3/IB
      COMPLEX CS(MD),CSS(MD),SUM,FACT
      DTR=57.29577858
      TPI=6.2831853
      N2=(N-1)/2
      DO 3 KM=1,K
          SUM=CMPLX(0.,0.)
          KOUNT=1
2          KM=KM-N2+KOUNT-1
          OFF=FLOAT(KM-KM)*TPI/FLOAT(N)

```

```

      IF(KM.LT.1) KM=2-KM
      IF(KM.GT.K) KM=2 * K - KM
      W=COS(OFF)+1.
      FACT=W*CS(KM)
      SUM=SUM+FACT
      IF(KOUNT.EQ.N) GO TO 1
      KOUNT=KOUNT+1
      GO TO 2
1     CONTINUE
      SUM=SUM/FLOAT(N)
      CSS(KM)=SUM
3     CONTINUE
      DO 6 KM=1,K
      CS(KM)=CSS(KM)
6     CONTINUE
      RETURN
      END

```

C
C
C
C

```

SUBROUTINE TAR(TA,TFILE,TLINE1,TLINE3,NPT,*)
INCLUDE 'CALCOM.FOR'
COMMON /BLK1/BUFF /BLK2/NP,FMIN,FINC /BLK3/IB
COMPLEX TA(MD)
INTEGER*2 TFILE(7)
BYTE LINE1(60),LINE3(60),BUFF(10),TLINE1(60),TLINE3(60)
EQUIVALENCE(LINE1(1),BUFF(1)),(LINE3(1),BUFF(121))
10    FORMAT(1X,/, ' INPUT THE TARGET FILE NAME')
      TYPE 10
      ACCEPT 120,(TFILE(IIN),IIN=1,7)
120   FORMAT(7A2)
      CALL RDFLE(TFILE,TA)
      NPT=NP
      DO 2346 I=1,60
      TLINE1(I)=LINE1(I)
2346  TLINE3(I)=LINE3(I)
      RETURN
      END

```

C
C
C
C

```

SUBROUTINE BTA(BT,BTFILE,NPBT,*)
INCLUDE 'CALCOM.FOR'
COMMON /BLK1/BUFF /BLK2/NP,FMIN,FINC /BLK3/IB
COMPLEX BT(MD)
INTEGER*2 BTFILE(7)
BYTE BUFF(10)
TYPE 20
20    FORMAT(1X,/, ' INPUT THE BACKGROUND FILE NAME FOR THE TARGET')
      ACCEPT 120,(BTFILE(IIN),IIN=1,7)
120   FORMAT(7A2)
      CALL RDFLE(BTFILE,BT)
      NPBT=NP

```

```

RETURN1
END

C
C
C
C
SUBROUTINE SPH(CAS,CFILE,TFILE,TLINE1,TLINE3,NPC,*)
INCLUDE 'CALCOM.FOR'
COMMON /BLK1/BUFF /BLK2/NP,FMIN,FINC /BLK3/IB
COMPLEX CAS(MD)
INTEGER*2 CFILE(7),TFILE(7)
BYTE LINE1(60),LINE3(60),BUFF(10),TLINE1(60),TLINE3(60)
EQUIVALENCE(LINE1(1),BUFF(1)),(LINE3(1),BUFF(121))
TYPE 40
40  FORMAT(1X,/, ' INPUT THE CALIBRATION TARGET FILE NAME')
ACCEPT 120,(CFILE(IIN),IIN=1,7)
120  FORMAT(7A2)
CALL RDFLE(CFILE,CAS)
NPC=NP
DO 4 I=1,7
IF(TFILE(I).NE.0) RETURN1
4    CONTINUE
DO 2346 I=1,60
TLINE1(I)=LINE1(I)
2346 TLINE3(I)=LINE3(I)
RETURN1
END

C
C
C
C
SUBROUTINE BSP(BC,BCFILE,NPBC,*)
INCLUDE 'CALCOM.FOR'
COMMON /BLK1/BUFF /BLK2/NP,FMIN,FINC /BLK3/IB
COMPLEX BC(MD)
INTEGER*2 BCFILE(7)
BYTE BUFF(10)
TYPE 41
41  FORMAT(1X,/, ' INPUT THE BACKGROUND FILE NAME FOR THE
$  CALIBRATION TARGET')
ACCEPT 120,(BCFILE(IIN),IIN=1,7)
120  FORMAT(7A2)
CALL RDFLE(BCFILE,BC)
NPBC=NP
RETURN1
END

C
C
C
C
SUBROUTINE EXA(EXS,EFILE,NPE,*)
INCLUDE 'CALCOM.FOR'
COMMON /BLK1/BUFF /BLK2/NP,FMIN,FINC /BLK3/IB
COMPLEX EXS(MD)
INTEGER*2 EFILE(7)

```

```

        BYTE BUFF(ID)
        TYPE 50
50      FORMAT(1X,/, ' INPUT THE EXACT CALIBRATION FILE NAME')
        ACCEPT 120, (EFILE(IIN), IIN=1,7)
120     FORMAT(7A2)
        CALL RDFLE(EFILE, EXS)
        NPE=NP
        RETURN1
        END

C
C
C
C
        SUBROUTINE WIN(DWIN, TDIST, TO, *)
        CME=2.998E+08
        CFT=9.836E+08

C
C
C
        COMPUTE TIME SHIFT IN DATA TO CENTER IT OVER THE HAMMING WINDOW
        TDIST=DISTANCE TO TARGET IN METERS

        TYPE *, 'ENTER ONE WAY DISTANCE TO TARGET IN METERS'
        TYPE *, '          DUAL AEL HORNS'
        TYPE *, 'OVER & UNDER PRIOR JULY 4, 1983 = 12.1 METERS'
        TYPE *, 'OVER & UNDER AFTER JULY 4, 1983 = 11.8 METERS'
        TYPE *, 'SIDE BY SIDE AFTER JULY 4, 1983 = 11.8 METERS'
        ACCEPT *, TDIST
        TO=2*TDIST/CME

C
C
C
        COMPUTE HAMMING WINDOW SIZE, (FEET, SECONDS)

        TYPE *, 'ENTER 3DB DOWN HAMMING WINDOW SIZE IN FEET'
        TYPE *, 'ENTER 0 FOR NO HAMMING WINDOW'
        ACCEPT *, DWIN
        RETURN1
        END

C
C
C
C
        SUBROUTINE TDW(INFILE, RS, NPMIN, ITPL, ISUP, GWID1, GWID2, WTP, ALPHA, DEMOD
*, SPAG, PAG)
        INCLUDE 'CALCOM.FOR'
        COMMON /BLK1/BUFF /BLK2/NP, FMIN, FINC /BLK3/IB
        COMMON /BLK4/NDIM, ANST, AINC
        COMPLEX*8 RS(5000)
        REAL*4 AM(5000), PH(5000)
        INTEGER*2 INFILE(15)

C
        IF (ITPL.EQ.1) GOTO 9014
        IF (ISUP.NE.1.OR.(GWID1.EQ.0.0.AND.GWID2.EQ.0.0)) THEN
            TYPE *, ' '
            TYPE *, 'TYPE STARTING AND END POINTS FOR WINDOW'
            ACCEPT *, GWID1, GWID2
            END IF
        ! For plotting

```

```

C      Calculate the number of points in time domain filter
C
      NTDPTS1=NINT(GWID1*4.096*NINT(FINC*1000.))
      NTDPTS2=NINT(GWID2*4.096*NINT(FINC*1000.))
      NTDPTS=NTDPTS2+NTDPTS1
      TYPE *, ' '
      TYPE *, 'NUMBER OF POINTS IN TIME DOMAIN FILTER ', NTDPTS

C
C      Convert from COMPLEX(x,y) to AMPLITUDE(dB) and PHASE(deg)
C      for compatibility with FTRAN modules.
C
8014  DO 8015 I=1, NPMIN
      AM(I)=20.*ALOG10(CABS(RS(I)))
      PH(I)=ATAN2D(AIMAG(RS(I)), REAL(RS(I)))
8015  CONTINUE
      IF (ITPL.EQ.1) THEN
        CALL FWN(AM, PH)
        END IF
        CALL IFT(AM, PH, ISUP, DEMOD)
        IF (ITPL.EQ.1) THEN
          CALL RPL(INFILE, AM, SPAG, PAG)
          END IF
          IF (ITPL.EQ.1) GOTO 8017
          CALL GAT(AM, PH, NTDPTS1, NTDPTS2, ISUP, WTP, ALPHA)
8016  CALL FFT(AM, PH, JNDIM, INFILE)
      NDIM=JNDIM
C
C      Convert data back into complex form and remove 0-FMIN
C      'fill-up' data points which will mess up plots
C
      DO 8029 I=1, (NDIM-IFIX(FMIN*100.))
      K=IFIX(FMIN*100.)+I
      RS(I)=CMPLX(COSD(PH(K)), SIND(PH(K)))*(10.*(AM(K)/20.))
8029  CONTINUE
C
C      Reset data parameters after time plot because forward
C      transform is not performed. (Forward transforming is unnecessary
C      indeed useless as window will appear in f. data and we have the
C      original f. file anyway.
C
8017  ITPL=0
      NDIM=NP
      ANST=FMIN*1000.
      AINC=NINT(FINC*1000.)
      RETURN
      END
C
      SUBROUTINE SUP(ISUP, ACFN, YDES, WTP, ALPHA, GWID1, GWID2, DEMOD, PAG)
      COMMON /BLK5/ARRA, NRPT
      COMMON /BLK6/PLOTOPT1, IP31, LPL1, NDIG1, FXB, FXE, FXS, FYB, FYE, FYS
      COMMON /BLK7/PLOTOPT2, IP32, LPL2, NDIG2, TXB, TXE, TXS, TYB, TYE, TYS
      DIMENSION ARRA(30)
      ISUP=1
      NA=1
      TYPE 53, NA

```



```

53     FORMAT(1X,'COMMAND: ',I2,' ',%)
      ACCEPT 55,ARRA(NA)
55     FORMAT(A3)
      CALL ESUP(ARRA,NA,IESUP)                                ! Eliminate bad commands
      IF(IESUP.EQ.1) GOTO 51
      IF(ARRA(NA).EQ.'END') GOTO 57
      IF(ARRA(NA).EQ.'RPT') THEN                                ! Repeat a section of commands
        TYPE *,' '
        TYPE 58
58     FORMAT(1X,'TYPE NUMBER OF REPETITIONS ',%)              ! For NRPT times
      ACCEPT *,NRPT
      GOTO 57
      END IF
      NA=NA+1
      GOTO 51

C
C     Input a series of control parameters
C
57     TYPE *,' '
      TYPE 61
61     FORMAT(1X,'Y OR N FOR AUTO FILE NAME                    ',%)
      ACCEPT 62,ACFN
62     FORMAT(A1)
      TYPE 63
63     FORMAT(1X,'Y OR N FOR BAD POINT REMOVAL                ',%)
      ACCEPT 62,YDES
      TYPE 69
69     FORMAT(1X,'Y OR N FOR FREQ.GREATER THAN 20 GHZ         ',%)
      ACCEPT 62,DEM0D
      TYPE 71
71     FORMAT(1X,'Y OR N FOR PLOT AGAIN OPTION                 ',%)
      ACCEPT 62,PAG
      TYPE 68
68     FORMAT(1X,'Y OR N FOR PLOT SET-UP IN FPL                ',%)
      ACCEPT 62,PLOTOPT1
      TYPE 7712
7712    FORMAT(1X,'Y OR N FOR PLOT SET-UP IN TPL                ',%)
      ACCEPT 62,PLOTOPT2
      IF(PLOTOPT1.EQ.'Y') THEN
        TYPE *,'          FPL PARAMETERS'
        TYPE 7700
7700    FORMAT(1X,'Y OR N FOR ANOTHER PLOT ON OLD ONE          ',%)
        ACCEPT 62,LPL1
        TYPE 7702
7702    FORMAT(1X,'INPUT NO. OF DIGITS RIGHT OF .XXX           ',%)
        ACCEPT *,NDIG1
        TYPE 7704
7704    FORMAT(1X,'INPUT MIN,MAX,INC FREQUENCY                 ',%)
        ACCEPT *,FXB,FXE,FXS
        TYPE 7706
7706    FORMAT(1X,'INPUT MIN,MAX,INC FREQ. AMPLITUDE            ',%)
        ACCEPT *,FYB,FYE,FYS
        END IF
        IF(PLOTOPT2.EQ.'Y') THEN
          TYPE *,'          TPL PARAMETERS'

```

```

TYPE 7700
ACCEPT 62,LPL2
TYPE 7702
ACCEPT *,NDIG2
TYPE 7708
7708 FORMAT(1X,'INPUT MIN,MAX,INC TIME',#)
ACCEPT *,TXB,TXE,TXS
TYPE 7710
7710 FORMAT(1X,'INPUT MIN,MAX,INC TIME. AMPLITUDE',#)
ACCEPT *,TYB,TYE,TYS
END IF
TYPE 64
64 FORMAT(1X,'Y OR N FOR HANNING OR BESSEL FILTER',#)
ACCEPT 62,WTP
IF(WTP.EQ.'N') THEN
TYPE 65
65 FORMAT(1X,'INPUT ALPHA',#)
ACCEPT *,ALPHA
END IF
TYPE 67
67 FORMAT(1X,'INPUT WINDOW START AND END POINTS nS',#)
ACCEPT *,GWID1,GWID2
RETURN
END

SUBROUTINE ESUP(ARRA,NA,IESUP)                                ! Find errors in commands
DIMENSION ARRA(30)
Q=ARRA(NA)
IF(Q.EQ.'TAR'.OR.Q.EQ.'BTA'.OR.Q.EQ.'SPH'.OR.Q.EQ.'BSP') GOTO 570
IF(Q.EQ.'WIN'.OR.Q.EQ.'EXA'.OR.Q.EQ.'EXI'.OR.Q.EQ.'HLP') GOTO 570
IF(Q.EQ.'CAL'.OR.Q.EQ.'WRT'.OR.Q.EQ.'FPL'.OR.Q.EQ.'TPL') GOTO 570
IF(Q.EQ.'TDW'.OR.Q.EQ.'LAB'.OR.Q.EQ.'RPT'.OR.Q.EQ.'CHK') GOTO 570
IF(Q.EQ.'END') GOTO 570
TYPE *,'ENTER A VALID COMMAND'
IESUP=1
RETURN
570 IESUP=0
RETURN
END

C
SUBROUTINE CSUP(ARR,I,KRPT,IEND,SPAG,KSTP)
COMMON /BLK5/ARRA,NRPT
DIMENSION ARRA(30)                                ! Control subroutine for SUP

IF(KSTP.NE.0.AND.I.EQ.KSTP) THEN
IESUP=0
IEND=1
RETURN
END IF

C
1984 ARR=ARRA(I)
C
IF(ARRA(1).EQ.'END') THEN                                ! Relinquish control set-up but
IEND=1                                                    ! keep parameter set-up
RETURN

```

```

C      END IF

      IF(I.GT.1.AND.ARRA(I).EQ.'END') THEN
      IEND=1
      ISUP=0
      RETURN
      END IF

C      IF(ARR.EQ.'LAB') THEN
      NLAB=I+1
      I=I+1
      GOTO 1984
      END IF
      I LAB (label) is starting point of
      I repetition process

C      IF(SPAG.EQ.'Y') THEN
      I=I-1
      ARR=ARRA(I)
      END IF
      I This allow plots to be
      I Redone

C      IF(NRPT.EQ.0) RETURN
      I Relinquish SUP mode after
      I repetitions are done

C      IF(ARR.EQ.'RPT') THEN
      ARR=ARRA(NLAB)
      KRPT=KRPT+1
      IF(KRPT.EQ.NRPT+1) THEN
      KSTP=I-1
      I=NLAB
      RETURN
      END IF
      I=NLAB
      END IF
      I SUP command structure is a bit like
      I a programmable calculator (especially
      I the Casio FX-601P)

C      RETURN
      END

C      SUBROUTINE HLP(*)
      TYPE *, ' '
      TYPE *, 'LIST OF COMMANDS'
      TYPE *, '"SUP"=SET UP A SERIES OF COMMANDS AND PARAMETERS'
      TYPE *, '"TAR"=ENTER DATA INTO TARGET ARRAY'
      TYPE *, '"BTA"=ENTER DATA INTO TARGET BACKGROUND ARRAY'
      TYPE *, '"SPH"=ENTER DATA INTO CALIBRATION TARGET ARRAY'
      TYPE *, '"BSP"=ENTER DATA INTO CALIBRATION TARGET BACKGROUND ARRAY'
      TYPE *, '"EXA"=ENTER DATA INTO EXACT CALIBRATION TARGET ARRAY'
      TYPE *, '"WIN"=CHANGE TARGET DISTANCE AND WINDOW WIDTH'
      TYPE *, '"CAL"=CALIBRATE DATA'
      TYPE *, '"CHK"=CHECK FILE STATUS AND PARAMETERS FOR CAL'
      TYPE *, '"TDW"=GATE IN TIME DOMAIN '
      TYPE *, '"FPL"=PLOT CALIBRATED DATA IN FREQUENCY DOMAIN'
      TYPE *, '"TPL"=PLOT CALIBRATED DATA IN TIME DOMAIN'
      TYPE *, '"WRT"=WRITE A CALIBRATED FILE'
      TYPE *, '"HLP"=PRINT LIST OF COMMANDS'

```

```
TYPE *, 'EXIT'=EXIT FROM PROGRAM GRACEFULLY'  
TYPE *, 'NOTE : MAX FILE NAME LENGTH = 12 CHARACTERS'  
TYPE *, ' '  
TYPE *, 'NOTE : THE "CAL" COMMAND DOES NOT WRITE A FILE IN CAL61'  
TYPE *, '      THIS IS ACHEIVED BY A SEPARATE "WRT" COMMAND '  
RETURN1  
END
```

```

C
C THIS SUBROUTINE REMOVES LARGE NON-PERIODIC SPIKES FROM DATA IN
C COMPLEX FORMAT. WRITTEN BY DONALD F. KIMBALL ON
C JANUARY 10, 1983
C
C INPUT TO SUBROUTINE REMOVE CONSISTS OF REAL AND IMAGINARY PARTS
C CONTAINED IN A SINGLE COMPLEX VARIABLE "RECT",
C AND THE NUMBER OF DATA POINTS. THE OUTPUT UNITS OF THE
C SUBROUTINE ARE THE SAME AS THE INPUT UNITS.
C
C SUBROUTINE CREMOVE(RECT,NP,NREMOV,NSPIKE,FINC)
C
C      NREMOV = no. of pts. removed
C      NSPIKE = index no. of pts. removed
C
C INCLUDE 'CALCOM.FOR'
C DATA CFT/ 9.836E+8 /
C INTEGER NSPIKE(MD)
C COMPLEX RECT(MD),CAVG,CSQAVG,CVAR,CSTDEV
C
C NAVG MUST BE AN EVEN NUMBER
C
C NSPIKE(1)=0
C NREMOV =0
C
C      note: NAVG must be an even number
C
C FIN = FINC * 1.E+9           ! frequency increment
C TZONE = 20.-                ! target zone in feet
C SEN = 9.                    ! SEN standard deviations
C ISKIP = (CFT/(TZONE * FIN)) - 1
C
C      ISKIP = no. of pts. to skip in average
C      ISKIP is derived from Shannon's theorem
C      ISKIP must be an odd number
C
C IF((ISKIP/2)*2 .EQ. ISKIP ) ISKIP = ISKIP + 1
C TYPE *, 'ISKIP = ',ISKIP
C IHOLE = (ISKIP - 1)/2
C TYPE *, 'IHOLE = ',IHOLE
C
C      dont use IHOLE points on either side test point
C
C NAVG = (2*CFT/(TZONE * FIN)) - ISKIP
C
C      NAVG, number of points to average over
C      this quantity is derived from the
C      the sinc/x filter.
C      NAVG must be an even number
C
C IF((NAVG/2)*2 .NE. NAVG ) NAVG = NAVG + 1
C IF(NAVG .LT. 4) NAVG = 4
C TYPE *, 'NAVG = ',NAVG
C
CC DO 606 J=1,NP

```

```

C      AVGDB=0.          ! initialize the average sumers
      CAVG=(0.,0.)
      CSQAVG=(0.,0.)
      SQAVGDB=0.
      NUM_SUM = 0        ! number of points added up
C
C      COMPUTE AVERAGE OF (NAVG) POINTS AROUND POINTS J-1,J,
C      AND J+1,BUT NOT INCLUDING THOSE POINTS IN THE AVERAGE.
C
      I = J - NAVG / 2 - IHOLE
      IF( I .LT. 1 ) I = 1
      IDIS = NP - J        ! how close to end
      IF( IDIS .LT. NAVG / 2 + IHOLE )
        I = I - ( NAVG / 2 + IHOLE - IDIS )
      IF( IDIS .LE. IHOLE ) I = I + ( IHOLE - IDIS )
C*
CC      TYPE *, ' J = ', J, 'SETTING I TO', I
C*
111  IF( IABS( I - J ) .LE. IHOLE ) GO TO 22 ! don't average over middle
C
C*
CC      TYPE *, ' CALCULATING FOR J,I,NP', J,I,NP
C*
      CAVG=CAVG+RECT(I)
      DB_NUM = 20*LOG10( CABS( RECT( I ) ) )
      AVGDB = AVGDB + DB_NUM
      SQAVGDB = SQAVGDB + DB_NUM ** 2
      CSQAVG = CSQAVG+CMPLX((REAL(RECT(I)))**2,(AIMAG(RECT(I)))**2)
      NUM_SUM = NUM_SUM + 1
22   I = I + 1
      IF( NUM_SUM .LT. NAVG ) GOTO 111
C
C
      CAVG=CAVG/NUM_SUM
      AVGDB=AVGDB/NUM_SUM
      SQAVGDB=SQAVGDB/NUM_SUM
      CSQAVG=CSQAVG/NUM_SUM
C
C      calculate variance and standard deviations
C
      VARDB=SQAVGDB-AVGDB**2
      CVAR=CSQAVG-CMPLX((REAL(CAVG))**2,(AIMAG(CAVG))**2)
      IF( VARDB .LT. 0. ) VARDB = 0.
      IF( REAL( CVAR ) .LT. 0. ) CVAR = CMPLX( 0., AIMAG( CVAR ) )
      IF( AIMAG( CVAR ) .LT. 0. ) CVAR = CMPLX( REAL( CVAR ), 0. )
      STDEVDB=SQRT(VARDB)
      CSTDEV=CMPLX(SQRT(REAL(CVAR)),SQRT(AIMAG(CVAR)))
C
C      SEE IF POINTS J-1,J,AND J+1 DEVIATES TOO FAR FROM THE AVERAGE BY
C      COMPARING THEM TO THE STANDARD DEVIATION
C
      IF(J-1.LT.1) GO TO 202
      IF(ABS(20*LOG10(CABS(RECT(J-1)))-AVGDB).GT.SEN*STDEVDB) GO TO 101
      IF(ABS(REAL(RECT(J-1)-CAVG)).GT.SEN*REAL(CSTDEV)) GO TO 101

```

```

101 IF(ABS(AIMAG(RECT(J-1)-CAVG)).LT.SEN*AIMAG(CSTDEV)) GOTO 202
    NREMOV=NREMOV+1
    NSPIKE(NREMOV)=J-1
    TYPE *, 'POINT ', J-1, ' REMOVED'
    RECT(J-1)=CAVG
202 IF(ABS(20*LOG10(CABS(RECT(J)))-AVGDB).GT.SEN*STDEVDB) GOTO 303
    IF(ABS(REAL(RECT(J)-CAVG)).GT.SEN*REAL(CSTDEV)) GOTO 303
    IF(ABS(AIMAG(RECT(J)-CAVG)).LT.SEN*AIMAG(CSTDEV)) GOTO 404
303 NREMOV=NREMOV+1
    NSPIKE(NREMOV)=J
    TYPE *, 'POINT ', J, ' REMOVED'
    RECT(J)=CAVG
404 IF(J+1.GT.NP) GO TO 606
    IF(ABS(20*LOG10(CABS(RECT(J+1)))-AVGDB).GT.SEN*STDEVDB) GOTO 505
    IF(ABS(REAL(RECT(J+1)-CAVG)).GT.SEN*REAL(CSTDEV)) GOTO 505
    IF(ABS(AIMAG(RECT(J+1)-CAVG)).LT.SEN*AIMAG(CSTDEV)) GOTO 606
505 NREMOV=NREMOV+1
    NSPIKE(NREMOV)=J+1
    TYPE *, 'POINT ', J+1, ' REMOVED'
    RECT(J+1)=CAVG
606 CONTINUE
    TYPE *, NREMOV, ' POINTS REMOVED'
    RETURN
    END

```

```

C
C      Subroutine FWN
C      Fortran name: FWNV.FOR, developed by A.Dominek to perform
C      pre-IFT windowing (to reduce pre-cursors) in FTRAN.FOR, modified
C      by N.F.Chamberlain for use in CAL81.FOR.
C
      SUBROUTINE FWN(AM,PH)
      COMMON /BLK1/BUFF /BLK2/NP,FMIN,FINC /BLK3/IB
      COMMON /BLK4/NDIM,ANST,AINC
      BYTE BUFF(33200)
C      INTEGER*2 INFILE(7)
      DIMENSION AM(5000),PH(5000)
      CHARACTER*2 WT,LP
      LOGICAL CE,WTY
      EXTERNAL BIO
      DATA LP/'LP'/
      PI=3.1415926
      NDIM=NP
      ANST=FMIN*1000.
      AINC=NINT(FINC*1000.)
      TYPE *,' '
      TYPE *,'STARTING TO WINDOW DATA TO REDUCE PRECURSORS IN TIME DOMAIN'
C      WRITE(6,*) 'INPUT T OF F TO CONSERVE SIGNAL ENERGY'
C      ACCEPT *, CE
      CE=0
      IF(CE) THEN
        S1=0.
        S3=0.
        DO 10 I=1,NDIM
          S3=S3+10.**[AM(I)/20.]*COSD(PH(I))
10      S1=S1+10.**[AM(I)/10.]
        END IF
C      WRITE(6,*) 'INPUT WINDOW TYPE, LP (LOW PASS) OR BP (BAND PASS)'
C      ACCEPT 20, WT
20      FORMAT(1A2)
C      IF(WT.EQ.LP) THEN
        IWTLB=1
        IF(IWTLB.EQ.0) THEN
          IW=NDIM
          DT=PI/FLOAT(IW)
          WRITE(6,*) 'INPUT T FOR HANNING OR F FOR KAISER-BESSEL'
          ACCEPT *, WTY
          IF(WTY) THEN
            DO 30 I=1,IW
              WFACT=.5*(1.+COS(DT*(I)))
C              WFACT=(COS(.5*DT*I)+.22*COS(1.5*DT*I))/1.22
              AA=10.**[AM(I)/20.]*WFACT
              IF(AA.LE.0.) AA=1.E-30
30      AM(I)=20.*ALOG10(AA)
            ELSE
C              WRITE(6,*) 'INPUT ALPHA'
C              ACCEPT *, ALPHA
              ALPHA=2.
              TYPE *,' '
              TYPE *,'ALPHA=2 IN BESSEL WINDOWING FILTER'

```



```

PIA=ALPHA*PI
CON=BIO(PIA)
DO 31 I=1,IW
ARG=PIA*SQRT(1.-(FLOAT(I)/FLOAT(IW))**2)
WFACT=BIO(ARG)/CON
AA=10.**((AM(I)/20.)*WFACT)
IF(AA.LE.0.) AA=1.E-30
31 AM(I)=20.*ALOG10(AA)
END IF
ELSE
C WRITE(6,*) 'INPUT T FOR HANNING OR F FOR KAISER-BESSEL'
C ACCEPT *, WTY
C IF(WTY) THEN
IWTY=1
IF(IWTY.EQ.0) THEN
IW=NDIM/2
IIW=2*IW-1
IF(FLOAT(NDIM)/2..EQ.FLOAT(IW)) THEN
DT=PI/FLOAT(IIW)
II=0
DO 40 I=1,IIW,2
II=II+1
WFACT=.5*(1.+COS(DT*I))
IF(WFACT.LE.0.) WFACT=1.E-4
AM(IW+II)=20.*ALOG10(10.**((AM(IW+II)/20.)*WFACT))
40 AM(IW-II+1)=20.*ALOG10(10.**((AM(IW-II+1)/20.)*WFACT))
ELSE
DT=PI/FLOAT(IW)
DO 50 I=1,IW
WFACT=.5*(1.+COS(DT*I))
IF(WFACT.LE.0.) WFACT=1.E-4
AM(IW+I+1)=20.*ALOG10(10.**((AM(IW+I+1)/20.)*WFACT))
50 AM(IW-I+1)=20.*ALOG10(10.**((AM(IW-I+1)/20.)*WFACT))
END IF
ELSE
C WRITE(6,*) 'INPUT ALPHA'
C ACCEPT *, ALPHA
ALPHA=2.
TYPE *, ' '
TYPE *, 'ALPHA=2 IN BESSEL WINDOWING FILTER'
PIA=ALPHA*PI
CON=BIO(PIA)
IW=NDIM/2
IIW=2*IW-1
IF(FLOAT(NDIM)/2..EQ.FLOAT(IW)) THEN
DT=1./FLOAT(IIW)
II=0
DO 60 I=1,IIW,2
II=II+1
ARG=PIA*SQRT(1.-(DT*I)**2)
WFACT=BIO(ARG)/CON
AM(IW+II)=20.*ALOG10(10.**((AM(IW+II)/20.)*WFACT))
60 AM(IW-II+1)=20.*ALOG10(10.**((AM(IW-II+1)/20.)*WFACT))
ELSE
DT=1./FLOAT(IW)

```

```

DO 70 I=1,IW
ARG=PIA*SQRT(1.-(DT*I)**2)
WFACT=810(ARG)/CON
AM(IW+I+1)=20.*ALOG10(10.**(AM(IW+I+1)/20.)*WFACT)
70 AM(IW-I+1)=20.*ALOG10(10.**(AM(IW-I+1)/20.)*WFACT)
END IF
END IF
END IF
IF(CE) THEN
S2=0.
S4=0.
DO 80 I=1,NDIM
S4=S4+10**((AM(I)/20.)*COSD(PH(I)))
80 S2=S2+10**((AM(I)/10.))
SC=SQRT(S1/S2)
SC1=S1/S2
WRITE(6,*) 'S1,S2,SC=',S1,S2,SC
WRITE(6,*) 'S3,S4,SC1=',S3,S4,SC1
DO 90 I=1,NDIM
90 AM(I)=20.*ALOG10(10.**(AM(I)/20.)*SC)
END IF
RETURN
END

```

```

C      Subroutine GAT
C      Part of SBCL61.FOR, a group of FFT subroutines.
C      Developed by A.Dominek to perform gating in the time domain,
C      modified by N.F.Chamberlain Jan. 1984 for use with CAL61.FOR.
C
SUBROUTINE GAT(AM,PH,NTDPTS1,NTDPTS2,ISUP,WTP,ALPHA)
COMMON /BLK1/BUFF /BLK2/NP,FMIN,FINC /BLK3/IB
COMMON /BLK4/NDIM,ANST,AINC
BYTE BUFF(33200)
C      INTEGER*2 INFILE(15)
C      DIMENSION AM(5000),PH(5000)
C      LOGICAL WTP,CE
C      LOGICAL CE
C      EXTERNAL BIO
C      PI=3.1415927
C      TYPE *,' '
C      TYPE *,'STARTING GATING ROUTINE IN TIME DOMAIN'
C      WRITE(6,*) 'INPUT T OR F TO CONSERVE SIGNAL ENERGY'
C      ACCEPT *, CE
C      CE=0
C      WRITE(6,*) 'INPUT STARTING AND ENDING INDEX NUMBERS'
C      ACCEPT *, IS,IE
C      IS=2048-NTDPTS1
C      IE=2048+NTDPTS2
C      IS1=IS-1
C      IF(CE) THEN
C      S1=0.
C      S3=0.
C      DO 10 I=IS,IE
C      S3=S3+AM(I)
10      S1=S1+AM(I)**2
C      END IF
C      IF(ISUP.NE.1) THEN
C      WRITE(6,*) 'INPUT Y FOR HANNING OR N FOR KAISER-BESSEL'
C      ACCEPT 11, WTP
11      FORMAT(A1)
C      END IF
C      DO 20 I=1,IS-1
20      AM(I)=0.
C      IF(WTP.EQ.'Y') THEN
C      NN=IE-IS+1
C      IW=NN/2
C      IIW=2*IW-1
C      IF(FLOAT(NN)/2..EQ.FLOAT(IW)) THEN
C      DT=PI/FLOAT(IIW)
C      DO 30 I=1,IIW,2
C      WFACT=.5*(1.+COS(DT*I))
C      AM(IW+IS1+I)=AM(IW+IS1+I)*WFACT
30      AM(IW+IS1-I+1)=AM(IW+IS1-I+1)*WFACT
C      ELSE
C      DT=PI/FLOAT(IW)
C      DO 40 I=1,IW
C      WFACT=.5*(1.+COS(DT*I))
C      AM(IW+IS1+I+1)=AM(IW+IS1+I+1)*WFACT
40      AM(IW+IS1-I+1)=AM(IW+IS1-I+1)*WFACT

```

```

END IF
ELSE
IF (ISUP.NE.1) THEN
WRITE(6,*) 'INPUT ALPHA'
ACCEPT *, ALPHA
END IF
PIA=PI*ALPHA
CON=BIO(PIA)
NN=IE-IS+1
IW=NN/2
IIW=2*IW-1
IF (FLOAT(NN)/2..EQ.FLOAT(IW)) THEN
DT=1./FLOAT(IIW)
DO 21 I=1,IIW,2
ARG=PIA*SQRT(1.-(DT*I)**2)
WFACT=BIO(ARG)/CON
AM(IW+IS1+I)=AM(IW+IS1+I)*WFACT
21 AM(IW+IS1-I+1)=AM(IW+IS1-I+1)*WFACT
ELSE
DT=1./FLOAT(IW)
DO 31 I=1,IW
ARG=PIA*SQRT(1.-(DT*I)**2)
WFACT=BIO(ARG)/CON
AM(IW+IS1+I+1)=AM(IW+IS1+I+1)*WFACT
31 AM(IW+IS1-I+1)=AM(IW+IS1-I+1)*WFACT
END IF
END IF
DO 50 I=IE+1,NDIM
50 AM(I)=0.
IF (CE) THEN
S2=0.
S4=0.
DO 60 I=IS,IE
S4=S4+AM(I)
80 S2=S2+AM(I)**2
SC=SQRT(S1/S2)
SC1=S3/S4
WRITE(6,*) 'S1,S2,SC=',S1,S2,SC
WRITE(6,*) 'S3,S4,SC1=',S3,S4,SC1
DO 70 I=IS,IE
70 AM(I)=AM(I)*SC
END IF
RETURN
END

```

```

FUNCTION BIO(X)
XX=X/2.
S=1.
S1=1.
FAC=1.
ACC=.00001
DO 10 I=1,100
FAC=FAC*I
S1=S1*XX
T=S

```



```

      N11=N1+I
      IF(N11.GT.NS) GO TO 51
      ANG=PH(I)*DTR
      AMP=10.**[AM(I)/20.]
40    A(N11)=CMPLX(COS(ANG),SIN(ANG))*AMP
      C    TRAILING ZEROS
      NMN=NS-N1-NDIM
      DO 50 I=1,NMN
50    A(N2+I)=CMPLX(0.,0.)
      C    CONTINUE
      C    CONSTRUCT NEGATIVE FREQ. IMAGE
60    A(NS+1)=A(NS)+CONJG(A(NS))
      DO 70 I=2,NS
      K=NST+2-I
70    A(K)=CONJG(A(I))
      ELSE
      NN=NDIM
      IF(FLOAT(NDIM)/2..EQ.FLOAT(NDIM/2)) NN=NDIM-1
      N2=NN/2
      IF(N2.GT.NS-1) WRITE(6,*)'TOO MANY SAMPLES', N2
      IF(N2.GT.NS-1) N2=NS-1
      W0=2.*PI*(ANST+N2*AINC)/1000.
      ANG=PH(N2+1)
      A(1)=10.**[AM(N2+1)/20.]*CMPLX(COSD(ANG),SIND(ANG))
      DO 72 I=1,N2
      II=N2+I+1
      ANG=PH(II)
72    A(I+1)=10.**[AM(II)/20.]*CMPLX(COSD(ANG),SIND(ANG))
      DO 73 I=N2+2,NS
73    A(I)=CMPLX(0.,0.)
      DO 74 I=1,N2
      II=NST-N2+I
      ANG=PH(I)
74    A(II)=10.**[AM(I)/20.]*CMPLX(COSD(ANG),SIND(ANG))
      DO 75 I=NS+1,NST-N2
75    A(I)=CMPLX(0.,0.)
      END IF
      CALL FORT(A,M,S,1,IERR)
      IF(IERR.NE.0) TYPE *, 'ERROR IN FORT',IERR
      C    DETERMINE TIME AXIS SCALING
      FFMX=AINC
      ANST=-1.E3/FFMX/2.
      FMAX=FMIN
      AINC=1.E8/FFMX/TNS
      NDIM=TNS
      IF(DEMOD.EQ.'Y') THEN
      A(1)=2.*A(1)
      W0=W0*AINC*1.E-5
      DO 76 I=1,NST-1
      II=I+1
      AA=2.*[REAL(A(II))*COS(W0*I)-AIMAG(A(II))*SIN(W0*I)]
76    A(II)=CMPLX(AA,0.)
      END IF
      C    SHIFT 'O TIME' TO CENTER OF PLOT
77    DO 80 I=1,NS

```



```

C      ACCEPT *, INWN
      NDIM=NP+NINT(FMIN*1000.*0.1)
      ANST=0
      AINC=NINT(FINC*1000.)
      INWN=0
      IF(INWN) THEN
        WRITE(6,*) 'INPUT WINDOW TYPE, LP (LOW PASS) OR BP (BAND PASS)'
        ACCEPT 1,WT
1      FORMAT(1A2)
        IF(WT.EQ.LP) THEN
          IW=NDIM
          DT=PI/FLOAT(IW)
          DO 15 I=1,IW
            WFACT=.5*(1.+COS(DT*(I-.5)))
            AM(I)=20.*ALOG10(CABS(A(I+1))/WFACT)
15          PH(I)=ATAN2D(AIMAG(A(I+1)),REAL(A(I+1)))
            ELSE
              NN=INT(ANST/AINC+.1)
              IW=NDIM/2
              IF(NDIM/2..EQ.IW) THEN
                DT=PI/FLOAT(IW)
                DO 30 I=1,IW
                  WFACT=.5*(1.+COS(DT*(I-.5)))
                  AM(IW+I)=20.*ALOG10(CABS(A(NN+IW+I))/WFACT)
                  AM(IW-I+1)=20.*ALOG10(CABS(A(NN+IW-I+1))/WFACT)
                  PH(IW+I)=ATAN2D(AIMAG(A(NN+IW+I)),REAL(A(NN+IW+I)))
30                  PH(IW-I+1)=ATAN2D(AIMAG(A(NN+IW-I+1)),REAL(A(NN+IW-I+1)))
                    ELSE
                      AM(IW+1)=20.*ALOG10(CABS(A(NN+IW+1)))
                      PH(IW+1)=ATAN2D(AIMAG(A(NN+IW+1)),REAL(A(NN+IW+1)))
                      DT=PI/(2.*IW-1)
                      DO 40 I=1,IW
                        WFACT=.5*(1.+COS(2.*DT*I))
                        AM(IW+I+1)=20.*ALOG10(CABS(A(NN+IW+I+1))/WFACT)
                        AM(IW-I+1)=20.*ALOG10(CABS(A(NN+IW-I+1))/WFACT)
                        PH(IW+I+1)=ATAN2D(AIMAG(A(NN+IW+I+1)),REAL(A(NN+IW+I+1)))
40                        PH(IW-I+1)=ATAN2D(AIMAG(A(NN+IW-I+1)),REAL(A(NN+IW-I+1)))
                          END IF
                          ELSE
                            NN=INT(ANST/AINC+.1)
                            DO 50 I=1,NDIM
                              AM(I)=20.*ALOG10(CABS(A(NN+I)))
50                              PH(I)=ATAN2D(AIMAG(A(NN+I)),REAL(A(NN+I)))
                                END IF
C      CALL LAB(INFILE)
      JNDIM=NDIM
      RETURN
      END

```



```

C      Subroutine RPL
C      Part of a group of plotting subroutines called PLOTV.FOR;
C      originally developed by A.Dominek to achieve time domain
C      plots in FTRAN.FOR, modified
C      for use with CAL61.FOR by N.F.Chamberlain, Jan. 1984.
C
      SUBROUTINE RPL(INFILE,AM,SPAG,PAG)
      COMMON /BLK1/BUFF /BLK2/MP,FMIN,FINC /BLK3/IB
      COMMON /BLK4/NDIM,ANST,AINC
      COMMON /BLK7/PLOTOPT2,IP32,LPL,NDIG,XB,XE,XS,TYB,YE,YS
      COMMON /PLT1/YB,DSY,DSX,ND1,ND2,TH(5000),ISYM
      BYTE BUFF(33200)
      REAL*4 AM(5000),AM1(5000)
      INTEGER*2 LINE1(30),LINE2(30),PARA(30),INFILE(15)
      LOGICAL LPL
      EQUIVALENCE ((LINE1(1),BUFF(1)),(LINE2(1),BUFF(61))),
1(PARA(1),BUFF(121))
      DATA LMASK/'88888888'X/
      YB=TYB
C
C      IF(LPL) THEN
C      IF(LPL.EQ.'Y') THEN
      ISYM=ISYM-1
      AINC=AINC*1.E-5
      DO 31 I=ND1,ND1+ND2-1
      AMT=AM(I)
      IF(AMT.LT.YB)AMT=YB
31      AM1(I-ND1+1)=AMT
      CALL STRYP(AM1,-YB,DSY,TH,0.,DSX,ND2,1.,ISYM)
      IF(PLOTOPT2.NE.'Y') THEN
      TYPE *,' '
      WRITE(6,*) 'INPUT Y OR N FOR ANOTHER CURVE ON SAME PLOT'
      ACCEPT 32, LPL
      END IF
32      FORMAT(A1)
      IF(LPL.EQ.'N') THEN
      CALL PLOT(0.,0.,999)
      CALL PLOTNOW(IMS)
C      CALL LIB$SPAWN('VPLOT')
      END IF
      ELSE
      ISYM=-1
      AINC=AINC*1.E-5
C
      CALL VPLOTS(0,0,IDUM)
      CALL PLOT(7.,1.75,-3)
      XL=8.
      ANEN=ANST+AINC*(NDIM+1)
      TYPE *,' '
      TYPE *, 'INI. TIME=',ANST,'FIN. TIME=',ANEN,'DEL TIME=',AINC
      IF(PLOTOPT2.NE.'Y') THEN
      TYPE *,' '
      TYPE *, 'INPUT BEGINNING/END TIME AND STEP TIME SIZE'
      ACCEPT *,XB,XE,XS
      END IF

```

```

ND2=INT((XE-XB)/AINC)+1
TH(1)=XB
AMAX=-1000.
AMIN=1000.
AINC=ABS(AINC)
DO 20 I=1,NDIM
IF(AM(I).LT.AMIN) AMIN=AM(I)
20 IF(AM(I).GT.AMAX) AMAX=AM(I)
DO 21 I=1,ND2
21 TH(I)=TH(I-1)+AINC
ND1=INT((XB-ANST)/AINC)+1
TYPE *,' '
TYPE 25,AMIN,AMAX
25 FORMAT(' Minimum is',F17.3,/, ' Maximum is',F17.3)
YL=6.
IF(PLOTOPT2.NE.'Y') THEN
TYPE *,' '
TYPE *,' INPUT BEGINNING/END MAGNITUDE AND STEP MAGNITUDE SIZE'
ACCEPT *,YB,YE,YS
END IF
IF(PLOTOPT2.NE.'Y') THEN
TYPE *,' '
TYPE *,' INPUT THE NUMBER OF DIGITS TO THE RIGHT OF .XXX'
ACCEPT *,NDIG
END IF
DO 30 I=ND1,ND1+ND2-1
AMT=AM(I)
IF(AMT.LT.YB) AMT=YB
30 AM1(I-ND1+1)=-AMT
XD=XE-XB
SMNX=XB
DSX=XD/XL
DXL=XL/XD
SPX=XS*DXL
IPX=ABS(XD/XS+0.5)
CALL FFAXIS(0.,0.,16HTIME IN NANOSECS,-16,XL,90.,SMNX,DSX,
1SPX,NDIG,1.,0)
YD=YE-YB
SMNY=YB
DSY=YD/YL
DYL=YL/YD
SPY=YS*DYL
IPY=ABS(YD/YS+0.5)
CALL FFAXIS(0.,0.,16HIMPULSE RESPONSE,16,YL,180.,SMNY,DSY,
1SPY,-1,1.,0)
YLG=-IPY*SPY
IP33=2*IP32
CALL STRYP(AM1,-YB,DSY,TH,0.,DSX,ND2,1.,ISYM)
C CALL GRID(YLG,0.,IPY,SPY,IPX,SPX,LMASK)
CALL SYMBOL(-6.6,0.,.10,6HFILE :,90.,6)
CALL SYMBOL(-6.6,.7,.10,%REF(INFILE),90.,IP33)
CALL SYMBOL(-6.4,0.,.10,%REF(LINE1),90.,60)
CALL SYMBOL(-6.2,0.,.10,%REF(LINE2),90.,60)
IF(PLOTOPT2.NE.'Y') THEN
TYPE *,' '

```

```

WRITE(6,*) 'INPUT Y OR N FOR ANOTHER CURVE ON SAME PLOT'
ACCEPT 32, LPL
END IF
IF(LPL.EQ.'N') THEN
CALL PLOT(0.,0.,999)
CALL PLOTNOW(IMS)
C CALL LIB$SPAWN('VPLLOT')
END IF
END IF
AINC=AINC*1.E5
C
IF(PAG.EQ.'Y') THEN
TYPE *, ' '
TYPE 1985
1985 FORMAT(1X,'Y OR N FOR PLOT AGAIN ',*)
ACCEPT 1986,SPAG
1986 FORMAT(A1)
END IF
C
RETURN
END
C
CCCCCCCCCCCCCCCCCCCCCCCCCCCCCCCCCCCCCCCCCCCCCCCCCCCCCCCCCCCCCCCC
C
C Subroutine APP, part of the plotting package PLOTV.FOR.
C Developed by A.Dominek to achieve amplitude and phase plots in the
C frequency domain in FTRAN.FOR, modified by N.F.Chamberlain Jan. 1984
C for use with CAL61.FOR
C
SUBROUTINE APP(INFILE,RS,SPAG,PAG)
C
COMMON /BLK1/BUFF /BLK2/NP,FMIN,FINC /BLK3/IB
COMMON /BLK4/NDIM,ANST,AINC
COMMON /BLK6/PLOPT1,IP31,LPL,NDIG,XB,XE,XS,YB,YE,YS
BYTE BUFF(33200)
DIMENSION AM(5000),PH(5000),AM1(2050)
COMPLEX*8 RS(5000)
INTEGER*2 LINE1(30),LINE2(30),PARA(30),INFILE(15)
COMMON/PLT2/XBB,DSX,YBP,YBA,DSYP,DSYA,YEA,TH(2050),ISYM
EQUIVALENCE (LINE1(1),BUFF(1)),(LINE2(1),BUFF(61)),
1(PARA(1),BUFF(121))
LOGICAL LPLLOT
DATA LMASK/'88888888'X/
C
DO 9015 I=1,NP
AM(I)=20.*ALOG10(CABS(RS(I)))
PH(I)=ATAN2D(AIMAG(RS(I)),REAL(RS(I)))
CONTINUE
IF(LPL.EQ.'Y') THEN
ISYM=ISYM-1
XB1=2.*XBB-ANST
XB1=XB1/1000.
TH(1)=XBB/1000.
AINC=AINC/1000.
DO 5 I=2,NDIM

```

```

5      TH(I)=TH(I-1)+AINCC
      DO 10 I=1,NDIM
      AMT=AM(I)
      IF(AMT.GT.YEA) AMT=YEA
      IF(AMT.LT.YBA) AMT=YBA
10     AM1(I)=AMT
      CALL PLOT(-.55,-.75,-3)
      CALL PLOT(.55,5.55,-3)
      CALL STRYP(TH,XB1,DSX,PH,YBP,DSYP,NDIM,1.,ISYM)
      CALL PLOT(0.,-4.8,-3)
      CALL STRYP(TH,XB1,DSX,AM1,YBA,DSYA,NDIM,1.,ISYM)
      IF(PLOTOPT1.NE.'Y') THEN
      TYPE *,' '
      WRITE(6,*) 'INPUT Y OR N FOR ANOTHER CURVE ON SAME PLOT'
      ACCEPT 32, LPL
      END IF
32     FORMAT(A1)
      IF(LPL.EQ.'N') THEN
      CALL PLOT(0.,0.,888)
      CALL PLOTNOW(IMS)
C      CALL LIB$SPAWN('VPLLOT')
      END IF
      ELSE
      CALL VPLOTS(0,0,IDUM)
      CALL PLOT(.55,5.55,-3)
      ISYM=-1
C      DO PHASE PLOT FIRST
C      CALCULATE THE X AXIS INFORMATION
      XL=6.
      XB2=ANST
      XE2=XB2+AINC*(NDIM-1)
      IF(XB2.GT.XE2) THEN
      XX=XB2
      XB2=XE2
      XE2=XX
      END IF
      XB1=XB2
      TYPE *,' '
      TYPE *,'THE INITIAL AND FINAL FREQUENCIES ARE', XB2/1000.,XE2/1000.
      IF(PLOTOPT1.NE.'Y') THEN
      TYPE *,' '
      TYPE *,'INPUT THE INITIAL, FINAL AND STEP SIZE FREQUENCIES IN GHZ'
      ACCEPT *, XB,XE,XS
      END IF
      XB3=XB*1000.
      XE3=XE*1000.
      XS3=XS*1000.
      XBB=XB3
      XB1=2.*XB3-XB1
      XB1=XB1/1000.
C      TYPE *,'INPUT STEP FREQUENCY SIZE'
C      ACCEPT *,XS3
      TH(1)=XB3/1000.
C      PMAX=PH(1)
C      PMIN=PH(1)

```

```

      AMAX=AM(1)
      AMIN=AM(1)
      AINCC=AINC/1000.
      DO 20 I=2,NDIM
      TH(I)=TH(I-1)+AINCC
C      IF(PH(I).LT.PMIN) PMIN=PH(I)
C      IF(PH(I).GT.PMAX) PMAX=PH(I)
      IF(AM(I).LT.AMIN) AMIN=AM(I)
20      IF(AM(I).GT.AMAX) AMAX=AM(I)
      XD=XE3-XB3
      SMNX=XB3/1000.
      DSX=XD/XL/1000.
      DXL=XL/XD
      SPX=XS3*DXL
      IPX=ABS(XD/XS3+0.5)
      CALL FFAXIS(0.,0.,16HFREQUENCY IN GHZ,-16,XL,0.,SMNX,DSX,
1SPX,2,1.,0)
C      CALCULATE THE Y AXIS INFORMATION
      YL=4.
C      TYPE *, 'THE MINIMUM AND MAXIMUM PHASE VARIATION IS',PMIN,PMAX
C      TYPE *, 'INPUT BEGINNING/END PHASE AND STEP MAGNITUDE SIZE'
C      ACCEPT *,YB,YE,YS
      YB2=-180.
      YE2=180.
      YS2=80.
      YD=YE2-YB2
      SMNY=YB2
      DSY=YD/YL
      DYL=YL/YD
      SPY=YS2*DYL
      IPY=ABS(YD/YS2+0.5)
      CALL FFAXIS(0.,0.,16HFASE IN DEGREES,16,YL,80.,SMNY,DSY,
1SPY,-1,1.,0)
      YLG=-IPY*SPY
C      PLOT THE CURVE,GRID AND IDENTIFICATION INFORMATION
      YBP=YB2
      DSY=DSY
      IP33=2*IP31
      CALL STRYP(TH,XB1,DSX,PH,YBP,DSYP,NDIM,1.,ISYM)
      CALL GRID(0.,0.,IPX,SPX,IPY,SPY,LMASK)
      CALL SYMBOL(.5,4.7,.10,6HFILE :,0.,6)
      CALL SYMBOL(1.2,4.7,.10,%REF(INFILE),0.,IP33)
      CALL SYMBOL(.5,4.8,.10,%REF(LINE1),0.,60)
      CALL SYMBOL(.5,4.3,.10,%REF(LINE2),0.,60)
      CALL SYMBOL(.5,4.1,.10,%REF(PARA),0.,60)
      CALL PLOT(0.,-4.8,-3)
C      PLOT THE MAGNITUDE NOW
      CALL FFAXIS(0.,0.,16HFREQUENCY IN GHZ,-16,XL,0.,SMNX,DSX,
1SPX,2,1.,0)
      TYPE *,' '
      TYPE 25,AMIN,AMAX
25      FORMAT(' Minimum is',F10.3,' DB',/, ' Maximum is',F10.3,' DB')
      IF(PLOTOPT1.NE.'Y') THEN
      TYPE *,' '
      TYPE *, 'INPUT BEGINNING/END MAGNITUDE AND STEP MAGNITUDE SIZE'

```

```

ACCEPT *,YB,YE,YB
END IF
IF(PLOTOPT1.NE.'Y') THEN
TYPE *,' '
TYPE *,'INPUT THE NUMBER OF DIGITS TO THE RIGHT OF .XXX'
ACCEPT *,NDIG
END IF
DO 30 I=1,NDIM
AMT=AM(I)
IF(AMT.GT.YE) AMT=YE
IF(AMT.LT.YB) AMT=YB
30 AM1(I)=AMT
YD=YE-YB
SMNY=YB
DSY=YD/YL
DYL=YL/YD
SPY=YS*DYL
IPY=ABS(YD/YS+0.5)
CALL FFAXIS(0.,0.,15,MAGNITUDE IN DB,15,YL,90.,SMNY,DSY,
1SPY,NDIG,1.,0)
YLG=-IPY*SPY
YEA=YE
YBA=YB
DSYA=DSY
CALL STRYP(TH,XB1,DSX,AM1,YBA,DSYA,NDIM,1.,ISYM)
CALL GRID(0.,0.,IPX,SPX,IPY,SPY,LMASK)
C TYPE *,'IS THIS THE LAST PLOT, T TO F'
C ACCEPT *,LPL
C IF(LPL) THEN
C CALL PLOT(0.,0.,999)
C CALL PLOTNOW(IMS)
C ELSE
C CALL PLOT(0.,0.,-999)
C END IF
C IF(PLOTOPT1.NE.'Y') THEN
C TYPE *,' '
C WRITE(6,*) 'INPUT Y OR N FOR ANOTHER CURVE ON SAME PLOT'
C ACCEPT 32,LPL
C END IF
C IF(LPL.EQ.'N') THEN
C CALL PLOT(0.,0.,+999)
C CALL PLOTNOW(IMS)
C CALL LIB$SPAWN('VPLLOT')
C END IF
C END IF
C IF(PAG.EQ.'Y') THEN
C TYPE *,' '
C TYPE 1987
1987 FORMAT(1X,'Y OR N FOR PLOT AGAIN ',*)
ACCEPT 1988,SPAG
1988 FORMAT(A1)
END IF
C RETURN
END

```

```

C
C      PROGRAM NAME : CATLOG.FOR
C      Modified from B3.FOR (by J.Chen) during 1984 by Neil Chamberlain.
C      Program now automatically fully scales a directory
C      of calibrated data files, in conjunction with FILESORT.COM.
C
C      THIS PROGRAM MAKES USE OF 2-18 GHZ CALIBRATED DATA
C      AND GENERATES A FULL-SCALE DATA FILE.
C
C      REAL*4 FA(1801),A218(1801),P218(1801)
C      INTEGER*2 LINE2(24)
C      COMPLEX*8 TA(1801),CA(1801),R(1801)
C      CHARACTER  INFILE*31,DIR_FILE*11,ID*48,T_POL*2,F_INC*4
C      CHARACTER  ELEV*2,S_FAC*4,W_D*3,ORIG*7,RFILE*10,T_SHIP*2,T_ASP*2
C
C      COMMON BUFF,NDIM,ANST,AINC
C      COMMON /BLK2/ T_SHIP,T_ASP
C
C      TYPE *,' '
C      TYPE *,'Input routine ..'
C
C      TYPE *,' '
C      TYPE *,'Input polarization type (FV,FH,FX)'
C      ACCEPT 7,T_POL
C      FORMAT(2A)
C
C      TYPE *,' '
C      TYPE *,'Input target elevation (15,27 deg)'
C      ACCEPT 7,ELEV
C
C      TYPE *,' '
C      TYPE *,'Input frequency increment Mhz'
C      ACCEPT *,FINC
C
C      TYPE *,' '
C      TYPE *,'Input frequency increment again'
C      ACCEPT 8,F_INC
C      FORMAT(A4)
C      TYPE *,' '
C      TYPE *,'Input a 7 char. description of source data'
C      ACCEPT 10,ORIG
C      FORMAT(A7)
C
C      TYPE *,' '
C      TYPE *,'Input directory file name'
C      ACCEPT 5,DIR_FILE
C      FORMAT(A11)
C      PRINT 1771,'Directory file name ',DIR_FILE
C      PRINT 1772
C      FORMAT('0')
C      PRINT 1771
C      FORMAT(1X,A22,A11)
C
C      TYPE *,' '

```

```

      TYPE *, 'Input number of files in directory'
      ACCEPT *, NLEN

C
      End of input routine
C
      Open directory file so that file headers may be read
C
      OPEN (UNIT=2, NAME = DIR_FILE ,READONLY,TYPE='OLD', ERR=999)
C
      DO 1111, I_MAIN=1,NLEN
      IF(I_MAIN.EQ.1) THEN
        TYPE *, ' '
        TYPE 15
15      FORMAT(1X, 'Starting scaling procedure')
        END IF
        READ(2,12) INFILE
12      FORMAT(A31)
        INFILE=INFILE(20:29)
        TYPE*, ' '
        TYPE 13, 'File', I_MAIN, ' ', INFILE
13      FORMAT(1X, A4, I3, A4, A10)
C
        CALL REA(INFILE, A218, P218)
C
        Convert data from dB and deg to nepers and radians.
        Note that data is taken and stored in the former format.
        Chen stores his data in dB and rad and this format is necessary
        for use in DBPLT, the full scale plotting routine.
C
        PI=4.*ATAN(1.)
        DTR=PI/180.
        DO 929 I=1,1601
        A218(I)=10.*(A218(I)/20.)
        P218(I)=P218(I)*DTR
929      CONTINUE
C
        IF(T_SHIP.EQ.'MD'.OR.T_SHIP.EQ.'LB') THEN
          SF=2400.
          WD=0.25
          S_FAC(1:4)='2400'
          W_D(1:3)='1/4'
          ELSE
            SF=1200.
            WD=0.5
            S_FAC(1:4)='1200'
            W_D(1:3)='1/2'
          END IF
C
        Compile a file name for the scaled target
C
        RFILE(1:2)=T_SHIP(1:2)
        RFILE(3:4)=T_POL(1:2)
        RFILE(5:6)=T_ASP(1:2)
        RFILE(7:8)=ELEV(1:2)
C

```



```

C      Compile a header to describe the scaled target
C
      ID(1:8) =RFILE(1:8)
      ID(9:9) = ' '
      ID(10:11)=T_ASP(1:2)
      ID(12:12)= ' '
      ID(13:15)='DES'
      ID(16:16)= ' '
      ID(17:19)='SF='
      ID(20:23)=S_FAC(1:4)
      ID(24:24)= ' '
      ID(25:29)='FINC='
      ID(30:33)=F_INC(1:4)
      ID(34:34)= ' '
      ID(35:37)='WD='
      ID(38:40)=W_D(1:3)
      ID(41:41)= ' '
      ID(42:48)=ORIG(1:7)
C
      TYPE *, ' '
      TYPE 33,ID
      PRINT 33,ID
33      FORMAT(1X,48A)
      PRINT *, ' '
C
      Calculate full scale frequencies
      according to scale factor
C
      DO 46 II=1,1601
      FA(II)=(2.+(II-1)/100.)/SF*1000.
46      CONTINUE
C
      CREATE A FULL-SCALE COMPLEX TARGET
      RETURN ACCORDING TO THE SCALE FACTOR
C
      DO 3540 IJ=1,1601
3540      CA(IJ)=CMPLX(SF*A218(IJ)*COS(P218(IJ)),SF*A218(IJ)*SIN(P218(IJ)))
C
      STORE THE INPUT-FILE NAMES IN A BUFFER
C
      DO 997 IK=1,24
997      LINE2(IK)= ' '
C
      SMOOTH THE FULL-SCALE DATA FILE BY CONVOLVING
      THE FILE WITH A HAMMING WINDOW
C
      CALCULATE PARAMETERS FOR THE CONVOLUTIONS, WHERE,
      FLOW IS THE LOWEST FULL-SCALE FREQUENCY
      FHIGH IS THE HIGHEST FULL-SCALE FREQUENCY
      FINC IS THE FULL-SCALE FREQUENCY INCREMENT
C
      FLOW=2./SF*1000.
      FHIGH=18./SF*1000.
      FLOW=INT(FLOW*10.)/10.+1
      FHIGH=INT(FHIGH*10.)/10.

```

```

I=1
K=0
ICNT=1601

C
TYPE *, ' '
TYPE *, 'FA(1)   =', FA(1), '   FA(ICNT)=', FA(ICNT)
TYPE *, 'FLOW    =', FLOW, '   FHIGH  =', FHIGH
TYPE *, 'ICNT    =', ICNT, '   NPT     =', NPT
TYPE *, 'SF      =', SF

C
C      PICK UP THE DESIRED FREQUENCY AND POSITION THE
C      CENTER OF THE HAMMING WINDOW AT THAT FREQUENCY.
C      ESTIMATE THE DATA VALUE OF THE DESIRED FREQUENCY BY
C      TAKING THE WEIGHTED AVERAGE OF THE NEIGHBORING DATA POINTS
C      COVERED BY THE HAMMING WINDOW, WITH THE WEIGHTINGS DETERMINED
C      THE HAMMING WINDOW.
C
DO 7720 RF=FLOW,FHIGH,FINC
7740 IF(RF.GE.FA(I).AND.RF.LE.FA(I+1))GO TO 7730
I=I+1
IF(I.GT.ICNT)GO TO 4812
GO TO 7740
7730 K=K+1
CALL INTER(R,CA,FA,ICNT,NS,I,K,WD,RF)
7720 CONTINUE
C
C      OUTPUT THE SMOOTHED FULL-SCALE DATA FILES
C
4812 CALL PDATA(RFILE,R,K,FLOW,FINC,SF,ID,LINE2)
C
TYPE *, 'NPT      =', K

1111 CONTINUE
CLOSE(UNIT=2,DISP='SAVE',ERR=1001)
GOTO 9090
689 TYPE *, 'Open error - file not found'
GOTO 11
1001 TYPE *, 'Close error'
STOP
9090 END

C
C      ||||||||||||||||||||||||||||||||||||||||||||||||||||||||||||
C
SUBROUTINE PDATA(RFILE,CA,NPT,FLOW,FINC,SF,ID,LINE2)
C
C      THIS SUBROUTINE WRITES A FILE ON A STORAGE UNIT
C
INTEGER*2 LINE2(24)
CHARACTER ID*48,RFILE*10
REAL*4 AM(801),PH(801)
COMPLEX*8 CA(801)
C
10 DO 210 I=1,NPT
IF(CABS(CA(I)).EQ.0.)CA(I)=(1.E-15,1.E-15)

```



```

30      PI=TWOP/2.
      IF(DPH.LT.PI)GO TO 20
      DPH=DPH-TWOP
      GO TO 30
20      IF(DPH.GT.-PI)GO TO 40
      DPH=DPH+TWOP
      GO TO 20
40      FBASE=FA(IBASE)
      DO 10 I=1,201
10      PH(I)=PH(I)-(DPH*FA(I)/FBASE)
      RETURN
      END

C
C      ||||||||||||||||||||||||||||||||||||||||||||||||||||||||||||
C
C      THIS SUBROUTINE ESTIMATES THE VALUES OF
C      PHASE RETURNS AT THE ENDS OF A DATA FILE,
C      USING A LINEAR INTERPOLATION
C
      SUBROUTINE EPH(PHM,PH,NS,NF,NI)
      REAL*4 PH(201)
      X=0
      Y=0
      XY=0
      X2=0
      DO 10 I=NS,NF,NI
      X=X+FLOAT(I)
      Y=Y+PH(I)
      XY=XY+FLOAT(I)*PH(I)
10      X2=X2+FLOAT(I)*FLOAT(I)
      XN=(NF-NS)*NI+1
      DELTA=XN*X2-X*X
      A=(XN*XY-X*Y)/DELTA
      B=(X2*Y-X*XY)/DELTA
      PHM=A*NS+B
      RETURN
      END

C
C      ||||||||||||||||||||||||||||||||||||||||||||||||||||||||||||
C
C      THIS SUBROUTINE READS A FILE AND EXTRACTS ASPECT AND SHIP-TYPE
C      INFORMATION FROM THE HEADER
C
      SUBROUTINE REA(INFILE,AM,PH)
      COMMON BUFF,NDIM,ANST,AINC
      COMMON /BLK2/ T_SHIP,T_ASP

C
      BYTE BUFF(33200)
      INTEGER*2 LINE2(30),PARAM(30)
      REAL*4 AP(4000),AM(1601),PH(1601)
      CHARACTER *2 T_SHIP,T_ASP,SHIP(6),ASP(14)
      CHARACTER *1 NUM(10),LINE1(60), INFILE*10,CFILE*60

C
      DATA SHIP/'AD','LR','LB','KH','KX','MD'/
      DATA ASP/'00','10','15','20','30','40','45','50','60','80','80'

```

```

1,'E2','17','18'/
DATA NUM/'0','1','2','3','4','5','6','7','8','9'/
C
C      DEFINE BUFFER STRUCTURE
C
EQUIVALENCE(LINE1(1),BUFF(1)),(LINE2(1),BUFF(61))
1,(PARAM(1),BUFF(121)),(AP(1),BUFF(361))
C
C      READ A FILE
C
CALL TR(INFILE)
C
C      Here begins the name and aspect extractor
C
DO 2222 I=1,60
CFILE(I:I)=LINE1(I)
2222 CONTINUE
K=0
DO 8888 I=7,30
C
IF (K.NE.0) GOTO 5577
DO 8888 J=1,10
IF (CFILE(I:I).EQ.NUM(J)) THEN
K=I
GOTO 8888
END IF
8888 CONTINUE
C
IF(K.EQ.0) GOTO 8888
DO 7788 L=1,10
IF(CFILE(I:I).EQ.NUM(L)) THEN
GOTO 8888
END IF
C
7788 CONTINUE
IF(L.EQ.11) THEN
L_STOP=I-1
GOTO 9866
END IF
8888 CONTINUE
9866 DO 6699 IC=7,20
IF(CFILE(IC:IC+2).EQ.'DES') THEN
N_FIND=IC+3
GOTO 7755
END IF
6699 CONTINUE
C
7755 DO 4444 I=N_FIND,N_FIND+8
IF(CFILE(I:I).EQ.'A') THEN
ISHIP=1
GOTO 3333
END IF
IF(CFILE(I:I).EQ.'M') THEN
ISHIP=6
GOTO 3333

```

```

      END IF
      IF(CFILE(I:I+1).EQ.'LR') THEN
        ISHIP=2
        GOTO 3333
      END IF
      IF(CFILE(I:I+1).EQ.'LB') THEN
        ISHIP=3
        GOTO 3333
      END IF
      IF(CFILE(I:I+1).EQ.'KH') THEN
        ISHIP=4
        GOTO 3333
      END IF
      IF(CFILE(I:I+1).EQ.'KX') THEN
        ISHIP=5
        GOTO 3333
      END IF
4444  CONTINUE
C
3333  IF(CFILE(K:L_STOP).EQ.'0') IASP=1
      IF(CFILE(K:L_STOP).EQ.'10') IASP=2
      IF(CFILE(K:L_STOP).EQ.'15') IASP=3
      IF(CFILE(K:L_STOP).EQ.'20') IASP=4
      IF(CFILE(K:L_STOP).EQ.'30') IASP=5
      IF(CFILE(K:L_STOP).EQ.'40') IASP=6
      IF(CFILE(K:L_STOP).EQ.'45') IASP=7
      IF(CFILE(K:L_STOP).EQ.'50') IASP=8
      IF(CFILE(K:L_STOP).EQ.'60') IASP=8
      IF(CFILE(K:L_STOP).EQ.'80') IASP=10
      IF(CFILE(K:L_STOP).EQ.'90') IASP=11
      IF(CFILE(K:L_STOP).EQ.'100') IASP=12
      IF(CFILE(K:L_STOP).EQ.'170') IASP=13
      IF(CFILE(K:L_STOP).EQ.'180') IASP=14
C
      TYPE *, ' '
      TYPE *, 'Information from source file'
C
      TYPE 105,CFILE,ASP(IASP),' DEG ',SHIP(ISHIP)
      PRINT 105,CFILE,ASP(IASP),' DEG ',SHIP(ISHIP)
      TYPE 106,LINE2
C      TYPE 106,PARAM
105    FORMAT(X,A60,A2,A5,A2)
106    FORMAT(X,30A2)
C
      T_SHIP(1:2)=SHIP(ISHIP)(1:2)
      T_ASP(1:2) =ASP(IASP)(1:2)
C
C      GET NUMERICAL INFORMATION FROM THE THIRD LINE
C      OF THE HEADER
C
      CALL DCDE(NDIM,ANST,AINC)
C
C      DIVIDE AN AMP-PHASE ARRAY INTO
C      AN AMP ARRAY AND A PHASE ARRAY
C

```

```

DO 188 NN=1,NDIM
AM(NN)=AP(2*NN-1)
IF(AM(NN).GT.40)AM(NN)=40.
188 PH(NN)=AP(2*NN)
C
C CHECK FOR BAD DATA POINTS, I.E., AM(I).GT.995
C
CALL ERRF(AM,PH,NDIM)
RETURN
END
C
C
C
C
C SUBROUTINE TR(INFILE)
COMMON BUFF,NDIM,ANST,AINC
C INTEGER*2 INFILE(15)
CHARACTER *10 INFILE
DIMENSION AM(1601),PH(1601)
BYTE BUFF(33200),TBUF(512)
INCLUDE 'SYS$LIBRARY:FORIO$DEF'
IB=1
ICNT=0
8106 OPEN(UNIT=8,NAME=INFILE,READONLY,TYPE='OLD',IOSTAT=IERR,ERR=8100)
C
C SET BLOCK LENGTH IN BYTES
C
82 IF(IB.EQ.1)LEN=512-8*4
IF(IB.GT.1)LEN=512-26*4
C
C READ A BLOCK OF 512 BYTES
C
READ(8,80,END=80) TBUF
80 FORMAT(512A1)
C
C STORE A BLOCK INTO THE BUFFER ACCORDING TO ITS LENGTH
C
DO 86 I=1,LEN
85 BUFF(ICNT+I)=TBUF(I)
IB=IB+1
ICNT=ICNT+ LEN
GO TO 82
80 DO 86 I=1,LEN
85 BUFF(ICNT+I)=TBUF(I)
C
C ELIMINATE BLANK SPACES IN BETWEEN EACH CHARACTER
C IN A FILE HEADER
C
DO 40 I=1,180
40 BUFF(I)=BUFF(2*I-1)
GO TO 331
8100 IF(IERR.EQ.FOR$IOS_FILNOTFOU)THEN
TYPE 1112,INFILE
1112 FORMAT(' FILE : ',A10,' WAS NOT FOUND',/,/, ' ENTER FILENAME AGAIN')
ELSE IF (IERR.EQ.FOR$IOS_FILNAMSPE)THEN
TYPE 1113,INFILE

```

```

1113  FORMAT(' FILE : ',A10,' WAS BAD, ENTER NEW FILENAME')
      ELSE
      TYPE *, 'UNRECOVERABLE ERROR, CODE=', IERR
      STOP
      ENDIF
      ACCEPT 1114, INFILE
1114  FORMAT(A10)
      GO TO 8106
331   CLOSE(UNIT=8, DISP='SAVE')
      RETURN
      END

C
C   ::::::::::::::::::::::::::::::::::::::::::::::::::::::::::::::::::::
C
      SUBROUTINE DCDE
      COMMON BUFF, NDIM, ANST, AINC
      DIMENSION AM(1601), PH(1601)
      BYTE BUFF(33200)
      INTEGER*4 IMIN, IINC, NDIM

C
C   NO OF DATA POINTS IS STORED IN FOUR CHARACTERS, AND
C   STARTING ANGLE AND ANGLE INC. IN 5 CHARACTERS
C
      CHARACTER*3 CNL1
      CHARACTER*4 CNL
      CHARACTER*5 CFF, CINC
      CHARACTER*1 ECH, TCAS
      DATA ECH, ZERO/' ', '0' /
      EQUIVALENCE (BUFF(123), CNL), (BUFF(131), CFF), (BUFF(140), CINC)
      EQUIVALENCE (BUFF(123), TCAS), (BUFF(124), CNL1)

C
C
C   CONVERT CHARACTERS INTO THEIR NUMERICAL EQUIVALENTS
C
      IF(ECH.EQ.TCAS) THEN
      DECODE(3,102,CNL1)NDIM
      ELSE
      DECODE(4,101,CNL)NDIM
      END IF
100   FORMAT(I5)
101   FORMAT(I4)
102   FORMAT(I3)
      DECODE(5,100,CFF)IMIN
      DECODE(5,100,CINC)IINC
      ANST=FLOAT(IMIN)
      AINC=FLOAT(IINC)
      RETURN
      END

C
C   ::::::::::::::::::::::::::::::::::::::::::::::::::::::::::::::::::::
C
      SUBROUTINE ERRF(AM, PH, NDIM)
      DIMENSION AM(1601), PH(1601)
      COMPLEX C1, C2, CD
      DO 1 I=1, NDIM

```



```

      IF(PH(I).GT.995.) WRITE(6,2) I,AM(I),PH(I)
1      CONTINUE
2      FORMAT(1X,16HERROR AT DATA PT,1I4,4HMAG=,1F10.4,4HPH=,1F10.4)
C      CHECK LEFT HAND END POINT
      IF(AM(1).GT.100.) THEN
        DO 200 I=2,NDIM
          IF(AM(I).LE.100. .AND. AM(I+1).LE.100.) THEN
            A1=10.**AM(I)/20.)
            C1=CMPLX(A1*COSD(PH(I)),A1*SIND(PH(I)))
            A2=10.**AM(I+1)/20.)
            C2=CMPLX(A2*COSD(PH(I+1)),A2*SIND(PH(I+1)))
            CD=C1-C2
            RD=REAL(CD)
            AD=AIMAG(CD)
            DO 212 II=1,I-1
              RC=REAL(C1)+RD*II
              AC=AIMAG(C1)+AD*II
              AM(II)=20.*LOG10(SQRT(RC*RC+AC*AC))
              PH(II)=ATAN2D(AC,RC)
212          CONTINUE
              GO TO 211
            ELSE
              END IF
          200      CONTINUE
          ELSE
            END IF
        C      CHECK RIGHT HAND END POINT
        211      IF(AM(NDIM).GT.100.) THEN
          DO 220 I=1,NDIM
            J=NDIM-I
            IF(AM(J).LE.100. .AND. AM(J-1).LE.100.) THEN
              A1=10.**AM(J)/20.)
              C1=CMPLX(A1*COSD(PH(J)),A1*SIND(PH(J)))
              A2=10.**AM(J-1)/20.)
              C2=CMPLX(A2*COSD(PH(J-1)),A2*SIND(PH(J-1)))
              CD=C1-C2
              RD=REAL(CD)
              AD=AIMAG(CD)
              DO 222 II=J+1,NDIM
                RC=REAL(C1)+RD*(II-J)
                AC=AIMAG(C1)+AD*(II-J)
                AM(II)=20.*LOG10(SQRT(RC*RC+AC*AC))
                PH(II)=ATAN2D(AC,RC)
222          CONTINUE
              GO TO 221
            ELSE
              END IF
          220      CONTINUE
          ELSE
            END IF
        C      CHECK INTERIOR POINTS
        221      DO 230 I=2,NDIM-1
          IF(AM(I).GT.100.) THEN
            DO 240 K=I+1,NDIM
              IF(AM(K).LE.100.) THEN

```

```

A1=10.**(AM(I-1)/20.)
C1=CMPLX(A1*COSD(PH(I-1)),A1*SIND(PH(I-1)))
A2=10.**(AM(K)/20.)
C2=CMPLX(A2*COSD(PH(K)),A2*SIND(PH(K)))
CD=(C1-C2)/(K-I+1)
RD=REAL(CD)
AD=AIMAG(CD)
DO 241 II=I,K-1
RC=REAL(C1)+RD*(II-I+1)
AC=AIMAG(C1)+AD*(II-I+1)
AM(II)=20.*LOG10(SQRT(RC*RC+AC*AC))
PH(II)=ATAN2D(AC,RC)
241 CONTINUE
GO TO 230
ELSE
END IF
240 CONTINUE
ELSE
END IF
230 CONTINUE

RETURN
END
C THIS IS THE END
C
C ||||||||||||||||||||||||||||||||||||||||||||||||||||||||||||||||

```

```

C      Program name  TAFCAL.FOR
C
C      Time And Frequency Classification ALgorithm (TAFCAL)
C
C      Originally developed by J.Chen
C      in two parts as FREQ.FOR and TIME.FOR
C      Modified by N.Chamberlain May 1984 to incorporate
C      classification at various polarizations,elevations and an
C      extended range of aspects.(with the capability of intro-
C      ducing known errors in aspect or elevation)
C
C      COMPLEX      C(110,30),NC(110,30),FFFT(32)
C      REAL          D(110,110),A(110,30),P(110,30),W(110,30)
C      REAL          AN(110,30),PN(110,30),WN(110,30)
C      REAL          WL(30),PX(30),PY(10,30),PYT(30),SAP(110)
C      REAL          SP(110),SNP(110),Y_PLOT(10,50),SFFT(8)
C      INTEGER       IPOL(5),IELEV(3),SNR,SNR_MAX,SNR_MIN
C      CHARACTER     POL(5)*1,ELE*5,TLINE*5,T_CHAR*4,TCON_EA(10)*1,TCON_EL(10)*1
C      CHARACTER     LINE(11)*70,PAR_CH*2,PAR(10)*2,AYN(10)*1,YN*1
C      CHARACTER     CON_ERA*1,CON_ERE*1
C
C      COMMON        /BLK1/ IPOL,IELEV,NS,C,A,P,IRA,IO,IGRAPH
C      COMMON        /BLK2/ SFFT,FFFT
C
C      Initialise header variables with blanks, so they can be searched
C
C      11111 DO I=1,11
C            DO J=1,70
C              LINE(I)(J:J)=' '
C            END DO
C          END DO
C
C      IGRAPH=1          ! Index for counting graphs
C      IER_AS=0          ! Initialize error in aspect index
C      IBIG_LOOP=1       ! This index enables the total number or runs,
C                        ! frequency and/or time to counted for plotting
C
C      Start input routine  ||||||||||||||||||| START INPUTS
C
C      TYPE          *, ' ***** Default to target directory *****'
C      TYPE          *, ' Do frequency before time if doing both '
C      TYPE          *, ' '
C      TYPE          *, ' Print classification distances ? Y or N'
C      ACCEPT        3,DIS
C      3 FORMAT      (A1)
C      IF            (DIS.EQ.'Y') THEN
C        IDIS=1
C      ELSE
C        IDIS=0
C      END IF
C
C      TYPE *, 'Input 1 OR D for new normalizing constant in AW feature'
C      ACCEPT *,INR
C
C      Parameters are entered by means of subroutines in order to make the

```

```

C      changing of parameters simpler and more flexible later on in program
C
      IQ=IBIG_LOOP
      CALL DOM(IQFT1,IQFT2,IQ,IGRAPH,&22)      ! Select classification domain
22     CALL PZN(IPOL,LINE,IQ,IGRAPH,&1)         ! I/P polarization parameters
1      CALL ELN(IELEV,LINE,IQ,IGRAPH,&8)       ! I/P elevation parameters
8      LINE(3)(1:30)='ELEV ASSUMED      KNOWN      '
      IF(IELEV(3).EQ.2) CALL EKJ(IEK,LINE,IQ,IGRAPH,&10) ! apriori ele knowl
10     IF(IEK.EQ.1.AND.IER_AS.EQ.0) CALL ERE(IER_EL,LINE,IQ,IGRAPH,&2)
2      CALL ASP(MINASP,MAXASP,INCASP,LINE,IQ,IGRAPH,&4) ! Select aspects
4      CALL AKJ(IAK,LINE,IQ,IGRAPH,&5)             ! apriori asp. knowledge
6      IF(IAK.EQ.1.AND.IER_EL.EQ.0) CALL ERA(IER_AS,LINE,IQ,INCASP,IGRAPH,&6)
6      CALL FRE(FMIN,FINC,NF,LINE,IQ,IGRAPH,&7)    ! Select frequencies
7      IF (IQFT2.EQ.0) CALL RAL(IRA,IQ,IGRAPH,&8)   ! Select Rel Amplitude
8      CALL NOS(IS3,IS4,NEX,IQ,IGRAPH,&554)        ! Select no expts & r.n seeds
554     IF(IQFT1.EQ.1) CALL NAG(JNAG,ANAG,&555)
555     CALL FEA(IYA,IYW,RR,IQ,IGRAPH,IB,LINE,&556)
C
C      End of input routine  !!!!!!!!!!!!!!!!!!!!!!!!!!!!!!!!!!!!!!!!!!!!!!! END INPUTS
C
5656    FMAX=FMIN+(NF-1)*FINC
C
C      Read data files  !!!!!!!!!!!!!!!!!!!!!!!!!!!!!!!!!!!!!!!!!!!!!!! READ DATA FILES
C
C      !!!!!!!!!!!!!!!!!!!!!!!!!!!!!!!!!!!!!!!!!!!!!!!!!!!!!!!!!!!!!!!!!!!!!!!
C      CALL DATA(MINASP,MAXASP,INCASP,FMIN,FMAX,FINC,NF,LINE) !!!!!!!!!!!!! DATA
C      !!!!!!!!!!!!!!!!!!!!!!!!!!!!!!!!!!!!!!!!!!!!!!!!!!!!!!!!!!!!!!!!!!!!!!!
C
C      Estimate signal powers for freq. and time classification
C
2880    PAVE=0.
      DO 910 I=1,NS
      DO 910 J=1,NF
      PAVE=PAVE+A(I,J)*A(I,J)
910    CONTINUE
C
      PAVE=PAVE/(FLOAT(NF)*FLOAT(NS))      ! Pave=sum(A**2/ns/nf)
      PAVE=10.*ALOG10(PAVE)                ! dB
      IN_PAVE=NINT(PAVE)                   ! Convert to nearest integer
      IN_MIN=IN_PAVE-30                   ! +/- 30 dB is a useful range
      IN_MAX=IN_PAVE+30                   ! for classification
      IN_INC=10                           ! This gives us 7 values of S/N
C
      IF(IBIG_LOOP.EQ.1.AND.IGRAPH.EQ.1) THEN      ! First run
      TYPE *, ' '
      TYPE *, 'Ave power (dB) = ',IN_PAVE
      TYPE *, 'Suggested MIN,MAX,INC of noise power for +/- 30 dB S/N '
      TYPE *,IN_MIN,IN_MAX,IN_INC
C
C      Specify minimum,maximum and increment of
C      additive gaussian noise powers, once signal power is known
C
      TYPE      *, ' '
      TYPE      *, 'Input MIN,MAX,INC of the noise power (dB) '
C      ACCEPT    *,IV1,IV2,IVT

```

```

IV1=IN_MIN
IV2=IN_MAX
IVT=IN_INC
SNR_MAX=NINT(PAVE)-IV1
SNR_MIN=NINT(PAVE)-IV2
ELSE
IV1=IN_PAVE+SNR_MIN
IV2=IN_PAVE+SNR_MAX
END IF
! Find limits of SNR

C
C
C
5555 IF(IQFT1.EQ.1) THEN
C
C
6664 DO 99237 I=1,NF
99237 WL(I)=300./((FMIN+(I-1)*FINC)
C
! Compute wavelengths

PI=4.*ATAN(1.)
TWOPI=2.*PI
NF1=NF-1
C
DO 1434 I=1,NS
DO 1434 J=1,NF-1
IF(IRA.EQ.1)A(I,J)=A(I,J)/A(I,J+1)
! Compute relative amplitude
C
C
C
Eliminate branch cuts
PC=P(I,J)
DP=P(I,J)-P(I,J+1)
IF(DP.GT.PI)PC=PC-TWOPI
IF(DP.LT.-PI)PC=PC+TWOPI
C
1434 W(I,J)=WL(J)*PC-WL(J+1)*P(I,J+1)
C
! Compute relative phase

IF(IRA.EQ.0)CALL VARN(A,NF,NS,VA,1)
IF(IRA.EQ.1)CALL VARN(A,NF1,NS,VA,1)
! Estimate variances of amplitudes
CALL VARN(W,NF1,NS,VW,1)
! Estimate variances of W's
C
505 RK=SQRT(VA/(RR*VW))
C
! Calculate normalization constant RK
C
C
Print out parameters
C
PRINT *, ' No of targets = ',NS
PRINT *, ' VAR(AMP) = ',VA
PRINT *, ' VAR(W) = ',VW
PRINT *, ' Ave. signal power (dB) = ',PAVE
PRINT 18221,RR
18221 FORMAT(1X,' VAR(A)/VAR(KW) = ',E12.5)
PRINT 18222,IYW,IYA
18222 FORMAT(' IYW = ',I1,' IYA = ',I1)
PRINT *, ' '
C
C
ELSE
C

```

```

IYA=0                      | Reset feature parameters for call
IYW=0                      | to MN

C
CALL FORT(FFFT,5,SFFT,0,IFERR)

C
C   Calculate square roots of total signal powers
C
DO 98274 I=1,NS
SP(I)=0
DO 9824 J=1,NF
9824 SP(I)=SP(I)+ABS(C(I,J))**2
98274 SP(I)=SQRT(SP(I))
C
PRINT *, ' No of targets ', NS
PRINT *, ' Ave signal power (dB) = ', PAVE
PRINT *, ' '

C
END IF

C
C   Calculate 80% confidence interval for 30% error
C   and encode into header line
C
5757 CON_IN=185.0*SQRT(0.7*0.3/NS/NEX)
IF(IQ.EQ.1.AND.IGRAPH.GT.1) THEN
DO I=1,70
LINE(8)(I:I)=' '
END DO
END IF
IF(IQ.EQ.1) THEN
ENCODE(23,1038,LINE(8))CON_IN
1038 FORMAT('80% CI (@30%) +/- ',F3.1,'%')
ELSE
DO I=70,20,-1
IF(LINE(8)(I:I).NE.' ') THEN
L9=I
GOTO 52
END IF
END DO
52 ENCODE(4,1037,LINE(8)(L9+5:L9+8))CON_IN
1037 FORMAT(F3.1,'%')
END IF

C
C   Encode number of targets into a header line
C
IF(IQ.EQ.1.AND.IGRAPH.GT.1) THEN
DO I=1,70
LINE(8)(I:I)=' '
END DO
END IF
IF(IQ.EQ.1) THEN
ENCODE(21,1040,LINE(8))NS
1040 FORMAT('NO OF TARGETS ',I5)
ELSE
DO I=70,21,-1
IF(LINE(8)(I:I).NE.' ') THEN

```

```

      LB=I
      GOTO 53
    END IF
  END DO
53      ENCODE(5,1039,TLINE)NS      ! Encode numerical data into a
1039      FORMAT(I5)                ! temporary variable
      LINE(8)(LB+5:LB+10)=TLINE(1:5) ! Add to existing header
    END IF

  C
  C      Encode classification features into a header
  C
      IF(IRA.EQ.1) T_CHAR(1:4)='R ' ! Rel amp
      IF(IRA.EQ.0) T_CHAR(1:4)='A ' ! Amp
      IF(IYA.EQ.0.AND.IYW.EQ.0) THEN ! Time
        TLINE(1:4)='T '
      ELSE IF(IYA.EQ.0.AND.IYW.EQ.1) THEN ! W only
        TLINE(1:4)='W '
      ELSE IF(IYA.EQ.1.AND.IYW.EQ.0) THEN ! Rel/amp only
        TLINE(1:4)=T_CHAR(1:4)
      ELSE IF(IYA.EQ.1.AND.IYW.EQ.1) THEN ! Rel/amp & W
        TLINE(1:4)=T_CHAR(1:1)
      TLINE(2:4)='6W '
    END IF

  C
      IF(IQ.EQ.1.AND.IGRAPH.GT.1) THEN
        DO I=1,70
          LINE(10)(I:I)=' '
        END DO
      END IF
      IF(IQ.EQ.1) THEN
        LINE(10)(1:19)='CLASS. FEATURES ' ! On first run include title
        LINE(10)(20:24)=TLINE(1:4) ! Add feature description
      ELSE
        DO I=70,20,-1 ! Search header for end of previous
          IF(LINE(10)(I:I).NE.' ') THEN ! entry
            L10=I ! Find length of previous entry
          GOTO 51
        END IF
      END DO
51      LINE(10)(L10+5:L10+9)=TLINE(1:4) ! Add new entry
    END IF

  C
  C      Vary the noise power from IV1 to IV2 dB ||||| VARY NOISE
  C      at an increment of IVT dB
  C
      J_COUNT=NINT(FLOAT(IV2-IV1)/FLOAT(IVT))+1 ! Run counter
      TYPE *, ' '
      TYPE *, ' Count down to end of classification run'
      IRMIS=0 ! Init. run index

  C
      DO 80 IV=IV1,IV2,IVT

  C
      IRMIS=IRMIS+1 ! Index so that RMIS can be arrayed
      TYPE *,J_COUNT
      J_COUNT=J_COUNT-1 ! Count down for long processing times

```

```

      RMIS=0                      ! Initialize the number of false alarms
C
      DO 888 IEX=1,NEX           ! Perform classifications NEX times
C
      IF(IDIS.EQ.1)PRINT *, '*****'
C
      Add noise to the original data files to generate
      test targets
C
      VM=10.*(FLOAT(IV)/10.)      ! dB to nepers
C
      .....
      CALL MN(VM,IS3,IS4,C,NC,NF,NS,IYA,IYW,IEX,SAP,SP)  !!!!!!! CALL MN
      .....
C
      IF(IQFT1.EQ.1) THEN !!!!!!! IF(IQFT2.EQ.1) THEN GOTO TIME DOMAIN CLASS.
C
      Calculate the noisy amplitude and phase returns
C
      DO 921 I=1,NS
      DO 921 J=1,NF
      AN(I,J)=ABS(NC(I,J))
821  PN(I,J)=ATAN2(AIMAG(NC(I,J)),REAL(NC(I,J)))
C
      Calculate the noisy W's
C
      DO 922 I=1,NS
      DO 922 J=1,NF-1
      PC=PN(I,J)
      DP=PN(I,J)-PN(I,J+1)
      IF(DP.GT.PI)PC=PC-TWOPI
      IF(DP.LT.-PI)PC=PC+TWOPI
822  WN(I,J)=WL(J)*PC-WL(J+1)*PN(I,J+1)
      IF(IRA.EQ.0)GO TO 398
C
      Calculate the noisy relative amplitudes
C
      DO 349 IR1=1,NS
      DO 349 IR2=1,NF-1
349  AN(IR1,IR2)=AN(IR1,IR2)/AN(IR1,IR2+1)
C
      398  IF(INR.EQ.1) THEN
      IF(IRA.EQ.0) CALL VARN(AN,NF,NS,VA,1)
      IF(IRA.EQ.1) CALL VARN(AN,NF1,NS,VA,1)
      CALL VARN(WN,NF1,NS,VW,1)
      RK=SQRT(VA/(RR*VW))
      END IF
C
      Compute the nearest neighbour distances
      between any two classes
C
      .....
      CALL DIST_F(IRA,IYW,IYA,A,W,AN,WN,NF,NS,RR,RK,D,JNAG,ANAG)
      .....
C

```



```

ELSE  ||||| TIME DOMAIN CLASS.

C
C Calculate the square roots of the total powers of
C the noisy targets
C
DO 8221 I=1,NS
SNP(I)=0
DO 8212 J=1,NF
SNP(I)=SNP(I)+ABS(NC(I,J))**2
8212 CONTINUE
8221 SNP(I)=SQRT(SNP(I))

C
C Compute cross coefficients between any two targets
C
NB=INT(FMIN/FINC)

C
C |||||
C 479 CALL DIST_T(C,NC,SP,SNP,NF,NS,D,NB) ||||| CALL DIST_T
C |||||
C
END IF

C
C Do classification and compute number of false alarms
C
C If the aspects are assumed known then
C consider only those classes whose aspect angles
C are the same as that of the target,otherwise
C consider all classes
C
KASP=(MAXASP-MINASP)/INCASP+1          ! No of aspect angles
IF(IAK.EQ.0)KASP=1                    ! aspects when aspect is known

C
C Find the nearest neighbour to the test targets
C or a class which has the max correlation coefficient
C with a target
C
IF(IEK.EQ.1.AND.IELEV(3).GT.1) THEN    ! Elevation known

C
C If elevation is known and there is more than 1 elevation, then
C consider only those classes whose elevations are known
C
IPP=2          ! Elev known
ELSE
IPP=1          ! Elev unknown
END IF

C
DO IP=1,IPP    ! Split target array into 2 parts if elev known

C
IKX1=NS*(IP-1)/2+1    ! --> ( 1 then NS/2 + 1 ) or 1
NS1=NS*IP/IPP         ! --&; ( NS/2 then NS ) or NS

C
DO 7263 IKX=1,KASP    ! 1-->No of aspects
IEXP0=1
IK1=IKX+IKX1-1
7171 DO 740 IT=IK1,NS1,KASP    ! 1,2,-->NS/2 & NS/2+1,2,-->NS

```

```

      DMIN=10000000000.      ! freq
      DMAX=-10.              ! time

C      IF(IER_EL.EQ.1) THEN      ! Change variables in do loop
      NS2=NS/IP              ! to introduce error of 15 deg in
      IKX2=(IPP-IP)*NS/2+1    ! elevation
      ELSE
      NS2=NS1                ! IER_EL=0 implies no elevation error
      IKX2=IKX1              ! therefore keep no noise elevations
      END IF                 ! the same as noisy elevations

C      IK2=IKX+IKX2-1
      DO 860 IU=IK2,NS2,KASP    ! Index for searching noiseless targets

C      IF(IER_AS.EQ.1) THEN
C      C      Introduce a deliberate error in aspect. There must be 2 or 3 aspects to
C      C      do this. If 1st shift up by INCASP, if last shift down by INCASP, if
C      C      middle shift up and down by INCASP. This simulates an error of +/-
C      C      INCASP degrees.
C
      IF(IKX.EQ.1) I=IU+1
      IF(IKX.EQ.3.OR.(KASP.EQ.2.AND.IKX.EQ.2)) I=IU-1
      IF(IKX.EQ.2.AND.KASP.EQ.3) I=IU+(-1)*IEXP0
      ELSE
      I=IU
      END IF

C      C      D(I,IT) is the distance between noiseless target I and noisy target IT
C      C
      IF(IQFT1.EQ.1) THEN      ! Freq classification
      IF(D(I,IT).GE.DMIN)GO TO 860    ! search for min distance
      DMIN=D(I,IT)
      IMIN=I
      ELSE
      IF(D(I,IT).LE.DMAX) GO TO 860    ! Time classification
      DMAX=D(I,IT)                    ! search for max corr. coeff.
      IMAX=I
      END IF

860      CONTINUE

C      C      If a target is misclassified increase the
C      C      number of false alarms by one
C
      IF (IER_AS.EQ.1) THEN
C      C      If a deliberate error is made in aspect, alter IMIN,IMAX to account
C      C      for this. So if algorithm picks S1 @ 10 deg as the closest neighbour
C      C      to S1 @ 0 deg, then this is considered a correct classification
C
      IF(IQFT1.EQ.1) IMINMAX=IMIN
      IF(IQFT2.EQ.1) IMINMAX=IMAX
      IF(IKX.EQ.1) IMINMAX=IMINMAX-1
      IF(IKX.EQ.3.OR.(IKX.EQ.2.AND.KASP.EQ.2)) IMINMAX=IMINMAX+1
      IF(IKX.EQ.2.AND.KASP.EQ.3.AND.IEXP0.EQ.1) IMINMAX=IMINMAX+1

```

```

      IF(IKX.EQ.2.AND.KASP.EQ.3.AND.IEXPO.EQ.2) IMINMAX=IMINMAX-1
      IMIN=IMINMAX
      IMAX=IMINMAX
      END IF

C
      IF(IER_EL.EQ.1.AND.IEK.EQ.1) THEN
C
C      Allow for deliberate error made in elevation in the same way as was
C      done for aspect
C
      IF(IQFT1.EQ.1) IMINMAX=IMIN
      IF(IQFT2.EQ.1) IMINMAX=IMAX
      IF(IP.EQ.1) IMINMAX=IMINMAX-NS/2
      IF(IP.EQ.2) IMINMAX=IMINMAX+NS/2
      IMIN=IMINMAX
      IMAX=IMINMAX

C
      END IF

C
      IF(IDIS.EQ.1.AND.IQFT1.EQ.1)PRINT *,' TARGET :',IT,' MIN = ',IMIN
      IF(IDIS.EQ.1.AND.IQFT2.EQ.1)PRINT *,' TARGET :',IT,' MAX = ',IMAX
      IF(IDIS.EQ.1)PRINT 730,(NINT(D(I1,IT)),I1=IK2,NS2)
C      IF(IDIS.EQ.2)WRITE(1,730)(D(I1,IT),I1=IK2,NS2)
730      FORMAT(1X,36I5,/)
C
      IF(IMIN.NE.IT.AND.IQFT1.EQ.1)RMIS=RMIS+1.      ! Increment errors
      IF(IMAX.NE.IT.AND.IQFT2.EQ.1)RMIS=RMIS+1.
740      CONTINUE
C
      IF(IKX.EQ.2.AND.IER_AS.EQ.1.AND.IEXPO.EQ.1.AND.KASP.EQ.3) THEN
      IEXPO=2
      GOTO 7171      ! If no of asps = 3, repeat for middle aspect
      END IF

C
7263      CONTINUE      ! number of aspects loop
      END DO      ! number of elevations loop
888      CONTINUE      ! number of experiments loop
C
      Calculate the maximum likelihood estimate
      of the error probability
      (Account for extra classifications done when there are 3 aspects
      and a deliberate error is introduced.)
C
      IF(IER_AS.EQ.1.AND.KASP.EQ.3) RMIS=RMIS/FLOAT(NEX*(NS+6))*100.
      IF(IER_AS.EQ.0.OR.KASP.EQ.2) RMIS=RMIS/FLOAT(NEX*NS)*100.

C
      SNR=NINT(PAVE)-IV      ! Signal to noise ratio
      IF(IDIS.EQ.0) PRINT 1113,SNR,RMIS
1113      FORMAT(' SIGNAL TO NOISE RATIO = ',I3,', % ERRORS = ',F5.1)
C
      Y_PLOT(IBIG_LOOP,J_COUNT+1)=RMIS      ! plotting array
      IF(IV.EQ.IV2) THEN
      PRINT *,' *****
      PRINT *,'
      END IF

```

```

80      CONTINUE
C
      IF(IER_AS.EQ.1) THEN
      IF(IQ.EQ.1.OR.IGRAPH.EQ.1) THEN
      TYPE *, ' '
      TYPE *, 'Continue to have error in aspect ? Y or N '
      ACCEPT 12986,CON_ERA
12986   FORMAT(A1)
      TCON_EA(IQ)(1:1)=CON_ERA(1:1)      ! Store previous entries for subsequent
      ELSE                                ! runs
      CON_ERA(1:1)=TCON_EA(IQ)(1:1)
      END IF
      IF(CON_ERA.EQ.'N') IER_AS=0
      END IF
C
      IF(IER_EL.EQ.1) THEN
      IF(IQ.EQ.1.OR.IGRAPH.EQ.1) THEN
      TYPE *, ' '
      TYPE *, 'Continue to have error in elevation ? Y or N '
      ACCEPT 12986,CON_ERE
      TCON_EL(IQ)(1:1)=CON_ERE(1:1)
      ELSE
      CON_ERE(1:1)=TCON_EL(IQ)(1:1)
      END IF
      IF(CON_ERE.EQ.'N') IER_EL=0
      END IF
C
      IBIG_LOOP=IBIG_LOOP+1                ! Increment curve counter
      IQ=IBIG_LOOP                        ! For convenience
C
C      Processing options
C
      IF(IGRAPH.EQ.1.OR.IQ.GT.(INUMG-1)) THEN
C
      TYPE *, ' '
      TYPE *, 'Type S to stop end plot'
      TYPE *, 'Type P to change current parameters '
      TYPE *, 'Type R to do new graph retaining old parameters'
      TYPE *, 'Type G to do new graph with new parameters'
C
      ACCEPT 1115,YN
1115   FORMAT(A1)
      AYN(IQ)=YN
      ELSE
      YN=AYN(IQ)
      END IF
C
      IF(YN.EQ.'S'.OR.YN.EQ.'G'.OR.YN.EQ.'R') GOTO 1117
C
C      Routine for changing parameters
C
      IF(IGRAPH.EQ.1.OR.IQ.GT.INUMG) THEN
C
      TYPE *, ' '
      TYPE *, 'Type P0 to change polarization'

```

```

TYPE *, 'AM to change rel/amplitude'
TYPE *, 'FR to change frequencies'
TYPE *, 'EL to change elevations'
TYPE *, 'EK to change un/known elev'
TYPE *, 'EE to change no/error in elev'
TYPE *, 'AS to change aspects'
TYPE *, 'AK to change un/known aspect'
TYPE *, 'AE to change no/error in aspect'
TYPE *, 'NE to change number of expts'
TYPE *, 'DO to change domains'
TYPE *, 'FE to change NN features'
TYPE *, 'NA to use Neils algorithm'

C
1118 TYPE *, 'Input change'
ACCEPT 1116, PAR_CH
1116 FORMAT(A2)
PAR(IQ)(1:2)=PAR_CH(1:2)
ELSE
PAR_CH(1:2)=PAR(IQ)(1:2)
END IF

C
IF(PAR_CH.EQ.'PO') CALL PZN(IPOL, LINE, IQ, IGRAPH, &5656)
IF(PAR_CH.EQ.'FR') CALL FRE(FMIN, FINE, NF, LINE, IQ, IGRAPH, &5656)
IF(PAR_CH.EQ.'AM') CALL RAL(IRA, IQ, IGRAPH, &5656)
IF(PAR_CH.EQ.'EL') THEN
CALL ELN(IELEV, LINE, IQ, IGRAPH, &7070)
7070 IF(IELEV(3).EQ.2) CALL EKJ(IEK, LINE, IQ, IGRAPH, &7072)
7072 IF(IEK.EQ.1.AND.IER_AS.EQ.0) CALL ERE(IER_EL, LINE, IQ, IGRAPH, &5656)
GOTO 5656
END IF
IF(PAR_CH.EQ.'EK') THEN
CALL EKJ(IEK, LINE, IQ, IGRAPH, &7074)
7074 IF(IEK.EQ.1.AND.IER_AS.EQ.0) CALL ERE(IER_EL, LINE, IQ, IGRAPH, &5757)
GOTO 5757
END IF
IF(PAR_CH.EQ.'EE'.AND.IEK.EQ.1) THEN
CALL ERE(IER_EL, LINE, IQ, IGRAPH, &5757)
ELSE IF(PAR_CH.EQ.'EE'.AND.IEK.EQ.0) THEN
TYPE *, 'Elevation must be known in order to introduce error'
GOTO 1118
END IF
IF(PAR_CH.EQ.'AK') THEN
CALL AKJ(IAK, LINE, IQ, IGRAPH, &7076)
7076 IF(IAK.EQ.1.AND.IER_EL.EQ.0) THEN
CALL ERA(IER_AS, LINE, IQ, INCASP, IGRAPH, &5757)
END IF
GOTO 5757
END IF
IF(PAR_CH.EQ.'AE'.AND.IAK.EQ.1.AND.IER_EL.EQ.0) THEN
CALL ERA(IER_AS, LINE, IQ, INCASP, IGRAPH, &5656)
ELSE IF(PAR_CH.EQ.'AE'.AND.IAK.EQ.0) THEN
TYPE *, 'Aspect must be known in order to introduce error'
GOTO 1118
END IF

```

```

IF(PAR_CH.EQ.'AS') THEN
CALL ASP(MINASP,MAXASP,INCASP,LINE,IQ,IGRAPH,&7078)
7078 IF(MINASP.NE.MAXASP) THEN
CALL AKJ(IAK,LINE,IQ,IGRAPH,&7080)
7080 IF(IAK.EQ.1.AND.IER_EL.EQ.0) THEN
CALL ERA(IER_AS,LINE,IQ,INCASP,IGRAPH,&72)
END IF
END IF
72 GOTO 5656
END IF
IF(PAR_CH.EQ.'NE') CALL NDS(IS3,IS4,NEX,IQ,IGRAPH,&5757)
IF(PAR_CH.EQ.'FE') CALL FEA(IYA,IYW,RR,IQ,IGRAPH,I9,LINE,&505)
IF(PAR_CH.EQ.'DO') THEN
CALL DOM(IQFT1,IQFT2,IQ,IGRAPH,&525)
525 IF(IQFT1.EQ.1) CALL FEA(IYA,IYW,RR,IQ,IGRAPH,I9,LINE,&505)
IF(IQFT2.EQ.1) GOTO 5555
END IF
IF(PAR_CH.EQ.'NA'.AND.IQFT1.EQ.1) CALL NAG(JNAG,ANAG,&5757)
C
GOTO 1118
C
C Plotting routine
C
1117 TYPE *,' '
TYPE *,' SNR_MIN SNR_MAX SNR_INC ',SNR_MIN,SNR_MAX,IVT
NDS=IBIG_LOOP-1
CALL V_PLOT(Y_PLOT,NDS,IRMIS,LINE,IGRAPH,SNR_MIN,SNR_MAX,IVT)
IF(YN.EQ.'S') THEN
STOP
END IF
IF(YN.EQ.'G') GOTO 11111
C
C End of first graph... continue if desired
C
INUMB=IQ
IBIG_LOOP=1
IQ=1
IGRAPH=IGRAPH+1
DO I=1,70
LINE(11)(I:I)=' '
END DO
C
TYPE *,'Type P0 to change polarization'
TYPE *,' AM to change rel/amplitude'
TYPE *,' FR to change frequencies'
TYPE *,' EL to change elevations'
TYPE *,' EK to change un/known elev'
TYPE *,' EE to change no/error 'in elev'
TYPE *,' AS to change aspects'
TYPE *,' AK to change un/known aspect'
TYPE *,' AE to change no/error in aspect'
TYPE *,' NE to change number of expts'
TYPE *,' FE to change features'
TYPE *,' DO to change domains'
TYPE *,' EX to exit from change session'

```



```

C      IF(JNAG.EQ.1) THEN
C      DO M=1,L_E
C      IF((D_T(M)-MEAN).GE.ANAG*SIGMA) D_T(M)=MEAN
C      END DO
C      END IF

C      DO M=1,L_E
C      D(I,IT)=D(I,IT)+D_T(M)
C      END DO

C      D(I,IT)=SQRT(D(I,IT))
20    CONTINUE
C      RETURN
C      END

C      C
C      C
C      C
C      C
C      C      This subroutine calculates the time domain correlation coefficients
C      C      for a set of noise contaminated targets.
C      C
C      SUBROUTINE DIST_T(C,NC,SP,SNP,NF,NS,D,NB)
C      C
C      C      REAL D(110,110),SP(110),SNP(110),S(8)
C      C      COMPLEX C(110,30),NC(110,30),RF(30),F(32)  !!!!!!! ARRAYS MAY NEED AL
C      C
C      DO 20 I=1,NS
C      DO 20 IT=1,NS
C      DO 23 K=1,NF
C      C
C      C      CALCULATE PRODUCTS OF RADAR RETURNS OF A CLASS
C      C      AND COMPLEX CONJUGATES OF A TARGET'S RETURNS
C      C
C      RF(K)=C(I,K)*CONJG(NC(IT,K))
C      C
C      23    CONTINUE
C      C
C      C      CALCULATE THE INVERSE FAST-FOURIER
C      C      TRANSFORM ( IFFT ) OF THE PRODUCTS
C      C
C      CALL IDIFT(RF,NF,NB,STM)
C      C
C      C      NORMALIZE THE OUTPUTS OF THE IFFT
C      C
C      D(I,IT)=STM/(2.*SP(I)*SNP(IT))
C      C
C      20    CONTINUE
C      20    RETURN
C      C      END
C      C
C      C      !!!!!!!!!!!!!!!!!!!!!!!!!!!!!!!!!!!!!!!!!!!!!!!!!!!!!!!!!!!!!!!!!!!!!!!!!!!!!!!!! MN

```

```

C
C      This subroutine adds gaussian noise to the original
C      data files to generate test targets
C
C      SUBROUTINE MN(VR,IS3,IS4,C,NC,NF,NS,IYA,IYW,IEX,SAP,SP)
C
C      COMPLEX NC(110,30),C(110,30)
C      REAL SAP(110),SP(110)
C
C      The Gaussian noise is additive and has variance VR
C      and mean 0.
C
C      Equal amounts of noise are added to the real
C      and imaginary parts of the data points.
C
C      VR1=VR/2.
C
C      DO 10 I=1,NS
C
C      Reset the seeds for each test target.
C
C      IS3=IS3-4
C      IS4=IS4-6
C      DO 10 J=1,NF
C
C      Generate two Gaussian numbers.
C
C      CALL GAUSS(IS3,0.,VR1,S3)
C      CALL GAUSS(IS4,0.,VR1,S4)
C
C      Generate a test target
C
C      NC(I,J)=CMPLX(REAL(C(I,J))+S3,AIMAG(C(I,J))+S4)
C
C      If the phase returns are unknown, set them to zero.
C
C      IF(IYA.EQ.1.AND.IYW.EQ.0)NC(I,J)=CMPLX(ABS(C(I,J))+S3,S4)
10  RETURN
END
C
C      |||||||||||||||||||||||||||||||||||||||||||||||||| DATA
C
C      This subroutine reads a data file generated by
C      the CATLOG.FOR scaling program
C
C      SUBROUTINE DATA(MINASP,MAXASP,INCASP,FMIN,FMAX,FINC,NF,LINE)
C
C      COMPLEX C(110,30)
C      REAL*4 A(110,30),P(110,30),W(110,30),AM(500),PH(500)
C      CHARACTER *2 FPOL,FEL,FLNAM(6),ASP(23),AIR(4),SHIP(6)
C      CHARACTER INFILE*14
C      CHARACTER*(*) LINE(11)
C      INTEGER IPOL(5),IELEV(3)
C
C      COMMON /BLK1/ IPOL,IELEV,NS,C,A,P,IRA,IQ,IGRAPH

```

```

C      DATA ASP/'00','05','10','15','20','25','30','35','40','45',
1'50','55','60','65','70','75','80','85','90','95',
2'E2','17','18'/
C      DATA SHIP/'AD','LR','LB','KX','KH','MD'/
C      DATA AIR/'B7','C0','C5','DC'/
C      IBASE=0                ! Counter to count each file accessed
C      IF(IQ.EQ.1.AND.IGRAPH.EQ.1) THEN
669  TYPE *, 'Input target type, SHIP or AIRCRAFT . S or A '
ACCEPT 770,AS
770  FORMAT(A1)
IF(AS.EQ.'S') THEN
IAS=1
ELSE IF(AS.EQ.'A') THEN
IAS=0
ELSE
GOTO 669
END IF
END IF
C      IF(IAS.EQ.0) THEN
PRINT *, ' Classification of aircraft'
LINE(1)(1:26)='CLASSIFICATION OF AIRCRAFT'
ELSE IF(IAS.EQ.1) THEN
PRINT *, ' Classification of ships'
LINE(1)(1:26)='CLASSIFICATION OF SHIPS'
END IF
C      IF(IAS.EQ.0)NST=4
IF(IAS.EQ.1)NST=6          ! There are 6 ships available for classif.
C      DO 772 I=1,NST
IF(IAS.EQ.0)FLNAM(I)=AIR(I)  ! Assign target name to temp variable
772  IF(IAS.EQ.1)FLNAM(I)=SHIP(I)
C      IF(INCASP.EQ.0)INCASP=1
IBC=(MAXASP-MINASP)/INCASP
C      ITPOLV=1
ITPOLH=1
ITPOLX=1
C      Start main loop for collecting target data  !!!!!!!!!!!!!!! MAIN LOOP
C      DO IP=1,IPOL(5)                ! Loop for as many polarizations
FPOL(1:1)='F'
IF(IPOL(1)*ITPOLV.EQ.1) THEN
FPOL(2:2)='V'
ITPOLV=0
GOTO 5050
ELSE IF(IPOL(2)*ITPOLH.EQ.1) THEN      ! Establish a new polarization
FPOL(2:2)='H'                        ! each time pass through loop

```

```

ITPOLH=0
GOTO 5050
ELSE IF(IPOL(3)*ITPOLX.EQ.1) THEN
FPOL(2:2)='X'
ITPOLX=0
END IF

C
5050 IEL15=1
      IEL27=1
C
      DO IE=1,IELEV(3)                                I Loop for as many elevations
      IF(IELEV(1)*IEL15.EQ.1) THEN
      FEL(1:2)='15'
      IEL15=0
      GOTO 5060
      ELSE IF(IELEV(2)*IEL27.EQ.1) THEN
      FEL(1:2)='27'
      IEL27=0
      END IF

C
5060 DO 40 I=1,NST                                     I Loop for as many targets
      DO 111 IAP1=MINASP,MAXASP,INCASP                 I Loop for as many aspects
      IBASE=IBASE+1

C
C      Convert aspect angle to an index so that file name can be formed
C
      IF(IAS.EQ.1) THEN
      IF(IAP1.GT.95) THEN
      IF(IAP1.EQ.100) IASP=21
      IF(IAP1.EQ.170) IASP=22
      IF(IAP1.EQ.180) IASP=23
      ELSE
      IASP=NINT(FLOAT(IAP1)/5.)+1
      END IF
      ELSE
      IASP=IAP1/15+1
      END IF

C
C      Compile filename :      R:**FV##15              ** = Target name
C                                  FH 27                ## = Target aspect
C                                  FX                     F = Full scale
C                                  V,H,X = Polarizations
C
      INFILE(1:2)='R:'
      INFILE(3:4)=FLNAM(I)
      INFILE(5:6)=FPOL
      INFILE(7:8)=ASP(IASP)
      INFILE(9:10)=FEL
      INFILE(11:12)='D'
      INFILE(13:14)='AT'
      INFILE=INFILE(3:14)
C      TYPE 6060,INFILE(1:8)
C      PRINT 6060,INFILE(1:8)
5060  FORMAT(1X,A8)
C

```

```

C      CALL TRT(INFILE,AM,PH,TFMIN,TFINC,SF)
C
C      Note the data files
C      are already scaled by the scale factor
C
      IMAX=(FMAX-TFMIN)/TFINC+1
      IMIN=(FMIN-TFMIN)/TFINC+1
      IC=FINC/TFINC
      NF1=0
      DO 2111 J=IMIN,IMAX,IC
C
C      Convert amplitude from dBcm**2 to nepers m**2
C      by antilogging and division by 100
C
      NF1=NF1+1
      A(IBASE,NF1)=10.**(AM(J)/20.)/100.
2111    P(IBASE,NF1)=PH(J)
111    CONTINUE
40     CONTINUE
      END DO
      END DO
C
C      End main loop for collecting target data ||| MAIN LOOP
C
      NS=IBASE
C      NS=Total number of targets = #pol x #asp x #elev x #target(=6 for ship)
C
C      Split up A,P matrix into 2 parts to allow V/H to be done
C
      IF(IPOL(4).EQ.1) THEN
        NS=NS/2
        DO I=1,NS
          DO J=1,NF1
            A(I,J)=A(I,J)/A(I+NS,J)
            P(I,J)=P(I,J)-P(I+NS,J)
          END DO
        END DO
      END IF
C
6664   DO 1436 I=1,NS
        DO 1436 J=1,NF
1436   C(I,J)=CMPLX(A(I,J)*COS(P(I,J)),A(I,J)*SIN(P(I,J)))
        IF(NF.LE,NF1)GO TO 1435
        DO 1437 I=1,NS
          P(I,NF)=0
C
C      If it is not possible to supply all of the frequencies requested
C      fill the remaining array points with zeros
C
          A(I,NF)=0
1437   C(I,NF)=0
1435   RETURN
      END
C
C      |||

```

```

C
C      This subroutine calculates the variance of a set of numbers
C
C      SUBROUTINE VARN(A,NF,NS,VA,INC)
C
C      REAL A(110,30)
C
C      RMEAN=0
C      DO 10 I=1,NS
C      DO 10 J=1,NF,INC
10      RMEAN=A(I,J)+RMEAN
C      RMEAN=RMEAN/(NS*(NF/INC))
C      VA=0
C      DO 20 I=1,NS
C      DO 20 J=1,NF,INC
20      VA=VA+(A(I,J)-RMEAN)**2
C      VA=VA/(NS*(NF/INC))
C      RETURN
C      END
C
C      :::::::::::::::::::::::::::::::::::::::::::::::::::::::::::::::::: GAUSS
C
C      This subroutine generates a Gaussian random number
C
C      SUBROUTINE GAUSS(IS,AM,V,S)
C
C      A=0.0
C      DO 50 I=1,12
C      A=A+RAN(IS)
50      CONTINUE
C      S=(A-6.)*SQRT(V)+AM
C      RETURN
C      END
C
C      :::::::::::::::::::::::::::::::::::::::::::::::::::::::::::::::::: IDIFT
C
C      This subroutine calculates the inverse Fourier transform of a set
C      of complex data points and finds the maximum of the results. It
C      assumes that the data points are symmetric around zero frequency
C
C      SUBROUTINE IDIFT(RF,NF,NB,STM)
C
C      COMPLEX F(32),RF(50)
C      REAL S(8)
C
C      COMMON /BLK2/S,F
C
C      NP=32
C      DO 40 I=1,NP
40      F(I)=(0.,0.)
C      K=0
C      DO 50 I=NB+1,NB+NF
C      K=K+1
C      F(I)=RF(K)
50      F(NP+2-I)=CONJG(RF(K))

```

```

C
C      Call a standard IFFT in the scientific library
C
C      CALL FORT(F,5,6,2,IFERR)
C      IF(IFERR.NE.0)PRINT *,' ERR IN IFFT'
C
C      Find the maximum of the outputs of the IFFT
C
C      STM=10000.
C      DO 500 I=1,NP
500    IF(REAL(F(I)).GT.STM)STM=REAL(F(I))
C      RETURN
C      END
C
C      ||||||||||||||||||||||||||||||||||||||||||||||||||||||||||||||||
C
C      Originally developed by J.Chen
C      Modified by N.Chamberlain May 1984 for inclusion in TAFCAL
C      This subroutine plots the results of classifications.
C
C      SUBROUTINE V_PLOT(YT,NDS,NPT,LINE,IGRAPH,INX1,INX2,INX3)
C
C      REAL X(50),Y(50),YT(10,50)
C      CHARACTER*(*) LINE(11)
C
C      IF(IGRAPH.EQ.1) THEN
5      TYPE *,'INPUT MIN, MAX, AND INC FOR S/N'
C      ACCEPT *,XMIN,XMAX,XINC
C      ELSE
C      XMIN=FLOAT(INX1)
C      XMAX=FLOAT(INX2)
C      XINC=FLOAT(INX3)
C      END IF
C      NPT=(XMAX-XMIN)/XINC+1.
C      J=0
C      DO 100 FW=XMIN,XMAX,XINC
100    J=J+1
C      X(J)=FW
C
C      DSX=(XMAX-XMIN)/5.
C      DSY=100./6.
C      SPAX=5./FLOAT(NPT-1)
C      SPAY=6./10.
C
C      CALL VPLOTS(0,0,0)
C      CALL PLOT(1.5,1.5,-3)
C      CALL NEWPEN(3)
C      CALL AXIS(0.,0.,'POST-PROCESSING S/N IN DB',-25,5.,0.,XMIN,DSX,SPAX,0)
C      CALL AXIS(0.,0.,'MISCLASSIFICATION PERCENTAGE',28,6.,90.,0.,DSY,SPAY,0)
C      CALL NEWPEN(1)
C      CALL GRID(0.,0.,NPT-1,SPAX,10,SPAY,'33333333')
C
C      DO 60 I=1,NDS
C      DO 70 J=1,NPT
C      Y(J)=YT(I,J)

```

```

70      CONTINUE
      ISYM=1*I
      CALL NEWPEN(3)
80      CALL STRYP(X,XMIN,DSX,Y,0.,DSY,NPT,0.5,ISYM)
      C
      DO 9876 I=1,11
      IF(LINE(I)(1:10).EQ.'          ') GOTO 9876
      HEI=8.4-FLOAT(I-1)*0.2
      ILEN=LEN(LINE(I))
      CALL NEWPEN(2)
      CALL SYMBOL(0.0,HEI,0.1,%REF(LINE(I)),0.0,ILEN)
9876    CONTINUE
      C
      CALL PLOT(0.,0.,899)
      CALL PLOTNOW(IMS)
      TYPE *,' '
      TYPE *,'Plot again ? Y or N'
      ACCEPT 99,PAG
99      FORMAT(A1)
      IF (PAG.EQ.'Y') GOTO 5
      CALL LIB$SPAWN('% RENAME [NFC4348.FSB]*.MET [NFC4348.MET]*.*'
      $,'NL:', 'NL:')
      RETURN
      END
      C
      C
      C
      C
      C      This subroutine inputs the required polarization parameters.
      C
      C      SUBROUTINE PZN(IPOL,LINE,IQ,IGRAPH,*)
      C
      C      INTEGER IPOL(5)
      C      CHARACTER POL(5)*1,TLINE*5,TPOL(10)*5
      C      CHARACTER*(*) LINE(11)
      C
      C      DO I=1,5
      C      IPOL(I)=0          ! Reset pol. control indicies
      C      END DO
      C
      C      IF(IGRAPH.EQ.1.OR.IQ.EQ.1) THEN
      C      TYPE          *,' '
      C      TYPE          *,'Input polarization(s) V,H,X'
      C      ACCEPT          7,POL
      C      FORMAT          (5A1)
      C      DO I=1,5
      C      TPOL(IQ)(I:I)=POL(I)
      C      END DO
      C      ELSE
      C      DO I=1,5
      C      POL(I)=TPOL(IQ)(I:I)
      C      END DO
      C      END IF
      C
      C      Assign pol. control parameters
      C

```



```

C      CHARACTER*(*) LINE(11)
C
C      IF(IGRAPH.EQ.1.OR.IQ.EQ.1) THEN
13      TYPE
C      TYPE
C      ACCEPT
C      FORMAT
9      TEL(IQ)(1:5)=ELE(1:5)
      ELSE
      ELE(1:5)=TEL(IQ)(1:5)
      END IF
      IF(IQ.EQ.1.AND.IGRAPH.GT.1) THEN
      DO I=1,70
      LINE(4)(I:I)=' '
      END DO
      END IF
      IF(IQ.EQ.1) THEN
      LINE(4)(1:19)='ELEVATION (DEG.) '
      LINE(4)(20:25)=ELE(1:5)
      ELSE
      DO I=70,20,-1
      IF(LINE(4)(I:I).NE.' ') THEN
      IEND_L=I
      GOTO 53
      END IF
      END DO
53      L4=IEND_L
      LINE(4)(L4+5:L4+10)=ELE(1:5)
      END IF
C
C      Set elevation control parameters
C
C      DO I=1,3
      IELEV(I)=0
      END DO
C
C      IF(ELE(1:2).EQ.'15'.OR.ELE(4:5).EQ.'15') IELEV(1)=1
C      IF(ELE(1:2).EQ.'27'.OR.ELE(4:5).EQ.'27') IELEV(2)=1
C      IELEV(3)=IELEV(1)+IELEV(2)
C      IF(IELEV(3)) 13,13,15
C
C      Print out
C
C      IF(IELEV(1).EQ.1) PRINT *, ' 15 deg. elevation'
15      IF(IELEV(2).EQ.1) PRINT *, ' 27 deg. elevation'
C
C      RETURN 1
C      END
C
C      ||||||||||||||||||||||||||||||||||||||||||||||||||||||||||||||||
C
C      This subroutine inputs the required a priori information for elevation
C
C      SUBROUTINE EKJ(IEK,LINE,IQ,IGRAPH,*)
C

```

```

      CHARACTER*(*) LINE(11)
      CHARACTER TEK(10)*1,EK*1
C
      IF(IQ.EQ.1.OR.IGRAPH.EQ.1) THEN
1      TYPE *,' '
      TYPE *,' Elevation known    --> Type K'
      TYPE *,' Elevation unknown  --> Type U'
      ACCEPT 10,EK
10     FORMAT(A1)
      TEK(IQ)(1:1)=EK(1:1)
      ELSE
      EK(1:1)=TEK(IQ)(1:1)
      END IF
C
      IF(EK.EQ.'K') THEN
      IEK=1
      PRINT*,' Elevation assumed known'
      ELSE IF(EK.EQ.'U') THEN
      IEK=0
      PRINT*,' Elevation assumed unknown'
      ELSE
      GOTO 1
      END IF
C
      IF(IEK.EQ.1.AND.LINE(3)(1:3).EQ.' ') THEN
      LINE(3)(1:30)='ELEV ASSUMED      KNOWN      '
      ELSE IF(IEK.EQ.0.AND.LINE(3)(1:3).EQ.' ') THEN
      LINE(3)(1:30)='ELEV ASSUMED      UNKNOWN     '
      END IF
      IF(IQ.GT.1.AND. IEK.EQ.0) LINE(3)(31:41)='/   UNKNOWN'
      IF(IQ.GT.1.AND. IEK.EQ.1) LINE(3)(31:41)='/   KNOWN   '
C
      RETURN 1
      END
C
C      ///////////////////////////////////////////////////////////////////
C
C      This subroutine inputs error in elevation
C
      SUBROUTINE ERE(IER_EL,LINE,IQ,IGRAPH,*)
C
      CHARACTER*(*) LINE(11)
      CHARACTER TLINE*3,TER_L(10)*1,ER_EL*1
C
      IF(IQ.EQ.1.OR.IGRAPH.EQ.1) THEN
1      TYPE *,' '
      TYPE *,'Type Y or N for error in elevation'
      ACCEPT 10,ER_EL
10     FORMAT(A1)
      TER_L(IQ)(1:1)=ER_EL(1:1)
      ELSE
      ER_EL(1:1)=TER_L(IQ)(1:1)
      END IF
C
      IF(ER_EL.EQ.'Y') THEN

```



```

C      RETURN 1
C      END
C      ||||||||||||||||||||||||||||||||||||||||||||||||||||||||||
C      This subroutine inputs required aspect angles.
C      SUBROUTINE ASP(MINASP,MAXASP,INCASP,LINE,IQ,IGRAPH,*)
C
C      CHARACTER TLINE*12
C      CHARACTER*(*) LINE(11)
C      INTEGER TMINA(10),TMAXA(10),TINCA(10)
C
C      Specify target aspect angles
C
C      IF(IQ.EQ.1.OR.IGRAPH.EQ.1) THEN
C      TYPE      *, ' '
C      TYPE      *, 'Input MIN,MAX,INC aspect angles'
C      ACCEPT    *, MINASP,MAXASP,INCASP
C      TMINA(IQ)=MINASP
C      TMAXA(IQ)=MAXASP
C      TINCA(IQ)=INCASP
C      ELSE
C      MINASP=TMINA(IQ)
C      MAXASP=TMAXA(IQ)
C      INCASP=TINCA(IQ)
C      END IF
C
C      IF(IQ.EQ.1.AND.IGRAPH.GT.1) THEN
C      DO I=1,70
C      LINE(6)(I:I)=' '
C      END DO
C      END IF
C      IF(IQ.EQ.1) THEN
1020      ENCODE(30,1020,LINE(6))MINASP,MAXASP,INCASP
C      FORMAT('MIN,MAX,INC ASPECT',3I4)
C
C      ELSE
1025      ENCODE(12,1025,TLINE)MINASP,MAXASP,INCASP
C      FORMAT(3I4)
C      DO I=70,30,-1
C      IF(LINE(6)(I:I).NE.' ') THEN
C      IEND_L=I
C      GOTO 53
C      END IF
C      END DO
53      LB=IEND_L
C      LINE(6)(LB+1:LB+1)=' '
C      LINE(6)(LB+2:LB+14)=TLINE(1:12)
C      END IF
C
C      PRINT      2849,MINASP,MAXASP,INCASP
2849      FORMAT      (' MIN,MAX,AND INC of the aspects .....',3I4)
C

```



```

C      END
C      |||
C      This subroutine inputs required a priori information for aspect angle
C
C      SUBROUTINE AKJ(IAK,LINE,IQ,IGRAPH,*)
C
C      CHARACTER*(*) LINE(11)
C      CHARACTER TAK(10)*1,AK*1
C
C      IF(IQ.EQ.1.OR.IGRAPH.EQ.1) THEN
1      TYPE      *, ' '
      TYPE      *, ' Aspect known      --> TYPE K'
      TYPE      *, ' Aspect unknown   --> TYPE U'
      ACCEPT    18,AK
18     FORMAT    (A1)
      TAK(IQ)(1:1)=AK(1:1)
      ELSE
      AK(1:1)=TAK(IQ)(1:1)
      END IF
C
C      IF      (AK.EQ.'K') THEN
      IAK=1
      PRINT*,    ' Aspect assumed known'
      ELSE IF  (AK.EQ.'U') THEN
      IAK=0
      PRINT*,    ' Aspect assumed unknown'
      ELSE
      GOTO 1
      END IF
C
C      IF(IAK.EQ.1.AND.IQ.EQ.1) THEN
      LINE(5)(1:30)='ASPECT ASSUMED      KNOWN      '
      ELSE IF(IAK.EQ.0.AND.IQ.EQ.1) THEN
      LINE(5)(1:30)='ASPECT ASSUMED      UNKNOWN      '
      END IF
      IF(IQ.GT.1.AND.IAK.EQ.0) LINE(5)(31:41)='/ UNKNOWN'
      IF(IQ.GT.1.AND.IAK.EQ.1) LINE(5)(31:41)='/ KNOWN  '
C
C      RETURN 1
C      END
C      |||
C      This subroutine selects relative amplitude feature.
C
C      SUBROUTINE RAL(IRA,IQ,IGRAPH,*)
C
C      CHARACTER TRA(10)*1,RA*1
C
C      IF(IQ.EQ.1.OR.IGRAPH.EQ.1) THEN
1      TYPE      *, ' '
      TYPE      *, ' Use relative amplitude ? Y or N'
      ACCEPT    17,RA

```

```

17      FORMAT      (A1)
      TRA(IQ)(1:1)=RA(1:1)
      ELSE
      RA(1:1)=TRA(IQ)(1:1)
      END IF

C
      IF      (RA.EQ.'Y') THEN
      IRA=1
      PRINT*, ' Relative amplitude used'
      ELSE IF (RA.EQ.'N') THEN
      IRA=0
      ELSE
      GOTO 1
      END IF

C
      RETURN 1
      END

C
C      !!!!!!!!!!!!!!!!!!!!!!!!!!!!!!!!!!!!!!!!!!!!!!!!!!!!!!!!!!!!!!!!!!!!!!!
C
C      This subroutine inputs seeds for random no. generator, and number
C      of experiments.
C
      SUBROUTINE NOS(IS3,IS4,NEX,IQ,IGRAPH,*)
C
      INTEGER TNEX(10)
C
      Input two arbitrary large odd integers
      which will serve as seeds for generating random numbers
C
      IF(IQ.EQ.1.OR.IGRAPH.EQ.1) THEN
15      TYPE      *, ' '
      TYPE      *, 'Input two arbitrary large odd integers'
      ACCEPT     *, IS3, IS4
      TYPE      *, ' '
      TYPE      *, 'Input number of experiments'
      ACCEPT     *, NEX
      TNEX(IQ)=NEX
      ELSE
      NEX=TNEX(IQ)
      END IF

C
      PRINT 30,IS3,IS4
      PRINT 20,NEX
30      FORMAT(' Large integers ..... ',2I8)
20      FORMAT(' Number of experiments ..... ',I3)
C
      RETURN 1
      END

C
C      !!!!!!!!!!!!!!!!!!!!!!!!!!!!!!!!!!!!!!!!!!!!!!!!!!!!!!!!!!!!!!!!!!!!!!!
C
C      This subroutine selects error in aspect angle
C
      SUBROUTINE ERA(IER_AS,LINE,IQ,INCASP,IGRAPH,*)

```



```

C      CHARACTER*(*) LINE(11)
C      CHARACTER TLINE*3,TER_A(10)*1,ER_AS*1
C
C      Note there must be 2 or 3 aspects to use the error subroutine
C
C      IF(IQ.EQ.1.OR.IGRAPH.EQ.1) THEN
1      TYPE *, ' '
      TYPE *, 'Type Y or N for error in aspect'
      ACCEPT 10,ER_AS
10     FORMAT(A1)
      TER_A(IQ)(1:1)=ER_AS(1:1)
      ELSE
      ER_AS(1:1)=TER_A(IQ)(1:1)
      END IF
C
C      IF(ER_AS.EQ.'Y') THEN
      IER_AS=1
      PRINT *, ' Error introduced in aspect',INCASP,' deg'
      ELSE IF(ER_AS.EQ.'N') THEN
      IER_AS=0
      PRINT *, ' No error in aspect'
      ELSE
      GOTO 1
      END IF
C
C      IF(LINE(11)(1:3).EQ.' ' .AND. IER_AS.EQ.1) THEN
      ENCODE(20,20,LINE(11))IQ
20     FORMAT('ASP ERR IN CURVE ',I3)
      ELSE IF(LINE(11)(1:3).NE.' ' .AND. IER_AS.EQ.1) THEN
      ENCODE(3,30,TLINE)IQ
30     FORMAT(I3)
      DO I=70,18,-1
      IF(LINE(11)(I:I).NE.' ') THEN
      L11=I
      GOTO 40
      END IF
      END DO
40     LINE(11)(L11+5:L11+8)=TLINE(1:3)
      END IF
C
      RETURN 1
      END
C
C      ||||||||||||||||||||||||||||||||||||||||||||||||||||||||||||||||
C
C      This subroutine selects nearest neighbour features.
C
C      SUBROUTINE FEA(IYA,IYW,RR,IQ,IGRAPH,I8,LINE,*)
C
C      CHARACTER*(*) LINE(11)
C      CHARACTER YWA(3)*1,TWA(10)*3,T_CHAR*4,TLINE*5
C      REAL TRR(10)
C
C      IF(I8.EQ.1.OR.IGRAPH.EQ.1) THEN

```

```

TYPE *,' '
TYPE *,'Input R=VAR(A)/VAR(W)'           ! Define the variance ratio
ACCEPT *,RR
TRR(IQ)=RR

C
C Specify the features as follows
C IYW = 1 —> use the W's
C IYW = 0 —> do not use the W's
C IYA = 1 —> use the amplitudes
C IYA = 0 —> do not use the amplitudes
C
1 TYPE *,' '
TYPE *,'Input required features A,W'
ACCEPT 557,YWA
557 FORMAT(3A1)
DO I=1,3
TWA(IQ)(I:I)=YWA(I)
END DO
ELSE
DO I=1,3
YWA(I)=TWA(IQ)(I:I)
END DO
RR=TRR(IQ)
END IF

C
C Assign feature control variables
C
IYW=0
IYA=0
DO I=1,3
IF(YWA(I).EQ.'A') IYA=1
IF(YWA(I).EQ.'W') IYW=1
END DO
IF((IYA+IYW).EQ.0) GOTO 1

C
RETURN 1
END

C
C
C
C This subroutine forms the input routine for an algorithm designed
C to reduce the effects of impulsive noise. This algorithm is still
C in an experimental stage and needs further development.
C
SUBROUTINE NAG(JNAG,ANAG,*)
C
CHARACTER YNAG*1
1 TYPE *,' '
TYPE *,'Use Neils Algorithm [ Y or N ]'
ACCEPT 10,YNAG
10 FORMAT(A1)
IF(YNAG.EQ.'Y') THEN
JNAG=1
TYPE *,' '
TYPE *,'Input value for standard deviation test [2]'

```

```

ACCEPT *,ANAG
PRINT *,'Nails Algorithm used'
PRINT *,ANAG
ELSE IF(YNAG.EQ.'N') THEN
  JNAG=0
  ELSE
  GOTO 1
  END IF
C
  RETURN 1
  END
C
C  ||||| END

```

```

C
C   THIS SUBROUTINE READS A FILE
C
      SUBROUTINE TRT(INFILE,AM,PH,FMIN,FINC,SF)
      INTEGER*2 LINE2(24)
      INTEGER*4 ID(12)
      CHARACTER INFILE*12
      REAL*4 AM(801),PH(801)
      INCLUDE 'SYS$LIBRARY:FORIOSDEF'
8106  OPEN(UNIT=8,NAME=INFILE,TYPE='OLD',READONLY,IOSTAT=IERR,ERR=8100)
      READ(8,30)(ID(I),I=1,12),LINE2,NP,FMIN,FINC,SF
      30  FORMAT(12A4,24A2,4A4)
      READ(8,40)(AM(I),I=1,NP),(PH(I),I=1,NP)
      40  FORMAT(128A4)
      GO TO 331
8100  IF(IERR.EQ.FOR$IOS_FILNOTFOU)THEN
      TYPE 1112,INFILE
1112  FORMAT(' FILE : ',A14,' WAS NOT FOUND',//,
1.  ' ENTER FILENAME AGAIN')
      ELSE IF (IERR.EQ.FOR$IOS_FILNAMSPE)THEN
      TYPE 1113,INFILE
1113  FORMAT(' FILE : ',A14,' WAS BAD, ENTER NEW FILENAME')
      ELSE
      TYPE *,'UNRECOVERABLE ERROR, CODE=',IERR
      STOP
      ENDIF
      TYPE *,'INPUTFILENAME'
      ACCEPT 1114,INFILE
1114  FORMAT(A14)
      GO TO 8106
331  CLOSE(UNIT=8,DISP='SAVE')
      RETURN
      END

C
C   THIS SUBROUTINE DECODES PARAMETERS READ
C   FROM THE DATA FILES, WHICH ARE CODED IN ASCII CODES
C
      SUBROUTINE DCDE(NP,FMIN,FINC)
      COMMON BUFF
      BYTE BUFF(6656)
      INTEGER*4 IMIN,IINC,NP

C
C   NO OF DATA POINTS IS STORED IN THREE CHARACTERS, AND
C   STARTING FREQ AND FREQ INC. IN 5 CHARACTERS
C
      CHARACTER*3 CNL
      CHARACTER*5 CFF,CINC
      EQUIVALENCE (BUFF(124),CNL),(BUFF(131),CFF),(BUFF(140),CINC)

C
C   CONVERT CHARACTERS INTO THEIR NUMERICAL EQUIVALENTS
C
      DECODE(3,100,CNL)NP
      100  FORMAT(I5)
      DECODE(5,100,CFF)IMIN

      DECODE(5,100,CINC)IINC
      FMIN=FLOAT(IMIN)/1000.
      FINC=FLOAT(IINC)/1000.
      RETURN
      END

```

```

      |
      |
      | Program name FILESORT
      | This procedure sorts through a directory
      | and compiles a file of desired filenames.
      | This file later becomes the source of a
      | control routine in CATLOG to enable large batches
      | of files to be scaled automatically.
      |
      | ON ERROR          THEN GOTO DONE
      | ON CONTROL_Y     THEN GOTO DONE
      |
      | INQUIRE F_TYPE "Input file type *.* "
      | INQUIRE D_OUT "Input output directory filename "
      |
      | DIRECTORY/VERSIONS=1/COLUMNS=1-
      |           /NODATE/NDSIZE/NOHEADING-
      |           /NOTRAILING/OUTPUT='D_OUT' 'F_TYPE'
      |
      | WRITE SYS$OUTPUT D_OUT
      | WRITE SYS$OUTPUT " "
      |
      | DIRECTORY/VERSIONS=1/COLUMNS=1/NOHEADING 'F_TYPE'
      |
      | DEFINE/USER_MODE SYS$INPUT SYS$COMMAND
      | RUN PC:NAMEFILE
      |
      | IF .NOT. $STATUS THEN GOTO DIR_ERR
      | DONE:
      | EXIT
      | DIR_ERR:
      | WRITE SYS$OUTPUT "Error:  'FMESSAGE($STATUS)'"
      | EXIT
      |
      |

```

```

*      | Command procedure : LINKCAL61.COM
*      | Linking routine for CAL61.FOR
*      |
*      LINK CAL61,SSCL61,FORT,SUBREMOVE,RCLIB/LIBRARY,-
*      PLOTV,PWNV,'PLOTLIB'

```

```

*      | Command procedure : LINKTAF.COM
*      | Linking routine for TAFCAL.FOR
*      |
*      LINK TAFCAL,TRT,PF:FORT,'PLOTLIB'

```

```

*      | Command procedure : LINKCAT.COM
*      | Linking routine for CATLOG.FOR
*      |
*      LINK CATLOG,RDFL

```